NASA TECHNICAL TRANSLATION

NASA TT F-373

NASA TT F-373

AUTOMATIC REGULATION AND CONTROL

SELECTED PARTS

by B. I. Andreychikov, et al.

Izdatel'stvo Akademii Nauk SSSR,
Moscow, 1962

NATIONAL AERONAUTICS AND SPACE ADMINISTRATION • WASHINGTON, D. C. • JULY 1966

NASA TT F-373

AUTOMATIC REGULATION AND CONTROL

SELECTED PARTS

By B. I. Andreychikov, et al.

Translation of "Avtomaticheskoye regulirovaniye i upravleniye."
Izdatel'stvo Akademii Nauk SSSR,
pp. 1-188 (Part I), 242-296 (Part III), 426-473 (Part VI),
Moscow, 1962

NATIONAL AERONAUTICS AND SPACE ADMINISTRATION

For sale by the Clearinghouse for Federal Scientific and Technical Information
Springfield, Virginia 22151 – Price $7.00

ANNOTATION

The present volume contains the reports presented at the VII Conference of Young Scientists of the Institute of Automation and Remote Control of the Academy of Sciences USSR, held in March 1960. The volume includes a wide range of scientific and technical questions in automatic regulation and control. The material of the volume is divided into seven sections: automatic control, automatic monitoring, computers, automation elements and devices, statistical methods in automation, theory of relay circuits and finite automata and automated electric drive.

Editor-in-Chief: Ya. Z. Tsypkin

CONTENTS

Page

Page

III. COMPUTERS

Page

34847

I. AUTOMATIC CONTROL

N66 34827

THE EFFECT OF DRY FRICTION AND FREE PLAY ON THE ERROR WITH REVERSAL IN SERVOSYSTEMS[1]

B. I. Andreychikov

The experience of the Institute of Automation and Remote Control of the Academy of Sciences USSR with machine tools using programed control has shown that large "bursts" of errors are observed at the points of reversal of machine tool servodrives. The cause of this phenomenon is the considerable dry friction loading and the free play in the transmission from the actuator motor to the position sensor. This phenomenon is manifested particularly strongly in the case where the actuator motor is not included in the rate-stabilizing feedback circuits. /3*

Physically the appearance of the large errors at reversal is explained as follows. At the time of reversal, after the actuator shaft has stopped, a definite time is required for the servosystem to develop on the motor shaft a torque equal to the dry friction torque and to take up the free play between the motor and the error sensor. Since during this time period the program continues to be applied to the input of the servosystem, or in the general case movement of the common axis continues while the actuator axis is immobile, a burst of error takes place. This burst will be larger for servosystems with greater inertia in the open-loop condition.

The present paper considers the analysis of these errors and presents recommendations for their reduction.

1. Reversal Errors Due to Dry Friction

Consider the processes which take place in the reversal region in the presence of dry friction torque. Prior to the moment of time t_0 (fig. 1), when the velocity of the output axis v_{out} reduces to zero, all processes in

---

*Numbers given in the margin indicate the pagination in the original foreign text.

[1]Values of free play and dry friction are assumed such that self-oscillations do not occur, but error "bursts" occur with reversal.

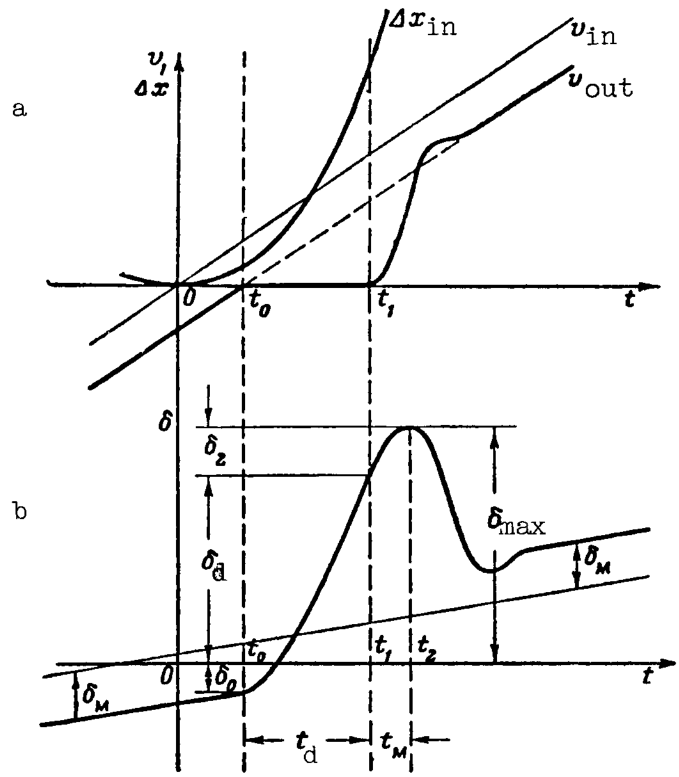

Figure 1. Processes in reversal region with dry friction or free play. a, Travel and velocity; b, error.

the servosystem are determined by the transfer function of the closed servosystem.

At the moment t_0 the motor stops and, under a definite condition which will be given below, remains immobile until the moment of time t_1 when the turning moment on its shaft reaches the value of the friction load torque. In the time interval $t_1 - t_0 = t_d$, termed the dead time, the servosystem is open, since the output shaft remains immobile in spite of the movement of /4 the input shaft, and the variation of the turning moment follows the transfer function of the open servosystem.

Beginning with the moment t_1 the motor shaft and the output shaft begin to move and the system again is closed. The system output quickly catches up with the input, but since the acceleration of the motor shaft is limited, for some time after t_1 the error will continue to increase, reaching its maximal

value δ_{max} at some instant of time t_2. In this case δ_{max} will exceed δ_d by a larger amount for a motor armature of higher inertia.

Knowing the form of the input action, the transfer functions of the closed and open systems, and also the initial conditions, we can precisely calculate all processes in the reversal region. However, this leads to extremely cumbersome calculations unsuitable for practical application.

Simple approximate equations for the error in the reversal region can be obtained in several cases. For this purpose we introduce the following assumptions:

(1) we limit ourselves to the class of input functions for which we can consider the velocity to vary linearly in the reversal region;

(2) for the open servosystem in the dead period of the output shaft we take account only of the first largest time constant, corresponding to the first conjugate frequency of the amplitude-frequency characteristic;

(3) in the time interval $t_1 - t_2$, as a result of the smallness of this interval and the large lag introduced by the rate stabilization, we consider the turning moment to vary in accordance with the law of the preceding /5
interval (ref. 1).

The idea of the derivation of the computational formulas amounts to the following. The error at the end of the dead time δ_d is determined as the algebraic sum of the error δ_0 and the increment of the input action during the dead period. The dead time t_d is determined from the condition of the motor-turning moment reaching the value equal to the moment of the static friction.

The maximal increment of the error after the dead period is determined by a study of the maximum of the expression for the error increment obtained, taking into account the third assumption.

The approximate expressions for the error δ_d depend on the initial conditions with respect to the error and the turning moment, i.e., actually on the form of the input action.

The initial conditions with respect to the turning moment are determined from the equation of equilibrium of the moments at the instant t_0

$$M_{t_0} = J\varepsilon - M_f, \qquad (1)$$

where ϵ is the angular acceleration of the motor shaft;

J is the moment of inertia of the motor, gearing and load, converted to the motor shaft;

M_f is the kinetic friction torque converted to the motor shaft.

According to (1), we can write the conditions for the existence of dead time

$$J\epsilon - M_f < M_{f_0}, \tag{2}$$

where M_{f_0} is the static friction moment.

We present without derivation the computational formulas for the errors and the initial conditions for certain input actions.

(a) Harmonic Input Action. The error at the end of the dead time is

$$\delta_d = \delta_0 + a_{in_0} t_0 t_d + \frac{a_{in_0} t_d^2}{2}, \tag{3}$$

where δ_0 is the value of the error at the instant of time t_0;

a_{in0} is the acceleration of the input action in the reversal region;

t_0 is the instant of stopping of the output shaft;

t_d is the dead time.

The time t_0 is determined from the expression

$$t_0 = \frac{2\pi\varphi_d}{\omega\, 360} \tag{4}$$

where φ_d is the value in degrees of the phase-frequency characteristic of the closed system for frequency ω.

According to figure 2 the expression for δ_0 has the form

$$\delta_0 = \delta_0' + \delta_M = \delta_{max} \sin\left(\varphi_d + \varphi_\delta - \frac{\pi}{2}\right) + \delta_M, \tag{5}$$

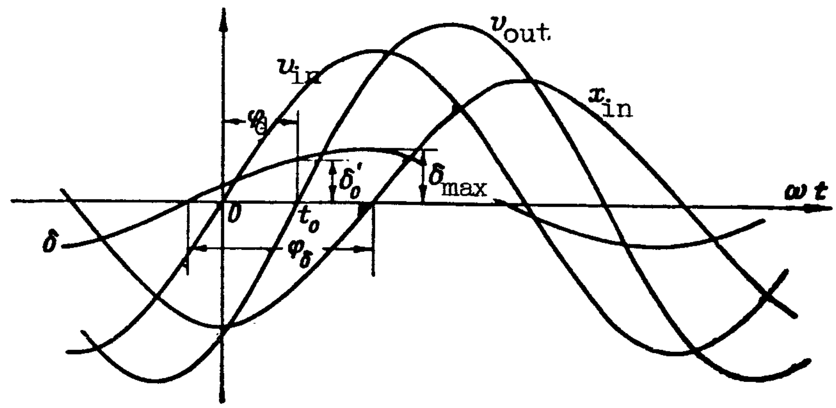

Figure 2. Determination of initial conditions with harmonic input signal.

where δ_{max} and φ_δ are determined with the aid of the amplitude-phase characteristic of the closed system with respect to the error;

δ_0' is the error at the instant t_0, without accounting for the friction torque;

δ_M is the torque error.

The dead time t_d is determined by means of graphical solution from /6
expression

$$-\frac{a_{in0}K_M}{6T_1}t^3+\frac{a_{in0}K_M t_0}{2T_1}t^2+\frac{\dot{\delta}_0 K_M}{T_1}t=M_{f0}-M_{t0}, \qquad (6)$$

where K_M is the system torque gain;

T_1 is the time constant corresponding to the first coupling frequency of the amplitude-frequency characteristic of the open system.

(b) Motion with Zero Initial Conditions ($\delta_0 = 0$, $M_{t\,0} = 0$, $t_0 = 0$). In this case

$$t_d=\sqrt[3]{\frac{6T_1M_{f0}}{a_{in0}K_M}}; \qquad (7)$$

$$\delta_d=\frac{a_{in0}t_d^2}{2}. \qquad (8)$$

(c) Motion with Nonzero Initial Conditions. For the worst case, when the system at the time t_0 is on the borderline of movement in the direction opposite to the future movement, the initial conditions will be

$$\left.\begin{aligned} M_{t\,0} &= -M_{f\,0}; \\ \delta_0 &= -\frac{M_{f\,0}}{K_M}; \\ t_0 &= 0, \end{aligned}\right\} \tag{9}$$

and the dead time and the error, respectively,

$$t_d = \sqrt[3]{\frac{12T_1 M_{f\,0}}{a_{in0} K_M}}; \tag{10}$$

$$\delta_d = -\frac{M_{f\,0}}{K_M} + \frac{a_{in0} t_d^2}{2}. \tag{11}$$

(d) Reversal with Any Slowly Varying Input Functions. Looking for the time t_0 corresponding to the extremum of x_{out}, we find that /7

$$t_0 = C_1 \tag{12}$$

where C_1 is the velocity error coefficient.

For precision servosystems we can set $C_1 = t_0 \approx 0$

and then

$$\delta_d = \delta_0 + \frac{a_{in0} t_d^2}{2}, \tag{13}$$

where

$$\delta_0 = \frac{a_{in0} C_2}{2} + \delta_M, \tag{14}$$

Here C_2 is the acceleration error coefficient and t_d is found from (6) with $t_0 = 0$.

With very slowly varying input actions, when t_d is large, we can neglect the third term in (6) and M_t is completely determined by the friction torque (this case is considered in reference 1).

(e) Increase of Error after the Dead Period. As has been mentioned previously, the solution is obtained by studying the maximum of the expression for the error increment, which was obtained by taking the third assumption into account.

The expression for the maximal increment of the error during the time $t_M = t_2 - t_1$ has the form

$$\delta_{2\max} = a_{in0} t_1 t_M + \frac{a_{in0}}{2} t_M^2 - \frac{a_{in0} K_M}{12 T_1 J K_p}\left(t_d^2 + 2 t_0 t_d + 2\frac{\delta_0}{a_{in0}}\right) t_M^3, \tag{15}$$

where K_p is the coefficient of the mechanical transmission from the motor shaft to the output displacement, and time t_M is found using formula

$$t_M = \frac{2 T_1 J K_p}{K_M\left(t_d^2 + t_0 t_d + \frac{2\delta_0}{a_{in0}}\right)}\left[1 + \sqrt{1 + \frac{t_1 K_M}{T_1 J K_p}\left(t_d^2 + 2 t_0 t_d + \frac{2\delta_0}{a_{in0}}\right)}\right]. \tag{16}$$

The maximal error at time t_2 is determined by the sum

$$\delta_{\max} = \delta_d + \delta_{2\max}. \tag{17}$$

The values of the error $\delta_{2\max}$ calculated using (15) are somewhat high, since the kinetic friction torque after the dead period was assumed constant and equal to the static friction torque. In actuality, as a result of the decreasing characteristic of the friction as a function of velocity, the acceleration of the motor will be accomplished more rapidly and the maximum error will be smaller.

2. Reversal Errors Due to Free Play Between Motor and Feedback Sensor

In addition to the assumptions made previously, we consider all the moments of inertia to be concentrated on the motor shaft. Using the same /8

method for the derivation of the equations, we obtain the following expressions for the estimation of the errors due to the free play.

(a) Harmonic Input Action. The error at the end of the dead time is determined by expression (3) except that in place of time t_d we must substitute dead time $t_{d\Delta}$, corresponding to the takeup of the free play and obtained by graphical solution from expression

$$\frac{K_v}{T_1}\left[\frac{a_{in0}}{24}t^4+\frac{a_{in0}t_0}{6}t^3+\frac{\delta_0}{2}t^2\right]=2\Delta, \tag{18}$$

where K_v is the figure of merit of the servosystem;

2Δ is the value of the free play.

We find the initial values of t_0 and δ_0 from section 1.

(b) Slowly Varying Input Action of Any Complex Form. According to paragraph (d) of section 1, in this case

$t_0 \approx 0,$

$\delta_0 = \dfrac{a_{in_0}\,C_2}{2}$ (torque error equal to zero by condition).

Taking into account (13), the error is determined by the expression

$$\delta_{d\Delta} = \frac{a_{in0}}{2}(C_2 + t_{d\Delta}^2), \tag{19}$$

where

$$t_{d\Delta} = \sqrt{-3C_2 + \sqrt{9C_2^2 + \frac{48T_1\Delta}{K_v a_{in0}}}} \tag{20}$$

(c) Startup. The most unfavorable case of startup is when the motion begins with the free play not taken up. This also includes the case of very slowly varying input actions.

Considering that the initial conditions $\delta_0 = 0$, $t_0 = 0$ correspond to both cases, we obtain

$$\delta_{d\Delta} = a_{in\ 0}/2\ t_{d\Delta}^2, \tag{21}$$

where

$$t_{d\Delta} = \sqrt{\frac{2\Delta 24 T_1}{K_v a_{in0}}} \tag{22}$$

(d) Errors after Takeup of Free Play. During the time of taking up of the free play, when the system is open, the error increases more rapidly than with tracking in the closed condition. Therefore, the movement of the output shaft after takeup of free play begins with higher acceleration and velocity than would be the case at the same moment of time in the absence of free play.

Here two cases are possible: (1) the velocity and the acceleration of the output shaft are equal to or greater than the corresponding values for the input action, and (2) these values are smaller for the output shaft than for the input action.

In the first case, the error accumulated at the end of the dead period /9 will also be the maximal value of the error in the region of the takeup of free play. For example, this will be true during reversal. In the second case, the error will continue to increase after the dead period, but will never reach a value greater than in the absence of free play. This case is observed with startup and small values of free play. With large values of free play the maximal value of the error will occur at the moment of termination of the dead period.

3. Reversal Errors Due to Simultaneous Action of Free Play and Dry Friction in the System

In addition to the assumptions discussed above, we consider that (1) all moment of inertia is concentrated on the motor shaft, i.e., on one side of the free play; (2) the friction torque is fully concentrated on the output shaft, i.e., on the other side of the free play. Under these assumptions the reversal process takes place as follows.

Prior to the instant of stoppage of the output shaft everything takes place just as in the presence of dry friction only (section 1).

After the instant of stoppage of the output shaft, i.e., after time t_0, there can arise the dead period t_{d_1}, due to the fact that the motor shaft begins its motion in the opposite direction not instantaneously, but only when the turning moment reaches a zero value. The processes taking place in this period are described by the equations considered in section 1, with replacement of M_{f_0} by zero. Therefore, the condition for the existence of the dead time t_{d_1} according to (2), is written in the form

$$J\varepsilon - M_f < 0. \tag{23}$$

On termination of the dead time t_{d_1} (or at the instant t_0 if $t_{d_1} = 0$) there begins the dead period $t_{d\Delta}$ due to free play. Expressions of section 2 are valid for this period, with the difference that the initial values will be determined by the final values of the preceding period, i.e., by the moment of time t_{d1} depending on dry friction.

On termination of dead period $t_{d\Delta}$ the system enters a new period, characterized by the appearance of the dry friction load and by closure of the servosystem. Assuming, as before, a linear variation of the turning moment on this segment or, what is the same, a linear variation of the acceleration of the output shaft (a_{out_1}) and also taking account of the retarding action of the moving friction torque, which we consider to be constant (a_{out_2}), we obtain the resultant acceleration

$$a_{out} = a_{out_1} - a_{out_2} = a_{in_0} K_v/T_1 (t'_0 + t_{d\Delta}) t + a_{out_0} - M_f/JK_p, \tag{24}$$

where $t'_0 = t_0 + t_{d_1}$ and t is measured from the instant of termination of the dead period t_{d_Δ}.

Depending on the values of the parameters appearing in (24), we can observe qualitatively different processes of the movement of the output shaft

$$(1)\ a_{out_0} - M_f/JK_p \geq a_{in_0}.$$

In this case we observe only a temporary reduction of the acceleration, not accompanied by a reduction of the velocity and increase of the error. The /10
maximal value of the error will correspond to the termination of the period t_{d_Δ}

$$(2)\ a_{out_0} - M_f/JC_p < a_{in_0}.$$

Here we observe a reduction of the velocity of the output shaft, but not to complete stoppage. The error will increase, reaching the maximum δ_{max} at the instant of time t_M (counting from the instant of the beginning of the movement of the output shaft)

$$\delta_{max} = \delta_0 + \Delta\delta_{d_1} + \Delta\delta_{d\Delta} + \Delta\delta_M, \tag{25}$$

where $\Delta\delta_{d_1}$ is the increment of the error during the dead period t_{d_1};

$\Delta\delta_{d_\Delta}$ is the error increment during the dead time t_{d_Δ};

$\Delta\delta_M$ is the error increment during the time t_M.

$$\Delta\delta_M = a_{in_0} t''_0 t_M + M_f/2JK_p \; t_M^2 - a_{in_0} K_v t''_0/6T_1 \; t_M^3 \tag{26}$$

$$t_M = \frac{M_f T_1}{JK_p a_{in_0} K_v t''_0}\left[1 + \sqrt{1 + \frac{2K_v}{T_1}\left(\frac{a_{in_0} t''_0 JK_p}{M_f}\right)^2}\right], \tag{27}$$

where $t''_0 = t_0 + t_{d_1} + t_{d_\Delta}$;

(3) $a_{out_0} - M_f/JK_p < a_{in_0}$.

In contrast to the preceding case, the reduction of the velocity of the output shaft continues to full stoppage.

The error increment during the time t_{M_1}, i.e., during the time of movement after t_{d_Δ}, is determined by expression

$$\Delta\delta_d\,(t) = a_{in_0}\; t''_0 t_{M_1} + M_f/2JK_p \; t_{M_1}^2 - a_{in_0}\; K_v \; t''_0/6T_1 \; t_{M_1}^3, \tag{28}$$

where

$$t_{M.1} = \frac{2T_1\,(M_f - a_{in_0} JK_p)}{JK_p a_{in_0} K_v t''_0}. \tag{29}$$

From (29) follow the conditions for stoppage of the output shaft

$$M_f \geq a_{out_0} \; JK_p. \tag{30}$$

After stoppage of the output shaft all processes in the system will be subject to the formulas considered above (section 1), in which as the initial conditions we must substitute the final values of the preceding segment.

(11)

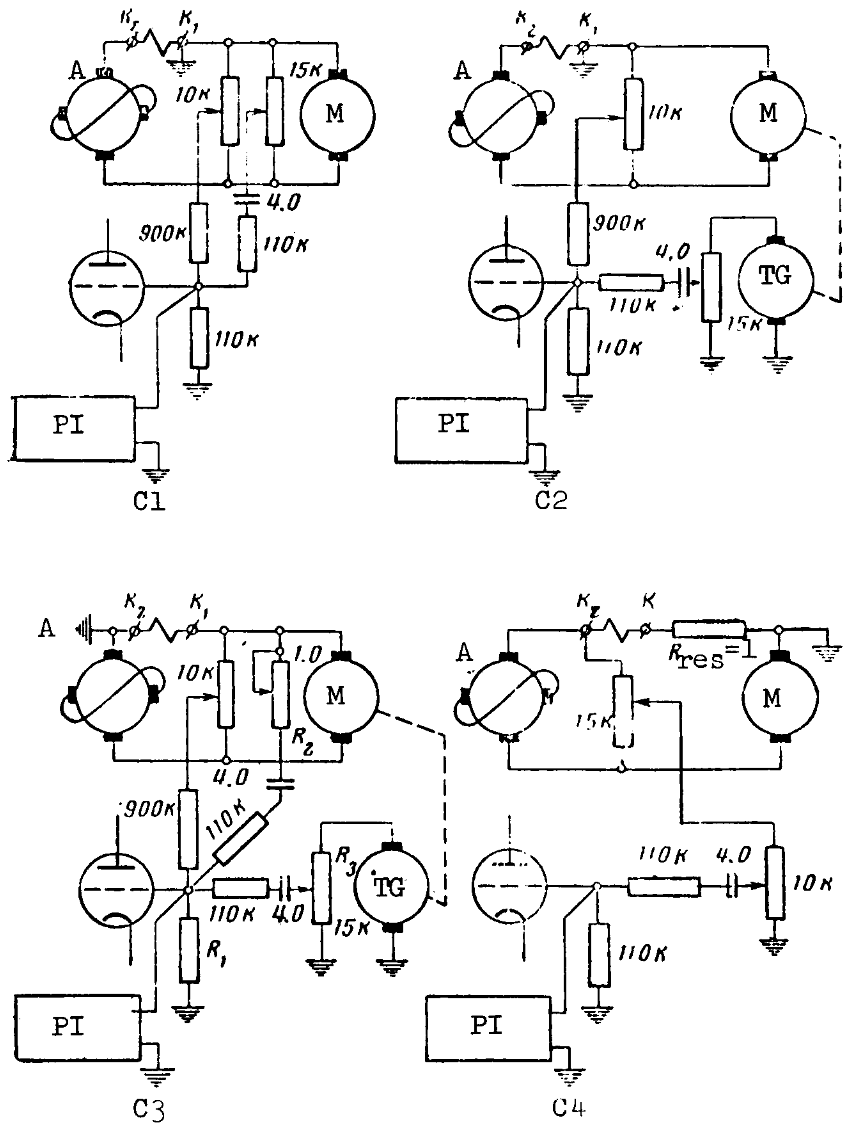

Figure 3. Correction circuits; C, circuit; PI, phase indicator; M, motor; TG, tach generator; A, amplidyne; res, response.

The maximal value of the error is written

$$\delta_{max} = \delta_0 + \Delta\delta_{d_1} + \Delta\delta_{d_\Delta} + \Delta\delta_{M_1} + \Delta\delta_{d_2} + \Delta\delta_{M_2}, \qquad (31)$$

where $\Delta\delta_{M_1}$ is the error increment in the period of slowing of the output shaft at the moment of complete stoppage;

TABLE 1. MAGNITUDE OF ERROR, mm.

	Circuit 1	Circuit 2				Circuit 3	Circuit 4	
	$\alpha = 20$, $K_v = 200\ sec^{-1}$, $n = 1.5$ rpm	$\alpha = 6$, $K_v = 100\ sec^{-1}$, $n = 1$ rpm	$\alpha = 18.7$			$\alpha = 22$, $K_v = 400\ sec^{-1}$, $n = 2$ rpm	$\alpha = 0$; $K_v = 1{,}200\ sec^{-1}$	
			$K_v = 100\ sec^{-1}$, $n = 1$ rpm	$K_v = 200\ sec^{-1}$				
				$n = 1.5$ rpm	$n = 2$ rpm		$n = 2$ rpm	$n = 1$ rpm
Reversal No. 1	0.04	0.02	0.02	0.01	0.01	0.01	0.02	0.02
Reversal No. 2	0.04	0.03	0.01	0.005	0.01	0.01	0.02	0.01
Reversal No. 3	0.06	0.03	0.02	0.015	0.02	0.01	0.02	0.025
Maximal error in remaining portions of profile	0.05	0.11	0.045	0.05	0.06	0.03	0.05	0.02

Remarks: α is the gain attenuation, determined by the proportional feedback encompassing the amplidyne and electric motor; K_v is figure of merit of servosystem (accounting for α); n is rate of rotation of stock.

$\Delta\delta_{d_2}$ is the error increment during the time of the second dead period caused by dry friction;

$\Delta\delta_{M_2}$ is the error increment after the second dead period due to dry friction.

$\dot{\delta}_0$, $\Delta\delta_{d_1}$, $\Delta\delta_{d_\Delta}$ are the same as in equation (25).

4. Correction Circuits Yielding Small Reversal Errors /12

As mentioned above, the error bursts in the reversal region are observed with an immobile output shaft, when the system is open and has considerable inertia. We evaluated this inertia by time constant T_1, which corresponds to the first conjugate frequency of the amplitude-frequency characteristic of the open system. Normally T_1 lies in the range of 5-10 sec.

It follows therefore that the error in the reversal region can be reduced by reducing T_1, i.e., by expansion of the low-frequency region of the amplitude-frequency characteristic. However, this is a difficult problem, associated with the stability and the factor of merit of the system.

The most rational method is the use of stabilization circuits, such that there is a change of the structure of the open system with stoppage of the output shaft. The idea amounts to the fact that with an immobile output axis there would not be any signal of the stabilizing rate feedback, which is precisely what introduces the high inertia necessary for stability of the system. An example of such feedback is tachometric feedback. While the output shaft is immobile, there is no damping action of this coupling, and the torque on the motor shaft rises practically instantaneously, since the inertia of the forward loop usually does not exceed hundredths of a second.

As a rule, this method of stabilization with high gains leads to instability of the inner loop in connection with nonsatisfaction of the condition necessary for high gains: the order of the equation describing the portion of the loop enclosed by the stabilizing device must not exceed by more than two the difference of the orders of the numerator and the denominator of the /13 operator of the stabilizing device (ref. 2). This condition is more easily satisfied, if the motor is not included in the stabilizing feedback.

To obtain a sufficient gain and small reversal errors we can use both forms of stabilizing feedback, introducing a minimal (necessary for stability of the inner loop) intensity of that not including the motor.

Figure 3 shows correcting feedback circuits as applied to a drive with an amplidyne amplifier. Table 1 presents experimental data taken from a servodrive for a machine tool with programed control, developed by the Institute of Automation and Remote Control of the Academy of Sciences USSR, together with the MOSNKh (Moscow Oblast Sovnarkhoz).[1]

---

[1]V. I. Simonenkov aided in preparation of the experiments.

Table 1 shows that the best results were obtained with circuits 2 and 3. For them the reversal errors are lower by a factor of four than, for example, for circuit 1, where the feedback does not include the motor. Circuit 3 also differs from circuit 2 by the presence of a small amount of rate feedback, not including the motor, which permitted bringing the response up to 400 sec^{-1} rather than 200 sec^{-1}. Circuit 4 is a tachometric bridge.

The circuits shown are not the only possible variants, but are presented as an illustration.

REFERENCES

1. Besekerskiy, V. A. Design of Low-Power Servosystems (Proyektirovaniye sledyashchikh sistem maloy moshchnosti). Sudpromgiz, 1958.

2. Meyerov, M. V. Synthesis of Structures of Systems for High-Accuracy Automatic Regulation (Sintez struktur sistem avtomaticheskogo regulirovaniya vysokoy tochnosti). Fizmatgiz, 1959.

N66 34828

DYNAMIC ACCURACY OF MACHINE TOOLS WITH PROGRAMED CONTROL

B. I. Andreychikov

1. Statement of the Problem

Metal cutting machine tools with programed control belong to that type of device whose purpose is the provision of a given relationship between individual spatial coordinates with a definite accuracy, while time enters into the reproduction process only as an intermediate parameter (ref. 1). /14

By accuracy of reproduction we understand the shortest distance from any surface given in the program to the surface obtained in the processing. The accuracy requirements can be formulated (ref. 2) as

$$\delta = | \rho_{in}(x, y) - \rho_{out}(x_1, y_1) | \leqslant \delta_0, \tag{1}$$

where $\rho_{in}(x, y)$ is the given surface;
$\rho_{out}(x_1, y_1)$ is the obtained surface;

δ_0 is a constant which characterizes the surfaces equidistant to $\rho_{in}(x, y)$ beyond whose limits the obtained surface $\rho_{out}(x_1, y_1)$ must not go;

δ is the reproduction inaccuracy.

The dynamic reproduction accuracy also depends, in addition to the transfer functions of the servosystems of the machine-tool feeds, on the form of the given surface $\rho_{in}(x, y)$ and the law of its variation with time $\rho_{in}(t)$.

Knowledge of these factors permits computation of the error at every point of the surface. However, in the general case this calculation is excessively cumbersome and is not suitable for practical use.

The following assumptions and limitations are introduced for the purpose of analysis and computation of the reproduction accuracy with an approximation acceptable for practical purposes and with acceptable complexity.

1. We replace the analysis of the accuracy of reproduction of 3-dimensional details by the analysis of the reproduction of their sections. The

errors introduced in this case are quite small, since the machining of a 3-dimensional detail is usually accomplished by "lines" or along a spiral line with small pitch.

2. We consider the plane contours and sections of 3-dimensional details to consist of straight lines and circular arcs. This assumption is valid, since we can always approximate, if not the entire contour, at least its most difficult portions with sharpest transitions by angles and arcs of circles of small radii, without introducing significant errors in the analysis of the dynamic accuracy of the servosystem.

3. In order to specify a definite temporal dependence we shall consider that with operation of the machine tool in rectangular coordinates, the /15
movement of the tool along its trajectory takes place with a constant tangential velocity, and with operation in polar coordinates the rotation of the stock is performed with a constant angular velocity.

2. Typical Part Profiles and Corresponding Input Functions

For the purpose of standardization of the analysis of the dynamic accuracy and for the comparison of the dynamic qualities of different machine tools using programed control with one another, it is necessary to have some typical profiles of the parts or typical portions of a profile, which will reflect sufficiently closely the most difficult portions of the part profile from the point of view of dynamic accuracy, and still will be sufficiently simple for calculation and experiment.

As a typical profile for the operation of a machine tool in rectangular coordinates we take a profile similar to that shown in figure 1, which represents all possible combinations of segments consisting of straight lines and circular arcs.

The characteristic portions of the typical profile are presented in table 1,[1] which also presents the corresponding typical input functions of the individual servosystems with the assumption of constant tangential velocity of the center of the cutting tool.

As typical profiles for operation of a machine tool in polar coordinates we also take the straight line and a circular arc rotating with a uniform angular velocity. The various variants for this case are presented in table 2,[1] which also shows the corresponding typical input functions for the lateral feed servosystem.

Figure 2 shows the input function for item I of table 2, where $\omega = 2.09$ rad/sec; $R = 60$ mm; $L_1 = 46.2$ mm and $L_2 = 42.5$ mm. The graphs of the input functions for the remaining points of table 2 are similar in form.

[1] See tables 1 and 2 in appendix to this article.

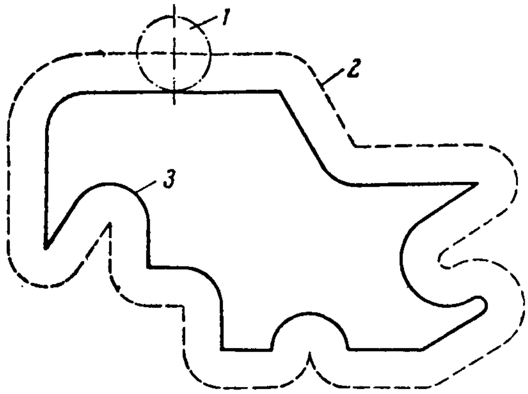

Figure 1. Typical profile of detail for machining in rectangular coordinates. 1, Cutter; 2, trajectory of center of cutter; 3, detail contour.

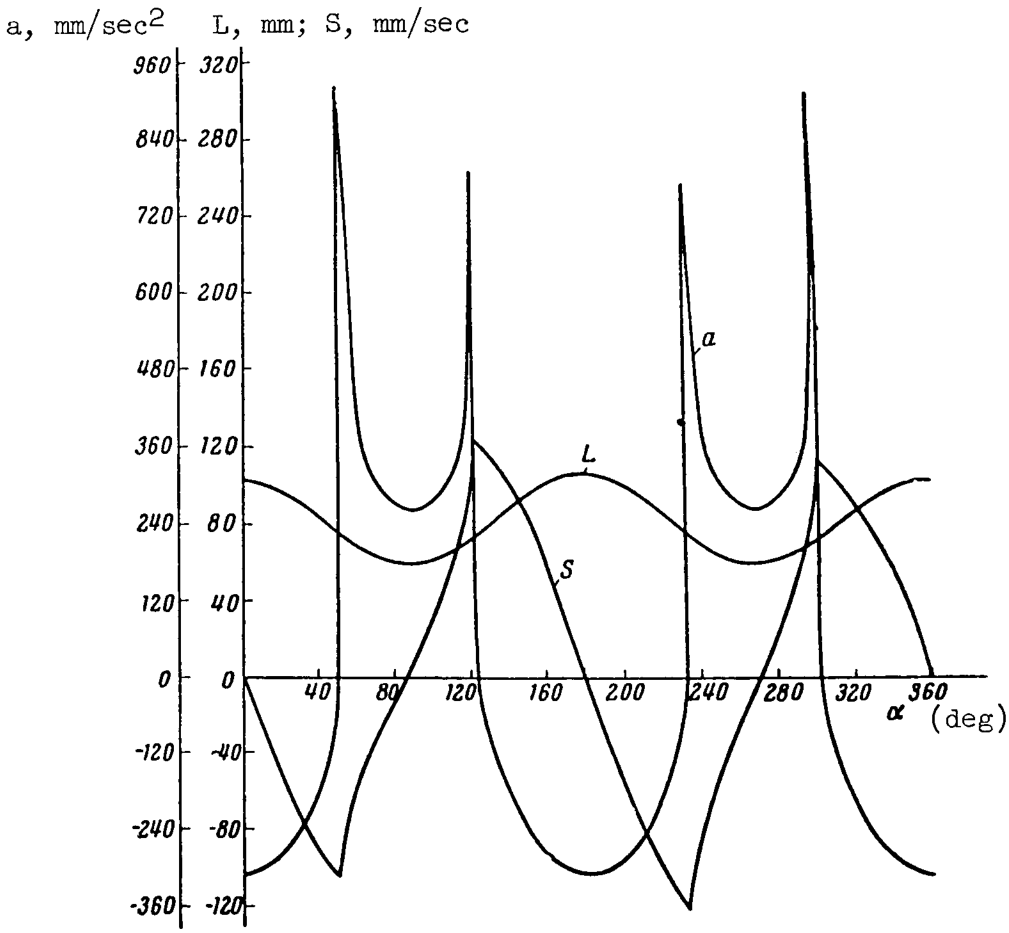

Figure 2. Input functions for operation in polar coordinates.

3. Technique of Calculation of Steady-State Error with Machining of a Circular Arc

Table 1 shows that the input functions with respect to the individual coordinates for machining of the circular arc with constant tangential velocity are harmonic. In this case the outputs of the servosystems with respect to the individual coordinates also vary, following a harmonic law; with identical frequency characteristics the amplitudes of the outputs and the phases with relation to their inputs will also be identical. Consequently the resulting contour will also be a circle, but with a radius differing in the general case from the radius of the given circle. By the accuracy definition given in section 1, the difference of the radii of the given and resulting circles is then the reproduction error.

Considering that the frequency of input action is determined by the magnitude of feed S and the radius of the given circle R,

$$\omega = S/R, \tag{2}$$

we obtain the expression for the error as a function of S, R, ω

$$\delta = R\,[1 - |\Phi(j\omega)|] = \frac{S}{\omega}\,[1 - |\Phi(j\omega)|], \tag{3}$$

where $|\Phi(j\omega)|$ is the amplitude-frequency characteristic (afc) of the closed servosystem. /17

As follows from (3), the error on the contour for a given R depends only on the afc of the closed system, while the phase-frequency characteristic (pfc) can be anything.

The steady-state error of reproduction of the circle can easily be determined from the nomogram representing the family of characteristics $R = S/\omega$ for various values of S (fig. 3). On the nomogram we plot the calculated or experimental afc of the closed system, from which for frequency ω, determined from the given values of R and S from the family of characteristics, we find the value 1 is $|\Phi(j\omega)|$, which, multiplied by R, supplies the looked-for error.

It is advisable to construct the family of errors, as is done in figure 3 for a given afc. Such a family of curves presents a complete picture of the steady-state errors with reproduction of a circular arc for a concrete servosystem.

4. Reproduction of a Straight Line in Rectangular Coordinates

With the reproduction of a straight line inclined at the angle α to the x-axis (fig. 4), the errors in the individual coordinates in the steady-state regime of movement with constant velocity become

$$\left.\begin{aligned}\delta_x &= \frac{S_x}{D_x} = \frac{S}{D_x}\cos\alpha;\\ \delta_y &= \frac{S_y}{D_y} = \frac{S}{D_y}\sin\alpha,\end{aligned}\right\} \qquad (4)$$

where S is the feed along the straight line; D is the factor of merit.

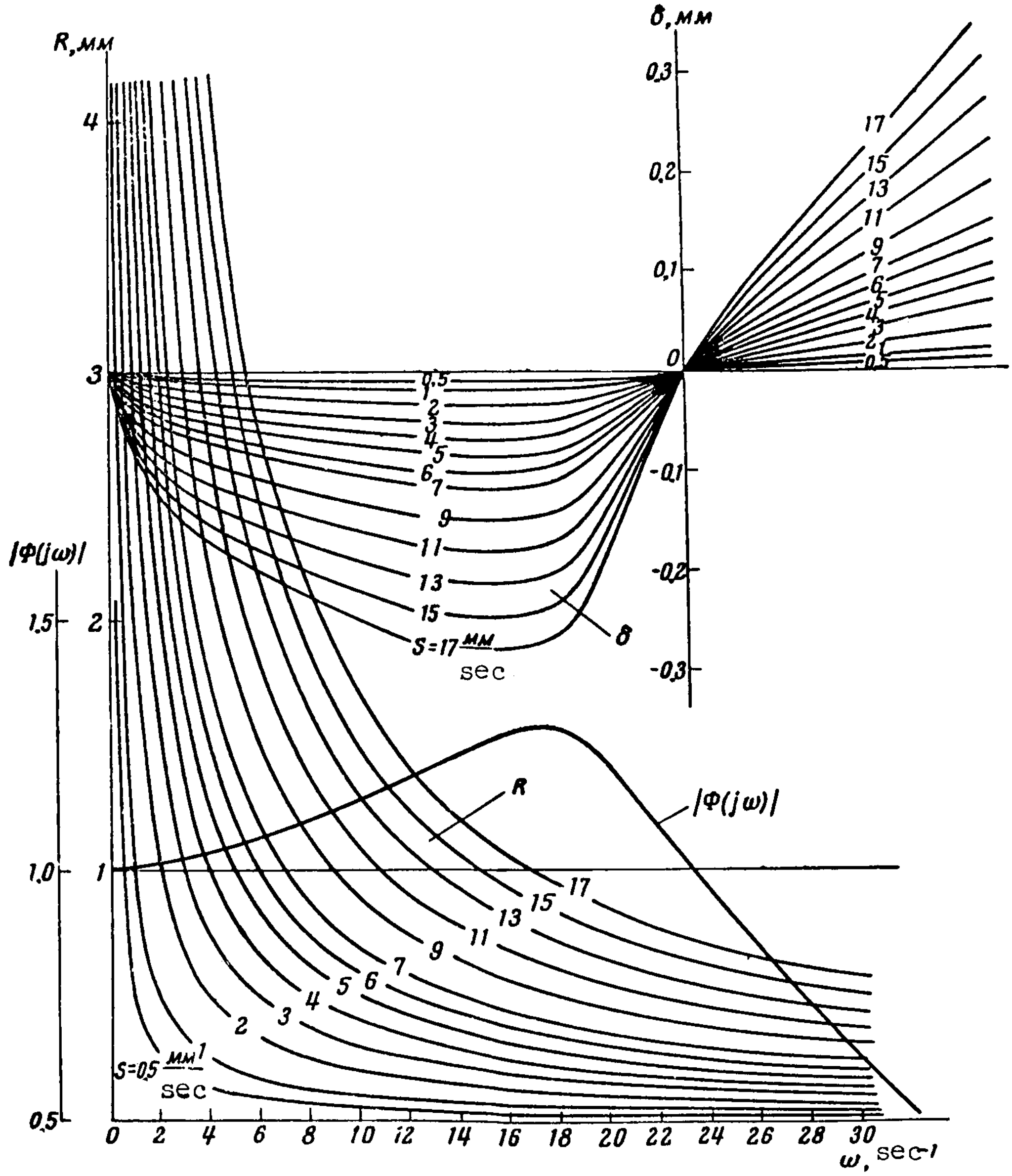

Figure 3. Nomogram for computation of steady-state error with machining of circular arc in rectangular coordinates.

From equation (4) it follows that with $D_x = D_y$, the straight line being reproduced coincides with the given straight line, i.e., the error on the contour is zero in spite of the presence of errors in the servosystems in each of the coordinates (fig. 4, 1 and 2).

5. Calculation of the Errors with Sharp Breaks of the Profile (Rectangular Coordinates)

We see from table 1 (No. IV-VII) that the input functions for the sharp breaks in the trajectory of the motion of the cutting tool are characterized by a velocity jump. Consequently the calculation of the errors in the individual coordinates is reduced to determining the reaction of the servosystem to velocity jumps.

The error in each coordinate will consist of the steady-state and transient components

$$\delta(t) = \Delta S\,[T_1(t) + C_1], \tag{5}$$

where ΔS is the velocity jump;
C_1 is the velocity error coefficient;
$T_1(t)$ is the component of the transient process with unit velocity jump.

Since the steady-state components do not give errors on the contour representing the straight line (section 4), it is necessary to consider only the transient component of the error, which will be in the region of the sharp breaks in the tool trajectory. /18

The transient component of error $T_1(t)$ can be computed, for example, from the equations and coefficients given (ref. 3) for the group of limit amplitude-frequency characteristics (lafc) of the open system.

Frequently the reaction of the system to a unit jump in position will be known from calculation or experiment. In this case use can be made of the familiar relation from the theory of automatic regulation, connecting the components in terms of the sequential derivatives

$$T_n(t) = \int T_{n-1}(t)\,dt, \tag{6}$$

where $T_n(t)$ is the component of the transient process with a unit jump of the nth derivative in the input action; /19
$T_{n-1}(t)$ is the same for the (n-1)th derivative.

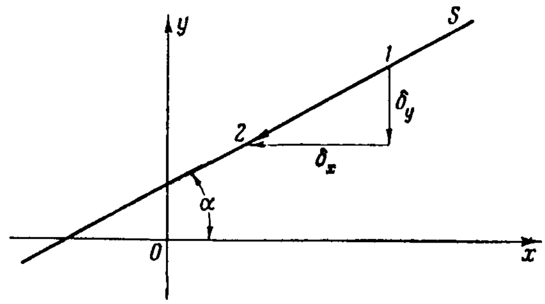

Figure 4. Error in reproduction of straight line in rectangular coordinates.

From (6) it follows that the component of the transient process with the velocity jump is an integral curve with relation to the component of the transient process of the system with a position jump.

For an approximate determination of the error with a velocity jump we can make use of the connection between the error and the system bandpass obtained in reference 3 on the basis of experimental data (for a definite group of transfer functions of the servosystems), namely; that for any system (of the indicated group) the maximal value of the error with a unit velocity jump is equal to approximately $1/\omega_c$, where ω_c is the cutoff frequency of the lafc of the open system.

On the basis of this discussion we can write the approximate value of the transient component with a single velocity jump

$$T_{x(y)max} \approx 1/\omega_c - C_1. \tag{7}$$

The transfer from errors in individual coordinates to the error on the contour is easily performed graphically.

6. Calculation of the Errors with Complex Input Functions (Polar Coordinates)

With machining in polar coordinates, the error on the contour is the result of the angular error in the rotational movement of the stock and the linear error in the translational movement of the stock or of the cutting tool.

The angular errors with rotation of the stock at a constant velocity lead to rotation of the entire part as a whole through the magnitude of this angular error without introducing distortions in the form of the part. For a whole series of parts this does not cause any error and affects only the mounting of the stock from the point of view of excess material. However, for parts in which such a rotation constitutes an error because the positioning of the section is associated with some basic surfaces which are worked on another

machine tool, we can easily introduce a correction for the constant angular error, for example, by means of displacement of the feedback sensor.

In connection with this analysis, it is the translational errors which are of interest. From a consideration of the input functions presented in table 2, we see that severe demands are made on the translational servosystem from the point of view of velocities, accelerations and the higher derivatives, which undergo sharp variations. /20

In view of the complexity of the input functions, the calculation is not so relatively simple as in the case of the rectangular coordinates. In practice, the reproduction errors are comparatively easily computed only with slow rotation of the stock, when the input functions of the servosystem can be considered to be in the class of the slowly varying functions, and when we can use the method of error coefficients (refs. 4 and 5).

For more rapid rotations of the stock it is necessary to have recourse to simulation. It would probably be useful to construct nomograms for the computation of the dynamic errors with application to the input functions of table 2, and the typical transfer functions of the servosystems similar to the way this was done for the case of the basic dynamic indices in refs. 5, 6 and 7.

7. Connection of the Error on the Contour with the Error of Translational Motion for Operation in Polar Coordinates

In the final analysis we are interested not in the error in the translation l movement of the cutter, but in the error on the contour, i.e., in the distance from the contour obtained during reproduction of the program to the given contour. As a rule the error on the contour will be smaller.

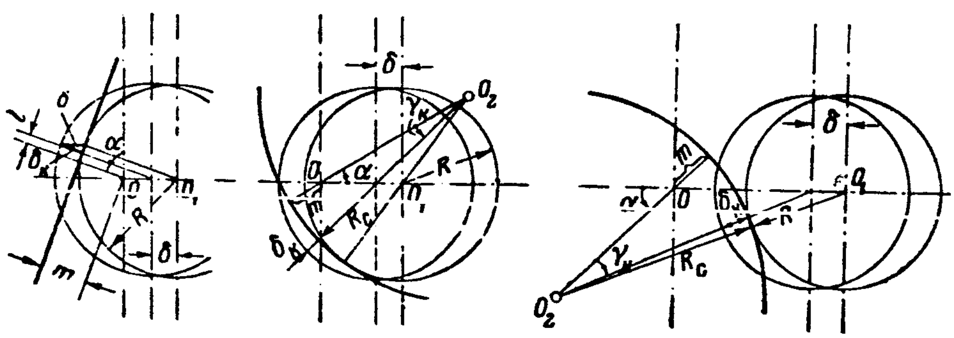

a b c

Figure 5. Relation of contour error to cross feed error. a, For straight line; b, for circular arc with center of rotation on side being machined; c, for circular arc with machining on opposite side from center of rotation.

On the basis of figure 5 we can write expressions relating the error on the contour with the error in the translational movement of the cutter:

For the section in the form of a straight line

$$\delta_k = \delta \left| \sin \alpha \right|; \tag{8}$$

$$l = (R \pm m) \left| \operatorname{ctg} \alpha \right| - \delta \left| \cos \alpha \right|; \tag{9}$$

where the plus sign before m corresponds to the angles $\alpha > 180^{\circ}$, the minus sign corresponds to angles $\alpha < 180^{\circ}$, and equality of m to zero corresponds to passage of the axis of rotation through the section (table 2, I).

For the section in the form of a circular arc with inside machining /21

$$\delta_k = R - R_c + \sqrt{\delta^2 + (R_c - R)^2 + 2\delta \sqrt{(R_c - R)^2 - (R_c \pm m)^2 \sin^2 \alpha}}; \tag{10}$$

$$\gamma_k = \frac{\pi}{2} - \left| \alpha \right| - \operatorname{arc\,tg} \frac{\delta + \sqrt{(R_c - R)^2 - (R_c \pm m)^2 \sin^2 \alpha}}{(R_c \pm m) \left| \sin \alpha \right|}. \tag{11}$$

For the section in the form of a circular arc with outside machining

$$\delta_k = R + R_c - \sqrt{\delta^2 + (R_c + R)^2 - 2\delta \sqrt{(R_c + R)^2 - (R_c \pm m)^2 \sin^2 \alpha}}; \tag{12}$$

$$\gamma_k = \left| \alpha \right| - \frac{\pi}{2} + \operatorname{arc\,tg} \frac{\sqrt{(R_c + R)^2 - (R_c \pm m)^2 \sin^2 \alpha} - \delta}{(R_c \pm m) \left| \sin \alpha \right|}. \tag{13}$$

In equations (10)-(13) the plus sign before m corresponds to the location of the axis of rotation of the section on the outside of the arc, the minus sign corresponds to location on the inside of the arc, and m = 0 corresponds to location on the section itself.

TABLE 1

	Typical profile segment		Typical input functions		
I	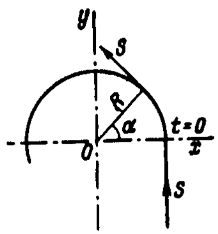	$t<0$: $x=R$. $t>0$: $x=R\cos\alpha$; $y=R\sin\alpha$.	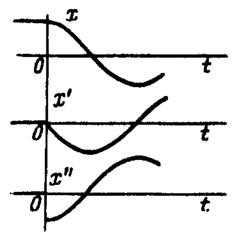	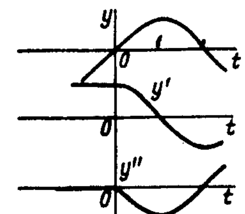	$t<0$: $x=R$; $x'=x''=0$; $y=st$; $y'=s$; $y''=0$. $t>0$: $x=R\cos\omega t$; $y=R\sin\omega t$; $x'=-s\cdot\sin\omega t$; $y'=s\cdot\cos\omega t$; $x''=-\frac{s^2}{R}\cos\omega t$; $y''=-\frac{s^2}{R}\sin\omega t$.
II	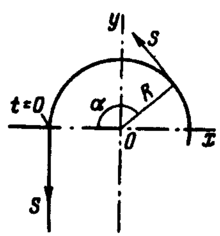	$t<0$: $x=-R\cos\alpha$; $y=R\sin\alpha$. $t>0$: $x=-R$	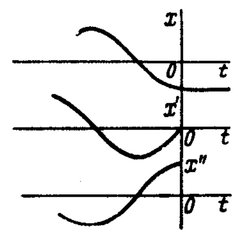	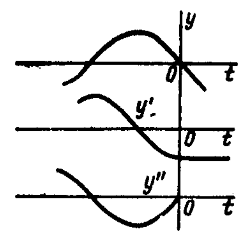	$t<0$: $x=-R\cos\omega t$; $y=R\sin\omega t$; $x'=s\cdot\sin\omega t$; $y'=s\cdot\cos\omega t$; $x''=\frac{s^2}{R}\cos\omega t$; $y''=-\frac{s^2}{R}\sin\omega t$. $t>0$; $x=-R$; $x'=x''=0$; $y=-st$; $y'=-s$; $y''=0$.
III	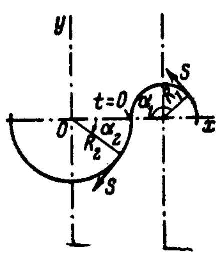	$t<0$: $x=R_1+R_2-R_1\cos\alpha_1$ $y=R_1\sin\alpha_1$. $t>0$: $x=R_2\cos\alpha_2$; $y=-R_2\sin\alpha_2$	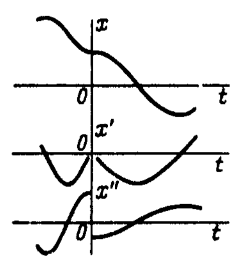	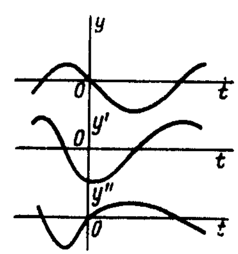	$t<0$: $x=R_1+R_2-R_1\cos\omega_1 t$; $y=-R_1\sin\omega_1 t$; $x'=s\cdot\sin\omega_1 t$; $y'=-s\cdot\cos\omega_1 t$; $x''=s^2/R_1\cdot\cos\omega_1 t$ $y''=s^2/R_1\cdot\sin\omega_1 t$. $t>0$; $x=R_2\cos\omega_2 t$; $y=-R_2\sin\omega_2 t$; $x'=-s\cdot\sin\omega_2 t$; $y'=-s\cdot\cos\omega_2 t$; $x''=-s^2/R_2\cdot\cos\omega_2 t$; $y''=s^2/R_2\cdot\sin\omega_2 t$.

TABLE 1 (Continued)

	Typical profile segment		Typical input functions		
IV	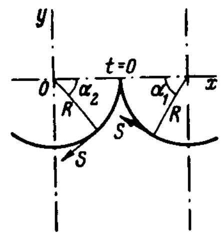	$t<0$: $x=2R-R\cos\alpha_1$ $y=-R\sin\alpha_1$. $t>0$: $x=R\cos\alpha_2$; $y=-R\sin\alpha_2$.	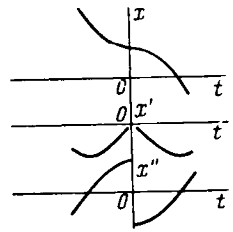	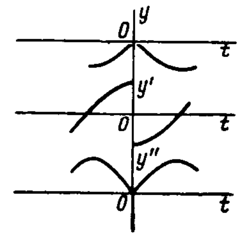	$t<0$: $x=2R-R\cos\omega t$; $y=-R\sin\omega t$; $x'=s\cdot\sin\omega t$; $y'=-s\cdot\sin\omega t$; $x''=s^2/R\cdot\cos\omega t$; $y''=s^2/R\cdot\sin\omega t$. $t>0$: $x=R\cos\omega t$; $y=-R\sin\omega t$; $x'=-s\cdot\sin\omega t$; $y'=-s\cdot\cos\omega t$; $x''=-s^2/R\cdot\cos\omega t$; $y''=s^2/R\cdot\sin\omega t$.
V	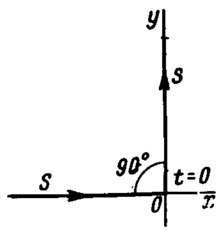	$t<0$: $y=0$. $t>0$: $x=0$.	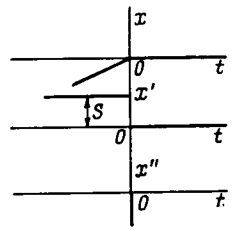	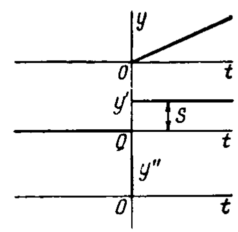	$t<0$: $x=st$; $x'=s$; $x''=y=y'=y''=0$. $t>0$: $y=st$; $y'=s$; $y''=x=x'=x''=0$ $t=0$: $x''=-\infty$; $y''=\infty$.
VI	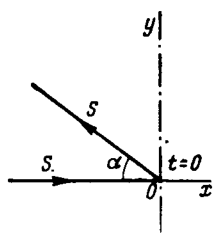	$t<0$: $y=0$. $t>0$: $y=x\ td\,\alpha$.	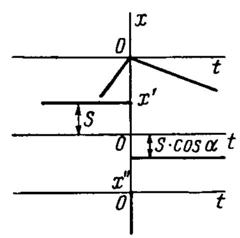	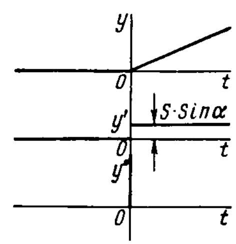	$t<0$: $x=st$; $x'=s$: $x''=y=y'=y''=0$. $t>0$: $x=-st\cos\alpha$: $y=st\sin\alpha$; $x'=-s\cdot\cos\alpha$; $y'=s\cdot\sin\alpha$; $x''=y''=0$. $t=0$: $x''=-\infty$; $y''=\infty$.
VII	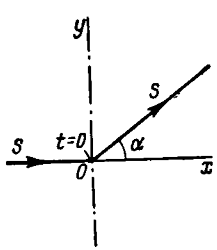	$t<0$: $y=0$. $t>0$: $y=x\,tg\,\alpha$.	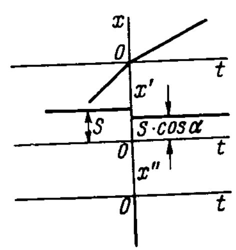	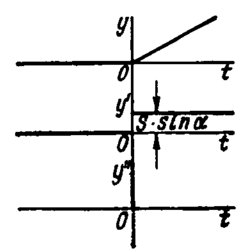	$t<0$: $x=st$; $x'=s$; $x''=y=y'=y''=0$. $t>0$: $x=st\cos\alpha$; $y=st\sin\alpha$; $x'=s\cdot\cos\alpha$; $y'=s\cdot\sin\alpha$; $x''=y''=0$. $t=0$: $x''=-\infty$; $y''=\infty$.

TABLE 2

I

Typical profile segment and rotation axis location

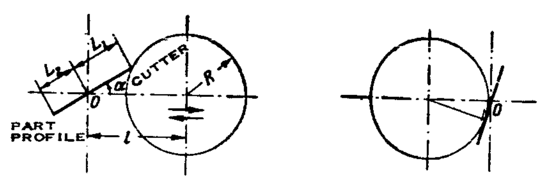

	Tool displacement as function of profile rotation angle	Maximal velocities and displacements
Rolling	$l_{\text{об}} = L_1\left(\cos\alpha + \sqrt{\left(\frac{R}{L_1}\right)^2 - \sin^2\alpha}\right)$ FOR $-\operatorname{arctg}\frac{R}{L_1} \leqslant \alpha \leqslant \operatorname{arctg}\frac{R}{L_1}$. $l_{\text{об}} = L_2\left(-\cos\alpha + \sqrt{\left(\frac{R}{L_2}\right)^2 - \sin^2\alpha}\right)$ FOR $\pi - \operatorname{arctg}\frac{R}{L_1} \leqslant \alpha \leqslant \pi + \operatorname{arctg}\frac{R}{L_2}$.	$\left\lvert s_{MAX}\right\rvert = \omega R\frac{\sqrt{1+\left(R\right)^2}}{\left(\frac{R}{L}\right)^2}$ $\left\lvert a_{MAX}\right\rvert = \omega^2 L\left[1+\frac{1}{\frac{R}{L}}\right]$ (On region boundary)
Sliding	$l_{\text{ск}} = \frac{R}{\sin\alpha}$ FOR $\operatorname{arctg}\frac{R}{L_1} \leqslant \alpha \leqslant \pi - \operatorname{arctg}\frac{R}{L_2}$. $l_{\text{ск}} = -\frac{R}{\sin\alpha}$ FOR $\pi + \operatorname{arctg}\frac{R}{L_2} \leqslant \alpha \leqslant -\operatorname{arctg}\frac{R}{L_1}$.	$\left\lvert a_{MAX}\right\rvert = \omega^2 L\frac{\left[\left(\frac{R}{L}\right)^2+2\right]\sqrt{1+\left(\frac{R^2}{L}\right)}}{\left(\frac{R}{L}\right)^3}$;

Typical input functions

Rolling	$-\operatorname{arctg}\frac{R}{L_1} \leqslant \alpha = \omega t \leqslant \operatorname{arctg}\frac{R}{L_1}$: $l_{\text{об}} = L_1\left(\cos\alpha + \sqrt{\left(\frac{R}{L_1}\right)^2 - \sin^2\alpha}\right)$; $s_{\text{об}} = -\omega L_1\left(\sin\alpha + \frac{\sin 2\alpha}{2\sqrt{\left(\frac{R}{L_1}\right)^2 - \sin^2\alpha}}\right)$; $a_{\text{об}} = -\omega^2 L_1\left(\cos\alpha + \frac{\cos 2\alpha}{\sqrt{\left(\frac{R}{L_1}\right)^2 - \sin^2\alpha}} + \frac{\sin^2 2\alpha}{4\left[\left(\frac{R}{L_1}\right)^2 - \sin^2\alpha\right]^{3/2}}\right)$.	$\pi - \operatorname{arctg}\frac{R}{L_2} \leqslant \alpha = \omega t \leqslant \pi + \operatorname{arctg}\frac{R}{L_2}$: $l_{\text{об}} = L_2\left(-\cos\alpha + \sqrt{\left(\frac{R}{L_2}\right)^2 - \sin^2\alpha}\right)$; $s_{\text{об}} = \omega L_2\left(\sin\alpha - \frac{\sin 2\alpha}{2\sqrt{\left(\frac{R}{L_2}\right)^2 - \sin^2\alpha}}\right)$; $a_{\text{об}} = \omega^2 L_2\left(-\cos\alpha + \frac{\cos 2\alpha}{\sqrt{\left(\frac{R}{L_2}\right)^2 - \sin^2\alpha}} + \frac{\sin^2 2\alpha}{4\left[\left(\frac{R}{L_2}\right)^2 - \sin^2\alpha\right]^{3/2}}\right)$.
Sliding	$\operatorname{arctg}\frac{R}{L_1} \leqslant \alpha = \omega t \leqslant \pi - \operatorname{arctg}\frac{R}{L_2}$ $_{\text{ск}} = \frac{R}{\sin\alpha}$; $s_{\text{ск}} = -\omega R\frac{\cos\alpha}{\sin^2\alpha}$; $a_{\text{ск}} = \omega^2 R\left(\frac{1}{\sin\alpha} + 2\frac{\cos^2\alpha}{\sin^3\alpha}\right)$.	$\pi + \operatorname{arctg}\frac{R}{L_2} \leqslant \alpha = \omega t \leqslant -\operatorname{arctg}\frac{R}{L_1}$: $l_{\text{ск}} = -\frac{R}{\sin^3\alpha}$; $s_{\text{ск}} = \omega R\frac{\cos\alpha}{\sin^2\alpha}$; $a_{\text{ск}} = -\omega^2 R\left(\frac{1}{\sin\alpha} + 2\frac{\cos^2\alpha}{\sin^3\alpha}\right)$.

об = rolling
CK = sliding

TABLE 2 (Continued)

II

Typical profile segment and rotation axis location

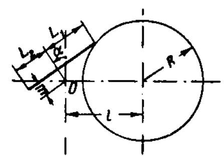 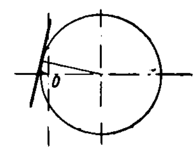

	Tool displacement as function of profile rotation angle	Maximal velocities and displacements
Rolling	$l_{об} = L_3\left(\cos\alpha_1 + \sqrt{R_1^2 - \sin^2\alpha_1}\right)$ FOR $-\operatorname{arctg}\frac{R+m}{L_1} \leqslant \alpha \leqslant \operatorname{arctg}\frac{R-m}{L_1}$. $l_{об} = L_4\left(-\cos\alpha_2 + \sqrt{R_2^2 - \sin^2\alpha_2}\right)$ FOR $\pi - \operatorname{arctg}\frac{R-m}{L_2} \leqslant \alpha \leqslant \pi + \operatorname{arctg}\frac{R+m}{L_2}$. $L_3 = \sqrt{L_1^2 + m^2};\quad L_4 = \sqrt{L_2^2 + m^2};$ $\alpha_1 = \alpha + \frac{\pi}{2} - \operatorname{arctg}\frac{L_1}{m};\ R_1 = \frac{R}{L_3};$ $\alpha_2 = \alpha - \frac{\pi}{2} + \operatorname{arctg}\frac{L_2}{m};\ R_2 = \frac{R}{L_4}.$	$\lvert s_{MAX}\rvert = \omega(R-m)\frac{\sqrt{1+\left(\frac{R-m}{L}\right)^2}}{\left(\frac{R-m}{L}\right)^2}$ $\lvert a_{MAX}\rvert = \omega^2 L\left[\ +\frac{1}{\frac{R-m}{L}}\right]$ (On region boundary
Sliding	$l_{ск} = \frac{R-m}{\sin\alpha}$ FOR $\frac{R-m}{L_1} \leqslant \alpha \leqslant \pi - \operatorname{arctg}\frac{R-m}{L_2}$ $l_{ск} = -\frac{R+m}{\sin\alpha}$ FOR $\pi + \text{ARCTG}\frac{R+m}{L_2}\quad \alpha \leqslant -\operatorname{arctg}\frac{R+m}{L_1}$	$\lvert a_{MAX}\rvert = \omega^2 L\frac{\left[\left(\frac{R-m}{L}\right)^2+2\right]\sqrt{1+\left(\frac{R-m}{L}\right)^2}}{\left(\frac{R-m}{L}\right)^3}.$

Typical input functions

Rolling	$-\operatorname{arctg}\frac{R+m}{L_1} \leqslant \alpha = \omega t \leqslant \operatorname{arctg}\frac{R-m}{L_1}$: $l_{об} = L_3\left(\cos\alpha_1 + \sqrt{R_1^2 - \sin^2\alpha_1}\right);$ $s_{об} = -\omega L_3\left(\sin\alpha_1 + \frac{\sin 2\alpha_1}{2\sqrt{R_1^2 - \sin^2\alpha_1}};\right)$ $a_{об} = -\omega^2 L_3\left(\cos\alpha_1 + \frac{\cos 2\alpha_1}{\sqrt{R_1^2 - \sin^2\alpha_1}} + \frac{\sin^2 2\alpha_1}{4\left[R_1^2 - \sin^2\alpha_1\right]^{3/2}}\right).$	$\pi - \operatorname{arctg}\frac{R-m}{L_2} \leqslant \alpha = \omega t \leqslant \pi + \operatorname{arctg}\frac{R+m}{L_2}$: $l_{об} = L_4\left(-\cos\alpha_2 + \sqrt{R_2^2 - \sin^2\alpha_2}\right);$ $s_{об} = \omega L_4\left(\sin\alpha_2 - \frac{\sin 2\alpha_2}{2\sqrt{R_2^2 - \sin^2\alpha_2}}\right);$ $a_{об} = -\omega^2 L_4\left(-\cos\alpha_2 + \frac{\cos 2\alpha_2}{\sqrt{R_2^2 - \sin^2\alpha_2}} + \frac{\sin^2 2\alpha_2}{4\left[R_2^2 - \sin^2\alpha_2\right]^{3/2}}\right).$
Sliding	$\operatorname{arctg}\frac{R-m}{L_1} \leqslant \alpha = \omega t \leqslant \pi - \operatorname{arctg}\frac{R-m}{L_2}$: $l_{ск} = \frac{R-m}{\sin\alpha};\quad s_{ск} = -\omega(R-m)\frac{\cos\alpha}{\sin^2\alpha};$ $a_{ск} = \omega^2(R-m)\left(\frac{1}{\sin\alpha} + 2\frac{\cos^2\alpha}{\sin^3\alpha}\right).$	$\pi + \operatorname{arctg}\frac{R+m}{L_2} \leqslant \alpha = \omega t \leqslant -\operatorname{arctg}\frac{R+m}{L_1}$: $l_{ск} = -\frac{R+m}{\sin\alpha};\quad s_{ск} = \omega(R+m)\frac{\cos\alpha}{\sin^2\alpha};$ $a_{ск} = -\omega^2(R+m)\left(\frac{1}{\sin\alpha} + 2\frac{\cos^2\alpha}{\sin^3\alpha}\right).$

TABLE 2 (Continued)

III

Typical profile segment and rotation axis location

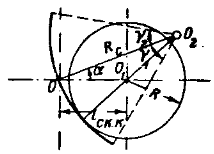

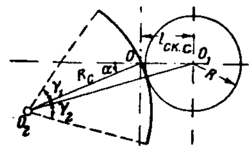

as in I where

Rolling

$$L_1 = 2R_c^2 \sin\frac{\gamma_1}{2},\ \alpha = \frac{\pi}{2} - \frac{\gamma_1}{2} - \alpha_1, \qquad \arcsin\frac{(R_c - R)\sin\gamma_1}{\sqrt{(R_c-R)^2 - 2(R_c - R)R_c\cos\gamma_1 + R_c^2}} \leqslant \alpha_1 = \omega t \leqslant \pi - \arcsin\frac{(R_c + R)\sin\gamma_1}{\sqrt{(R_c+R)^2 - 2(R_c + R)R_c\cos\gamma_1 + R_c^2}}$$

$$L_1 = 2R_c \sin\frac{\gamma_2}{2},\ \alpha = \frac{\pi}{2} + \frac{\gamma_2}{2} - \alpha_2, \qquad \arcsin\frac{(R_c + R)\sin\gamma_2}{\sqrt{(R_c+R)^2 - 2(R_c + R)R_c\cos\gamma_2 + R_c^2}} \leqslant \alpha_2 = \omega t \leqslant \pi - \arcsin\frac{(R_c - R)\sin\gamma_2}{\sqrt{(R_c-R)^2 - 2(R_c - R)R_c\cos\gamma_2 + R_c^2}}$$

	Tool displacement as function of profile rotation angle	Maximal velocities and displacements
Sliding — Concave	$l_{CK.K} = R_c\left(\cos\alpha - \sqrt{\left(\frac{R_c - R}{R_c}\right)^2 - \sin^2\alpha}\right)$ FOR $-\arcsin\frac{(R_c - R)\sin\gamma_2}{\sqrt{(R_c-R)^2 - 2(R_c-R)R_c\cos\gamma_2 + R_c^2}} \leqslant \alpha \leqslant \arcsin\frac{(R_c - R)\sin\gamma_1}{\sqrt{(R_c-R)^2 - 2(R_c-R)R_c\cos\gamma_1 + R_c^2}}$	$\lvert S_{CK.K\,MAX}\rvert = \omega R_c\left[a - \frac{a\sqrt{1-a^2}}{\sqrt{\left(\frac{R_c - R}{R_c}\right)^2 - a^2}}\right]$; $\lvert a_{CK.K\,MAX}\rvert = \omega^2 R_c\left\{\sqrt{1-a^2} - \frac{(1-2a^2)\left[\left(\frac{R_c-R}{R_c}\right)^2 - a^2\right] + a^2(1-a^2)}{\left[\left(\frac{R_c-R}{R_c}\right)^2 - a^2\right]^{3/2}}\right\}$, WHERE $a = \frac{(R_c - R)\sin\gamma_{1(2)}}{\sqrt{(R_c-R)^2 - 2(R_c-R)R_c\cos\gamma_{1(2)} + R_c^2}}$.
Sliding — Convex	$l_{CK.C} = R_c\left(-\cos\alpha + \sqrt{\left(\frac{R_c + R}{R_c}\right)^2 - \sin^2\alpha}\right)$ $-\arcsin\frac{(R_c + R)\sin\gamma_1}{\sqrt{(R_c+R)^2 - 2(R_c+R)R_c\cos\gamma_1 + R_c^2}} \leqslant \alpha \leqslant \arcsin\frac{(R_c + R)\sin\gamma_2}{\sqrt{(R_c+R)^2 - 2(R_c+R)R_c\cos\gamma_2 + R_c^2}}$	Convex, same equations replacing $(R_c - R)$ by $(R_c + R)$

Typical input functions

Sliding

Concave $(\alpha = \omega t)$:

$$l_{CK.K} = R_c\left(\cos\alpha - \sqrt{\left(\frac{R_c - R}{R_c}\right)^2 - \sin^2\alpha}\right);$$

$$S_{CK.K} = \omega R_c\left(-\sin\alpha + \frac{\sin 2\alpha}{2\sqrt{\left(\frac{R_c - R}{R_c}\right)^2 - \sin^2\alpha}}\right);$$

$$a_{CK.K} = \omega^2 R_c\left(-\cos\alpha + \frac{4\cos 2\alpha\left[\left(\frac{R_c - R}{R_c}\right)^2 - \sin^2\alpha\right] + \sin^2 2\alpha}{4\left[\left(\frac{R_c - R}{R}\right)^2 - \sin^2\alpha\right]^{3/2}}\right).$$

Convex $(\alpha = \omega t)$:

$$l_{CK.C} = R_c\left(-\cos\alpha + \sqrt{\left(\frac{R_c + R}{R_c}\right)^2 - \sin^2\alpha}\right);$$

$$S_{CK.C} = \omega R_c\left(\sin\alpha \quad \frac{\sin 2\alpha}{2\sqrt{\left(\frac{R_c + R}{R_c}\right)^2 - \sin^2\alpha}}\right);$$

$$a_{CK.C} = \omega^2 R_c\left(\cos\alpha - \frac{4\cos 2\alpha\left[\left(\frac{R_c + R}{R_c}\right)^2 - \sin^2\alpha\right] + \sin^2 2\alpha}{4\left[\left(\frac{R_c + R}{R_c}\right)^2 - \sin^2\alpha\right]^{3/2}}\right).$$

R_c = convex

CK. K = sliding concave

CK. C = sliding convex

TABLE 2 (Continued)

IV

Typical profile segment and rotation axis location

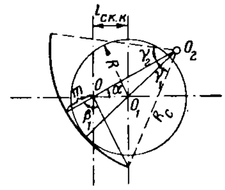

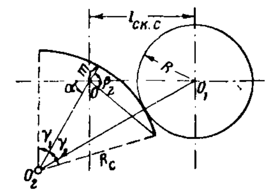

Rolling

as in I where

$$L_1 = \sqrt{(R_c - m)^2 - 2(R_c - m)R_c\cos\gamma_1 + R_c^2};\ \alpha = \pi - \alpha_1 - \arcsin\frac{R_c\sin\gamma_1}{L_1}\ \text{FOR}\ \beta_1 \le \frac{\pi}{2};\ \alpha = -\alpha_1 + \arcsin\frac{R_c\sin\gamma_1}{L_1}\ \text{FOR}\ \beta_1 \ge \frac{\pi}{2};$$

$$\operatorname{arctg}\frac{(R_c\gamma - R)\sin\gamma_1}{(R_c - m) - (R_c - R)\cos\gamma_1} \le \alpha_1 = \omega t \le \pi - \gamma_1 - \operatorname{arctg}\frac{(R_c - m)\sin\gamma_1}{(R_c + R) - (R_c - m)\cos\gamma_1}.$$

$$L_1 = \sqrt{(R_c - m)^2 - 2(R_c - m)R_c\cos\gamma_2 + R_c^2};\quad \alpha = -\alpha_2 + \arcsin\frac{R_c\sin\gamma_2}{L_2}\ \text{FOR}\ \beta_2 \le \frac{\pi}{2};\ \alpha = \pi - \alpha_2 - \arcsin\frac{R_c\sin\gamma_2}{L_2}\ \text{FOR}\ \beta_2 \ge \frac{\pi}{2};$$

$$\gamma_2 + \operatorname{arctg}\frac{(R_c - m)\sin\gamma_2}{(R_c + R) - (R_c - m)\cos\gamma_2} \le \alpha_2 = \omega t \le \pi - \operatorname{arctg}\frac{(R_c - R)\sin\gamma_2}{(R_c - m) - (R_c - R)\cos\gamma_2}.$$

		Tool displacement as function of profile rotation angle	Maximal velocities and displacements
Sliding	Concave	$l_{ck.\,k} = (R_c - m)\left(\cos\alpha - \sqrt{\left(\frac{R_c - R}{R_c - m}\right)^2 - \sin^2\alpha}\right)$ FOR $-\operatorname{arctg}\frac{(R_c - R)\sin\gamma_2}{(R_c - m) - (R_c - R)\cos\gamma_1} \le \alpha \le$ $\le \operatorname{arctg}\frac{(R_c - R)\sin\gamma_1}{(R_c - m) - (R_c - R)\cos\gamma_2}$.	$-s_{ck.\,k.\,MAX}\Big\vert = \omega(R_c - m)\left[a - \frac{a\sqrt{1 - a^2}}{\sqrt{\left(\frac{R_c - R}{R_c - m}\right)^2 - a^2}}\right];$ $\vert a_{ck.\,k.\,MAX}\vert = \omega^2(R_c - m)\left\{\sqrt{1 - a^2} - \frac{(1 - 2a^2)\left[\left(\frac{R_c - R}{R_c - m}\right) - a^2\right] + a^2(1 - a^2)}{\left[\left(\frac{R_c - R}{R_c - m}\right)^2 - a^2\right]^{3/2}}\right\}$, WHERE $a = \frac{(R_c - R)\sin\gamma_{1\,(2)}}{\sqrt{(R_c - R)^2 - 2(R_c - R)(R_c - m)\cos\gamma_{1\,(2)} + (R_c - m)^2}}$. Convex, same equations replacing $(R_c - R)$ by $(R_c + R)$
	Convex	$l_{ck.\,c} = (R_c - m)\left(-\cos\alpha + \sqrt{\left(\frac{R_c + R}{R_c - m}\right)^2 - \sin^2\alpha}\right)$ FOR $-\gamma_1 - \operatorname{arctg}\frac{(R_c - m)\sin\gamma_1}{(R_c + R) - (R_c - m)\cos\gamma_1} \le \alpha \le$ $\le \gamma_2 + \operatorname{arctg}\frac{(R_c - m)\sin\gamma_2}{(R_c + R) - (R_c - m)\cos\gamma_2}$.	

Typical input functions

	Concave ($\alpha = \omega t$):	Convex ($\alpha = \omega t$):
Sliding	$l_{ck.\,k} = (R_c - m)\left(\cos\alpha - \sqrt{\left(\frac{R_c - R}{R_c - m}\right)^2 - \sin^2\alpha}\right);$	$l_{ck.\,c} = (R_c - m)\left(-\cos\alpha + \sqrt{\left(\frac{R_c + R}{R_c - m}\right)^2 - \sin^2\alpha}\right);$
	$s_{ck.\,k} = \omega(R_c - m)\left(-\sin\alpha + \frac{\sin 2\alpha}{2\sqrt{\left(\frac{R_c - R}{R_c - m}\right)^2 - \sin^2\alpha}}\right);$	$s_{ck.\,c} = \omega(R_c - m)\left(\sin\alpha - \frac{\sin 2\alpha}{2\sqrt{\left(\frac{R_c + R}{R_c - m}\right)^2 - \sin^2\alpha}}\right);$
	$a_{ck.\,k} = \omega^2(R_c - m)\left(-\cos\alpha + \frac{4\cos 2\alpha\left[\left(\frac{R_c - R}{R_c - m}\right)^2 - \sin^2\alpha\right] + \sin^2 2\alpha}{4\left[\left(\frac{R_c - R}{R_c - m}\right)^2 - \sin^2\alpha\right]^{3/2}}\right).$	$a_{ck.\,c} = \omega^2(R_c - m)\left(\cos\alpha - \frac{4\cos 2\alpha\left[\left(\frac{R_c + R}{R_c - m}\right) - \sin^2\alpha\right] + \sin^2 2\alpha}{4\left[\left(\frac{R_c + R}{R_c - m}\right)^2 - \sin^2\alpha\right]^{3/2}}\right)$

TABLE 2 (Continued)

V

Typical profile segment and rotation axis location

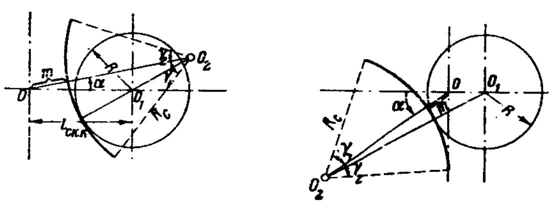

All as in IV for $\beta_1 \geq \frac{\pi}{2}$ and $\beta_2 \geq \frac{\pi}{2}$, replacing $(R_c - m)$ by $(R_c + m)$.

REFERENCES

1. Sarachik, P. and Ragazzini, J. R. A 2-Dimensional Feedback Control System. Applications and Industry. May, 1957.

2. Petrov, B. N. Analysis of Automatic Profiling Systems (Analiz avtomaticheskikh kopiroval'nykh sistem). Thesis, Moscow, 1945.

3. Bernson, G. Determination of Transient Processes from the Frequency Characteristics of the Open-loop System (Opredeleniye perekhodnykh protsessov po chastotnym kharakteristikam razomknutoy sistemy). IN: Frequency Methods in Automation, I. L., 1957.

4. Theory of Servosystems (Teoriya sledyashchikh sistem). Translated from English, edited by James, Nichols and Phillips, I. L., 1953.

5. Fundamentals of Automatic Regulation (Osnovy avtomaticheskogo regulirovaniya). Collection of Articles edited by V. V. Solodovnikov, Mashgiz, 1958.

6. Chestnut, G. and Mayer, R. Design and Analysis of Servosystems and Regulation Systems (Proyektirovaniye i raschet sledyashchikh sistem i sistem regulirovaniya). Part I, Gosenergoizdat, 1959.

7. Bulakov, A. A. Programed Control of Metal Cutting Machine Tools (Programmnoye upravleniye metallorezhushchimi stankami). Gosenergoizdat, 1959.

N66 34829

DISSIPATIVITY IN THE LARGE OF A THREE-DIMENSIONAL NONAUTONOMOUS NONLINEAR AUTOMATIC CONTROL SYSTEM

T. G. Babunashvili

1. Statement of the Problem

In the analysis of automatic control systems (ACS) we encounter systems whose phase trajectories have the following properties: in the system phase space there exists the bounded, open set M_1 which contains the coordinate origin (which is assumed to be the point of the equilibrium state of the ACS) and the bounded set M_2 which contains the set M_1, such that each trajectory passing at the moment of time t_0 through the set M_1 will not leave the set M_2 for all $t > t_0$ (stability in the Lagrange sense (ref. 1)); moreover, there exists the number $T > t_0$, such that each trajectory "embeds itself" completely in the set M_1 for all $t > T$ (dissipativity in the large (ref. 2)). /22

Shirokorad (ref. 3) found the conditions for the existence of this property of the phase trajectories for a definite class of three-dimensional nonlinear nonautonomous ACS with constant parameters. Using these conditions we can determine the above mentioned sets (the analysis problem). The method can also be used in the synthesis of ACS having the property of dissipativity in the large.

In the present paper we study the question of the dissipativity in the large of a three-dimensional ACS described by the equations

$$\ddot{\gamma} + A(t)\dot{\gamma} + B(t)\mu = 0; \qquad \dot{\mu} = f(\sigma); \qquad \sigma = k\gamma - \mu,$$

where $\gamma, \dot{\gamma}, \mu$ are the system coordinates;
k is the regulator transfer function;
σ is the control parameter;
$f(\sigma)$ is an essentially nonlinear class A[1] function (ref. 4);

[1]Class A includes functions, piecewise continuous with a finite number of discontinuities of the first kind, and which satisfy the conditions $f(\sigma) = 0$ with $|\sigma| \le \sigma_*$ and $\sigma f(\sigma) > 0$ with $|\sigma| \le \sigma_*$. Here σ_* is a fixed nonnegative number which characterizes the zone of insensitivity of the regulator to changes of σ.

$A(t)$, $B(t)$ are time-dependent object parameters;
$A(t)$, $B(t)$ are bounded, continuous, positive functions in the interval $0 \leq t < +\infty$.

In the considered case the question is complicated by the presence of variable parameters. The given ACS has a very complex structure of the phase space, since its forms change with variation of the time. In this work we show that the method developed by Shirokorad can be applied to systems with time-varying parameters with satisfaction of the conditions of the Olech theorem (ref. 5) for $A(t)$ and $B(t)$. /23

We encounter problems of this sort in the theory of automatic regulation of those systems for which there exists the so-called starting regime. We will clarify this by an example.

We consider a symmetric finless rocket with a cruciform arrangement which is controlled by means of an exhaust jet rudder and an elevator and by spoilers in roll.

The rocket jet of a solid motor provides (as a result of the coriolis effect) sufficient natural damping of the rocket about its lateral axes. For this reason the signal of a rate gyro, which determines the artificial damping of the rocket, is not introduced into two channels of the autopilot (rudder and elevator).

In the course of the launch period (from the instant of release to the engagement of the guidance system) the rocket is not guided--the guidance system is not connected. However, the autopilot, of course, operates during the launch period as an automatic control system. As will be shown below, with sufficiently high natural damping and if the autopilot actuator satisfies certain definite conditions (these conditions are satisfied with sufficiently powerful hydraulic actuators), in the course of the launch period comparatively large deviations of the system coordinates are possible, which will not permit engagement of the guidance system. At the end of some time T the system coordinates will vary in limits (the set M_1) which will permit engagement of the guidance system.

Thus, during the launch period the autopilot, although it may not provide stability relative to the launch line, will at the termination of a definite time bring the system coordinates into such a state (the set M_1) that it is possible to guide the rocket at the termination of the launch period.

In operation of the system it is necessary to know both the possible maximal deviations of the coordinates and the time T at the end of which the guidance system can be engaged.[1] Because of the system symmetry it is sufficient to consider one of the channels. For definiteness let us take the elevator channel.

[1]For example, knowing the possible deviations of the pitch angle, we can construct the region which the rocket will not leave during launch.

If we designate the time-varying coefficients of the natural damping and the effectiveness of the exhaust jet control surface by $a_1(t)$ and $a_3(t)$, respectively, the equation of motion of the rocket about its lateral axis $\vec{Oz_1}$ will have the form

$$\ddot{\vartheta} + a_1(t)\,\dot{\vartheta} + a_3(t)\,\delta = 0, \tag{1}$$

where $a_1(t)$ and $a_3(t)$ are continuous bounded positive functions in the interval $0 \le t < +\infty$.

ϑ is the angle between the longitudinal axis of the rocket and the launch line (for the sake of simplicity it is assumed that there is no roll oscillation and that the $\vec{Oz_1}$ axis lies in the horizontal plane);

δ is the angle of deviation of the exhaust jet elevator surface from the neutral position.

The autopilot elevator channel is described by the equations /24

$$\delta = f(\sigma); \quad \sigma = i\vartheta - \delta, \tag{2}$$

where i is the gain with respect to the angle δ ($i > 0$).

We are required to show that the nonautonomous, nonlinear, three-dimensional ACS described by the system of equations (1) and (2) is dissipative in the large in the Massera sense (and, consequently, is Lagrange-stable in the positive direction).

In addition, we are required to determine the time T, the open set M_1, which in our case is represented in the form of the parallelepiped Π

$$-r \leqslant \underline{\sigma}_2 < \sigma < \overline{\sigma}_2 \leqslant r, \quad |\vartheta| < r, \quad |\dot{\vartheta}| < r \ (\underline{\sigma}_2 \text{ and } \overline{\sigma}_2 \text{ are numbers} \tag{3}$$

and the set M_2, which is represented in the form of a sphere with the center coinciding with the coordinate origin and having the radius R, such that

$$\sigma^2(t) + \dot{\vartheta}^2(t) + \vartheta^2(t) < R^2 \text{ for all } t > t_0. \tag{4}$$

2. Problem Solution

We represent the systems (1) and (2) in the form

$$\ddot{\vartheta} + a_1(t)\dot{\vartheta} + a_3(t) i\vartheta = a_3(t)\sigma(t);$$
$$\dot{\sigma} = i\dot{\vartheta} - f(\sigma), \tag{5}$$

and assume that the damping coefficient $a_1(t)$ is so large that the Olech conditions (ref. 5) are satisfied, namely, there exist the negative numbers $\underline{\lambda}_1 \leqslant \overline{\lambda}_1 < \underline{\lambda}_2 \leqslant \overline{\lambda}_2$, such that the roots $\lambda_1(t)$ and $\lambda_2(t)$ of the algebraic equation

$$\lambda^2(t) + a_1(t)\lambda(t) + a_3(t) i = 0 \tag{6}$$

satisfy the inequalities $\underline{\lambda}_1 \leqslant \lambda_1(t) \leqslant \overline{\lambda}_1$ and $\underline{\lambda}_2 \leqslant \lambda_2(t) \leqslant \overline{\lambda}_2$ for all $t \geq t_0$, where t_0 is the moment of separation of the rocket from the launcher. Without losing generality we can assume that $t_0 = 0$.

Let us assume a priori that the function $\sigma(t)$ is known on the time segment $[0, \overline{\tau}]$. Then we integrate the first of equations (5), using the Olech theorem (ref. 5). We obtain the expression

$$\vartheta(t) = C_1 \exp\int_0^t \xi_1(\tau)\,d\tau + C_2 \exp\int_0^t \xi_2(\tau)\,d\tau + \int_0^t \frac{\left[\exp\int_\tau^t \xi_2(\tau)\,d\tau - \exp\int_\tau^t \xi_1(\tau)\,d\tau\right] a_3(\tau)\sigma(\tau)\,d\tau}{\xi_2(\tau) - \xi_1(\tau)}, \tag{7}$$

where $\xi_1(\tau)$ and $\xi_2(\tau)$, according to the Olech theorem, satisfy the inequalities

$$\underline{\lambda}_1 \leqslant \xi_1(\tau) \leqslant \overline{\lambda}_1, \quad \underline{\lambda}_2 \leqslant \xi_2(\tau) \leqslant \overline{\lambda}_2 \quad \text{when} \quad 0 \leqslant \tau < +\infty, \tag{8}$$

and

$$C_1 = \frac{\vartheta(0)\xi_2(0) - \dot{\vartheta}(0)}{\xi_2(0) - \xi_1(0)}, \quad C_2 = \frac{\dot{\vartheta}(0) - \vartheta(0)\xi_1(0)}{\xi_2(0) - \xi_1(0)}.$$

Differentiating both sides of (7), we obtain the expression for $\dot{\vartheta}(t)$ /25

$$\dot{\vartheta}(t) = C_1\xi_1(t)\exp\int_0^t \xi_1(\tau)\,d\tau + C_2\xi_2(t)\exp\int_0^t \xi_2(\tau)\,d\tau -$$

$$- \xi_1(t)\int_0^t \frac{\exp\int_\tau^t \xi_1(\tau)\,d\tau\cdot a_3(\tau)\cdot\sigma(\tau)\,d\tau}{\xi_2(\tau)-\xi_1(\tau)} + \xi_2(t)\cdot\int_0^t \frac{\exp\int_\tau^t \xi_2(\tau)\,d\tau\cdot a_3(\tau)\,\sigma(\tau)\,d\tau}{\xi_2(\tau)-\xi_1(\tau)}. \tag{9}$$

Making use of the limiting inequality (8) and assuming that the initial point of the trajectory $P_0\{\sigma(0),\ \vartheta(0),\ \dot{\vartheta}(0)\}$ belongs to the sphere with center coinciding with the coordinate origin and with the radius r, from (7) and (9) we obtain the estimates

$$|\vartheta(t)| < i(mr + k\bar{\sigma}) \text{ and } |\dot{\vartheta}(t)| < i(nr + l\bar{\sigma}), \tag{10}$$

where

$$m = \frac{(2-\underline{\lambda}_2-\underline{\lambda}_1)}{\underline{\lambda}_2-\bar{\lambda}_1}\cdot\frac{1}{i}; \qquad n = \frac{\underline{\lambda}_1(\lambda_2-1)+\underline{\lambda}_2(\underline{\lambda}_1-1)}{\underline{\lambda}_2-\bar{\lambda}_1}\cdot\frac{1}{i};$$

$$k = \frac{\bar{a}_3}{\underline{\lambda}_2-\bar{\lambda}_1}\cdot\left(-\frac{1}{\bar{\lambda}_2}-\frac{1}{\bar{\lambda}_2}\right)\cdot\frac{1}{i}; \qquad l = \frac{2\bar{a}_3}{\underline{\lambda}_2-\bar{\lambda}_1}\cdot\frac{1}{i};$$

$$\bar{\sigma} = \max_{\text{when } 0<t<\tau} |\sigma(t)|; \qquad \bar{a}_3 = \text{borne}\sup_{\text{when } t>0} a_3(t),$$

where r is subject to determination.

Now let us assume that function f(σ) satisfies the conditions of reference 4.

There exists a sufficiently large r > 0, such that the roots of the equations

$$i(m\omega + k\sigma_1) = f(\sigma_1); \quad i(n\omega + l\cdot\sigma_2) = f(\sigma_2), \tag{11}$$

where $\bar{\sigma}_1 > 0$ and $\bar{\sigma}_2 > 0$, corresponding to ω = r, and $\underline{\sigma}_1 < 0$ and $\underline{\sigma}_2 < 0$ with ω = -r, lie in the interval $[-r, r]$.

Moreover, these roots satisfy the inequalities

$$-\frac{r}{ki} < \underline{\sigma}_1 < \bar{\sigma}_1 < \frac{r}{ki}, \quad -\frac{r}{li} < \underline{\sigma}_2 < \bar{\sigma}_2 < \frac{r}{li}. \tag{12}$$

Then, if $\underline{\sigma}_2 < \sigma(0) < \overline{\sigma}_2$, then

$$\underline{\sigma}_2 < \sigma(t) < \overline{\sigma}_2 \text{ when } t > 0. \tag{13}$$

Let us prove this by contradiction. Let us assume that the inequality (13) is not satisfied. Then the following two cases are possible.

1. There exists a minimal $\overline{\tau} > 0$, for which $\sigma(\overline{\tau}) = \overline{\sigma}_2$ and $\dot{\sigma}(\overline{\tau}) \geqslant 0$. But in this case, using the second of equations (5), the second inequality (10) and the assumption relative to the function, we obtain the contradiction

$$\dot{\sigma}(\overline{\tau}) = i\dot{\vartheta}(\overline{\tau}) - f[\sigma(\overline{\tau})] < i(nr + l\overline{\sigma}_2) - f(\overline{\sigma}_2) = 0.$$

2. There exists the minimal $\overline{\tau} > 0$, for which $\sigma(\overline{\tau}) = \underline{\sigma}_2$ and $\dot{\sigma}(\overline{\sigma}) \leqslant 0$. We /26 obtain the contradiction

$$\dot{\sigma}(\overline{\tau}) = i\dot{\vartheta}(\overline{\tau}) - f[\sigma(\overline{\tau})] > i(-nr + l\underline{\sigma}_2) - f(\overline{\sigma_2}) = 0.$$

Consequently, (13) is satisfied.

From inequalities (10) and (13) it follows that each positive phase trajectory passing at the instant of time t = 0 through the point $P_0\{\sigma(0), \vartheta(0), \dot{\vartheta}(0)\}$, lying within the parallelepiped (3), is found in the sphere with radius $R = r\left[(m\cdot i+1)^2 + (n\cdot i+1)^2 + \left(\frac{1}{k\cdot i}\right)^2\right]^{\frac{1}{2}}$ with t > 0.

This property is termed stability of the phase trajectory in the positive direction (ref. 1).

Now let us show that there exists T > 0, such that as soon as t > T, the phase trajectory P(t) will remain in the parallelepiped $(P(t) \in \Pi)$, if $P(0) \in \Pi$.

There exist the numbers $\epsilon_1 > 0$ and $\epsilon_2 > 0$ for which the inequalities

$$\left.\begin{aligned} -\frac{r-\varepsilon_1}{k\cdot i} < \underline{\sigma}_1 < \overline{\sigma}_1 < \frac{r-\varepsilon_1}{k\cdot i}\,; \\ -\frac{r-\varepsilon_2}{k\cdot i} < \underline{\sigma}_2 < \overline{\sigma}_2 < \frac{r-\varepsilon_2}{k\cdot i}\,, \end{aligned}\right\} \tag{14}$$

are satisfied, which follows from (12).

Let us write a more exact limiting condition for $\vartheta(t)$ and $\dot{\vartheta}(t)$

$$-imr\cdot\exp(\bar{\lambda}_2\cdot t)+ik\underline{\sigma}_1<\vartheta(t)<ik\bar{\sigma}_1+imr\cdot\exp(\bar{\lambda}_2\cdot t); \tag{15}$$

$$-inr\cdot\exp(\bar{\lambda}_2\cdot t)+ik\underline{\sigma}_2<\dot{\vartheta}(t)<i\cdot k\cdot\bar{\sigma}_2+imr\cdot\exp(\bar{\lambda}_2\cdot t); \tag{16}$$

with the value of $t\geqslant-\frac{1}{\bar{\lambda}_2}\ln\frac{imr}{\varepsilon_1}$ inequality (15) takes the form $|\vartheta(t)|<r$, if we take account of the first inequality (14), and with the value $t\geqslant-\frac{1}{\bar{\lambda}_2}\ln\frac{inr}{\varepsilon_2}$, inequality (16) takes the form $|\dot{\vartheta}(t)|<r$, if we take account of the second inequality (14). Of the sets $\varepsilon_1(0<\varepsilon_1<r-k\bar{\sigma}_1)$ which satisfy the first inequality (14), the upper bound of the sets corresponds to the value $t = T_1$, at which the coordinates of the system $\vartheta(t)$ begin to appear in the open parallelepiped, i.e., the inequality $|\vartheta(t)|<r$ begins to be satisfied.

Thus, substituting the value of the upper bound of the set ϵ_1 in the formula for t, we obtain the value

$$T_1=-\frac{1}{\bar{\lambda}_2}\ln\frac{imr}{r-k\bar{\sigma}_1}. \tag{17}$$

Using similar reasoning we obtain the value

$$T_2=-\frac{1}{\bar{\lambda}_2}\ln\frac{inr}{r-k\bar{\sigma}_2}, \tag{18}$$

at which the inequality $|\dot{\vartheta}(t)|<r$ begins to be satisfied. Let us denote by T the larger of T_1 and T_2. Taking account of inequality (13) and this last inequality, we can write: $-r\leqslant\underline{\sigma}_2<\sigma(t)<\bar{\sigma}_2\leqslant r$, $|\vartheta(t)|<r$, $|\dot{\vartheta}(t)|<r$ with $t > T$ with the condition $\underline{\sigma}_1<\sigma(0)<\sigma_1$, $|\vartheta(0)|\leqslant r$ and $|\dot{\vartheta}(0)|\leqslant r$.

Thus, if the velocity characteristic of the control surface actuator /27
satisfies conditions (11) and (12), the given automatic regulation system is stable in the sense of Lagrange and Massera. Then, using equation (11), we determine the ensemble of sets r, $\underline{\sigma}_2$ and $\bar{\sigma}_2$, i.e., the sets of the parallelepipeds. Further, starting from the system operational specifications, we

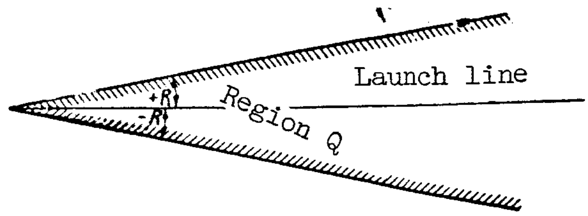

Figure 1. Rocket launch safety region Q.

select r (from the set $r_{min} \leq r \leq r_{max}$). After selecting r, using the equation for R we determine the value of the maximal deviation of the coordinates, i.e., the value of R. Then, using the inequality $|\vartheta(t)| < R$, we can construct the region in which the rocket will remain with motion in the vertical plane.

Actually, since $\vartheta(t)$ is the angle of deviation of the rocket axis from the launch line, by drawing two lines at the angles R and -R relative to the launch line (fig. 1), we obtain region Q, in which the rocket will remain until engagement of the guidance system. By variation of the launch line we can eliminate foreign objects from region Q during the launch period. Further, using equations (17) and (18) we determine the values of T_1 and T_2, the larger of which will be T, i.e., the time at the end of which the guidance system can be engaged.

Thus, knowledge of the value of R, more precisely the region Q and T, is necessary in order to ensure launch safety.

In conclusion we note that this theory can be related not only to the particular case of the rocket, but also to any ACS (refs. 6 and 7) whose equations can be reduced to the form (5).

REFERENCES

1. Nemytskiy, V. V. and Stepanov, V. V. Qualitative Theory of Differential Equations (Kachestvennaya teoriya differentsial'nykh uravneniy). Gostekhizdat, 1947.

2. Massera, I. L. The Number of Subharmonic Solutions of Nonlinear Differential Equations of the Second Order. Ann. Math., Vol. 50, No. 1, 1949.

3. Shirokorad, B. V. Existence of a Cycle Outside the Conditions of Absolute Stability of a Three-Dimensional System (O sushchestvovanii tsikla vne usloviy absolyutnoy ustoychivosti trekhmernoy sistemy). Avtomat. i telemekh., Vol. 19, No. 10, 1958.

4. Letov, A. M. Stability of Nonlinear Control Systems (Ustoychivost' nelineynykh reguliruyemykh sistem). Gostekhizdat, 1955.

5. Olech, C. Asymptotic Behavior of the Solutions of Second Order Differential Equations. Bull. de l'Acad. Polonais des Sci., Vol. VII, No. 6, 1959.

6. Murray, F. I. and Müller, K. S. Existence Theorems for Ordinary Differential Equations. New York, University Press, 1954.

7. Serdenjecti, S. Optimalizing Control in the Presence of Noise Interference. Jet Propulsion, Vol. 26, No. 6, 1956.

N66 34830

STUDY OF AN OPTIMAL SYSTEM FOR CONTROL OF FLYING SHEARS FOR A JOBBING MILL

B. B. Buyanov

The theory of optimal systems, receiving extensive development in recent years (ref. 1), which provides for maximal speed of response with limitations on certain parameters has found successful application in the automation of various processes. One of the examples of the use of an optimal system is the automatic device developed at the Institute of Automation and Remote Control of the Academy of Sciences USSR for the control of the drive of the flying shears of a jobbing mill. /28

The flying shears are installed at the end of the rolling line and shear off the rolled metal into strips of the required length. The electric drive for the shears continuously rotates a drum carrying the shears and is synchronized with the last stand of the mill by a tachometric circuit. Without the optimal system the shears simply perform a measured cutoff of the rolled stock. Since the leading edge of the rolled metal is flattened, in order to remove the low-grade leading edge portion the entire lot of section metal, after cooling and baling, has 200-300 mm of the end cut off on a cold-cut shear, which leads to prohibitive loss of metal. Thus there arose a need for the creation of an automatic controlling device which would provide for a measured cutoff of the leading ends which were being discarded. The new system control must be optimal in speed of response, since it is necessary to cancel any errors in the very short time which is determined by the distance between the last mill stand and the shears, and also by the rolling speed. Increase of the time for elimination of the error can lead to reduction of the rolling speed and consequently to reduction of the mill productivity.

The controlling portion of the optimal system for the drive of the flying shears must solve the following problems:

(1) determine the mismatch in the system at the instant of the exit of the leading end of the stock from the mill rollers;

(2) transmit the controlling signal to the shear drive circuit;

(3) determine the moment of change of the sign of the controlling signal;

(4) turn off the controlling signal at the end of the transient period.

The principles of the construction of the controlling devices for the flying shears' optimal system have been considered in references 2 and 3.

Let us recall briefly the purpose of the primary elements of the circuit (fig. 1). For the determination of the error, use is made of the photorelay PR and the integrator I with the travel switch TS. At the instant of illumination of the photorelay the electronic timing relay TDR breaks the integrator input circuit and the travel switch circuit. At the output of the integrator the voltage is stored proportional to the distance traveled by the shears from /29 the instant of convergence, i.e., the system error. Variation of the delay of the time-delay relay TDR regulates the length of the first piece of metal.

The drive control unit DCU transmits and changes the sign of the control signal to the electric drive of the shears. The computer unit CU performs the determination of the instant of switching of the control signal. The voltage at the output of the computer is proportional to the portion of the mismatch which has been eliminated. Since the static torque of the drive is quite low, the switching takes place at the instant of generation of half of the stored error. Turnoff of the control action is accomplished by the electronic null relay NR at the instant of equality of the velocities of the shears and the stand rollers.

The optimal control system was tested on the flying shears of the "240" jobbing mill of the Chelyabinsk Metallurgical Plant (CMP). A preliminary investigation was made of a similar system on a physical model. The real time constants of the motor and generator were retained in the modeling of the power drive on the low power machines. The system was well tuned. The nature of the behavior of the transient processes during the error elimination was close to optimal (fig. 2).

From the oscillogram, which presents the variations of the speed n, the measurement distance S, and the motor current I with differing values of mismatch, we can see the good quality of the current diagram. The steep current rise (about 0.1 sec), the small overshoots, the stability of the value of the current for a period of 4 sec, the similarity of the shape of the current curve during deceleration and acceleration provided for high accuracy of the elimination of the error.

A special circuit was used for the measurement of the effective travel for different amounts of mismatch. When the steady state velocity was sufficiently high so that the elimination of the maximal mismatch was accomplished without reversing of the drive, the accuracy of the determination over the entire range did not exceed ±1 percent of the measured cut, which with a strip length of /30 12 m amounts to ±12 cm (in the present case each convergence of the blades corresponds to a measured cut).

The flying shears of the CMP "240" jobbing mill have certain peculiarities in their design. Figure 3 shows the kinematic diagram of the flying shear arrangement. The upper drum 1 of the shear rotates in bearings on a movable frame (not shown in the figure) and is somewhat raised. Therefore, with rotation of drums 1 and 2 at the instant of convergence of the blades, there remains a gap between them which is sufficient for free passage of the strip, and no cutting takes place. The eccentric shaft 4 is connected with the upper drum by means of a gear. The latch 5 is freely seated on the shaft 4 and with rotation of the shaft it performs an oscillating movement.

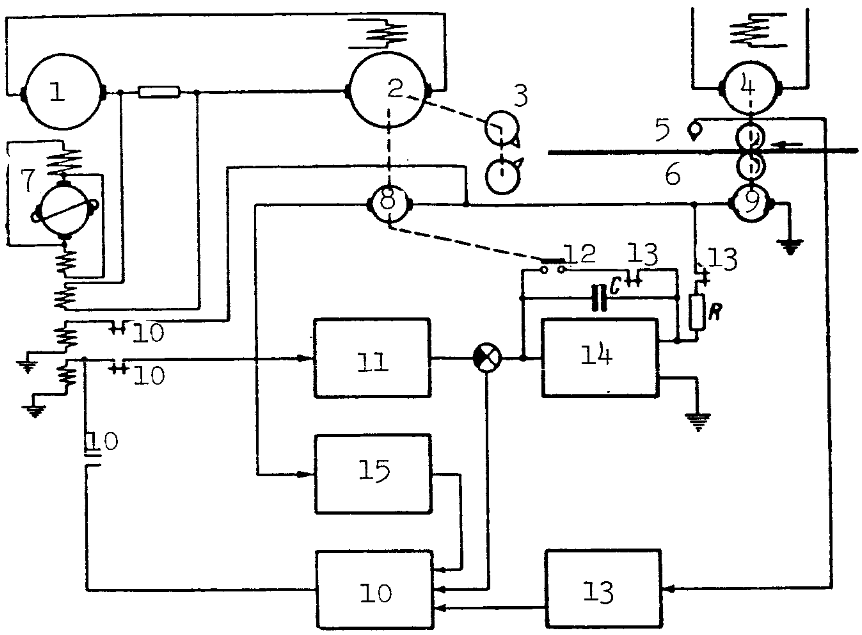

Figure 1. Block diagram of control portion of optimal system: 1, generator; 2, motor; 3, shears; 4, roll motor; 5, photorelay; 6, rolls; 7, amplidyne; 8, shear tach-generator; 9, rolls tach-generator; 10, drive control unit; 11, computer; 12, limit switch; 13, electronic timing relay; 14, integrator; 15, null relay.

During two revolutions of the drums the latch makes a complete cycle in its movement, which corresponds to 3 m along the length of the circle described by the edges of the lands.

With every convergence of the blades the latch is located in the upper or lower position. Cutting is possible only in the lower position of the latch. The electromagnet 8 must be engaged in order to make a cut. This electromagnet draws in the core and by means of lever 7 rotates the small link 6, which with the roller on its lower end firmly presses the latch to the flat surface on the shear frame. Since the drums and the eccentric shaft continue to rotate, the upper drum together with large link 3 and the mobile frame are dropped by the magnitude of double the eccentricity and close up the gap between the blades. The blades converge at this same instant and the cut is made.

The cutting instruction is transmitted from the cutting circuit so that the nominal length of the metal strip amounts to 25-30 m. However, the travel switch closes with each convergence of the blades, and therefore the maximal measurement distance of the system does not exceed 3 m.

A salient feature of the testing of the experimental installations under industrial conditions is the inadmissibility of interruption in the production

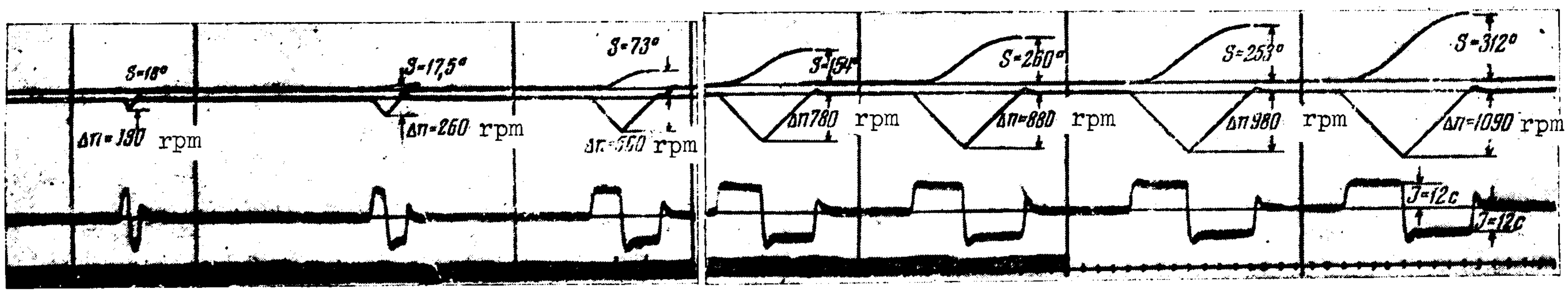

Figure 2. Oscillogram of transient process in physical model.

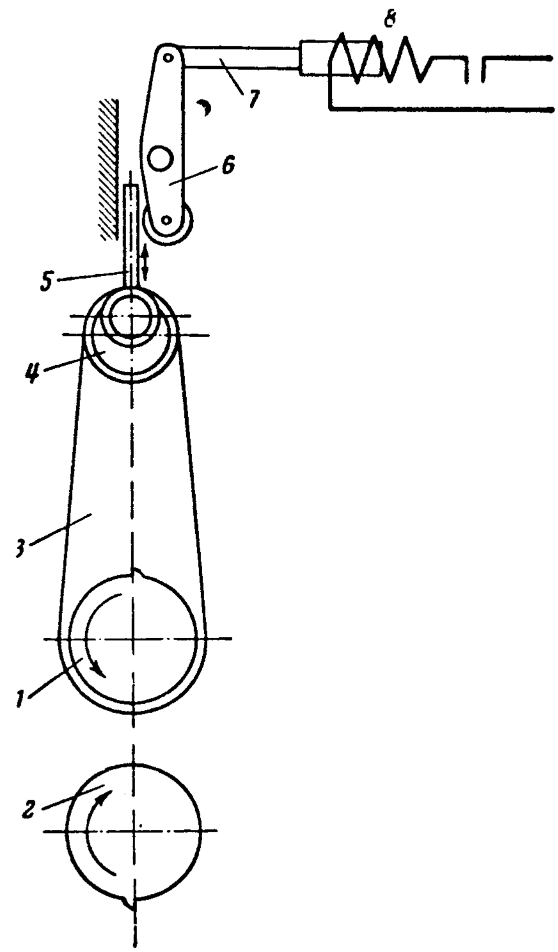

Figure 3. Kinematic diagram of flying shears.

process. Therefore an experimental circuit[1] (fig. 4) was assembled and debugged for the testing of the optimal system[2] in parallel with the present system for the control of the drive of the flying shears. The transfer from the present system to the experimental system was accomplished with selector switches.

Let us examine the circuit of the flying shear drive which was used in the testing of the optimal system. The dc motor (21 kW, 110A, 1500 rpm) is controlled using a generator-motor system. The motor excitation current is not regulated. In the circuit of the excitation winding EW we included the no-field lockout relay NLR, which disconnects the system in case of an open circuit in the motor excitation. The additional resistors AR and 1AR, as well as the maximal current relay MCR, are connected in the main circuit of the GM system. /31

[1]V. A. Kovtunovich, F. S. Balakin and I. Ye. Barbner of the Chelyabinsk Metallurgical Plant automation laboratory participated in this work.

[2]The numbers of the diagram correspond to the numbers of the contacts of the LN-1 disconnect plug used to connect the noted points of the circuit.

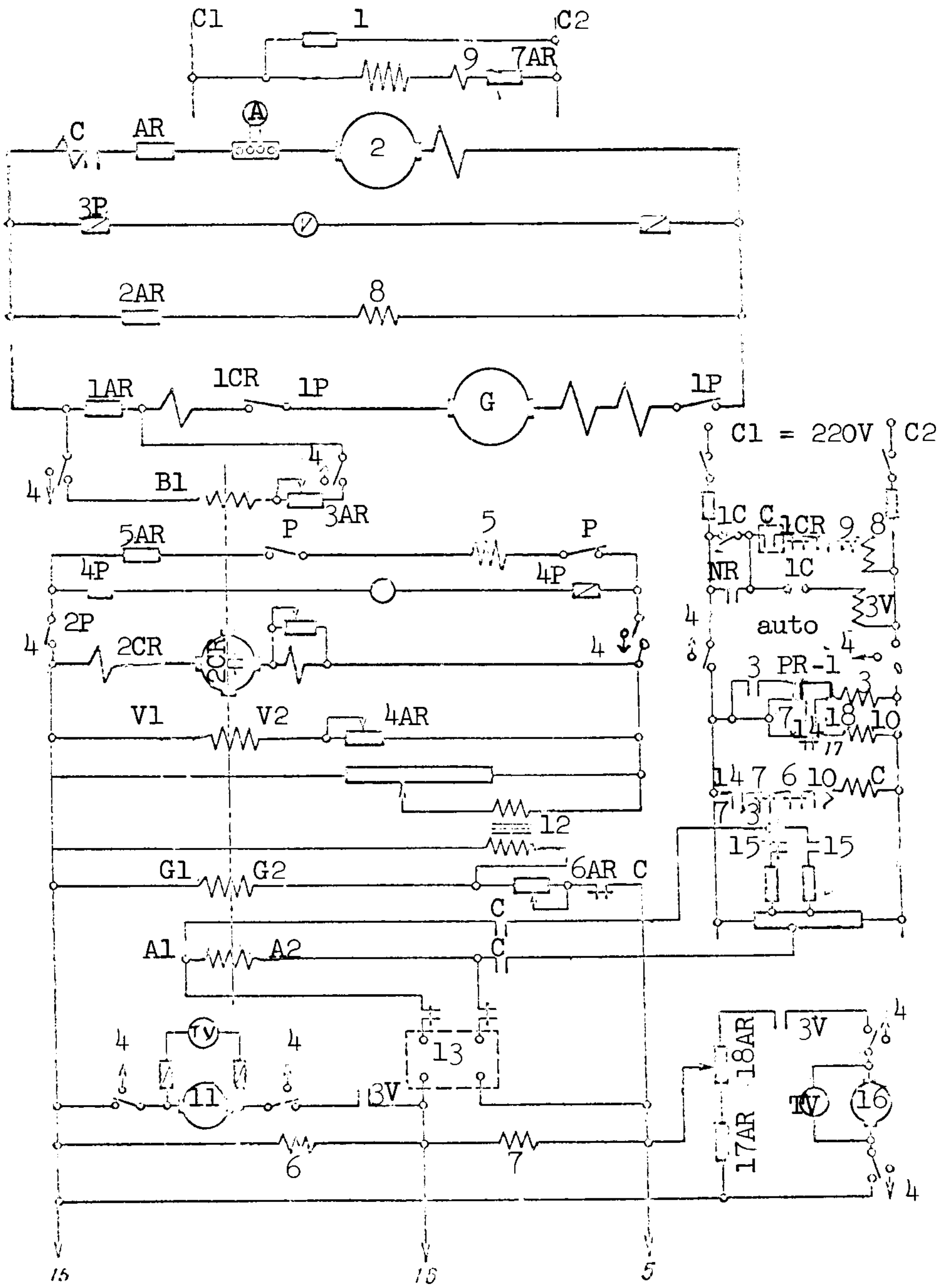

Figure 4. Diagram of drive for flying shears. 1, Motor exciter winding; 2, motor; 3, intermediate relay; 4, to circuit; 5, generator exciter winding; 6, overspeed relay; 7, mismatch limiting relay; 8, maximum voltage relay; 9, no-field lockout relay; 10, timing relay; 11, tach-generator shear; 12, transformer; 13, transistorized amplifier; 14, time-delay relay, 15, drive control unit; 16, tach-generator roll; C, contactors; PR, photorelay; CR, overcurrent relay; AR, additional resistors; G, generator.

The main circuit current feedback voltage is taken from the resistor 1R. The maximal voltage relay MVR is connected across the terminals of the generator.

The winding of the generator exciter WGE is supplied from the reserve amplidyne A (3CR). In order to reduce the time constant of the WGE winding circuit, the additional resistor 5AR is connected in series with it. The amplidyne is protected from overloads by the overload current relay 3CR, whose normally closed contacts break the transverse circuit of the A, if the armature current exceeds the permissible magnitude.

The control windings of A are used in the following way. The A1-A2 winding--the speed winding--serves to synchronize the speed of rotation of the shears with the mill speed. The control signal is applied to this winding during measurement of the error. The speed winding is connected to the /33 difference of the voltages of the tach-generators of the motors of the rollers TGR and the shear TGS through the transistorized amplifier TA. The winding b1-b1--current winding--serves to limit the main circuit current in the transient regime (proportional current feedback).

The magnitude of the current of the main circuit is established by the controllable resistor 3CR. The winding b1-B2 creates a negative proportional feedback with respect to the voltage of the A, which reduces the lag of the A. The winding g1-g2 is both driving and stabilizing. As a driver it is connected to the voltage of the tach-generator TGR through the divider 17AR-18AR, which permits the variation of the relation between the speed of rotation of the blades and the speed of travel of the metal in the direction of either having the metal lead or lag the blades. The stabilization loops are adjusted so that the damping action of the transformer ST retards the motor acceleration process as little as possible and at the same time is sufficient to suppress the oscillations arising in the system.

The shear motor is energized from the switch 1K which energizes relay 3B. The driver winding is connected to the voltage of the tach-generator TGR and the input of the transistorized amplifier TA is connected to the difference of the voltages TGR and TGS. The switchings in the circuits of the control windings of A in the transient regimes are accomplished by an automatic control device.

During the time of debugging and testing of the optimal drive control system, improvements and changes were made in the circuit. Thus, after the first trial cuts of the leading end it was found that the speed of the motor after elimination of the error did not always return to the original speed, since the hysteresis of A and the generator has a strong effect because of the low gain of the speed feedback. The transistorized amplifier TA shown in figure 4 was developed to eliminate this deficiency. This amplifier increased the system gain and the accuracy of maintenance of the speed of the shear motor.

The functional circuit of the amplifier is shown in figure 5. The amplifier operates into a low-resistance load (10 ohm) and has a linear input-output characteristic. The load current varies from -1.5 to +1.5 A with a change of the input signal of ±1.5 V. A feature of the operation of the amplifier is that

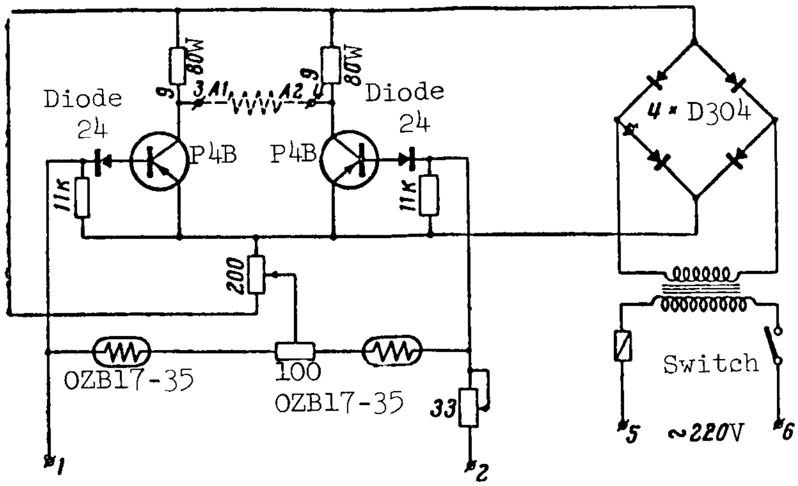

Figure 5. Diagram of semiconductor amplifier.

during startup or shutdown of the shear motor the total voltage of the roller tach-generator TGR is applied to its input in the present case on the order of 100 V. Therefore, the input circuit of the amplifier has a somewhat unusual form. The current stabilizers serve for the limitation of the triode base currents with high voltages on the amplifier input, while the diodes D24 in the base circuit prevent breakdown of the triodes, since their reverse resistance is significantly higher than the base-emitter resistance of the triode. /34

The speed control system had a tendency to oscillate. Stable operation of the system in the transient regimes was achieved by increase of the stabilization and some deterioration of the duty cycle of the current diagram. After these changes the rise of the motor current to the maximal value $I_{max} = (1.3\text{-}1.4)I_{nom}$ lasted for 0.3-0.4 sec (fig. 6).

As indicated by the tests, the time for the measurement of the maximal mismatch, equal to 3 m (two revolutions of the blade drum), was 2.6 sec with an acceleration corresponding to the current $I_{max} = (1.3\text{-}1.4)I_{nom}$. In order to provide the time of 2.6 sec necessary for elimination of the maximal mismatch with a metal speed of 5.5-6 m/sec, the photorelay was moved close to the exit finishing mill stand (about 15 m from the shear). However, even with these conditions there was no time margin for the regulation of the length of the leading end with the aid of the delay of the time-delay relay TDR (fig. 4).

With this relatively poorly debugged drive it was decided to carry out tests to clarify the capabilities of the optimal system and to determine the deviations in the length of the cutoffs of the leading ends (accuracy of the system).

The quantity of the tests was limited, since the rolling on the finishing stands is performed simultaneously in two strips and the flying shears have two cutting systems and two pairs of blades with a common electric drive.

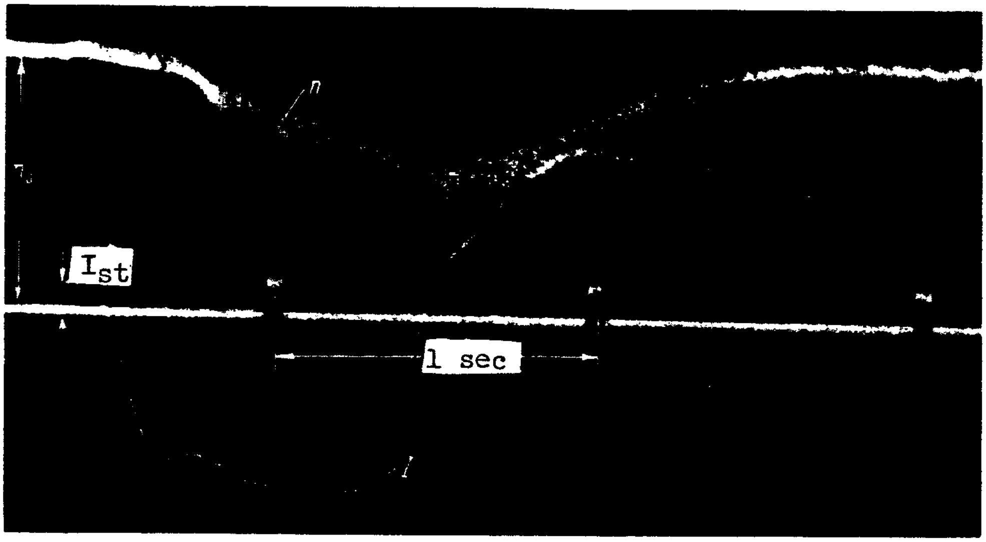

Figure 6. Oscillogram of transient process in optimal system.

In order to avoid breakdown during the time of measured cutoff of the strip in one filament with measurement of the mismatch for the other filament, the /35 testing of the optimal system was performed with rolling of the metal in only one filament, which reduces the productivity of the mill. Tests of the system for accuracy of the cutoff of the leading end were performed for two differing relationships of the velocity of the strip and the metal. With a fixed adjustment of the control device we obtained a mean scatter in the length of the leading end of ±120 mm. The maximal deviation did not exceed ±200 mm. In spite of the low accuracy of the measurement of the maximal mismatch (3 m), the results obtained satisfy the operational requirements.

Conclusions

The tests made on the optimal system for the control of the drive of flying shears showed that the system satisfies the posed requirements. The system provides adequate accuracy of measured cutoff of the discarded leading ends of the strips, which reduces the metal scrap. The accuracy of the system could be improved considerably by means of improving the static and dynamic characteristics of the drive. To do this it is necessary to increase the acceleration of the system in the transient process, improve the shape of the current curve and provide for strict maintenance of the speed during the measured cutoffs.

REFERENCES

1. Lerner, A. Ya. Design of High-Speed Automatic Control Systems with Limitation of the Values of the Coordinates of the Regulated System (Postroyeniye bystrodeystvuyushchikh sistem avtomaticheskogo regulirovaniya pri ogranichenii znacheniy koordinat reguliruyemogo ob"yekta). Izd-vo AN SSSR, Vol. II, 1954.

2. Chelyustkin, A. B. Application of Computer Technology for the Control of Metallurgical Plants (Primeneniye vychislitel'noy tekhniki dlya upravleniya metallurgicheskimi agregatami). Metallurgizdat, 1960.

3. Domanitskiy, S. M. Systems of Optimal Control of the Drive of Flying Shears for a Rolling Mill (Sistemy optimal'nogo upravleniya privodom letuchikh nozhnits prokatnogo stana). Elektrichestvo, No. 1, 1960.

N66-34831

ANALYZER FOR DISTRIBUTION CURVES OF RANDOM PROCESSES IN THE INFRALOW FREQUENCY REGION

I. N. Bocharov

Introduction

Complex electronic automatic systems used under production conditions /36 have received increasingly broad application recently. Under these conditions, random electrical interferences (noise) have a tremendous influence on the operation of these systems. In this connection there is increased interest both in the Soviet Union and abroad in the noise problem, particularly the study of the frequency and amplitude spectra of noise.

In addition, at the present time work is being done on the creation of self-adjustable systems working directly in conjunction with random process generators, which are used, for example, to generate random initial conditions. In working with such systems we must know the basic characteristics of the noise generators, including such characteristics as the distribution curves, the autocorrelation and cross correlation functions. There are analytical methods for the determination of all these relations, but they are all lengthy and tedious and lack adequate accuracy.

During operation with automatic systems in the presence of input noise it is frequently necessary by means of nonlinear transformations of the noise to give the noise amplitude distribution a particular nature. In this case, operational control of the transformation process is required, which clearly cannot be accomplished with the aid of the existing methods of analysis of the distribution curves.

The literature contains descriptions of instruments automating this process. Thus, reference 1 presents a description of an instrument intended for the automatic analysis of the amplitude distribution of radar noise. The instrument operates in the 0-1,000 cps range. The distribution curve of the noise applied to the instrument input is drawn out on a recorder. This instrument has low sensitivity and a considerable error (to 5 percent). However, the authors state that their method has major advantages over the existing methods of analysis.

Reference 2 describes another instrument for automatic analysis of distribution curves. The instrument operates over a very wide range of frequencies of the input signal (from 0-1,000 kcps) and has high sensitivity. However, a major drawback is its complexity and high cost. Thus, the fundamental part of the instrument is a special cathode ray tube which requires high voltage, and complex video amplifiers are necessary.

The instrument considered in the present report is intended for automatic recording of the distribution curves. The instrument is of simple design and has an error of less than 2 percent. /37

Operating Principle and Block Diagram

The instrument is based on principles known from the literature (refs. 1 and 4).

Every point of the distribution curve of an electric signal characterizes the probability that the signal amplitude lies within the interval ΔU, which is included between the levels U and U + ΔU (fig. 1).

The distribution curve itself is expressed in the form of the ratio of $\Sigma\Delta t$ (time that the signal is in the interval ΔU) to T (total time of observation). This ratio can be written in the form

$$\frac{\Sigma\Delta t}{T} = \int_{U}^{U+\Delta U} P[f(t)]\,df, \tag{1}$$

where P[f(t)] is the probability density of the input signal;
t is the time during which the signal is between U and U + ΔU;
T is the total time in the course of which the interval ΔU is at the level U (averaging time).

At the output of the instrument we obtain voltage E, which is proportional to the ratio $\Sigma\Delta t/T$; therefore from equality (1) we have

$$E = K\frac{\Sigma\Delta t}{T} = K\int_{U}^{U+\Delta U} P[f(t)]\,df. \tag{2}$$

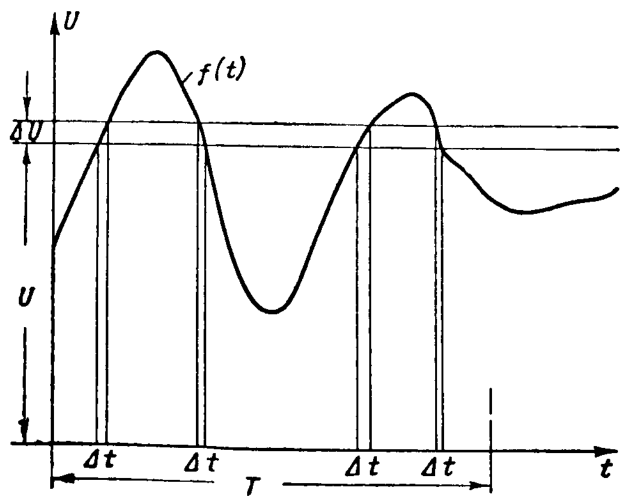

Figure 1

The structure of the block diagram of the instrument, i.e., the operations which the instrument must perform, can be judged from equation (2). In particular, the instrument must: /38

(1) slice out a strip of width ΔU at the level U relative to the zero level in the input signal;

(2) transform the portions of the input signal included in the bounds of the interval ΔU into a series of unipolar pulses of standard height and with length proportional to the time during which the input signal intersects the given interval;

(3) integrate these pulses;

(4) change the level from $-U_{a\ max}$ to $+U_{a\ max}$;

(5) assign and maintain the time of integration T, and on termination of this time return the instrument to the original position.

Figure 2a shows a block diagram and figure 2b a functional diagram of the instrument.

The "shift" block is intended for shifting the input signal relative to the zero level. It consists of a cathode follower with a capacitor connected to the input (fig. 2b). With arrival of the clock pulse, the outer end of the capacitor is connected by relay contacts to the output of the U_{sh} block and is charged to the instantaneous value of U; its other end, connected to the grid of the cathode follower, is at the same time connected to the ground. On opening of the relay the grid end of the capacitor is disconnected from the ground and its outer end is connected to the input of the instrument.

The capacitor acts like a battery, introducing a constant component equal to U into the input signal. In this case there will be a signal, shifted relative to zero by magnitude U, at the output of the cathode follower.

Since the interval $\Delta U = \pm 1/2\Delta U$ is specified relative to zero, giving the increment U_{sh} with each clock pulse we can "look at" all levels of the input signal from $-U_{a\ max}$ to $+U_{a\ max}$.

The ΔU block is intended for the formation of the interval ΔU. It consists of two limiting germanium diodes DGTs27 and a cathode follower at the output (fig. 2b).

The ΔU block slices a strip of width ΔU from the input signal. At the block output a series of trapezoidal pulses arises, whose leading and trailing edges are formed by the corresponding portions of the input signal crossing the interval; the amplitude of this series is equal to ΔU. These pulses are applied to the input of the "rectifier" block, which consists of a differential cascade with cathode input.

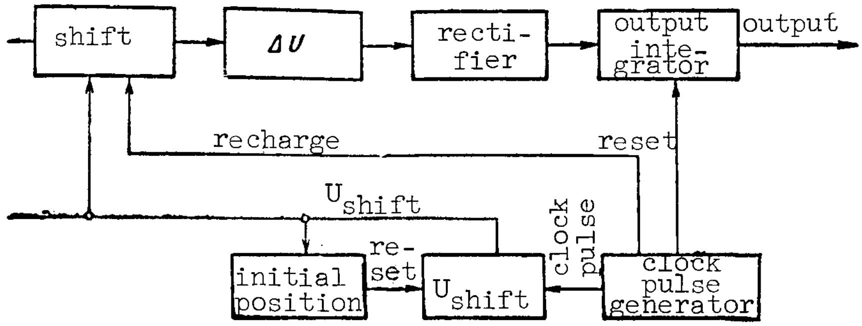

a

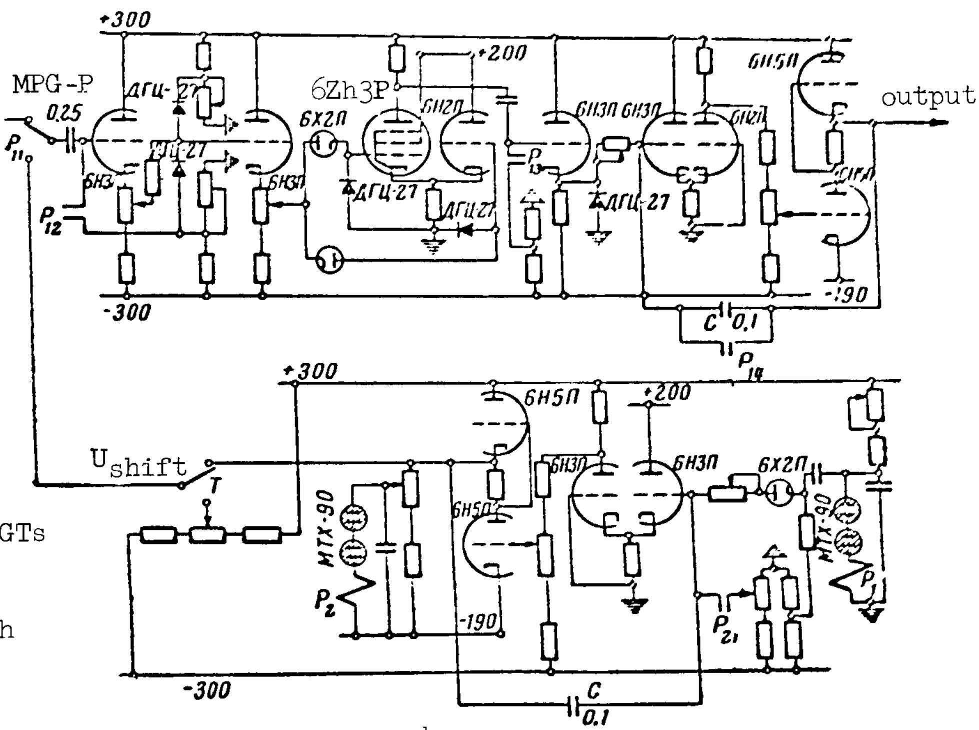

ΔГЦ = DGTs
Н = N
П = P
Х = Kh

b

Figure 2

Here the leading and trailing edges of the trapezoidal pulses are transformed into unipolar triangular pulses, equal in height and with areas proportional to the time of intersection of the interval by the corresponding portions of the input signal.

The obtained unipolar pulses are applied to the output integrator and are integrated. The time of integration (averaging) is specified by the generator of the clock pulses (CP Generator block) and is equal to the interval between

clock pulses. With arrival of the clock pulse the voltage E at the output of the integrator is reset to zero, and U simultaneously receives the increment ΔU_{sh} in the U_{sh} block.

Thus U varies stepwise in time. The duration of each step is equal to the interval between the clock pulses, i.e., the averaging time, in the course of which there takes place the determination of the probability, more precisely, of the quantity proportional to the probability that the signal is at the given level.

This quantity is precisely the voltage E obtained at the output of the integrator before the arrival of the following clock pulse.

If the analyzer output is applied to the vertical plates of an oscil- /40
loscope and as the horizontal scan we use U_{sh}, we obtain on the oscilloscope screen a series of vertical lines separated from one another by ΔU_{sh} and proportional in magnitude to the probability that the input signal is at the given level. The envelope of these lines is then the distribution curve.

With recording of the output signal on a single-coordinate recorder, U_{sh} must vary linearly, otherwise the shape of the distribution curve will be distorted.

Instrument Accuracy

The accuracy of the approximation of the distribution curve obtained on the analyzer to the theoretical curve depends on satisfaction of the requirements of the theory of probability, according to which the averaging time T must tend to infinity at the same time that the width of the interval ΔU tends to zero. However, the theory is applicable only to time-stationary processes, while in the majority of cases the processes studied are not completely stationary, and with increase of the averaging time the errors caused by the non-stationarity of the process increase. Moreover, with long averaging time the drifts of the amplifiers begin to have an effect.

These considerations impose limitations on duration T. In our experiments with the instrument the averaging time varied from 1-10 sec.

As for the interval ΔU, reduction of its width severely increases the demands on the frequency properties of the circuit elements. Actually, with the passage of a signal, a sinusoid for example, through the interval ΔU, a pulse arises at the output of the "rectifier" block (fig. 2) with a duration equal to the time of crossing of the interval by the input signal. It is easy to show that this time is inversely proportional to the amplitude and frequency of the input signal and directly proportional to the width of the interval.

Thus, other conditions being equal, the width ΔU is limited by the passband of the circuit elements to which this pulse is applied. In recording the

diagrams in our tests, ΔU was chosen equal to 3 V with a range of the input signal of 120-140 V.

Furthermore, the accuracy of operation of the instrument depends on the operation of the circuit elements. It follows from our statements that the primary requirement on the circuit elements is a wide passband (in practice /41 from zero to thousands of cps with a frequency of the input signal up to 1 kcps). In the instrument diagram we see that the primary elements which limit the passband are the "rectifier" block and the "output integrator" block. The remaining elements use cathode followers which have a wide passband.

The criterion of accuracy of operation of the instrument with differing frequencies of the input signal was taken to be the identity of the distribution curve of sinusoids with the same amplitudes and differing frequencies.

It is easy to show that the probability density of a sinusoidal signal does not depend on its frequency (other conditions being the same). In the diagrams shown in figure 3 we see that at frequencies to 100 cps the distribution curves are completely identical (fig. 3a and b), while at 1,000 cps (fig. 3c) the curve, retaining its basic shape, is raised twice as high above the

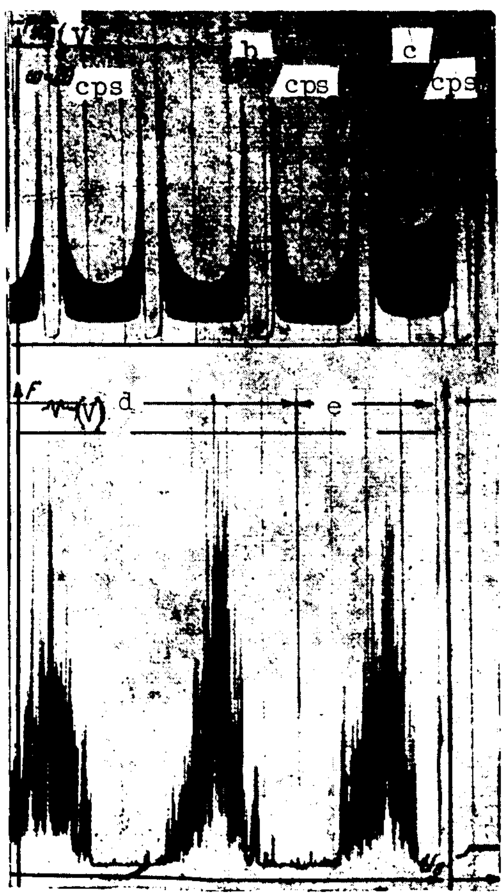

Figure 3

.zero level. This rise of the curve is caused by the broadening of the intermediate pulses while they retain the amplitudes resulting from the self-capacitance of the circuit elements (primarily the vacuum tube diodes). With further increase of the frequency of the input signal, there begins to be distortion of the shape of the curve, caused by the frequency characteristics of the circuit.

Figure 4 presents a graph of the distribution curves of a sinusoidal voltage as constructed from equation (2) and as recorded experimentally, and table 1 presents the corresponding values. The analytic distribution curve of the sinusoid according to equation (1) has the form

$$F_{\sin} = K \frac{1}{\sqrt{1-\frac{U^2}{A^2}}}, \tag{3}$$

where K is a constant coefficient; A is the amplitude value of the sinusoid.

Equation (3) is valid as $\Delta U \to 0$.

Figure 4 shows that the experimental and theoretical curves are in good agreement, with the error Δ not exceeding 2 percent of the theoretical value of $F_{\sin}$ at any point in the range of variation of the ratio U/A up to 0.8. /42

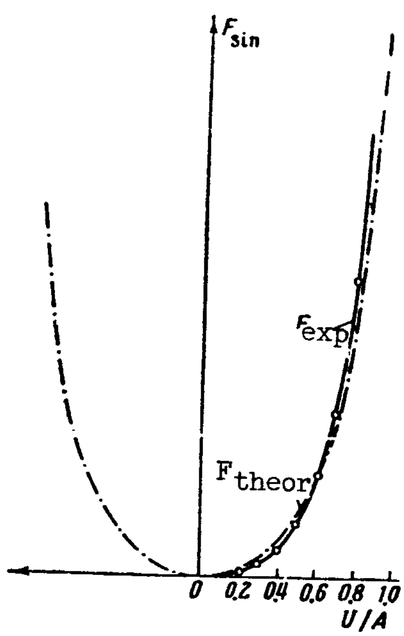

Figure 4

TABLE 1

Parameter	Value of parameter										
U/A	0	0.1	0.2	0.3	0.4	0.5	0.6	0.7	0.8	0.9	1
F_{theor}	1	1	1.02	1.05	1.09	1.16	1.25	1.4	1.67	2.3	∞
F_{exp}	1	1	1.01	1.03	1.07	1.14	1.27	1.42	1.78	2.72	-
Δ, %	-	0	1	1.9	1.84	1.73	1.6	1.43	10	18.3	-

Experiments

On the first prototype model of the instrument we verified the possibility of recording distribution curves of differing shapes and frequencies of the input signal in the range from 0-1,000 cps. Distribution curves were recorded of sinusoidal signals (fig. 3) and also of random processes.

For the recording of the distribution curves of the random processes we made use of the noise generator described in reference 3. This generator theoretically gives noise with a Gaussian distribution of amplitudes and a uniform frequency spectrum from zero to several cps. Figure 3e presents the distribution curves of the random processes obtained with this generator.

In addition to the distribution curves of the noise from the generator output, we also recorded the distribution curves of noise which had been subjected to various nonlinear transformations. In addition to the distribution curves of the sinusoidal signals mentioned above, we recorded the distribution curves of certain other regulator signals whose distribution curves are easily calculated, namely triangular and sawtooth curves with truncated lower vertices.

In all cases the obtained distribution curves correspond to the theoretical curves with adequate accuracy.

Conclusions

An instrument has been developed and tested for the recording of distribution curves of random signals. Tests of the instrument showed that it provides for rapid (1-5 min) recording of the distribution curves with a deviation from the theoretical curves not exceeding 2 percent. Verification of the accuracy was made using sinusoidal distribution curves.

The adequately high accuracy and the rapidity of obtaining the distribution curves in comparison with the analytical methods give us the possibility of operational control of the sources of the studied processes for obtaining distribution curves of a specified shape.

The performance of this instrument can be improved by better circuit elements.

REFERENCES

1. Zoll, D. J. Simple Plotter Analyzes Radar Noise Rapidly. Electronics, p. 162, 14 March 1958.
2. Zient, H. Probability Density Measurement with an Electrode Mounted in the Face of a Cathode-Ray Tube. Review of Scientific Instruments, Vol. 30, No. 2, p. 110, 1959.
3. Petrovskiy, A. M. Fluctuating Noise Generator for Infralow Frequencies (Generator fluktuatsionnykh shumov dlya infrazvukovykh chastot). Avtomatika i telemekhanika, Vol. 14, No. 4, 1953.
4. Fel'dbaum, A. A. Computers in Automatic Systems (Vychislitel'nyye ustroystva v avtomaticheskikh sistemakh). Fizmatgiz, 1959.

N66 34832

OPTIMAL CONTROL OF SYSTEMS

A. G. Butkovskiy

At the present time the development of automation has reached the level where the functions of the human operator controlling a system are increasingly performed by automatic control. The determination of the function of the control, and the specification of the fixed program are performed so that the system will operate optimally in some sense, for example, will yield the highest productivity, will have the highest efficiency, will produce a product with minimal cost of production, etc. /43

Along with the maximization or minimization of some parameter, the operator must also take care that certain constraints are observed; structural, technological and others. For example, in order to minimize the time for the heating of the charge in an open-hearth furnace it is necessary to supply the furnace with the greatest amount of fuel; however, raising the temperature above some definite limit leads to melting of the furnace lining and may put the furnace out of commission. Again, in the production of rectified spirits in a spirit column, an excessive abstraction of spirits will cause the spirit strength to fall below the specified value.

The human operator controlling a system is faced in the general case with the difficult problem of how to vary the control parameters and how to specify the regulator settings in order to maximize or minimize some process index, while a whole series of other parameters and indices must remain within certain set limits. Such control of a process requires considerable experience and a high level of skill on the part of the operator.

The modern science of control, or cybernetics, has already posed the problem of transferring the complex control functions to a controller which will control the system in the best (optimal) way under all operating conditions.

In order to control any system--a furnace or a rolling-mill stand, a chemical or nuclear reactor, an aircraft or an automobile, a ship or a rocket, we must study first of all the system itself, i.e., we must know what will happen to the output parameters of the system if we begin to vary the control parameters in a particular fashion.

Of course, it is also desirable to know the exact quantitative relationships between the inputs and the outputs of the system, to know the inequalities and the equations which describe the behavior of the system. A quite extensive class of controllable objects may be described by systems of ordinary

differential equations. The relationship between the k input control parameters $U_1, U_2, \ldots, U_k$ and the n output coordinates $x_1, x_2, \ldots, x_n$ is given /44 in the form of differential equations

$$\frac{dx_i}{dt} = f_i(x_1, \ldots, x_n, U_1, \ldots, U_k). \tag{1}$$

Knowledge of equations (1) permits the determination of the variation with time t of coordinates $x_1(t), \ldots, x_n(t)$, if the control is changed in accordance with some law.

The more complex the system, the more output coordinates it has, the more control parameters it has, the higher will be the order of the system of equations which describe this system. In practice we always strive to reduce the order of the system of equations, reducing it to a minimum, for example, by ignoring certain insignificant time constants. Even the severely simplified equations of the system give an adequate amount of information about the system to enable optimal control of the system.

In many cases the variable x_0 which must be optimalized (minimized or maximized) can be written in the form

$$x_0 = \int_{t_0}^{t_1} f_0(t, x_1(t), \ldots, x_n(t), U_1(t), \ldots, U_k(t))\,dt, \tag{2}$$

where f_0 is some known function of the coordinates and the controls of the system, where $x_1(t), \ldots, x_n(t), U_1(t), \ldots, U_k(t)$ are connected by equations (1).

Variational calculus, a branch of mathematics, gives us the differential equations (Euler equations) to which the controls $U_1, \ldots, U_k$ must be subjected in order to have the integral (2) maximal or minimal. Many practical problems are complicated by the fact that some or all variables cannot go beyond certain specified limits. This is explained by the natural constraints in the system (for example, when the handling capacity of a pipeline, speed of rotation of a motor, angle of deflection of an aircraft control surface, deflection of a motor vehicle or ship control, etc. are limited).

Thus, we have the series of constraints

$$|U_1(t)| \leqslant M_1, \ldots, |U_k(t)| \leqslant M_k,\ t_0 \leqslant t \leqslant t_1. \tag{3}$$

In the general case the control vector $U = (U_1, \ldots, U_k)$ must not go beyond the limits of some closed region Ω.

The variational problem described above with constraints (3) is not resolved in classical variational calculus. In the present formulation the necessary condition for optimality is given by the Pontryagin maximum principle (ref. 1), which was discovered relatively recently. We note that the Pontryagin maximal principle can also be used when the functions $U_1, \ldots, U_k$ are not bounded. If, however, the functions f are continuous and twice differentiable with respect to $U_1, \ldots, U_k$, the maximum principle is equivalent to the Euler equation. The essence of this principle amounts to the following.

Knowing the original system of equations (1) and the integral (2), we compose the auxiliary system of (n + 1)th order relative to the new functions $\psi_0(t), \psi_1(t), \ldots, \psi_n(t)$

$$\frac{d\psi_i}{dt} = -\sum_{\alpha=0}^{n} \frac{\partial f_\alpha}{\partial x_i} \psi_\alpha, \quad i=0,1,\ldots, n. \tag{4}$$

We further compose the function

$$H = H(t, x_1, \ldots, x_n, \psi_0, \psi_1, \ldots, \psi_n, U_1, \ldots, U_k) = \sum_{\alpha=0}^{n} \psi_\alpha f_\alpha. \tag{5}$$

It has been proved that the optimal control parameters $U_1, \ldots, U_k$ /45 must be selected so that at every fixed moment of time t, $t_0 \leq t \leq t_1$ with fixed values of $x_1, \ldots, x_n, \psi, \ldots, \psi_n$, function H will reach its maximum when the vector $U = (U_1, \ldots, U_k)$ varies in the closed region Ω.

Thus the maximum principle gives the possibility of finding the optimal control as a function of $x_1, \ldots, x_n, \psi_0, \ldots, \psi_n, t$

$$U = U(x_1, \ldots, x_n, \psi_0, \ldots, \psi_n, t). \tag{6}$$

Substituting (6) into (4) and (1) we obtain the equation for all the optimal trajectories $x_1, \ldots, x_n$. From this collection we must choose only that trajectory which passes through the given initial and final points. For example, while conserving the fuel in an aircraft, we must still get from one point to

another; a weapon must be pointed rapidly, but also must be pointed accurately at the target.

The problem of optimal control has been completely solved in reference 2, for a wide class of linear systems with real characteristic roots and a single control action U, $|U| \leq M$. This reference also presents the solution of the problem of the synthesis of the optimal system of the given class. By the synthesis of the optimal system we mean the finding of the control $U = (U_1, \ldots, U_k)$ as a function of the vector $x = (x_1, \ldots, x_k)$, i.e.,

$$U = U(x). \tag{7}$$

This function is found by the exclusion of the vector $\psi = (\psi_0, \psi, \ldots, \psi_n)$ from equations (1), (4) and (6).

The function $U(x) = 0$ forms in the system phase space a switching surface, with penetration of which by the representative point of the system the control vector U changes its sense.

Thus, knowing the function $U = U(x)$ we can construct a computer which, receiving at every instant of time $t(t_0 \leq t \leq t_1)$ information on the state of the system, i.e., measuring its coordinates $x_1, \ldots, x_n$ generates the control $U_1, \ldots, U_k$.

Reference 3 describes the construction of an optimal servosystem consisting of a sequential connection of two motors. In a power servosystem a hydraulic servomotor is frequently selected as the second actuator. Making use of the fact that the time constant of a hydraulic motor is tens of times less than the time constant of an electric motor, we can neglect the time constant of the hydraulic motor.

Thus, the order of the equation is reduced to third

$$x_1 = \frac{K_1}{p} x_2, \; x_2 = \frac{K_2}{p} x_3, \; x_3 = \frac{K_3}{Tp+1} U_1, \; |U_1| \leqslant M.$$

Making use of the theory presented in reference 2, the author determined the switching function $U = U(x) = 0$, which was realized on an electronic computer. Tests of this optimal system showed that the time for the transient process was cut in half, compared to the linear control system. The optimal system has little and sometimes no overcontrol.

Another practical application of the theory of optimal systems is given /46
in reference 4. It was required to construct an optimal system for the control

of the electric drive for the flying shears of a rolling mill. The transfer function of the drive is well approximated by a function of the form

$K(p) = e^{-\tau p}\frac{K}{p^2}$. The input action U is bounded in magnitude $|U| \leq M$. Systems with delay are not described by equations (1). However, even in this case we can create a simple control which will minimize the time for the transient process.

The theory of the optimal systems also considers the problems with the condition that the system coordinates $x_1, \ldots, x_n$ are not bounded. Reference 5 presents constructions of optimal processes for linear systems of 2nd, 3rd and 4th order, with account taken of the boundaries imposed on the system coordinates. However, the solution of this problem is still incomplete.

The example of the practical application of the optimal control principle described in reference 6 is interesting applying it to a periodic-operation chemical reactor. This reactor is a part of an aggregate for the production of margarine and other food products. Pure hydrogen acts on the initial product in an autoclave reactor for the purpose of improving the taste properties, improving the stability and raising the melting point. In the presence of a catalyzer with a definite temperature and pressure, the hydrogen reacts with the components of the initial product X and Y with concentrations x and y, respectively, and transforms them into the different constituents $\overline{Y}$ and Z with concentrations $\overline{y}$ and z, respectively, according to equations

$$\left.\begin{aligned} &X + H_2 = Y; \\ &X + H_2 = \overline{Y}; \\ &Y + H_2 = Z; \\ &\overline{Y} + H_2 = Z; \\ &Y = \overline{Y}; \\ &\overline{Y} = Y \end{aligned}\right\} \qquad (8)$$

with the reaction constants $K_1, K_2, \ldots, K_6$, respectively. The kinetics of this process is described, taking into account (8), by the system of ordinary differential equations

$$\left.\begin{aligned} &\frac{dx}{dt} = -(K_1 + K_2)x; \\ &\frac{dy}{dt} = K_1 x - (K_3 + K_5)y + K_4\overline{y}; \\ &\frac{d\overline{y}}{dt} = K_2 x - (K_4 + K_6)\overline{y} + K_5 y; \\ &x + y + z + \overline{y} = 1. \end{aligned}\right\} \qquad (9)$$

In the general case the coefficients K_i, $i = 1, 2, \ldots, 6$ have the form

$$K_i = a_i p^{n_i} e^{-b_i/T},$$

where p is the absolute pressure in the reactor, T is the absolute temperature in the reactor, a_i, b_i, n_i are constants which depend on the catalytic activity, the degree of mixing, etc.

It is obvious that we can influence the course of the reaction, other conditions being constant, by pressure p and temperature T. For reasons of simplicity we leave the temperature constant and control only the pressure. The coefficients in equations (9) then take the form /47

$$K_i = A_i p^{n_i}$$

where A_i, n_i are constants.

Another simplification is the condition that the concentration x can be neglected, therefore (9) takes the form

$$\left.\begin{aligned} \frac{dy}{dt} &= -(K_3 + K_5)\, y + K_4 \bar{y}; \\ \frac{d\bar{y}}{dt} &= -(K_4 + K_6)\, \bar{y} + K_5 y. \end{aligned}\right\} \tag{10}$$

The following problem was posed: find that relation of the variation of the pressure in the reactor P with time t, $p = p(t)$, such that the initial concentrations $(y_0, \bar{y}_0)$ are transformed into the specified final concentrations $(y_1, \bar{y}_1)$ after the shortest time $t = t_1 - t_0$.

The Euler equations for this problem, nonlinear equations of the second order, which gave the set of all optimal controls $p = p(t)$, were solved on a model with fast time scale. It was necessary to repeat the solution frequently in order to select the initial value of the pressure $p_0 = p(t_0)$, for which the trajectory of the process $y = y(t)$, $\bar{y} = \bar{y}(t)$ passed through the points $(y_0, \bar{y}_0)$ and $(y_1, \bar{y}_1)$. The resulting initial value $p_0 = p(t_0)$ was transmitted to the pressure control which maintained this value.

Since the mathematical relations (10) approximate the process well only for a small time interval, every five minutes with the aid of a special physical analyzer with a computer, the new initial coordinates $(y_0, \bar{y}_0)$ are introduced, and the initial value of the pressure p_0 is found again. In each interval between computations the value of the pressure is maintained constant, equal to

the initial value on this interval. The use of this method of control shortened the process time by 23 percent.

Reference 7 considers the problem of the control of a chemical reactor for the purpose of the best approximation of its operation to the optimal regime. To the kinetic equations are added the heat transfer equations which characterize the thermal regime of the aggregate. The resulting nonlinear equations were linearized in the vicinity of the steady-state optimal regime. The problem of optimization was resolved by the method of dynamic programing on a digital computer.

Let us turn to the optimization methods based on the principle of the search for the optimal regime of operation. Actually, if the dependencies between the control and output coordinates of the system are not known, we cannot a priori determine the optimal trajectories with which the optimum of any process index is achieved. To start, let us assume that there is one control parameter U_1 and one output coordinate x_1, which we wish to maintain at the maximum, and we do not know the static relation $x_1 = f(U_1)$, but we do know that the curve $x_1 = f(U_1)$ has a single maximum.

Let us assume that at the initial moment of time we are at the point U_1, $x_1 = f(U_1)$ and that $x_1 = f(U_1) \neq \max$. We give an increment to U_i $(U_1 + \Delta U_1)$ then we obtain the increment Δx_1. If ΔU_1 is of the same sign as Δx_1, we must continue to give an increment to U_1 of the same sign as ΔU_1, otherwise we must reverse the sign of the increment of U_1. After a series of steps we again /48
obtain a change of the sign of the increment Δx_1. This means that x_{opt} has been passed, the transient process is terminated and the regime of "hunting" about the maximum begins. The hunting is necessary in order to determine immediately the displacement of the maximum of the function $x_1 = f(U_1)$ under the influence of distrubing forces.

This search method is termed stepping. There are other methods for the search for the optimum of a function of a single variable: the method of peak-holding, the method of introduction of special test signals. These methods are described in reference 8. Instruments which automatically search out the optimal regime are termed automatic optimizers. Optimizers with a single input variable are finding ever-increasing application. They are already used today to maintain the optimal fuel-air ratio in boilers and furnaces, for economy of fuel consumption in internal combustion and jet engines, to maintain the optimal regime of operation of radio stations, optimal speed of rotation of turbine drills and for other purposes.

Here the optimizer finds a natural application, since it is impossible or very difficult to compute ahead of time the optimal value of the input parameter for all possible varying operational conditions.

In connection with the introduction of optimizers for the control of systems, there arise new problems of analysis of their operation. We are required to calculate the parameters and the adjustment of the optimizer so that it will operate stably, will search out the optimum in the shortest time and will maintain it most precisely.

It is obvious that these calculations can be made only after knowing adequately the characteristics of the system itself. The difficulty of the analysis is that the problem is essentially nonlinear. With the introduction of optimizers in practice, it was found that the operation of the optimizer is significantly affected by the noise which is almost always present in the system at both input and output of the system. The noise at the input of the system must be detected, while the noise at the output of the system and the input of the optimizer must be filtered out. In this case it is necessary to repeat the test steps in order to be certain of the correctness of the result obtained. However, the test movements cannot be continued too long, since during this time the optimum may shift to a different position. This leads to the problem of finding the optimal filter for the optimizer.

The presence of noise in the system prolongs the process of search for the extremum, increases the hunting. Therefore, special attention in references 9 and 10 was devoted to the creation of noise-resistant optimizers.

The application of optimizers, therefore, requires a profound study not only of the dynamic and static, but also the statistical properties.

In many cases the controlled system has several control parameters $U = (U_1, \ldots, U_k) \in \Omega$, where Ω is a closed region. It is required that a transition be made from some initial state $U(t_0) = U_0 \in \Omega$ into another state $U_{opt} \in \Omega$, in order that some criterion F take an extremal value. For simplicity let us assume that F(U) has a single optimum, for example, a maximum. There are several algorithms for the search for the value $U = U_{opt}$ for which F is optimal.

If we follow the gradient method, by giving in turn the increments ΔU_i to each U_i with the remaining parameters fixed, we find

$$\frac{\partial F}{\partial U_i} \cong \frac{\Delta F}{\Delta U_i}, \; i = 1, \; 2, \ldots, \; k,$$

i.e., the coordinates of the vector of the gradient of the function F.

After this, each control parameter U_i receives an increment proportional to $\Delta F/\Delta U_i$ with the same coefficient of proportionality for all $i = 1, 2, \ldots, k$. Furthermore, at the new point we again determine the gradient of F and again take a step in the direction of this vector, and so on to the point $U = U_{opt}$. /49.

There is also the method of steepest descent, proposed by Kantorovich. Following this method, we must determine grad F, and move in this direction until F ceases to increase. At the point where F ceases to increase, we again determine grad F and continue the motion along this new direction again until F ceases to increase and so on, until reaching $U = U_{opt}$. Generally, the Kantorovich method leads to finding the maximum more quickly than the gradient method.

Reference 11 presents a comparison of these two methods. It was found that far from the optimum we should recommend the method of steepest descent which leads to the objective more quickly, while near the optimum we should shift to search by the gradient method, which quite accurately maintains the already found optimum. These results were verified on an automatic optimizer, which can search out the optimum of a function of 12 variables.

In the method of sequential variation of the input parameters, first one parameter is varied, with the others fixed, until a partial optimum is reached; after this, the following parameter is varied, with the others fixed, until reaching a partial optimum and so on, until reaching the total optimum.

There is also the scanning method, in which the entire region Ω of admissible values is "probed" until the optimum of F is found. This method can be useful when the function F has several optimums and is not a smooth function.

In the design and development of multichannel optimizers there are also the problems of finding an algorithm which yields a stable, rapid and precise search in the presence of noise at the input and output of the system, and with the constraints imposed on the output coordinates of the system.

These complex problems still do not have general methods of solution; they are far more difficult than the corresponding problems associated with one-dimensional search.

The range of application of the multichannel optimizers is also being expanded. Studies are now being made on the application of the multichannel optimizers for the control of distillation columns, chemical reactors and for the design of electrical machinery.

Multichannel optimizers for 10 or more variables can find wide application as automata for the solution of variational problems, for example, using the Euler method. The essence of the method is that the desired function or functions $U_1(t), \ldots, U_k(t)$ with $t_0 \leq t \leq t_1$, which must give the optimum of some

functional, can be piecewise linearly approximated on n intervals. Thus, each function is defined by a set of n + 1 numbers and, consequently, the functional is transformed to a function of (n + 1)k numerical parameters. Finding the optimum of this functional can now be performed on an automatic optimizer with (n + 1)k channels (ref. 12).

At the present time development work is starting on control systems which combine in themselves systems for compensation of disturbances and for automatic search. The construction of the compensation system presupposes the knowledge of the equations describing the behavior of the controlled system. Knowing the magnitudes of the disturbances, measuring them, we can use a model of the system to determine that variation of the control action which will compensate for the disturbance. Such regulation would give a zero error. However, the matter is complicated by the fact that the exact equations of the system, from which we construct the model, are not known. /50

Even if the structural diagram of the model quite faithfully represents the system, its parameters (time constants, gains, delay times, etc.) may not correspond to the parameters of the system. Moreover, the parameters of the system can change in the process of operation in the course of time. Here is where the automatic search systems--automatic optimizers--come to our aid. The input of the optimizer is the magnitude of some variable which characterizes the error of undercompensation x(t), due to the noncorrespondence of the parameters of the system to the parameters of the model.

As the magnitude of the variable we take one of the following expressions

$$\max_{t_0<t<t_1}|x(t)|;\ \int_{t_0}^{t_1}|x(t)|\,dt;\ \int_{t_0}^{t_1}x^2(t)\,dt \text{ etc.}$$

In the process of its operation the optimizer changes the model parameters to minimize the specified variable. Reference 13 gives a description of such a system for the control of the drives of a three-stand cold-rolling mill. The requirement is to obtain strip with minimal thickness variation at the stand output. The thickness variation is characterized by the function x(t) = S - s(t), where S is the specified strip thickness and s(t) is the actual value of the thickness at the moment t.

The disturbance is the thickness variation of the strip arriving at the input to the stand. This thickness variation must be compensated by variation of the tension of the strip between the second and third rollers. Variation of the tension is achieved by means of variation of the ratio of the angular velocities of rotation of the rollers of the second and third stands.

The compensating computer has the transfer function

$$K(p)=\frac{e^{-p\tau}}{Tp+1}.$$

As the optimality variable we take $\int_{t_0}^{t_1} x^2(t)\,dt$, whose magnitude is minimized by the automatic optimizer by variation of the parameters τ and T.

Reference 12 presents the general block diagram of such a self-adjusting system. The controlling machine must consist of three blocks: the direct control block, constructed on the basis of some initial knowledge of the system characteristics; the block for the determination of the system dynamics either from the normal operation of the system or with the aid of special test signals; these test signals are supplied by a third block. As data is accumulated on the statics and dynamics of the system, the second block acts on the controlling block. The entire process is realized by a set of defined cycles of programs for a digital computer.

At the present level of development of automation equipment, all these control principles can be successfully applied for the control of concrete systems.

REFERENCES

1. Boltnyanskiy, V. G. The Maximum Principle in the Theory of Optimal Processes (Printsip maksimuma v teorii optimal'nykh protsessov). Dokl. AN SSSR, matematika, Vol. 119, No. 6, 1958. /51

2. Fel'dbaum, A. A. Synthesis of Optimal Systems for Automatic Regulation (K voprosu o sinteze optimal'nykh sistem avtomaticheskogo regulirovaniya). Transactions of the Second All-Union Conference on the Theory of Automatic Regulation, Izd-vo AN SSSR, Vol. II, 1955.

3. Sung Chien. Synthesis of the Control Portion of an Optimal Servosystem (Sintez upravlyayushchey chasti optimal'noy sledyashchey sistemy). Transactions of a Conference on Discrete Automatic Control Systems, Izd-vo AN SSSR, 1958.

4. Butkovskiy, A. G. and Domanitskiy, S. M. Synthesis of the Control Portion of Optimal Systems for Certain Systems with Delay (O sinteze upravlyayushchey chasti optimal'nykh sistem dlya nekotorykh ob"yektov s zapazdyvaniyem). Conf. Disc. Autom. Cont. Syst., Izd-vo AN SSSR, 1958.

5. Lerner, A. Ya. Design of High-Speed Automatic Regulation Systems with Limitation of the Values of the Coordinates of the Regulated System (Postroyeniye bystrodeystvuyushchikh sistem avtomaticheskogo regulirovaniya pri ogranichenii znacheniy koordinat reguliruyemogo ob"yekta). Tr. Sec. All-Union Conf. Theory Autom. Reg., Izd-vo AN SSSR, Vol. II, 1955.

6. Lefkowitz and Eckman. Application and Analysis of a Computer. ASME Publication, N 58-A-281, 1957.

7. Kalman, R. The Optimal Control of Chemical and Petroleum Process. Joint Symposium: Instrument and Computation in Process Development and Plant Design. London, May, 1959.

8. Ch'ien-Hsüeh-sên. Engineering Cybernetics, I. L., 1956.

9. Fel'dbaum, A. A. Effect of Random Factors on the Automatic Search Process (O vliyanii sluchaynykh faktorov na protsess avtomaticheskogo poiska). Tr. Conf. Disc. Autom. Cont. Syst., Izd-vo AN SSSR, 1958.

10. Norkin, K. B. and Torgashin, A. V. Single-Channel Automatic Optimizers (Odnokanal'nyye avtomaticheskiye optimizatory). Bulletins of the Central Information Institute for Ferrous Metallurgy (TsIIN), Metallurgizdat, No. 5, 361, 1959.

11. Stakhovskiy, R. I. Comparison of Search Methods for an Automatic Optimizer (O sravnenii nekotorykh metodov poiska dlya avtomaticheskogo optimizatora). Tr. Conf. Disc. Autom. Cont. Syst., Izd-vo AN SSSR, 1958.

12. Fel'dbaum, A. A. Application of Computers in Automatic Systems (O primenenii vychislitel'nykh ustroystv v avtomaticheskikh sistemakh). Avtomatika i telemekhanika, Vol. 17, No. 11, 1956.

13. Doganovskiy, V. A. Electronic Simulation of a Continuous Rolling Mill (Elektronnoye modelirovaniye nepreryvnogo prokatnogo stana). Byull. TsIIN, ChM. Metallurgizdat, No. 5, 361, 1959.

N66 34833

AUTOMATIC OPTIMIZER FOR THE CONTROL OF CHEMICAL PRODUCTION PROCESSES

B. G. Volik

1. Introduction

The optimization of production processes, i.e., that control which maintains as constant the extremum of some process index (cost, quantity or quality of finished product, etc.), may be achieved in two ways: directly on the system being controlled or on a model of the system with subsequent transfer of the values of the controlling quantities to the real system. /52

The optimizer described is intended for the search for the extremum of the quantity φ being optimized directly on the system by means of action on the two control quantities x_1, x_2, with the presence of the two boundaries $H_1 (x_1, x_2)$ and $H_2 (x_1, x_2)$.

Figure 1 shows the lines of equal values of φ and H_1, H_2 in the plane of the control quantities x_1, x_2.

In the design of the optimizer, experimental and theoretical studies were made of the characteristics of the most common chemical production processes (distillation processes and certain catalytic processes), which are of importance for the construction of the optimizer scheme. These characteristics are the following.

1. As a rule the extremum of $\varphi (x_1, x_2)$ for chemical production facilities does not have a sharply expressed nature. This is explained by the fact that in the designing of the processes all parameters are selected so as to provide the highest economic indices. The necessity for optimization in such cases can be due to the deviations from the established regime caused by some disturbance, for example, by the variation of the composition of the raw material, by change of the properties of the aggregates (deposition of some substances on the walls of the apparatus, variation of the catalyzer properties, etc.).

The deviations of the composition of the raw material basically cannot reach high values, if the production is sufficiently highly automated. The effect on the optimal regime of the variation of the properties of the aggregates cannot be accounted for by the usual regulation systems. The elimination

of even slight deviations from the optimal regime can have a major economic effect.

2. The limits of variation of the control quantities x_1, x_2 with the search for the extremum of φ are bounded by the process parameters H_1 (x_1, x_2) and H_2 (x_1, x_2). This can be, for example, the quality of the finished product, the temperature at some point of the process, pressure, flow rate, etc.

3. Long duration of the transient processes φ (t) with respect to the control channels x_1 and x_2 (can reach several tens of minutes). /53

4. Extended stay in the "forbidden" zone (hatched in figure 1) is not permissible, since this may be associated with irreversible loss of valuable products, with deterioration of the quality, with reduction of equipment safety, etc.

5. We impose low-frequency noise, (1-10) 10^{-3} cps, on the measured quantities, which is due to the nature of the process and the operation of the customary regulation systems.

6. In the automation of chemical production primary use is made of pneumatic regulators and instruments.

Given these characteristics of the systems of chemical production, we can establish the following requirements for the optimizer.

(a) High accuracy of maintenance of the extremum. This requirement is associated with the frequency of the disturbances which displace the point of extremum, by the inertia of the system and by the presence of noise. The accuracy is higher, the longer the average duration of the period of the disturbance which displaces the extremum with respect to the duration of the transient processes φ (t) in the channels x_1 and x_2, and the stronger the suppression of the noise.

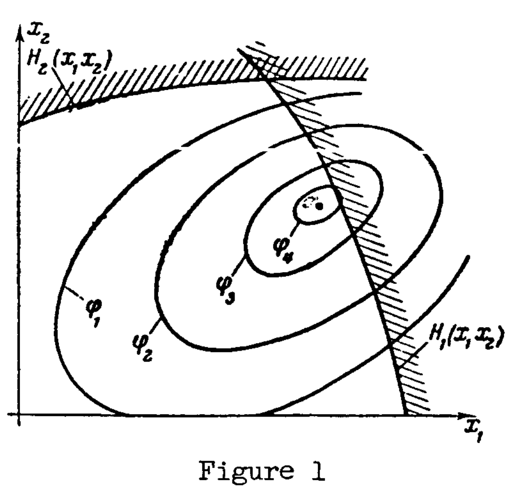

Figure 1

(b) The minimal staytime in the "forbidden" zone.

(c) The possibility of wide variation of the program and the output data of the optimizer. This is dictated by the presence of a large number of objects with differing parameters.

2. Structural Diagram of Optimizer

Selection of Search Method. For inertialess systems it has been established (ref. 1) that the best accuracy of tracking of the extremum is provided by the gradient method. However, comparison with the method of sequential stepping search (Gauss-Seidel) for systems with high inertia in the case of two control channels shows that it will not retain its advantage. The influence of the noise, which cannot be completely suppressed, and the long intervals of time between test steps in x_1 and x_2 can lead to a considerable error in the computation of grad φ, which determines the direction and the magnitude of the working steps in x_1 and x_2 in the direction of the extremum of φ. Another circumstance which limits the application of the gradient method is the impossibility of escape from the "forbidden" zone along the gradient of H, since an inadmissibly long time interval is required for the test steps for the computation of grad H.

For our optimizer we have used the method of sequential stepping search with a constant step (ref. 1).

Structural Diagram of Optimizer. In essence the optimizer performs the function of an operator which controls the process and operates on the sensors of the regulators x_1 and x_2, with the objective of achieving the extremum of φ. The presence of the usual regulation systems is dictated by the necessity for precisely fixing the achieved values of x_1 and x_2 and to smooth the local disturbances in x_1 and x_2. The optimizer circuit is built with electrical elements. This does not cause major difficulties in the application of the optimizer, since it can be installed in an explosion-proof housing. /54

Figure 2 shows the structural diagram of an automatic optimization system which includes the following devices.

(1) The controlled object (O), by which we understand the object itself and also the measuring instruments p_1, p_2, ..., p_n, H_1, H_2 and the usual systems for the regulation of the individual process parameters.

(2) The pneumatic-electric (PE) and the electric-pneumatic (EP) transformers, which are required for the connection of the optimizer with the pneumatic measuring and regulating apparatus.

(3) The computer (C), which determines the quantity being optimized φ, which must be expressed in the form of a dc voltage (0-100 V).

If the quantity being optimized (for example, the yield of the finished product) is measured directly on the object, the computer is the transformer of the ac voltage U from the output of the PE into the dc voltage φ

$$\varphi = kU.$$

For the case when the quantity being optimized is the ratio of the consumptions of two products, it is convenient to make use of an electromechanical divider, which does not require preliminary transformation of the ac voltage into dc.

(4) The automatic optimizer. The elements of the optimizer have the following purposes:

(a) the averaging device (AD) smooths the low-frequency noise;

(b) the logic device (LD) (ref. 2) determines the direction of the movement of the executive devices x_1 and x_2 during search for the extremum; /55

(c) the executive device (ED) acts on the sensors of the regulators for the control quantities x_1 and x_2 on command from the control block;

(d) the device for switching of the control channels (SCC). As has already been noted, the search is accomplished alternately in the channels x_1 and x_2; therefore it is necessary to have an independent device for the performance of this operation.

(e) the control unit (CU) which determines the operational regime of the optimizer both in the search process and with violation of the constraints.

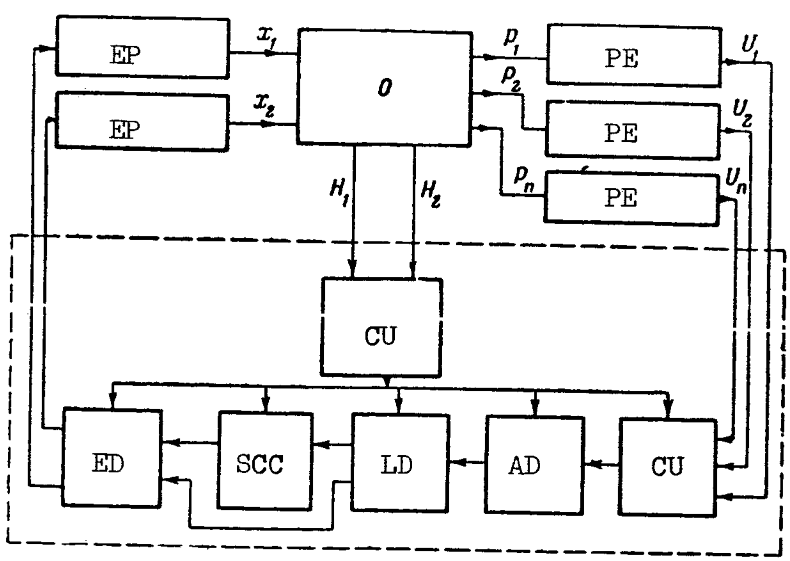

Figure 2

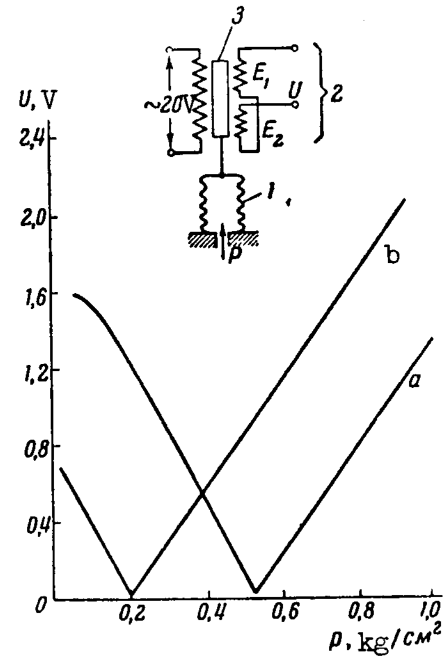

Figure 3

3. The Pneumoelectric Transformers

At the present time our industry is producing pneumoelectric transformers of the PPE-6 type, which are intended for telemetric transmission of signals.

The transformer (fig. 3) consists of the bellows 1 and the inductive system 2 with the moving plunger 3. The secondary windings of the inductive system are connected in opposition so that the output voltage $U = E_1 - E_2$. The displacement of the bellows is transmitted through a system of levers to the plunger. With a pressure of 0.627 kg/cm^2 on the converter the phase is changed by 180° (fig. 3, curve a). This shift is eliminated by shifting of the initial position of the plunger so that with an initial pressure of 0.2 kg/cm^2 $U \cong 0$. Consequently, with a change of the pressure from 0.2 to 1 kg/cm^2 we can obtain a voltage U from 0-2 V with a constant phase (fig. 3, curve b).

The primary requirement on the converter is linearity of the characteristic $U = f(p)$. Experimental tests have shown that the deviation of the characteristic from a straight line amounts to no more than 0.3 percent of the converter scale (2 V), which can be considered satisfactory in the present case.

4. Averaging Device

The input quantities p_1, p_2, ..., p_n, in addition to the useful signals, also contain low-frequency noise, which in the final analysis enters into the quantity φ being optimized. The quantity φ cannot be applied in this form directly to the input of the logic device, since the probability of false search would be too great. Thus we have the problem of suppression of the noise, which in the general case can vary in frequency, and which excludes the possibility of the use of a synchronous filter. The use of an aperiodic element as a filter is also inadvisable, since excessive time is required for the averaging, and this retards the search process.

The most acceptable unit is the integrator with time of integration t_{in}, which is a multiple of the average value of the period of the noise T_{av}. /56

$$t_{in} = kT_{av}, \; k = 1, 2, \ldots, n.$$

It is evident that the larger t_{in}, the better the noise suppression will be, but this leads to slowing down of the search. It is advisable to establish $t_{in} = (2\text{-}3)\, T_{av}$.

For this purpose we select an electronic integrator (fig. 4) in the form of a dc amplifier[1] with parametric compensation for the zero drift (fig. 4).

$$U_{in} = \frac{1}{R_u C_u} \int_0^{t_{in}} \varphi \, dt.$$

To minimize the parasitic leakage reducing the accuracy of integration, we make use of the polystyrene condenser $C_u = 1$ μF. From the given values $U_{in\ max} = 100$ V, $\varphi_{max} = 100$ V and $C_u = 1$ μF, it is not difficult to determine R_u, after first selecting the time of integration. Operational experience has shown that the electronic integrator operates reliably with $t_{in} \leq 20$ min. Here the accuracy of integration lies in the range of 1 percent of the scale (100 V).

[1] Developed by L. N. Fitsner, A. V. Torgashin and K. B. Norkin.

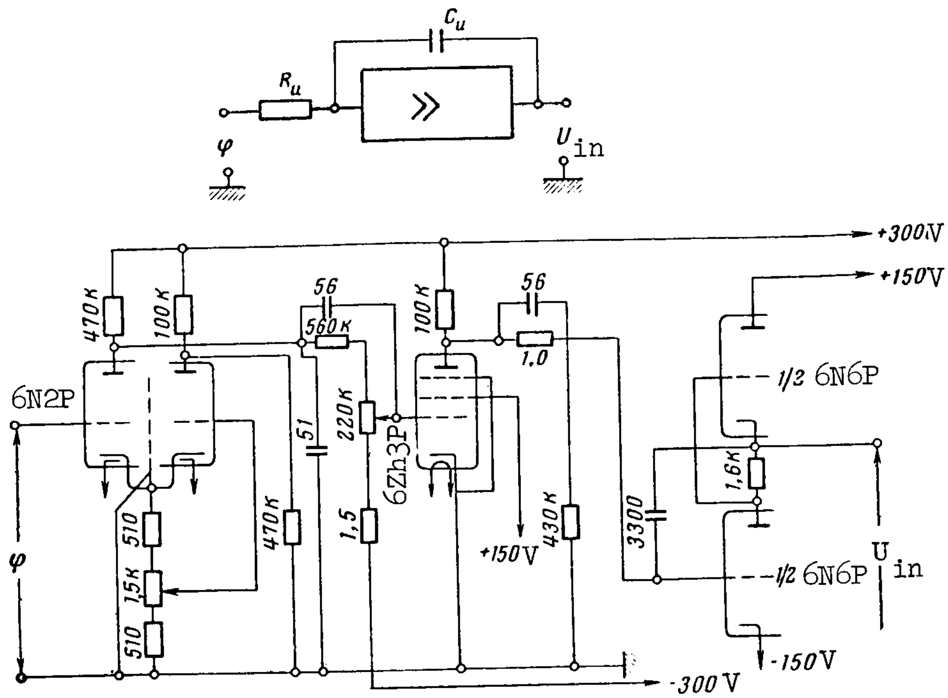

Figure 4

5. Logic Device /58

The logic device (ref. 2) realizes the stepping search principle. Its function includes storage of the quantity being optimized, comparison of it with the preceding value and determination of the direction of movement of the executive devices as a function of the result of the comparison.

The logic device (fig. 5a) consists of the memory capacitor C_3 (polystyrene condenser), the single-transistor P2b amplifier with relay output P_{01} (relay PR-4) and the trigger P_{02}, P_{03} with two stable states. The voltage U_{in} is applied to the input. The polarity of the voltage U_{in} in figure 5 corresponds to search for the minimum of φ. When we apply to the input the voltage U_{in_2}, which is less than the preceding U_{in_1}, the amplifier is saturated and the relay P_{01} is not triggered. However, when $U_{in_2} > U_{in_1}$ the relay P_{01} is operated, the trigger P_{02}, P_{03} is thrown, and the direction of movement of the executive device is established, corresponding to the search for a minimum.

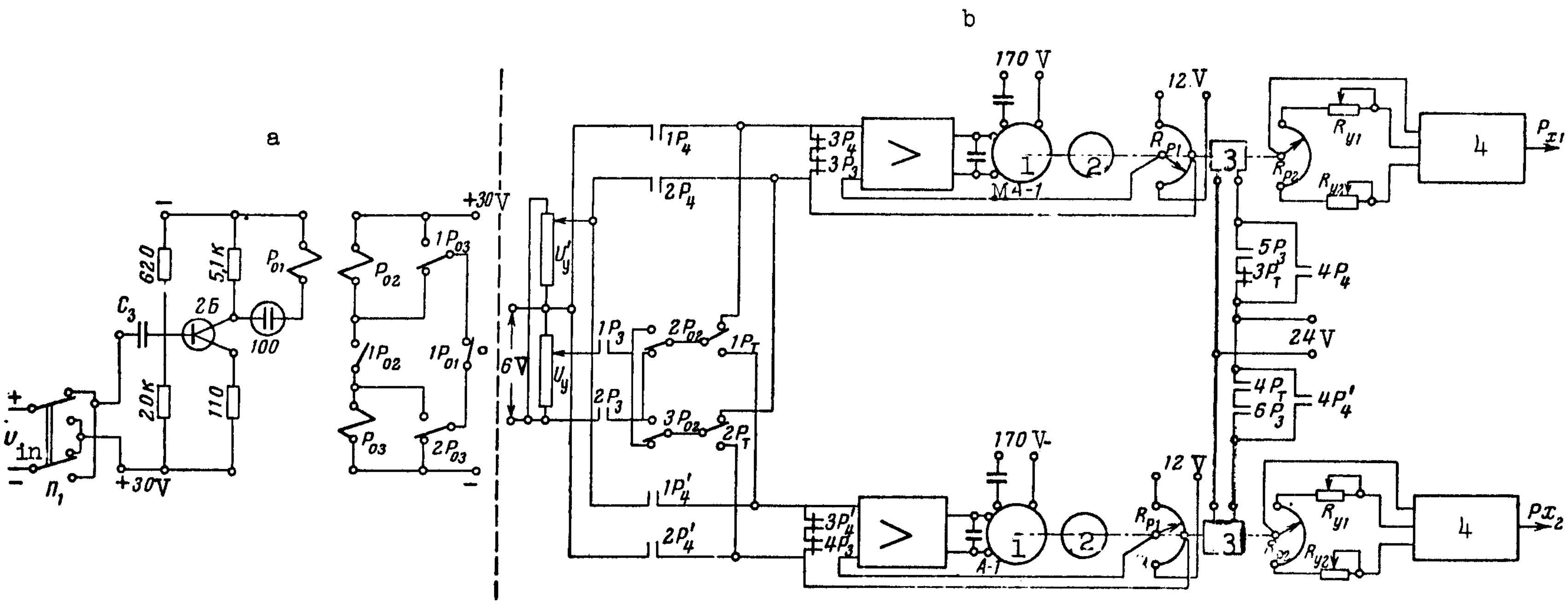

Figure 5. 1, Motor; 2, reducer; 3, electromagnetic clutch; 4, electropneumatic converter.

With search for the maximum of φ it is necessary to change the polarity of U_{in} at the input of the logic device by means of the switch P_1. The sensitivity of the logic device is about 1.2 V, which provides for quite high search accuracy.

6. Basic Circuit of the Executive Devices

The executive devices are intended for the variation of the control quantities x_1 and x_2 by the magnitude of the established step every time on command from the control block. Each executive device (fig. 5b) is (ref. 4) an electromechanical servosystem, consisting of an amplifier, a two-phase motor, a reduction gearing with i = 1/100 and the feedback slidewire R_{p1}. The output shaft of this system is coupled by the electromagnetic clutch EMC (ref. 3) to the output summing slidewire R_{p2}. With actuation of the relay P_3 of the control unit, first the clutch is engaged (as a result of the adjustment of the contacts of P_3 and the higher inertia of the servosystem) and then voltage U_y is applied to the input of the servosystem. The output shaft of the servosystem is rotated through an angle proportional to this voltage.

With deactivation of relay P_3 the clutch declutches the shafts of the slidewire P_{p2} and of the servosystem, which is established in the initial position. The slidewire P_{p2} performs the functions of summing and storage. It is the driver for the electropneumatic converter, which acts directly on the controlled system.

Voltage U_y passes to the input of the servosystems of the executive devices through contacts $2P_{02}$, $3P_{02}$ of the logic device, which determines the direction of the movement of each executive device during search, and through the contacts $1P_T$, $2P_T$ of the device for switching the control channels, which determines the search for the extremum in the channel x_1 or x_2.

In case of violation of the constraints H_1 (H_2), the relay P_4 (P'_4) of the control block actuates and the corresponding executive device takes a step in the previously established direction, regardless of the state of the logic device and the control channel in which the search is being conducted at the given moment.

The magnitude of the step can be established in the range from $\Delta R_{p1} = 0$ to $\Delta R_{p1} = R_{p_1}/2$ by variation of the magnitude of the input voltage U_y and U'_y.

7. Device for Switching the Control Channels /59

When the extremum of φ is reached in one of the channels, control of the optimizer must be switched to search in the other channel. The necessity for transfer of control from one channel to the other also varies with violation of the constraints during search in one of the channels. This operation is accomplished by the device for switching the control channels (fig. 6), which consists of a ring circuit (ref. 5) and a trigger composed of MTKh-90 triodes.

The moment of channel switching with search for the extremum is determined by the number of changes of state of relay P_{02} of the trigger of the logic device. For the determination of the extremum in one channel it is sufficient to register one actuation and one release of relay P_{02}, because this characterizes the moment of passage of the extremum.

With both actuation and release of relay P_{02}, relay P_B is used to apply a pulse to the ring circuit which fires the succeeding cell. After two pulses relay P_k is actuated which excites the trigger and brings the ring circuit into the initial position (the extreme left cell is activated). The trigger is also thrown by the contacts of relays P_5 and P_6, which actuate with violation of the constraints, and by the manual control button K_T.

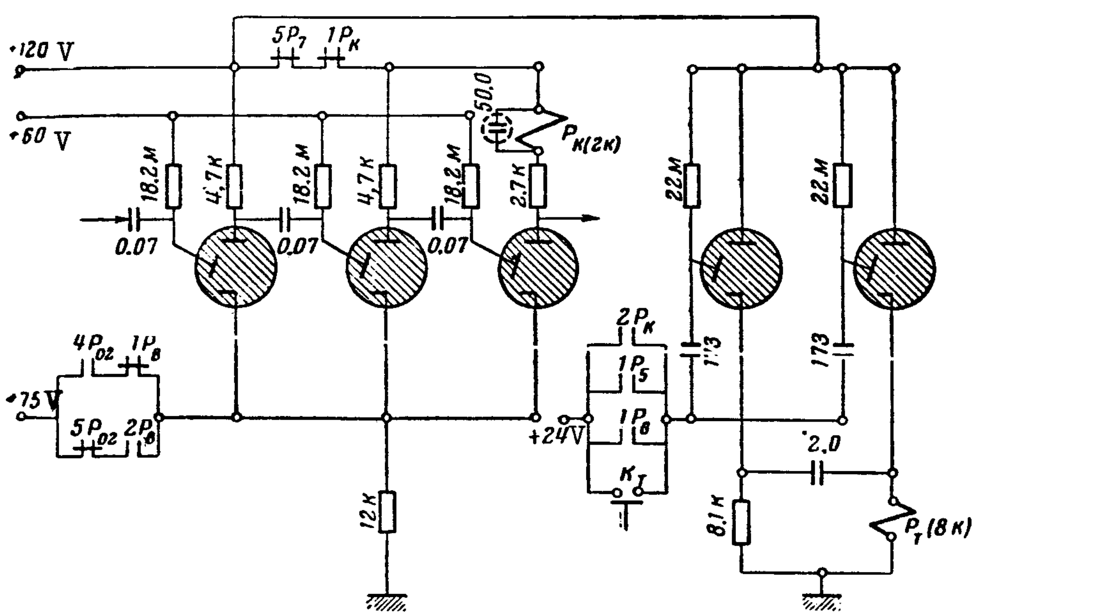

Figure 6

We note that an increase of the number of control channels only requires replacement of the trigger of the ring circuit with a number of cells equal to the number of control quantities. It is necessary to include in each cell a relay which activates its control channel.

8. Functional Diagram of the Control Unit

The control unit (fig. 7) connects all the elements of the optimizer in accordance with a prespecified program for the purpose of performing the selected search algorithm, while taking account of the constraints of the control system.

Two regimes of operation can be established in the optimizer: the regime of search for the extremum of the quantity being optimized in the admissible region of variation of the control quantities and the regime of recovery from the "forbidden" zone. The control circuit must control both of these regimes of operation. /60

Search Regime. The program for the operation in time (fig. 7) of all elements of the optimizer is assembled on the terminals of the stepping selector SS. The time of transfer from one terminal of the SS to another is determined by the frequency of closure of the contacts CI of the interruptor which consists of the synchronous motor S_M (SM-2), the gearing and the cam. At the beginning of the first row of the stepper selector a number of contacts m are left free, which is proportional to the decay time of the transient process $\varphi(t)$ on the control system 0, with a variation of the control quantities x_1 and x_2 by the step magnitude Δx_1 and Δx_2. The integrator I is connected to the following n-m contacts with the aid of relay P_1. On the (n + 1)th contact, relay P_2 connects the output of integrator I to the logic device LD, on the (n + 2)th contact relay P_3 connects one of the executive devices ED which generate a step in x_1 or x_2 and drains the charge from the capacitor C_I of the integrator I.

The stepping selector SS passes over the remaining contacts in a fraction of a second, with transfer of the arm of the 3rd row to the (n + 4)th contact, where it is connected to self-drive by its latching contact 1 SS. Prior to beginning of integration, the capacitor C_I of the integrator is shorted across the contacts a, b of the 4th row on the (k-1)th terminal, and thus the charge which has been accumulated from the amplifier zero drift is drained off.

Regime of Recovery from the "Forbidden" Zone. In the preliminary study of the system it is necessary to establish which of the control actions must be varied and in which direction, in order to recover the process from the "forbidden" zone with violation of each constraint.

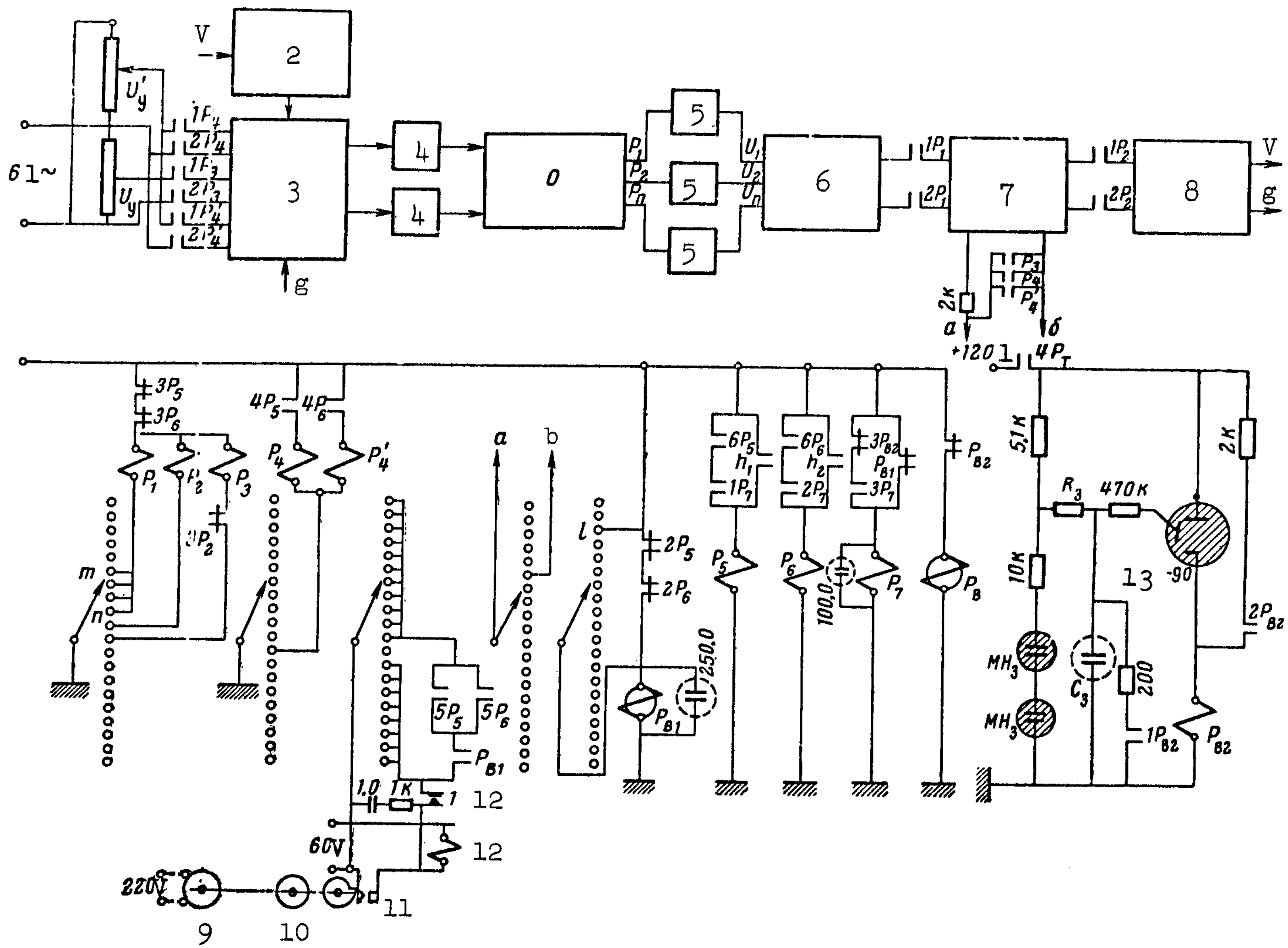

Figure 7. 1, V; 2, control channel switching unit; 3, actuator; 4, electropneumatic converter; 5, pneumoelectric converter; 6, computer; 7, integrator; 8, logic unit; 9, motor; 10, reducer; 11, breaker; 12, stepping switch; 13, thyratron.

As we have already mentioned, the bounding values can be pressure, flow, product quality, temperature, etc. The optimizer imposes one requirement on the instruments used to measure the constraints: they must have a contact device (h_1 or h_2), which is activated on reaching the bounded admissible value of the bounded quantity. If the quantity being measured is expressed in the form of air pressure, it is convenient to use a contact manometer for this purpose. In the case of measurement of the quantity being bounded by a potentiometer or an automatic bridge, a contact device can be mounted on the potentiometer shaft.

With closure of the contacts h_1 (h_2) relay P_5 (P_6) actuates, and in any position other than the (n + 3)th terminal this connects the stepper selector SS to self-drive. The timing relay P_{T_1} is constantly energized, and with actuation of P_5 (P_6) it releases with a time delay sufficient to return the arm of the stepper selector to the (n + 3)th terminal from any position. At this position, relay P_4 (P'_4) engages the executive device which is capable of reestablishing the normal regime of operation of the system. The stepping selector passes the remaining terminals in self-drive. After this a time delay of l terminals (established experimentally on the system) follows at the end of which relay P_{T_1} is again connected to the lth terminal. If the constraint is reestablished, the circuit transfers to the search regime, but now in another channel, since relay P_5 (P_6) by means of contacts $1P_5$ ($1P_6$) has changed the state of the trigger (relay P_T) which switches the control channels.

If, however, the constraint has not be reestablished, then self-drive of the selector is again engaged and on the (n + 3)th terminal the same executive device again generates a step from the "forbidden" zone.

Low-frequency noise is superposed on the bounded quantities; it is therefore possible to have several steps in a row from the "forbidden" zone without the time delay between them, which accounts for the transient process on /62 the system. Actually, as a result of the noise there may occur a regime of alternation of search and recovery from the "forbidden" zone. In order to eliminate this phenomenon, use is made of relays P_7 and P_{T2}. The P_{T2} thyratron timing relay has an actuation delay of t_1, which is equal to that established after actuation of relay P_4 (P'_4) (l terminal). Because of P_7, relay P_5 (P_6) in the course of the time t_1 remains engaged regardless of the contacts h_1 (h_2).

Relay P_7 (contacts $5P_7$) also brings the ring circuit into the initial position, which excludes possible errors in the determination of the moment of passage of the extremum with transfer to the other control channel. For the case of recovery from the "forbidden" zone, the step of the executive devices U'_y should be chosen somewhat greater than U_y, which improves the quality.

9. Electropneumatic Converters

At the present time, as the electropneumatic converter we can make use of the EPP-4 electropneumatic relay--which is a relay electropneumatic servosystem whose feedback slidewire must be connected in a bridge circuit with the output slidewire R_{p2} of the executive device. If we connect in series with R_{p2} the variable resistors R_{D1} and R_{D2} (fig. 5), we can change both the initial pressure from which the search is conducted and the scale of the step Δx_1 (Δx_2). The conversion can also be performed with the aid of the EMD-232 regulator.

Conclusions

The proposed circuit for an automatic optimizer is noise-resistant and provides for sufficiently precise tracking of the extremum of the quantity being optimized. It permits varying the step magnitude and the operational program over wide limits, which is particularly important in the experimental study of processes. The circuit for the executive devices can also be used for optimizers with variable, dependent step.

REFERENCES

1. Fel'dbaum, A. A. Computers in Automatic Systems (Vychislitel'nyye ustroystva v avtomaticheskikh sistemakh). Fizmatgiz, 1959.

2. Norkin, K. B. and Torgashin, A. V. Single-Channel Automatic Optimizers (Odnokanal'nyye avtomaticheskiye optimizatory). TsIIN ChM, No. 5, 1959.

3. Vorob'yeva, T. M. Clutches with Electric Control (Mufty s elektrickeskim upravleniyem). Gosenergoizdat, 1961.

4. Diligenskiy, S. N., Krug, Ye. K., Minina, O. M. and Polonnikov, D. Ye. Electronic Control and Regulation Devices for Complex Automation of Production Processes (Elektronnyye ustroystva kontrolya i regulirovaniya dlya kompleksnoy avtomatizatsii proizvodstvennykh protsessov). PNTPO, No. P-58-104/12, 1958.

5. Collection of Papers on Questions of Electromechanics (Sbornik rabot po voprosam elektromekhaniki). Institut elektromekhaniki, AN SSSR, No. 2, 1958.

N66 34834

ANALYSIS OF AN EXTREMAL REGULATION SYSTEM WITH PEAK-HOLDING IN THE PRESENCE OF NOISE

V. G. Gradetskiy and Yu. I. Ostrovskiy

In the adaptive systems of the search type, which include the extremal /63 regulation systems (ERS), random noise has a significant effect on the system operation. The effect of noise on search time in the transient process was considered in reference 1 for a series of types of extremal systems. Reference 2 used the considerations of the discrete Markov chains for the study of the steady-state process of automatic search in a discrete extremal system in the presence of noise, and determined the steady-state error and the optimal magnitude of the step with which this error is minimal. Studies of Fel'dbaum, Ostrovskiy, Morosanov, Grishko and several other authors have been devoted to the investigation of various types of extremal systems.

One of the possible methods of improving the noise resistance of peak-holding ERS is the use of a noise filter.

Figure 1 shows a structural diagram of the system. The controlled system is represented in the form of a series connection of the linear element L_1, the inertialess nonlinearity c which represents the static characteristic of the system, and the linear element L_2. On the diagram EC is the extremal control; F is the noise filter; A is the actuator. The transfer functions of the linear elements L_1 and L_2 are

$$W_1 = H_1(\omega) \cdot e^{j\theta_1(\omega)} \text{ and } W_2 = H_2(\omega) \cdot e^{j\theta_2(\omega)}. \tag{1}$$

The static characteristic in the zone of the extremum is approximated /64 by the quadratic parabola

$$y^* = -k(x^*)^2. \tag{2}$$

On the input of the system are disturbances $\varphi(t)$, which shift the static characteristic of the system and change the optimal position of the control corresponding to the extremum of this characteristic.

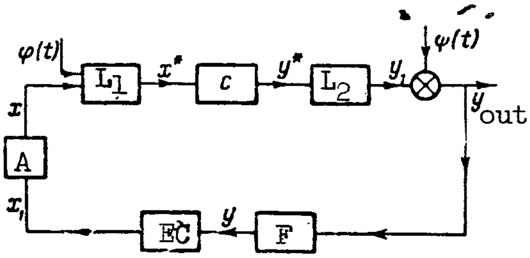

Figure 1

On the input of the control is noise $\psi(t)$, which has no effect on the optimal position of the control.

The primary parameter, which characterizes the quality of the operation of the ERS with peak holding, is the search loss D, defined as the difference between the maximal value of the quantity being optimized, which could be achieved with ideal tracking of the moving extremum, and the average value of the quantity being optimized, which is actually obtained.

The problem of the selection of the optimal adjustments of the extremal control and of the optimal noise filter in the general case can be stated as follows. The static and dynamic characteristics of the regulated system and the regulator are known. Statistical data are available on the disturbances and noise acting on the system. We are required to find the filter structure and define its parameters, and also the parameters of the remaining portion of the system (gain k, control insensitivity zone δ_0 and search speed a) so as to provide for the minimal possible search loss D under the given conditions.

However, in this general formulation the problem is quite complex. We present below an approximate semi-empirical method of analysis.

1. We select an admissible value of the search loss in the steady-state regime with fixed extremum and speed of search $a = dx/dt$. The search speed is selected so that we provide tracking of the extremum, which is shifting as a result of the action of the disturbances. The dynamic and static characteristics of the system and the static characteristics of the noise are assumed to be known.

2. We determine the frequency and amplitude of the self-oscillations for the ideal (no noise) system. Here use is made of the harmonic balance method.

3. Using the first harmonic of the coordinate y thus obtained as the mathematical expectation of the quantity being optimized, we find the magnitude of the control insensitivity zone δ_0, for which the average frequency and amplitude of the self-oscillations in the presence of the noise have the same value as in the ideal system.

Here we assume that:

(a) The mean square frequency of noise ω_ψ considerably exceeds the mean frequency of switching of the sign of the search speed. Therefore, we can assume that the closing of the system by the extremal control does not have any significant effect on the spectrum of the noise present at the control output with the open system.

(b) The frequency of false switchings is negligibly small. By "false" we understand switching of the direction of movement of the control, which takes place with movement of the system in the direction of the extremum.

4. We determine the mean frequency of false switchings. If the preceding assumption is justified, with the selected values of a and δ_0 we will obtain the specified value of the search loss D. False switchings increase the search /65 loss and slow down the search for the extremum with its displacement.

5. If the frequency of the false switchings is high, a noise filter is introduced into the system. The filter structure is assumed to be known. Its adjustment is selected so that, with given search speed and search loss in the ideal system, there is a minimal frequency of the false switchings in the real system (in the presence of noise). If with optimal adjustment of the filter the fréquency of the false switchings still remains high, the given search loss cannot be provided with the given value of the search speed.

Thus the proposed technique for analysis provides the possibility of establishing whether or not a given combination of search speed and search loss can be realized in the system with a low frequency of false switchings. In the case of a positive answer to this question, we can obtain the adjustments of the extremal control and the noise filter. We make use of an indirect variable for evaluation of the quality of the operation of the system--the minimum of the frequency of false switchings. In the case when even with optimal adjustment of the filter the frequency of false switchings remains high, the suggested method cannot determine the actual magnitude of the search loss.

Initial Data for Analysis

If the search speed and search loss are given, then the corresponding frequency ω of the first harmonic at the output of the extremal control and the amplitude A_{y_1} of the first harmonic at its input for the ideal (no noise) system can be determined using the method of harmonic balance (ref. 3) from equations

$$\frac{\omega^2}{H_1^2(\omega)} = \frac{8ka^2}{\pi^2 D}, \tag{3}$$

$$A_{y_1} = \frac{8ka^2 H_1^2(\omega) \cdot H_2(2\omega)}{\pi^2 \omega^2}, \tag{4}$$

where $H_1(\omega)$ and $H_2(2\omega)$ are the moduli of the linear portion of the system; k is the coefficient in equation (2).

The coordinate at the regulator input can be represented in the form

$$y = y_1 + \psi,$$

where y_1 is the mathematical expectation of the quantity being optimized. The quantity ψ can be given by the average number N of crossings in unit time of the arbitrary level ψ_i, reckoned from the mathematical expectation of the quantity ψ. The graph of $N(\psi_i)$ can be constructed from the oscillogram of the quantity y with the open system (with the extremal control disconnected). The finding of the points for the construction of such a graph can be easily automated.

Determination of the Magnitude of the Insensitive Zone with Account for the Noise

The maximal value y_{max} of the coordinate y which can be achieved in the course of the period τ and registered by the memory device is a random quantity (fig. 2).

Let $\tilde{y}_{max}$ be the mathematical expectation of this random quantity; t_0 the moment of switching of the sign of the search speed with noise; $\tilde{t}_0$ the mathematical expectation of the random quantity t_0; $\tilde{y}_{min}$ the value of the coordinate y at the moment $\tilde{t}_0$. /66

Let us set $\tilde{t}_0 = t_s$, where t_s is the moment of switching in the ideal system (without noise), and let us select the zone of insensitivity of the control in accordance with the condition

$$\delta_0 = \tilde{y}_{max} - \tilde{y}_{min}. \tag{5}$$

We can then assume approximately that the average values of the frequency and the amplitude of the first harmonic, and also the search losses in the presence of noise, are equal to the corresponding values of these parameters for the ideal system. Then

$$\delta_0 > \delta_{01},$$

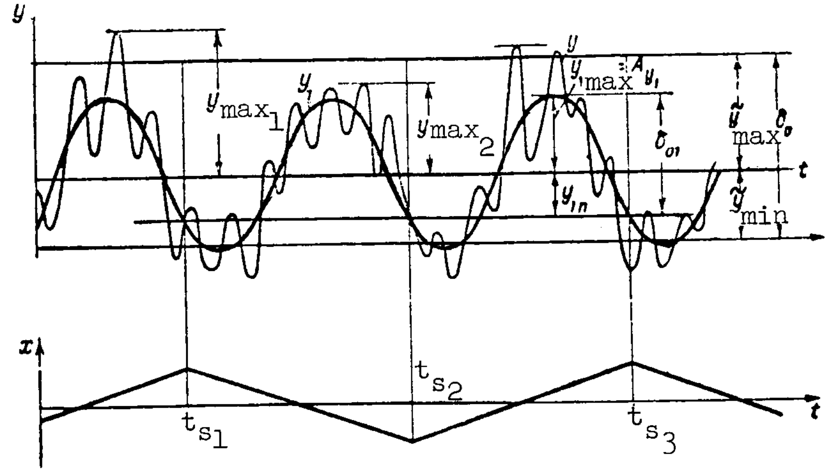

Figure 2

where δ_{01} is the magnitude of the zone of insensitivity for the ideal system (fig. 2).

We present below the semi-empirical methods for the determination of the quantities $\tilde{y}_{max}$, $\tilde{t}_0$ and $\tilde{y}_{min}$.

(a) Determination of the Quantity $\tilde{y}_{max}$

Let us make a preliminary determination of the mathematical expectation of the value of the stationary random function of time ψ, which is achieved in the course of the interval of time Δ of fixed duration.

Consider a series of intervals of time Δ.

Let random quantity $\psi_{max}(\Delta)$ be the greatest value of the stationary random function of time ψ achieved in the course of one interval Δ,

$\tilde{\psi}_{max}(\Delta)$ is the mathematical expectation of random quantity $\psi_{max}(\Delta)$;

$\overline{\omega}_{\psi}$ is the average circular frequency of quantity ψ;

$P_0(\psi_i)$ is the probability that during time Δ there is not a single overshoot of random quantity ψ which exceeds some fixed level ψ_i;

$P_0(0)$ is the probability of zero crossings of the level $\psi_i = 0$ during time Δ.

For sufficiently large intervals Δ, when $\Delta \gg 2\pi/\overline{\omega}_{\psi}$, we can set $P_0(0) \cong 0$. Then $\psi_{max}(\Delta) > 0$ and /67

$$F(\psi_i) = P(\psi_{max} < \psi_i) = P_0(\psi_i), \tag{6}$$

where $F(\psi_i)$ is the distribution function of quantity ψ_{max}.

Let $N(\psi_i)$ (crossings per second) be the mathematical expectation of the number of crossings of level ψ_i in the upward direction per unit time.

Every such crossing is an overshoot beyond level ψ_i, and we shall consider it as an individual event R. The mathematical expectation of the number of events R during time Δ is

$$\lambda(\psi_i, \Delta) = \Delta \cdot N(\psi_i). \tag{7}$$

For a sufficiently high level, the probability of more than one crossing of this level during the time can be considered close to zero (ref. 4).

We shall assume that the values of a random quantity between which the time interval is greater than $2\pi/\overline{\omega}_\psi$ are practically independent. The distribution of the number of independent events R occurring in interval Δ is subject to the Poisson law

$$P_m = \frac{\lambda^m}{m!} \cdot e^{-\lambda}, \tag{8}$$

where P_m is the probability that in interval Δ there will occur m events R. From (6) and (8) for the case m = 0

$$F(\psi_i) = P_0(\psi_i) = e^{-\lambda(\psi_i,\, \Delta)}. \tag{9}$$

Taking account of (6) and assuming, as before, that with $\Delta \gg 2\pi/\overline{\omega}_\psi$ the probability of at least one crossing of level $\psi_i = 0$ is close to unity, the mathematical expectation of the greatest level achieved in time Δ will be

$$\tilde{\psi}_{max} \cong \int_{-\infty}^{+\infty} \psi_i \frac{dP_0(\psi_i)}{d\psi_i} d\psi_i = \int_0^{\infty} \psi_i \cdot e^{-\lambda} \frac{d\lambda}{d\psi_i} d\psi_i. \tag{10}$$

With a normal distribution law of the quantity ψ (ref. 4)

$$N_{norm} = \frac{\overline{\omega}_{\psi}}{2\pi} \cdot e^{-\frac{\psi_i^2}{2\sigma^2}}; \tag{11}$$

$$\lambda_{norm} = \frac{\overline{\omega}_{\psi} \cdot \Delta}{2\pi} \cdot e^{-\frac{\psi_i^2}{2\sigma^2}}. \tag{12}$$

Here σ^2 is the variance of the quantity ψ.

Substituting in (10) we obtain

$$\frac{\widetilde{\psi}_{max}}{\sigma} \cong \varkappa \int_0^{\infty} v^2 \cdot e^{-\left(\varkappa e^{-\frac{v^2}{2}} + \frac{v^2}{2}\right)} dv, \tag{13}$$

where /68

$$\varkappa = \frac{\overline{\omega}_{\psi} \cdot \Delta}{2\pi}, \quad v = \frac{\psi_i}{\sigma}.$$

For the approximate determination of quantity $\widetilde{\psi}_{max}(\Delta)$ from experimental data with an arbitrary distribution law, we partition the region of the values of ψ_i from $\psi_i = 0$ to $\psi_i = \psi_{i\ M}$ into m fixed levels ψ_i (here $\psi_{i\ M}$ is the greatest value of the quantity ψ which occurs during the experiment).

From an oscillogram or by some other method we directly determine the number $N(\psi_i)$ of crossings of every level ψ_i in unit time. Then

$$\widetilde{\psi}_{max} \cong \sum_{i=0}^{m-1} P_i \psi_{i\,av} = \sum_{i=0}^{m-1} \frac{\psi_i + \psi_{i+1}}{2} [e^{-\Delta N(\psi_{i+1})} + e^{-\Delta N(\psi_i)}]. \tag{14}$$

Here P_i is the probability that the greatest value for a given interval Δ of quantity ψ will be found in the interval between levels ψ_i and ψ_{i+1}.

Equation (14) can be used only with $\Delta \gg 2\pi/\overline{\omega}_{\psi}$. If $\Delta = 0$, quantity ψ_{max} coincides with the instantaneous value of ψ. In this case

$$\tilde{\psi}_{max}(0) = 0. \tag{15}$$

Having determined $\tilde{\psi}_{max}$ with $\Delta \gg 2\pi/\varpi_{\psi}$ and with $\Delta = 0$, we construct the approximate graph of $\tilde{\psi}_{max} = F(\Delta)$, starting from the assumption that this function is monotonic.

For the determination of the quantity $\tilde{y}_{max}$ we make use of the following empirical method. Consider the interval of time $\Delta < \tau$ located symmetrically relative to the maximum of function $y_1 = A_{y_1} \cdot \cos 2\omega_1 \cdot t$. The nonrandom function of time y_1 can be considered as a particular case of a random function with the mathematical expectation

$$\tilde{y}_1(\Delta) = \frac{1}{\Delta} \int_{-\frac{\Delta}{2}}^{+\frac{\Delta}{2}} A_{y_1} \cos 2\omega_1 t \, dt = \frac{A_{y_1} \cdot \sin \omega_1 \Delta}{\omega_1 \Delta}. \tag{16}$$

The greatest overshoot ψ_{max} in interval Δ can with equal probability take place at any point of this interval. Let $z(\Delta)$ be the value of function $y = y_1 + \psi$ at the moment when $\psi = \psi_{max}$ and $\tilde{z}(\Delta)$ the mathematical expectation of the quantity $z(\Delta)$

$$\tilde{z}(\Delta) = \tilde{y}_1(\Delta) + \tilde{\psi}_{max}(\Delta). \tag{17}$$

With variation of the interval Δ from $\Delta = 0$ to $\Delta = \tau = \pi/\omega$ $\tilde{y}_1(\Delta)$ diminishes from $y_1(0) = A_{y_1}$ to $y_1(\tau) = 0$ while $\tilde{\psi}_{max}(\Delta)$ increases from $\tilde{\psi}_{max}(0) = 0$ to $\tilde{\psi}_{max}(\tau)$.

With $\Delta = \Delta_M \leq \tau$ the quantity $\tilde{z}(\Delta)$ reaches the maximal value $\tilde{z}(\Delta)_{max}$. It has been experimentally established that for fluctuations which are subject to the normal probability distribution law quantity $\tilde{y}_{max}$ can be approximately /69
determined from the relation

$$\tilde{y}_{max} - A_{y_1} \cong c \cdot [\tilde{z}(\Delta)_{max} - A_{y_1}], \tag{18}$$

where $c \cong 1.1$ is a constant coefficient.

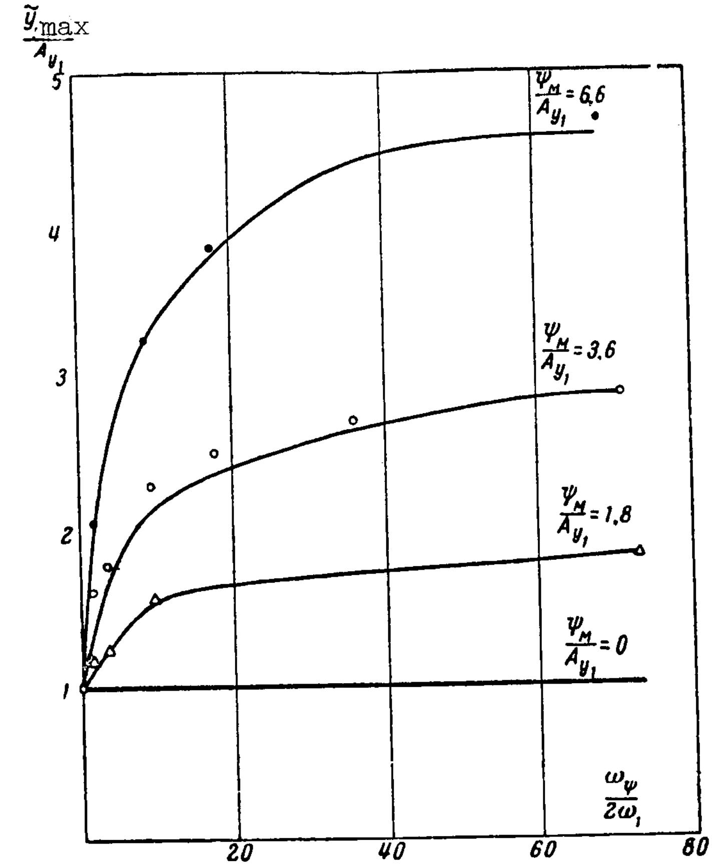

Figure 3

Considering that the analysis is of a preliminary nature, we can set $c = 1.0$ then

$$\tilde{y}_{max} \cong \tilde{z}\,(\Delta)_{max}. \tag{18'}$$

Figure 3 presents curves of the relations $\tilde{y}_{max}/A_{y_1} = F(\overline{\omega}_\psi/2\omega_1)$ obtained from (18) for different relative noise levels and the corresponding points obtained from experiments on a simulation setup with a ball-type random fluctuation generator (arrangement of the experimental setup is presented below).

The curves show that

ψ_M is the greatest overshoot of the quantity which occurred in the course of the experiment;

$\tilde{\psi}_{max}$ was determined from the experimental data using equation (14).

(b) Determination of the Quantity $\tilde{y}_{min}$

We approximate the law of variation of the quantity $y_1 = A_{y_1} \cos 2\omega_1 t$ /70 in the switching zone by the linear function $y_1' = -k_1 t$ setting

$$k_1 = \left(\frac{dy_1}{dt}\right)_{t=\frac{\pi}{4\omega_1}} = 2A_{y_1}\omega_1.$$

We place the coordinate origin 0_1 at the point $t = 0$. We select the arbitrary time segment T_n so that the probability of crossing the level $y = 0$ by the random quantity $y = -k_1 t + \psi$ in the time interval $-\infty < t < -T_n$ will be negligibly small, and we find the approximate expression for the mathematical expectation $\tilde{t}_I$ of the moment of the first crossing of the level $y = 0$ with variation of t from $t = -T_n$ to $t = 0$.

We partition the interval of time T_n into i segments of duration Δ seconds each; n is the order number of the segment.

We assume that for the duration of the segment with number n

$$y_1 = -k_1 t_{av} = \text{const},$$

where

$$t_{av} = (n - i)\Delta + \Delta/2.$$

Let $P_0(n)$ be the probability of zero crossings of the level $y_0 = 0$ in the duration of the segment with the order number n; $1 - P_0(n)$ is the probability of at least one crossing of the level during this segment.

The product of the probabilities $\prod_{n=1}^{m-1} P_0(n)$ is the probability of absence of crossings of level $y_0 = 0$ on all time segments from $n = 1$ to $n = m - 1$ inclusive.

The probability that the first crossing of the level y_0 occurs on segment m, whose midpoint is removed from the coordinate origin by the time $t_{av}(m)$ is

$$P_m = [1 - P_0(m)] \cdot \prod_{n=1}^{m-1} P_0(n). \tag{19}$$

If the probability that the first crossing of the level y_0 takes place after the moment t = 0 is sufficiently small, the mathematical expectation of the moment of the first crossing can be represented approximately in the following form

$$\tilde{t}_1 \cong \sum_{m=1}^{m=i} [t_{av}(m)]\,[1 - P_0(m)] \cdot \prod_{n=1}^{n=m-1} P_0(n). \qquad (20)$$

For the case m = 0 we obtain the probability of zero crossings of level ψ_i in time Δ

$$P_0(n) = e^{-\Delta \cdot N(\psi_i)} = e^{-\Delta \cdot N[y_i(\Delta)]}, \qquad (21)$$

where

$$y_1(n) = \left[(1 - n) \cdot \Delta + \frac{\Delta}{2}\right] \cdot k.$$

The plot of figure 4, constructed in dimensionless coordinates for the normal distribution law, presents the relation /72

$$\overline{\omega}_\psi \tilde{t}_1 = F(\lambda),$$

where

$$\lambda = \frac{k}{\overline{\omega}_\psi \sigma}.$$

The plot of figure 5 presents the calculated relation $\tilde{t}_I = f(k^{-1})$ and the experimental points obtained on the simulation setup with the ball noise generator. The average circular frequency is $\overline{\omega}_\psi = 13$ (sec^{-1}). The maximal overshoot of the random quantity, which occurred in the process of the experiment, was $-\psi_M = 40$ mm in the oscillogram scale.

We draw the straight line $y_1' = -k_1 \cdot t$ through the point with the coordinates t_n, $y_1'(t_n)$, which corresponds to the moment of switching in the absence of noise (fig. 6). We locate point O_1 on the straight line y_1' at distance $\tilde{t}_I$ from the moment t_n and draw through this point the straight line $\tilde{y}_{min}$ parallel to the

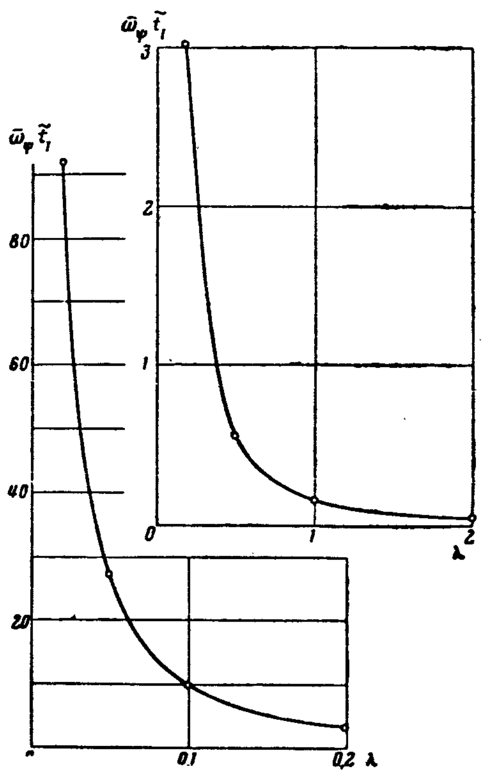

Figure 4

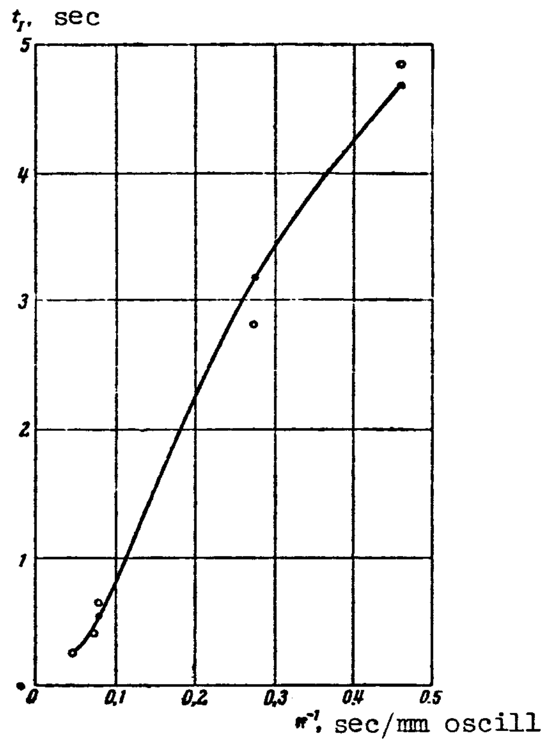

Figure 5

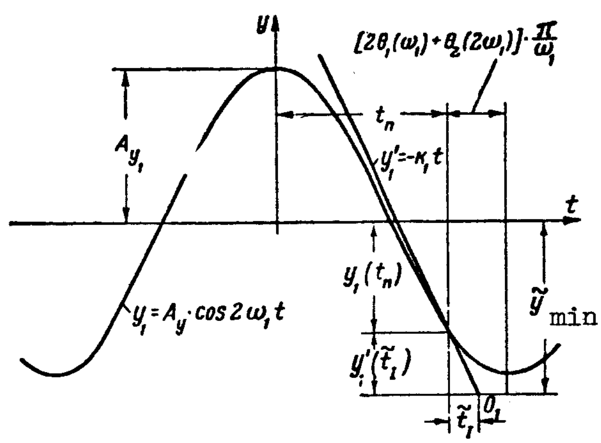

Figure 6

abscissa axis. Then moment t_n will be the mathematical expectation of the moment of the first crossing of level $\tilde{y}_{min}$ by random quantity $y = y_1' + \psi$. Whence

$$-\tilde{y}_{min} = y_1(t_n) + y_1'(\tilde{t}_1). \qquad (22)$$

Using the method of harmonic balance for the ideal system, we find

$$y_1(t_n) = A_{y_1} \cos[2\theta_1(\omega) + \theta_2(2\omega)],$$

whence

$$\tilde{y}_{\min} = -\{A_{y_1} \cos[2\theta_1(\omega) + \theta_2(2\omega)] + \dot{k_1}\tilde{t}_1\}. \tag{23}$$

Determination of the Mean Frequency of False Switchings

We determine the mean number of false switchings with movement in the direction toward the extremum, setting, as before,

$$\frac{dy_1'}{dt} = k_1 = \text{const},$$

where

$$k_1 = 2A_{y_1}\omega.$$

Assume that a false switching takes place at moment t_f, when the negative overshoot of the random component of ψ reaches level ψ_f and the following equality is satisfied

$$\psi_f = \bar{y}_r - \delta_0, \tag{24}$$

where y_r is the maximal value of coordinate y, which was registered by the memory device prior to moment t_f.

We locate the coordinate origin at point $t = t_f$, setting $y_1'(t_f) = 0$.

We denote Δ_f is the mean value of the time interval between neighboring false switchings;

$\tilde{z}(\Delta)$ is the mathematical expectation of the greatest value of random quantity $y = y_1' + \psi$ in the interval Δ.

Then /73

$$\tilde{z}(\Delta) = \tilde{y}_1'(\Delta) + \tilde{\psi}_{\max}(\Delta) \text{ and } \tilde{y}_1' = \frac{k_1}{2} \cdot \Delta = A_{y_1}\omega_1\Delta. \tag{25}$$

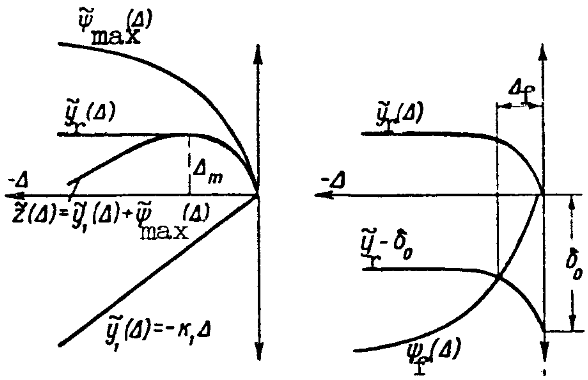

Figure 7

If we consider the time intervals prior to the moment of false switching ($\Delta < 0$), then we have $\tilde{y}_1(\Delta) < 0$, $\tilde{\psi}_{max}(\Delta) > 0$ (fig. 7a). With $\Delta = \Delta_M$ quantity $z(\Delta)$ reaches its greatest value $z_M(\Delta)$. It has been established experimentally that with $\Delta_f \gg \Delta_M$ the mathematical expectation of the largest value of quantity y, registered by the memory device, is $\tilde{y}_r \cong \tilde{z}_M(\Delta)$ (fig. 7a). With $\Delta_f < \Delta_M$ the mathematical expectation of quantity y, registered by the memory device during time Δ_f between neighboring false switchings is

$$y_r \cong z(\Delta_f).$$

At the moment when the difference between quantity y_r and the instantaneous value of coordinate y reaches the boundary of the zone of insensitivity δ_0, i.e., at the moment when level $\psi_f = y_r - \delta_0$ is crossed, there occurs a false switching. The false switchings can take place only in the course of the half of each period τ when $dy_1/dt > 0$. Therefore, the average number of false switchings in unit time

$$L = \frac{N(\psi_f)}{2} = \frac{1}{2\Delta_f}, \tag{26}$$

where $N(\psi_f)$ is the average number of crossings of level ψ_f in unit time. /74
It is convenient to determine quantity Δ_f graphically, constructing curves

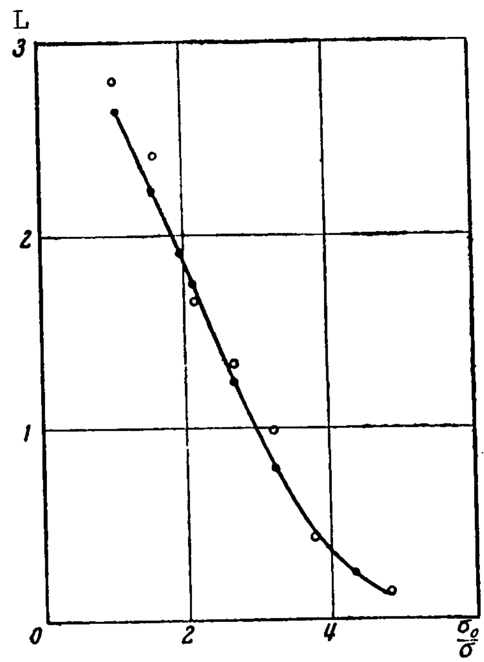

Figure 8. L, False switchings per sec.

$\tilde{y}_r(\Delta)$, $\tilde{y}_r - \delta_0$ and $\psi_f(\Delta)$ (figs. 7a and b). The quantity Δ_f is found as the abscissa of the point of intersection of the latter two curves.

Figure 8 presents the calculated relation $L = F(\delta_0/\sigma)$ for the case $dy_1/dt = 0$ and the experimental points obtained on the simulator.

Choice of Adjustment of Noise Filter

The analysis technique presented here can be used for the selection of the adjustment of the noise filter. In this case the filter structure is assumed given (for example, a sequential chain of aperiodic elements with identical time constants T_F) and we are required to determine quantity T_F.

With increase of the quantity T_F there is a reduction of the noise variance σ^2 at the control input. If the zone of insensitivity of the control remains unchanged, reduction of the variance reduces the frequency of false switchings. In this case, however, increase in inertia of the system leads to increase of the search loss for the ideal system. In order to hold quantity D constant, it is necessary to reduce quantity δ_0. Reduction of the dead zone with a constant value of the variance leads to increase of the frequency of false switchings. The frequency of false switchings reaches a minimum for a definite value of T_F.

TABLE 1

Parameter	Value						
Filter time constant T_F, sec	0	0.2	0.5	1	2	3	4
Dead zone	27.3	9.05	3.94	1.90	0.807	0.313	0.141
L, No. of false switchings per period	0.183	0.081	0.0185	$3.32 \cdot 10^{-4}$	$5.7 \cdot 10^{-7}$	$8.46 \cdot 10^{-5}$	0.005

Table 1 presents as an example the values of L for different values of T_F. In the computation we assumed that the linear portion of the system is a first order element.

$$W_1 = 1, \quad W_2 = \frac{1}{T_0 p + 1}.$$

For the ideal system, the self-oscillation frequency is $\omega = \frac{2a}{\pi}\sqrt{\frac{2k}{D}} = 0.15$ sec^{-1}. The noise at the filter input is white noise in the frequency range from $\omega_{n\ min} = 1$ sec^{-1} to $\omega_{n\ max} = 20$ sec^{-1}, $\sigma_0 = 5$ D. The filter consists of two sequential aperiodic elements. The noise spectral density at the filter input in the given case is constant

$$F_0 = \frac{\sigma_0^2}{\omega_{n\ max} - \omega_{n\ min}}.$$

The variance and the mean circular frequency of the noise at the filter /75 output

$$\sigma^2 = \int_0^\infty \frac{F_0 \cdot d\omega_n}{[1 + (\omega_n T_F)^2]^2};$$

$$\omega_\psi = \frac{1}{\sigma}\sqrt{\int_0^\infty \frac{F_0\ \omega_n^2 d\omega_n}{[1 + (\omega_n T_F)^2]^2}}.$$

Assuming a series of values of T_F, we find $\tilde{y}_{max}$, $\tilde{y}_{min}$, δ_0, y_r, L. From table 1 it follows that with increase of T_F the frequency of false switchings first diminishes sharply, reaches a minimum with a definite value of T_F, and then begins to increase again.

Experimental Investigation

The experimental study of the operation of ERS with the presence of noise was made on an electronic simulator (fig. 9). The entire system including the control was simulated. As the source of random fluctuations we made use of the NG ball noise generator. The linear portion of the system is represented by an aperiodic element (the resolving amplifier y_2 is located after the non-linearity $y^* = 1/100(x^*)^2$). The determination of the quantities $\tilde{y}_{max}$ and $\tilde{\tau}_i$ was accomplished with the system open. The harmonic signal from a separate generator was applied to the system output, where it was summed with the random quantity ψ. The results of these experiments are presented in figures 3 and 5. The determination of the frequency of false switchings with $dy_1/dt = 0$ was also performed with the open system (fig. 8). In the study of the closed system the maximal value of the coordinate y at the system output was registered by /76
polystyrene condenser C_3. The comparison of the maximal and instantaneous values was performed on the amplifier y_6.

After transition through the maximum, the current value of the coordinate is compared with its extremal value, and when the difference $\delta = y_{max} - y$

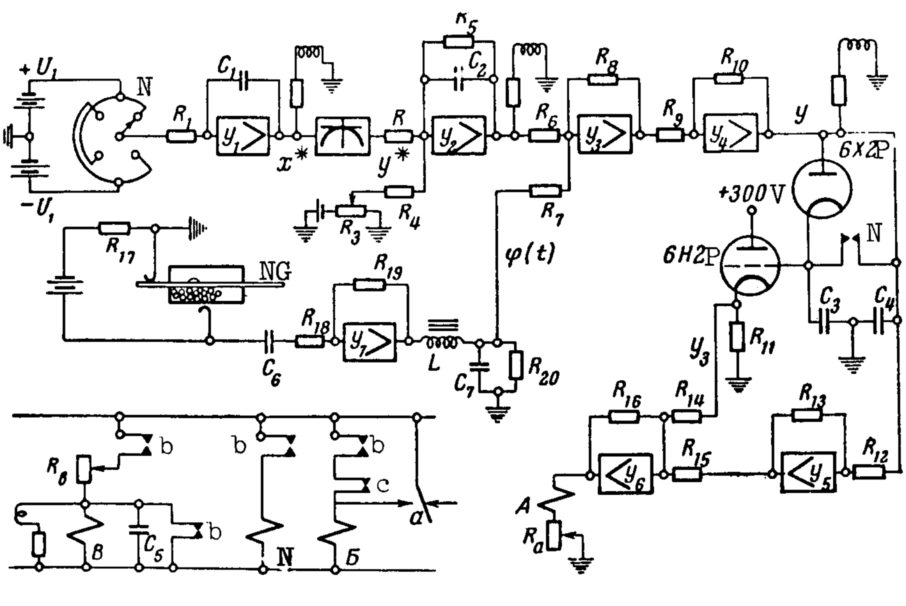

Figure 9. NG, noise generator.

reaches the specified value δ_0, there is a reversal of the direction of variation of the coordinate x and the value is stored.

Figure 10 presents the relation $D/a^2k = f(\omega)$ constructed from equation (3) and the points obtained with processing of the experimental data. The numbers of the points correspond to the numbers of the oscillograms in table 2. For each point the average number of false switchings per period is indicated. Figure 11 shows as an example a portion of the oscillogram No. 5. /77

Table 2 presents the comparison of the experimental and calculated values of the number of false switchings and the dead zones which obtain with a given value of the search loss D. The maximal error in the determination of the magnitude of the dead zone, taking into account the noise present in this series of experiments, amounted to 13 percent; the average error was 8.5 percent.

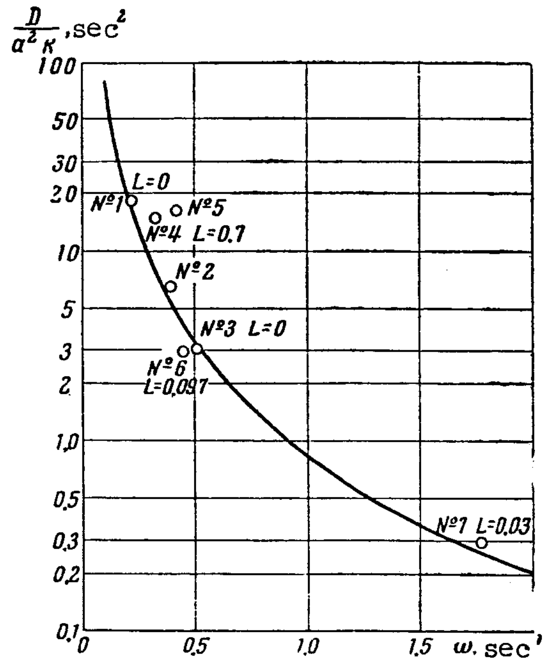

Figure 10

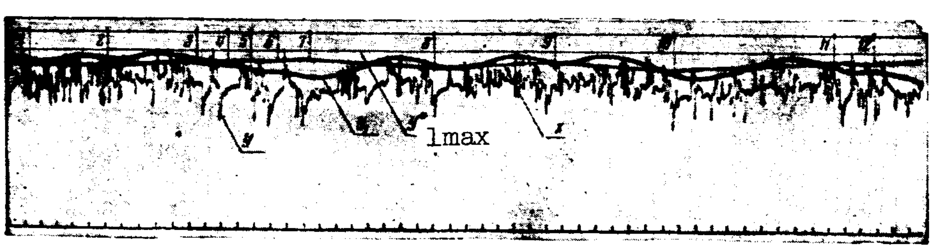

Figure 11

TABLE 2

Parameter	Experiment No.						
	1	2	3	4	5	6	7
ω_1, sec^{-1}	0.218	0.397	0.51	0.33	0.42	0.45	1.78
σ, mm oscillogram	6.3	6.3	6.3	7.7	7.7	7.7	7.0
D, mm oscillogram	17.1	23.8	43.1	11.2	13.0	16.9	73.7
a^2k, mm/sec^2	0.92	3.65	14.2	0.75	0.78	5.82	24.8
δ_0, mm oscillogram:							
computed w/o noise	17.7	11.5	19.1	4.4	2.28	12.1	16.8
computed with noise	38.7	32.2	35.5	41.2	41.3	38.7	24.8
actual	36	36	36	36	36	36	23
L, false switchings per period:							
computed	0	0	0	16.7	20.2	1.26	2.8
actual	0	0	0	6	15	1	1

Calculation, using the method of harmonic balance without accounting for the noise in the present case yields a maximal error of 1,400 percent and an average error of 400 percent.

Conclusions

The proposed method of analysis does not pretend to be mathematically rigorous. However, in spite of several quite crude assumptions the results obtained are quite crude assumptions the results obtained are quite well confirmed by experiment; the method can, therefore, be recommended for practical analysis of systems for extremal regulation in the presence of noise. It is necessary to keep in mind that the lack of rigor of the derivations makes it impossible to indicate with sufficient justification the bounds of applicability of this method, which must be considered to be semi-empirical.

REFERENCES

1. Fel'dbaum, A. A. Effect of Random Factors on the Automatic Search Process (O vliyanii sluchaynykh faktorov na protsess avtomaticheskogo poiska). Conference on the Theory and Application of Discrete Automatic Systems, 1958.

2. Fel'dbaum, A. A. The Steady-State Process in the Simplest Discrete Extremal System with the Presence of Random Noise (Ustanovivshiysya protsess v prosteyshey diskretnoy ekstremal'noy sisteme pri nalichii sluchaynykh pomekh). Avtomatika i telemekhanika, Vol. 20, No. 8, 1959.

3. Ostrovskiy, Yu. I. Peak-Holding Pneumatic Extremal Regulator (Pnevmaticheskiy ekstremal'nyy regulyator s zapominaniyem maksimuma). Candidate's Dissertation, IAT AN SSSR, 1959.

4. Bunimovich, V. I. Fluctuation Processes in Radio Receivers (Fluktuatsionnyye protsessy v radiopriyemnykh ustroystvakh). Izd-vo Sovetskoye radio, 1951.

5. Ostrovskiy, Yu. I. Some Questions of the Theory of Peak-Holding Extremal Regulation Systems (Nekotoryye voprosy teorii sistem ekstremal'nogo regulirovaniya s "zapominaniyem" ekstremuma). Conf. Theor. & Appl. Disc. Autom. Syst., 1958.

6. --- A Pneumatic Extremum Regulator (Pnevmaticheskiy ekstremum-regulyator). Avtomat. i telemekh., Vol. 18, No. 11, 1957.

7. Serdenjecti, S. Optimalizing Control in the Presence of Noise Interference. Jet Propuls., Vol. 26, No. 6, 1956.

N66 34835

OPTIMAL EXTREMAL SYSTEMS

N. V. Grishko

Frequently extremal control is used in the presence of considerable /78
noise which cannot be reduced directly. In this case, for the realization and the complete utilization of the capabilities of extremal control we require systems having a minimal mean square error of tracking the extremum with random inputs. In particular, such a system was required in the development of the control system for the internal combustion engine with a variable load (ref. 1).

In the design of a high-quality extremal system the following engineering problems are posed: (1) finding the structure of the extremal system; (2) obtaining engineering recommendations on the optimal adjustment of the system; (3) preliminary evaluation of the economic advisability of application of extremal control; (4) checking the advisability of complicating the structure of the extremal system in order to improve its quality (and in this connection, verification of the need for improving the theoretical methods of analysis) and so on.

We have made a theoretical study of extremal control with random inputs in order to resolve this problem.

1. Formulation of the Problem

In order to formulate the problem of the theoretical study, we shall first describe the system to be controlled and shall give a definition of the performance variable.

Let us assume for simplicity that the model of the extremal control system is inertialess with a parabolic[1] static characteristic

$$y = y_m - (x - x_m)^2, \tag{1}$$

where $x_m(t)$ and $y_m(t)$ are the extremum coordinates, varying in time in accordance with a stationary law.

---

[1]With the aid of a change of variables the coefficient of the parabola is taken as unity.

Let the extremum tracking error be the following time-average[1]

$$\overline{y_m(t) - y(t)} = K. \tag{2}$$

We take the magnitude of the error K as the variable of the performance of the extremal control and of the extremal systems. It can easily be shown that in the given case this performance variable reduces to the variable of the mean square error: $\overline{(x - x_m)^2}$.

Every control system realizes some set of mathematical operations (i.e., it realizes some operator). The problem then consists in the following: for the given controlled system find (at least one in the class of all possible sets) that optimal set of mathematical operations, transforming y(t) into x(t), such that the tracking error K will have the smallest value $K_{min,min}$. /79

Section 5 presents a brief description of the entire course of the solution of the problem and indicates the salient features of the solution.

2. Results of the Determination of the Optimal Characteristics of One Extremal System

Let us describe the extremal system shown in figure 1. In the following sections we shall see that the consideration of this system is of general importance (sections 4 and 5).

The extremal system generates signals $x_2(t)$ of period T_2 which are applied to the input of the system (through a summator) and to the multiplier (X); prior to multiplication, the oscillations x_2 are first transformed into the oscillations $x_{2k}(t)$ of the same period T_2 but of a different form than $x_2(t)$. The oscillations $x_{2k}(t)$ and the output of the extremal system y(t) are multiplied in the multiplier. This product is then averaged in device A over time T_p (we assume that the number of oscillations during the averaging time $T_p/T_2 = z$ is integral).

It can be shown that the resulting average value with noise accuracy is the estimate of the distance of the system from the extremum. By closure of a switch at the end of time T_p the value of the distance from the extremum is transmitted to device B, where the primary component of the law for the tracking of extremum

[1]The formulation of the problem with indication of the method for its solution was presented at the Conference on the Theory and Application of Discrete Automatic Systems on 26 September 1958.

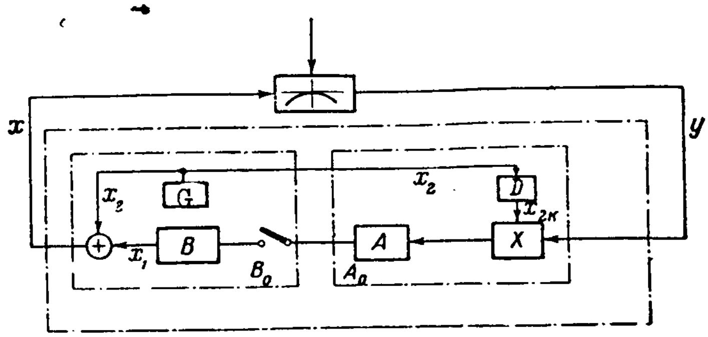

Figure 1. Diagram of extremal system: A_0, sensor for distance from extremum; B_0, device which generates the extremum tracking law; G, test signal generator; D, convertor of signals x_2 into signals x_{2K}; X, multiplier; A, averager over time T_p; B, arbitrary continuous linear portion of the extremal system.

x_1 is developed. After summating x_1 with x_2, we obtain the law of the tracking for the extremum $x(t) = x_1 + x_2$. The B device is a linear continuous system with the weighting function $g_B(t, s)$.

The particular case of this system in the electronic realization was investigated experimentally (ref. 2).

We particularly emphasize that this extremal system can operate with systems other than (1). Of course, it works with an inertial system and with /80
other forms of static characteristics, for example, those formed by two straight lines (only if they have a single extremum).

Thus, this extremal system with the chosen structure is defined by the following arbitrary characteristics $g_B(t, s)$, $x_2(t)$, $x_{2k}(t)$, T_p.

In order to find the optimal system from the selected class it is sufficient to find the optimal indicated characteristics.

The optimal characteristics of the extremal system are determined by variational methods on the basis of the obtained analytic expression for the mean square error K in terms of the specified characteristics of the given controlled system and the arbitrary characteristics of the chosen extremal system

$$K = K_1 + K_2 = K_{1x_m} + K_{1y_m} + K_2 + r^{*}; \tag{11'}$$

$$K_2 = \overline{x_2^2(t)} = \frac{1}{T_2}\int_0^{T_2} x_2^2(\theta)\, d\theta; \tag{1'}$$

$$K_{1x_m} = 2\int_{-\infty}^{\infty} g_{01}(\tau)\,\Delta R_{x_m}(\tau)\, d\tau - \iint_{-\infty}^{\infty} g_0(\tau, \theta)\,\Delta R_{x_m}(\tau - \theta)\, d\tau\, d\theta; \tag{6'}$$

$$\Delta R_{x_m}(\tau_1) = R_{x_m}(0) - R_{x_m}(\tau_1)^{**}, \quad \tau_1 = \tau - \theta; \tag{8'}$$

$$K_{1y_m} = \frac{1}{\alpha^2}\iint_{-\infty}^{\infty} g_0(\tau, \theta)\, R_{x_{2k}}(\tau - \theta)\, R_{y_m}(\tau - \theta)\, d\tau\, d\theta; \tag{10'}$$

$$\alpha = \frac{2}{T_2}\int_0^{T_2} x_2(\theta)\, x_{2k}(\theta)\, d\theta; \tag{7'}$$

$$g_{01}(\tau) = \frac{1}{T_p}\int_0^{T_p} g_G(u,\ u - \tau)\, du; \tag{4'}$$

$$g_0(\tau, \theta) = \frac{1}{T_p}\int_0^{T_p} g_G(u,\ u - \tau)\, g_G(u,\ u - \theta)\, du; \tag{5'}$$

$$R_{x_{2k}}(\tau_1) = \frac{1}{T_2}\int_0^{T_2} x_{2k}(u)\, x_{2k}(u - \tau_1)\, du. \tag{9'}$$

The weighting function $g_G(t, s)$ is defined by the following system of equations

$$g_V t,\ s) = \sum_{t_p=-\infty}^{\infty} g_B(t, t_p)\, g_A(t_p, s); \tag{2'}$$

$$g_G(t, s) = g_V(t, s) - \int_{-\infty}^{\infty} g_G(t, u)\, g_V(u, s)\, du. \tag{3'}$$

The computation of quantity K with given characteristics of the extremal system is performed in the order indicated by numbers (1') to (11'). /81

---

* r is a relatively small term which for the optimal system is smaller, the more intense the noise with a sufficiently flat correlation function $R_{x_m}(\tau_1)$.

** $R_{x_m}(\tau_1)$ and $R_{y_m}(\tau_1)$ are the correlation functions of the laws of variation of the coordinates of the extremum of $x_m(t)$ and $y_m(t)$.

The results of the determination of the optimal characteristics in the sense of the minimum of K are the following:

(1) $x_{2k\ opt}(t) = \text{sign} \cos 2\pi/T_2\, t$; with $x_2(t) = \text{sign} \cos 2\pi/T_2\, t$;

(2) $x_{21\ opt}(t) = \text{sign} \cos 2\pi/T_2\, t$; with $x_{2k} = \text{sign} \cos 2\pi/T_2\, t$. (We assume that $x_2(t) = x_{2m}x_{21}(t)$, where x_{2m} is the amplitude of the oscillations x_2 and $x_{21}(t)$ are oscillations such that $\frac{1}{T_2}\int_0^{T_2} x_{21}^2(t)\, dt = 1$.) In the general case $x_{2k\ opt}(t) = x_{21\ opt}(t)$.

(3) $T_{2\ opt} \to 0$. (In the consideration of the inertial system $T_{2\ opt} > 0$, since as $T_2 \to 0$ the effectiveness of the oscillations x_2 decreases, which from some instant leads to increase of the quantity K. Thus in practice $T_2 > 0$, but it is small);

(4) $z_{opt} = 1$, i.e., $T_{p\ opt} = T_2$;

(5) $g_{B\ opt}(\tau)$ is the weighting function of the continuous portion of the optimal extremal system and is determined from the optimal weighting function of the entire system as a whole $g_{G\ opt}(\tau)$. In turn, this weighting function is determined by some method of the theory of optimal servosystems using the correlation functions of $x_m(t)$ and $y_m(t)$ from the Wiener-Hopf integral equation

$$R_{x_m}(\tau) - \int_{-\infty}^{\infty} g_{G\,opt}(s)\, R_{x_m+n}(\tau - s)\, ds = 0,$$

where $R_{x_m}(\tau)$, $R_{x_{m+n}}(\tau)$ are the correlation functions

$$n = 1/\alpha\, x_{2k\ opt}(t)\, y_m(t);\ \alpha = 2/T_{2\ opt} \int_0^{T_{2\ opt}} x_{2k\ opt}(t)\, x_{2\ opt}(t)\, dt;$$

(6) $x^4_{2m\ opt} = 1/4 \iint_{-\infty}^{\infty} g_{G\ opt}(\tau)\, g_{G\ opt}(\theta) R_n(\theta - \tau) d\tau d\theta.$

Results (1) to (4) are mathematically very simple and therefore are of interest as engineering recommendations. The determination of the last two characteristics is performed by the methods of the theory of optimal servosystems;

in this sense the problem on the optimal extremal systems in its most fundamental aspect, most difficult for computation, reduces to the problem on optimal servo-systems.

The resulting optimal characteristics at the same time correspond to the hardware simplifications of the extremal system.

Substituting in the expression for K the value of the optimal characteristics of the extremal system, we obtain the expression for the minimal value of the tracking error K_{min}

$$K_{min} = 2 \int_{-\infty}^{\infty} g_{G\ opt}(\tau)\ \Delta R_{x_m}(\tau)d\tau -$$ /82

$$- \iint_{-\infty}^{\infty} g_{G\ opt}(\tau) g_{G\ opt}(\theta)\ \Delta R_{x_m}(\tau - \theta)\ d\tau d\theta +$$

$$+ 1/4 \iint_{-\infty}^{\infty} g_{G\ opt}(\tau)\ g_{G\ opt}(\theta)\ R_{x_{2k\ opt}}(\tau - \theta)\ R_{y_m}(\tau - \theta)\ d\tau d\theta + x_{2m\ opt}^2,$$

where $\Delta R_{x_m}(\tau) = R_{x_m}(0) - R_{x_m}(\tau)$.

On the basis of this expression we can make a preliminary estimate of the economic advisability of the use of extremal control (see Introduction).

3. The Pneumatic Extremal System

The resulting optimal characteristics were used in the development of the extremal system described below, which is outstanding in the simplicity of its circuit. In this case the extremum tracking error is just as small as for the system considered in section 2.

The extremal system is assembled from ready-made pneumatic devices which are in mass production.

Let us describe the operation of the extremal system (fig. 2). For simplicity we first assume that the output of the floating readout system y_{fl} is equal to zero. The control unit 4 by switching of contacts k_1, ..., k_4 applies the output of the system in the course of the first half of period T_2, for example, to the "plus" input of integrator 1, and in the course of the second half--to the "minus" input.

The two integrator inputs are denoted "plus" and "minus" as a function of the sign of the integral, obtained with application of pressure only to this one input. Simultaneously, the square-wave signals x_2 are applied to the input

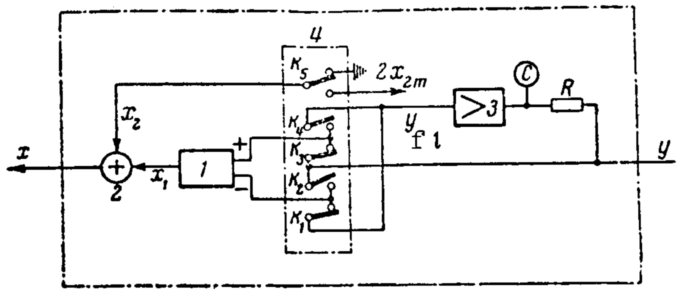

Figure 2. Diagram of pneumatic realization of optimal extremal system: 1, integrator; 2, summator; 3, C, R, inertial element representing floating readout system; K_1-K_5, pneumatic contacts of control unit.

of the system. They are generated with the aid of contact k_5 and some constant pressure equal to $2x_{2nn}$ (this pressure is obtained with the aid of a resistance divider--a throttle). If the system is not at an extremum, the magnitudes of the system output and, consequently, their integrals on the indicated half-periods have a different magnitude. The sum of these integrals, having opposite signs, give during a period an increment at the integrator output, which with proper phasing will bring the system closer to the extremum. We note that in this case the oscillations associated with the processes of integration over the period penetrate to the system input and reduce the quality of the extremal control. These oscillations are larger, the larger the absolute magnitude of the system output.

Now let us assume that the floating readout system is engaged. If the value of its output $y_{f1}(t)$ varies between the values of the output of the object $y(t)$ for two half-cycles, the integrals indicated above have identical signs. This means that the primary component of the movement toward extremum x_1 (with a step change of its position) is monotonic and there are no oscillations about the extremum (with the exception of test signals x_2). /83

Actually, the processes in the extremal system are somewhat more complex, since the magnitudes of the outputs of the system and the floating readout system vary during the time of operation.

The period and the amplitude of signals x_2 are subject to adjustment, as are the time constants of the integrator and of the floating readout system.

Simplification of this system, while obtaining it from the system described in section 2, is based on the following:

(1) since the signals $x_{2k\ opt}(t)$ are rectangular, no multiplier is required; it is sufficient to have only a simple relay contact circuit;

(2) the signals $x_{2\ opt}(t)$ are also rectangular, and therefore it is sufficient to have a relatively simple generator for the rectangular (and not sinusoidal, ref. 3) signals;

(3) since $z_{opt} = 1$, no counter for the test signals is necessary;

(4) since $g_{G\ opt}(t, s)$ is the unit weighting function and $T_{p\ opt} = T_{2\ opt} \to 0$, we can approximately set $T_p = 0$, which permits further significant simplification of the system by means of removal of the separate averager A and the pulser. Here A and B are combined.

The pneumatic system, as a technical realization, differs from the system considered in section 2 by greater interconnection of the processes in time, and by the combination of several functions in one device.

The described linear system has as a general weighting function an exponent which is optimal (in the class of linear systems) in the conditions when the variation of $x_m(t)$ has the nature of random switchings, while the signals $y_m(t)$ are "white noise." Under other conditions a system with a different weighting function will be optimal. For example, with a sawtooth variation of the position of the extremum the system in which there is a more complex device (ref. 2) in place of a single integrator (fig. 2) will have better performance.

We note that the linear systems are optimal only with Gaussian distribution of the functions $x_m(t)$ and $y_m(t)$ in the class of all possible systems. Consequently, under the conditions indicated above, the nonlinear system will be absolutely optimal.

Optimal tuning of the system can be performed automatically with the aid of another like system, which takes as the parameter being optimized the following approximate expression for the variable of performance K

$$K \approx \frac{k}{N} \sum_{i=1}^{N} (\Delta x_1 + n^*)_i^2 + k x_{2m}^2,$$

where $\Delta x_1 = x_1 - x_m$.

The right side of this expression can be measured directly with operation of the extremal system together with a real system, while the quantity K_{min}

cannot be measured. The first term is the average value of the square of the pulses obtained at the output of a special meter for the distance from the extremum, similar to the arrangement A of the extremal system described in section 2. The measurement time $T_{p\ meas\ opt}$ is selected so that the measurement error

n^* will be minimal, i.e., the time of measurement is chosen on the basis of the accuracy of measurement and not on the tracking accuracy, which is not the same. Of course, now $T_{p\ meas\ opt}$ is larger than T_2 with considerable noise. /84

In the expressions presented above for K, k is the average value of the coefficient of the parabola which approximates the static characteristic of the system; we emphasize that as a rule it can be measured in practice.

4. Comparison of Extremal Systems

The comparison of the systems from the point of view of the performance criterion K can be made as follows.

Assume that we are given a system with fixed characteristics. In the present case these characteristics are the functions of time $x_m(t)$ and $y_m(t)$.

Let us assume that we can, by some method, find for each of the systems being compared the value of the performance variable in question. By varying the characteristics (tuning) of the extremal system, we find those optimal characteristics of the system with which the magnitude of the tracking error K (performance variable) reaches a minimum. Comparing the values of the minima of the performance variable, we determine the ordering among the systems being compared with respect to performance. As a result we find under the given conditions the best system for which the magnitude of the minimum of K is the smallest.

This investigation is carried out through the entire range of variation of the system characteristics. As a result, we determine the region of variation of the operating conditions in which the system remains optimal.

We can thus find the system (or combination of systems) which has the best tracking of the extremum in these conditions.

The finding of the minimal values of the performance variable can be performed experimentally full scale or on a model of the extremal system, together with a model of the extremal system. In the experimental determination of the performance variable, the confidence level of the results of the comparison of the extremal systems is very high. However, this method of comparison has several drawbacks: (a) the requirement for the realization of each of the systems being compared; (b) the need for a large amount of experimental work for the computation of K_{min} over a wide range of variation of the characteristics of

the controlled system for various objects; (c) with such a comparison we are not certain that there is not another, possibly better, system and so on.

The performance variables can also be computed analytically. Individual extremal systems have been studied theoretically, and methods have been obtained for the computation of the performance criterion K for them (section 2 and reference 4; reference 5 presents a method of computation of another performance variable--the minimum number of false switchings--which the author indicates is, in practice, close to the performance variable K). With the analytic determination of K_{min}, the volume of the computations associated with the necessity for the variation of the tracking conditions is reduced. This is explained by the fact that the tracking conditions must be varied with an accuracy to certain functions of $x_m(t)$ and $y_m(t)$.

For the system described in section 2 it is sufficient to vary the functions $x_m(t)$ and $y_m(t)$ only with an accuracy to their correlation functions. However, methods for the computation of K_{min} have not been worked out for all systems, and this makes the comparison of the systems difficult. In both the experimental determination of K_{min} and the independent, formal computation of K_{min} for the individual systems we do not obtain assurance of the absence of better principles of operation of the extremal systems.

The comparison of the systems described in the beginning of this section can also be attempted without the separate determination of K_{min} independently for each system. For this we must make a logical comparison of the algorithms of the systems under comparison. In this case it may be found that certain systems are particular cases of others or are close with respect to some variables. It may be found that as a result of certain general properties one of the systems /85 is obviously worse than the others, etc. On the basis of these considerations we can evaluate both the nature of the variation of K_{min} with variation of the system characteristics and also the relations between the magnitudes of K_{min} for various systems.

With this comparison, realization of all systems is not required. Experimental or analytic determination of K_{min} is required only for certain forms of the system characteristics.

It is important that logical comparison of extremal systems can indicate ways for their improvement, but it is particularly important that this comparison permits obtaining some confidence in the low probability of the appearance of new essential improvements, i.e., permits obtaining some guarantee of the nonobsolescence of the system.

It is desirable to perform these analyses rigorously everywhere, which is apparently possible on the basis of some aggregate of elementary initial assumptions. The comparison of extremal systems presented below is brought up to the state of quite clear engineering inductive arguments. The deficiency of the results obtained from the comparison is precisely that they are only probable

(we can continue refining these arguments and make them, as mentioned, more rigorous, reaching mathematical rigor). The correctness of the inductive derivations can be verified experimentally (or analytically). It is evident that it is sufficient at the present to do this with less than full mathematical rigor.

As a rule, the comparison of the systems is possible only on a quite high level of abstraction in general terms, such, for example, as "size of the system memory" and so on.

The principle of the comparison of the extremal systems is based on the results of the considerations presented in section 5. There the general structure of the extremal system is obtained with the aid of clear engineering considerations. This structure consists of two basic parts: the device which senses the distance from the extremum and the device which works out the law for the tracking of the extremum. The optimal combination of the properties of the ensemble of these devices provides for optimal tracking of the extremum. The comparison of the extremal properties system is performed in accordance with the general structure of the system along two basic lines: the first line is the method of measurement of the distance from the extremum, and special attention is devoted to the noise resistance with respect to low-frequency noise; the second line is the method of formulation of the tracking law, and particular attention is devoted to the "size of the system memory."

As a result of extensive comparison of the various systems as equal members, an orderliness was found among the known extremal systems from the point of view of the magnitude of error K_{min} under given conditions of operation of a system. We then thought that one of the systems described in section 2 apparently solves the problem of tracking the extremum with random signals better than the others. If we draw an analogy with the theory of optimal servosystems, we can state that it yields the optimal solution of the posed problem in the class of linear extremal systems.

The arguments presented below can be considered a type of survey of the extremal systems.

After the arguments are considered in detail, it will be desirable to picture them together as a whole. To facilitate this, figures 3 and 5 present conditional diagrams: the interpretations of the arguments and of their results. Since we have these diagrams, we will not give special importance to the sequential description of the arguments (or the description of the diagram of figure 3, which is equivalent).

1. In section 4 we have already indicated the relationship of the systems described in sections 2 and 3. First, let us consider which extremal systems are a particular case of the system from section 2, both in the sense of /86 the method of measurement and in the sense of the algorithm by which the extremum tracking law is worked out.

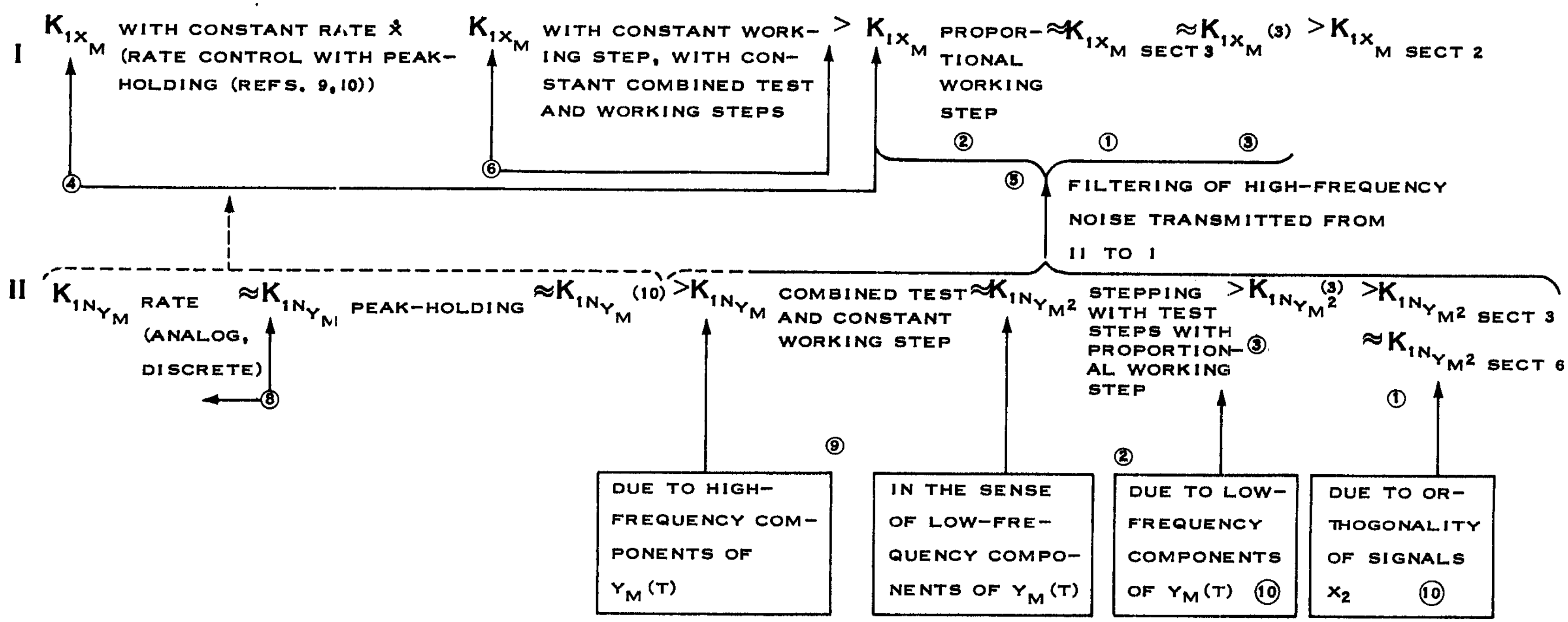

Figure 3. Conditional diagram of comparison of extremal systems. K_{1x_m}, error of extremum tracking due to hunting about extremum and variation of extremum position; $K_{1n_{y_m}}$, same due to noise n_{y_m} associated with oscillations of magnitude of extremum $y_m(t)$; $K_{1n_{y_m 2}}$, same as $K_{1n_{y_m}}$, but with account for error from test signals x_2.

2. It is not difficult to see that the pulse system with test steps and with proportional operational step is such a system. To obtain this system, we must substitute in the system of section 2

(a) $z = 1$;

(b) $x_2 = x_{2k}$ = sign sin $(2\pi/T_2)t$ (and not sign cos $(2\pi/T_2)t$, which does not permit more complete filtering of the low-frequency noise). Sometimes simple storage of the value of the output is used in place of averaging over half-cycles;

(c) the device B is simply an integrating element, i.e., there is no rate tracking, etc.

3. The extremal system (ref. 3) is of the type considered in section 2 almost as much as the type of section 3. The difference is that the test signals x_2 in the system of reference 3 are sinusoidal. The sinusoidal nature of the test signals caused hardware complications: a multiplier and a generator for the sinusoidal signals were required, rather than a simple relay-contact circuit.

In a study of the system from section 2 a method was found for determining the optimal weighting function of the linear portion of the system; this question is not considered in reference 3.

Above we compared the extremal system of section 1 with two linear systems. Now let us compare it with some nonlinear systems (ref. 6).

First, let us consider the algorithms used for the generation of the extremum tracking law.

4. Consider the relay extremal systems in which the magnitude of the rate of travel of the regulator is constant in absolute magnitude, but changes sign at definite instants of time. Such systems include: the derivative extremal system (ref. 7); the peak-holding extremal system (ref. 8); the system with harmonic "probing" (ref. 9); and also the system in reference 10.

As we have mentioned, the regulator moves with a constant velocity. In this respect the indicated extremal systems are analogous to the relay servo-systems.

From the experience accumulated in the field of theory and practice of servosystems it is known (ref. 11) that the relay (nonlinear) systems have lower performance (in the sense of the mean square error) than the analog (continuous) systems. If the laws of the distribution of the useful signal and the noise are not Gaussian, further reduction of the mean square error is possible with introduction of nonlinearity into the servosystem. Moreover, this nonlinearity may be different from the nonlinearity of the simple relay systems. /87

By analogy we can conclude from this that the extremal systems with such a relay output device will have lower performance than the linear (continuous) systems, for example, those in section 1 with continuous (no jumps) variation of the position of the extremum $x_m(t)$.

This conclusion seems to be directly valid. These relay systems have a very "short memory." After every switching of the sign of the rate, the system immediately forgets the history of the variation of the position of the extremum. Actually, the new direction of the motion of the regulator (after switching) will be the same with differing laws of variation of the position of the extremum, if only the condition of the switching of the sign of the rate is satisfied.

In the continuous systems account is taken of the entire necessary history of the process of the variation of the position of extremum $x_m(t)$ within the limits of the correlatability of the process. In principle the provision of astatism of any order is possible, for example, the tracking of an extremum which is being displaced with constant speeds (ref. 2). Even with an unchanged position of the extremum, for best holding (less hunting about the extremum) it is necessary to make use of the fact that the position of the extremum was fixed prior to this.

The theoretical investigation of the system of section 2 has shown that for minimal tracking error the system memory must be fully concentrated in device B and removed from device A (a very "short" memory is required in the A device for filtering of only the low-frequency noise).

Thus, the result of the measurement with the aid of the A device contains at the end of each period $T_p = T_2$ a large error from the high-frequency noise. Nevertheless, the result must be transmitted to the B device for rapid processing (rapid transformation into the tracking law). Incidentally, even in the B device an averaging is performed, a smoothing of the high-frequency noise. It was found that this process itself gives a high tracking performance in the linear systems.

Let us examine the relay systems from this point of view. In them, on the other hand, the memory device B is very short, and it does not perform any averaging of the high-frequency noise. Therefore, the averaging of the high-frequency noise must be performed in the A device. This in itself delays the transmission of the information on the distance from the extremum to device B. And this is important, as we saw above, in spite of the fact that this information contained an error from the high-frequency noise. Moreover, as a result of the functional circuit itself the signals on the distance from the extremum in the relay systems is transmitted comparatively infrequently, and device B does not receive any information between these signals.[1]

REMARK. The absence of astatism of the second (and higher) order in the extremal systems (and in particular in the relay systems) will apparently have

[1] In addition, there is no possibility for astatism of high order.

less effect on the tracking performance than in servosystems. This is due to the fact that the region of variation of x(t) is limited (by the stops of the regulator), therefore long-duration variation of the position of the extremum with a significant constant velocity is not possible. Consequently, in the /88 extremal control it appears that the possibility of tracking an extremum which is being displaced with constant velocity is not so important. On the other hand, the relative accuracy of tracking of the extremum is apparently lower than in the servosystems (radar, for example).

The required accuracy of the extremum tracking is determined by the cost of the process being controlled; high cost may require a very high accuracy.

Let us consider the systems which have separate test and operating steps, where the operating step has a constant magnitude, and also the systems in which the functions of the test and operating steps are combined into a single step of constant magnitude (ref. 12). These systems, first slowly approach the extremum with a sharp significant variation of its position; second, they have a large magnitude of the hunting about the extremum when reaching it. These systems therefore have a large value of the extremum tracking error in comparison with the system of section 1.

We note that the system of section 2, with a static extremal characteristic formed by two straight lines, is transformed into a system with a constant working step (far from the extremum). In the region of the extremum the magnitude of the working step is reduced to zero. Only the test signals remain around the extremum. This favorably differentiates the system of section 2 from the systems with essentially constant working steps. Where it is not possible to obtain information on the distance from the extremum, which is more accurate than sign accuracy, the system advances with constant (large) steps, which near the extremum fade out.

We note that the system of reference 12 can be also realized with a variable step, whose size depends on the ratio of the increment of the system output in the preceding step to the magnitude of this step. But the minimal magnitude (absolute) of this step must always be greater than zero, so that the system does not "stick" after reaching the extremum.

This use of a variable step then eliminates the indicated deficiency of the system of reference 12. However, from the point of view of stability to low-frequency noise it is still inferior to the system of section 1 (see below).

It can be shown that the system just described and the system of reference 12 with a given inertia of the system are faster-acting than the system with a proportional step (see beginning of section 4) and the system of sections 2 and 3. However, this is not the case. With the same law of the test signals which was selected from the point of view of filtering the low-frequency noise, the response speed remains the same with an inertial system.

Let us compare the sensors of the extremal systems.

Let us consider the rate-type extremal systems (refs. 7-10). In these systems the sensors put out a signal for the change of the sign of the rate of movement of the regulating organ.

5. In principle there is apparently no difference in how the derivative dy/dx is measured by these sensors. It can be measured either by direct differentiation with the aid of an analog device or in the finite-difference form $\frac{\Delta y}{\Delta x} = \frac{y_2 - y_1}{\Delta x}$. With the measurement in the finite-difference form, we can perform the averaging of quantities y_2 and y_1, which reduces the effect of the high-frequency noise. Therefore this method of measurement is better than using an analog differentiating device.

However, both methods of measurement in this direct form have an essential deficiency: they are not capable of filtering out the low-frequency oscillations of quantity y(t). The low-frequency components can be caused both by /89 the low-frequency variations of quantity $y_m(t)$ and by the slow variations of the magnitude of the distance from the extremum.

6. The method of measurement in the extremal systems with peak-holding is, in principle, evidently little different from the methods just described for the measurement of the distance from the extremum. Here the ratio $\Delta y/\Delta x = y_2 - y_1/\Delta x$ is also computed, since it is, in principle, not essential that quantity y_2 be the maximal value and that y_1 be the variable value.

In the derivative system the signal for the change of the sign of the velocity of the servomotor is sent when the magnitude of the derivative reaches some value. In the peak-holding system the situation is the same. As soon as the difference $(y_2)_{max} - y_1$ reaches some value, (ref. 8) a signal is sent to reverse the servomotor. The analogy consists in the fact that quantity δ corresponds to some completely definite absolute value of derivative $|d_y/d_x|$; between δ and $|d_y/d_x|$ there is a one-to-one functional relation, which is defined by the form of the corresponding extremal characteristic of the system.

Thus, when we speak of the quantity δ we can implicitly understand the derivative. Consequently, the method of measurement of the distance from the extremum in these two systems does not differ in principle.

There may be differences in the time of averaging of y_2 and y_1, in the values of Δx in the computation of $\Delta y = y_2 - y_1$, and so on. In the peak-holding system quantity Δx is apparently larger and Δy is also larger. This permits somewhat lower requirements of the sensitivity of the sensor or, in

other words, for a given sensitivity it permits a more precise holding of the extremum. But this is important only in the case when the high-frequency and, particularly, the low-frequency noise is absent, when the position of the extremum changes very slowly.

With intense oscillations of $x_m(t)$ and $y_m(t)$ large dynamic deviations from the extremum appear: the deviation due to the noise. Under these conditions the primary role is played by the noise resistance and not the sensitivity of the system. With large forced deviations the measurement of the distance from the extremum by means of the measurement of y_2 and y_1 (where y_2 is not necessarily the maximal value) can be accomplished better than in the peak-holding system. Actually, since the selection of the periods of the averaging of quantities y_2 and y_1 is arbitrary (if we do not require that y_2 be the maximal value), averaging can be performed more efficiently in the absence of this limitation.

Moreover, there is the possibility of repeating several times (!) the measurement of the distance from the extremum, while the system is on one side of the extremum. At the same time the peak-holding system must each time pass through the extremum for the succeeding act of the measurement of the distance from the extremum. In the period of time between switchings, the extremal system with peak holding does not receive information on its position relative to the extremum, other than the very fact of the storage of the maximum. On the other hand, another system, as mentioned above, can, in principle, perform a repetition of the measurement of the distance from the extremum many times, and thus filter the noise to a greater degree by tracking the extremum.

We note that under these conditions the extremum tracking error will generally be larger. However, our problem is to obtain a system which will provide a minimum of this large quantity.

With excessively complex tracking conditions the advantages of the optimal system are hardly apparent. The extremum tracking error may be of the same order as in the absence of the extremal system.

In very simple tracking conditions, i.e., with $x_m \approx$ const and $y_m \approx$ const, the advantages of the optimal system (optimal with statistical inputs) are also not apparent, because for any extremal system the error is close to zero and is determined only by the system sensitivity. /90

In practice, extremal control takes place under conditions of high-frequency and low-frequency noise, and the noise resistance of the systems is of primary importance. Under excessively complex tracking conditions, high tracking accuracy is generally impossible, and the use of extremal control itself is not advisable. We must find other ways of controlling the process.

When we speak of noise, we mean that these are noises which cannot be directly reduced in practice. We are forced to use the noise-resistant extremal

systems which provide minimal error of tracking (maintaining) of the extremum with random inputs.

As we mentioned, these methods of measurement have a common drawback--they are unstable to low-frequency noise. Actually, let us assume, for example, that a quantity varies slowly over some period of time approximately according to a linear law. Because of the fact that y_2 and y_1 are measured at different sequential intervals of time, the magnitude of the distance from the extremum may be measured inaccurately; there may even be an error in sign. This can lead to false reversals ("false steps," see below) and can "bottom" the system, bring it to the stop. Moreover, the bottoming can take place very rapidly, since the hunting rate is quite high.

We must note, it is true, that the range of variation of $y_m(t)$ is limited in practice, as is the range of variation of $x_m(t)$ (see above). Therefore, $y(t)$ cannot for an extended time have an approximately constant rate of change $y(t)$ (differing from zero, of one sign). In this sense, the phenomenon just considered is not so dangerous if the system does not get stuck near the stops; it can lead only to a considerable reduction of the tracking performance.

7. This same deficiency, i.e., inability to filter out the low-frequency noise, is also present in the extremal system described in reference 12, which combines the test and operating steps. For example, in the regions where $y_m(t)$ increases approximately uniformly, the extremal system will be in a stable position to the side of the extremum. The magnitude of the distance of the position from the extremum is greater, when the rate of change of $y_m(t)$ and the magnitude of the averaging period are greater.

8. Under these conditions the extremal system described in section 2 will not react at all to time-linear variations of quantity $y(t)$ (coupled with variation of $y_m(t)$ or of Δx_1); only the nonlinear variations will become apparent. However, they will be minimally apparent due to the fact that the optimal period T_2 of the test signals x_2 is selected as small as possible and is limited only by the inertia of the system.

The system described in section 3 and in reference 3 does react to linear variations of $y(t)$ (compared with the system described in section 2). However, in contrast to the system of reference 12 (section 7), as a result of the presence of the floating readout system it performs only small oscillations about the extremum, varying its value linearly. The oscillation amplitude is smaller, when the rate of change of $y(t)$ and the period of the test signals T_2 are smaller. Since the optimal period of the test signals is made as small as possible, these oscillations about the extremum are small.

The system considered in section 2 does not in principle react to /91 linear variations of $y(t)$; this is explained by the fact that the test signals during the averaging period $T_p = T_2$ have the law sign cos $(2\pi/T_2)t$ and not sign sin $(2\pi/T_2)t$. With reduction of T_2 and with a cosinusoidal law of x_2 there is a reduction of the effect of the nonlinear variations of $y(t)$ (with reduction of T_2 and with a sinusoidal law of x_2 there is a reduction of the effect of linear variations of $y_m(t)$.

The oscillations of the systems of section 3 and of reference 3, noted above, are caused by the fact that the sensor of the distance from the extremum is combined with the device generating the tracking law. Since these devices are not separate, like the system of section 2, the processes associated with the variation of the distance from the extremum penetrate to the input of the system in the form of additional (in addition to $x_2(t)$) oscillations.

We note that in the extremal systems several of the functions which have been combined in a single device are transferred into another device. Thus, for example, the study of the extremal system of section 2 has shown that the extremum tracking error is minimal, if the function of the averaging of the high-frequency noise is completely transferred from device A to device B.

Actually $T_{p\ opt} \to 0$. Thus, device A is assigned the problem of filtering out only the low-frequency noise. This requires the principle of optimal tracking. Although with the requirement for precise measurement of the value of the tracking error the optimal time of measurement T_p must be greater than zero in order to average the high-frequency noise, it must not be so large as to average the function Δx_1 excessively (this averaging can take place not only discretely during time $T_{p\ meas\ opt}$, but also continuously with the aid of a suitable optimalizing filter). If we are required to optimally tune the operating extremal system (see section 2) automatically, $T_{p\ meas\ opt}$ will have still another (third) value, selected optimally from these new considerations.

It was remarked above that the system of reference 12 does not have a higher response speed in the sense of limiting the inertia of the system than the system of section 2. It is not difficult to see that in principle the period of the test signals T_2 is the same, i.e., minimal (section 2). However, the processing, the use of the test signals in the system of section 2 are different than in the system of reference 12. This achieves filtering out the low-frequency noise.

In the systems of section 3 and of reference 3, the processing of the test signals with the presence of the floating readout system is such that the

low-frequency noise does not lead to shifting of the extremum of the extremal system, in contrast to the system of reference 12 and other similar systems.

We have dealt in detail with the low-frequency noise stability, because this is particularly important for the precise, sensitive systems which are close to the extremum most of the time. This is the case, for example, with the peak-holding systems.

From the system comparison presented, we conclude that experimental verification requires first of all comparison of the relay and continuous analog systems, for example, the peak-holding systems and the systems considered in section 3, and also comparison of the stepping system (with a combination of the test and operating step of constant magnitude) with the system described in sections 2 and 3.

5. Clarification of the General Structure of the Extremal System

In section 4 we made a comparison of the known extremal systems. But one important question remained: is there not some other principle of extremal control, unknown to us, which will give a better solution of the problem posed in section 1.[1] Quite detailed, special engineering analyses have been made in order to reduce, to some extent, the possibility of such an omission. /92

These analyses were carried out independently of the known structures of the extremal systems discussed in section 4. Special attention was devoted to the verification of the absence (in the analyses) of other avenues than those available; we thereby verified the nonexistence of solutions of the problem other than those found. These deductive engineering analyses are a concretization of the formulation of the problem by eliminating excessive "futile" generality.

As a stage of these analyses the general structure of the extremal system was obtained (fig. 4). With the same generality as in the formulation of the problem in section 1, this structure is considerably more concrete.

We shall not present here these engineering analyses, because they are simple in themselves and their result (fig. 4) is quite evident.

Since the circuit of the extremal system in figure 4 is similar to the system of figure 1, we shall limit ourselves to only certain clarifications of its salient features. Both components of the tracking law are applied to the device A_1 for the computation of the derivative. The A_1 unit puts out not only the sum $\Delta y/\Delta x + n_{\dot{y}}$, where $n_{\dot{y}}(t)$ is the error in the measurement of the derivative, but also certain information on the error $n_{\dot{y}}$ in the form $\varphi_1[n_{\dot{y}}]$. Since

[1]This needs to be clarified with regard to the question on the obsolescence of control systems.

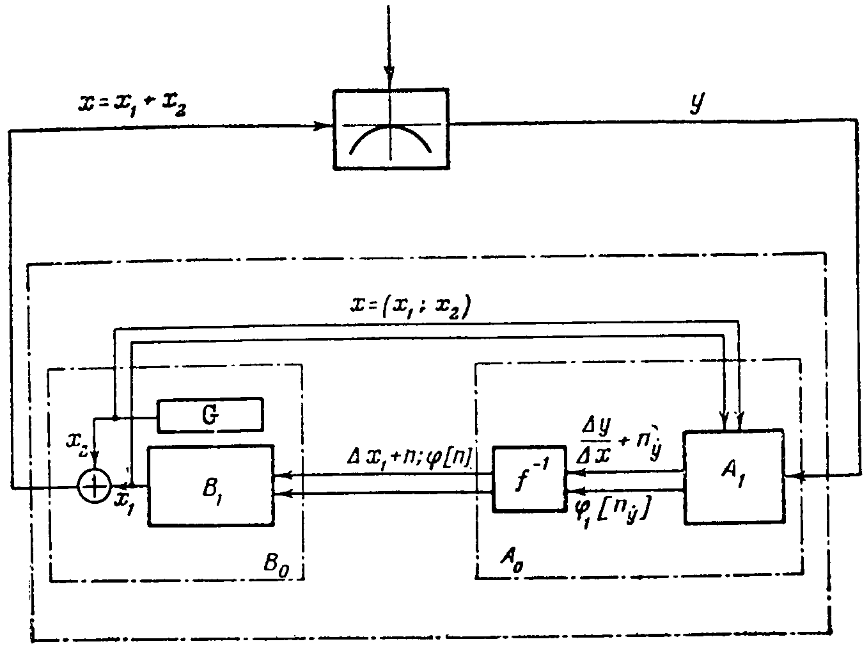

Figure 4. General structure of extremal system: A, device which computes derivative dy/dx; f^{-1}, device converting derivative value into value of distance from extremum; B_1, device which generates basic law of tracking of extremum x_1 (remaining notations same as in figure 1).

there is the relation $dy/dx = f(\Delta x_1)$, with the aid of the functional transformer f^{-1} from the measured derivative the distance from the extremum is computed with error $\Delta x_1 + n$. In addition, some information on the error (noise) is transmitted in the form $\varphi[n]$. For a parabolic extremal characteristic, f^{-1} is the operation of multiplication by a constant quantity.

The system (fig. 4) is not completely concrete, because devices A_1 and B_1 are not fully defined.

The extremal system described in section 2 (fig. 1) was obtained from the system shown in figure 4 by means of concretization of devices A_1 and B_1. We have limited these devices to the class of linear systems by considering the simplicity of realization and analysis. We have thus constricted our system (fig. 1). We note further that in the measurement of the derivative in this system (fig. 1) no use is made of the law of $x_2(t)$, because it is ineffective for this when the performance of the extremal system is high and the variation of the position of extremum of $x_m(t)$ is smooth with infrequent jumps.

Thus, as a result of the performance of the deductive and engineering analyses we have clarified and limited the search region of the optimal extremal system. This region is clearly defined by the diagram in figure 4.

The relationship among all known systems, including the general structure of the extremal system in figure 4, can be visually represented in figure 5, which supplements the previously considered diagram of figure 3. Figure 5 is an attempt to somehow picture a multidimensional space reflecting the dependence of the tracking error K on the tracking conditions ($x_m(t)$, $y_m(t)$) and on the properties of the extremal systems. Here primary attention is given to clarification of the relationship between the systems in the sense of "structural properties." As these properties we chose such concepts as: system-memory size T_m, astatism of second, third order, etc., and also the phase of the oscillations in interval T_p, the form of the oscillations and the frequency of the oscillations, the measurement time T_p, etc.

We imagine that each of these characteristics is an axis of the multi- /94 dimensional space. On each of these axes we determine the position of the various extremal systems from the point of view of corresponding structural property. In spite of the external differences, the known systems have common features--from the more abstract points of view, in the more general concepts such as "system memory," etc. We thereby determine that there exists a structural difference, a "distance" between the systems. For example, the memory of the relay systems is very small in magnitude, while in the system of section 2 the memory is arbitrary and can be large. From this point of view the distance between these systems can be great.

Another Example. The method of measurement in the peak-holding system, in the rate system with combination of test and operating steps, is characterized as follows. For a single measurement event (after which a rate reversal or a step is accomplished) the measurement is performed in two sequential time segments. It is not difficult to see that this corresponds to the sinusoidal law of oscillations x_2 in the system of section 2, which can have not only a sinusoidal, but also a cosinusoidal law of $x_2(t)$. In this sense there is also a structural difference--a "distance"--between the systems mentioned above and the system of section 2. At the same time there is structural similarity between the systems listed above (other than the system of section 2).

So far we have spoken of structural differences. When operating under certain conditions, the value of variable K can be found for each of the systems. The structural difference of the systems can lead to difference in the sense of K as well. We have discussed these differences in section 4. We note that the structural difference also may not lead to differences of the systems with respect to K. For example, the value of K_{min} is approximately the same for the various (stable) extremal systems under excessively simple and excessively complex conditions of operation. In the first case K is equal to zero; in the second case it is equal to the value of K in the absence of the extremal system.

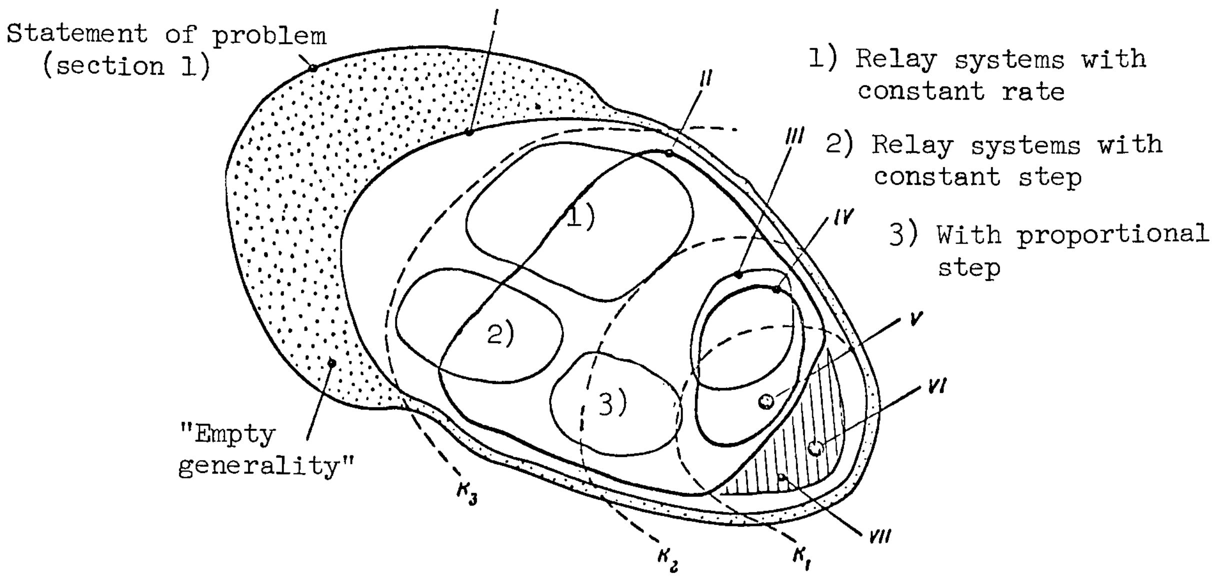

Figure 5. Conditional representation of relations among systems from point of view of their structural properties and dependence of K on general structural properties of systems in tracking conditions of medium complexity: I, general structure of system of figure 4; II, analytic study of system of section 2; III, Vasu system (ref. 3); IV, pneumatic system of section 3; V, system of section 2, giving K_{min}; VI, system, giving $K_{min,min}$; VII, higher performance nonlinear, nonstationary systems.

Thus, differences with respect to K are observed in tracking conditions of medium difficulty. They manifest themselves as follows. For example, with slow variation of $x_m(t)$ and with intense high-frequency oscillations of $y_m(t)$ quite a large system memory is required. The system of section 2 can have this large memory, while the peak-holding system cannot. Therefore, the value of K_{min} for the system of section 2 will be correspondingly smaller.

Another Example. The cosinusoidal law of x_{2k} is required in order to filter out the low-frequency noise, when $T_2 \gg 0$ (because of the high inertia of the system). The peak-holding system does not have this structural possibility and therefore will be inferior to the system of section 2.

Thus, these structural differences of the systems in the indicated conditions were important in the sense of K (the situation is similar with the other structural properties).

From each of the properties we can find the optimal characteristics (which correspond to "points" on the axes), which in the aggregate give K_{min}. Figure 5

shows the optimal points on the property axes for certain average conditions, and the coordinate origin is shifted to these points. The axes are superposed on one another and intersect. The distribution of the properties with respect to the axes is shifted so as to "group" them and obtain real systems. Then the line of equal K (fig. 5) will encircle the optimal system.

With variation of the conditions $[x_m(t), y_m(t)]$ the optimal characteristics change; the axes are therefore displaced relative to one another.

The system of section 2 gave us K_{min}. But we know that there exists the absolute minimum $K_{min,min}$. It has already been noted that under certain conditions, with a Gaussian distribution of $x_m(t)$ and $y_m(t)$, the system considered in section 2 can give the absolute minimum $K_{min} = K_{min,min}$ similarly to the /95
linear servosystems.

Thus, with the aid of the general structure of the system (fig. 4) and the system from section 2 we have evidently determined a "corridor," along which further improvement and perfection of the performance of the extremal systems will proceed. Just as in the servosystems, the improvement of the performance will, in the general case, be based on the introduction into the extremal systems of nonstationarity and nonlinearity,[1] in connection with the corresponding complexity of the tracking conditions.

With further perfection of extremal control we will arrive at a situation where the system will cease to be purely extremal in the usual sense, i.e., having only the single input y (section 6).

Let us summarize the entire course of the solution of the problem posed in section 1.

In the process of the inductive engineering consideration of the analysis of the formulation of the problem we have determined (independently of the existing systems) certain very general properties of the solution of the problem, and as a stage of these analyses have obtained the general structure of the desired extremal system (section 5).

This general structure is not completely concrete. By imposing additional requirements of linearity and others, we concretize the system. Because of the imposed limitations, the obtained concrete system (section 2) is in the general case only an approximate solution of the original problem, and provides only a partial rather than an absolute minimum of error K. In essence it is the solution of a new, more restricted problem. Moreover, as a result of the limitations the system described in section 2 is simple in realization and analysis.

[1]In this case the nonlinearity in the general case can be different from the nonlinearity of the relay systems (section 4).

The resulting concrete system (section 2) was studied analytically for the purpose of determining its optimal characteristics. The resulting optimal characteristics, presented in section 2, gave us the possibility of obtaining a simple circuit of the extremal system (section 3) with the same performance as the system of section 2. Section 4 presented the logical comparison of the known extremal systems and the systems described in sections 2, 3 and 5.

As a result of these analyses we came to the conclusion that the system of section 2 is the best of the existing systems; some of the known systems are clearly inferior, and certain of the best systems are a particular case of the system of section 2. This is true in spite of the fact that the system of section 2 itself was obtained with certain limitations imposed on it (fig. 4) in its concretization. Further improvement of the performance of the systems will take place in the form of a concretization of the system shown in figure 4, with increasingly weak additional limitations.

6. The Place of Extremal Control

Let us clarify the place occupied by extremal control in the process of the improvement of automatic control systems. This question arose in connection with the solution of the concrete problem of the control of the internal combustion engine with a variable stationary load (ref. 1). The resulting control system combined algorithm control and search operations. The system structure was not entirely conventional. It was not entirely clear, for example, whether it was a temporary system which would rapidly transform itself into some other systems. Thus it was necessary to clarify the connection of this system with the automatic control systems "surrounding" it. The study of this system led to the following ideas and generalizations.

Ideas on the Process of Improvement of a Control System

We shall evaluate our system (ref. 1) as a stage of some process of the improvement of a control system, consisting of the transfer of the control functions from the search portion of the system to the portion operating in accordance with the algorithm (in brief, the C → F process). /96

Let us consider this process, using a very simple example. Let us assume that we are to automate some new, insufficiently studied technological process. The automation process itself always starts with the existence of at least some information on the system; the aggregate of this information is quite varied in completeness and reliability; this information is the starting condition for the automation process.

Let us assume that we know that the technological process is defined by parameters x_j $(j = 1,\ldots,n)$. Here certain of the parameters x_{ju} are the control parameters; it is also known that x_{jb} are the uncontrolled parameters which are the external inputs and the variations of the process characteristics.

For the system we must formulate the criteria of the performance of the processes in the system $y(x_j)$ which can be calculated from some set of economically significant parameters x_j. We are required to control the process, so that the time average $\bar{y}$ will be an extremum.

We also assume that the dynamic properties of the system can be neglected, that the process is continuous and that the values of y are computed continuously. Then for every instant of time there exists that position $x_{ju\ max}$* for which y(t) reaches an extremum. However, with variation of the characteristics of the system and the external inputs x_{jb}, the position of the extremum with respect to the regulating elements $x_{ju\ max}(t)$ varies with time. If we knew the causal connection U between x_{jb} and $x_{ju\ max}$ ($x_{ju\ max} = U\,[\ldots x_{jb} \ldots]$) completely, we could synthesize the control device F, which would transform in accordance with some algorithm x_{jb} into x_{ju} ($x_{ju} = F\,[\ldots x_{jb} \ldots]$), so that $x_{ju}(t)$ would track $x_{ju\ max}(t)$, which changes with time. However, we do not know the relation U. This relation must be determined, but control of the system must be initiated as soon as possible. Therefore, we first establish extremal control system C, since the control device F is not available, and begin to study the system as a function of time, while it is controlled by extremal system C.

Study of the individual properties of the system requires differing intervals of time.

Experience with the introduction of extremal control has shown that by controlling the process manually, we can learn in a short time the nature of the shape of the extremal characteristic (and thereby the average value of the exponent of the parabola which approximates the extremal characteristic). After short periods of time we can also learn the nature of the (stationary) high-frequency noise.

Somewhat more time is required to obtain oscillographic records of the (stationary) laws of the slow variation of the magnitude[1] and the position of the extremum: $y_m(t)$ and $x_m(t) = x_{ju\ max}$. We emphasize that we simply record the laws[2] of $y_m(t)$ and $x_m(t)$.

*$x_{ju\ max}(t)$ is the same as $x_m(t)$ in section 2.

[1]This is necessary in order to adjust the gain of the sensor of the quantity y as high as possible without saturation of the sensor output.

[2]It is unimportant that we can, for example, compute the autocorrelation functions of them and others.

Here we only assume which external inputs x_{jb} determine them and know /97 practically nothing of the mechanism of these causal relations U (with the exception of what is given by the theory of the technological process). Determination of the causal relations U requires considerable time.[1] But this is the time at the end of which we can, in principle, have device F, which will give the greatest value for $\overline{y}$ = max max (correspondingly $K \to 0$).

The process of the improvement of the control of the system begins with the formulation of extremal system C. To do this, we establish correlators, which compute during the time of operation of the extremal system the correlation functions $R_{x_{ju}x_{jb}}(\tau)$.

In those cases in which these functions are identically not equal to zero, we introduce devices F_j with arbitrary parameters f_{js} ($s = 1,\ldots,m$), which transform the given x_{jb} into $x_{juF(x_{jb})}$. In the considered simplest case F_j is a functional converter. It can also be simply an amplifying element. In the first approximation the magnitude and the sign of the amplification factor are taken in accordance with the magnitude and the sign of the correlation function $R_{x_{ju}x_{jb}}(\dot{0})$. Then the functional converter, in the general case nonlinear, is optimally tuned by the same extremal system C. Now in the general case it acts on both x_{ju} and on adjustment f_{is} of device F_j.

Thus, in the present case the law $x_{ju}(\ldots \dot{x}_{jb} \ldots)$ consists of two components. The first component is generated by all devices F_j. It is equal to the sum of the components $x_{juF(x_{jb})}$ of all x_{jb}, for which the corresponding correlation functions were not equal to zero. The second component x_{juC} is generated by extremal system C. In the course of time the first component becomes the primary one. The component generated by the extremal system becomes ever smaller. However, this is necessary for the following reasons: first, when the extremal system has not yet managed to adjust device F optimally or when it is out of adjustment, for example, because of variation of its characteristics; second, when device F is still so simple that it cannot generate the required law for the tracking of extremum x_{ju}; third, when certain disturbances of process x_{jb} still remain unknown to us, or we do not have sensors for them, etc.

In view of this process of adjustment of parameters f_{is}, information is continually arriving on the properties of the system, and as this information arrives, it is "embedded" in control device F. Thus the volume of information

[1] Tnat is, it is necessary to establish specifically what we actually know about the system and what intervals of time we require to determine the particular properties of the system we need.

on the system is increased. The quality of the control is improved on the basis of this knowledge. In this case the extremal system, as a search system, is increasingly "removed" from the system. This process ($C \to F$) does not exclude the participation of the human operator, who resolves questions of a higher level than those which at a given moment of time the machine, which partially replaces him, is capable of solving.

This physical process ($C \to F$) of improving the control performance must be automated (for example, as described above). It is a concrete example of "self-instruction" of a control system. Here self-instruction is understood in the sense that with unchanged properties of the tracking conditions the system CF in the course of time will maintain and track the extremum better and better. In constant, but difficult tracking conditions the accuracy of peak-holding is low, but it improves in the learning process. In constant, but simple conditions the accuracy of peak-holding is high and also improves, i.e., it improves in both cases. In the simple conditions it is naturally higher in absolute /98
magnitude than in the complex conditions.

The described outline of the process can be more complex. It is apparent that differing variants of this process are possible.

In connection with this concept of the existence of a process of transfer of the control functions from the search portion of system C to the portions of the system which operate in accordance with an algorithm (briefly $C \to F$), the problem arises of determining the property of an optimal dynamic process for the improvement of control systems in connection with the optimal process of the accumulation of knowledge of the system being controlled during the control period.

It is apparent that this problem will be resolved, first, with the aid of organized, planned, inductive and logical analyses. At some stage we may use the methods of operational research, game theory, prediction theory and finally, classical mathematical methods. As usual, the problem will first be resolved by the consideration of individual idealized models in order to determine sequentially the individual properties of the problem solution, without attempting, of course, to obtain the complete solution immediately, which is unusually difficult when considered as a whole.

We shall make several more individual remarks on the described process to clarify various aspects.

Optimality Criterion

The considered technological problem is already so broad that the criterion of optimality of the process of improving the control system is directly reduced to the criterion of optimality of economic planning. It is natural to take the criterion of optimality of the process $C \to F$ to be the average $I = \overline{y_m - y} + \overline{s(t)}$,

where $s(t)$ is assessable with a possible accuracy of the expenditure of energy,

equipment and manpower. The question of the criterion of optimality of planning is quite complex and is still far from solution.[1]

We note that on the basis of these last considerations it is advisable to discuss the question of the optimality criterion with application to the technical problems of automatic control since, on the one hand, it is of interest as a particular case as one of the salient features of the criterion of optimality of the entire economic planning, and, on the other hand, here there are apparently the means available in a larger degree to show how to formulate the optimality criterion with mathematical precision.

Limitations on the C → F Process

It may turn out that F does not improve the control performance very much in comparison with the control using extremal system C. This occurs with a small number of regulating elements x_{ju}, with a slowly varying position of extremum $x_{ju\ max}(t)$ and with a low-inertia system. In this case, from the economic point of view, the extremal system can be retained as the control means, since it is cheaper than F, with a complex law of conversion of F.

On the other hand, if, for example, with a single regulating element the variation of the position of the extremum is relatively strong, while the time lag of the system from x-y is relatively large, the extremal system is not /99 capable of tracking extremum y.

Thus, for one-dimensional (or few-dimensional) systems the process of conversion of the control function from C → F is either economically inadvisable or is impossible in principle. In this sense the region in which the C → F conversion may be required for one-dimensional systems is not very broad.

However, for multidimensional systems, which are the most important in practice, the region of the performance of the C → F process is sharply expanded in connection with the fact that the possibility of purely extremal control of the multidimensional system is limited.

Actually, with a large number of regulating elements x_{ju}, with a sufficiently high rate of change of the position of the extremum with respect to the regulating elements $x_{ju\ max}(t)$ and, finally, with a high time lag of the system from x_{ju} to y, the purely extremal system C in principle is not capable of tracking the extremum y. It can be shown that under these conditions the use of several test signal frequencies in practice does not strongly expand the

[1]This was shown at the Conference on the Application of Mathematical Methods in Economics at the Institute of Economics of the Academy of Sciences USSR on 4-8 April 1960.

region of application of the purely extremal control, since the possible number of these frequencies is not great.

The C → F Process for Multidimensional Systems

For multidimensional systems the region of existence of the C → F process is sharply expanded. This is caused by the fact that in such systems the extremal system is capable of tracking the extremum of y, using a single regulating element (but not using all of them). Therefore the C → F process is in principle possible. Moreover, it will apparently be economically advisable, since control system F provides for tracking of the extremum, while the purely extremal system C cannot do this in principle. This consideration increases the importance of the solution of the problem on the optimal process C → F.

REMARK I. If purely extremal control of a univariate system is not possible because of the high rate of change of $x_m(t)$ with adequately high inertia, we can try to establish by guesswork a sufficiently arbitrary device F. It may be found that it influences quantity y, and with suitable optimal adjustment (with the aid of C) of its arbitrary parameters f_s it will provide for an extremum of y. A similar approach can be taken with multivarite systems.

REMARK II. We have discussed above the continuous processes where y is computed continuously and where an optimal position for the regulating element x_{ju} (with a low-inertia system) at each instant is desired. With a cyclic process we seek the optimal law of motion of the regulating element during the course of the cycle, and the optimality of the process is determined not from the instantaneous value of some set of parameters x_j, but from a functional of the parameters for the cycle. An example of this is the open-hearth melt cycle, the motion of a rocket, an individual working cycle of an internal combustion engine and the operation of an engine with a variable load (ref. 1).

Let us point out some salient features of the C → F process, using the last example. With a stationary law of variation of the load, the properties of the optimal law of fuel feed remain the same, i.e., extremal system C is required only to maintain the optimal value of parameters f_s of device F. With a change of the properties of the laws of variation of the load, the extremal system/100 must search out this nonstationarity by changing adjustment f_s. Continuing the C → F process, we introduce the "nonstationarity sensor" and set F' at a higher level than F. The quantity F' is also optimally adjusted with the aid of the same extremal system C, now acting on f_s' as well. This is continued, until it is sufficient to hold constant the optimal parameters f_s^n of device F^n. This physical process may be infinite, but in practice it is limited by economic considerations.

In this process with the same object the criterion of optimality of y remains the same as before.

For extremal system C the adjustments f_s, $f'_s, \ldots, f^n_s$ are in principle the same as for x_{ju}.

In this process for extremal system C the number of places of action will obviously increase: in addition to x_{ju}, action on $f_s, \ldots, f^n_s$ is also required. In the course of the development of the $C \rightarrow F$ process, the extremal system performs an analysis of quantity y at increasingly long intervals of time. In this case the time variation of the adjustments of $f^n_s(t)$ becomes increasingly slow with increase of n. For a fixed system some adjustment f^n_s may be constant.

We must point out that with respect to extremal system C the system is (in the general case) the combination of the original technological process and the controlling devices F, F', ..., F^n.

In essence extremal system C is also a device F of a particular form, but in practice it is frequently repeated in the control circuits.

REMARK III. In addition to the indicated use, the correlators can also be utilized for the determination of the dynamic properties of the system. They make it possible to evaluate the dynamic properties from x_{jb} to $x_{ju\ max}$ and also from x_{ju} to y.

In order to improve the tracking performance with an inertial system, a system with delays, controlling device F must possess dynamic properties (under these conditions F is an operator and not a functional transformer). The dynamic properties must be adjusted by extremal system C, but the search operations can be speeded up if we use for the adjustment in the first approximation the results of the computation of the indicated correlation functions.

In addition to the correlators, we can make use of more complicated devices which compute, for example, the laws of distribution which reduce the dependence $x_{ju\ max} = U[\ldots x_{jb} \ldots]$, which in the general case is nonlinear (and dynamic).

REMARK IV. While accounting for the optimal process of improvement of control systems, there is no sense in speaking, for example, of the existence of equipment for complete complex automation. What is understood by this terminology will be some quite distant stage of the mentioned process. Physically, this process is infinite; but it is further defined, i.e., limited by economic and other considerations. This is the normal situation when economics further defines an incompletely defined physical problem.

In this case improvement of control devices is moving not only along the line of increased complexity of the functional circuits, which free the human operator from control of the production process on ever higher levels of

activity, but also along the line of increasing the reliability, stability and service-life of the system elements. Otherwise, with unreliable and unstable elements the work expended on servicing the control system itself increases. The increase of these labor costs begins to exceed what was saved by the introduction of the improved functional circuit. In the course of improvement of the elements, the automation system will somewhat "shift" in the direction of the realization of ever more complex systems to free man from labor at /101
increasingly higher levels of activity. And although still more complex systems will then be known, they will be economically nonoptimal, because their introduction will lead at a given level of reliability and service-life of the elements to an increase of the total expenditure of human labor on the control and service of the system itself. It is apparent that it is not known at the present time what limits automation: the absence of functional circuits or of reliable hardware. Automation of control will continue to develop, until at some level control becomes one of the forms of satisfaction of human needs.

In conclusion we point out that the resolution of this problem in the field of improvement of automatic control has great national economic significance, particularly in the period of extensive introduction of automatic control in new, unstudied processes, for example, in the chemical industry where the study of new chemical processes and the search for optimal control of these processes is imminent. It is apparent that the improvement of the control systems will be repeated in many analogous production processes.

In connection with this great variety of places for the application of automatic control, the resolution of the posed problem is becoming particularly important. Of course this problem is complex; on the other hand, the importance of the resolution of this technological problem for the most rapid solution of our basic economic problem in the competition of the two social systems does not require any special clarification.

REFERENCES

1. Grishko, N. V. Synthesis of an Extremal Control System for an Internal Combustion Engine with Variable Stationary Load (Sintez ekstremal'noy upravlyayushchey sistemy dlya dvigatelya vnutrennego sgoraniya pri peremennoy statsionarnoy nagruzke). IN: Collection of works of the VIth Scientific Engineering Conference of Young Scientists on Automatic Control, Institut avtomatiki i telemekhaniki (IAT), AN SSSR, 1959.

2. --- Extremal Regulator with Extremum Tracking (Ekstremal'nyy regulyator s otslezhivaniyem ekstremuma). Avtomatika i telemekhanika, Vol. 20, No. 4, 1959.

3. Vasu, G. Experiments with Optimalizing Control Applied to Rapid Control of Engine Pressures with High-Amplitude Noise Signals. Trans., ASME, April, 1957.

4. Fel'dbaum, A. A. The Steady State Process in the Simplest Discrete Extremal System with Random Noise (Ustanovivshiysya protsess v prosteyshey diskretnoy ekstremal'noy sisteme pri nalichii sluchaynykh pomekh). Avtomat. i telemekh., Vol. 20, No. 8, 1959.

5. Ostrovskiy, Yu. I. Some Questions on the Theory of Peak-Holding Extremal Regulation Systems (Nekotoryye voprosy teorii sistem ekstremal'nogo regulirovaniya s "zapominaniyem" ekstremuma). Report at the Conference on the Theory and Application of Discrete Automatic Systems. IAT, AN SSSR, 1959.

6. Pugachev, V. S. Theory of Random Functions and Its Application to the Problems of Automatic Control (Teoriya sluchaynykh funktsiy i yeye primeneniye k zadacham avtomaticheskogo upravleniya). GITTL, 1957.

7. Morosanov, N. S. Methods of Extremal Control (Metody ekstremal'nogo regulirovaniya). Avtomat. i telemekh., Vol. 20, No. 11, 1957.

8. Ostrovskiy, Yu. I. Pneumatic extremum regulator (Pnevmaticheskiy ekstremum-regulyator). Avtomat. i telemekh., Vol. 18, No. 11, 1957.

9. Serdenjecti, S. Optimalizing Control in the Presence of Noise Interference. Jet Propulsion, Vol. 26, No. 6, 1956.

10. Rastrigin, L. A. Extremal Control by the Method of Random Search (Ekstremal'noye regulirovaniye metodom sluchaynogo poiska). Avtomat. i telemekh., 1961.

11. Iosif'yan, A. G. and Kogan, B. M. Fundamentals of Servodrive (Osnovy sledyashchego privoda). Gosenergoizdat, 1954.

12. Ostrovskiy, Yu. I. and Eskin, M. Extremum Regulator for Turbine Drilling of Oil Wells (Ekstremum regulyator dlya turbinnogo bureniya neftyanykh skvazhin). Avtomat. i telemekh., Vol. 17, No. 9, 1956.

AUTOMATIC SELECTION OF INTERPOLATION SEGMENTS FOR A MACHINE TOOL WITH LINEAR INTERPOLATOR

V. V. Karibskiy and A. P. Yevseyeva

For the machining of details on machine tools with digital program /102 control it is necessary to specify the movement of the table so that the tool moves along a specified trajectory with the required accuracy. In the calculation of the motion trajectory we usually specify the detail contour in a Cartesian system of coordinates by either an equation or a table. In the latter case a series of coordinates of reference points is given (fig. 1), with an indication of the interpolation law in the spaces between them.

In machine tools with a linear interpolator, each segment of the curve is further divided into smaller segments within the limits of which the curve is replaced by a straight line. The ends of the straight line segments lie on the given curve $y = \varphi(x)$ and the maximal distance between the given curve and the approximating straight line must not exceed the acceptable error δ. The determination of the values of the straight line segments of the broken line from the specified approximation accuracy is one of the most time-consuming elements in compiling the machining program. The problem consists in finding the algorithm and the composition of the program for the automatic computation of the values of the projections of the interpolating segments on the axes X and Y from the given error δ.

Let us consider the two methods for the resolution of the posed problem.

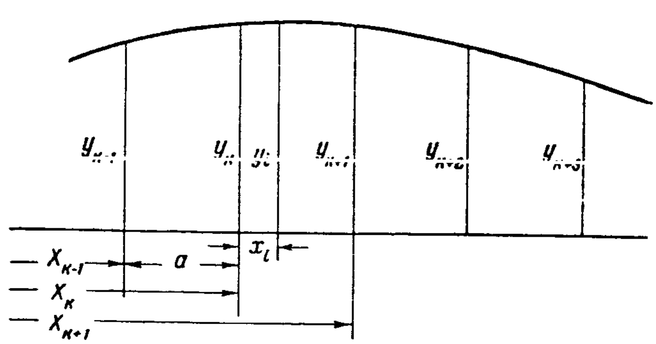

Figure 1

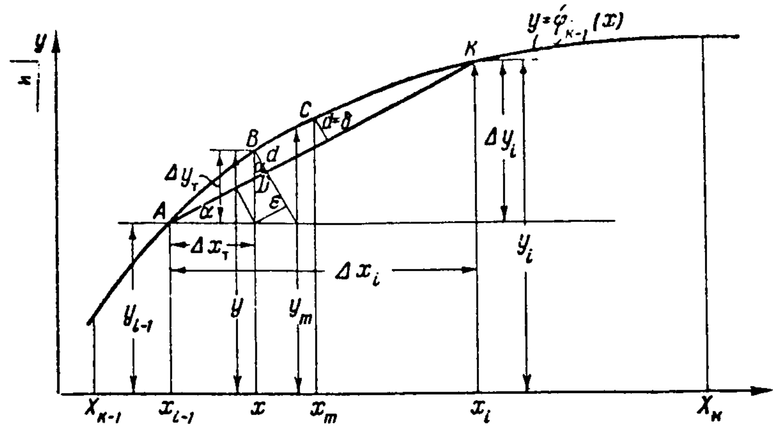

Figure 2

1. Exact Method of Solution

Assume that on the segment $[X_{k-1}; X_k]$ there is given the equation /103 $y = \varphi_{k-1}(x)$ of the original curve (fig. 2). For the determination of $\Delta x_i = x_i - x_{i-1}$; $\Delta y_i = y_i - y_{i-1}$ it is necessary to find the equation of the straight line passing through the given points A and K, whose coordinates must be determined, having in mind that the maximal distance from the straight line d to the curve $\varphi_{k-1}(x)$ must equal the specified deviation δ.

The value of d for any instantaneous value of $\Delta x_т = x - x_{i-1}$ is determined from geometric constructions (fig. 2) using equation

$$d = (y - y_{i-1})\cos\alpha - (x - x_{i-1})\sin\alpha, \tag{1}$$

where

$$\cos\alpha = \frac{\Delta x_i}{\sqrt{\Delta x_i^2 + \Delta y_i^2}};$$

$$\sin\alpha = \frac{\Delta y_i}{\sqrt{\Delta x_i^2 + \Delta y_i^2}}.$$

At the point $C(x_m; y_m)$ where the tangent is parallel to the secant AK, d reaches the maximal value.

To obtain the equations which determine x_m and tan α, let us form two equations, setting $d_{max} = \delta$,

$$\delta = (y_m - y_{i-1})\cos\alpha - (x_m - x_{i-1})\sin\alpha; \tag{2}$$

$$\varphi'_{k-1}(x_m) = \operatorname{tg}\alpha. \tag{3}$$

Solving equations (2) and (3) jointly, we find the values of tan α and x_m.

Further, considering that point K is the point of intersection of the found straight line and the curve $\varphi_{k-1}(x)$, we find the coordinates of point K from the equations

$$y_i - y_{i-1} = (x_i - x_{i-1})\operatorname{tg}\alpha; \tag{4}$$

$$y_i = \varphi_{k-1}(x_i) \tag{5}$$

and the values of the segments Δx_i and Δy_i: /104

$$\Delta x_i = x_i - x_{i-1};$$

$$\Delta y_i = y_i - y_{i-1}.$$

Unfortunately, this method is not very suitable for practical applications, because it is associated with a large number of cumbersome computations. For example, for the typical case when $y = \varphi(x) = Ax^3 + Bx^2 + Cx + D$, equations (2) and (3) take the form

$$\delta = (Ax_m^3 + Bx_m^2 + Cx_m + D - y_{i-1})\cos\alpha - (x_m - x_{i-1})\sin\alpha; \tag{2'}$$

$$\operatorname{tg}\alpha = 3Ax_m^2 + 2Bx_m + C. \tag{3'}$$

The solution of these equations on a computer requires considerable time and may introduce additional errors during the calculation. Therefore, it is more advisable to perform suitable algebraic transformations and reduce the system of equations to an equation with a single unknown, after which the computational process is automated.

For our example, after exclusion of tan α from the first equation, we will have an equation of 6th degree in x_m

$$f_{k-1}(x_m) = a_0x_m^6 + a_1x_m^5 + a_2x_m^4 + a_3x_m^3 + a_4x_m^2 + a_5x_m + a_6 = 0, \tag{6}$$

where

$$a_0 = 4A^2;$$

$$a_1 = 4AB - 12A^2x_{i-1};$$

$$a_2 = 9A^2x_{i-1} - 14ABx_{i-1} + B^2 - 9A^2\delta^2;$$

$$a_3 = 12ABx_{i-1}^2 - 4ACx_{i-1} - 4B^2x_{i-1} - 4AD + 4Ay_{i-1} - 12AB\delta^2;$$

$$a_4 = 6ACx_{i-1}^2 + 6ADx_{i-1} - 6Ax_{i-1}y_{i-1} + 4B^2x_{i-1}^2 - 2BD + 2By_{i-1} - - 2BCx_{i-1} - 4B^2\delta^2 - 6AC\delta^2;$$

$$a_5 = 4BCx_{i-1}^2 + 4BDx_{i-1} - 4Bx_{i-1}y_{i-1} - 4BC\delta^2;$$

$$a_6 = C^2x_{i-1}^2 + 2CDx_{i-1} - 2Cx_{i-1}y_{i-1} - \delta^2C^2 + y_{i-1}^2 - 2Dy_{i-1} + D^2 - \delta^2.$$

The real root of equation (6), which is of interest to us, can be found by solving this equation by one of the approximate methods (refs. 1 and 2), after first computing the coefficients $a_0; a_1 \dots a_6$ and determining the limits of the desired root.

However, with a more detailed consideration of the described method we find that for its realization a large number of cumbersome computations are required. Moreover, for each new function $y = \varphi(x)$ it is necessary to perform a series of algebraic transformations and to solve the system of equations (2) and (3). Therefore, we considered it more advisable to make use of the approximate method for the solution of this problem on the Ural computer (ref. 3).

2. Approximate Method of Solution

The approximate method of determination of the values of segments /105 Δx and Δy is based on a series of sequential trials. First we assume the arbitrary segment Δx_i and for this value we compute Δy_i. Then, using the equation for d

$$d = \frac{(y - y_{i-1})\Delta x_i - (x - x_{i-1})\Delta y_i}{\sqrt{\Delta y_i^2 + \Delta x_i^2}}$$

we compute the values of $d_1; d_2; d_3; d_4$, corresponding to the values of $\Delta x_T = x - x_{i-1}$, equal to $0.2\Delta x_i$, $0.4\Delta x_i$, $0.6\Delta x_i$ and $0.8\Delta x_i$, where each time a comparison is made of the values of d with δ. If $d < \delta$ at all four points, the initial value of Δx_i is increased by $0.2\Delta x_i$, and all the operations are

cyclically repeated, until at some cycle we obtain $d \geq \delta$. As soon as this condition is satisfied, quantities Δx_i and Δy_i obtained in the preceding cycle are printed out.

If the initial value of Δx_i was such that with the computation of d condition $d > \delta$ was satisfied, we make a reduction of Δx_i by $0.2\Delta x_i$ and again compute the values of d at the four points. This process is continued until the condition $d \leq \delta$ is satisfied at all four points.

As soon as this occurs, the current values of Δx_i and Δy_i are printed out and a transition is made to the following elementary segment, i.e., to the computation of the following value of Δx_i, where the initial value of the following segment is taken to be the value printed out for the preceding segment. For monotonically varying smooth curves, such an assumption of the initial value of Δx_i ensures rapid determination of the required value of Δx_i.

With this method of calculation all segments obtained lie in a tolerance of 20 percent with relation to the maximal possible segment on the given portion of the curve. To illustrate this approximate method, we compiled the program for the calculation of an airplane wing profile contour.

Logical Scheme of the Program

The profile contour is specified at equal intervals along the X-axis (fig. 1) by the coordinates of the reference points: Y_1; Y_2; ...; Y_k.

Between the reference points Y_k and Y_{k+1} the intermediate ordinates are determined from the Gaussian interpolation equation

$$y_i = Y_k + \Delta_{k+0.5} \cdot u + \frac{u(u-1)}{2!}\Delta_k^2 + \frac{u(u-1)(u+1)}{3!}\Delta_{k+0.5}^3 + \frac{u(u-1)(u+1)(u-2)}{4!}\Delta_k^4 + \ldots, \tag{7}$$

where y_i is the desired ordinate;

Y_k is the ordinate just preceding the desired ordinate;

x_i is the current value of x on the given interval $x_i = \sum_{l=0.5}^{i} \Delta x_l$ (here $l = 0.5, 1.5, \ldots, i$);

$\Delta_{k+0.5}$ is a first order difference;

Δ_k^2 is a second order difference;

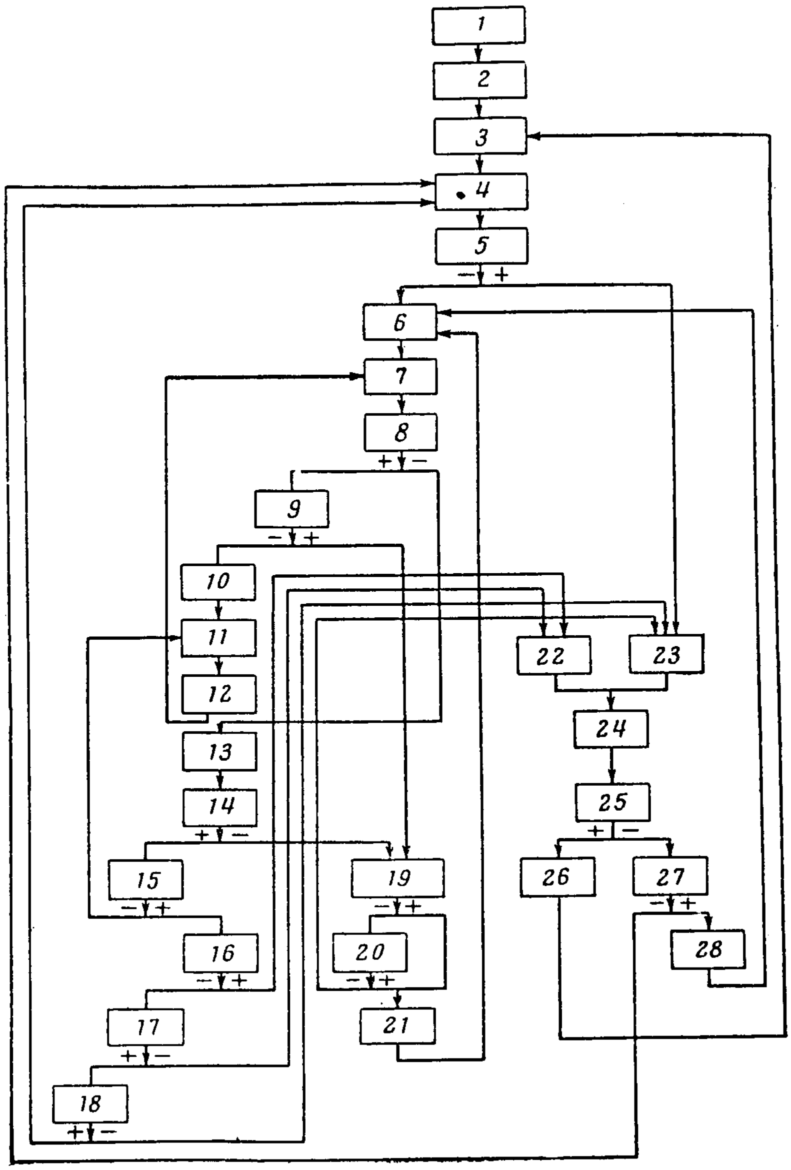

Figure 3. Caption on opposite page.

Figure 3. Approximate method for calculation of airplane wing profile contour. 1, conversion of Δ, Δ^2 and Δ^3 from decimal system to binary; 2, computation of A, B, C; 3, beginning of X_k segment; 4, entry into adder of Δx_{i+1} and calculation of $\sum_{l=0.5}^{i} \Delta \bar{x}_l + \Delta \bar{x}^*_{i+1}$; 5, determination of the sign of $(\sum_{l=0.5}^{i} \Delta \bar{x}_e + \Delta x^*_{i+1}) - (x_{k+l} - x_k)$; 6, entry into the adder of Δx_{i+1} and calculation of $\sum_{i=0.5}^{i} \Delta \bar{x}_l + \Delta \bar{x}^*_{i+1}$; 7, calculation of $\Delta \bar{y}^*_{i+1}$; 8, comparison of 0 with 0, 1, 2, 3 with the calculation of d_1, d_2, d_3, d_4; 9, check of $\Delta \bar{y}^*_{i+1} < \Delta \bar{y}_{max}$; 10, calculation of $\sqrt{\Delta \bar{x}^*_{i+1} + \Delta \bar{y}_{i+1}}$; 11, determination of the sign of the difference between the counter content and the number 3; 12, calculation of $\bar{x}_T$; 13, calculation of $\bar{d}$; 14, comparison of δ with $\bar{d}$; 15, check of the sign of the difference between the counter content and the number 3; 16, check of the sign of $(\sum_{l=0.5}^{i} \Delta \bar{x}_l + \Delta \bar{x}^*_{i+1}) - (\bar{x}_{k+1} - \bar{x}_k)$; 17, recording of the four-fold computation of $\bar{d}$ and check of the fact of reduction of $\Delta \bar{x}^*_{i+1}$; 18, increase of Δx^*_{i+1} and check of $\Delta \bar{x}^{ym}_{i+1} < \bar{x}_{max}$; 19, check of the sign of $\sum_{l=0.5}^{i} \Delta x_l + \Delta \bar{x}^*_{i+1}) - (\bar{x}_{k+1} - \bar{x}_k)$; 20, check of the fact of the four-fold computation of $\bar{d}$; 21, reduction of Δx^*_{i+1} and recording of the fact of a reduction; 22, conversion of the current values of $\Delta\bar{x}$ and $\Delta\bar{y}$ into the binary-decimal system; 23, conversion of the preceding values of $\Delta\bar{x}$ and $\Delta\bar{y}$ into the binary-decimal system; 24, printout of $\Delta\bar{x}$ and $\Delta\bar{y}$; 25, comparison of with $\bar{x}_{k+1} - \bar{x}_k)$; 26, restoration of zeros in operating cells and $\sum_{l=0.5}^{i} \Delta \bar{x}_l$ transfer to $(x_{k+2} - x_{k+1})$; 27, verification of the sign of $\sum_{l=0.5}^{i} \Delta \bar{x}_l + \Delta \bar{x}^*_{i+1} - (\bar{x}_{k+1} - \bar{x}_k)$; 28, calculation of $(\bar{x}_{k+1} - \bar{x}_k) - \sum_{l=0.5}^{i+1} \Delta \bar{x}_l$.

$\Delta^3_{k+0.5}$ is a third order difference, etc.;

$u = x_i / a$ (here a is the distance between the reference points of the profile).

The differences are determined as follows /107

$$Y_k - Y_{k-1} = \Delta_{k-0.5}; \quad Y_{k+1} - Y_k = \Delta_{k+0.5}; \quad Y_{k+2} - Y_{k+1} = \Delta_{k+1.5};$$

$$\Delta_{k+0.5} - \Delta_{k-0.5} = \Delta^2_k; \quad \Delta_{k+1.5} - \Delta_{k+0.5} = \Delta^2_{k+1}.$$

$$\Delta^2_{k+1} - \Delta^2_k = \Delta^3_{k+0.5};$$

The program provides for finding the values of the projections Δx_i and Δy_i, which are obtained as a result of approximation of the curve $\varphi(x)$ by the broken line with the error δ. In our case $\varphi k(x)$ is determined by equation (7), in which the terms containing differences higher than 3rd are not taken into account.

Since in the program for the computations we operate with the increments of the ordinates and not with the ordinates themselves, the equations which are used in the calculations are written in the form

$$\Delta\bar{y} = \bar{y}_i - \bar{Y}_k = A\bar{x}_i^3 + B\bar{x}_i^2 + C\bar{x}_i, \tag{8}$$

where
$$A = \frac{\bar{\Delta}^3_{k+0.5}}{a^3 \cdot 3!};$$
$$B = \frac{\bar{\Delta}^2_k}{a^2 \cdot 2!};$$
$$C = \frac{\bar{\Delta}_{k+0.5}}{a \cdot 1!} - \frac{\bar{\Delta}^2_k}{a \cdot 2!} - \frac{\bar{\Delta}^3_{k+0.5}}{a \cdot 3!};$$

$$d = \frac{\Delta \bar{y}_{\text{T}} \cdot \Delta \bar{x}_i - \Delta \bar{x}_{\text{T}} \cdot \Delta \bar{y}_i}{\sqrt{\Delta \bar{x}_i^2 + \Delta y_i^2}}. \tag{9}$$

Here $\bar{x}$, $\bar{y}$, $\bar{d}$ and $\bar{\Delta}$ are the representations of the quantities x, y, d and Δ in the scale selected for the calculations.

The numerical material in the program is given in the form of $\bar{\Delta}$, $\bar{\Delta}^2$ and $\bar{\Delta}^3$ for each interval. Since in the digital computers the storage of the numerical material in the machine memory and the performance of the logic and arithmetic operations on them is accomplished in the binary system, the necessity arises for preliminary conversion of the initial decimal numbers into the binary system (this is shown in the first block in fig. 3). From the

initial data we find the coefficients A, B, C of equation (8) for all segments of the contour and store them in the memory.

For the determination of $\Delta\bar{x}_i$ and $\Delta\bar{y}_i$ we proceed as follows. We take the segment $\Delta\bar{x}_i^*$, which is taken equal to the printed-out value of $\Delta\bar{x}_{i-1}$, then we divide $\Delta\bar{x}_i^*$ into 5 portions and for each value of $\Delta\bar{x}$, equal to $0.2\Delta\bar{x}_i^*$; $0.4\Delta\bar{x}_i^*$; $0.6\Delta\bar{x}_i^*$; $0.8\Delta\bar{x}_i^*$, we calculate $\bar{d}$ from equation (9). For each of the enumerated values in equation (9) only the numerator changes, the denominator remaining the same. Consequently, when we compute $\bar{d}$ for $0.2\Delta\bar{x}_i^*$, we calculate the denominator of expression (9); in all remaining cases this branch of the program is bypassed by the introduction into the program of a special comparison element.

We must note that $\Delta\bar{y}_i^*$, corresponding to the $\Delta\bar{x}_i^*$, assignable in the /108 linear interpolator, cannot exceed the definite value $\Delta\bar{y}_{max} = \Delta\bar{x}_{max}$ because of structural considerations. If this condition is not satisfied, $\Delta\bar{x}_i^*$ are reduced by $0.2\Delta\bar{x}_i^*$. Comparison of the indication of the special counter with the number 3 provides for the computation of $\bar{d}$ four times: for $0.2\Delta\bar{x}_i^*$; $0.4\Delta\bar{x}_i^*$; $0.6\Delta\bar{x}_i^*$ and $0.8\Delta\bar{x}_i^*$. The result of the comparison is stored. With the computation of $\Delta\bar{y}_T$ using expression (8)

$$\bar{x}_T = \sum_{i=0,5}^{i} \Delta\bar{x}_i + 0.2\Delta\bar{x}_i^*,$$

where ι = 0.5, 1.5, 2.5,...,i, since with computation of $\Delta\bar{x}_i$ on each $(\bar{X}_{k+1}; \bar{X}_k)$ segment the coordinate origin is transferred to to the point with the coordinates $\bar{X}_k$; $\bar{Y}_k$. After the computation of each value of $|\bar{d}|$ a comparison of $|\bar{d}|$ with $|\bar{\delta}|$ is made.

Depending on the result of the comparison, we either transfer to the computation of the following value of $|\bar{d}|$ with $|\bar{\delta}| > |\bar{d}|$, or to the reduction of $\Delta\bar{x}_i^*$ by $0.2\ \Delta\bar{x}_i^*$ with $|\bar{\delta}| < |\bar{d}|$.

If the given value of $\Delta\bar{x}_i^*$ satisfies the condition $|\bar{\delta}| > |\bar{d}|$ in all four cases and prior to this $\Delta\bar{x}_i^*$, has not been diminished, we increase $\Delta\bar{x}_i^*$ by $0.2\ \Delta\bar{x}_i^*$ and perform all computations from the beginning.

Increasing is continued until $|\bar{d}|$ becomes greater than $|\bar{\delta}|$. In this case the preceding value of $\Delta\bar{x}_i^{\bullet}$, for which $|\bar{\delta}| > |\bar{d}|$ is printed out, where every time, after printing, a computation is made of the sum $\sum_{l=0.5}^{i} \Delta\bar{x}_l = \sum_{l=0.5}^{i-1} \Delta\bar{x}_l + \Delta\bar{x}_l$. If with the condition $|\bar{\delta}| > |\bar{d}|$ there was a reduction, we transfer to printing of the current results. Reduction of $\Delta\bar{x}_i^{\bullet}$ takes place in two cases: when the $\Delta\bar{y}_i^{\bullet}$, computed using equation (8) for the value of $\Delta\bar{x}_i^{\bullet}$, exceeded the limit Δy_{max} and when $|\bar{\delta}| < |\bar{d}|$ with verification of this condition after computation of $|\bar{d}|$. Reduction of $\Delta\bar{x}_i$ in the case $|\bar{\delta}| < |\bar{d}|$ for any of the values: $0.2\Delta\bar{x}_i^{\bullet}$; $0.4\Delta\bar{x}_i^{\bullet}$; $0.6\Delta\bar{x}_i^{\bullet}$ and $0.8\Delta\bar{x}_i^{\bullet}$, if there was no increase, continues until for all these values $|\bar{\delta}|$ becomes greater than $|\bar{d}|$. In this case the current value of $\Delta\bar{x}_i^{\bullet}$ is printed out. If there was a reduction, then with $|\bar{\delta}| < |\bar{d}|$ the preceding value is printed out.

Prior to printing, the values of $\Delta\bar{x}_i$ and $\Delta\bar{y}_i$ are converted by a special preliminary program from the binary notation system to binary-decimal. After printing of the values of $\Delta\bar{x}_i$ and $\Delta\bar{y}_i$ a comparison is made of the quantities $\sum_{l=0.5}^{i+1} \Delta\bar{x}_l$ and $(X_{k+1} - X_k)$. If these quantities are not equal, then we verify the sign of

$$\left(\sum_{l=0.5}^{i} \Delta\bar{x}_l + \Delta\bar{x}_i^{\bullet}\right) - (\bar{X}_{k+1} - \bar{X}_k).$$

If the difference is a negative quantity, a new value of $\Delta x_{i+1}^{\bullet} = \Delta x_l$ is assumed and all the computations discussed above are performed. However, when the difference is a positive quantity, this indicates transfer beyond the limits of the segment $[\bar{X}_{k+1} - \bar{X}_k]$.

Transfer beyond the limits $[\bar{X}_{k+1} - \bar{X}_k]$ to segment $[\bar{X}_{k+2} - \bar{X}_{k+1}]$, which is characterized by its coefficients A_{k+1}, B_{k+1} and C_{k+1}, can take place in two ways.

(1) If with transfer to the new segment $\Delta\bar{x}_{i+1}^{\bullet} \left(\sum_{l=0.5}^{i} \Delta\bar{x}_l + \Delta\bar{x}_{i+1}^{\bullet}\right) > \bar{X}_{k+1} - \bar{X}_k$ (fig. 4), in this case the preceding value of $\Delta\bar{x}_{i+1}$ and $\Delta\bar{y}_{i+1}$, is printed out, which

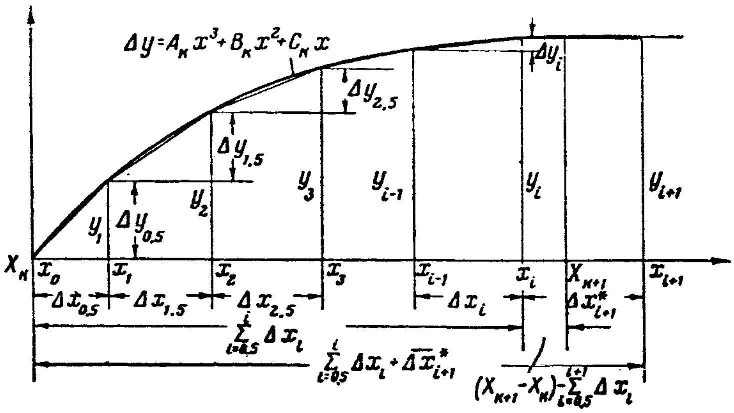

Figure 4

in the present case will be equal to zero, because each time after printing there is a restoration of zero in the cells from which the preceding values were printed out.

After comparison of $\sum_{l=0.5}^{i+1} \Delta\bar{x}_l$ with $(\bar{X}_{k+1}-\bar{X}_k)$ we find the difference $(\bar{X}_{k+1}-\bar{X}_k)-\sum_{l=0.5}^{i+1} \Delta\bar{x}_l$, which we take as the next value of $\Delta\bar{x}^*$, and we compute $|\bar{d}|$ for the values $0.2\,[(\bar{X}_{k+1}-\bar{X}_k)-\sum_{l=0.5}^{i+1} \Delta\bar{x}_l]$; $0.4\,[(\bar{X}_{k+1}-\bar{X}_k)-\sum_{l=0.5}^{i+1} \Delta\bar{x}_l]$;...; $0.8\,[(\bar{X}_{k+1}-\bar{X}_k)-\sum_{l=0.5}^{i+1} \Delta\bar{x}_l]$. If in all four cases $|\bar{d}| < |\bar{\delta}|$ we then print out the current results. There may be a case when the segment $(\bar{X}_{k+1}-\bar{X}_k) -\sum_{l=0.5}^{i+1}\Delta\bar{x}_l$ is too large; we reduce it by $0.2[(\bar{X}_{k+1}-\bar{X}_k)-\sum_{l=0.5}^{i+1} \Delta\bar{x}_l]$ until $|\bar{d}|$ is less than $|\bar{\delta}|$ in all four cases, then print out the current values of $\Delta\bar{x}_{i+1}$ and $\Delta\bar{y}_{i+1}$, and perform all the computations described above with the new difference.

(2) Transfer beyond the boundary $(\bar{X}_{k+1}-\bar{X}_k)$ of the segment occurs with increase of the next Δx^*_{i+1} by $0.2\,\Delta\bar{x}^*_{i+1}$ (fig. 5). In this case a printout is made of the preceding results, and after comparison of $\sum_{l=0.5}^{i+1} \Delta\bar{x}_l$ with $(\bar{X}_{k+1}-\bar{X}_k)$ a verification is made of the condition $\left(\sum_{l=0.5}^{l} \Delta\bar{x}_l+\Delta\bar{x}^*_{i+1}\right)-(\bar{X}_{k+1}-\bar{X}_k)$. As a result we find, as in the preceding case $(\bar{X}_{k+1}-\bar{X}_k)-\sum_{l=0.5}^{i+1} \Delta\bar{x}_l$.

After computation of $\bar{d}$ for 0.2; 0.4; 0.6 and $0.8\,(\bar{X}_{k+1}-\bar{X}_k)-\sum_{l=0.5}^{i+1} \Delta\bar{x}_l$ /110 and verification of the condition $|\bar{d}|<|\bar{\delta}|$, the current results are printed

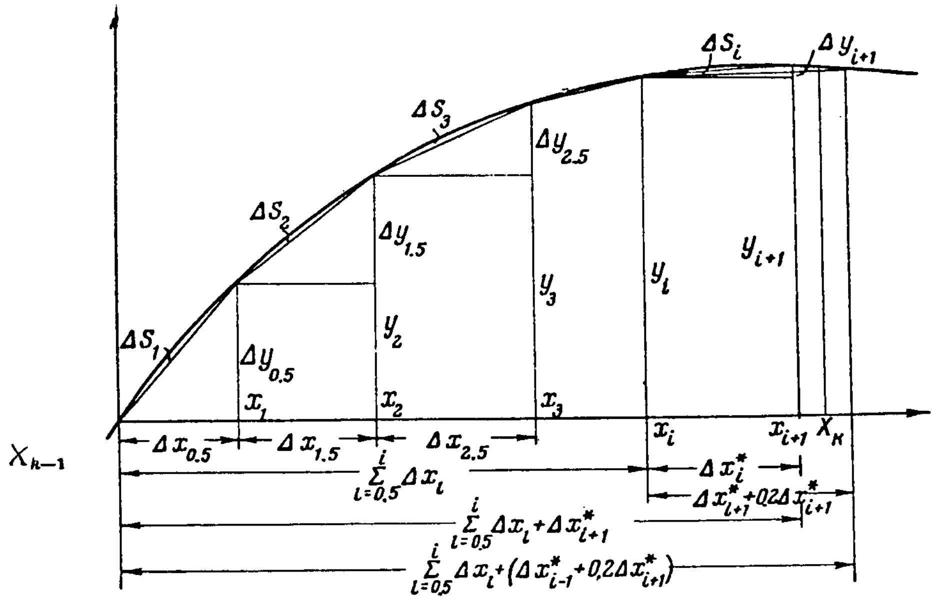

Figure 5

out and we find the new sum $\sum\limits_{l=0.5}^{i+2} \Delta \bar{x}_l$, which is equal to $(\bar{X}_{k+1} - \bar{X}_k)$. Consequently, we terminate the operational cycle with the given coefficients and, on the cycle termination command, transfer to the beginning of the program.

This program was computed out on the Ural computer, where for the computation of 36 segments, each of which was given by the equation $y = A_k x^3 + B_k x^2 + C_k x + D$, only 30 min was required, while the computation of a single check point by an experienced human computer using a desk keyboard machine required 60 min.

In conclusion we can state that the approximate method is more universal than the exact method, because for any continuous function φ(x) the basic program does not change, only the preparatory program for the computation of the function φ(x) changes. In the remaining particular cases the exact method may be more effective, since it is logically simpler than the approximate method.

The use of a universal digital computer for the automation of the process of the preparation of the program for the control of a machine tool is advisable, because it accelerates the process of the preparation of the program and reduces the number of possible errors.

REFERENCES

1. Bezikovich, A. S. Approximate Computations (Priblizhennyye vychisleniya). Gostekhizdat, 1953.

2. Krylov, A. N. Lectures on Approximate Calculations (Lektsii o priblizhennykh vychisleniyakh). Gostekhizdat, 1954.

3. Bondarenko, V. N., Plotnikov, I. T. and Polozov, P. P. Programing for the Ural Digital Computer (Programmirovaniye dlya tsifrovoy vychislitel'noy mashiny "Ural"). Gostekhizdat, 1957.

N66 34837

SPECIALIZED COMPUTER FOR THE SPECIFICATION OF THE MOTION OF A SYSTEM ALONG A STRAIGHT LINE, PARABOLA AND CIRCLE

V. V. Karibskiy

Specialized digital computers--interpolators--are used in cases when it is necessary to provide movement between two reference points along a straight line, parabola or circle, i.e., in accordance with the equations of the form /111

$$y = Bx; \tag{1}$$

$$y = Ax^2 + Bx; \tag{2}$$

$$y = \sqrt{R^2 + x^2}; \tag{3}$$

where A and B are constant coefficients, R is the radius of the circle.

Interpolation devices have found particularly wide application in systems for digital program control of milling machines for specifying the displacements of the working element.

In our case the interpolator generates control pulses to two-coordinate machine tools in the coordinates X and Y, distributed in time in accordance with the specified interpolation law, where with the transmission of a single pulse there is a displacement of the working element by unit length of the selected scale.

It can be shown that for the quadratic parabola with $\Delta x = 1$

$$\Delta y_1 = A + B:$$

$$\Delta y_k = \Delta y_{k-1} + 2A;$$

$$y_k = \sum_{k=1}^{k} \Delta y_k.$$

On the basis of these equations we propose a simple algorithm for the solution of equation (2).

To do this, it is sufficient to transmit, for the first pulse along the X-axis, a number of pulses along the Y-axis equal to the whole part of the quantity A + B and to store the fractional part; with the second pulse in the X-axis we send to the Y-axis a number of pulses equal to the whole part of the quantity A + B + 2A, and the fractional part is added to the fraction part of the quantity A + B. If the sum exceeds 1, we send to the Y-axis a single additional pulse, and so on.

Thus, with increase of the quantity x by unity, the preceding value /112 of the quantity Δy_k is changed by 2A, as a result of which we have Δy_{k+1}, from which the whole part is transmitted in the form of pulses.

For A = 0, we have the particular case of a parabola in the form of a straight line.

For the solution of equation (3) we can also propose a relatively simple algorithm, for whose realization we do not require either multiplication or extraction of the square root.

Let us assume that the movement along a circle starts from the point with the coordinates $x = 0$; $y = R$ and proceeds clockwise. It can be shown that the 1st pulse in the Y-axis must be given with $x_1^2 = 2R - 1$, the 2nd pulse with $x_2^2 - x_1^2 = 2R - 3$, and so on. For $\Delta x_k^2 = x_k^2 - x_{k-1}^2 = 2R - (2k - 1)$. With these conditions the error of specification of the circle will not exceed unity of the selected scale. However, in view of the discrete nature of the variation of quantity x, the equalities presented above cannot always be realized, since $x_1, x_2, \ldots, x_k$ may have fractional parts. It is necessary to change over to the inequalities $x_1^2 \geq 2R - 1$, $x_2^2 - x_1^2 \geq 2R - 3$, and so on; $x_i^2 - x_{i-1}^2 \geq 2R - (2k - 1)$, where $x_1, x_2, \ldots, x_i$ in equalities may have fractions.

On the basis of this discussion the solution of equation (3) can be performed as follows. Quantity x^2 is accumulated in the summator 1 (fig. 1). This is accomplished quite easily using the circuit proposed by Yermilov /113 (ref. 1). Then 2R - 1 is set in the summator 2. With transmission of an impulse in the X-axis, quantity 2R - 1 is subtracted from the content of summator 1; if the difference is negative, 2R - 1 is added again and the 2nd pulse is sent to the X-axis and x^2 is set in summator 1, i.e., the number 2^2 and the subtraction is performed again, and so on, until the difference becomes positive.

If after a successive subtraction the difference becomes positive or equal to zero, the addition of 2R - 1 to the summator content is not performed. A single pulse is sent to the Y-axis and the number 2 is subtracted from the quantity 2R - 1. We again then perform a subtraction from the content of summator 1 of the number 2R - 3, and continue the described sequence

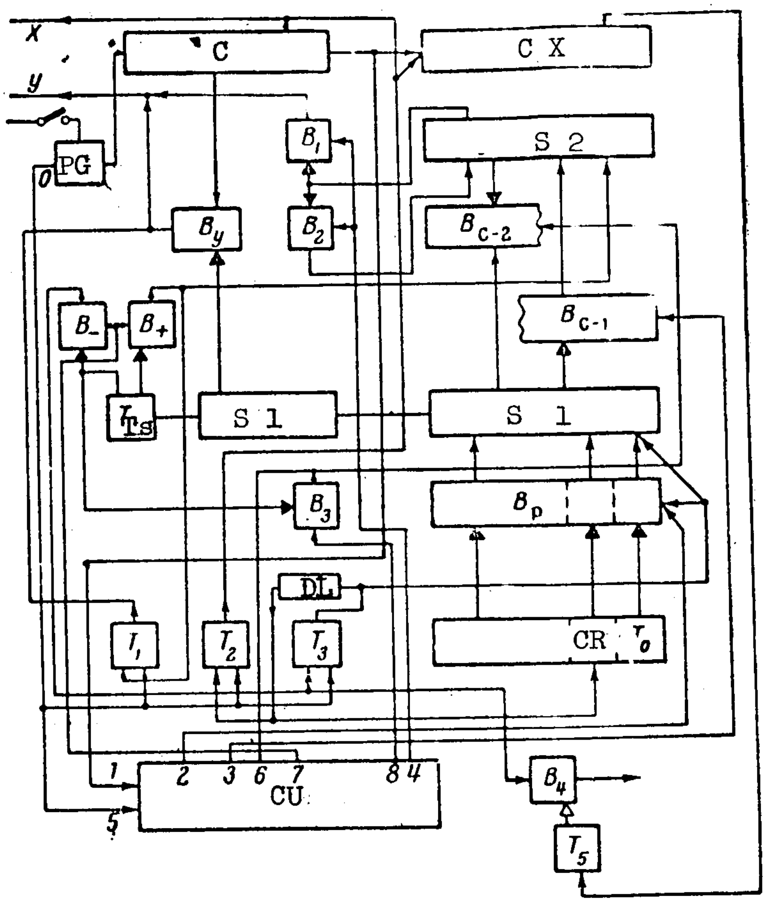

Figure 1. C, counter; S, summator; CU, control unit; CR, counter-register; PG, pulse generator; T_S, T_{sign}; DL, delay line; O, output.

of actions until the difference becomes negative. As soon as this occurs, we again send a pulse to the X-axis. In the process of the computation, at every moment of time there the quantity $x^2 - \sum_{k=1}^{\Delta y} 2R - (2k - 1)$, is formed in summator 1, where Δy is the number of pulses transmitted along the Y-axis and x is the number of pulses sent along the X-axis.

The circuit shown in simplified form in figure 1 is constructed in accordance with the algorithms described for the solution of equations (1)-(3).

The circuit consists of two summators of the accumulating type with transmission of the carry unit through the delay line (DL) from the lower place to the higher, a counter register, a counter for readout of the X-coordinate, a control unit and several auxiliary logic elements for the transmission of pulses. In the counter-register, the summators and in the readout counter the direction from the lower to the higher digits is shown

by arrows. The arrows on the lines connecting the blocks indicate in what direction pulses can flow in a given line, where it is assumed that a pulse cannot pass through the line against the arrow. The gates B_{C2}, B_{C1} and B_p are open, when the triggers controlling them are in the "1" position.

1. Interpolation of a Parabola

The interpolation of a parabola involves the operation of the counter-register, which operates only as a register (transfer of a pulse from place to place is forbidden), the gates of the register B_p, summator 1, gates of summator 1 - B_{C1}, summator 2, counter X, gates B_y and pulse generator PG which delivers pulses from output 0.

The initial values are introduced before beginning of the operation of the interpolator: A + B is entered in summator 1; 2A in the counter-register; in the X-counter in the supplementary code Δx is entered--the magnitude of the projection of the interpolation segment of the X-axis, expressed by a number of pulses. In addition, the direction of the movement along the X-axis is specified; the direction of movement along the Y-axis is determined by the automatic circuit from the sign of the contents of summator 1.

Then the generation of the parabola proceeds in accordance with the described algorithm. After each elementary cycle, the whole part (wp) of Δy_k, located in summator 1 (wp), with the aid of the pulse generator PG and the linear interpolator (counter, B_y and summator 1 (wp)) is delivered to the Y-axis in the form of a number of pulses, while during this time a single pulse is sent to the X-axis.

The fractional parts of the increments Δy are summed in summator 2, and as soon as unity is accumulated there, an additional pulse formed as the result of the overflow of summator 2 is applied to the Y-axis. The formation of the following increment Δy_{k+1} is accomplished by the addition from the counter-register of the number 2A to summator 1 through gates B_p, while the fractional part of Δy_{k+1} is added to the contents of summator 2 through gates B_{C1}. All arithmetic operations take place in the interval between two pulses of generator GP with the aid of the series of pulses delived by /114 by the control unit, which by input 1 is triggered by the pulse of the termination of the elementary cycle, after which, sequentially in time from the outputs 2, 3 and 4, three pulses are applied to the circuit to perform the arithmetic operations.

2. Interpolation of a Circle

For the generation of the circle we basically use the same blocks, namely the X-counter, summator 2, gates B_{c-2}, triggers T_1 - T_3, gates B_-, B_+, B_3, B_4, T_{sign}, summator 1, counter-register, delay line (DL) and pulse generator (PG). The trigger of the lowest place of the counter-register T_0 does not participate in the operation and is in "zero" position all the time.

Consider the case when the motion begins from the point with the coordinates x = 0, y = R and proceeds in clockwise direction.

Prior to the beginning of the operation, in the X-counters in the auxiliary code we introduce the magnitude of the displacement along the X-axis, i.e., Δx, in summator 2 we enter quantity 2R - 1 and in summator 1 and in the counter-register--zero. Prior to initiation of the operation, T_1 and T_2 are set to the "zero" state, and T_3 is set to "unity." The first pulse of the generator establishes T_3 in the "zero" state; here the pulse from the output of T_3 sets the number 1 in summator 1 and in the counter-register, while T_2 is set in the "unity" state. Then we proceed to subtract from the content of summator 1 the content of summator 2; if the difference is negative, trigger T_3 is set to the "unity" state with the aid of gate B_-. Then the content of summator 1 is added to the content of summator 2, i.e., we recover 1 in summator 1.

The second generator pulse sets T_2 and T_3 to "zero." Pulses go from the output of T_2 to the X-axis and to the X-counter, and as a result of setting T_3 to the "zero" state, the number 2 is formed in the counter-register, the number 4 is formed in summator 1, i.e., the square of 2. Furthermore, in accordance with the algorithm, 2R - 1 is subtracted from the number 4 and, if the difference is negative, the described sequence of operations is repeated.

With formation of a positive difference in summator 1, with the aid of trigger T_{sign} and gate B_+ the number 2 is subtracted from the content of summator 2, i.e., the number 2R - 3 is formed, and the trigger T_1 is set to "unity." The addition of the content of summator 2 to the content of summator 1 is forbidden in this cycle, i.e., the recovery of the content of summator 1 does not take place. The next generator pulse sets T_1 in the "zero" state, as a result of which a pulse is sent from the output of T_1 to the Y-axis, etc.

All these operations are accomplished with the aid of a sequence of three pulses delivered by the control block at the outputs 6, 7 and 8 in response to each generator pulse arriving at input 5.

Thus, in accordance with the sign of the difference formed in summator 1, the generator pulses are distributed to the X- and Y-axes in accordance with the equation of the circle. In the case when movement along the circle begins from an arbitrary point with the coordinates x_0, y_0, the initial values (initial settings) must be the following: the value of the given displacement Δx in the auxiliary code is set in the X-counter; $2y_0 - 1$ is in summator 2; $1 - x_0^2 - R^2 + y_0^2$ in summator 1; x_0 in the counter-register, where y_0 is equal to the value of y'_0, increased to the nearest whole number.

The maximal radius of the circle is $R = 2^{n-1}$, where n is the number of places of summator 2 without account for the sign place.

REFERENCE

1. Yermilov, B. L. Some types of digital functional converters (Nekotoryye tipy tsifrovykh funktsional'nykh preobrazovateley). Conference on the Theory and Application of Discrete Automatic Systems. Izd-vo AN SSSR, 1958.

AIRCRAFT LONGITUDINAL STABILITY WITH AN AUTOPILOT HAVING LAG

V. S. Kislyakov

With the aid of the asymptotic methods of Krylov and Bogolyubov (refs. 1 and 2) a study is made of the longitudinal stability of the short-period motion of an aircraft controlled by an autopilot. The presence of a time lag is assumed in the autopilot (ref. 3). /115

The longitudinal stability of an aircraft on the assumption that the autopilot has a time lag was considered in references 3-6. The present paper considers this problem in two versions: linear and nonlinear. The studies are made with the aid of the asymptotic methods developed by Academicians Krylov and Bogolyubov. The justification for the possibility of the use of the asymptotic methods is contained in references 7 and 8.

Equations of Motion

Consider the controllable system consisting of an aircraft and autopilot without feedback, whose short-period motion in pitch is described by the system of combined differential-difference equations

$$\left.\begin{aligned} \ddot{\vartheta}(t) + \overline{M}_z^{\omega_z}\dot{\vartheta}(t) + \overline{M}_z^{\alpha}\vartheta(t) + \overline{M}_z^{\delta}(t) &= 0; \\ \dot{\delta}(t) &= f[\sigma(t-\tau)], \\ \sigma(t) &= k_{\vartheta}\vartheta(t) + k_{\dot{\vartheta}}\dot{\vartheta}(t) + k_{\ddot{\vartheta}}\ddot{\vartheta}(t) \end{aligned}\right\} \qquad (1)$$

where ϑ is the pitch angle;

δ is the elevator deflection angle;

$\overline{M}_z^{\omega_z}$ $\overline{M}^{\alpha}$, $\overline{M}_z^{\delta}$ are the aerodynamic coefficients;

$k_{\vartheta}, k_{\dot{\vartheta}}, k_{\ddot{\vartheta}}$ are the autopilot transfer numbers (adjustments);

τ is the constant time lag.

It is assumed that $f[\sigma(t - \tau)]$ belongs to the subclass A' of the class A of functions (ref. 9), satisfies the Dirichlet conditions and can be represented in the form of a linear part and a small nonlinear contribution:

*Hereafter we consider $+k_{\ddot{\vartheta}}\ddot{\vartheta}(t)$, the case $k_{\ddot{\vartheta}} = 0$.

$$f[\sigma(t-\tau)] = k\sigma(t-\tau) + \varepsilon\varphi[\sigma(t-\tau)], \tag{2}$$

where $k = \left[\frac{\partial f[\sigma(t-\tau)]}{\partial\sigma(t-\tau)}\right]_{\sigma(t-\tau)=0}$;

ϵ is a small parameter.

Equivalent Linearization of the System of Equations (1) Using the Krylov-Bogolyubov Method

Using the Krylov-Bogolyubov equivalent linearization method (ref. 7, see also refs. 4 and 10), we shall look for the linear element equivalent in the first approximation to the nonlinear element (2). We write the differential equation of the linear element in the form /116

$$\dot{\delta}(t) = a_1(A)\sigma(t) + a_2(A)\dot{\sigma}(t), \tag{3}$$

where $a_1(A)$ and $a_2(A)$ are the coefficients of the linear element, dependent on amplitude A.

According to reference 7, coefficients $a_1(A)$ and $a_2(A)$ are determined by the equations

$$\left.\begin{aligned} a_1(A) &= \left(k + \frac{\varepsilon q_1(A)}{A}\right)\cos\omega\tau - \frac{\varepsilon h_1(A)}{A}\sin\omega\tau; \\ a_2(A) &= -\left(k + \frac{\varepsilon q_1(A)}{A}\right)\frac{\sin\omega\tau}{\omega} - \frac{\varepsilon h_1(A)}{A\omega}\cos\omega\tau, \end{aligned}\right\} \tag{4}$$

where $q_1(A)$ and $h_1(A)$ are the coefficients of the expansion in a Fourier series for $n = 1$.

Let $\varphi[\sigma(t - \tau)]$ be an odd function, which with an adequate degree of accuracy can be represented as

$$\varepsilon\varphi[\sigma(t-\tau)] \approx -\rho\sigma^3(t-\tau), \tag{5}$$

where ρ is a small constant (taken as a small parameter).

In this case coefficients $a_1(A)$ and $a_2(A)$ will be determined by the formulas

$$\left.\begin{aligned} a_1(A) &= \left(k - \frac{3}{4}\rho A^2\right)\cos\omega\tau; \\ a_2(A) &= -\left(k - \frac{3}{4}\rho A^2\right)\frac{\sin\omega\tau}{\omega}. \end{aligned}\right\} \tag{6}$$

The combined equivalent system of equations will be

$$\left.\begin{array}{l}\ddot{\vartheta}(t)+\overline{M}_z^{\omega_z}\dot{\vartheta}(t)+\overline{M}_z^{\alpha}\vartheta(t)+\overline{M}_z^{\delta}\delta(t)=0;\\ \dot{\delta}(t)=\left(k-\frac{3}{4}\rho A^2\right)\cos\omega\tau\cdot\sigma(t)-\left(k-\frac{3}{4}\rho A^2\right)\frac{\sin\omega\tau}{\omega}\cdot\dot{\sigma}(t);\\ \sigma(t)=k_{\vartheta}\vartheta(t)+k_{\dot{\vartheta}}\dot{\vartheta}(t).\end{array}\right\} \quad (7)$$

By means of exclusion of $\sigma(t)$ and $\delta(t)$, the system of equations (7) can be reduced to a differential equation of third order

$$\dddot{\vartheta}(t)+B_1\ddot{\vartheta}(t)+B_2\dot{\vartheta}(t)+B_3\vartheta(t)=0; \quad (8)$$

where

$$B_1=\overline{M}_z^{\omega_z}-\left(k-\frac{3}{4}\rho A^2\right)k_{\dot{\vartheta}}\overline{M}_z^{\delta}\frac{\sin\omega\tau}{\omega};$$

$$B_2=\overline{M}_z^{\alpha}+\left(k-\frac{3}{4}\rho A^2\right)k_{\dot{\vartheta}}\overline{M}_z^{\delta}\cos\omega\tau-\left(k-\frac{3}{4}\rho A^2\right)k_{\vartheta}\overline{M}_z^{\delta}\frac{\sin\omega\tau}{\omega};$$

$$B_3=\left(k-\frac{3}{4}\rho A^2\right)k_{\vartheta}\overline{M}_z^{\delta}\cos\omega\tau.$$

Following the method of asymptotic approximations of Krylov and Bogolyubov, we shall look for the periodic solution of the system of equations (1) in the form of the formal series in the small parameter ρ /117

$$\vartheta(t)=A_i\cos\psi_i+\rho u_1(A_i\psi_i)+\rho^2u_2(A_i\psi_i)+\ldots,\quad i=1,2,3 \quad (9)$$

where $u_1(A,\psi)$, $u_2(A,\psi),\ldots$ are periodic functions with the period 2π. An additional condition expressed in the absence of the first harmonic with expansion of these functions in Fourier series is imposed on the functions.

We shall discuss first the linear version of the problem, which is of known independent interest.

Linear Version (Generating System $\rho = 0$)

In this version the controllable system aircraft-autopilot is described by the system of so-called equations of the first approximation

$$\left.\begin{array}{l}\ddot{\vartheta}(t)+\overline{M}_z^{\omega_z}\dot{\vartheta}(t)+\overline{M}_z^{\alpha}\vartheta(t)+\overline{M}_z^{\delta}\delta(t)=0;\\ \delta(t)=p_1\vartheta(t-\tau)+p_2\dot{\vartheta}(t-\tau),\end{array}\right\} \quad (10)$$

where $p_1 = \bar{k}k_\vartheta$, $p_2 = \bar{k}k_{\dot\vartheta}$, $\bar{k} = k - \Delta k\,(\Delta k \to 0$ as $\rho \to 0)$.

In this case the equivalent linear equation will be

$$\dddot{\vartheta}(t) + c_1\ddot{\vartheta}(t) + c_2\dot{\vartheta}(t) + c_3\vartheta(t) = 0, \tag{11}$$

where

$$c_1 = \overline{M}_z^{\omega_z} - p_2\overline{M}_z^{\delta}\frac{\sin\omega\tau}{\omega};$$

$$c_2 = \overline{M}_z^{\alpha} + p_2\overline{M}_z^{\delta}\cos\omega\tau - p_1\overline{M}_z^{\delta}\frac{\sin\omega\tau}{\omega};$$

$$c_3 = p_1\overline{M}_z^{\delta}\cos\omega\tau.$$

The latter is obtained from equation (8) with $\rho = 0$.

It is known that the region of asymptotic stability of the aircraft-autopilot system constructed in the plane of the transfer numbers of the autopilot p_1 and p_2 is limited by a boundary curve. This is the so-called curve of the D-partition (ref. 11). The latter separates the region of asymptotic stability of the system from the region of periodic oscillations. Let us determine this curve. In order that the differential equation (11) have a periodic solution, it is sufficient that the characteristic equation corresponding to it

$$\lambda^3 + c_1\lambda^2 + c_2\lambda + c_3 = 0 \tag{12}$$

have purely imaginary roots.

Setting $\lambda = j\omega$ and separating the equation into real and imaginary parts, we find

$$\left.\begin{aligned} -\omega^3 + \omega c_1 = 0;\\ -\omega^2 + c_3 = 0.\end{aligned}\right\} \tag{13}$$

Therefore, the numerical values of p_1 and p_2, which determine the points of the boundary of the region of asymptotic stability (points of the boundary of the region of periodic oscillations), are found from the equations /118

$$\left.\begin{aligned} p_1 &= \frac{\omega\,[\overline{M}_z^{\omega_z}\omega + (\overline{M}_z^{\alpha} - \omega^2)\sin\omega\tau\cos\omega\tau - \overline{M}_z^{\omega_z}\omega\sin^2\omega\tau]}{\overline{M}_z^{\delta}\cos\omega\tau};\\ p_2 &= \frac{(\omega^2 - \overline{M}_z^{\alpha})\cos\omega\tau + \overline{M}_z^{\omega_z}\omega\sin\omega\tau}{\overline{M}_z^{\delta}}.\end{aligned}\right\} \tag{14}$$

Determination of the Critical and Permissible Autopilot Lag Times

Let us further determine τ_{cr} (critical) which, as experience shows, has a significant effect on the permissible adjustments of the autopilot and particularly on the quantity p_2. For simplicity let us consider the case when $p_1 = 0$. Then equation (11) has the form

$$\ddot{\vartheta}(t) + \overline{M}_z^{\omega_z}\dot{\vartheta}(t) + \overline{M}_z^{\alpha}\vartheta(t) + p_2\overline{M}_z^{\delta}\vartheta(t-\tau) = 0. \tag{15}$$

We introduce as a new independent variable the dimensionless time $u = \frac{t}{0,64\tau}$.

Then we have
$$\frac{d}{dt} = \frac{1}{0.64\tau}\frac{d}{du};$$
$$\frac{d^2}{dt^2} = \frac{1}{0.64^2\tau^2}\frac{d^2}{du^2}.$$

The transformed equation will be

$$\ddot{\vartheta}(u) + 0.64\tau\overline{M}_z^{\omega_z}\dot{\vartheta}(u) + 0.64^2\tau^2\overline{M}_z^{\alpha}\vartheta(u) + 0.64^2\tau^2 p_2\overline{M}_z^{\delta}\vartheta\left(u - \frac{\pi}{2}\right) = 0. \tag{16}$$

Using the Krylov-Bogolyubov method of equivalent linearization, we transform equation (16) to the form

$$\ddot{\vartheta}(u) + a_1\dot{\vartheta}(u) + a_2\vartheta(u) = 0, \tag{17}$$

where

$$a_1 = 0.64\tau\overline{M}_z^{\omega_z} - \frac{0.64^2\tau^2 p_2\overline{M}_z^{\delta}\sin\frac{\pi}{2}\Omega}{\Omega};$$
$$a_2 = 0.64^2\tau^2\overline{M}_z^{\alpha} + 0.64^2\tau^2 p_2\overline{M}_z^{\delta}\cos\frac{\pi}{2}\Omega.$$

The characteristic equation corresponding to (17) has the form

$$\lambda^2 + a_1\lambda + a_2 = 0. \tag{18}$$

The boundary of the region of stability of equation (18) can be determined from the condition

$$\Delta_{n-1} = a_1 = 0, \tag{19*}$$

where Δ_{n-1} is the (n - 1)th Hurwitz determinant.

Condition (19) obtains with

$$\overline{M}_z^{\omega_z} - 0.64\tau p_2 \overline{M}_z^{\delta} \frac{\sin\frac{\pi}{2}\Omega}{\Omega} = 0. \tag{20}$$

Thus, τ_{cr} will be equal to /119

$$\tau_{cr} = \frac{\overline{M}_z^{\omega_z}}{0.64 p_2 \overline{M}_z^{\delta} \frac{\sin\frac{\pi}{2}\Omega}{\Omega}}. \tag{21}$$

Since $\sin\frac{\pi}{2}\Omega/\Omega$ is a limited quantity $0 \leqslant \sin\frac{\pi}{2}\Omega/\frac{\pi}{2}\Omega \leqslant 1$, a rough estimate of τ_{cr} can be obtained from formula

$$\tau_{cr} \approx \frac{\overline{M}_z^{\omega_z}}{p_2 \overline{M}_z^{\delta}}. \tag{22}$$

This rough estimate does not differ from the exact value by more than 20 percent with the variation $0 \leq \Omega \leq 0.7$.

Let us determine the permissible value of the lag time τ_{per} for which there is asymptotic stability of the aircraft-autopilot system. This is guaranteed by the inequality

$$\Delta_{n-1} = a_1 > 0, \; a_2 > 0. \tag{23}$$

We rewrite inequality (23) in the form

$$\overline{M}_z^{\omega_z} - 0.64\tau p_2 \overline{M}_z^{\delta} \frac{\sin\frac{\pi}{2}\Omega}{\Omega} > 0. \tag{24}$$

---

*The case $a_2 = 0$ is of less interest.

Thus, τ_{per} (permissible) is determined from the condition

$$\tau_{per} < \tau_{cr} = \frac{\overline{M}_z^{\omega_z}}{0.64 p_2 \overline{M}_z^{\delta} \dfrac{\sin\frac{\pi}{2}\Omega}{\Omega}} \tag{25}$$

or roughly from the condition

$$\tau_{per} < \tau_{cr} \approx \frac{\overline{M}_z^{\omega_z}}{p_2 \overline{M}_z^{\delta}}. \tag{26}$$

EXAMPLE. Let us take specific aerodynamic coefficients corresponding to a turbojet fighter (ref. 12) which has the following specifications: G = 6900 kg; L = 10.6 kg; S = 21.4 m^2; b_A = 1.95 m; the aerodynamic coefficients with $C_y = 0.4$; $\overline{M}_z^{\omega_z *} = 14.3$; $\overline{M}_z^{\alpha} = 115.5$. Coefficient $\overline{M}_z^{\delta}$, computed from the equation for the value $m_z^{\delta} = -0.01$, taken from the graph (see ref. 12 p. 225), is equal to[1]

$$\overline{M}_z^{\delta} = -\frac{\mu m_z^{\delta}}{\overline{r}^2} = \frac{324 \cdot 0.01 \cdot 57.3}{0.92} = 200.$$

Substituting the numerical values of the coefficients into (14) and picking various values of ω, we determine with the aid of the D-partition curve the region of stability of the considered system in the plane of the transfer numbers of the autopilot p_1 and p_2. /120

The results of the computation for values of the lag τ equal to 0, 0.01, 0.1, 0.2 and 0.4 sec are presented in the figure. From the figure we see that with increase of τ the region of stability of the aircraft-autopilot system is notably decreased.

For comparison we also present the numerical estimate which is obtained from equation (22) and the results of an exact calculation for the values of the autopilot transfer numbers $p_1 = 0$, $p_2 = 7.13$ and $p_1 = 0$, $p_2 = 0.9$. In the first case τ_{cr} = 0.01 sec (exact result is τ_{cr} = 0.01 sec). In the second case τ_{cr} = 0.08 sec (exact result is τ_{cr} = 0.1 sec).

---

*In the notation of reference 12, a_1 and a_2 are used in place of $\overline{M}_z^{\omega_z}$, $\overline{M}_z^{\alpha}$.

[1] The numerical value of $\overline{M}_z^{\delta}$, computed in reference 6 and equal to 3.54 must be considered in error, because in its calculation the author did not take account of the dimensionality of the remaining aerodynamic coefficients.

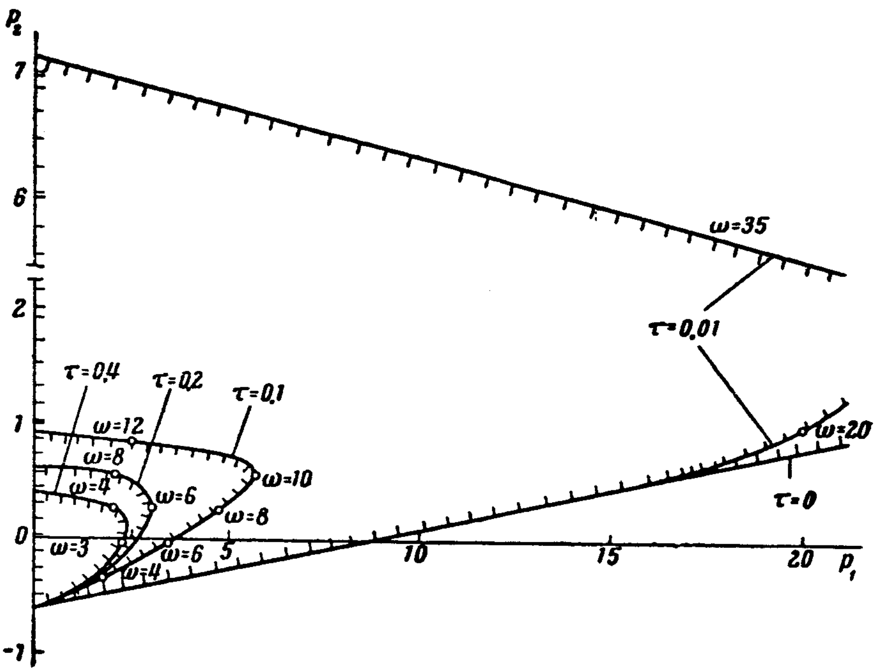

D-partition curves for various τ, constructed in the plane of autopilot transfer numbers.

Let us compare this numerical estimate of τ_{per} with that obtained using the Razumikhin equations from the stability conditions obtained by Lyapunov's method (ref. 6). For the values $p_1 = 0.0175$, $p_2 = 0.35$ and $\overline{M}_z^\delta = 200$, $\tau_{per} < \tau_{cr}$, the value found using the Krylov-Bogolyubov method[1] will be $\tau_{per} < 0.4$ sec. Using Razumikhin equations for the values $c_1 = 1$, $c_2 = 20$ and $\overline{M}_z^\delta = 3.54$ ($p_1 M_z^\delta = c_1 \overline{M}_z^\delta$; $p_2 \overline{M}_z^\delta = c_2 \overline{M}_z^\delta$), the maximal permissible value of the lag $\tau_{per\ max} = 0.017$ sec. Thus, the estimates determined using the Razumikhin equations are quite rough.

Nonlinear Version ($\rho \neq 0$)

Let us turn to equation (8). With fixed values of the amplitude A, equation (8) is a linear differential equation. Its corresponding characteristic equation will be /121

$$\lambda^3 + B_1\lambda^2 + B_2\lambda + B_3 = 0. \tag{27}$$

[1]In the linear version the Krylov-Bogolyubov method gives an exact result (ref. 8).

Let us determine the periodic oscillations (auto-oscillations) which are possible on the boundary of the region of asymptotic stability of the aircraft-autopilot system. Setting $\lambda = j\omega$ in equation (27) and dividing the equation into real and imaginary parts, we obtain

$$\left.\begin{aligned} -\omega^3 + B_2\omega = 0; \\ -\omega^2 B_2 + B_3 = 0. \end{aligned}\right\} \tag{28}$$

Substituting the values of the coefficients B_1, B_2 and B_3, we find the expression for the amplitude of the periodic oscillations

$$A = \left(\frac{k\overline{M}_z^{\delta} (\omega k_{\dot{\vartheta}} \sin \omega\tau + k_{\vartheta} \cos \omega\tau) - \omega^2 \overline{M}_z^{\omega_z}}{\frac{3}{4} \rho \overline{M}_z^{\delta} (\omega k_{\dot{\vartheta}} \sin \omega\tau + k_{\vartheta} \cos \omega\tau)} \right)^{1/2}. \tag{29}$$

The frequencies of the periodic oscillations ω_i are determined from a graphical solution of the transcendental equation

$$\operatorname{tg} \omega\tau = -\frac{k_{\vartheta}(\omega^2 - \overline{M}_z^{\alpha}) - \overline{M}_z^{\omega_z} k_{\dot{\vartheta}} \omega^2}{\omega [k_{\dot{\vartheta}}(\omega^2 - \overline{M}_z^{\alpha}) + k_{\vartheta} \overline{M}_z^{\omega_z}]}. \tag{30}$$

Thus, as the first approximation for the solution of equation (1), we have the expression

$$\vartheta(t) = A_i \cos \omega_i t \quad (i = 1, 2, 3), \tag{31}$$

in which the amplitudes A_i $(i = 1, 2, 3)$ are determined from equation (29), and the corresponding frequencies which satisfy equations (29) and (30) are determined from the graphical solution of the transcendental equation (30). Similar to the way this was done for the equation of the first order in reference 7, it is easy to show that only a finite number of frequencies m = 3 satisfy equations (29) and (30).

With the second approximation of the solution of equation (1), neglecting quantities of the order of smallness of ρ^2, we have

$$\vartheta(t) = A_i \cos \omega_i t + \rho u_1(A_i, \psi_i) \quad (i = 1, 2, 3). \tag{32}$$

In our case

$$u_1 = \frac{1}{32}\frac{\cos 3\omega\,(t-\tau)}{\omega^2}. \tag{33}$$

Then the second approximation has the form

$$\vartheta(t) = A_i \cos\omega_i t + \frac{\rho}{32}\frac{\cos 3\omega_i\,(t-\tau)}{\omega_i^2} \tag{34}$$

and so on.

Stability Analysis of the Periodic Solutions

For the study of the stability of the periodic solutions, we consider /122 the (n - 1)th Hurwitz determinant of equation (27)

$$R_{(A)} = \Delta_2 = B_1 B_2 - B_3. \tag{35}$$

Since $R_{(A)}$ is a function of the amplitude, the oscillations described by equation (27) can be stable with some values of A and unstable with others. The oscillations on the boundary of the region of asymptotic oscillatory stability will be stable if

$$\left(\frac{dR_{(A)}}{dA}\right)_{R(A)=0} = \left(\frac{\partial R_{(A)}}{\partial A}\right)_{R(A)=0} + \left(\frac{\partial R_{(A)}}{\partial \omega}\right)_{R(A)=0}\frac{d\omega}{dA} > 0. \tag{36}$$

Similar to the way this is done in reference 7, i.e., determining from expression (35) the values of $\frac{\partial R_{(A)}}{\partial A}$ and $\frac{\partial R_{(A)}}{\partial \omega}$ and using for finding $\frac{d\omega}{dA}$ any of the equalities (28), it is easy to show that in the considered case $\left(\frac{dR_{(A)}}{dA}\right)_{A\to 0} = 0$, i.e., A = 0 is the bifurcation point.

The oscillations are stable in the small, since the quantity $\frac{dR_{(A)}}{dA}$ with $A \to 0$ remains positive. In this case, according to Bautin, the boundary is "safe" in the small.

Conclusions

From the study using the Krylov-Bogolyubov methods of the longitudinal stability of an aircraft with autopilot performing short-period motions, we can draw the following conclusions.

1. The presence of lag in the autopilot has a significant effect on the stability of the aircraft. This effect is manifested primarily in a considerable narrowing of the region of stability of the system as constructed in the plane of the transfer numbers of the autopilot.

2. Neglect of the lag can lead to the selection of autopilot adjustments outside the region of asymptotic stability of the system, i.e., to instability.

3. The permissible magnitude of the lag in the autopilot $\tau_{per} < \tau_{cr}$ depends on and is determined by the value of the coefficients $\overline{M}_z^{\omega_z}$ (see ref. 12) and $\overline{M}_z^{\delta}$. With a given value of the lag τ the aerodynamic coefficients $\overline{M}_z^{\omega_z}$ and $\overline{M}_z^{\delta}$ determine the permissible adjustments of the autopilot.

4. The steady-state periodic oscillations (auto-oscillations) which occur on the boundary of the region of asymptotic stability of the considered system are stable in the small, i.e., the boundary according to Bautin is safe in the small.

REFERENCES

1. Krylov, N. M. and Bogoluybov, N. N. Introduction to Nonlinear Mechanics (Vvedeniye v nelineynuyu mekhaniku). Izd-vo AN USSR, 1937.

2. Bogolyubov, N. N. and Metropol'skiy, Yu. A. Asymptotic Methods in the Theory of Nonlinear Oscillations (Asimptoticheskiye metody v teorii nelineynykh kolebaniy). Gostekhizdat, 1955.

3. Kotel'nikov, V. A. Longitudinal Stability and Controllability of an Airplane with the AVP-12 Autopilot (Prodol'naya ustoychivost' i upravlyayemost' samoleta s avtopilotom AVP-12). Trudy, No. 2, 1941.

4. Tsypkin, Ya. Z. Systems with Feedback Lag (Sistemy s zapazdyvayushchey obratnoy svyaz'yu). Trudy NISO, No. 24, 1947.

5. Salukvadze, N. Ye. Effect of Typical Nonlinearities on Autopilot Adjustment (Vliyaniye nekotorykh tipichnykh nelineynostey na nastroyku avtopilota). Avtomatika i telemekhanika, Vol. 20, No. 5, 1959.

6. Razumikhin, B. S. Application of the Lyapunov Method to Some Motion Stability Problems (Primeneniye metoda Lyapunova k nekotorym zadacham ustoychivosti dvizheniya). Dissertation, IM AN SSSR, 1958.

7. Kislyakov, V. S. Application of the Krylov-Bogolyubov Method of Construction of Asymptotic Approximations for the Study of Systems with Lag (Primeneniye metoda postroyeniy asimptoticheskikh priblizheniy Krylova i Bogolyubova dlya issledovaniya sistem s zapazdyvaniyem). Avtomat. i telemekh., No. 4, 1960.

8. --- Justification for Application of the Method of Harmonic Linearization for the Study of Periodic Oscillations of Systems with Lag (Obosnovaniye primeneniya metoda garmonicheskoy linearizatsii dlya issledovaniya periodicheskikh kolebaniy sistem s zapazdyvaniyem). Avtomat. i telemekh., No. 11, 1960.

9. Letov, A. M. Stability of Nonlinear Control Systems (Ustoychivost' nelineynykh reguliruyemykh sistem). Gostekhizdat, 1955.

10. Popov, Ye. P. Approximate Analysis of Auto-Oscillations and Forced Oscillations of Nonlinear Systems (Priblizhennoye issledovaniye avtokolebaniy i vynuzhdennykh kolebaniy nelineynykh sistem). Izv. AN SSSR, OTN, No. 5, 1957.

11. Neymark, Yu. I. D-Partition of Quasipolynomial Space (D-razbiyeniye prostranstva kvazipolinomov). PMM, Vol. 13, 1949.

12. Ostoslavskiy, I. V. and Kalachev, V. S. Airplane Longitudinal Stability and Control (Prodol'naya ustoychivost' i upravlyayemost' samoleta). Gostekhizdat, 1951.

13. Kislyakov, V. S. Some Questions on the Theory of Systems of Automatic Control with Lag Described by Linear Differential Equations with Lagging Argument (Nekotoryye voprosy teorii sistem avtomaticheskogo regulirovaniya s zapazdyvaniyem, otobrazhayemyye lineynymi differentsial'nymi uraveniyami s zapazdyvayushchim argumentom). IN: Automatic Control (Avtomaticheskoye upravleniye), Izd-vo AN SSSR, 1960.

N66 34839

A METHOD OF SYNTHESIS OF CONTROLLED SYSTEMS

A. I. Moroz

1. Statement of the Problem

We have the system of differential equations describing the controlled /124 system

$$\dot{\eta}_k = \sum_{\alpha=1}^{n} b_{k\alpha}\eta_\alpha + m_k\xi \quad (k = 1, \ldots, n). \tag{1}$$

Here η_k are the generalized coordinates of the system; ξ is the control coordinate. The coefficients b_{ka} and m_k are considered given. Consider the phase space of the variables $\eta_1, \eta_2, \ldots, \eta_n, \xi$. We select in this space the initial point $M^0(\eta_1^0, \eta_2^0, \eta_n^0, \ldots, \xi^0)$ (we consider that $(\eta_1^0)^2 + (\eta_2^0)^2 + \ldots + (\eta_n^0)^2 + (\xi^0)^2 \neq 0$].).

A. M. Letov posed the problem amounting to the following. We are required to determine the control law ξ for the system such that the imaging point from the initial position M^0 arrives on the sphere of arbitrarily selected radius δ after the specified time t^* and for all $t > t^*$ remains within this sphere.

2. Method of Solution

We note that the equation of the control has not yet been specified. We consider that the closed system system-control has the property that the differential equations corresponding to it have the first integral:

$$\eta_1^2 + \eta_2^2 + \ldots + \eta_n^2 + \xi^2 = R_0^2 e^{-2\rho t}, \tag{2}$$

where

$$R_0^2 = \sum_{k=1}^{n} (\eta_k^0)^2 + (\xi^0)^2, \quad \rho > 0.$$

By suitable choice of ρ, we can for fixed $\delta > 0$ and time t^* make $\Sigma\eta_k^2 + \xi^2 \leqslant \delta$ and this will be satisfied for all $t \geq t^*$.

Each differential equation must have a control variable in order to satisfy (2). For this we differentiate equation (2) with respect to t and, replacing in the left side all $\dot{\eta}_k (k = 1, 2, \ldots, n)$ from (1), and in the right side replacing $R_0^2 e^{-2\rho t}$ from (2), we express $\dot{\xi}$ in terms of the remaining variables.

Thus we obtain the differential equation of the control /125

$$\dot{\xi} = -\sum_{k=1}^{n} m_k \eta_k - \rho\xi - \frac{\sum_{k}^{n}\sum_{\alpha}^{n} (b_{k\alpha} + \delta_{k\alpha}\rho)\,\eta_k\eta_\alpha}{\xi},$$

where δ_{ka} is the Kronecker symbol.

Thus, the differential equations having the first integral

$$\sum_{k=1}^{n} \eta_k^2 + \xi^2 = R_0 e^{-2\rho t}$$

and describing the closed controlled system are the following

$$\left.\begin{aligned} \dot{\eta}_k &= \sum_{\alpha=1}^{n} b_{k\alpha}\eta_\alpha + m_k\xi; \\ \dot{\xi} &= -\sum_{k=1}^{n} m_k\eta_k - \rho\xi - \frac{\sum_{k}^{n}\sum_{\alpha}^{n} (b_{k\alpha} + \delta_{k\alpha}\rho)\,\eta_k\eta_\alpha}{\xi}. \end{aligned}\right\} \tag{3}$$

We have a nonlinearity in the right side of the system. With $\xi = 0$ the conditions of the Cauchy problem are not satisfied. The effect of the nonlinearity on the solution of system (3) is studied in the present paper.

For simplicity and clarity (without limitation of generality in principle) we set k = 1 and denote η_1 by η; b_1 by b and m_1 by n.

3. Analysis of the System

We have the problem of analysis of the system of differential equations

$$\left.\begin{aligned} \dot{\eta} &= b\eta + n\xi; \\ \dot{\xi} &= -n\eta - \rho\xi - \frac{(b+\rho)\,\eta^2}{\xi}. \end{aligned}\right\} \tag{4}$$

The nonlinearity in the right side will drop out if we select $\rho = -b$, but this case is not of interest because then the connection of the control to the system does not offer any improvement; in the future we shall therefore consider that $\rho \neq -b$. The solution of the Cauchy problem for the given system exists and is unique in any closed part of the plane where the right sides of the equations are continuous and satisfy the Lipshits condition, i.e., in closed parts of the plane which do not contain the axis $\xi = 0$.

For the study of the behavior of the integral curves in the phase plane $\xi\eta$ we consider the equation

$$\frac{d\xi}{d\eta} = -\frac{\rho\xi^2 + n\xi\eta + (b+\rho)\eta^2}{\xi(b\eta + n\xi)}. \tag{5}$$

Let us always set $\rho > 0$.

Let us characterize the quadratic form $\rho\xi^2 + n\xi\eta + (b+\rho)\eta^2 = U(\xi, \eta)$.

1. $U(\xi, \eta)$ is sign-definite, if

$$\rho(b+\rho) - \frac{n^2}{4} > 0. \tag{6}$$

Whence it follows that $\rho > -b$. /126

The possible cases are

$$n > 0,\ b > 0; \tag{7}$$

$$n > 0,\ b < 0; \tag{8}$$

$$n < 0,\ b < 0; \tag{9}$$

$$n < 0,\ b > 0. \tag{10}$$

We see that all of them give qualitatively the same pattern in the phase plane. For definiteness we shall consider (7) and (9).

Let $\rho = n = b = 1$, satisfying (6) and (7).

On the straight line $\xi + \eta = 0$ the phase trajectories have vertical tangents, since the slope at the points of this straight line $d\xi/d\eta = \infty$.

With $\eta = 0$, $\frac{d\xi}{d\eta} = -1$.

We find the asymptotic direction of the integral curves, for which we set $\xi = \alpha\eta$, where α is a still-unknown number designating the slope of the asymptote.

Whence $d\xi/d\eta = \alpha$ and, substituting this into equation (2), we obtain the algebraic equation for the determination of α

$$n\alpha^3 + (b + \rho)\alpha^2 + n\alpha + (b + \rho) = 0.$$

We have the single root $\alpha = -\frac{b+\rho}{n}$. By substitution we verify that $\xi + 2\eta = 0$ is a solution of equation (5), i.e., this straight line is the integral curve of our system. It should be noted that the isoclines (curves where the tangent to the phase trajectory has the same direction) will be the straight lines

$$\xi = -\frac{kb + n \pm \sqrt{(kb - n)^2 - 4\rho(kn + b + \rho)}}{2(kn + \rho)}\eta,$$

where k is the slope of the tangent to the integral curve. The behavior of the integral curves in cases (6) and (7) is shown in figure 1. The imaging point moves as shown by the arrows. For definiteness let us set $\rho = 2$, $b = -1$, $n = -1$, satisfying (6) and (9). The vertical tangent to the phase trajectory will be on the straight line $\xi + \eta = 0$. By the same method we find the asymptote--the integral curve $\xi - \eta = 0$. This case is shown in figure 2.

2. Let $\rho(b + \rho) - \frac{n^2}{4} < 0.$ (11)

Then $U(\xi, \eta)$ breaks down into two linear forms, i.e.,

$$U(\xi, \eta) = U_1(\xi, \eta)U_2(\xi, \eta).$$

The possible cases on which the behavior of the integral curves depend are

$$b + \rho < 0, \quad (12)$$

$$b + \rho > 0. \quad (13)$$

On the straight lines $U_1(\xi, \eta) = 0$ and $U_2(\xi, \eta) = 0$ the integral /127 curves have a horizontal tangent. All these constructions are carried out in order to isolate the regions where the phase trajectories only increase or only decrease. Since the isoclines are straight lines and the numerator and denominator in (2) break down into linear forms, the slope of the tangents will change sign only on the straight lines where $d\xi/d\eta$ becomes zero or infinite.

For definiteness let us set $\rho = 1$, $b = -2$, $n = -1$, where they satisfy (11) and (12). The equation of the phase trajectory, which is the asymptote, will

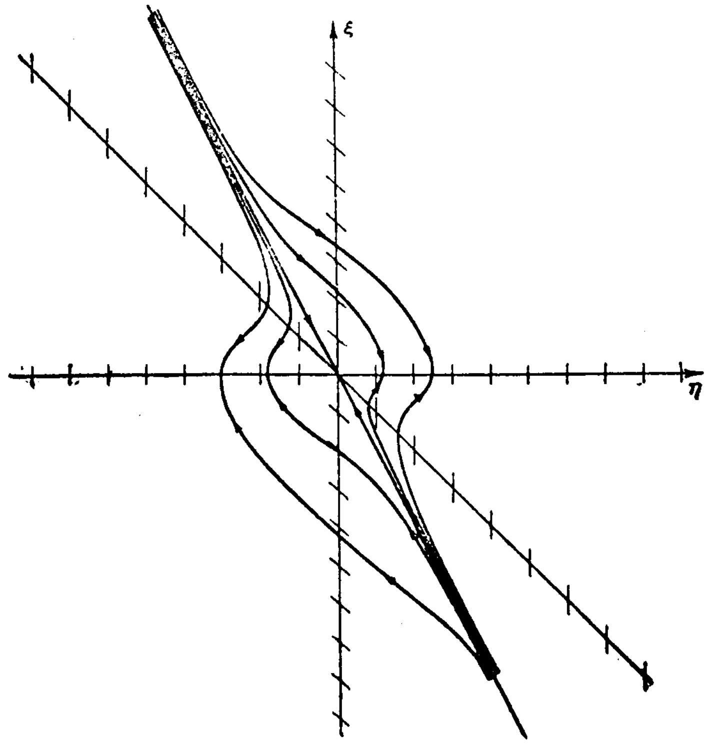

Figure 1

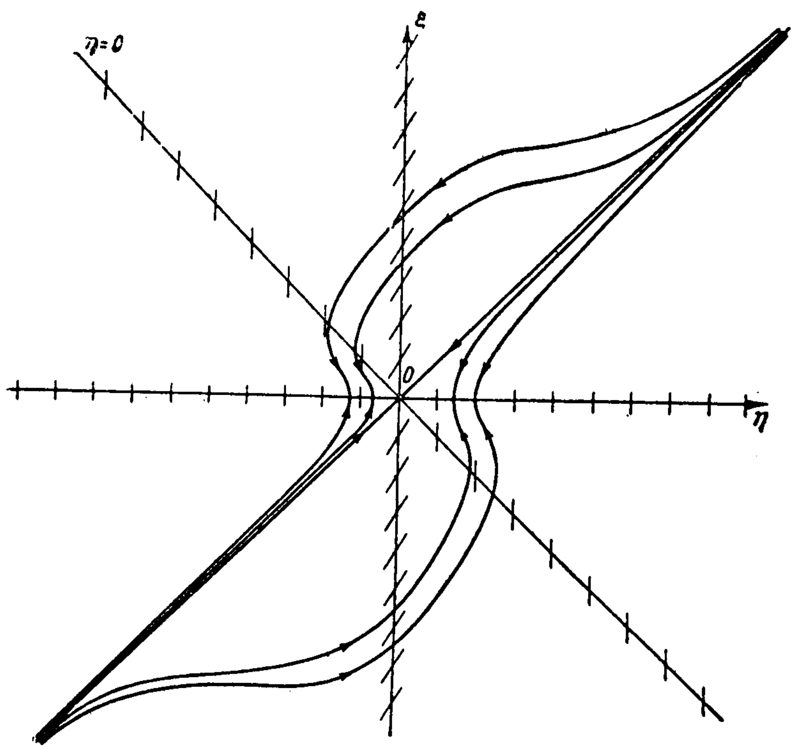

Figure 2

be $\xi + \eta = 0$. With $\eta = 0$ $d\xi/d\eta = 1$. The integral curves intersect the axis $\eta = 0$ at an angle whose tangent is equal to 1. On the straight line $\xi + 2\eta = 0$, $d\xi/d\eta = \infty$. The nature of the construction of the integral curves in the case (11) and (12) is shown in figure 3.

The nature of the behavior of the curves does not depend on the sign of n. Figure 4 presents the same case with $n > 0$. Arrows indicate the direction in which the imaging point moves along the trajectory. With conditions (11) and (12) the coordinate origin will be a stable singular point. But this version is unsatisfactory, since the connection of the control to the system does not offer us anything concrete (at least we cannot state that the characteristic of the system of interest to us is improved).

Let conditions (11) and (13) be satisfied and $n > 0$. For definiteness we set $\rho = 2$, $b = 1$, $n = -3$. The asymptote is the integral curve $3\xi - \eta = 0$. Using the same methods as before, we determine the nature of the behavior of the integral curves in the phase plane. From figure 5 we see that in this case the imaging point comes to the axis $\xi = 0$ and remains there. The case $n > 0$ is analogous. Now we can draw certain conclusions.

In all cases of interest to us the nature of the behavior of the phase trajectories is the same. The imaging point moves from infinity to the straight line $\xi = 0$, where it remains. It cannot leave the straight line, because it would have to go counter to the motion in the phase plane specified by the system of differential equations. In other words, if there is specified a disturbance of the system under the condition that the control is in the null position, then the control signal will not arise, i.e., the connection of the control to the system will not have the required effect. Attempts have been made to eliminate this deficiency, which is the result of the nonlinearity in the right side of the system (the smaller $|\xi|$, the higher is the rate of its decrease, i.e., in the vicinity of axis $\xi = 0$ there is a decrease of $|\xi|$).

We can "impose" on the system any first integral, hoping by suitable choice of the integral to find a positive solution of the problem.

Assume that the system has the first integral

$$\eta^2 + \xi^{2/3} = R_0^2 e^{-2Qt}.$$

Such a system is

$$\dot{\eta} = n\xi + b\eta;$$

$$\dot{\xi} = -3\rho\xi - 3(b+\rho)\xi^{\frac{1}{3}}\eta^2 - 3n\xi^{\frac{4}{3}}\eta.$$

The right sides satisfy the conditions of the Cauchy problem on any finite portion of the plane. The single singular point is at the coordinate origin.

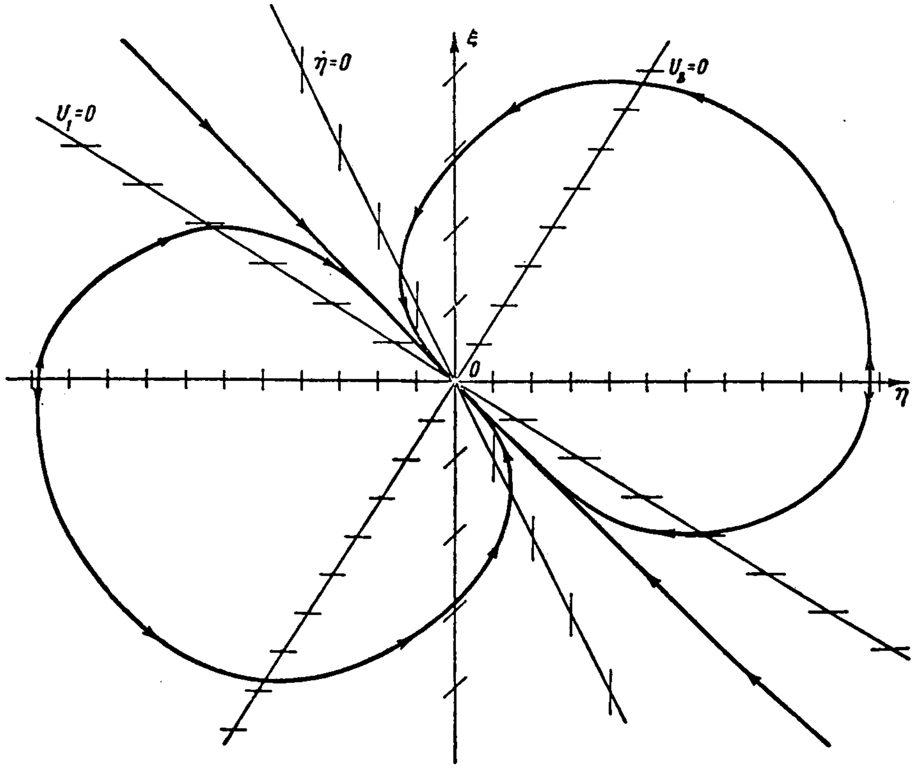

Figure 3

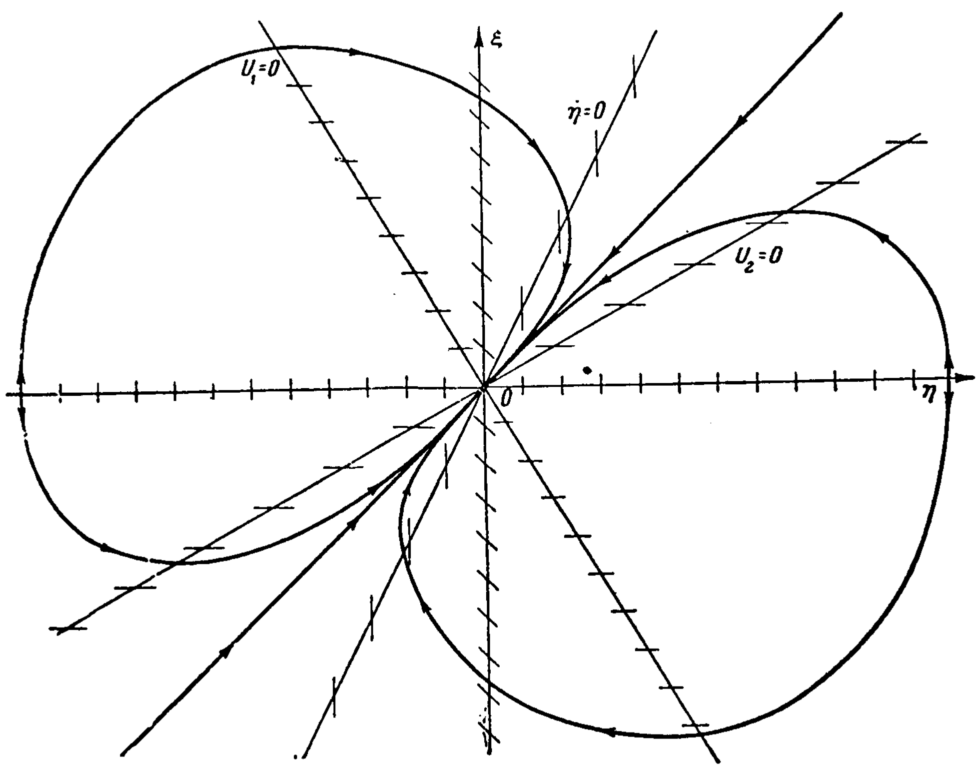

Figure 4

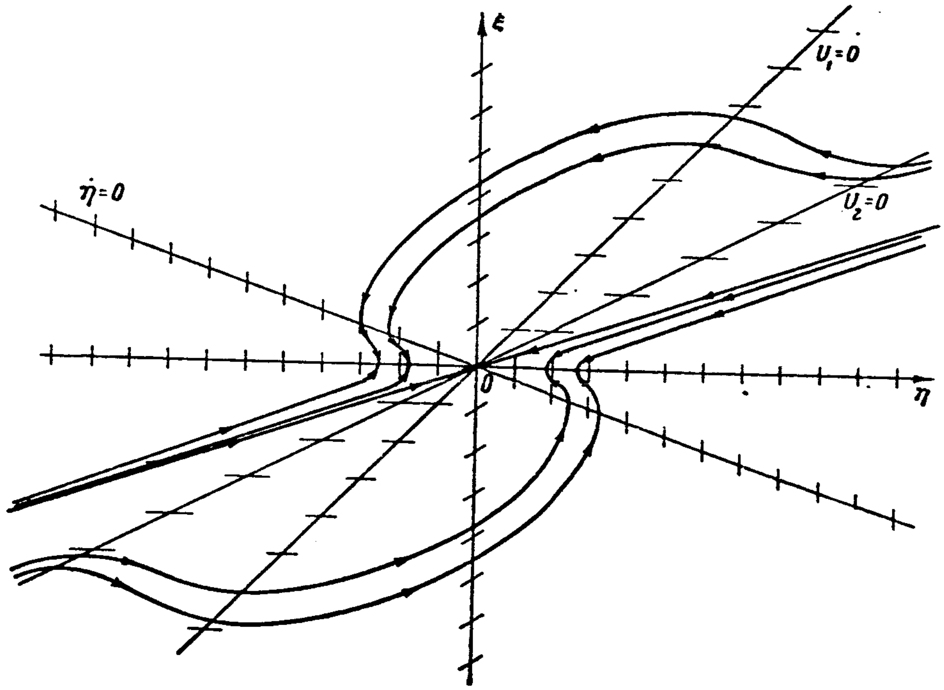

Figure 5

Let us study it. Consider the linear system which corresponds to the non-linear system

$$\dot{\xi} = -3\rho\xi;$$
$$\dot{\eta} = n\xi + b\eta.$$

Its characteristic equation is /131

$$\begin{vmatrix} -3\rho-\lambda & 0 \\ n & b-\lambda \end{vmatrix} = (3\rho+\lambda)(\lambda-b) = 0.$$

If $\rho > 0$ and $b < 0$, the coordinate origin is a stable node. For definiteness, let $\rho = 2$, $b = -1$, $n = 1$. Then the equation for which we are studying the phase pattern will be

$$\frac{d\eta}{d\xi} = \frac{\eta-\xi}{3\left(2\xi+\xi^{\frac{1}{3}}\eta^2+\xi^{\frac{4}{3}}\eta\right)}.$$

This case is shown in figure 6.

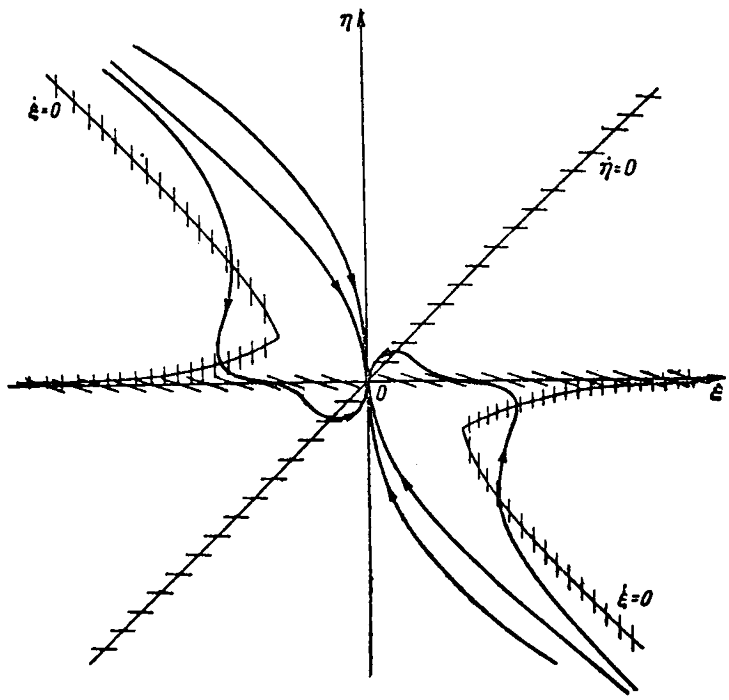

Figure 6

Here we have the same deficiency as before. With $\xi = 0$ $\dot{\xi} = 0$, i.e., the controlling action does not arise with the passage of time. Consequently, if $\xi^0 \neq 0$, is not specified at the initial moment the control will not function.

We will now show that if we consider $\rho(\xi) = \rho = \text{const}$, it is impossible to solve the posed problem by selection of the first integral.

Consider the function $R^2(\xi, \eta)$.

(1) $R^2(\xi, \eta)$ is continuous and everywhere differentiable with respect to ξ, where $\xi \neq 0$ and with $\xi = 0$ there exists the one-sided derivative with respect to ξ; $(\xi, \eta) \in D$ (here D is a closed region);

(2) $R^2(\xi, \eta) > 0$;

(3) $R^2(0, 0) = \min$.

To eliminate these deficiencies it is necessary that $\left.\frac{\partial R^2}{\partial \xi}\right|_{\xi=0} \neq 0$ and $\left.\frac{\partial R^2}{\partial \xi}\right|_{\xi=0} \neq \infty$.

If, however, the partial derivative does not tend to zero or infinity, then it is necessary that $\left.\frac{\partial R^2}{\partial \xi}\right|_{\xi=0+0} \cdot \left.\frac{\partial R^2}{\partial \xi}\right|_{\xi=0-0} > 0$.

But these requirements cannot be satisfied, because conditions 1-3 are imposed on $R^2(\xi, \eta)$. This is all valid for the case $\rho(\xi) = \rho = \text{const}$, where $\rho > -b$ ($\rho < -b$ is not of interest to us). In the future the functions $\rho(\xi)$ will be found, for which this defect will be eliminated; however, other difficulties appear here.

Hereafter, we shall consider systems which have a first integral of the form

$$\xi^2 + \eta^2 = R_0^2 e^{-2\int_0^t \rho(\xi)dt},$$

where $\rho(\xi) \neq \text{const}$.

We shall now choose $\rho(\xi)$ so that we can avoid the deficiencies discussed above. To do this, we require the following of $\rho(\xi)$

(1) $\rho(\xi)$ is continuous with $|\xi| \leqslant M$;

(2) $\rho(\xi) = -b$ with $\xi = 0$;

(3) $\rho(\xi) > -b$ for $\xi \neq 0$;

(4) for any $\epsilon > 0$ there exists $\delta > 0$ such that if $|\xi| > \delta$, then $|\rho(\xi) - \rho^*| < \varepsilon$.

An example of such a function may be

$$\rho(\xi) = \frac{(\rho^* + b)\xi^2}{1 + \xi^2} - b$$

or /132

$$\rho(\xi) = (b + \rho^*) e^{-\frac{2}{\xi^2}} - b.$$

The differential equations of the closed controlled system for such $\rho(\xi)$ will be

$$\left.\begin{aligned} \dot{\xi} &= b\xi - n\eta - \frac{(b + \rho^*)(\xi^2 + \eta^2)\xi}{1 + \xi^2}; \\ \dot{\eta} &= n\xi + b\eta \end{aligned}\right\} \qquad (14)$$

or

$$\left.\begin{aligned}\dot{\xi} &= b\xi - n\eta - \frac{(b+\rho^*)(\xi^2+\eta^2)\,e^{-\frac{s}{\xi^2}}}{\xi};\\ \dot{\eta} &= n\xi + b\eta.\end{aligned}\right\} \quad (15)$$

We have the problem of studying the phase plot of these equations. To do this we consider the system (14) with the coefficients (this does not restrict the generality) $\rho^* = 2$, $b = -1$, $n = 1$. $\frac{d\eta}{d\xi} = \infty$. On the curve $\xi\eta^2 + (1+\xi^2)\eta + 2\xi^3 + \xi = 0$ (fig. 7). The tangent to the integral curve at the points of the straight line $\xi - \eta = 0$ is horizontal. The system has a single singular point at the coordinate origin. Let us consider at the point (0, 0) the shortened system /133

$$\begin{aligned}\dot{\xi} &= -\xi - \eta;\\ \dot{\eta} &= \xi - \eta.\end{aligned}$$

Its characteristic equation is $(1+\lambda)^2 + 1 = 0$. The roots are $\lambda_1 = -1 + i$, $\lambda_2 = -1 - i$, i.e., we have a stable focus. On the straight line $\xi = 0$ $\frac{d\eta}{d\xi} = 1$. The behavior of the integral curves is shown in figure 7.

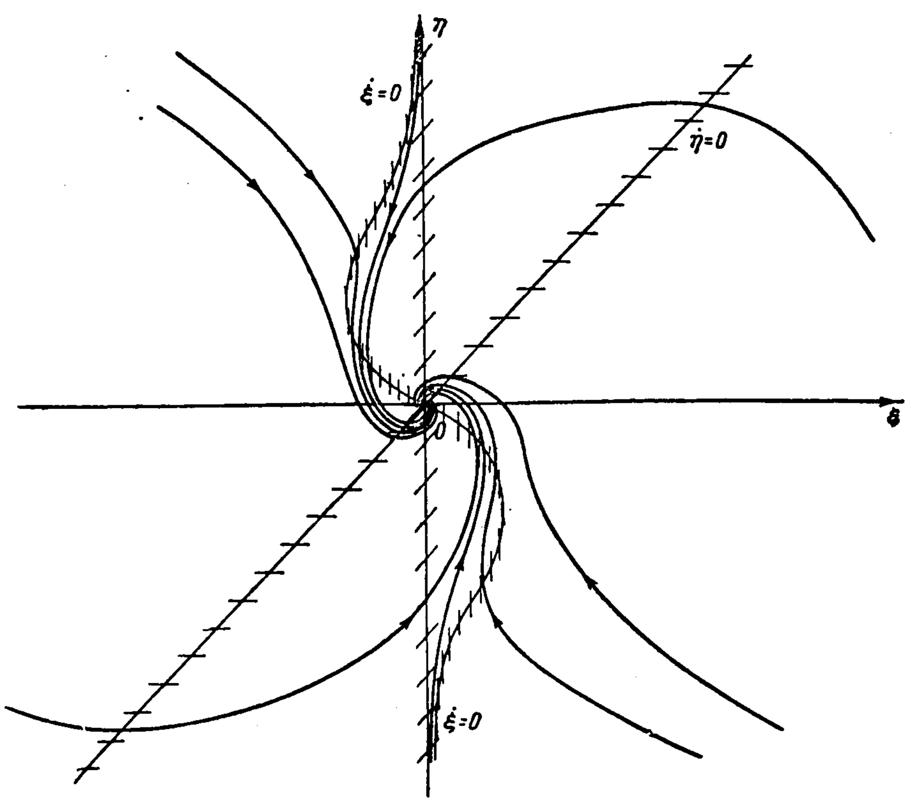

Figure 7

The same is also obtained for the system (15).

For the points of the plane where $|\xi| > \delta$ ($\delta > 0$ is some fixed number) the damping of the periodic process is determined by the parameter ρ^*.

We can describe about the coordinate origin a sphere of arbitrarily small radius $\delta > 0$ and state the problem as follows. Select the function $\rho(\xi)$ and the parameter ρ^* so that the imaging point arrives from the initial position

$$M^0(\eta_1^0, \eta_2^0, \ldots, \eta_n^0, \xi^0) \quad R_0^2 = \sum_{k=1}^{n} (\eta_k^0)^2 + (\xi^0)^2 \neq 0,$$

where $|\xi^0| \geqslant \xi_{fix}$ to this sphere in the specified time t^*. This problem has been solved.

If, however, M^0 is such that $\xi^0 = 0$, then let us see what difficulties arise in the solution of this problem.

In case (14) with $\xi = 0$, $\eta \neq 0$ we will have $\dot{\xi} \neq 0$, i.e., with the occurrence of a disturbance of the system, a control signal appears. The function $\rho(\xi)$ is chosen so that if at the initial instant $\xi \neq 0$ and is sufficiently large, then

$\xi^2 + \eta^2 \leqslant R_0^2 e^{-2(\rho^* - \varepsilon^*)t}$, where $\varepsilon^* > 0$, i.e., if we make a suitable choice of ρ^*, we can make the degree of damping of the transient process whatever we need.

However, near the axis $\xi = 0$ $\rho(\xi) \cong -b$, i.e., the problem cannot be solved (it is not possible to obtain any desired degree of damping by selection of ρ^*). The function $\rho(\xi)$ depends on the parameter ρ^*, and if we increase ρ^*, then with any fixed ξ the ordinate of $\rho(\xi)$ increases approximately proportionately, and

it would seem that, since $\xi^2 + \eta^2 = R_0^2 e^{-2\int_0^t \rho(\xi)\,dt}$, the degree of damping must increase. However, as we see from figure 7, the integral curves, which take the initial values on the straight line $\xi = 0$ (which is the case in practice), cannot pass through the parts of the plane where ξ takes large values, because there is a separating integral curve (separatrix), beyond which these trajectories cannot go. With increase of ρ^* the separatrix is "squeezed" to the axis $\xi = 0$. Thereby the region of variation of ξ is narrowed, i.e., $\rho(\xi)$ takes values corresponding to smaller ξ, i.e., we do not obtain any effect from the increase of ρ^*.

Generally speaking, since $\rho(\xi^2) \geqslant -b$ and only $\rho(0) = -b$, then $\int_0^t \rho(\xi^1)\,dt$ from the theorem on the mean of ($\xi^2(t)$ varies from 0 to $\xi_{max}^2 > 0$ equal to $\rho(\overline{\xi_0^2})t$, where $0 \leqslant \overline{\xi_0^2} \leqslant \xi_{max}^2$ and since $\rho(\xi^2) > -b$ with $\xi \neq 0$, then $\rho(\overline{\xi_0^2}) > -b + \omega$, where $\omega > 0$ is some number, i.e., the characteristic of the closed system is improved,

but, as can be verified, there exists ω_0 such that all $\omega < \omega_0$, no matter how much we increase ρ^*.

Consider the differential equations having a first integral of the form

$$\left(\xi + \rho \sum_{k=1}^{n} \eta_k\right)^2 = R_0^2 e^{-2\rho t} . \tag{16}$$

Let $k = 1$, and denote η_1 by η. Expression (16) takes the form /134

$$(\xi + \rho\eta)^2 = R_0 e^{-2\rho t},$$

where ρ = const.

Here R^2 is equal to zero or reaches a minimum not only at the coordinate origin, but also on the straight line $\xi + \rho\eta = 0$. From the form of this first integral we still cannot determine how the transient process behaves, but the equations which we obtain are linear and can be studied easily.

We have

$$2(\xi + \rho\eta)(\dot{\xi} + \rho\dot{\eta}) = -2\rho R_0^2 e^{-2\rho t} = -2\rho(\xi + \rho\eta)^2.$$

Whence the equation of the control

$$\dot{\xi} = -(\rho + n\rho)\xi - (\rho^2 + \rho b)\eta.$$

Combining with it the differential equation describing the system, we obtain

$$\dot{\xi} = -(\rho + n\rho)\xi - (\rho^2 + \rho b)\eta;$$
$$\dot{\eta} = n\xi + b\eta.$$

The characteristic equation of this system (singularity only at 0) is

$$\begin{vmatrix} -(\rho + n\rho) - \lambda & -\rho^2 - \rho b \\ n & b - \lambda \end{vmatrix} = \lambda^2 + [\rho(1+n) - b]\lambda + n\rho^2 - \rho b = 0.$$

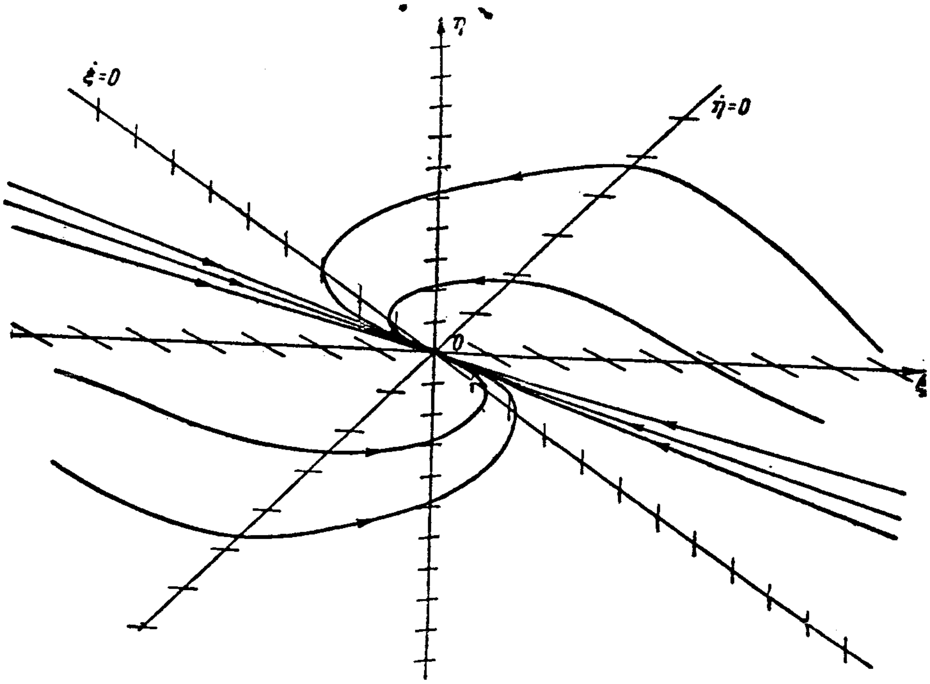

Figure 8

Its roots are /135

$$\lambda_{1,2} = \frac{b-\rho(1+n)}{2} \pm \sqrt{\frac{b^2-2b\rho(1+n)+\rho^2(1+n)^2-4n\rho^2+4\rho b}{4}}$$

or

$$\lambda_1 = b - \rho n;$$
$$\lambda_2 = -\rho.$$

From this we see that by selecting ρ adequately large, we can make the degree of damping of the transient process as large as desired. Here the new requirement that $n > 0$ appears. This case is shown in figure 8.

Conclusions

The question on how the posed problem has been solved can be answered as follows. With the use of the original method of solution, when the integral which was "imposed" on the system had the form

$$R^2(\xi, \eta) = R_0^2 e^{-2Qt},$$

where $R^2(\xi, \eta)$ is a positive function which becomes zero only at the point (0, 0) and ρ = const, the solution of the system was such that the imaging point in the phase space came to the $\xi = 0$ axis and remained there, i.e., thereafter there was no damping of the transient process. Thus the problem was not solved.

The posed problem is solved when ρ is a function of ξ selected by the method indicated above and the initial position in the phase space is chosen so that $|\xi_0| \geq \xi_{fix}$; with $|\xi_0| < \xi_{fix}$ the transient process in the closed controlled system damps more rapidly than without the control, but the degree of this damping cannot be made anything desired.

If $R^2(\xi, \eta)$ is selected from the functions which vanish not only at the coordinate origin, then by means of the selection ρ = const the degree of damping can be made arbitrarily large.

Consequently, the method proposed by Letov permits solution of the posed problem, if the limitations listed above are satisfied.

N66 34840

OPTIMAL CONTROL IN SECOND-ORDER RELAY-PULSE SYSTEMS

V. N. Novosel'tsev

In the study of pulse systems for automatic control limitations of the form /136

$$|u| \leqslant N.$$

are usually imposed on the control actions of the system.

This limitation permits, with arbitrary initial conditions, the selection from the admissible range of actions of those with which we can obtain an accurate result with unlimited accuracy (refs. 1 and 2). However, in real systems for automatic control the requirement on the accuracy of the end result is usually limited to some quantity ϵ.

The present paper considers the system for the automatic control of the two-dimensional motion of a material point. Optimal control has as its objective the displacement of the point from an arbitrarily specified initial position to the coordinate origin. If after termination of the control process the point is near the coordinate origin at the distance $\rho \leq \epsilon$ and the final velocity of the point is equal to zero, then the problem is considered solved. This statement is equivalent to the introduction of the "success function" $g(x)$ having the form shown in figure 1.

The considered system is described by two finite-difference equations

$$\left.\begin{aligned} x([k+1]h) - x(kh) &= y(kh)h; \\ y([k+1]h) - y(kh) &= u[(k+1)h] \end{aligned}\right\} \qquad (1)$$

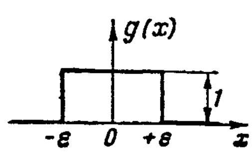

Figure 1

where x, y are the coordinates of the point on the phase plane corresponding to the distance traveled by the point and its velocity; u is the control action (acceleration of the point).

Since we are required to reach the coordinate origin $x = y = 0$ /137 with respect to x only with an accuracy to ϵ, it is possible to limit ourselves, from the entire range of values of the control action $|u| \leq 1$ usually used (without limitation of generality in the expression presented above we can consider $N = 1$), to only a discrete set of control actions. The simplest are the sets containing 2 or 3 values of the control action ±1 and ±1.0).

$$\{u\} = \{+1, -1\}; \tag{2}$$
$$\{u\} = \{+1, 0, -1\}. \tag{3}$$

If the repetition interval of the pulses h in the relay-pulse system is specified, the quantity y can take only values equal to ah, and x can take only the values abh^2, where a and b are whole numbers. The minimal value of the segment of the path traveled by such a system during the time between pulses is clearly equal to h^2. It is convenient to take this distance to be unity.

Thus the path traveled by the point in one cycle can be equal to ±1, ±2, ±3, and so on. In the relay-pulse system with a dead zone it is also possible to have an equilibrium position when $x([k+i]h) = x(kh)$; $i = 1, 2, \ldots$

Consider the question of the possibility of constructing an optimal control with various values of ϵ. It is evident that if in the selected scale of time and space $2\epsilon < 1$, the construction of the optimal control for arbitrary initial conditions is not possible, since there exists an innumerable set of points whose movement into the region $g(x) = 1$ is not possible. Such a point, for example, is the point $x = \frac{1-2\varepsilon}{2}$, $y = 0$. At the same time, with the condition $2\epsilon \geq 1$, it is obvious that there are no such points, and in principle it is possible to carry out the construction of optimal control for any initial conditions. Of particular interest is the boundary case $2\epsilon = 1$, and we shall turn to the consideration of this case.

Hereafter, we consider only points whose coordinates x and y are whole numbers. Such an assumption is natural for coordinate y, since otherwise the system can never be found in a state of rest $(y = 0)$. The assumption that x is a whole number does not restrict the considered problem, because, taking our previous remarks into account, it is evident that optimal control of an integral point, leading to the coordinate origin, is also valid for those points for which the initial value of the coordinate x differs from a whole number by the magnitude $\rho \leq \epsilon$.

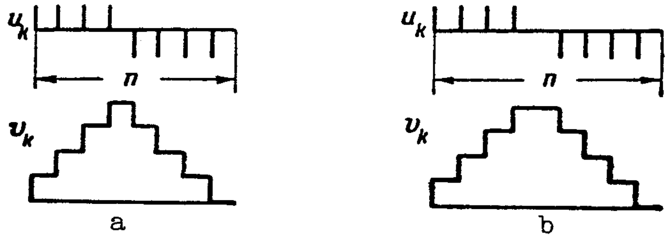

Figure 2

Let there be given the point for which $y_0 = 0$. Let us find the maximal value of path S_n traveled by the point after n steps under the condition that after termination of the process the velocity of the point is equal to 0, i.e., $y_n = 0$, $(n > 1)$. For system (2) the problem obviously is meaningful only with n even; in this case

$$\sum_{u_i>0}^{l} u_i = -\sum_{u_j<0}^{p} u_j; \; i, j = 1, 2, \ldots, n; \; l + p = n. \tag{4}$$

As is easily shown (for example, ref. 3), in this case the control has the form shown in figure 2a, and the maximal path traveled is

$$S_{max} = \frac{n^2}{4}.$$

This remark remains valid for even n for system (3) as well. However, for relay-pulse system (3) it is also possible to construct the control for odd n. In this case the maximal possible path is the area bounded by /138 the broken line of figure 2b. This area is equal to $\frac{n^2-1}{4}$.

Let us turn now to the construction of the optimal control for system (1) with conditions (2) or (3).

First, we construct the optimal control for the points of the x axis of the phase plane, and then, with the aid of the expression obtained, we construct the control for any point of the phase plane.

The expressions presented above for S_{max} can now be treated as follows: the points most remote from the coordinate origin, from which the point (0,0) can be reached after 2, 3, 4, ..., 2m, 2m + 1, ... steps, have the coordinate

x equal, respectively, to 1, 2, 4, ... , m^2, $m(m + 1)$, ...; ($m = 1, 2...$). In this case the optimal control for the points ($x > 0$) can be written as

$$\left.\begin{aligned} &x = m^2;\\ &u_k^0 = -\operatorname{sign}\left[\frac{K^\circ}{2} - k\right], \text{ (we consider } \operatorname{sign} 0 = 1);\\ &K^\circ = 2m; \end{aligned}\right\} \quad (5)$$

$$\left.\begin{aligned} &x = m(m+1);\\ &u_k^0 = -\operatorname{sign}\left[\frac{K^\circ - 1}{2} - k\right] + \delta_{kz};\\ &K^\circ = 2m + 1;\\ &z = \frac{K^\circ + 1}{2}; \qquad \delta_{kz} = \begin{cases} 1 & k = z\\ 0 & k \neq z \end{cases} \end{aligned}\right\} \quad (6)$$

After determining the optimal control (5) and (6), we can find the time for the optimal transient process for all integral points of the x-axis.

Actually, on the x-axis we have, according to (5), points m^2 for which the optimal process lasts 2m steps. Consequently, for all points $x > 2m$ of the x-axis the process lasts longer than 2m steps.

Furthermore, according to (6) there is a region for which the optimal process takes more than 2m + 1 steps. The lower boundary of this region is point $m(m + 1)$. But this implies that for all points $m^2 < x \leq m(m + 1)$ the optimal process takes no less than ($2m + 1$) steps, i.e., if we can construct a process lasting ($2m + 1$) steps, it will clearly be optimal, i.e., $K^o = 2m + 1$.

This applies to relay-pulse system (3). For relay-pulse system (2), it is obvious that K^o can be only even and in this case with $m^2 < x < (m + 1)^2$, $K^o = 2m + 2$ everywhere. /139

We now turn to the construction of the optimal control for any point of the x-axis with satisfaction of one of the conditions (2) or (3). Case (2) was considered in detail in reference 3, where it was shown that for such points the optimal control has the following form: if the position of the point is defined by expression

$$x_0 = n^2 + p, \; 1 < p \leqslant 2n + 1, \; y_0 = 0,$$

then

$$
\left.\begin{aligned}
K^\circ &= \begin{cases} 2n, & p=1; \\ 2n+2, & p=2,3,\ldots,2n+1; \end{cases} \\
u_k^0 &= -\operatorname{sign}\left[\frac{K^\circ}{2}-k-1\right]-2\delta_{kz}; \\
z &= K^\circ - E\left(\frac{p+1}{2}\right)
\end{aligned}\right\} \tag{7}
$$

(in this case, if k = 2, 4, ..., 2n, then after K^0 steps in our case it is necessary to add two more steps to reach the coordinate origin $u_{K^0+1}^0 = -u_{K^0+2}^0 = -1$).

On the basis of the found expression we can construct the optimal control for any initial conditions and can represent it in the form of a convenient "switching line," separating the phase plane into two regions, for which the control action is constant and has different signs. The switching line for the relay-pulse system is shown in figure 3a. The equation of the switching line presented in reference 3 can be rewritten in symmetrical form

$$
\left.\begin{aligned}
u^0 &= \begin{cases} -1, & \text{if } x \geqslant F(x,y); \\ +1, & \text{if } x < F(x,y); \end{cases} \\
F(x,y) &= \frac{y^2+3|y|+1}{2}\operatorname{Sign} x.
\end{aligned}\right\} \tag{8}
$$

Thus, the solution for relay-pulse system (2) is known. Let us construct now the optimal control for relay-pulse system (3).

We again consider the points of the x-axis (for definiteness we set x > 0). We select the segment of the axis containing points with the coordinates

x $(n + 1)^2 \geq x > n^2$ with some n. Then, according to our previous discussion,

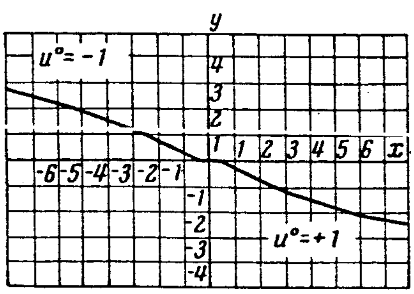

a

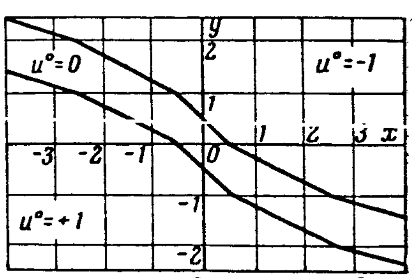

b

Figure 3

for relay-pulse system (3) we can determine the corresponding quantities K^0

$$K^\circ = \begin{cases} 2n+1, & \text{if } n^2 < x \leqslant n(n+1); \\ 2n+2, & \text{if } n(n+1) < x \leqslant (n+1)^2. \end{cases} \tag{9}$$

Let $K^0 = 2n + 1$, $n^2 < x \leq n(n + 1)$. Then, according to (6), for the points farthest removed from the coordinate origin $x = n(n + 1)$, the optimal control u^0 has the form

$$\underbrace{-1, -1, \ldots, -1}_{n}, \underbrace{0, +1, \ldots, +1}_{n} \tag{10}$$

If the initial point is located closer to the coordinate origin by ι units, then the optimal control must change its form so that S_{2n+1} /140 is equal to $n(n + 1) - \iota$, $(1 \leq \iota < n)$. Such a value of S_{2n+1} can be obtained with permutation in the sequence (9) of the quantities 0 and +1 (or -1), separated from one another by ι steps

$$-1, \ldots, -1, \underbrace{0, -1, \ldots, -1}_{\iota}, +1, \ldots, +1 \tag{11a}$$

or

$$-1, \ldots, -1, \underbrace{+1, \ldots, +1, 0}_{\iota}, +1, \ldots, +1. \tag{11b}$$

We choose as the optimal control for such points the sequence (11b). Now let $K^0 = 2n + 2$, and let x be determined by the expression $n(n + 1) < x \leq (n + 1)^2$. For point $(n + 1)^2$, according to (5), we have the optimal sequence of control actions of the form

$$\underbrace{-1, \ldots, -1}_{n+1}, \underbrace{+1, \ldots, +1}_{n+1}, \tag{12}$$

With an even number of steps, (4) must be satisfied, therefore, by manipulations of sequence (12) we shall simultaneously replace the pairs + 1 and -1 by zeros.

If the initial point is defined by the coordinate $x = (n + 1)^2 - \iota$, then quantity S_{2n+2}, corresponding to the optimal sequence of controlling actions,

must be smaller by l than with sequence (12). Such a quantity S_{2n+2} can be obtained, in particular, if we replace by "0" the controlling action in the (n + 1)th step; we shall replace by "0" the quantity "-1" removed from it by l steps

$$-1,\underbrace{\dots,-1,0,}_{n}+\underbrace{1,\dots,+1,0}_{l}+1,\dots,+1. \qquad (13)$$

It is also possible to use the sequence which is "inverted" with respect to (13)

$$u'_{K^*-k+1}=-u_k^0.$$

Sequences of the type (11a) and (13) thus give the optimal control for the points of the x-axis, which are defined, respectively, by expressions

$x = n(n + 1) - l$ and $x = (n + 1)^2 - l$, where $1 \le l \le n - 1$.

With $l = 0$ and $x = n(n + 1)$ or $x = (n + 1)^2$ the optimal control is determined by expressions (5) or (6), respectively.

For relay-pulse system (3) we can, on the basis of (11b) and (13), just as for relay-pulse system (2), construct switching lines which partition the phase plane into regions with definite values of the optimal control action. In the present case optimal control is accomplished by the realization of two switching lines defining the regions with values $u^0 = +1$; 0; or -1, respectively. /141

In order to obtain the optimal switching lines, we consider the integral points lying on the half-line $y = -n$, $x > 0$ on the phase plane (x, y) (fig. 4).

The optimal control for all points of the considered range, according to (11b), (13), (5) and (6), begins with the application of $u^0 = -1$ with

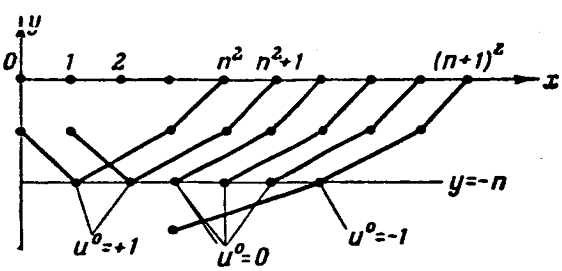

Figure 4

k = 1, 2, ..., n. After this the imaging point is on the straight line y = -n, and

$$S_n = -\frac{n(n+1)}{2}.$$

Considering the dependence of u^0 on x with y = -n, we can note that

$$\left.\begin{array}{l} u^0 = -1 \text{ with } x = \frac{(v+1)(v+2)}{2}; \\ u^0 = 0 \text{ with } \frac{(v+1)(v+2)}{2} > x \geqslant \frac{v(v+1)}{2}; \\ u^0 = +1 \text{ with } \frac{v(v+1)}{2} > x > \frac{v(v-1)}{2}, \end{array}\right\} \quad (14)$$

where $v = |y|$

At the same time with $x > \frac{(v+1)(v+2)}{2}$ we have $u^0 = -1$, since, according to the formulas for optimal control, the first change of the magnitude of the optimal action for such points occurs no earlier than at the (n + 1)th step.

It is easy to show also that with $x \leqslant \frac{v(v-1)}{2}$ it is necessary that $u^0 = +1$. Actually, the point $x = \frac{v(v-1)}{2}$ with the use of $u_k^0 = +1$, (k = 1, 2, ..., y)moves directly to the coordinate origin, while the points $x < \frac{v(v-1)}{2}$ with displacement to the coordinate origin inevitably cross the x-axis in the region of negative values of x.

Since consideration of the problem with x < 0 is completely analogous to the discussion above, the intersection of the optimal trajectory with the x-axis must occur with the minimal possible value of x. This proves the need in this case for $u^0 = +1$.

Now (14) can be rewritten in the form /142

$$u^0 = \begin{cases} -1, & \text{if } x \geqslant \frac{v^2+3v+2}{2}; \\ 0, & \text{if } \frac{v^2+3v+2}{2} > x > \frac{v^2+v}{2}; \\ +1, & \text{if } x < \frac{v^2+v}{2} \end{cases} \quad (15)$$

with (y = -n, x > 0.

Since (15) is valid for any n, this relationship expresses the partition of the phase semiplane $x > 0$ into three regions with fixed values of u^0. The boundaries of these regions can be considered to be the broken lines joining the integral points

$$\left.\begin{aligned} x &= \frac{v^2+3v+3}{2} \\ x &= \frac{v^2+v}{2}. \end{aligned}\right\} \qquad (16)$$

and

Thus, the optimal control for relay-pulse system (1) with limitation (3) has the form (11b), (13) depending on initial conditions, and a convenient representation of the optimal control with the aid of two switching lines (16) is possible. These switching lines are shown in figure 3b.

We can write an equation analogous to equation (8) for the relay-pulse system with the limitation (2). It has the form

$$u^0 = \begin{cases} -1 & x \geqslant F_1'(v, x); \\ 0 & F_1'(v, x) > x \geqslant F_2'(v, x); \\ +1 & x < F_2'(v, x), \end{cases}$$

where

$$\left.\begin{aligned} F_1' &= \begin{cases} \dfrac{v^2+3v+1}{2}, & \text{if} \quad x \geqslant 0 \\ -\dfrac{v^2+v-1}{2}, & \text{if} \quad x < 0; \end{cases} \\ F_2' &= -F_1'(v-x). \end{aligned}\right\} \qquad (17)$$

The block diagrams of the optimal control system for the relay-pulse systems which are realizable according to (8) and (17) are shown in figure 5.

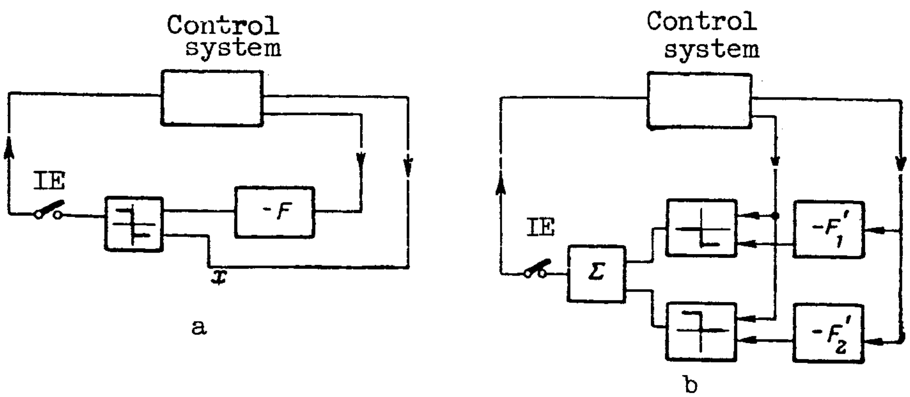

Figure 5

In conclusion we should say a few words on the possibilities of the use of pulse systems with discrete assemblies of control actions in general.

Here we have considered pulse systems with a set of control actions containing two or three values. Comparing (7) and (9), we can see that the use of three values of the control action shortens the time of the optimal transient process in our system in comparison with the case of two values.

The reduction of the time of the transient process in this case can amount to 0, 1, 2, or 3 steps, depending on the position of the initial point. We should note that further increase of the number of levels used for control does not lead to reduction of the time for the transient process in this simple system, although with an increase of the number of discrete control levels used we can obtain greater accuracy of the final result.

REFERENCES

1. Krasovskiy, N. N. A Problem of Optimal Control (Ob odnoy zadache optimal'nogo regulirovaniya). Prikladnaya matematika i mekhanika, Vol. 21, No. 5, 1957.

2. Kalman, R. E. Optimal Nonlinear Control of Saturating Systems by Intermittent Action. IRE Wescon, Convention Record, Vol. 1, p. 4, 1957.

3. Novosel'tsev, V. N. The Optimal Process in a Relay-pulse System (Optimal'nyy protsess v releyno-impul'snoy sisteme). Avtomat. i telemekh., Vol. 21, No. 5, 1960.

N66 34841

34841

TRANSMITTER AUTOTUNING SYSTEM USING AN AUTOMATIC OPTIMIZER

K. B. Norkin

1. Operating Principle of System

A large number of nonautomated transmitters are in operation at the present time. The development of a system for the automatic control of radio transmitters is an important problem. /144

The choice of the criterion of optimal operation of the transmitter is difficult in view of the variety of the possible operating regimes (frequency and amplitude modulation, telegraphic regime, single-side band operation, etc.). For a simplified solution of the problem we can consider that the transmitter operates satisfactorily, if its output stage is tuned in resonance with the frequency of the master oscillator and the antenna coupling has the specified value.

The magnitude of the plate current i_k of the power stage tube can serve as an indicator of resonant tuning of the circuit. The variation of i_k with circuit tuning is shown in figure 1, where the angle of rotation α of the shaft of the tuning knob of the output stage loop is plotted along the horizontal axis. The relationship $i_k(\alpha)$ has an extremum. If we increase the antenna coupling, the form of the relation $i_k(\alpha)$ is altered (dashed curve in fig. 1). An electrical signal proportional to the plate current can be obtained easily by means of the measurement of the voltage drop across a small resistor included in the cathode circuit of the output stage tube.

Thus, the simplified problem posed above can be solved as follows. One system must provide for positioning of the transmitter tuning knob, so that the output loop is tuned to resonance. Another system must provide for loading the plate circuit to the specified value i_k with resonance. Loading is accomplished by means of increasing the antenna coupling. The first system can operate only with the use of automatic search. The second system is a conventional automatic regulation system (ARS).

On the basis of the considerations just mentioned, the Institute of Automation and Remote Control of the Academy of Sciences USSR (IAT) and the /145

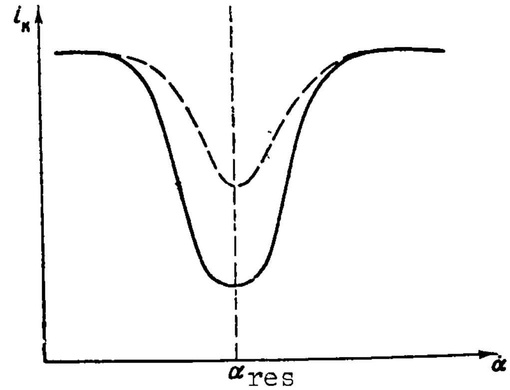

Figure 1

October Radio Transmitting Center have developed a system for autotuning of the output stage loop and a system for automatic loading.

In the system use is made of the single-channel, noise-resistant, automatic optimizer with proportional action 1AO1-1 (ref. 1) developed at IAT and the antenna coupling regulator (ACR), which is a very simple three-position regulator with a dead zone.

Tuning of the transmitter was accomplished using the circuit shown in figure 2. The retuning of the plate circuit in the transmitter Tr was accomplished with the use of the reversing motor M_1. The motor was controlled by the automatic optimizer. As mentioned above, the tuning of the circuit to resonance with the master oscillator corresponds to the minimal value of the dc component of the current i_k. The magnitude of i_k was determined by measuring the voltage drop across the resistor R_k. This voltage was applied to the input of the optimizer AO.

Simultaneously with the tuning of the plate loop in resonance, the motor M_2 was used to regulate the antenna coupling by maintaining i_k equal to a definite value. The antenna coupling was increased or decreased with the aid of the antenna coupling regulator (PCA in fig. 2). In this case the systems for search and regulation operated jointly.

This system maintained the minimum of the plate current with high accuracy. The presence of a considerable ac frequency component (50 cps) in the plate current had practically no effect on the search process. The joint operation of the search and regulation systems with proper selection of rates of travel did not introduce any significant cross talk.

The transmitter ~~tuning~~ lasted 10-20 sec. The tuning time depended on the magnitude of the established constant of integration and the magnitude of the initial misalignment of the transmitter. The error in holding the minimum of the anode current did not exceed 0.5 percent. After termination of the

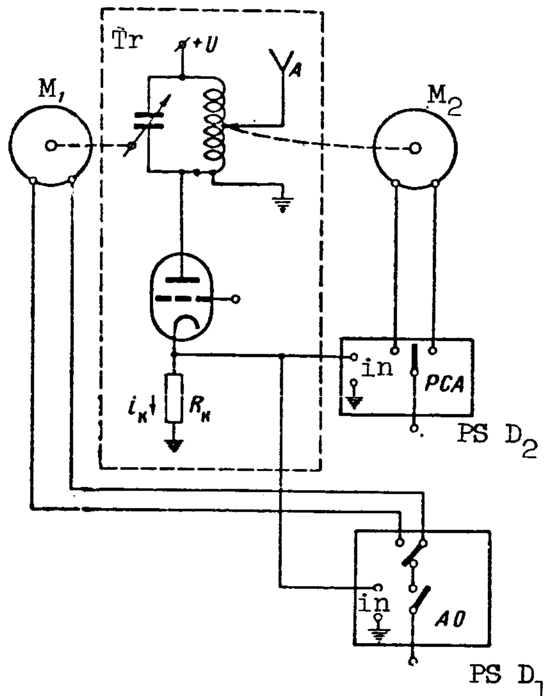

Figure 2. M, motor; Tr, transmitter; in, input; PCA, antenna coupling controller; PS, power supply; AO, automatic optimizer.

search process, the optimizer hunted about the extremum point due to the presence of noise. The hunting period depended on the magnitude of the constant of integration and was equal to about 10-25 sec. The primary noise sources were integrator drift and the variation of the transmitter voltages and the parameters of the anode circuit due to heating.

An operational system of autotuning has been developed and introduced in the October Radio Center on the basis of this simplified circuit. In addition to the units mentioned, it includes an exciter selector unit and a coarse tuning unit. The coarse tuning unit, constructed using positional servosystems, performed the preliminary establishment of the circuit near the operational frequency. /146

In the process of the development and the introduction of the autotuning system several problems arose concerning optimal selection of the tuning parameters of the automatic optimizer. The results obtained can be used for many other cases.

2. Selection of the Optimizer Tuning Parameters

The block diagram of the automatic optimizer used is shown in figure 3.

When relay P_1 operates, the memory device m is connected to the inertial filter T_F and stores the voltage in its output. The integrator returns to the

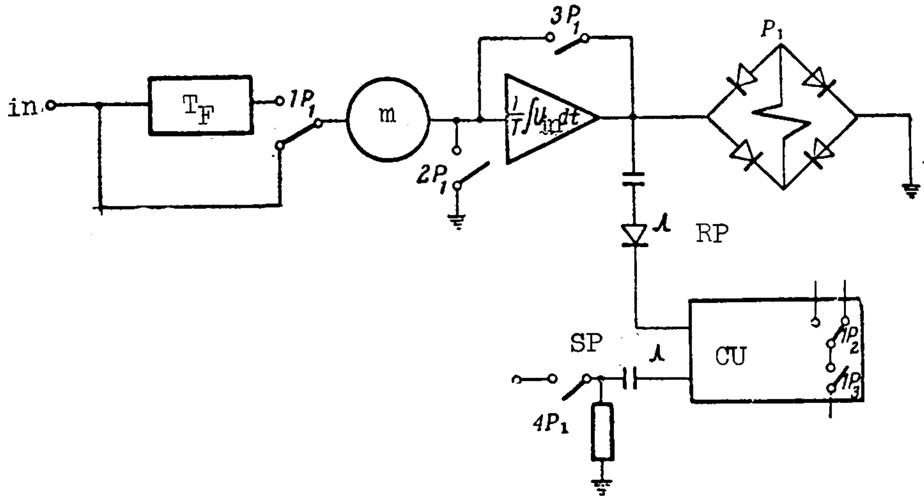

Figure 3. In, input; m, memory; RP, reverse pulse; SP, step pulse; CU, control signal shaping unit.

zero initial conditions, and a preparatory pulse is sent to CU, the control signal shaping unit block.

After dropout of relay P_1, the voltage stored in m is connected in opposition to the input voltage. Thus a computation is made of the difference ΔU_{in} between the instantaneous and the stored averaged values of the input voltage. Simultaneously, there is closure of contact $1P_3$ in CU for a length of time which determines the length of the operational step of the actuator. The direction of the operational step is determined by the position of contact $1P_2$ of CU. If after the operational step the difference ΔU_{in} has an unfavorable sign, then a pulse arrives in CU, which causes the throwing of contact $1P_2$.

Relay P_1 operates, if the magnitude of the output voltage reaches the specified triggering threshold. It is evident that in this circuit the larger the magnitude of the difference ΔU_{in}, the higher are the triggering frequency and the rate of motion toward the extremum.

The following factors have a significant effect on the operation of the optimizer: the dynamic properties and the static characteristics of the system of the automatic search, the drift of these characteristics in the course of time, the magnitude of the integrator constant T_i, the value of the time constant of T_F of the inertial filter, and the length of the step Δx. Moreover,

since in the operation of the optimizer the determination of the small difference of two large quantities is of essence, it is important to consider the operation of the optimizer in the presence of noise, in the general case white noise of a definite spectral density (S_0). /147

The proper selection of the optimizer adjustments and the analysis of the transient processes is complicated by the circumstance that the input coordinate x varies in discrete steps Δx.

For the consideration of the operation of the optimizer it is necessary to specify certain concepts and definitions more accurately.

We represent the system of the automatic search in the form of a series connection of an inertialess nonlinear element (whose output signal is U_y) and an inertial linear element (whose output signal is U_i).

The equation of the linear element, relating the instantaneous value of the input U_y and the instantaneous value of the output U_i, will be

$$U_i + a_1\dot{U}_i + a_2\ddot{U}_i + \ldots = U_y. \tag{1}$$

The equation of the nonlinear element

$$U_y = f_0(x). \tag{2}$$

In this equation x corresponds to the position of the regulating element, and U_y is the static value of the output. The function f_0 must satisfy the following conditions: its derivative $\frac{df_0}{dx}$ is bounded, has only one zero and is monotonic near the zero. For convenience of analysis we shall consider that $\frac{dU_y}{dx} = 0$ with x = 0. The function $f_0(x)$ is the static characteristic of the system. The drift of this static characteristic will not be considered.

During the process of the optimizer operation certain values of the output quantity of the system are stored

$$U_{si} = f_0(x_i, t_i), \tag{3}$$

where x_i and t_i are constants;

U_{si} is compared with the instantaneous value of U_i.

(subscript s = storage.)

It is evident that

$$U_{si} = U_i(t_i - \Delta t), \tag{4}$$

where Δt is a variable delay which with each step increases linearly from zero to some value and then again decreases to zero.

The input signal of the optimizer ΔU_{in} is the difference between two values of U_i. It corresponds to the value of U_{si}, i.e., to the value at the moment of storage. Another value of U_i is taken with a new position of the regulating element at the moment of time t.

$$\Delta U_{in} = U_i(t) - U_{sk}. \tag{5}$$

It is evident that ΔU_{in} is a function of time.

The optimizer sensitivity ΔU is defined as the minimal value of the input signal, which is always adequate for the system to select the correct direction of movement.

The problem of the analysis of the operation of the system with this optimizer will be that of finding

$$x_i = f_1(t) \tag{6}$$

and the relation /148

$$U_i = f[f_0(x), t, t_0, x_0, U_0, \dot{U}_0, \ddot{U}_0 \ldots] \tag{7}$$

with definite optimizer parameters T_i, T_F and Δx.

The problem of the synthesis of the optimizer parameters consists in the selection for a given system of the values of T_i, T_F and Δx, which will permit approaching in an optimal fashion the desired form of the transient process $U_i = f_{des}(t)$ (des = desired).

If in the solution of the synthesis problem we are not able to satisfy exactly the prescribed value of $f_{des}(t)$, we must select f(t) so that the integral

$$D = \int_{t_0}^{\infty} | f(t) - f_{\text{des}}(t) | \, dt \tag{8}$$

will be minimal. In the present case D is the search loss.

The position of the regulating element in the search process can vary only in discrete steps, i.e.,

$$x_i = x_{i-1} + \Delta x \tag{9}$$

and then

$$U_y = U_{y-1} + \frac{dU}{dx} \Delta x. \tag{10}$$

If U_k is the value of U_y with x = 0 (fig. 4), then, obviously, $\Delta U_0 = U_{k-1} - U_k$ must not be larger than the permissible error of maintenance of the extremum of θ. However, since of necessity $\theta > \Delta U$ and if $\Delta U_0 = \theta$, then there will of necessity be oscillations about the extremum in the system.

In order that the motion near the extremum be of a random nature rather than systematic, it is necessary that

$$0 = | f_0(0) - f_0(2\Delta x) | \tag{11}$$

and

$$\Delta U_0 = | f_0(0) - f(\Delta x) | = \Delta U, \tag{12}$$

i.e., it is necessary to permit system hunting in the range of two steps about the extremum (11) and to provide the maximal input signal of the optimizer in the center of the hunting zone equal to the sensitivity (12).

If $\Delta U < \Delta U_0$, then a stable cycle of four steps may be formed after termination of the search process. The frequency of the steps will diminish with reduction of ΔU_0. If ΔU_0 satisfies equation (12), the hunting frequency will be minimal and will not change with further reduction of Δx, because in this case the hunting will be determined primarily by the self-noise of the optimizer, i.e., will not depend on the input signal. Since reduction of the step leads

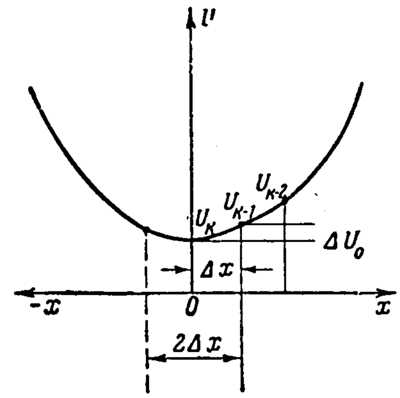

Figure 4

to slowing of the search, it is not advisable to take Δx smaller than the value corresponding to (12).

In the case where $x_i = \pm 100$ percent, the optimizer sensitivity is 0.05 percent of the input voltage scale, and $U_y = 0.02x_i^2 - 100$ percent, the required maximal value of the step Δx is determined from equations /149

$$f_0(0) = -100\%; \quad f_0(\Delta x) = 0.02\,\Delta x^2 - 100\%;$$
$$\Delta U_0 = f_0(0) - f_0(\Delta x) = 0.05,$$

where 0.05 is the optimizer sensitivity;

$$\Delta x = \sqrt{2.5} = 1.6\%.$$

In this case the greatest error in the maintenance of the extremum (without account for the effect of noise and drift of the static characteristics of the system) will be

$$\theta = 0.08 \cdot 2.5 = 0.2\%.$$

As we see from this analysis, Δx is very small; consequently, with sufficient frequency of the steps we can take the variation of x to be continuous.

For the case of a 1st order inertial system and negligibly small inertia of the filter T_F, the nature of the transient process can be determined by direct computation.

If the search for the minimum of the function U is performed and N steps have been made from the moment of beginning the search, then

$$U_n = U_N + (U_{N-1} - U_N + \xi_{n-1}) e^{-\frac{t-t_{n-1}}{T_0}}; \tag{13}$$

$$U_{n-1} = U_{N-1} + (U_{N-2} - U_{N-1} + \xi_{n-2}) e^{-\frac{t_{n-1}-t_{n-2}}{T_0}} \tag{14}$$

where T_0 is the object time constant;

t_{n-1} is the time of transmission of the command for the (n - 1)th step;

U_N is the static value of U at the Nth step;

U_n is the real value of U at the nth step;

ξ_{n-1} is the difference $U_{N-1} - U_{n-1}$ existing at the beginning of the nth step, i.e., the lag of the dynamic output of the system from the static output.

With operation of the optimizer a computation is made of the difference between the value of U at the end of the preceding step and the current value, and this difference is integrated by an integrator with the gain $-1/T_i$.

The output voltage of the integrator is equal to

$$U_{out} = -\frac{1}{T_i} \int_{t_{n-1}}^{t} (U_n - U_{n-1})\, dt^{**}$$

or else

$$T_i' = -\int_{t_{n-1}}^{t} [U_N - U_{N-1} - \xi_{n-1} + (U_{N-1} - U_N + \xi_{n-1}) e^{-\frac{t^{**}-t_{n-1}}{T_0}}]\, dt^{**}.$$

Taking $y_{N-1} - y_N + \xi_{n-1}$ outside the integral sign, we obtain

$$T_i' = [U_{N-1} - U_N + \xi_{n-1}] \int_{t_{n-1}}^{t} (1 - e^{-\frac{t^{**}-t_{n-1}}{T_0}})\, dt^{**}$$

and after integration we obtain /150.

$$\frac{T_i'}{(t-t_{n-1})+T_0(e^{-\frac{t-t_{n-1}}{T_0}}-1)}=U_{N-1}-U_N+\xi_{n-1}. \quad (15)$$

By definition

$$\xi_n=(U_{N-1}-U_N+\xi_{n-1})e^{-\frac{t_n-t_{n-1}}{T_0}}. \quad (16)$$

If we introduce

$$T_i'=k_i T_0;\ t_n-t_{n-1}=k_T T_0,$$

equations (15) and (16) can be rewritten in the form convenient for computation

$$\frac{k_i}{k_T+e^{-k_T}-1}=y_{N-1}-y_N+\xi_{n-1}=y^* \quad (17)$$

$$\xi_n=y^* e^{-k_T}. \quad (18)$$

If we assume a value of k_i, after obtaining ξ_{n-1} we determine k_T from equation (17) and find ξ_n from equation (18).

Thus, equations (17) and (18) are recurrence relations which permit the determination of sequential values of ξ_i. In this case, with differing values of k_i we obtain differing graphs of ξ_i. We consider optimal that graph with which y* changes sign two steps after passing the extremum.

Figure 5 shows the graphs of ξ_i for various values of k_i.

For convenience of computations we constructed the graph of the function

$$y^*=\frac{1}{k_T+e^{-k_T}-1}. \quad (19)$$

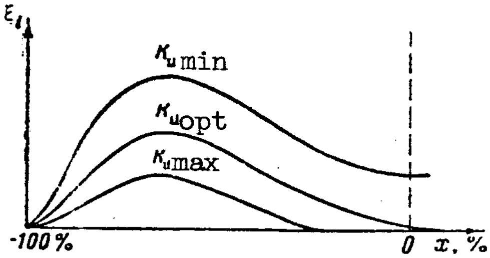

Figure 5

From the value of y* in a given step we determined k_T and e^{-k_T} and then used equation (18) to find ξ for the succeeding step.

The curves of figure 5 show that with an inertial system it is not advisable to establish excessively small integrator constants k_i, because with $k_i = 0.1$ we already observe some over-regulation, which for a given optimizer can lead to an extended dwell period prior to change of the direction of movement.

Oscillograms reflecting the process of the search and selection of optimal adjustment of the optimizer have been obtained experimentally. The variations of the input coordinate x and the coordinate at the output of the inertialess nonlinear element were recorded. The step length Δx was equal to 3 percent of the scale of the variation of the input voltages.

It was found that the best value of the integrator time constant was $T_i = 0.015$ sec, which corresponds to $k_i = 0.37$. The deviation from the computed value is due to the fact that in the analysis the increment was taken equal to 1 percent.

In the analysis of the optimizer noise stability we can represent the /151 input signal in the form of the useful signal U_i and the noise $\xi(t)$. Since in the operation of the optimizer a storage of the useful signal (and noise) is performed, and then a subtraction of the current value of U_i from the stored signal, with small input signals ΔU_{in} we can limit ourselves to the consideration of the passage of stationary white noise of spectral density S_0 through the optimizer.

With passage of white noise through an inertial filter, the time-average value of the noise at the filter output is equal to (ref. 2)

$$\sigma_1 = \sqrt{\frac{S_0}{4T_F}}. \tag{20}$$

A randomly taken value of the output voltage of the filter (ξ_2) is stored. The average value of the stored voltage is equal to σ_1. This quantity, and also the quantity $\xi(t)$, are applied to the integrator input. At the integrator output there will be the quantity

$$\eta(t) = \frac{1}{T_i}\int_0^\tau \xi(t)\,dt + \frac{1}{T_i}\int_0^\tau \xi_2 dt. \tag{21}$$

Squaring and taking the mean value, we obtain

$$\overline{\eta^2(t)} = \frac{1}{T_i^2}\int_0^\tau\int_0^\tau \overline{\xi_1(t_1)\,\xi_1(t_2)}\,dt_1\,dt_2 + \frac{2}{T_i^2}\int_0^\tau \overline{\xi_1(t_1)\,\xi_2}dt_1\,dt_2 + \frac{1}{T_i^2}\int_0^\tau\int_0^\tau \overline{\xi_2^2}dt_1\,dt_2. \tag{22}$$

The second integral in equation (22) is equal to zero, since $\overline{\xi_1(t_1)} = 0$.

Consequently we can write

$$\sqrt{\overline{\eta^2(t)}} = \frac{1}{T_i}\sqrt{\frac{S_0 t}{1} + \frac{\overline{\xi^2} t^2}{2}} \tag{23}$$

and with account for equation (20), since

$$\sigma_1 = \sqrt{\frac{S_0}{4T_F}},$$

we obtain

$$\sqrt{\overline{\eta^2(t)}} = \frac{1}{T_i}\sqrt{S_0 t + \frac{S_0 t^2}{8T_F}} = \frac{\sqrt{S_0}}{T_i}\sqrt{t + \frac{t^2}{8T_F}}. \tag{24}$$

Relation (24) defines the dispersion of the output voltage of the integrator as a function of time. Since the transformations performed with the random quantity $\xi(t)$ are linear, at every instant of time there are observed normal distributions of the probable deviations with the mean-square deviation $\sigma = \sqrt{\overline{\eta^2(t)}}$, which is easily determined from equation (24).

The probability of the appearance of a noise signal above some value U is determined by the familiar equation for normal distribution.

With application to the integrator input of a signal equal to the sensitivity, we obtain at the output

$$\eta_2(t) = \frac{1}{T_i} \Delta U t. \tag{25}$$

When $\eta_2(t) = U_{av}$ of the integrator, the time t is equal to /152

$$t = \frac{U_{av} T_i}{\Delta U}. \tag{26}$$

With operation of the optimizer, the probable mean value at the output of the integrator after the time t, determined by equation (26), must be in a definite relationship with U_{av}. This relation is determined by the admissible probability of a false step, which must always be less than half. If we take $U/U_{av} = 1$, we obtain

$$U_{av} = \frac{\sqrt{S_0}}{T_i} \sqrt{\frac{U_{av} T_i}{\Delta U} + \frac{U_{av}^2 T_i^2}{\Delta U^2 8 T_F}} \tag{27}$$

Relation (27) establishes the connection between U_{av}, S_0, ΔU and T_i, T_F. If T_i and T_F are taken so that relation (27) is satisfied, the probability of a correct step is determined by the equation

$$P(\sigma) = \frac{1}{\sigma\sqrt{2\pi}} \int_{-\sigma}^{\sigma} e^{-\frac{x^2}{2\sigma^2}} dx \cong 68\%.$$

The rate of movement of the optimizer diminishes for small input signals. An additional time appears, which it is advisable to use for the separation of the signal from the noise.

It follows from equation (20) that the noise level at the output of an RC-filter is constant in time. It is rational to use a filter for which the noise level at the output diminishes with time.

The simplest realization of such a filter is shown in figure 6. At the first instant after opening the contact, the voltage on condenser C is equal $y_i + \eta(t_0)$, where y_i is the useful signal and $\eta(t_0)$ is a random quantity whose

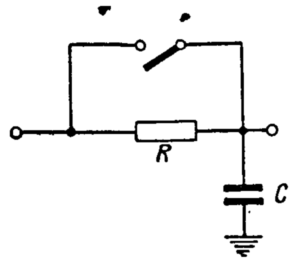

Figure 6

mean square value is determined by the noise level at the optimizer input. A long time after opening the contact, the voltage on condenser C is equal to $y_i + \eta(t)$, where $\eta(t)$ is a random quantity whose mean square value is determined by equation (20). At an intermediate instant of time the mean square of $\eta(t)$ takes an intermediate value.

With this connection of the memory filter T_F, its time constant does not affect the dynamics of the search process, because the achievement of the steady-state values of $\eta(t)$ is delayed in this case, while the dispersion of the integrator output voltage increases (24) with time.

If $T_n' = T_n U_{av}$ is defined on the basis of the optimal dynamics of the /153
search process, we should set

$$T_F = T_n'^2 / S_0. \tag{28}$$

The noise stability will decrease with increase of T_F. For improved noise stability of the system T' should be increased.

REFERENCES

1. Fitsner, L. N. and Norkin, K. B. The 1A01-1 Automatic Optimizer. Advanced Scientific, Engineering and Production Experiment (Avtomaticheskiy optimizator 1A01-1. Peredovoy nauchno-tekhnicheskiy i proizvodstvennyy opyt). Izd. filiala Vsesoyuznyy institut nauchnoy i tekhnicheskoy informatsii, Report 42, No. P-59-15/1, 1959.

2. Lenshk, J. H. and Bettin, R. J. Random Processes in Automatic Control Problems. I. L., 1958.

N66 34842

BOUNDEDNESS OF TRANSIENT REGIMES IN A PENTAVARIATE AUTOMATIC CONTROL SYSTEM

R. P. Parsheva

Using as an example a controllable winged rocket (with liquid rocket engine and with airspeed stabilizer), the present paper studies a pentavariate automatic control system (ACS), equipped with an autopilot with proportional feedback and a three-dimensional field of control with respect to attitude, pitch rate and deviation of flight altitude from a constant preset value. /154

1. Statement of the Problem

We consider a pentavariate autonomous ACS with a single nonlinearity: equations of motion of the rocket

$$\left.\begin{aligned}&\ddot{\vartheta} + a_1\dot{\vartheta} + a_2\alpha + a_3\delta = 0;\\ &\dot{\theta} = a_4\alpha + a_5\delta;\\ &\dot{H} = V\theta;\\ &\vartheta = \theta + \alpha;\end{aligned}\right\} \tag{1}$$

autopilot equations

$$\left.\begin{aligned}\sigma = \vartheta + \mu\dot{\vartheta} + \nu H - \frac{1}{i}\delta;\\ \dot{\delta} = f(\sigma).\end{aligned}\right\} \tag{2}$$

Here ϑ is the rocket pitch angle; θ is the flight path angle; α is the angle of attack; H is the deviation of the flight altitude from the specified value; σ is the control surface signal; δ is the deflection of the elevator; i, μ, ν - are autopilot parameters; a_1, a_2, a_3, a_4, a_5 - are the aerodynamic constants of the rocket.

Introducing the variable $z = \dot{\vartheta}$ and excluding α and δ, system (1) can be written in the form

$$
\left.\begin{aligned}
&+(a_1+a_3i\mu)z+(a_2+a_3i)\vartheta-a_2\theta+a_3i\nu H=a_3i\sigma;\\
&\dot{\vartheta}\qquad -z\qquad\qquad =0;\\
&\dot{\theta}\qquad -a_5i\mu z-(a_4+a_5i)\vartheta+a_4\theta-a_5i\nu H=-a_5i\sigma;\\
&\qquad\qquad -V\theta\qquad =0.
\end{aligned}\right\} \quad (3)
$$

The integral curve (trajectory) of the closed pentavariate ACS passing through the point $X(0)=\{\sigma_0, Z_0, \vartheta_0, \theta_0, H_0\}$, with t = 0 is denoted by /155

$X[t, X(0)]$, where $X(t)=\{\sigma(t), z(t), \vartheta(t), \theta(t), H(t)\}$, $(X(0)=X[0, X(0)])$ are vectors which image the motion of the point.

If there exists a sphere S with radius R within which there is located the entire trajectory X(t), i.e., $|X(t)|<R$ $[|X(t)|\equiv(\sigma^2+z^2+\vartheta^2+\theta^2+H^2)^{\frac{1}{2}}]$ for each t ≥ 0, then trajectory X(t) is termed Lagrange-stable in the positive direction.

Let us show that there exists the open parallelepiped Π

$$
-r\leqslant\xi<\sigma<\dot{\xi}\leqslant r;\quad |z|<r;\quad |\vartheta|<r,\quad |\theta|<r,\quad |H|<r, \tag{4}
$$

(where ξ and $\dot{\xi}$ are some numbers) such that each trajectory X(t) of system (3) passing through point $X(0)\in \Pi$ with t = 0 will not leave the sphere $S\,[X(t)\in S]$ with t > 0, i.e., is Lagrange-stable in the positive direction. Moreover, there exists the number T > 0, such that $X(t)\in\Pi$ with t > T, or system (3) is dissipative in the large (belongs to the Masser class D).

If the function σ = σ(t) is known, then the general solution of system (3) is equal to the sum of the general solution of the homogeneous system and the partial solution of the entire system. The characteristic equation of the system has the form

$$
\begin{vmatrix}
a_1+a_3i\mu+\lambda & a_2+a_3\lambda & -a_2 & a_3i\nu\\
1 & -\lambda & 0 & 0\\
-a_5i\mu & -(a_4+a_5i) & a_4+\lambda & -a_5i\nu\\
0 & 0 & -V & \lambda
\end{vmatrix}=0 \tag{5}
$$

or

$$
\lambda^4+A_1\lambda^3+A_2\lambda^2+A_3\lambda+A_4=0, \tag{6}
$$

where

$$A_1 = a_1 + a_4 + i\mu a_3;$$
$$A_2 = a_2 + a_1 a_4 + i a_3 + i a_3 a_4 \mu - i a_5 (\nu V + a_2 \mu);$$
$$A_3 = i(a_3 a_4 - a_5 (a_1 \nu V + a_2));$$
$$A_4 = \nu V_i (a_3 a_4 - a_2 a_5).$$

Depending on the form of the roots of the characteristic equation, we have different cases.

2. Determination of the Form of the Roots of the Characteristic Equation

The method of determination of the regions in which the roots have the form we need is given by Bottema (ref. 1). By the transformation $\lambda = \lambda_0 - \frac{A_1}{4}$ equation (6) is brought to the form

$$\lambda_0^4 + a\lambda_0^2 + b\lambda_0 + c = 0, \qquad (7)$$

where /156

$$a = \frac{8A_2 - 3A_1^2}{8};$$
$$b = \frac{A_1^3 + 8A_3 - 4A_1 A_2}{8};$$
$$c = \frac{256A_4 + 16A_1^2 A_2 - 64A_1 A_3 - 3A_1^4}{256}.$$

The form of the roots of equation (7) depends on the sign of the quantity D

$$27D = 4(a^2 + 12c)^3 - (2a^3 - 27ac + 27b^2)^2. \qquad (8)$$

By replacement of the variables $u = 12\frac{c}{a^2}$, $v = \frac{27}{2}\frac{b^2}{a^3}$ expression (7) is brought to the form

$$\frac{27}{4}D = a^6 K,$$

where

$$K \equiv (u+1)^3 - (1-3u+v)^2.$$

The curve $u^3 - 6u^2 + 6uv - v^2 + 9u - 2v = 0$ can be written parametrically

$$u = (m-2)(m-4);$$
$$v = (m-1)(m-4).$$

The curve K = 0 is shown in figure 1.

In the following paragraphs we shall construct the solution for the case when the roots of the characteristic equation are real and different. The necessary and sufficient condition that all roots of equation (7), and consequently of (6), are real and different has the form $D > 0$, $a < 0$, $a^2 - 4c > 0$. The region satisfying these three conditions is hatched in figure 1.

3. Stability of the Solution of the Homogeneous System of Equations

The solution of the homogeneous system of equations is stable (the roots of the characteristic equation are negative or have negative real parts) if and only if the coefficients of the characteristic equation satisfy the stability

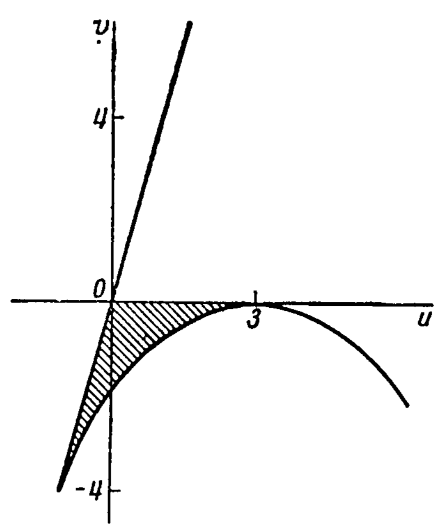

Figure 1

conditions, for example, those of Fuller[1] (ref. 2). For an equation of 4th order the Fuller conditions are written in the form

$$A_1 > 0, \quad A_3 > 0, \quad A_4 > 0, \quad \Delta = \begin{vmatrix} A_1 & A_3 & 0 \\ 1 & A_2 & A_4 \\ 0 & A_1 & A_3 \end{vmatrix} > 0.$$

The conditions $A_1 > 0$, $A_3 > 0$, $A_4 > 0$ are satisfied, since a_5 is small in comparison with c a_1, a_2, a_3, a_4. If we neglect the terms containing a_5, condition $\Delta > 0$ is written /157

$$a_2 + a_1 a_4 + i a_3 a_4 \mu + i a_3 - \nu V (a_1 + a_4 + i \mu a_4) > 0.$$

The graph of the function $f(i\mu, \nu V) = a_2 + a_1 a_4 + i a_3 a_4 \mu + i a_3 - \nu V (a_1 + a_4 + i \mu a_4) = 0$ is an equilateral hyperbola with center at the point $C\left(-\frac{a_1 + a_4}{a^3}; a_4\right)$, and asymptotes parallel to the coordinate axes.

If $D = a_3 (a_4^2 - a_2 - i a_3^2) > a$, the region of possible values of νV and $i\mu$ are hatched in figure 2.

If $D = a_3 (a_4^2 - a_2 - i a_3^2) < 0$, then in the hatched region of figure 3, $f(i\mu,$ $)$.

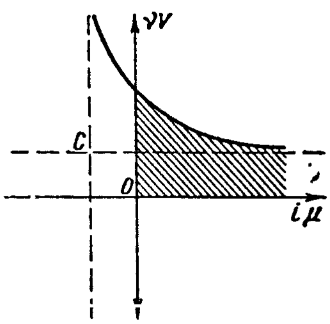

Figure 2

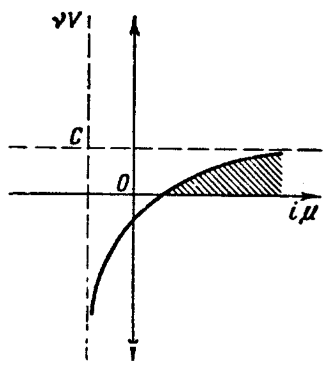

Figure 3

---

[1]These conditions are equivalent to the familiar Routh-Hurwitz condition

4. Finding the General Solution of System (3)

Since we assume that the roots of the characteristic equation are all real, negative and different, the fundamental system of solutions of the homogeneous system of equations has the form

$$z^{(j)} = b_{j1}e^{\lambda_j t},\ \vartheta^{(j)} = b_{j2}e^{\lambda_j t},\ \theta^{(j)} = b_{j3}e^{\lambda_j t},\ H^{(j)} = b_{j4}e^{\lambda_j t},$$

where $b_{j1}, b_{j2}, b_{j3}, b_{j4}$ are the minors of the terms of any row of the determinant (5) $\Delta(\lambda_j)$ (the value of the root λ_j is substituted in place of λ), for which they are not all equal to zero.

The general solution of the homogeneous system

$$\begin{aligned}
z &= C_{11}b_{11}e^{\lambda_1 t} + C_2 b_{21}e^{\lambda_2 t} + C_3 b_{31}e^{\lambda_3 t} + C_4 b_{41}e^{\lambda_4 t};\\
\vartheta &= C_1 b_{12}e^{\lambda_1 t} + C_2 b_{22}e^{\lambda_2 t} + C_3 b_{32}e^{\lambda_3 t} + C_4 b_{42}e^{\lambda_4 t};\\
\theta &= C_1 b_{13}e^{\lambda_1 t} + C_2 b_{23}e^{\lambda_2 t} + C_3 b b_{33}e^{\lambda_3 t} + C_4 b_{43}e^{\lambda_4 t};\\
H &= C_1 b_{14}e^{\lambda_1 t} + C_2 b_{24}e^{\lambda_2 t} + C_3 b_{34}\partial^{\lambda_3 t} + C_4 b_{44}e^{\lambda_4 t}.
\end{aligned}$$

The constants C_1, C_2, C_3, C_4 are determined from the initial conditions and depend linearly on them.

The method of construction of the particular solutions of system (3) is given in the article by Murray and Miller (ref. 3). We use W(x) to denote the determinant of the matrix of the fundamental solutions /158

$$W(x) = C_1C_2C_3C_4e^{(\lambda_1+\lambda_2+\lambda_3+\lambda_4)x}\begin{vmatrix} b_{11} & b_{21} & b_{31} & b_{41}\\ b_{12} & b_{22} & b_{32} & b_{42}\\ b_{13} & b_{23} & b_{33} & b_{43}\\ b_{14} & b_{24} & b_{34} & b_{44}\end{vmatrix}$$

We denote

$$W_0 = \begin{vmatrix} b_{11} & b_{21} & b_{31} & b_{41}\\ b_{12} & b_{22} & b_{32} & b_{42}\\ b_{13} & b_{23} & b_{33} & b_{43}\\ b_{14} & b_{24} & b_{34} & b_{44}\end{vmatrix}$$

W_{ij} is the algebraic complement of the term b_{ij} of the determinant W_0. For our system (3) the particular solutions z_1, ϑ_1, θ_1, H_1 will have the form

$$\left.\begin{aligned}
z_1 &= \int_0^t \left(\sum_{j=1}^4 b_{j1} e^{\lambda_j (t-x)} \frac{W_{1j}}{W_0}\right) a_3 i\sigma\, dx - \int_0^t \left(\sum_{j=1}^4 b_{j1} e^{\lambda_j (t-x)} \frac{W_{3j}}{W_0}\right) a_5 i\sigma\, dx;\\
&= \int_0^t \left(\sum_{j=1}^4 b_{j2} e^{\lambda_j (t-x)} \frac{W_{1j}}{W_0}\right) a_3 i\sigma\, dx - \int_0^t \left(\sum_{j=1}^4 q_{j2} e^{\lambda_j (t-x)} \frac{W_{3j}}{W_0}\right) a_5 i\sigma\, dx;\\
\theta_1 &= \int_0^t \left(\sum_{j=1}^4 b_{j3} e^{\lambda_j (t-x)} \frac{W_{1j}}{W_0}\right) a_3 i\sigma\, dx - \int_0^t \left(\sum_{j=1}^4 b_{j3} e^{\lambda_j (t-x)} \frac{W_{3j}}{W_0}\right) a_5 i\sigma\, dx;\\
H_1 &= \int_0^t \left(\sum_{j=1}^4 b_{j4} e^{\lambda_j (t-x)} \frac{W_{1j}}{W_0}\right) a_3 i\sigma\, dx - \int_0^t \left(\sum_{j=1}^4 b_{j4} e^{\lambda_j (t-x)} \frac{W_{3j}}{W_0}\right) a_5 i\sigma\, dx.
\end{aligned}\right\} \tag{9}$$

The general solution of system (3) has the form

$$\left.\begin{aligned}
z &= \sum_{j=1}^4 c_j b_{j1} e^{\lambda_j t} + z_1; \quad & \vartheta &= \sum_{j=1}^4 c_j b_{j2} e^{\lambda_j t} + \vartheta_1;\\
\theta &= \sum_{j=1}^4 c_j b_{j3} e^{\lambda_j t} + \theta_1; \quad & H &= \sum_{j=1}^4 c_j b_{j4} e^{\lambda_j t} + H_1.
\end{aligned}\right\} \tag{10}$$

After differentiation of the first equation of system (10) we will have

$$\begin{aligned}
\dot{z} &= \sum_{j=1}^4 c_j \lambda_j b_{j1} e^{\lambda_j t} + \left[\left(\sum_{j=1}^4 b_{j1} \frac{W_{1j}}{W_0}\right) a_3 - \left(\sum_{j=1}^4 b_{j1} \frac{W_{3j}}{W_0}\right) a_5\right] i\sigma +\\
&+ i \int_0^t \left[\left(\sum_{j=1}^4 \lambda_j b_{j1} = \frac{W_{1j}}{W_0} e^{\lambda_j (t-x)}\right) a_3 - \sum_{j=1}^4 \left(\lambda_j b_{j1} \frac{W_{3j}}{W_0} e^{\lambda_j (t-x)}\right) \dot{a_5}\right] \sigma\, dx.
\end{aligned} \tag{11}$$

5. Stability According to Lagrange

Using the method of Shirokorad (ref. 4), we show the boundedness of the solution of system (3) as $t \to \infty$ (i.e., stability in the Lagrange sense).

Let us assume that the initial point $X(0)$ belongs to the sphere S with center at the coordinate origin and radius r, i.e., $X(0) \in S$, and let us consider in the interval $(0, \tau)$ of variation of time t the limiting inequalities resulting from (10) and (11) /159

$$\left.\begin{array}{ll}|\bar{z}|<m_1r+l_1\bar{\sigma}, & |\theta|<m_3r+l_3\bar{\sigma},\\ |\vartheta|<m_2r+l_2\bar{\sigma}, & |H|<m_4r+l_4\bar{\sigma},\\ |\dot{z}|<m_1\lambda r+L\bar{\sigma}, & \bar{\sigma}=\max|\sigma(t)|,\ 0\leqslant t\leqslant\tau,\end{array}\right\} \tag{12}$$

where

$$\lambda=\max(\lambda_j),\quad m_k=\varphi_k(b_{ij}),$$

$$l_k=i\Omega(a_3K_{2k-1}-a_5K_{2k}),\quad L=2_i[a_3-4K_6a_5],$$

$$K_{2k-1}=\max\left|b_{j1}\frac{W_{1j}}{W_0}\right|,\quad K_{2k}=\min\left|b_{j1}\frac{W_{3j}}{W_0}\right|,\quad \Omega=-\sum_{j=1}^{4}\frac{1}{\lambda_j}.$$

Then for quantity $y=z+\mu\dot{z}+\nu V\theta$ we can obtain the bound

$$|y|<L_1r+L_2\bar{\sigma}, \tag{13}$$

where $L_1=m_1+m_1\lambda\mu+\nu Vm_3,\ L_2=i[(\Omega K_1+2i\mu+\nu V\Omega K_5)a_3-a_5(\Omega K_2+ + 8K_6\mu+\nu V\Omega K_6)].$

Let us assume that function f(x) of class[1] A satisfies the following conditions of "dissipativity." There exists a sufficiently large r > 0, such that the roots of the equation

$$L_1\omega+L_2\xi=if(\xi) \tag{14}$$

(the values $\xi > 0$ correspond to ω = r and $\underline{\xi}<0$ with ω = -r) lie in the interval $[-r,r]$ and, moreover, the following inequalities are satisfied

$$-\frac{r}{L_2}<\underline{\xi}<\xi<\frac{r}{L_2}, \tag{15}$$

since $L_2>l_k\,(k=1,\ 2,\ 3,\ 4)$ are clearly satisfied and

$$-\frac{r}{l_k}<\underline{\xi}<\xi<\frac{r}{l_k}.$$

[1]The class A includes definite piecewise-continuous functions of the 1st kind with a finite number of discontinuities.

Then the following inequalities are satisfied

$$\underline{\xi} < \sigma(t) < \xi \text{ with } t > 0, \tag{16}$$

if only $\xi < \sigma(0) < \xi$. Assume that this is not satisfied. Then there can be two cases. In the first case there exists the smallest $\tau > 0$, for which $\sigma(\tau) = \xi$ and $\dot{\sigma}(\tau) \geqslant 0$. But in this case we obtain a contradiction, since $\dot{\sigma}(\tau) = y(\tau) - f[\sigma(\tau)] < L_1 r + L_2 \xi - if(\xi) = 0$. In the second case, when there exists the smallest $\tau > 0$, for which $\sigma(\tau) = \xi$ and $\dot{\sigma}(\tau) \leqslant 0$, the same contradiction is obtained.

From inequalities (13) and (16) stability in the Lagrange sense is /160
obtained in the positive direction of each trajectory of (3) passing at the moment of time t = 0 through point X(0) lying within the parallelepiped Π, since each such positive semitrajectory (t > 0) does not leave the sphere S with radius R.

Let us now prove the existence of the number T for which the trajectory $X[t, X(0)] \in \Pi$ with t > T if $X(0) \in \Pi$. From (15) it follows that there exists $\varepsilon > 0$ such that the inequalities

$$\begin{gathered} -\frac{r-\varepsilon}{L_2} < \underline{\xi} < \xi < \frac{r-\varepsilon}{L_2} \\ -\frac{r-\varepsilon}{l_k} < \underline{\xi} < \xi < \frac{r-\varepsilon}{l_k} \quad (k = 1,\ 2, 3,\ 4). \end{gathered} \tag{17}$$

are satisfied.

We denote by $T = \max T_k\ (k = 1,\ 2,\ 3,\ 4)$, where

$$T_k = -\frac{1}{\lambda_a} \ln \frac{m_k r}{\varepsilon}, \qquad \lambda_a = -\min |\lambda_j|.$$

Evaluating more precisely than in (12) the expressions $z(t)$, $\vartheta(t)$, $\theta(t)$, $H(t)$ from (10), we obtain the limiting inequalities

$$\begin{aligned} -m_1 r \exp(\lambda_a t) + l_1 \xi < z(t) < l_1 \xi + m_1 r \exp(\lambda_a t), \\ -m_2 r \exp(\lambda_a t) + l_2 \xi < \vartheta(t) < l_2 \xi + m_2 r \exp(\lambda_a t), \\ -m_3 r \exp(\lambda_a t) + l_3 \xi < \theta(t) < l_3 \xi + m_3 r \exp(\lambda_a t), \\ -m_4 r \exp(\lambda_a t) + l_4 \xi < H(t) < l_4 \xi + m_4 r \exp(\lambda_a t). \end{aligned}$$

From inequalities (16) and (17) it follows that

$$-r \leqslant \underline{\xi} < \sigma(t) < \xi \leqslant r, \quad |z(t)| < r, \quad |\vartheta(t)| < r, \quad |\theta(t)| < r, \quad |H(t) < r$$
with $t > T$,

if

$$\underline{\xi} < \sigma(0) < \xi, \quad |z_0| \leqslant r, \quad |\vartheta_0| \leqslant r, \quad |\theta_0| \leqslant r, \quad |H_0| \leqslant r.$$

Conclusions

Thus we have defined a finite region in which there is embedded every trajectory after passage of a fixed and trajectory-independent starting regime time, if only at the moment of start t = 0 the trajectory begins in this region. We have also defined the region which is not left by any trajectory with t ≥ T. These two regions permit defining the boundaries of safe launch of rockets and the boundaries of altitude oscillations of winged rockets in horizontal flight.

REFERENCES

1. Bottema, O. The Routh-Hurwitz Condition for the Biquadratic Equation. Indicationes Mathematical (Amsterdam), Vol. 59, ser. A, No. 4, 1956.

2. Fuller, A. T. Stability Criteria for Linear Systems and Reliability Criteria for RC-networks. Proc. Cambridge Phil. Soc., Vol. 53, pt. 4, October, 1957.

3. Murray, F. I. and Miller, S. Existence Theorems for Ordinary Differential Equations. New York University Press, 1954.

4. Shirokorad, B. V. On the Existence of a Cycle Outside the Conditions of Absolute Stability of a Trivariate System (O sushchestvovanii tsikla vne usloviy absolyutnoy ustoychivosti trekhmernoy sistemy). Avtomat. i telemekh.,Vol. 19, No. 10, 1958.

N66 34843

PROGRAM CONTROL SYSTEM WITH FREQUENCY SEPARATION OF THE CHANNELS

V. N. Shadrin

1. Introduction

Program control is considered to be one of the dominant trends in the field of automation of production processes. A specified program can be used for the control of the machining of parts of various configurations on metal-working machine tools, for the control of the operation of gantry cranes and devices for gas-cutting of steel sheets, control of the operation of special machine tools for the assembly of complex telephone cables, for the assembly of radio circuits, etc. /161

The control program can be recorded on punched cards, punched tape, movie film, magnetic tape and magnetic drum. Of the listed program carriers, the magnetic tape is considered the most convenient from the operational point of view. At the present time program control has received the widest acceptance in the metal-cutting industry, particularly program control for milling machines.

The program on magnetic tape can be presented in continuous or pulse form.

At the present time the program control systems (PCS) with continuous recording of the information use the principle of phase modulation. In this case, to each displacement of the coordinates of the machine table there corresponds a definite shift in phase between the coordinate signals and the reference signals, which is recorded on the tape together with the operational signals.

For control of the machine in three coordinates it is necessary to record four signals on the tape, one reference signal and three operational (one for each coordinate). Two signals must be left for the control of the auxiliary operations (lubrication, cooling, etc.). Thus, up to six signals may be required for the program control of a milling machine. For the control of other processes, for example the assembly of telephone cables or the assembly of radio components, up to 10-20 signals may be required. Various methods of multichannel magnetic recording can be used for the storage of this quantity of signals on the magnetic tape. Among the methods used at the present time for the recording of the program for continuous system of program control systems are spatial (multitrack recording) and frequency separation of the channels.

Frequency separation is based on the separation of the operational signals by the use of different carriers, which are amplitude-modulated by the /162 operational signals. Normally the operational frequencies are chosen in the range of 400-500 cps, while the carriers are in the range from 1,300-5,000 cps. Since the operational frequencies are phase-modulated, while the carriers are amplitude-modulated, this method of recording can be termed FM-AM frequency division.

2. Frequency Separation of Channels

The block diagram of a PCS with frequency separation of the channels is presented in figure 1. Here the following notation is used: MT is the machine

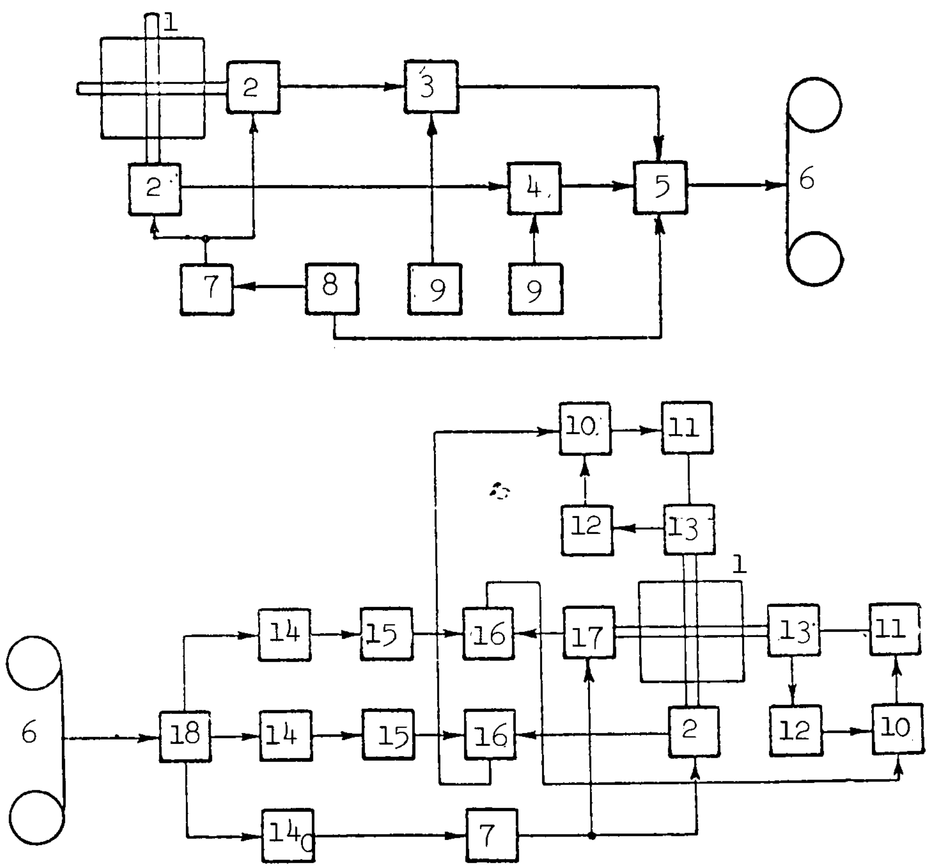

Figure 1. 1, MT, machine table; 2, RT, rotary transformer; 3, FM, frequency modulator; 4, AMo, amplitude modulator; 5, AM, amplifier-mixer; 6, RC, record carrier (magnetic tape); 7, PS, phase splitter; 8, RSG, reference signal generator; 9, CFG, carrier frequency generator; 10, CU, control unit; 11, M, motor; 12, CE, correcting element; 13, TG, tach generator; 14, F, filter; 15, DM, demodulator; 16, PD, phase discriminator; 17, RT, rotary transformer; 18, RA, reproduce amplifier.

tool table; RT is a rotary transformer; PS is a phase splitter; RSG is the reference signal generator; CFG is the carrier frequency generator; AMo are amplitude modulators; AM is an amplifier-mixer; RC is the recording carrier (magnetic tape); RA is the reproduction amplifier; F are carrier frequency filters; F_0 is the reference signal filter; DM are demodulators; PD are phase discriminators; CU is the control unit; M is a motor; TG are tach generators and CE is the correcting element.

The upper portion of figure 1 shows the recording regime, the lower part is the reproduce regime.

The circuit operates as follows. In the record regime the reference signal from the RSG arrives at the phase-splitter, which splits the signal phase at an angle of $\pi/2$; the signal then goes to the rotary transformer RT. /163
The signals at the output of the RT will have phases proportional to the position of the machine table. In AM the phase-modulated operational signals amplitude modulate the carrier coming from the CFG. The amplitude modulated carrier and the reference signals are mixed in AM and recorded on the RC by the record amplifier MEZ-15 on a single track.[1]

In the reproduce regime the signals recorded on the magnetic tape are reproduced by the magnetic heads, are amplified in the RA amplifier and are separated from one another by the bandpass filters F. The reference signal is filtered out by the filter F_0 and is applied to the phase splitter and then to the RT. The signals from the RT are compared with the operational signals arriving from the demodulators DM to the phase meters PD. In the case of phase mismatch between the signals, at the output of the PD appear signals, which through the control unit CU rotate the dc actuator motor M, until the phase mismatch is eliminated. The table drive has rate feedback through the correcting element CE.

Bandpass six-element differential bridge filters are used in the PCS for the separation of the operational signals during reproduction. Filters of this type have a rectilinear phase characteristic in the passband and satisfactory attenuation in the stopband. According to studies which have been made, these filters retain linearity of the phase characteristic to values of the losses in the inductive elements of the filter of the order of $d = 0.02$. To avoid significant phase distortions due to the reflection phase and the reflection interaction phase, the matching coefficient of the filter with the load must be chosen exactly equal to unity.

Figures 2 and 3 present attenuation b_r and phase b curves of the ideal differential-bridge filter, and also phase a and reflection attenuation a_r and coupling reflection a_{cr} with losses $d_L = 0.02$ and a load matching coefficient $\alpha = 0.5$.

---

[1] The MEZ-15 is a standard tape recorder with recording of the program on tape 6.35 mm wide.

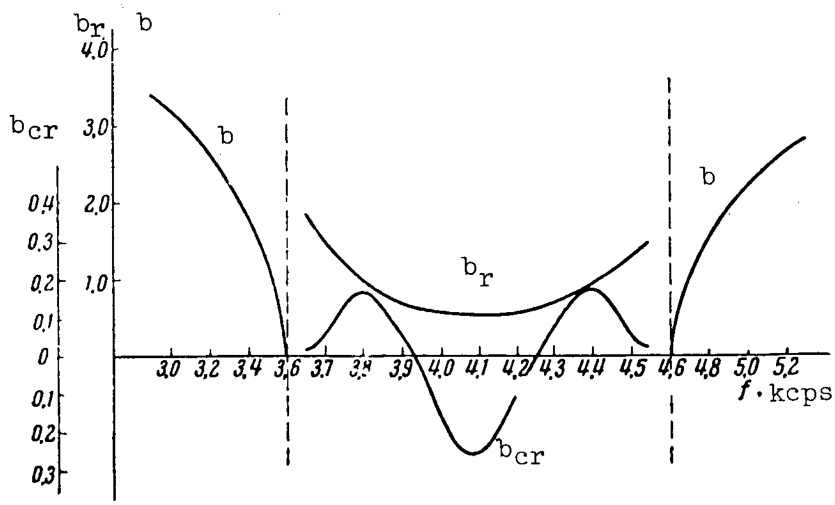

Figure 2. r, reflection; cr, coupling reflection.

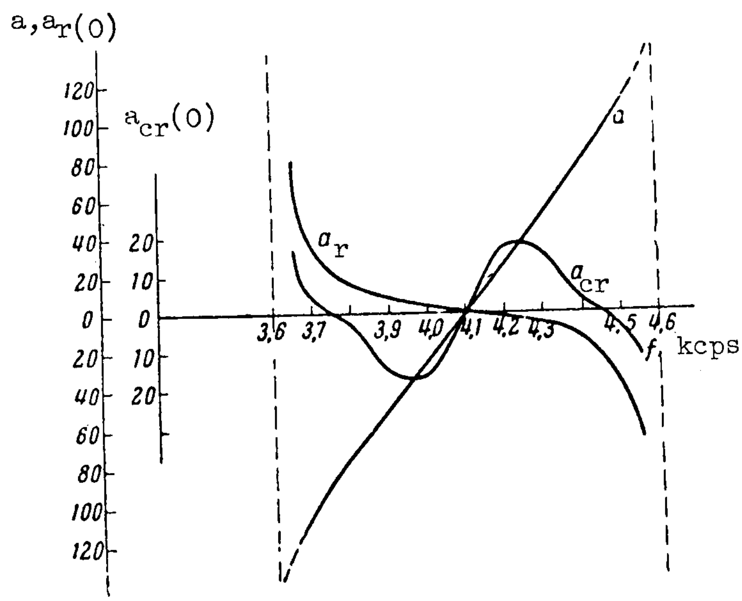

Figure 3. r, reflection; cr, coupling reflection.

The magnetic record-reproduce channel of the continuous system for program control with magnetic recording can be considered a type of communication channel in which the transmitter is the record unit, the communication channel is the magnetic tape and the receiver is the reproduce unit.

Any communication channel can be characterized by the accuracy, the noise stability and the handling capacity. By accuracy of the continuous program control systems with magnetic recording we mean the accuracy of the transmission of the phase shift through the magnetic record-reproduce channel, as measured at

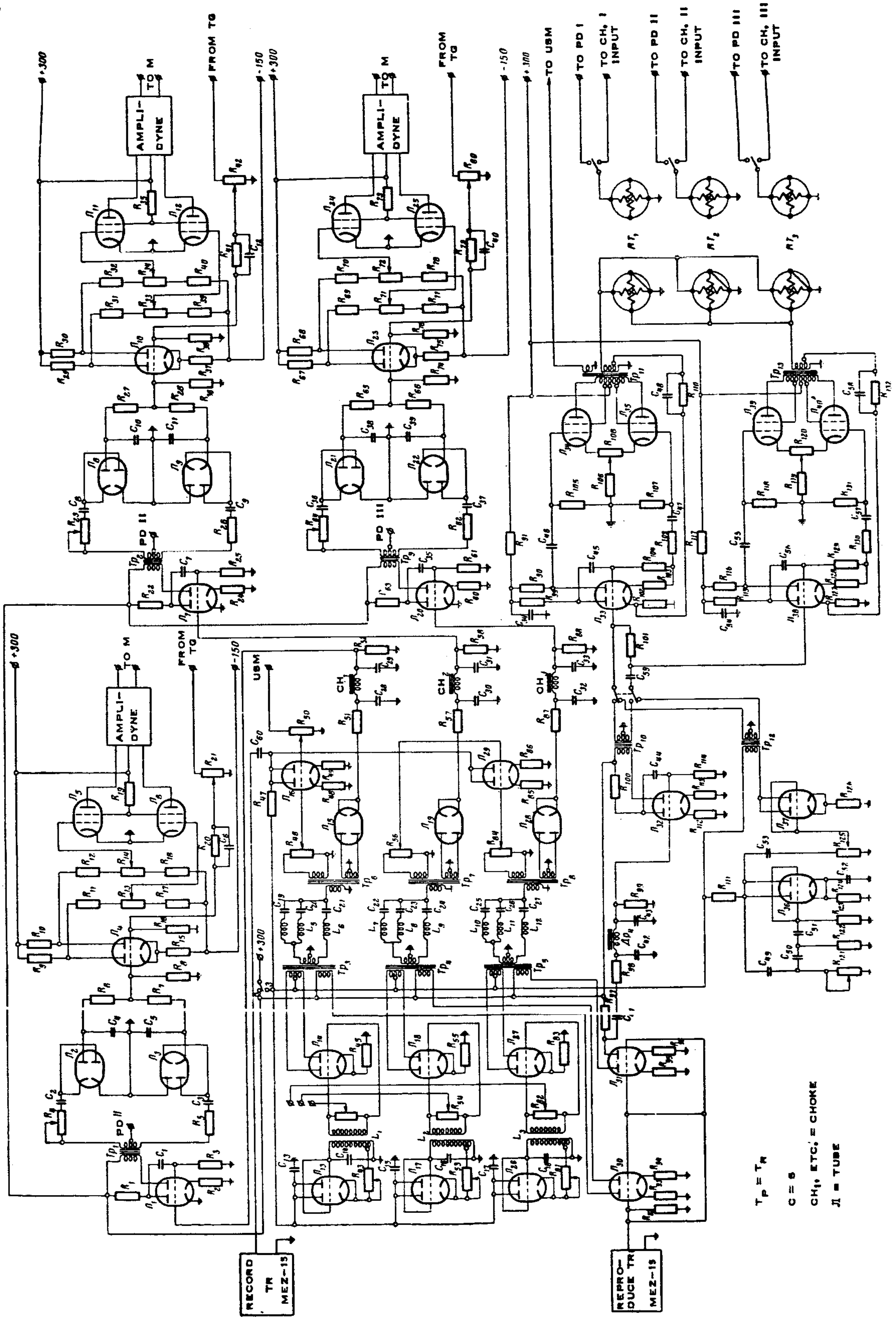
AMPLI-DYNE
TO M
FROM TG
+300
-150
AMPLI-DYNE
TO M
FROM TG
-150
+300
TO USM
TO PD I
TO CH. I INPUT
TO PD II
TO CH. II INPUT
TO PD III
TO CH. III INPUT
PD II
PD III
AMPLI-DYNE
TO M
FROM TG
-150
+300
USM
PD II
RECORD TR MEZ-15
REPRODUCE TR MEZ-15
T_P = T_R
C = S
CH1, ETC. = CHOKE
Л = TUBE

Figure 4

the input of the servosystem; by noise stability we mean the capability of the system to counteract the harmful effect of random noise, and by handling capacity we mean the maximal quantity of information which can be recorded on a one-meter length of the carrier with a given recording method.

The accuracy of the transmission of the information depends on the phase distortions in the magnetic record channel, on the distortions in the circuit for the recording, reproduction and conversion of the information and in the circuit for the engagement of the rotary transformer RT.

Thus, the maximal phase shift

$$\Delta P = \Delta P_{mr} + \Delta P_{c} + \Delta_{RT}. \tag{1}$$

(Subscripts in this and the following three equations: mr = magnetic recording; c = circuit; RT = rotary transformer; cm = cross modulation; n = noise; ct = crosstalk; Pd = phase distortion; f = frequency.) /165

In turn

$$\Delta P_{mr} = \Delta P_{cm} + \Delta P_{n}, \tag{2}$$

where ΔP_{cm} are the phase distortions due to the noise from cross modulation in the head-tape-head system; ΔP_n are the random phase oscillations due to the noise of the magnetic recording channel, and

$$\Delta P_c = \Delta P_{ct} + \Delta P_{Pd} \tag{3}$$

where ΔP_{ct} is the phase shift from crosstalk due to insufficient filtering between neighboring channels; ΔP_{Pd} are the phase distortions in the phase meter due to nonlinear distortions of the signals being reproduced.

The noise stability of the continuous program control systems with frequency separation of the channels as calculated by the methods of the Kotel'nikov theory of potential noise stability can be expressed by the following relation (ref. 1)

$$\sigma^{*}\text{FM-AM} = 2\,\frac{N}{\alpha_r}\,\frac{\sigma}{\Delta P U_0}\ , \tag{4}$$

where N is the number of channels; σ is the specific value of the noise; ΔP is the signal phase deviation; U_0 is the nominal signal voltage; α_r is the utilization coefficient of the dynamic range of the magnetic recording with frequency separation of the channels.

As we see from the expressions presented, with increase of the number of channels the noise stability of the FM-AM PCS deteriorates proportionately. Thus, the handling capacity is worse, the larger the magnitude of the random phase oscillations with reproduction of the recorded signals.

3. Schematic Diagram

The schematic diagram of the FM-AM PCS is presented in figure 4. This figure shows the circuit for the generation, recording and reproduction of the signals combined into a single system, which can be termed the frequency block. The frequency block is mounted in the case of the MEZ-15 tape recorder. The record and reproduce amplifiers and the tape transport mechanism of the tape recorder are used for the recording and preamplification of the signals from the frequency block. The power supply system for this block is not shown in the figure.

The circuit shown provides for control of the operation of the milling machine in two coordinates (longitudinal and lateral). Control of the vertical feed can be provided, if desired. The circuit contains 40 tubes and consumes about 500 W of power from the mains.

According to measurements, the phase distortions from cross modulation amount to $\pm 4^{\circ}$, the random oscillations are $\pm 2^{\circ}$, the phase distortions from crosstalk are $\pm 2^{\circ}$ and the errors of the RT circuit and the phasemeter are in the limits of $\pm 2^{\circ}$.

Figure 5 presents the curve of the phase distortions measured at the input of the servosystem by the compensation method. As we see from the figure,

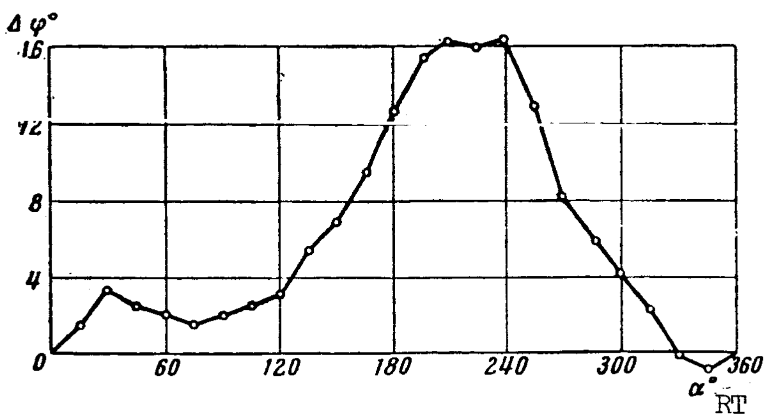

Figure 5

the maximal error amounts to $\pm 8^{o}$ (without account for random oscillations). With a transfer number $i = 1/60$ mm/deg, the static error of the information transmission system, referred to the part, amounts to 0.14-0.15 mm. This relatively large error limits the use of the FM-AM system for the control /166 of processes requiring high accuracy.

Conclusions

Higher accuracy could be obtained by reducing the distortions from cross modulation, crosstalk and by reduction of the error of the RT and increase of the transfer ratio i.

The program control system with frequency separation of the channels is simple and convenient for maintenance and makes use of standard components (magnetic heads, amplifiers and tape drive mechanism of the production MEZ-15 tape recorder).

As a result of the nonlinear characteristic of the system (magnetic head--tape--magnetic head) noise arises from cross modulation between the channels, which causes additional phase distortions of the signal. According to measurements made, the overall distortions amount to $\pm 8^{o}$ with use of excitation from the generator of the MEZ-15. Of this about $\pm 4^{o}$ is due to noise from cross modulation.

Therefore the FM-AM PCS can be recommended for the control of production processes not requiring high[1] accuracy.

REFERENCE

1. Shadrin, V. N. Noise Stability of Analog Program Control Systems with Magnetic Recording (Pomekhoustoychivost' nepreryvnykh sistem programmnogo upravleniya s magnitnoy zapis'yu). Avtomat. i telemekh., Vol. 20, No. 8, 1959.

[1]The static accuracy is ± 0.15 mm with a sensitivity of $i = 1/60$ mm/deg.

N66 34844

THREE-CHANNEL OPTIMIZER

Ye. A. Fateyeva

Introduction

The problem which arises in the regulation of the rectification process amounts to the provision for the specified precision of the separation of the mixture of liquids and the maximal intensification and economy of the process (ref. 1). /167

The rectification column is a complex process whose characteristics depend on many parameters. It is desirable during the time of the process to maintain a minimum of the ratio of the steam consumption per unit of the resulting product of required quality.

The rectification process proceeds as follows. The heated initial mixture Q, which is subject to separation, enters the central portion of the column. Superheated steam Q_1 is supplied to the lower portion of the column and the finished product Q_2 is obtained in the upper part. The separation of the mixture of fluids takes place by the interaction of the mixture with the steam. As a result of heat exchange, the component with the lower boiling point is transformed into a vapor and rises, while the component with the higher boiling point flows downward, forming the so-called still product.

The efficiency of the rectification process is determined by the ratio of the consumption of superheated steam to unit finished product Q_1/Q_2. This relation is complex and is determined experimentally. It has a minimum with definite relationships of the steam consumption, initial mixture and still product. In addition, two limitations are imposed on the regulation process:

$$H_1 < H_1^*; \; H_2 < H_2^*,$$

where H_1^* is the limiting index of the quality of the finished product; H_2^* is the limiting index of the quality of the still product.

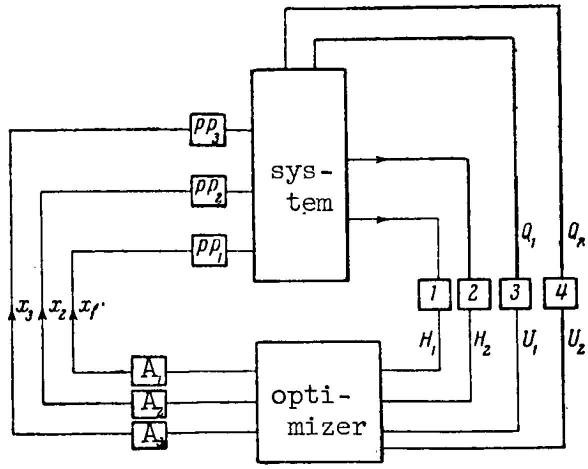

Figure 1. Block diagram of rectification process control. H_1, index of quality of finished product; H_2, index of quality of still product; x_1, flow of superheated steam; x_2, flow of initial mixture; x_3, flow of still product; PP_1, PP_2, PP_3, flow controllers; A_1, A_2, A_3, actuators; 1, 2, 3, 4, electro-pneumatic converters.

The described regulator (fig. 1) is intended for maintaining a minimal value of the ratio Q_1/Q_2 by means of the variation of two or three parameters x_1, x_2, x_3 (x_1 is the superheated steam flow rate, x_2 is the initial mixture flow rate, x_3 is the still product flow rate).

We consider the pressure drop ratio in the corresponding lines as the quantity to be minimized, y. To obtain quantity y, the regulator has a computer (divider), whose inputs are the pneumoelectric pressure and voltage converters.

The quantities H_1^* and H_2^* are given. They are also introduced into the regulator through the pneumoelectric converters and contacts. The regulator outputs x_1, x_2 and x_3 are the commands for the corresponding pneumatic /168 flow regulators. EMD-232 electronic instruments are used to connect the output of the electric regulator and the pneumatic regulators.

The search cycle must continue for 125 min.

Principle of Optimizer Operation

The objective of the three-channel optimizer amounts to the findings of the minimum and its stabilization in the process of the operation of the process. The quantity being minimized $y=k\frac{U_1}{U_2}$ is computed in the computer and delivered in the form of an ac voltage. The optimizer performs the search for the minimum using the gradient principle. The block diagram is shown in figure 2.

The disturbance Δn_1 (test step) is applied at a definite instant of time to the actuator, and consequently to the process. This disturbance causes a change of the quantity Δy being minimized. This change is integrated.

The quantity proportional to the integral and, consequently, to Δy is applied to the memory block MB_1; on the actuator A_2 the test step Δn_2 (similar to the introduction n_1) is introduced into the system. This also causes a change of y, which also is integrated and stored in MB_2.

After this, an operational step is performed, i.e., to A_1 and A_2 there are transmitted from the memory block the quantities Δx_1 and Δx_2 which are proportional, respectively, to Δy_1 and Δy_2. This causes a change of the object parameters, after which there is established a new value of the quantity y. With this the search cycle is terminated.

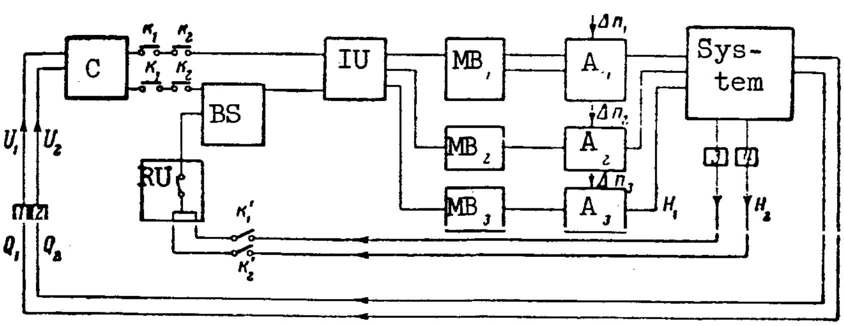

Figure 2. Control block diagram. C, Computer; BS, balanced servosystem; RU, relay unit; IU, integral unit; MB, memory block; A, actuators; 1, 2, 3, 4, pneumoelectric converters; Δn, test step disturbance (remaining notation same as in figure 1).

Then the test step Δn_1 is again applied, Δx_1 is calculated, Δn_2 is applied, Δx_2 is calculated and the operational step is performed and so on.

With reaching of the extremum, auto-oscillations are established in the system whose amplitude in the coordinates x_1 and x_2 cannot be made less than Δn_1 and Δn_2. /169

In the case of regulation of the processes with respect to three parameters x_1, x_2 and x_3--still another memory block MB_3 is provided in the optimizer. In this case test step Δn_3 is made prior to the working step and a corresponding computation of Δx_3 is made.

The fact that the computation of Δx takes place as a test integration with respect to signal y considerably improves the noise stability of the system and increases its accuracy. Improvement of the accuracy is also aided by the use of a balanced servosystem, which increases the integration limit of the electromechanical integrator providing the application of quantity Δy to the integrator. The balanced servosystem has inertia, which also improves the noise stability of the regulator.

In case the quality indices H_1 and H_2 exceed slightly the limiting values in the system in the operational process, the optimizer is switched to the H_1 and H_2 sensors. The optimizer computes ΔH_1 and ΔH_2 and provides for variation of the corresponding quantities Δx_1, Δx_2 and Δx_3 which alter the system parameters so that H_1 and H_2 are established within the acceptable limits.

However, if H_1 and H_2 considerably exceed the limiting values, the system of contacts k'_1 and k'_2 is switched. With operation of contact k'_1, coordinate x_1 is decreased by 10 percent (or by some other set amount); with operation of contact k'_2, coordinate x_2 is changed similarly.

The following elements compose the optimizer (fig. 3): switching device (SD), relay block (RB), computer (C), balanced servosystem (BS), integral block (IB), memory block (MB), actuator (A), supply block (SB).

Switching Unit

The switching unit is intended for continuous and sequential connection of all elements of the circuit (fig. 3). It is assembled using the stepping

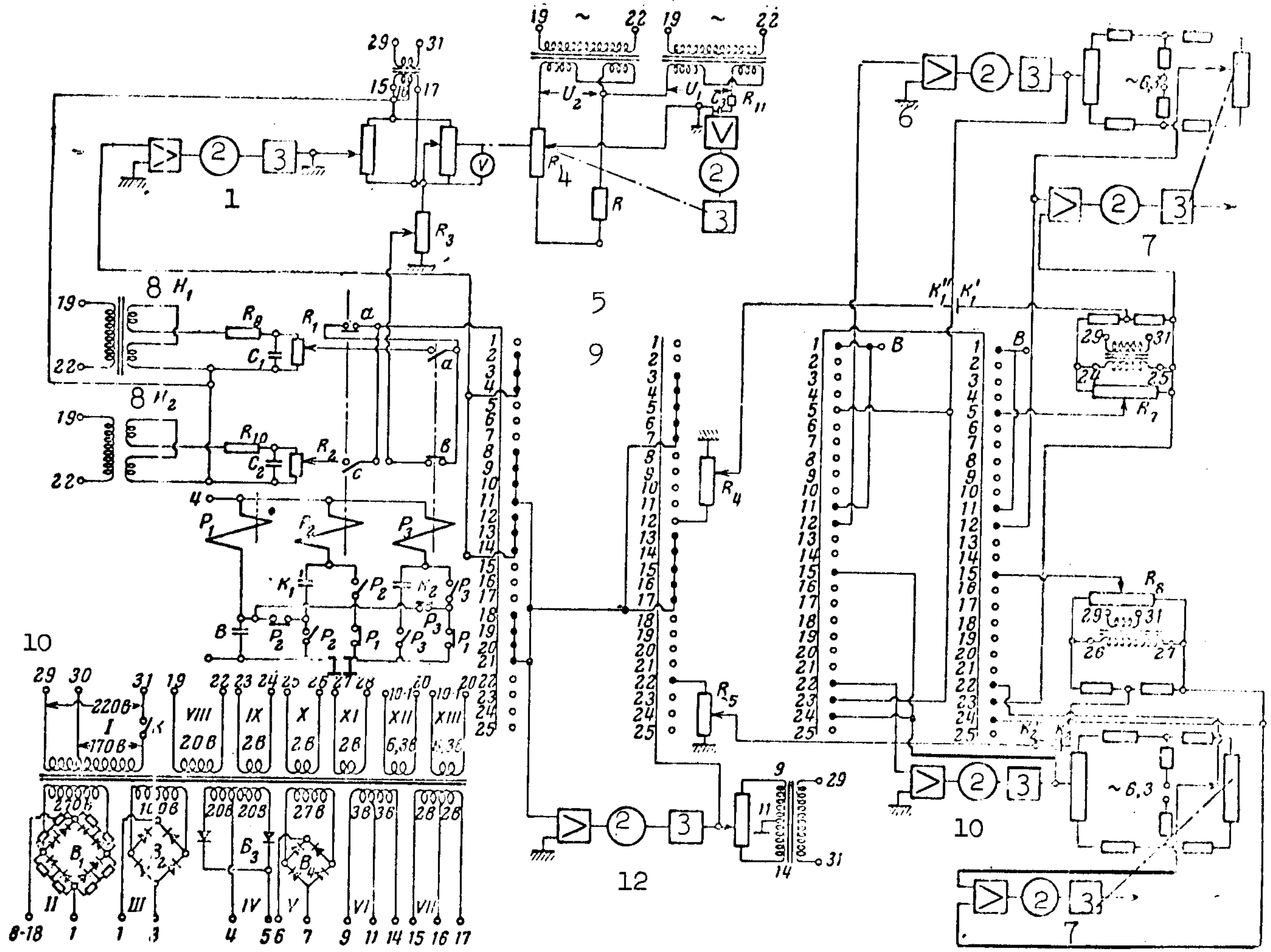

Figure 3. 1, Balanced servosystem; 2, motor; 3, reducer; 4, slidewire; 5, divider; 6, power supply; 7, actuator; 8, sensor; 9, switching device; 10, power supply; 11, relay block; 12, integral unit.

switch SW-50 of the wiper type and is driven by an electromagnet. Operation of the electromagnet occurs when a cam closes the corresponding contacts. The cam is rigidly mounted on the output shaft of the gearbox which is driven by the motor CM-2. Cams with differing profiles and gearboxes with differing gear ratios can be used to obtain varying cycle times. /171

With operation of the cam and the gearbox ($i = 10$) the time of revolution of the cam or time between switchings of the pickoff from one terminal to another is equal to 5 min, while the time for the entire cycle $T_c = 25 \cdot 5 = 125$ min.

The contact field of the stepping switch consists of four rows of contacts (with split pickoffs), corresponding numbers of which are closed simultaneously.

The stepping switch operates as follows. With closing of segment 1, contacts B (segment[1] 1_{3-4}), which engage the relay block, are closed. If the quantities H_1 and H_2 are within the acceptable limits, in the future with closure of segments 2-7 the balanced servosystem (segments 2_1 - 4_1) is connected to the quantity y. If H_1 and H_2 are outside of the acceptable limits, the balanced servosystem is connected to the H_1 and H_2 sensors. Simultaneously the integral block (segments 3_2 - 7_2) is reset to zero.

When the stepping switch is on segment 5, the test step Δn_1 (segments 5_{3-4}) is applied to actuator A_1. At this time the balanced servosystem is disengaged.

With closure of segments 8-11 the change Δy_1, due to the test step Δn_1, is integrated. In segment 11 the system is again tested from the point of view of the limitations of H_1 and H_2. With the transfer to segment 12 the computed integral $\int \Delta y_1 dt$ is transmitted to the memory block MB_1 (segments 12_{2-3-4}). Then KCC is again connected to y or H (segments 12_1 - 14_1), the integral block is again reset to zero (segments 13_2 - 17_2). On segment 15 the test step Δn_2 is applied to the actuator A_2 (segments 15_{3-4}). The integration of the change Δy_2 from the test step Δn_2 (segments 18_1 - 21_1) and transmission to the memory block MB_2 is again performed.

---

[1] The segment subscripts denote the number of the row of the contact field.

Finally, with closure of segments 23 and 24 signals Δx_1 and Δx_2, proportional to increments Δy_1 and Δy_2, are applied to the corresponding actuators A_1 and A_2 (operational steps). The operational steps are made nearly simultaneously. Segment 25 is vacant. Then segment 1 is closed again and so on, and the entire operational cycle is repeated.

Thus the switching unit provides for continuous operation of the optimizer.

Switchover of the regulator from two quantities x_1 and x_2 to three quantities x_1, x_2, x_3 is accomplished by replacement of the stepping switch with a switching device, whose assembly provides for minimization with respect to three input quantities.

Relay Block

The relay block of the optimizer serves to switch the balanced servosystem amplifier input and the integrating block amplifier from the memory block to the sensor for the limited quantity when it gets beyond the operational zone.

The relay block consists of three telephone relays of the RM type and is fed by full-wave rectified voltage of 20 V (fig. 3). When the optimizer is functioning in the operational zone, contacts K_1 and K_2 of the signal devices are open. At some instant of time segments B (1 or 11) of the stepping /172 switch SW-50 are connected to the circuit of relay P_1. Relay P_1 operates, while relays P_2 and P_3 will be de-energized, since their circuits are opened by contacts K_1 and K_2. Therefore the brush of the stepping switch will be connected through the unopened contacts a of relay P_2 and b of relay P_3 to the computer. In this position of the brushes of the stepping switch SW-50 the signal from the computer will be applied to the balanced servosystem amplifier input and then to the integrating block amplifier input.

With departure of the limited controlled quantity H_1 from the operating zone, its signal device closes signal contact d. The brushes of the stepping switch in position on segments B again close the circuit of relay P_1. Since K_1 is closed, the circuit of relay P_2 will be engaged and relay P_2 will operate. By operating, relay P_2 opens its contact p_2^I and is latched by the contact p_2^{II}

connected in series with the contact of the signaling device K_1. Therefore, relay P_2 is disconnected from point 1 and remains connected (sic) when segments B open. Contact a of relay P_2 opens, while contact c closes, and the optimizer will be connected to the sensor of the limited quantity through contacts b and c of relays P_2 and P_3.

With return of the limited quantity H_2 to the operating zone, the input of the balanced servosystem amplifier remains connected to sensor H_1 until the following triggering of relay P_1. The secondary latching of relay P_2 by contacts p_1 and p_2^{III} serve for this purpose.

With departure from the operational zone of the limited quantity H_2, the contact of signaling device K_2 is closed. The relays P_3 and P_1 operate at the instant of passage of the brushes of the stepping switch through segments B. The contact b of relay P_3 opens and contact d connects the sensor of the limited quantity H_2 to the input of the optimizer. So that reverse switching does not occur prior to the succeeding operation of relay P_1, the circuit of relay P_3 with the contact of the signaling device K_2 is also latched by the unopened contact of relay P_1 and by contact P_3^{III} of relay P_3.

It must be noted that the limitations are generated by the optimizer sequentially. So that there is no simultaneous connection of the input of the balanced servosystem amplifier to both limited quantities, the unclosed contacts of relays P_2 and P_3 are provided. They disconnect one of the limited quantities at the time of the determination of the other by the optimizer.

Computer

The computer is a divider (fig. 3) and is intended to obtain the quantity $y = k(U_1/U_2)$ being minimized. The divider is built using a servosystem. It consists of an amplifier, the MA-1 motor with gearbox and two slidewires whose arms are rigidly coupled.

In the expressions presented, U_1 and U_2 are the voltages obtained from the pneumoelectric converters. These converters consist of inductive sensors with plungers rigidly connected to a bellows. The output voltage of the sensor is proportional to the position of the plunger, i.e., to the pressure drop in the corresponding lines.

The voltage U_2 is applied to the series connected slidewire R_p and resistor R. The servosystem is in equilibrium when the voltage taken from a part of the slidewire is equal to the voltage U_1, i.e.,

$$U_1 = \frac{U_2 r}{R_p + R},$$

where r is the instantaneous resistance.

The position of the slidewire arm is proportional to the voltage /173
$y = k(U_1/U_2)$. The quantity being minimized y is applied to the indicator. The resistor provides for the use of the entire scale of the instrument with the specified ranges of variations of U_1 and U_2.

The second slidewire is connected in the bridge circuit with the balanced servosystem.

The amplifier A and all amplifiers of the servosystems of the optimizer are constructed on the basis of the EU-17 amplifier with power feed from a common source (ref. 2).

Balanced Servosystem

The balanced servosystem is intended for the subtraction of the level of the signals y applied to the integral block. If at any moment prior to application of the test step the average value of quantity y corresponds to value y_1, the balanced servosystem provides for application to the integral block of signal $\Delta y = y - y_1$, where y is the instantaneous value of the quantity being minimized. This considerably improves the accuracy of the integration, the search for the extremum in comparison with the case when the increment Δy is computed as the difference of the two integrals

$$\int_0^T y\,dt - \int_T^{T+t} y\,dt,$$

because the characteristic of the electromechanical integrator is nonlinear.

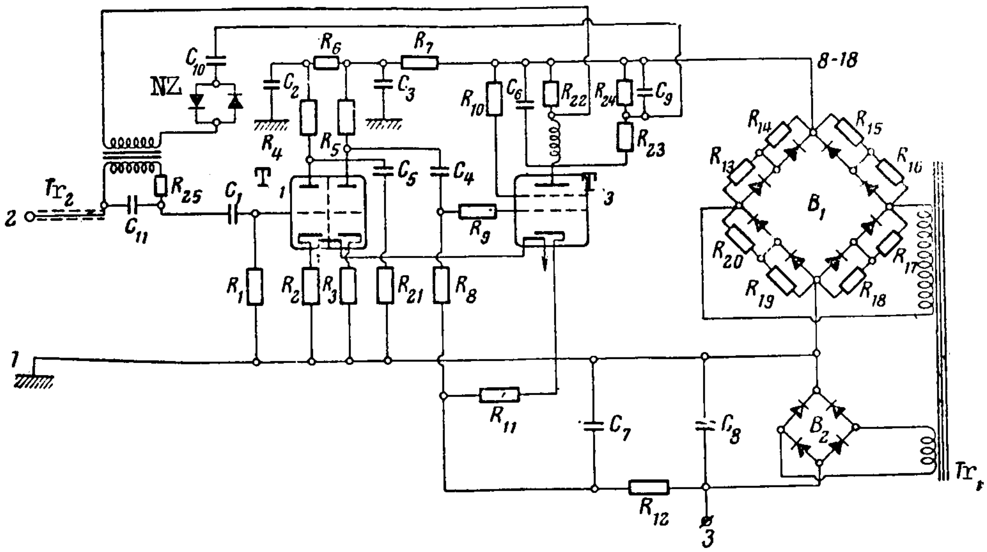

Figure 4

The servosystem consists of the amplifier of a two-phase asynchronous motor MA-1, a gearbox with a high gear ratio ($i = 100 - 500{,}000$), which can be adjusted.

As we mentioned above, the high gear-ratio reducer makes the system sluggish to high-frequency noise. This provides for averaging of quantity y.

The Integral Block

The integral block is intended for the integration of the increment of the quantity being minimized Δy, while the system searches for the minimum. As the integral block, use is made of the block of the proportional regulator ΔYC. This block consists of the amplifier (fig. 4), the two-phase asynchronous motor MA-1 with variable reducer ($i = 100 + 500{,}000$) and a slidewire. The slidewire arm is coupled with the output shaft of the motor. The voltage between the arm and the midpoint of the feedback slidewire supply winding is proportional to the integral $\int \Delta y dt$, if the system was in equilibrium at the beginning of integration.

The computation of the integral will be more accurate, the greater the range of the linear zone of the characteristic of the motor $n = f(U_{in})$ (fig. 5),

where n is the motor speed, U_{in} is the input voltage.

Linearization of the characteristic is achieved by introduction of rate feedback to the amplifier input. The feedback voltage is taken from a bridge circuit which is balanced relative to the rate of rotation of the motor. The rate feedback circuit contains a nonlinear element, which provides low gain of the feedback circuit with low signals (clips the harmonics) and with high large signals has a characteristic with high gain. The introduction of the rate

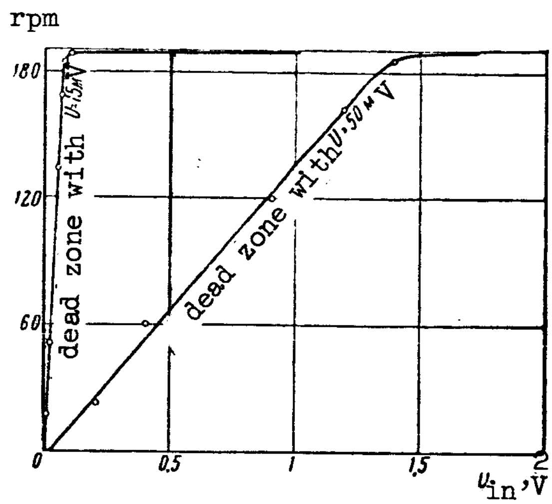

Figure 5

feedback is limited by the increase of the dead zone, on the one hand, and by the occurrence of amplifier generation on the other hand. /174

The constant of integration is changed with change of the reducer gear ratio.

Memory and Actuator Devices

Three memory and three actuating devices are provided in the system. Each memory device is made using a servosystem which consists of an amplifier, a two-phase asynchronous motor MA-1 with reducer, and a feedback slidewire. This slidewire is connected in a bridge circuit with the slidewire of the corresponding actuator. As an actuator, use is made of the EMD-232 electronic instrument. The position of the meter slidewire arm is determined by the pressure and is an adjustment of the corresponding pneumatic regulators on the object.

At the moment of the application of the test step, there is a closing of the input circuit of the actuator amplifier, which is transmitted to the system. After computation of $\int \Delta y dt$ the quantity proportional to $\int y dt$ is transmitted to the memory unit (the amplifier input circuit is closed). With the operational step the actuator amplifier is connected directly to the output of the bridge circuit and thus the transmission of the signal to the controlled object is performed. With closure of the emergency contacts K'_1 and K'_2 a signal is immediately applied to the actuator and the quantities x_1 and x_2 are changed by prespecified values (fig. 2).

Power Supply Block

The power supply for all elements of the optimizer is provided from a single common transformer, composed of laminated Sh-40 iron core 45 mm on a side.

The electrical circuit of the transformer is shown in figure 3. The amplifier filament supply consists of two windings, each of which go to /175 three amplifiers. The rectifiers B_1, B_2, B_3, B_4 are mounted on a block attached to the case of the transformer. The resistors $R_{13-20} = 75 k\Omega$ (fig. 4), shunted with the DG-Ts24 rectifiers, reduce the scatter with respect to reverse breakdown voltage. The supply for the relays and the stepping switch is taken from the rectifiers B_3 and B_4.

Adjustment of the Parameters

Several adjustments are provided in the optimizer, whose control resistors are brought out to the front panel.

The resistors R_1 and R_2 (fig. 3) change the scale of the quantities H_1 and H_2 applied to the regulator input. Resistor R_3 changes the scale of the quantity y when the balanced servosystem is connected for the generation of the quantity being minimized y and then changes the a scale of the quantity Δy applied to the integral block. The resistors R_4 and R_5 regulate the scale of the quantity $\int \Delta y dt$ applied to the corresponding memory device, i.e., they regulate the coefficient of proportionality between the quantities $\int \Delta y dt$ and Δx; R_7, R_8, R_9 regulate the magnitude of the test step which is applied to the corresponding actuator. The switch K is intended for complete disconnection of the regulator. The indicating meter is intended for the measurement of the quantity $y = k(U_1/U_2)$ being minimized and is connected into the circuit (fig. 3).

Conclusions

Thus, an electromechanical optimizer has been developed which performs a search using the gradient principle. This optimizer has high noise-stability and regulation accuracy because the generation of the operational step is accomplished by integration of the variation of the quantity being minimized, and because an inertial balanced servosystem is used, which increases the limits of the electromechanical integration.

REFERENCES

1. Kasatkin, A. G. Basic Processes and Equipment of Chemical Technology (Osnovnyye protessy i apparaty khimicheskoy tekhnologii), Avtomat. i telemekh. No. 11, 1957.

2. Advanced Scientific-Engineering Experience. Electronic Devices for Control and Regulation for Complex Automation of Production Processes (Peredovoy nauchno-tekhnicheskiy opyt. Elektronnyye ustroystva kontrolya i regulirovaniya dlya kompleksnoy avtomatizatsii proizvodstvennykh protsessov). Report 42, 1958.

N66 34345

ANALYSIS OF THE DYNAMIC CHARACTERISTICS OF SYSTEMS FOR THE AUTOMATIC CONTROL OF AIR-CONDITIONING INSTALLATIONS

M. M. Khasanov

During the present decade a large number of installations for air /176 conditioning (installations for the creation of an artificial climate) will be introduced into the national economy of the USSR. The introduction of these installations will not only create in the production areas favorable working conditions, but will also ensure provision of environmental air parameters necessary for the efficient conduct of technological processes.

In the modern air-conditioning installations the process of the preparation of the air is to a considerable degree automated. However, analysis of the automatic control systems (ACS) for these installations shows that they have essential deficiencies in many cases.

This is the result of the fact that a proper choice is not always made of the method of regulation or the type of regulator; sometimes use is made of circuits and equipment which do not meet the high specifications, because the dynamic characteristics of the production shop and the installations for air conditioning as a whole have received little study.

Therefore, the specified air parameters are not always maintained throughout the year within the limits or following the laws demanded in recent times by the production technology of various plants.

In order to design ACS with a wide range of control to satisfy the ever-increasing demands of production technology of the various branches of industry, the circuit shown in figure 1 has been selected on the basis of an analysis of the latest schemes for air conditioning. We call this scheme the generalized air-conditioning circuit. An ACS has been developed for this circuit. By modifying the generalized ACS for the conditioning installation in accordance with the requirements of a specific regulated system we can obtain quite a number of particular, simpler and more economically advantageous schemes, which have received wide application in industry.

Figure 1 shows the controlled system and the completely automated air-conditioning installation. In the controlled system--a production area--we must maintain within given limits the temperature and relative humidity, pressure, air velocity and air purity. The specified value of the air pressure and velocity of air movement are usually provided by the selection /177 of a fan and a system of air distribution in the production area, and the

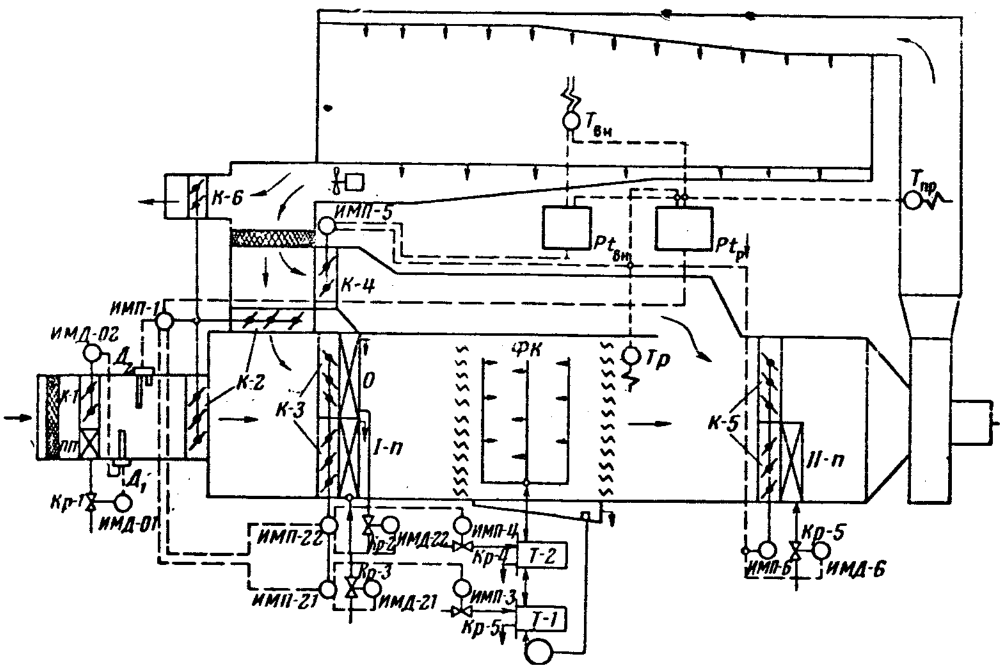

Figure 1. Functional diagram of automated air conditioning installation. Nomenclature shown in tables 1 and 2.

purity is provided by means of the filters F and washing in the spray chamber SC. The specified value of the air temperature is provided by heating the air by means of the preheater H, the first stage heater I-H and the second stage heater II-H, and also by the addition to the fresh air of some quantity of air recirculated in the first or second mixing chambers or air which is cooled with the aid of the surface cooler O. The specified value of the relative humidity of the air is provided by moistening it in the spray chamber SC, for which the spray water can be heated in the heat exchanger HE-1 or cooled in the heat exchanger HE-2.

Among these control parameters the primary ones are the temperature and the relative humidity of the air, which are, moreover, interrelated quantities.

In order to design a simpler ACS and to facilitate its adjustments, we have separated the loops for the control of the relative humidity and for the control of the temperature of the air in the production area. This ACS, which contains two basic control loops ACSϑ_p and ACSϑ_{in}, combines the operation of its individual elements into a single complex with a minimal number of controllers (one for each controlled parameter), and will, we believe, provide excellent regulation.

However, for the design of a scientifically sound ACS we must determine the static and dynamic characteristics of the controlled system and of the elements of the air-conditioning installation, because it is impossible to

say anything about the system and the selection of the regulator without studying the system as a whole.

In view of the fact that the characteristics which are suitable for the solution of the general problems for several reasons cannot be obtained experimentally, there arises the necessity for determining them analytically.

Table 1 presents the equations and transfer functions of the dynamic elements of the ACSϑ_p loop for the dew point temperature downstream of the /178 spray chamber SC; table 2 presents the equations and transfer function of the dynamic elements of the ACSϑ_{in} for the air temperature inside the production area.

The equation of the controlled object of the ACSϑ_{in} loop was derived on the basis of analysis of the production area. As the most typical example we studied the spinning room of the cotton textile industry. The equation and the dynamic parameters of the control system of the ACSϑ_p loop were determined from experimentally recorded curves of the transient process (ref. 1). The equations of the remaining elements of the automated air-conditioning installation were obtained for a given ACS using the familiar methods (refs. 2-4).

Figures 2 and 3 present the block diagrams of the ACSϑ_p and ACSϑ_{in} loops of the air-conditioning installation, where the numbers and the indices of the

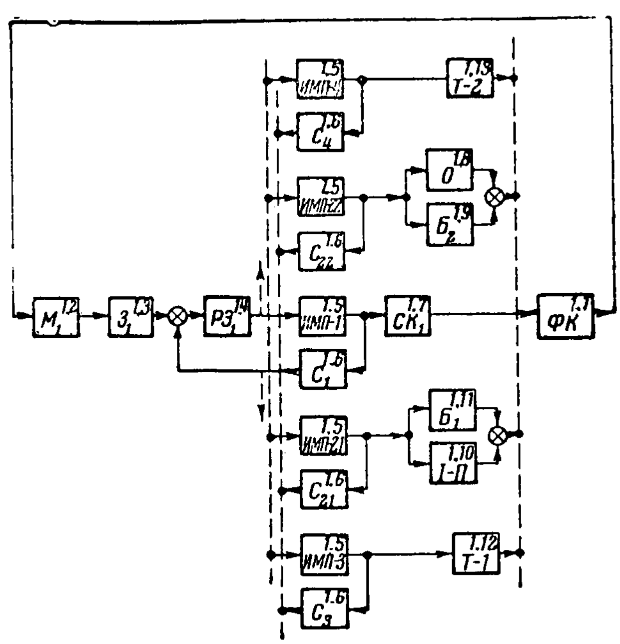

Figure 2. Structural diagram of ACS for control of dew point temperature. Nomenclature shown in tables 1 and 2.

TABLE 1. SUMMARY TABLE OF EQUATIONS AND TRANSFER FUNCTIONS FOR DYNAMIC ELEMENTS OF ACSϑ_p LOOP.

No. in fig. 2	Name and symbol for element		Element differential equation	Element transfer function
1.1	Controlled system, spray chamber	ΦK SC	$(T_{\phi 1}^2 p^2 + T_{\phi 2} p + 1)\Delta\vartheta_p = k_\phi \Delta\vartheta_{вх1}$	$W_\phi(p) = \frac{k_\phi}{T_{\phi 1}^2 p^2 + T_{\phi 2} p + 1)}$
1.2	Electronic bridge	$М_1$ EB_1	$\Delta\rho_{м1} = k_{м1}\Delta\vartheta_p$	$W_{м1}(p) = k_{м1}$
1.3	Master driver shaft	$З_1$ MDS_1	$\Delta u_{з1} = k_{з1}\Delta\rho_{м1}$	$W_{з1}(p) = k_{з1}$
1.4	Relay element	$РЭ_1$ RE_1	$y_1 = \Phi_1(u)$'	
1.5	Actuator	ИМП A	$T_{d1} p \Delta\rho_{д1} = k_{д1} y_1$	$W_{d1}(p) = \frac{k_{д1}}{T_{д1} p}$
1.6	Follow-up shaft	$С_1$ FS_1	$\Delta u_{с1} = k_{с1}\Delta\rho_{д1}$	$W_{с1}(p) = k_{с1}$
1.7	Mixing chamber	$СК_1$ MC_1	$\Delta\vartheta_{ск1} = k_{ск1} k_{к2}\Delta\rho_{д1}$	$W_{ск1}(p) = k_{ск1} k_{к2}$

ПР = limits ВХ = input Тр = transfer М = bridge б = bypass

ПП = Н (heater) ВН = inner Р = control Т = heat exchange Д = motor

К = cathode Ф = spray П = preheater

TABLE 1 (Continued)

No. in fig. 2	Name and symbol for element		Element differential equation	Element transfer function
1.8	Surface cooler	О SC_0	$(T_{01}^2 p^2 + T_{02} p + 1)\ \Delta\vartheta_0 = k_0\ k_{кз} \times \times (\tau_{01}^2 P^2 + \tau_{02} P + 1)\ \Delta\rho_{д1}$	$W_0(p) = \dfrac{k_0\ k_{кз}(\tau_{01}^2 p_2 + \tau_{02}\, p + 1)}{(T_{01}^2\ P_2 + T_{02} P + 1)}$
1.9	Bypass duct	$Б_2$ BD_2	$\Delta\vartheta_{б2} = k_{б2} k_{кз}\, \Delta\rho_{д1}$	$W_{б2}(p) = k_{б2} k_{кз}$
1.10	First preheater oven	$1\ П$ I-PO	$(T_{1п1}^2 p^2 + T_{1п2} p + 1)\Delta\vartheta_{1п} = k_{1п}\, k_{кз} \times \times (\tau_{01}^2 P^2 + \tau_{02}\, P + 1)\ \Delta\rho_{д1}$	$W_{1п}(p) = \dfrac{k_{1п}\, k_{кз}\, (\tau_{1п1}^2 p^2 + \tau_{1п2} p + 1)}{(T_{1п1}^2 p^2 + T_{1п2} p + 1)}$
1.11	Bypass duct	$Б_1$ BD_1	$\Delta\vartheta_{б1} = k_{б1}\, k_{кз} \Delta\rho_{д1}$	$W_{б1}(p) = k_{б1} k_{к}$
1.12	Heat exchanger	Т-1 HE-1	$(T_{1т1}^2 p^2 + T_{1т2} p + 1)\Delta\vartheta_{2т} = k_{1т}\, k_{кps} \Delta\rho_{д1}$	$W_{1т}(p) = \dfrac{k_{1т}\, k_{кps}}{(T_{1т1}^2 p^2 + T_{1т2} p + 1)}$
1.13	Heat exchanger	Т-2 HE-2	$(T_{2т1}^2 p^2 + T_{2т2} p + 1)\Delta\vartheta_{2т} = k_{2т}\, k_{крч}\, \Delta\rho_{д1}$	$W_{2т}(p) = \dfrac{k_{2т} k_{крч}}{(T_{1т1}^2 p^2 + T_{2т2} p + 1)}$
1.14	Mixing chamber downstream of oven (cooler)	СКК MCD	$\Delta\vartheta_{в} = k_{кз} \left[(k_{в}\, k_{п} \dfrac{(\tau_{п1}^2 p^2 + \tau_{п2} p + 1)}{(T_{п1}^2 p^2 + T_{п2} p + 1)} + k_{б}^1) - k_{б} \right] \Delta\rho_{д1}$	$W_{скк}(p) = k_{кз}\ [(k_{в} W_{п}(p) + k_{б}^1) - k_{б}$

TABLE 2. SUMMARY TABLE OF EQUATIONS AND TRANSFER FUNCTIONS FOR DYNAMIC ELEMENTS OF ACSϑ_{in} LOOP.

No. in fig. 2	Name and symbol for element		Element differential equation	Element transfer function
2.1	Controlled system, production area	Об CS	For heat exchange $(T^3_{об1}p^3 T^2_{об2}p^2 + T_{об3}p + 1)\Delta\vartheta_{вн} = (\tau^2_{об1}p^2 + \tau_{об2}p + 1)\Delta\vartheta_{вх2}$ For material exchange $(T^2_{об1}p^2 + T_{об1}p + 1)\varphi_{вн} = k'_{об}(\tau_{об'1}p + 1)\varphi_{вх2}$	$W_{об}(p) = \frac{(\tau^2_{об1}p^2 + \tau_{об2}p + 1)}{(T^3_{об1}p^3 + T^2_{об2}p^2 + T_{об3}p + 1)}$ $W'_{об}(p) = \frac{k'_{об}(\tau_{об'1}p + 1)}{(T^2_{об'1}p^2 + T_{об'2}p + 1)}$
2.2	Electronic bridge	M_2 EB_2	$\Delta\rho_{м2} = k_{м2}\Delta\vartheta_{вн}$	$W_{м2}(p) = k_{м2}$
2.3	Master driver shaft	$З_2$ MDS_2	$\Delta u_{з2} = k_{з2}\Delta\rho_{м2}$	$W_{з2}(p) = k_{з2}$
2.4	Relay element	$РЭ_2$ RE_2	$y_2 = \Phi_2(u)$	
2.5	Actuator	ИМП A	$T_{д2}p\Delta\rho_{д2} = k_{д2}y_2$	$W_{д2}(p) = \frac{k_{д2}}{T_{д2}p}$

TABLE 2 (Continued)

No. in fig. 3	Name and symbol for element		Element differential equation	Element transfer function
2.6	Follow-up shaft	C_2 FS_2	$\Delta u_{c2} = k_{ск2} \Delta k_{c2} \Delta \rho_{д2}$	$W_{c2}(p) = k_{c2}$
2.7	Mixing chamber	CK_2 MC_2	$\Delta \vartheta_{ск2} = k_{ск2} k_{к4} \Delta \rho_{д2}$	$W_{ск2}(p) = k_{ск2} \cdot k_{к4}$
2.8	Bypass duct	$Б_3$ BD_2	$\Delta \vartheta_{б3} = k_{б3} k_{к5} \Delta \rho_{д2}$	$W_{б3}(p) = k_{б3} k_{к5}$
2.9	Second preheater oven	*II-П* II-PO	$(T^2_{2п1} p^2 + T_{2п2} p + 1) \Delta \vartheta_{2п} = k_{2п} k_{к5} (\tau^2_{2п1} p^2 + \tau_{2п2} p + 1) \Delta \rho_{д2}$	$W_{2п}(p) = \frac{k_{2п} k_{к5} (\tau^2_{2п1} p^2 + \tau_{2п2} p + 1)}{(T^2_{2п1} p^2 + T_{2п2} p + 1)}$
2.10	Air-distribution system	B AS	$\vartheta_1(t) = \vartheta_1(t - \tau)$	$W_{в}(p) = e^{-p\tau}$
2.11	Mixing chamber down-stream	CKK MCO	$\Delta \vartheta_{6} = k_{к5}\left[\left(k_{в} k_{п} \frac{(\tau^2_{п1} p^2 + \tau_{п2} p + 1)}{(T^2_{п1} p^2 + T_{п2} p + 1)}\right) + k'_{б}\right]\Delta \rho_{д2}$	$W_{скк}(p) = k_{к5}[(k_{в} W_{п}(p) + k'_{б}) - K_{б}]$

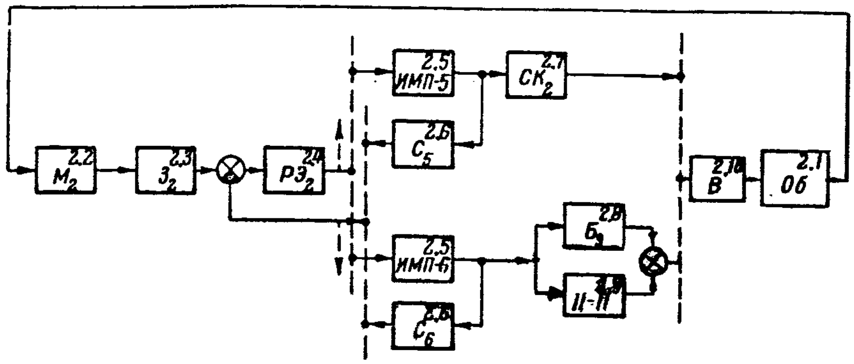

Figure 3. Structural diagram of ACS for control of air temperature inside production area. Nomenclature shown in table 2.

dynamic elements of the loops correspond to the numbers of the elements of tables 1 and 2.

The generalized circuit of the ACS for the air-conditioning installation was developed in such a way that it changes its structure with change of the magnitude and sign of the disturbing action applied to it. The scheme of the variation of the structures of the ACS loops are shown by arrows in figures 2 and 3.

For the analysis of these ACS loops we must determine the transfer function of those structural diagrams which are created with the most unfavorable conditions of operation of the controlled process. These conditions for the considered class of systems correspond to two regimes of operation, namely, the regime of operation of the system under winter (minus) and summer (plus) maximal temperatures of the outside air, and in certain cases also the regime of operation when the minimal amount of power is expended on the "preparation" of the air.

From figures 2 and 3 we see that the ACS loops include a relay ele- /180
ment which, as well as the actuator, is enclosed by the internal proportional feedback.

Analysis of one of the possible and highest response regimes of operation of the ACS studied shows that the external actions applied to the relay element enclosed by the internal feedback vary considerably more slowly than the action of the internal feedback. Therefore, we can assume that the given relay servo-system provides satisfactory tracking of the disturbance applied to it (refs. 5 and 6). However, for the existence of a continuous smooth control regime several conditions must be satisfied (ref. 6).

Computations show that these conditions are usually satisfied for /181
the considered class of systems. Therefore, we can assume with complete justification that the smooth control regime will also exist in the remaining operating regimes. Then, under certain conditions, the relay system can be

replaced by a linearized system, in which the amplifier with relay characteristics is replaced by an amplifier whose gain tends to infinity. In this case the relay element, the actuator and the feedback element can be replaced by a single linear element with a transfer function equal to the inverse of the magnitude of the transfer function of the internal feedback element.

The study of the critical regimes of operation of the ACS was performed, using as example the typical installation of the year-round air-conditioning plant of one of the spinning shops of the textile plant in Reutov, Moscow oblast. The concrete diagram of the air-conditioning installation for /182 this shop was obtained after corresponding computation of its winter and summer heat balance from the generalized diagram of figure 1 by means of exclusion of the heat exchanger equipment HE-1, HE-2 and the loop for preheating of air.

The determination of the effect of the gain on the stability of the ACS loops of the air-conditioning installation was performed with the aid of the generalized criterion of stability (D-partition). Figures 4a and b and 5a and b

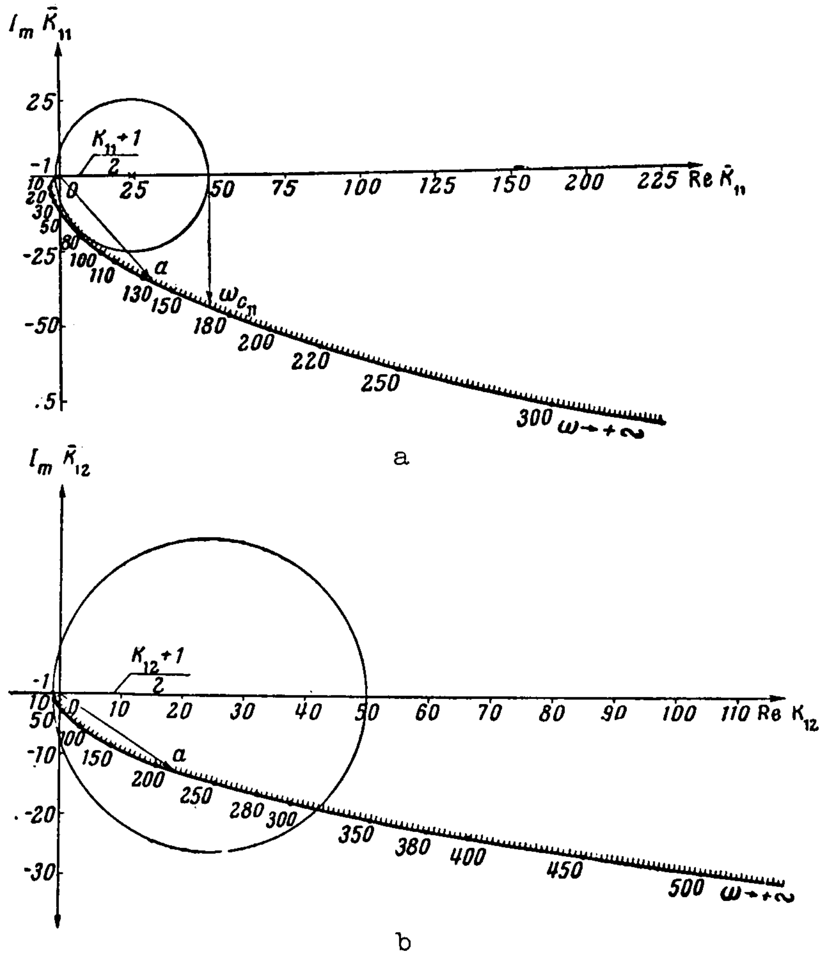

Figure 4. Curve of D-partition with respect to gain of ACSϑ_p loop. a, For summer critical regime of operation; b, for winter critical regime of operation.

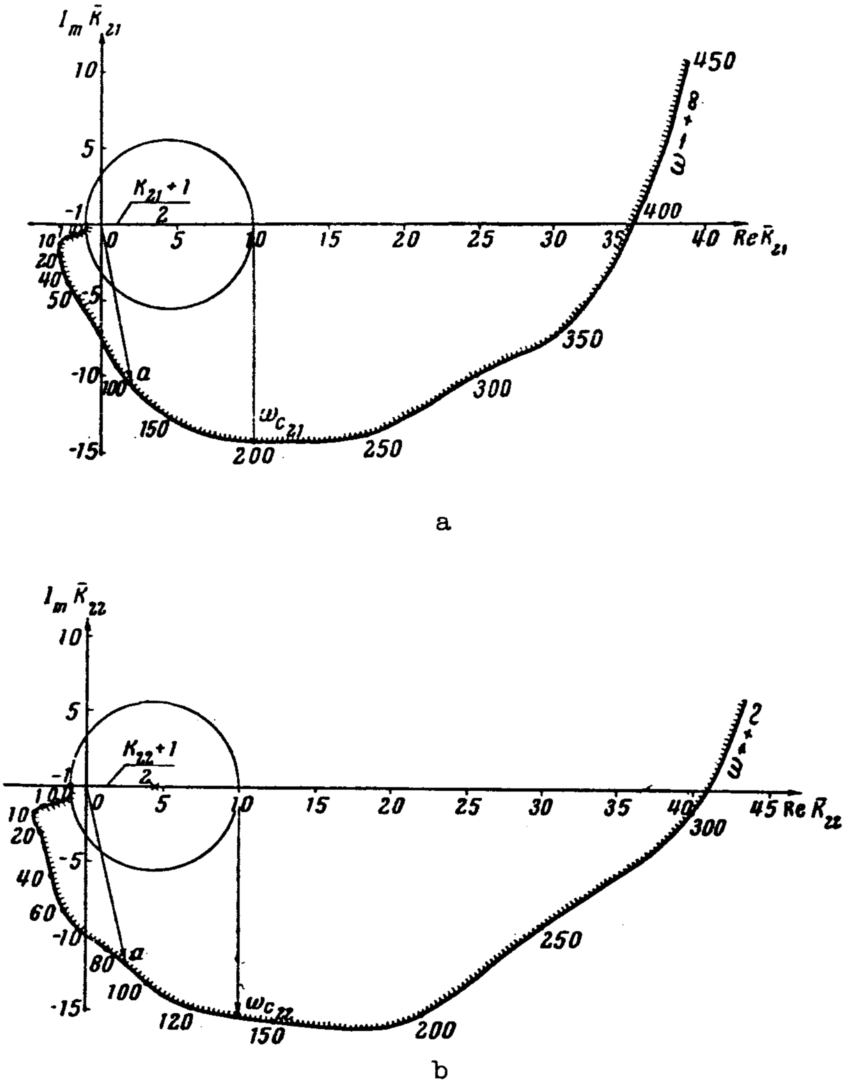

Figure 5. Curve of D-partition with respect to gain of ACSϑ_{in} loop.

a, For summer critical regime of operation; b, for winter critical regime of operation.

show the D-partition curves with respect to the system gain K for the critical regimes of operation of the ACSϑ_p loop and the ACSϑ_{in} loop, respectively (ω_c is the frequency of the interval of positivity of the real characteristic, 0a is the vector K for a given value of the frequency).

A preliminary evaluation of the performance of the ACS can also be made from these D-partition curves. However, for a more precise evaluation of the performance indices of the system and their correspondence to the spec- /187
ified values, the real frequency characteristics were constructed from these

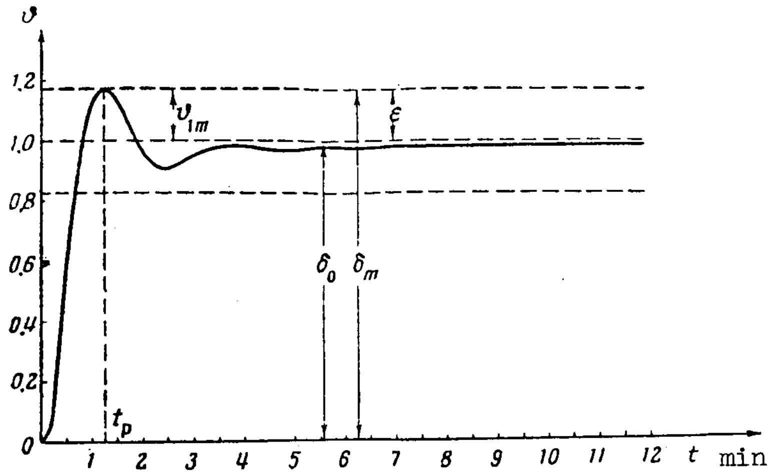

a

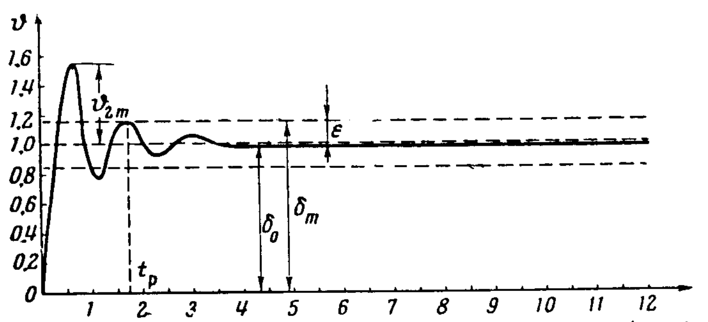

b

Figure 6. Curve of transient process of ACSϑ_p loop.

a, For summer critical regime of operation; b, for winter critical regime of operation; ϑ_{1m}, initial deviation; t_p, control time; δ_0, variation of control; ϵ, regulator deadband; δ_m, maximal static error; ϑ_{2m}, maximal acceptable overcontrol.

curves (ref. 7). After replacement of the frequency characteristics by the sum of the trapezoids, the curves of the transient process were constructed (ref. 8).

Figures 6a and b and 7a and b present the curves of the transient process for the critical regimes of operation of the ACSϑ_p and ACSϑ_{in} loops, respectively. Analysis of the curves of the transient process shows that the system

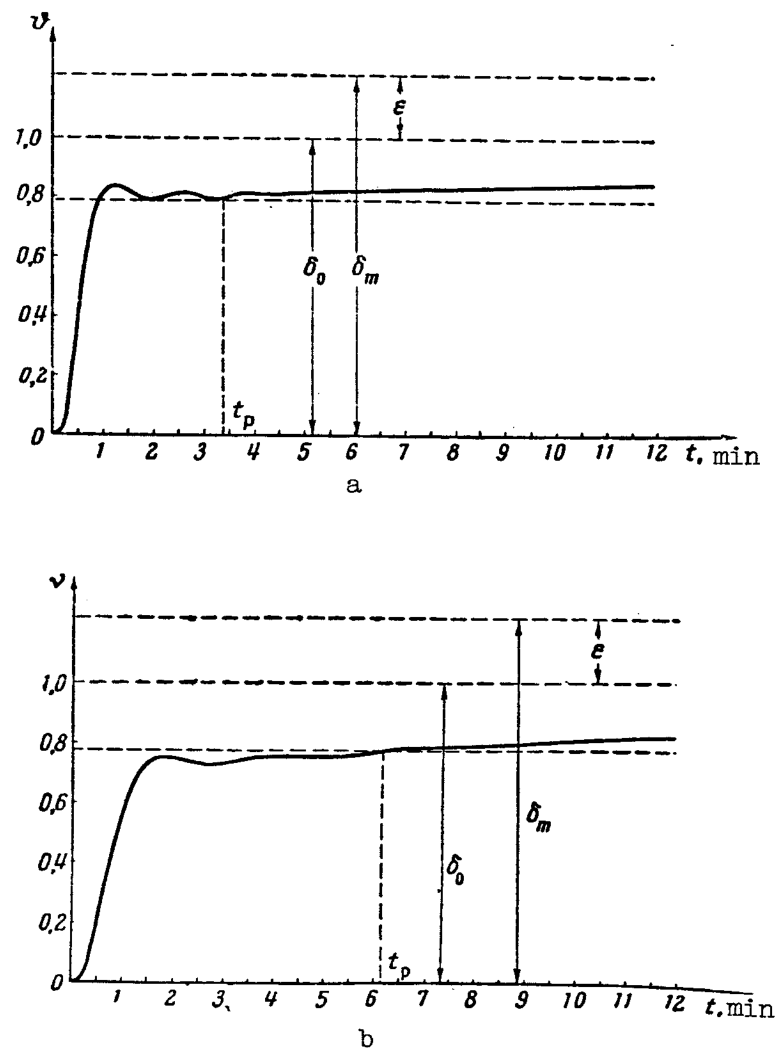

Figure 7. Curve of transient process of ACSϑ_{in} loop.

a, For summer critical regime of operation; b, for winter critical regime of operation. Notations same as in figure 6.

satisfies the technical specifications, since its performance indices fall in the specified limits.

Conclusions

A generalized ACS diagram has been developed for an air-conditioning installation which permits the use of a single static regulator for each regulated parameter with a large number of regulating elements operating sequentially from it.

The equations of the controlled system and of the elements of the generalized diagram of the ACS for this installation have been derived in general form.

The critical regimes of operation of the ACS have been studied, using as example a typical installation for air conditioning, and the performance indices of this system have been determined. This permits a rational approach to the development of an efficient ACS for air-conditioning installations in various branches of industry.

REFERENCES

1. Tsypkin, Ya. Z. Determination of the System Dynamic Parameters Which Are Describable by Linear Equations of no Higher Than Second Order from Oscillograms of the Transient Process (Opredeleniye dinamicheskikh parametrov sistemy opisyvayemykh linneynymi uravneniyami ne vyshe vtorogo poryadka po ostsillogrammam perekhodnogo protsessa). Trudy BZEI, No. 6, IN: Electrical Engineering (Elektrotekhnika). Gosenergoizdat, 1955.

2. Lossiyevskiy, V. L. Fundamentals of Automatic Control of Technological Processes (Osnovy avtomaticheskogo regulirovaniya tekhnologicheskikh protsessov). Oborongiz, 1949.

3. Amelin, A. T. Finding the Dynamic Characteristics of Technological Processes by the Analytic Method (Nakhozhdeniye dinamicheskikh kharakteristik tekhnologicheskikh protsessov analiticheskim metodom). Avtomat. i telemekh., Vol. 14, No. 3, 1953.

4. Dudnikov, Ye. G. Fundamentals of Automatic Control of Thermal Processes (Osnovy avtomaticheskogo regulirovaniya teplovykh protsessov). Gosenergoizdat, 1956.

5. Fundamentals of Automatic Control (Osnovy avtomaticheskogo regulirovaniya). Edited by V. A. Solodovnikov, Mashgiz, 1954.

6. Tsypkin, Ya. Z. Theory of Relay Automatic Control Systems (Teoriya releynykh sistem avtomaticheskogo regulirovaniya). GITTL, 1955.

7. Meyerov, M. V. Introduction to the Dynamics of Automatic Control of Electrical Machines (Vvedeniye v dinamiku avtomaticheskogo regulirovaniya elektricheskikh mashin). Izd-vo AN SSSR, 1956.

8. Solodovnikov, V. A. Application of Trapezoidal Frequency Characteristics to the Analysis of the Performance of Automatic Control Systems (O primenenii trapetsoidal'nykh chastotnykh kharakteristik k analizu kachestva sistem avtomaticheskogo regulirovaniya). Avtomat. i telemekh., No. 5, 1959.

N66 34846

SIMULATION OF CERTAIN SYSTEMS WITH DISTRIBUTED PARAMETERS

A. G. Butkovskiy

The theoretical consideration of the questions of optimal control of systems with distributed parameters leads to the necessity of constructing models of such systems (ref. 1). The simulation of processes described by equations in partial derivatives has, moreover, great importance in the integrated study of these processes. /242

The present paper considers the method of simulation of two forms of processes which are described by the following two types of partial derivative equations

$$\text{I.} \qquad bv\frac{\partial Q}{\partial y}+b\frac{\partial Q}{\partial t}+Q=u \tag{1}$$

with $0\leqslant y\leqslant L,\ 0\leqslant t\leqslant T.$

The boundary condition has the form

$$Q(0,t)=Q_0(t), \qquad 0\leqslant t\leqslant T. \tag{2}$$

The initial condition has the form

$$Q(y,0)=Q_{in}(y), \qquad 0\leqslant y\leqslant L. \tag{3}$$

Here the following notation is used

$Q = Q(y, t)$ is the distribution function describing the process in the system

b is a coefficient which depends on the difference $\eta = y - \int_0^t v(p)\,dp$;

$v = v(t)$ is a positive function of the time t;

$u = u(y, t)$ is a known function of its arguments which can be the control function in the process of the control of the process.

$$\text{II.} \qquad \frac{\partial Q}{\partial t} = a\frac{\partial^2 Q}{\partial x^2} - \nu\frac{\partial Q}{\partial y} \tag{4}$$

with $0 \leqslant x \leqslant S, \quad 0 \leqslant y \leqslant L, \quad 0 \leqslant t \leqslant T.$

The boundary conditions have the form /243

$$\left.\frac{\partial Q}{\partial x}\right|_{x=S} = \beta[u(y, t) - Q(S, y, t)]; \quad 0 \leqslant y \leqslant L, \quad 0 \leqslant t \leqslant T; \tag{5}$$

$$\left.\frac{\partial Q}{\partial x}\right|_{x=0} = \gamma[v(y, t) - Q(0, y, t)]; \quad 0 \leqslant y \leqslant L, \quad 0 \leqslant t \leqslant T; \tag{6}$$

$$Q(x, 0, t) = Q_0(x, t); \; 0 \leqslant x \leqslant S, \; 0 \leqslant t \leqslant T. \tag{7}$$

The initial condition has the form

$$Q(x, y, 0) = Q_{in}(x, y). \tag{8}$$

Here the notation is

$Q = Q(x, y, t)$ is the distribution function in two spatial dimensions which describes the process in the system;

a_{in} is the coefficient of thermal conductivity, dependent on the difference $\eta = y - \int\limits_0^t \nu(p)\,dp$;

$\nu = \nu(t)$ is a positive function of the time t;

β and γ are constant coefficients;

$u = u(y, t)$ and $v = v(y, t)$ are known functions of their arguments, which can be the control functions in the control process.

Equations of type I and II are among the basic equations of mathematical physics; they describe numerous thermal, diffusional, stochastic and electric processes in various systems. Such equations describe the processes in many production facilities, where the material being processed moves through the processing zone.

As an example of the construction of a model of a system described by equations of type I and II, let us consider the processes of heating of metal in a through-flow furnace, for example, in a continuous furnace. The through-flow heating furnace is a typical system with spatially distributed parameters. The primary parameter which characterizes the furnace operation--the temperature Q of metal being heated in the furnace--is distributed both along the length of the furnace and through the thickness of the metal and is a function of three variables $Q = Q(x, y, t)$.

Normally, bilateral heating of the metal is accomplished in the continuous furnace, and the process temperature is characterized by two functions, also distributed along the length of the furnace: $u = u(y, t)$--the temperature of the upper semispace of the furnace and $v = v(y, t)$--the temperature of the lower semispace of the furnace.

In the design of a system for optimal control of a continuous furnace to synchronize its operation with a rolling mill, the need arose for construction of a model of the process of heating the metal in the furnace, i.e., the calculation of temperature Q of the metal being heated in the furnace as a function of spatial coordinates x and y and of time t, i.e., $Q = Q(x, y, t)$.

In the theoretical analysis of the problem it was found that the temperature in the furnace $u = u(y, t)$ and $v = v(y, t)$, considered as the controlling action during heating, even in the simplest case (ref. 1) must depend on the distribution of Q (fig. 1). For simplicity we shall first describe the case of unilateral heating of "thin" stock (criteria $Bi \leq 0.25$) from the initial temperature $Q_0(t) = 0$. In this case the heating process is

described by an equation of type I, where b is the coefficient characterizing the heat transfer condition, which depends on the thickness of the /244

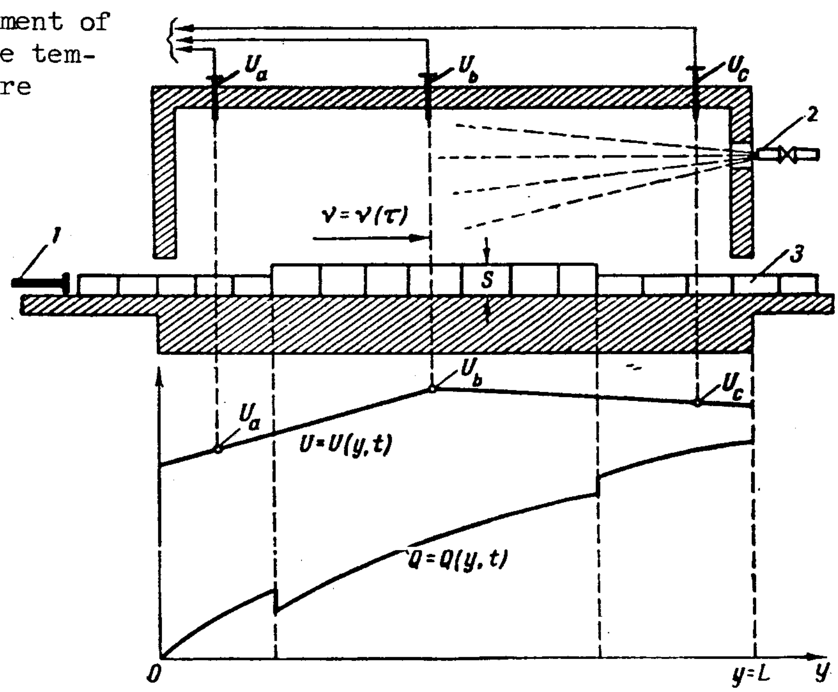

Figure 1. Graph of furnace temperature $U = U(y,t)$ and of stock temperature along furnace length $Q = Q(y,t)$ at some fixed moment of time t. 1, Pusher; 2, burner; 3, stock being heated.

stock being heated, its specific heat and the heat transfer coefficient in the furnace. Other conditions being the same, coefficient b is proportional to the porosity of the stock.

The function $\nu = \nu(t) \geq 0$, $0 \leq t \leq T$ is the rate of movement of all stock being heated in the furnace as a function of time t measured by the velocity sensor; the function $u = u(y, t)$ is the temperature in the working space of the furnace, which is measured with the aid of temperature sensors at several points of the furnace. From these points a piecewise-linear approximation of the temperature u is constructed; the function $Q = Q(y, t)$ is the temperature of the metal in the furnace as a function of coordinate y and time t.

Let us fix the point associated with the moving metal which at the instant of time $t = 0$ is at the point $y = 0$. Let $U = U(t)$ be the temperature of the furnace which acts on this point in the course of the entire time of its stay in the furnace, until it reaches the coordinate $y = L$. Then the equation of the heating of this point has the form

$$b\frac{dq}{dt} + q = U(t), \tag{9}$$

where $q = q(t)$ is the temperature of the point in question as a function of the time t.

It is evident that $U(t) = u\left(\int_0^t \nu(p)\,dp, t\right)$, i.e., $U(t)$ is equal to the temperature in the furnace $u = u(y, t)$ where instead of y the expression $\int_0^t \nu(p)\,dp$ is substituted, and the integration must be performed until moment t_1, /245 which satisfies the condition $\int_0^{t_1} \nu(p)\,dp = L$. It is also evident that if we integrate equation (9) from the moment of time t_0 to the moment t_1, $0 \leq t_0 \leq t_1$, with the initial condition $q(t_0) = Q_0$ (Q_0 is the metal temperature at entry into the furnace, at point $y = 0$), then $q(t_1)$ is the temperature of the metal at point $y = \int_{t_0}^{t_1} \nu(p)\,dp$ at the moment of time t_1. i.e.,

$$q(t_1) = Q(y, t_1),$$

where

$$y = \int_{t_0}^{t_1} \nu(p)\,dp.$$

Thus the computation of the distribution $Q = Q(y, t)$ at moment t requires knowledge of the functions b, ν, and u at the time interval $[t - \tau, t]$ before, where τ is determined from condition

$$\int_{t-\tau}^{t} \nu(p)\, dp = L. \tag{10}$$

These functions can be stored on individual tracks of a magnetic drum, which turns with a sufficiently high speed so that we can solve the equation at a high rate. For the reproduction of a function of two variables $u = u(y, t)$ we must store several functions. In particular, for the case shown in figure 1 it is necessary to store the three functions

$$U_a = U_a(t); \qquad U_b = U_b(t); \qquad U_c = U_c(t).$$

With the aid of a controllable functional converter having the functions $U_a = U_a(t)$, $U_b = U_b(t)$ and $U_c = U_c(t)$, we can reproduce the function $u = u(y, t)$.

For storage of each of the five indicated functions of time U_a, U_b, U_c, b and ν, the corresponding track of the drum is divided into $n = T/\Delta t$ sectors, where T is the maximal possible time of stay of each piece being heated in the furnace, and Δt is the interval of time between two neighboring recordings of the functions, which is chosen from the condition of the accuracy of their approximation.

At the moments of time t_i, $i = 1, 2, \ldots$, separated from one another by Δt, in alternate sectors of each track the instantaneous or averaged, over the time Δt, value of the function corresponding to this track is recorded i.e., U_{ai}, U_{bi}, U_{ci}, b_i, ν_i. The recording is made in the direction opposite to that of the rotation of the drum. After filling of the last nth sector, the next recording is again made in the 1st sector after the interval Δt, then in the 2nd sector, etc. Thus, all required functions for the time T past are stored on the drum.

Let us assume that at the given moment of time t it is necessary to compute the temperature of the metal at the end of the furnace with $y = L$. Assume that the last recording was made in the rth sector.

Consequently, the reproduce channels must be energized at the moment when that sector in which the recording was made at the moment $t - \tau$ passes the reproduce head, where τ is determined from the condition (10) in discrete form

$$\sum_{i=k}^{r} \nu_i = \frac{L}{\Delta t}. \tag{11}$$

The determination of number k of this sector is performed in two /246. revolutions of the drum as follows: beginning with sector r, where the last recording was made, summation is performed of the quantities ν_i over all n sectors of the drum, as a result of which we obtain the quantity $R_n = \Sigma\nu_i$, the constant quantity L (furnace length) is subtracted from R_n; in the following revolution the summation begins with the same sector r as in the first revolution, but with the sign reversed. At the moment when there is zero at the output of the summator, the reproduce heads will be located opposite the sector in which the recording was made at the moment of time $t - \tau$. At this moment the reproduce channels are energized and information from all five tracks is applied to the controlled functional converter and control model (9) (fig. 2). The value of function B stored in this sector is stored on the condenser. This stored value is applied to control model (9) in the course of the entire solution.

At the moment when the rth sector, where the last recording was made at the moment of time t, passes under the reproducing heads at the output of control model (9), we obtain a voltage proportional to the value of the temperature of the metal at point $y_0 = L$, which is stored (for example, is recorded in a free track of the drum, see fig. 2). At this moment the reproduce channels are blocked. After this, the reproduce channel is enabled at the moment of the beginning of the passage of the sector with the number (k + 1) under the reproduce head. When the rth sector reaches the reproduce heads, there will be a voltage at the output of control model (9), corresponding to the metal temperature at the point $y_1 = \sum_{i=k+1}^{r} \nu$. The obtained temperature value and the coordinate are stored in the following sectors of the 6th and 7th tracks of the drum. After each revolution of the drum the number of the

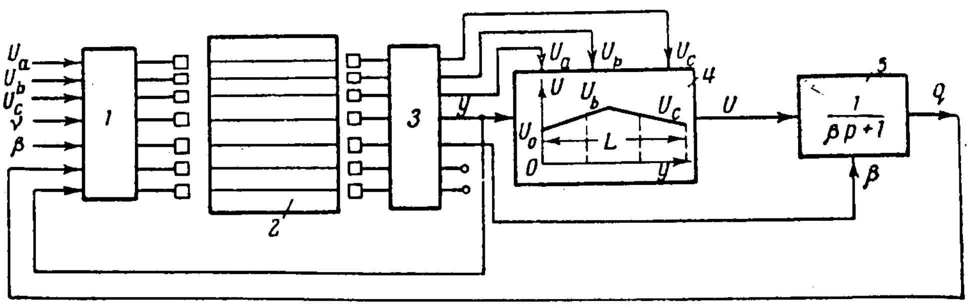

Figure 2. Structural diagram of system model with distributed parameters. 1, Drum recording unit; 2, magnetic drum with seven tracks; 3, reproduce unit; 4, controllable functional converter; 5, aperiodic element, which models heating of stock with variable time constant β.

sector with which the solution begins is increased by unity, and so on to the rth sector. Since the drum can revolve rapidly, during the time interval Δt the temperature distribution along the entire length of the furnace is computed.

In principle, the modeling of the equations of type II is analogous to the modeling of the equations of type I. The block diagram of the simulation of equations of type II differs from the scheme of figure 2 only in the block 5. An equation of type II describes the heating of metal in through-flow furnaces with the criterion Bi > 0.25 ("thick" body). In the case when the boundary condition (6) has the form /247

$$\left.\frac{\partial Q}{\partial x}\right|_{x=0} = 0,$$

this corresponds to the situation where the model of equation (9) is replaced by the model of the following system of ordinary differential equations

$$\left.\begin{aligned} \frac{dq_1}{dt} &= \mu\,[U(t) - q_1] + \mu_1 (q_2 - q_1); \\ \frac{dq_i}{dt} &= \mu_1 (q_{i-1} - 2q_i + q_{i+1}),\ i = 2, 3, \ldots, m-1; \\ \frac{dq_m}{dt} &= \mu_1 (q_{n-1} - q_n)], \end{aligned}\right\} \tag{12}$$

where

$$\mu = \frac{\beta}{c\gamma s},\quad \mu_1 = \frac{\lambda}{c\gamma s^2} = \frac{a}{s^2},\quad s = \frac{S}{m}.$$

These equations, as is known, approximate the one-dimensional equation of thermal conduction

$$\frac{\partial q}{\partial t} = a\frac{\partial^2 q}{\partial x^2} \tag{13}$$

with the boundary conditions

$$\left.\frac{\partial q}{\partial x}\right|_{x=S} = \beta(U - q) \text{ and } \left.\frac{\partial q}{\partial x}\right|_{x=0} = 0,$$

where $a = \frac{\lambda}{c\gamma}$ is the thermal conduction coefficient.

REFERENCES

1. Butkovskiy, A. G. and Lerner, A. Ya. Optimal Control of Systems with Distributed Parameters (Ob optimal'nom upravlenii ob"yektami s raspredelennymi parametrami). Avtomat. i telemekh., Vol. 21, No. 6, 1960.

2. Fitsner, L. N. and Norkin, K. B. Nonlinear Converter Controlled by Electric Voltages (Nelineynyy preobrazovatel' upravlyayemyy elektricheskimi napryazheniyami). Otchet IAT AN SSSR, 1959.

? 4 ? 4 7

N 66 34847

DIGITAL COMPUTERS FOR COMPILING MILLING MACHINE PROGRAMS

V. A. Brik

A prototype has been developed in Laboratory No. 7 of the Institute of Automation and Remote Control of the Academy of Sciences, USSR, of a VPO-1 specialized computer intended for compilation of the program for machining on a milling machine, with digital program control of parts whose profiles consist of rectilinear segments and arcs of circles. Details of this type constitute the overwhelming majority of all parts used in general machine design. /248

The salient feature of the device is that it generates the machining program in the form of binary coded numbers--the codes of the linear increments of the coordinates, thereby replacing the contour of the part by a set of a relatively large number of linear segments which must be machined with the aid of the linear interpolator mounted on the machine tool. Thanks to this method there is, on the one hand, a reduction of the volume of information introduced into the machine tool (in comparison with the unitary code), and on the other hand, only a relatively simple computer is installed directly at the machine (linear interpolator), which can operate with high reliability.

The foundation of the VPO-1 is a new mathematical algorithm (refs. 1 and 2), by which the coordinates of the sequential points of the circle and straight line are calculated, respectively, using equations

$$\left.\begin{aligned} x(n+1) &= x(n)\left(1-2^{-2k-1}\right) \mp y(n)\,2^{-k};\\ y(n+1) &= y(n)\left(1-2^{-2k-1}\right) \pm x(n)\,2^{-k}; \end{aligned}\right\} \quad (1)$$

$$\left.\begin{aligned} x(n+1) &= x(n)+h_1;\\ y(n+1) &= y(n)+h_2, \end{aligned}\right\} \quad (2)$$

where h_1 and h_2 are given quantities and k is a whole positive number, specified as a function of the radius of the circle.

The device operates in the binary notation system and therefore multiplication by 2^{-k} or 2^{-2k-1} reduces to a single shift of the multiplicand.

The linear increments generated by the device are computed from the equations

$$\left.\begin{array}{l}\Delta x(n)=x(n+1)-x(n);\\ \Delta y(n)=y(n+1)-y(n).\end{array}\right\} \qquad (3)$$

Simultaneously the device computes the differences /249

$$\left.\begin{array}{l}x_k-x(n+1);\\ y_k-y(n+1),\end{array}\right\} \qquad (4)$$

where x_k and y_k are the given coordinates of the end of the segment.

When both differences become smaller than the small quantity $M = 2^{-6}$, the device transmits the differences (4), thus canceling out all error accumulated over the segment, after which the machining of the new segment is started.

The initial data for each linear segment of arc must be located on one line of the punched card introduced into the computer. After the machining of a given segment, the punch card is shifted and the machining of the following segment is initiated. The number of segments can be anything desired.

$N = 19$ bits are used in the device for the representation of the numbers, of which the first 13 are true, while the remaining 6 are assigned to the accumulated error. The magnitude of the error was determined on the basis of experimental and theoretical analysis (ref. 3).

The present paper describes the circuit of the prototype of the VPO-1. The device is basically constructed from standard cells from the Ural universal digital computer. Therefore we shall use here the notation adopted in reference 4.

A general view and a simplified block diagram of the operational model of the device are shown in figure 1a and b. It consists of the input unit IU, the control unit CU and the arithmetic unit AU. All required data for the operation of the device are introduced into it from the input unit. For the case of the circular arc, these data are the coordinates of the initial point x(0) and y(0), the coordinates of the end of the segment x_k and y_k, the quantity k, the line-arc symbol (L-A) and the binary symbol indicating the direction of motion along the circular arc.

In the case of the machining of a straight line, the values of the elementary increments h_1 and h_2, the quantities x_k and y_k, the symbol L-A are introduced from the IU. A portion of the data from the IU is continuously applied to the CU in the course of operation of the entire time of the computations associated with the given segment. This includes quantity k, symbol L-A and the symbol of the direction of motion along the arc. Some data from the AU are also supplied to the control unit.

All processing of the information takes place in the arithmetic unit AU, consisting basically of two binary registers Re1 and Re2, the shifter Sh and

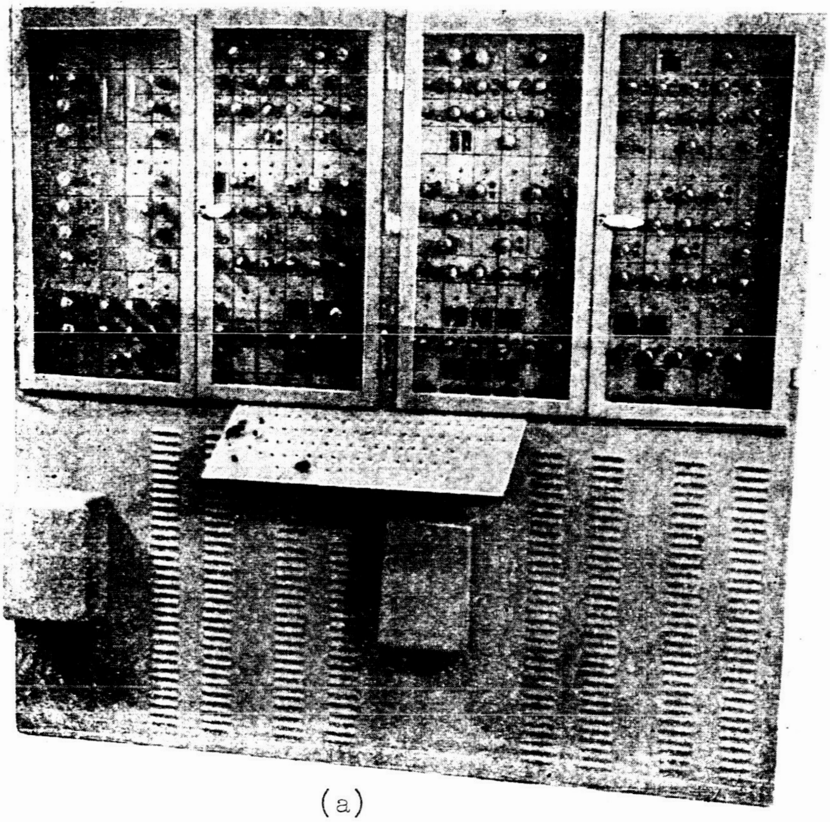

(a)

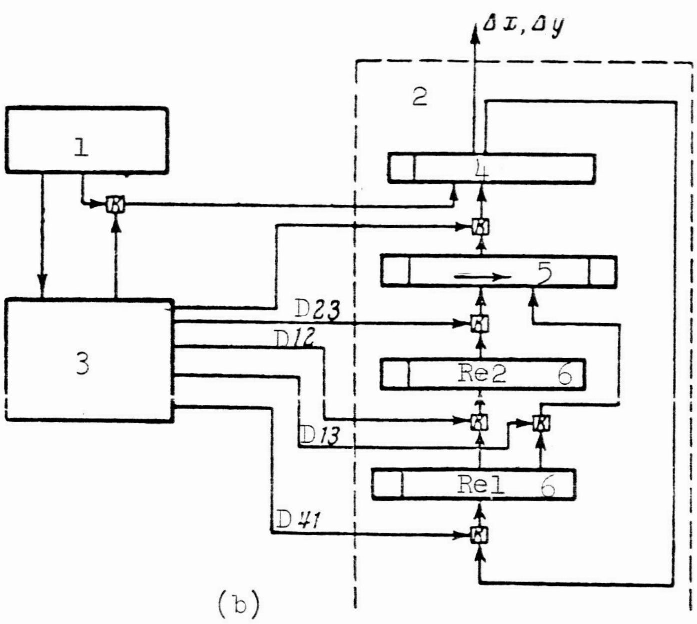

(b)

Figure 1. 1, Punchcard input unit; 2, arithmetic unit; 3, control unit; 4, summator; 5, shifter; 6, binary registers Re.

the summator Su. The registers Re1 and Re2 serve, in essence, only as an operational memory for the temporary storage of information.

Addition and subtraction of positive and negative numbers is performed in the summator with the use of an inverse code.

In accordance with the data introduced into it, the control unit generates the controlling pulses which in the required sequence, following a fixed program, control the input of the data into the AU, the processing of the data, and the output of the results. The CU includes the pulse timing generator (multivibrator), the pulse counter and a large diode circuit (decoder).

The frequency of the timing generator determines the rate of operation of the entire device. The pulse counter contains 9 binary place bits (triggers) with definite combination of which the control unit delivers, with the aid of the decoder, definite control signals. Thus the entire device operates in accordance with a fixed program, determinable by the sequence of the control pulses delivered by the decoder, and this sequence is in turn defined by /251 the changes of states of the triggers of the pulse counter (and also by the state of the sign triggers in the shifter and in the summator, introduced by the quantities k, L-A and others).

The binary registers of the machine each contain N = 19 significant bits and one sign bit. The output information (Δx and Δy) is located in the sign place and in the 7-15 places of the summator.

The quantity k can have the values 4, 5 and 6, which correspond to the generation of 100, 200 and 400 equally spaced points on a circle.

The control signals available in the device include:

S1 is the signal to reset the first register, Re1, to zero;

S3 is the reset signal for the shifter Sh;

S4 is the signal to reset the summator Su;

D12 is the signal to deliver a number from Re1 to Re2 (direct code);

D13 is the signal to deliver a number from Re1 to Re3 (direct code);

A is the signal for direct code delivery of the first 15 bits from Sh to summator Su;

D is the signal for the delivery by inverse code of the first 15 bits from Sh to Su. In this case unity is added to the sign bit of the summator;

S is the signal for the delivery by direct code of the 16-19 bits from Sh to Su;

Γ is the signal for the delivery by inverse code of the 16-19 bits from Sh to Su;

. D is the signal for adding unity to the 16-19 bits of Su;

RO is the roundoff signal;

RO4 is the signal for the entry of unity or zero to the 16-19 bits of Su (units are entered if in Su there is a negative number; zeros are entered otherwise). This signal is generated with the aid of the signals $D41_d$ and $D41_0$;

$D41_d$ is the signal for the delivery of a number from Su to Rel by direct code (for the transfer of a positive number);

$D41_0$ is the signal for the delivery of a number from Su to Rel by inverse code (for the transfer of a negative number);

Sh is the signal for a shift by one place of a number in the shifter; the shift is performed in the direction of the less significant places. The signals Sh are generated with the aid of the auxiliary signals Sh3 and Sh4;

Ex(0) is the signal for the entry of x(0) or h_1 from the punchcard IU into Su;

Ey(0) is the signal for the entry of y(0) or h_2 from IU into Su;

Ex_k is the signal for the entry of x_k from IU into Su;

Ey_k is the signal for the entry of y_k from IU into Su;

DΔx is the signal for the delivery from the device of the sequential increment Δx;

DΔy is the signal for the delivery of Δy;

DSa is the signal used to verify the approach to the end of a segment, namely to analyze the quantity x_k-x (n + 1) or the quantity y_k-y (n + 1);

Sc is the signal for the termination of the cycle of computations of each point;

Sp2 is the signal on the entry of the point x (n + 1), y (n + 1) into a definite zone about the point x_k, y_k;

St is the signal to stop the device.

Prior to initiation of the processing of a new segment the signal PrR ("preparatory reset") is sent, which establishes the pulse counter and certain other elements of the device in the initial position. The operation of the device in the machining of a single segment (rectilinear or circular) consists of three stages.

The first stage is entry of initial data and preparation for first cycle.

The second stage is the cyclic computation of the coordinates of the sequential points of the segment and the delivery of the increments of the coordinates with simultaneous verification of the distance from the current point to the specified end of the segment.

The third stage (with approach to the end) is the computation and the delivery of the last differences $\Delta x = x_k - x\ (n + 1)$ and $\Delta y = y_k - y\ (n + 1)$ and stopping the device.

The operations in these stages for the cases of the arc and the straight line differ somewhat from one another. /252

In the design of the unit we chose that sequence of operations which provides a minimal number of different operations of number transfers, register resets, etc. To achieve this result we had to permit the performance in the summator of the operation $x\ (n) \mp y\ (n)\ 2^{-k}$ and the operation $y\ (n) \pm x\ (n)\ 2^{-k}$ which causes overfilling of the summator. However, analysis shows that this overfilling does not distort the final results, i.e., the quantities $x\ (n + 1)$ and $y\ (n + 1)$.

The detailed algorithm of operation will be considered below in the description of the control unit CU.

Arithmetic Unit

The block diagram of the arithmetic unit is shown in figure 2. All signal controlling pulses (other than the shift signal) have a duration of 180 or 50 μsec and are formed in the CU with the aid of two standard series of positive pulses: S180 (duration 180 μsec) and S50 (duration 50 μsec). Both series have constant and identical frequencies (with a constant frequency of the clock generator), but are shifted in time relative to each other. The S180 series, as can be seen from figure 2, is also used for the formation (after assembly) of the input pulses in the shifter and summator.

Figure 2 does not show the details of the four blocks (shift, stop and two roundoff blocks) which will be considered below.

The purpose of the signals D12, D13, $D41_d$, $D41_0$, S1, S4, S3, Sh can be understood from a listing of the control signals.

The numbers in Re1, Re2 and Sh are represented in a direct code; the negative numbers differ from positive numbers only in that a one is in the sign place.

In the summator Su addition and subtraction of the numbers is accomplished in an inverse code; the summator is of the parallel type with sequential carry of unity through the delay line, as used in the Ural computer.

The transfer of positive numbers from Su to Re1 is accomplished by a direct code with the aid of the signal $D41_d$, while the transfer of the negative numbers

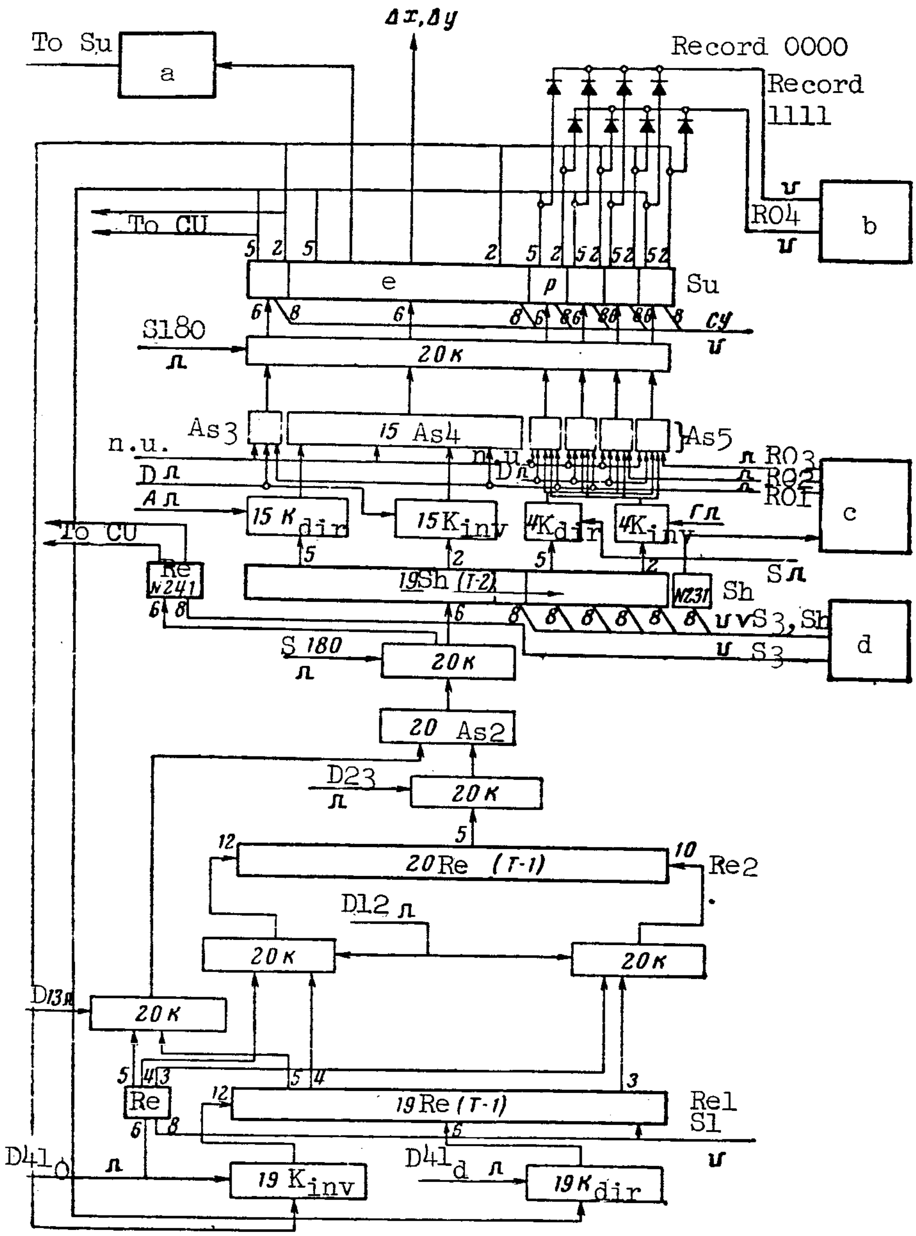

Figure 2. a, Stop unit; b, roundoff unit No. 2; c, roundoff unit No. 1; d, shift unit; e, summator. In all figures, K = cathode.

is performed by an inverse code with the aid of the signal $D41_0$, so that the mantissa of the number is always represented in Rel by a direct code. The transfer to Rel goes to various inputs of the triggers. Thanks to this scheme of transfer there are none of the usual assemblies and forming diode gates. With the transfer of a negative number from Su to Rel (with the aid of $D41_0$),

unity is entered in the sign place of Re1 with the aid of the pulse $D41_0$ itself.

The signal S1 for the reset of the first register is applied directly before the delivery of numbers from Su into Re1.

The transfer of a number from Re1 to Re2 is accomplished simultaneously on the various inputs of the triggers T-1, which permits avoiding the preliminary reset of Re2 to zero.

Since with multiplication by 2^{-k} and 2^{-2k-1} it is only necessary to shift the mantissa of the number in Sh, the pulses for shift Sh are not applied to the sign place of the shifter (cell Re241).

The shifter has one additional trigger (cell 231) for the most significant of the shifted places. This place controls the operation of the first round-off block (this will be considered in more detail below).

The letters "n.u." in figure 2 denote the conductors along which the quantities $x(0)$, $y(0)$, h_1, h_2, x_k, y_k travel from IU.

Let us consider the operation of the four small additional blocks shown in figure 2.

Shift Block

/254

The block diagram is shown in figure 3. The reset pulses S3 are formed by the decoder, shaped in the cells 2I-1 266, F-6 273 and 2I-5 275 and are fed to the reset buses of the sign place and all the other places of the shifter. The durations of the S3 pulses, just as all the other reset pulses in the unit, are equal to 50 μsec. The shift pulses are formed from a continuous series of pulses arriving at the monovibrator Mo 341. After the monovibrator there is a gate controlled by the trigger T-1 267. The gate must open at the required moment, pass k or 2k + 1 pulses and again close. The opening or closing of the gate is accomplished by setting of the trigger T-1 267 in the unit or zero state with the aid of the pulses Sh3 (shift initiate) and Sh4 (shift terminate) which are generated by the decoder and are formed by the pulses from the monovibrator Mo 214, which lag in time from the output of the pulses of the cell Mo 341. Passing through the gate, the differentiating network, the shaper F-6 273 and the power amplifier (invertor) 2I-5, the pulses of the monovibrator Mo 341 are converted into short (duration about 2.5 μsec) shift pulses which are fed to the reset bus of the shifter (excluding the sign trigger). Each pulse causes a shift of the number by one place (in the direction of the lower-order places).

Roundoff Block No. 1

The block (fig. 4) consists of a small summator (sign and two significant places), in which the roundoff units are summed which arrive from the auxiliary place of the shifter (trigger T-2 231). If the shifted number is transferred

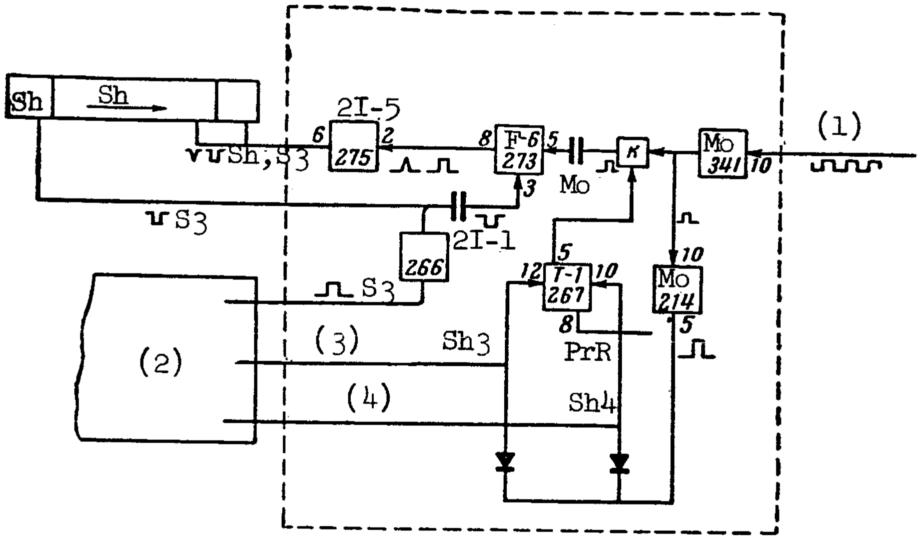

Figure 3. 1, From input of control unit pulse counter; 2, decoder; 3, begin shift; 4, end shift.

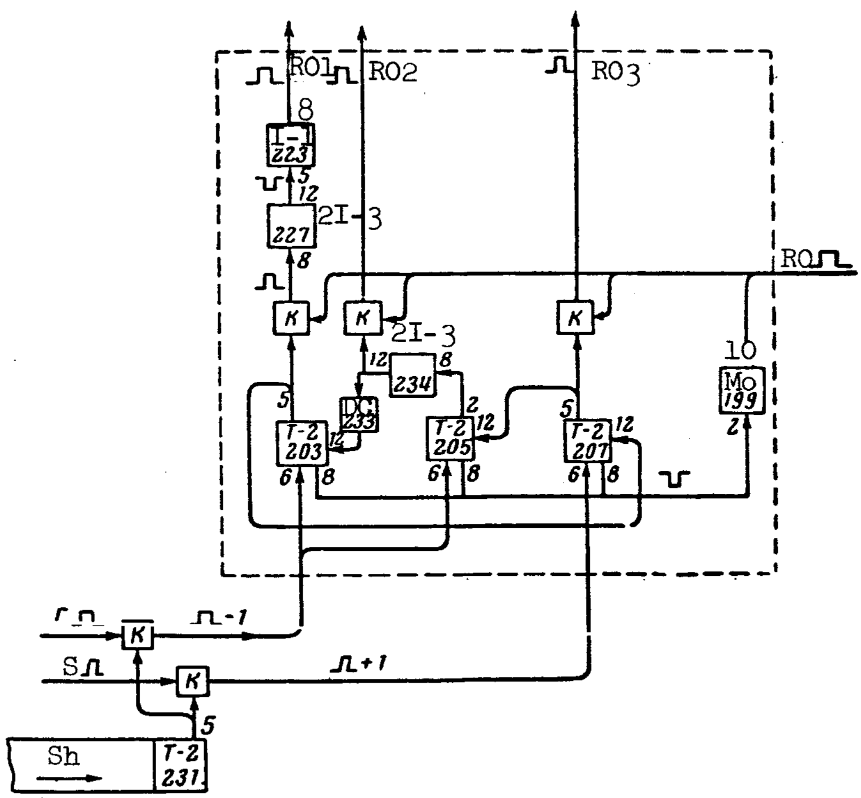

Figure 4

from the shifter into the summator by a direct code (i.e., by the signal S) and the cell T-2 231 is in the "1" position, then to the summator of the roundoff block there is added +1 (pulse to the complementing input of the lowest place of the summator--cell T-2 207). If, however, the shifted number is transmitted from Sh to Su by an inverse code (i.e., is subtracted with the aid of the signal Γ) then to summator of the roundoff block there is added -1 /255
(by the inverse code, i.e., pulses are applied to the complementing inputs of the triggers T-2 205 and 203).

During the time of the computation of the next value of x (n + 1) or y (n + 1), there is one multiplication by 2^{-k} and one multiplication by 2^{-2k-1}. With the transfer of the shifted numbers into the summator, there is storage of the roundoff units (if there are any) in the summator of the roundoff block. The roundoff of the number in the summator takes place after the computation of x (n + 1) or y (n + 1). To accomplish this the decoder delivers the pulse RO with the aid of which the roundoff block, in accordance with the state of the summator of the roundoff block, generates the roundoff pulses RO1, RO2 and RO3 which are applied, as we see in the block diagram /256
of the AU, to the sign place and the 1-17 places (RO1), the 18th place (RO2) and the 19th place (RO3) of the summator.

Table 1 shows the possible combinations of roundoff pulses which are sent to the summator Su and also shows by what magnitude they change the number in the summator Su.

After performance of the roundoff, the summator of the roundoff block is reset to zero by a negative pulse generated by the monovibrator Mo 199.

TABLE 1

State of summator of roundoff unit	Pulses delivered	Change of number in summator Su
0 0 0	-	0
0 0 1	RO3	$+ 2^{-N}$
0 1 0	RO2	$+ 2 \cdot 2^{-N}$
1 1 1	RO1, RO2, RO3	0
1 1 0	RO1, RO2	$- 2^{-N}$
1 0 1	RO1, RO3	$- 2 \cdot 2^{-N}$

Roundoff Block No. 2

The block (fig. 5) performs the reduction (in modulus) of the number in the summator Su to the nearest whole number of units of the 15th place. The

roundoff is performed directly following the transfer of the number from Su to Rel on the signal $D41_0$ or $D41_d$.

If there is a negative number in Su, then after its transfer on the signal $D41_0$ the monovibrator Mo 338 delivers a positive pulse, which is amplified by

the cell 2I-5 130 and triggers T-2 179-182 to the unit states (setting takes place through the anode circuits). If, however, there is a positive number in Su, the pulse S4 triggers the monovibrator Mo 337, whose output pulse is also amplified by the cell 2I-5 130 and triggers these cells to the zero states. In this case, with the aid of the diode circuit shown in figure 5, there is simultaneously a blocking of the carry pulse from the 16th place to the 15th, i.e., from cell trigger T-2 179 to cell trigger T-2 178 (the carry pulse can occur if prior to roundoff the cell was triggered by T-2 179 to the unit state).

The blocking circuit operates as follows. The square positive pulse /257 from the output of the monovibrator Mo 337 blocks the diode D in the circuit of the grid input of the trigger T-2 178. Therefore, the peaked negative carry pulse, which can appear at the output of the delay circuit DC, does not pass to the input of the trigger T-2 178 in the absence of a positive pulse at the output of the monovibrator.

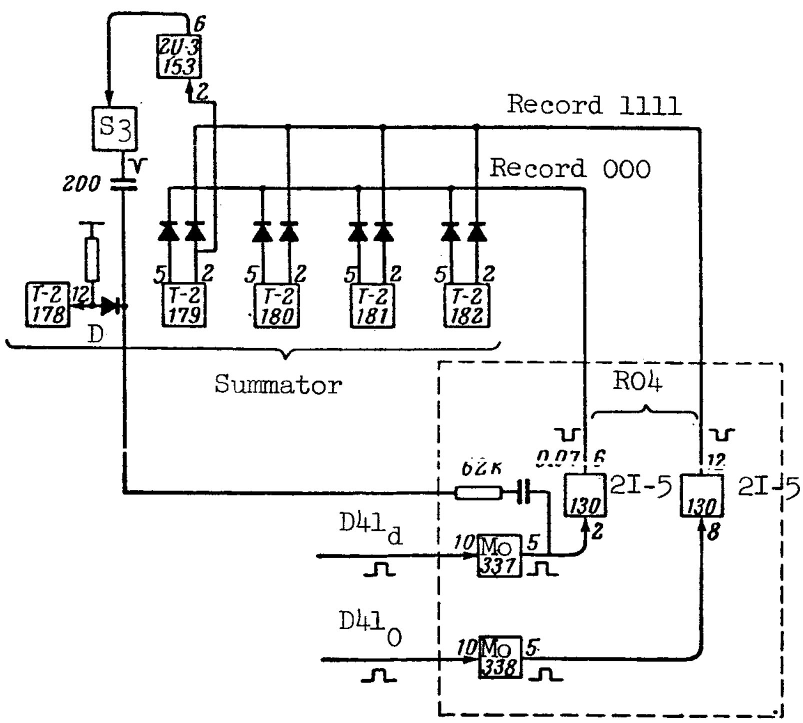

Figure 5

Stop Unit

The purpose of the stop unit (fig. 6) is:

(a) transfer of the device from the second stage operational regime (cyclic computation) to the third stage operational regime (exit from a segment) with satisfaction of the conditions

$$\left.\begin{array}{l} |x_k - x(n+1)| < M; \\ |y_k - y(n+1)| < M, \end{array}\right\} \tag{5}$$

where $M = 2^{-6}$;

(b) stopping of the device after completion of the exit from a segment.

The unit operates as follows. The seven inputs of one of the two diode coincidence circuits CC7 are connected with the single anodes of the sign place and the first six significant places of the summator Su, and the inputs of the second coincidence circuit CC7 are connected with the zero anodes of the same triggers. Consequently, in those cases when only zeros or only units are in these places (i.e., when the modulus of the number in the summator is less than 2^{-6}), at the output of one of the two circuits CC7 and at the output of the assembly As2 (cell 114) a high potential appears, which is applied to the coincidence circuit CC3.

A pulse appears at the output of CC3 with satisfaction of three conditions: with a high potential at the output of As2, with a high enabling potential PSv, and with the presence of the pulse DSv.

A high potential PSv appears at the output of the three-stage counter (T-2 131, 105, 106), to whose input there are applied pulses from the output of the 1st place of the counter of the CU (see description to figure 8 below). A single pulse is applied at the end of each cycle. Prior to beginning the operation, the three-stage counter is reset to zero by the signal AsP. The fourth pulse sets trigger T-2 106 in the unit state; in this case the gate at the counter input is blocked and a high level of the signal PSv appears, which is retained until termination of the machining of the segment.

Thanks to this, the verification of the observance of conditions (5) begins only with the fifth point. This is done for the case when $x_0 = x_k$, $y_0 = y_k$, as in this case the device could stop before the instantaneous point could manage to depart from the initial point in at least one of the coordinate axes by a distance farther than M.

The pulses DSv are applied twice in the course of each cycle at those moments when the quantity x_k-$x(n + 1)$ or y_k-$y(n + 1)$ is found in the summator.

Consequently, with observance of conditions (5) and with the condition n ≥ 5, where n is the cycle number, at the output of the coincidence circuit CC3 (cell 114) twice in one cycle there appears the pulse Sp1 applied to the two-stage counter (T-1 115 and T-2 112), which at the end of each cycle is set to zero with the aid of the pulse Cr ("cyclic reset"), which is generated by the decoder.

The two pulses ST1 which appear sequentially flip the trigger T-1 115 twice and set the trigger T-2 112 in the unit state. Then, at the output of the monovibrator Mo 110 there appears the negative pulse ST2, which sets the pulse counter in the control unit in the position from which the third stage--exit from the segment--starts.

At the end of the third stage the decoder delivers the pulse ST1 which sets the trigger T-1 392 in the unit state. The low potential which then

/258

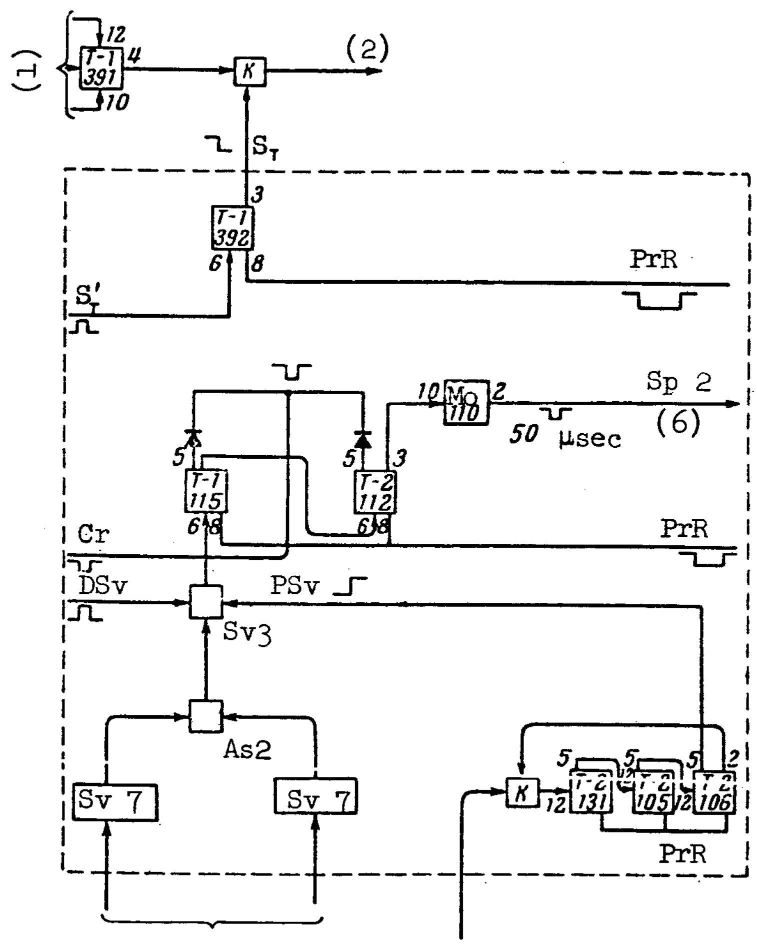

Figure 6. 1, From CG; 2, to control unit counter; 3, 50 μsec; 4, from sign place and six highest places of summator; 5, from 1st trigger of control unit counter; 6, to control unit.

appears on the zero anode of the trigger (signal ST) blocks the gate through which the pulses from the clock generator pass to the control unit counter. Thus the device stops. Prior to beginning of the operation of the device the "stop trigger" T-1 392 is set in the zero state by the preparatory reset pulse PRP.

Input Unit

The input unit (fig. 7) is intended for the input into St and into CU of the following information: k, L-A, the symbol for the direction of rotation, x(0) (or h_1), y(0) (or h_2), x_k and y_k. The first three signals are entered

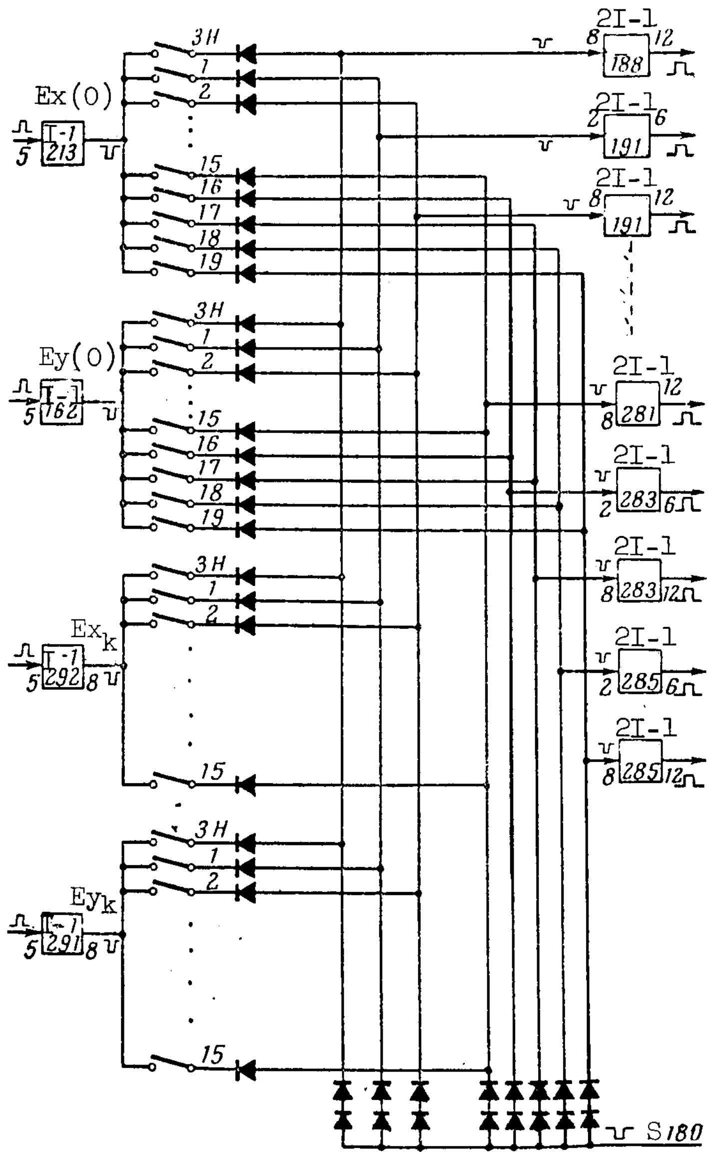

Figure 7

into the control unit (fig. 8) with the aid of switches, which are not shown in figure 7. The switches are connected to the source of high (+ 130 V) and low (+ 80 V) voltage (voltage divider). For example, in the case of machining a straight line the switches are used to apply a high potential to the L bus and a low potential to the A bus.

The input of the remaining information (to the summator) is accomplished with the aid of the circuit shown in figure 7. The signals Dx(0), Dy(0), Dx_k, Dy_k are generated in the CU, amplified by the cells I-1 and are /259

applied to the switches located on the control panel and simulating the contacts of the punchcard brushes. With a closed switch the pulse passes through the switch and diode, is shaped by the negative pulses of the series S180, is amplified by the cell 2I-1 (188) and is applied through the assembly and shaping gate to the sign trigger of the summator (the output of cell 2I-1 enters the cable denoted in figure 2 by the letters n.u.). The other switches and cells of figure 7 operate similarly.

The positive quantities x and y (and h) are assembled on the switches in direct code, the negative quantities are set using an inverse code.

Control Unit /260

The control unit (fig. 8) consists basically of the clock generator CG, a nine-stage pulse counter, cathode followers connected with the counter triggers, a diode decoder and several circuits for amplification and shaping of the output pulses of the decoder.

Two switches for the control of the regime of operation of the device, the trigger T-1 391, and a gate are located between the pulse generator and the counter. With actuation of the "automatic regime," the generator pulses go to the complementing input of trigger T-1 391 which is flipped by each input pulse, thus delivering a continuous series of pulses which pass through the gate (if it is not blocked by the low level of the signal ST, see description of the stop unit in the AU) and are applied to the counter.

If the automatic regime switch is in the left position, the pulses from the generator are applied through one of the two gates to the 10th or 12th output of the trigger T-1 (391), where each switching of the "manual" switch causes triggering of the gates and, consequently, one reversal of the trigger.

The pulse counter of the control unit must provide for operation of the device in three stages; in accordance with this the counter itself operates in three stages, or in three regimes.

The first regime (corresponding to the stage of the initiation of a segment) begins with the preparatory reset of PrR setting the counter in the initial state 001000000. During the time of the first stage, the counter is gradually filled to the state 011111111. The following input pulse sets the state 100000000. After this the second stage begins in the device. Each cycle of operation begins with the state 100000000 and terminates with the state /261

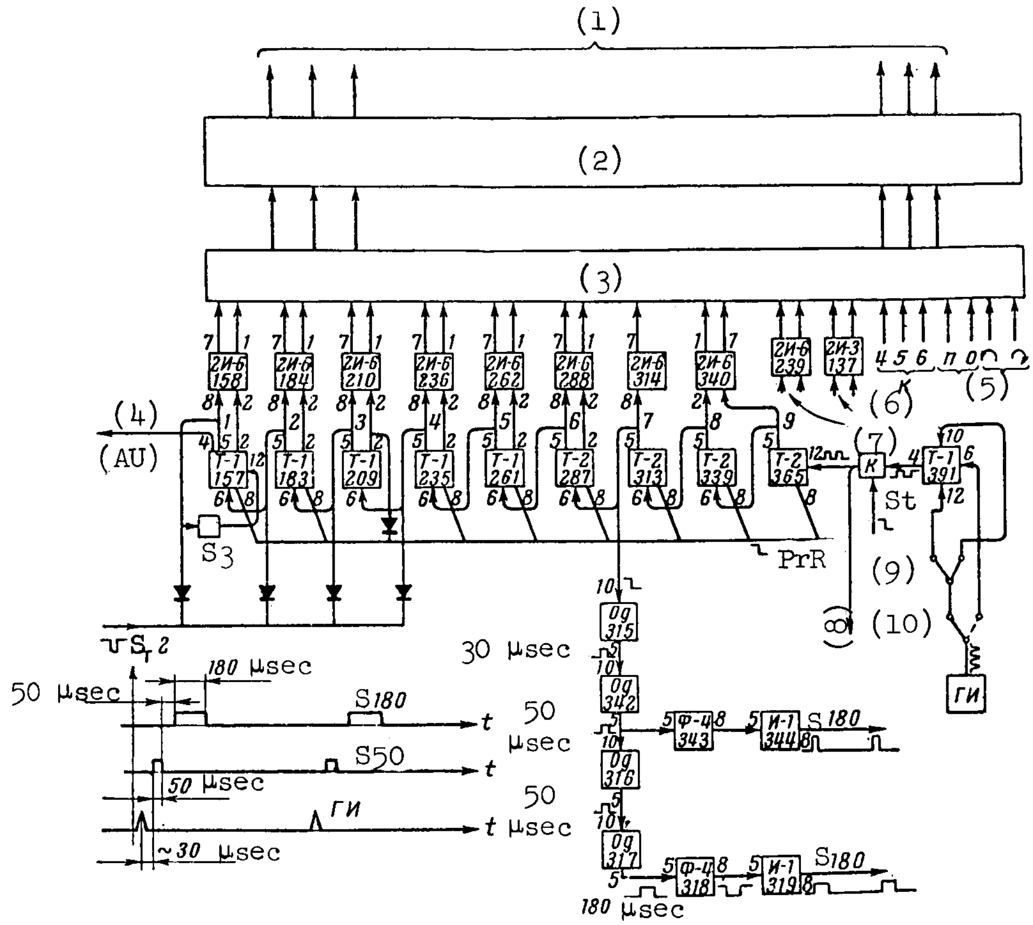

Figure 8. 1, Control signals; 2, circuits for shaping control signals; 3, decoder; 4, to stop unit; 5, direction; 6, sign of number in Su; 7, sign of number in Sh; 8, to shift unit; 9, "manual"; 10, "auto". И = I; Og = Mo; ГИ = CG; φ = F.

111111111. The following pulse resets the entire counter to zero, but after a short time (about 4 μsec) the first trigger, thanks to the feedback circuit from the output through the delay line SD back to the input, is again set in the unit state. This takes place every time after the entire counter is filled with ones.

Thus the filling of the counters from the state 100000000 to the state 111111111 takes place periodically, each period corresponding to a single cycle, i.e., to the transition from the preceding discrete point of the segment to the following point. The cyclic computations are continued until the approach of the present point to the specified end of the segment. With approach to the end, the stop unit of the AU (see above) generates the pulse ST2 (at that moment when the counter is in the state 111101000). The pulse ST2 through the anode circuits sets the counter in the new state 000001000, from which the third stage--the exit from the segment--begins. This stage

terminates when the counter arrives in the position 000110000. At this moment the signal ST appears and the device stops.

In figure 8 we see that the output signals of the seventh trigger are used for the formation of the standard series S180 and S50. With each transition of the third trigger from the one state into the zero state, one pulse of the series S180 and one of the series S50 are generated. The time delays of the monovibrator are selected so that the pulse S50 appears 30 μsec after inversion of the trigger, and the S180 pulse appears 50 μsec after termination of the S50 pulse (fig. 8).

The pulses of the standard series S50 and S180 are delayed in order that at the moment of appearance of the S50 pulse (which is used for the formation of a series of signals in the decoder) all the transient processes in the pulse counter and in the decoder associated with the arrival of the successive clock pulse from the trigger T-1 391 have already decayed, which facilitates the formation of the output signals of the decoder.

The decoder, located in the CU, consists of a large diode logic circuit (535 diodes). The decoder generates a series of signals which control the operation of the device: D12, D13, $D41_d$, $D41_0$, A, D, S, Γ, D, S1, S3, S4, Sh_3, Sh_4 and others.

Each of the output signals appears under definite, fixed once and for all, combinations of states of the input logic variables, each of which can have two values: 0 or 1, i.e., is selected by a high or low potential. These logic variables are: the state of the triggers of the counters in the control unit, the quantities k introduced from the punchcard, L-A, the direction symbol, the states of the triggers of the sign summator and of the shifter--26 variables in all, as shown in figure 8.

Since the triggers can have only a comparatively small loading, the decoder is not connected directly to the triggers, but to the cathode followers connected with the anodes of the corresponding triggers.

The circuits for the generation of the individual signals are all approximately the same. The detailed algorithm for operation of the device is composed so that there is a minimal number of standard circuits with a mini- /262
mal number of diodes in the decoder. Several steps were taken to achieve this goal.

The standard circuit (for generation of the signals D23 and Ex_k) is shown in figure 9.

The signal D23 is generated with the aid of three coincidence circuits and an assembly which combines the outputs of the three coincidence circuits and the shaping gate, in which use is made of the standard series S180 for shaping the signal D23 (and also the signal Ex_k). If the number of coincidence circuits is greater than 4-5, we install in the assembly after the coincidence

circuits KBMP diodes, which have high reverse impedance (of the order of 10 MΩ), which prevents reduction of the useful signal at the output of any of the coincidence circuits due to leakage through the reverse resistance of the diode assembly. The greatest number of coincidence circuits used for the generation of a single signal is equal to 12 (signals A, D, S, Sh3).

Almost all output pulses of the decoder are formed by the series S180 or the series S50. The shaping permits us to obtain a standard duration of the control pulses, synchronize them with the main series S180 and S50 and improve the flanks (particularly the rear).

Because of some disparity of the levels of the voltages of the logic variables and for several other reasons, on the decoder outputs, in addition to the large (about 40 V) positive useful pulses, there are false pulses of lower amplitude (to 5 V). Therefore, for the further shaping and amplification of the control signals use is made of invertors having a constant negative grid bias sufficient for cutoff of the false pulses. During shaping and amplification the control pulses acquire the required polarity: the reset pulses become negative, the pulses for the input, transfer, output of data from the device and certain other pulses become positive.

The CU counter digits are not used for the generation by the decoder /263
of the control signals other than the signal Sh3. These digits participate only in the generation of the signal for shift initiate Sh3, while the pulses arriving at the counter input from the clock generator are also used for the formation of the shift pulses themselves Sh (fig. 3).

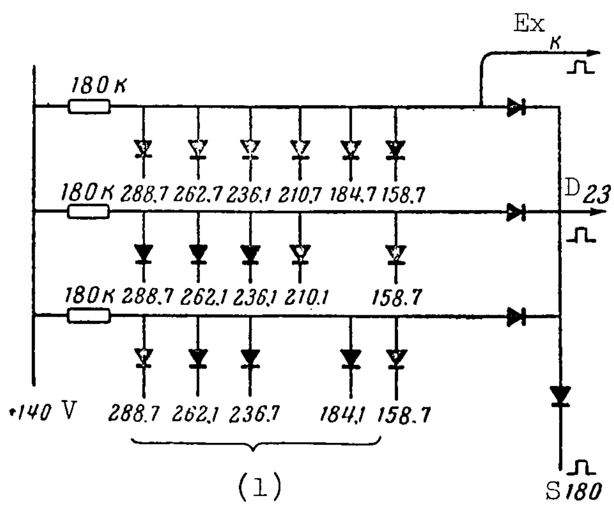

(2)	6	5	4	3	2	1
(3)	1	1	0	1	1	1
	1	0	0	0		1
	1	0	1		0	1

Figure 9. 1, Outputs of cathode followers; 2, counter places; 3, combinations for which D23 is delivered.

Table 2 shows in detail the sequence of the delivery of the various pulses and the performance of the operations in the device. At the bottom of the table are the states of the 1-4th triggers of the counter, on the right are the states of the 5-6th triggers of the counter. The signals and operations indicated in table 2 are located at the points of intersection of the corresponding rows and columns of the table. Thus, for example, the signal Cr is delivered with the following state of the counter: 111110.

This arrangement of the table emphasizes the fact that in the compilation of the algorithm an attempt was made to have every signal, for example S3, appear, insofar as possible, with the same states of the 5th and 6th triggers of the counter, which permits simplification of the logic circuits.

The following clarifications of table 2 must be made:

(1) The computation of the increments (3) and also of the quantities (4) is performed in the device with account only for the first 15 digits, since lower order digits may contain an error. Therefore, in computations using these equations the quantities $x(n)$, $y(n)$, $x(n + 1)$ and $y(n + 1)$ are reduced in modulus to the nearest whole number of units of the 15th digit, for which use is made of the RO4 operation and the Δ operation (see below).

(2) The letter "o" denotes those signals generated only in the machining of the circles, and the letter "s" denotes those which appear only in the machining of a straight line.

(3) The "+" symbol denotes addition and is to be understood as: in this place in the program the signals A and S are produced, if the number in the shifter is positive, and if it is negative, then D and Γ are produced. The "-" symbol denotes subtraction, i.e., the delivery of D and Γ with a positive number in the shifter, and the delivery of A and S with a negative number.

(4) The notations $\pm$ A and $\mp$ A used in the table denote addition or subtraction performed in the machining of the circle, where the upper sign denotes the operation performed with movement along the arc in the counterclockwise direction, and the lower sign denotes the operation with clockwise movement.

(5) The operation Δ denotes the subtraction from the number in the summator of the number located in the shifter, where the latter is rounded off to the nearest smaller whole number of positive or negative units of the 15th digit. In other words, here the signals B and D are delivered, if the number in Sh is positive, or the signal A is delivered otherwise.

(6) We must keep in mind that $Ex(0)$ and Eh_1 are one and the same signal (as are the signals $Ey(0)$ and Eh_2), since the numbers $x(0)$ and h_1 and the numbers $y(0)$ and h_2 are arranged on the punchcard in the same places and are introduced into Su by pulses from the same cells.

TABLE 2

Start												Output from section				
0010		0011		0100		0101		0110		0111		0000		0001		
														Δ	$y_k - y(n+1)$ $y(n+1)$ $x(n+1)$ $y(n+1)$ ——— $y_k - y(n+1)$ $y(n+1)$ $x(n+1)$ $y(n+1)$	00
C4 $Bx(0)_0$	0 . . . . ——— $x(0)$	C3 C4	0 0 . . . . . . 0 ——— 0 0 . . . . . . $x(0)$	$By(0)_0$	0 0 0 0 ——— $y(0)$ 0 $x(0)$ $x(0)$	B13	0 0 0 0 ——— $y(0)$ $y(0)$ $x(0)$ $y(0)$									01
												$B\Delta x$	$x_k - x(n+1)$ . . . . . . $x(n+1)$ $y(n+1)$ ——— $x_k - x(n+1)$ $y(n+1) \cdot 2^{-k}$ $x(n+1)$ $y(n+1)$	$B\Delta y$ Cm	$y_k - y(n+1)$ $y(n+1)$ $x(n+1)$ $y(n+1)$ ——— $y_k - y(n+1)$ $y(n+1)$ $x(n+1)$ $y(n+1)$	10
C1 B41 OK4*	0 . . . . 0 ——— $x(0)$ . . . . $x(0)$	B12 OK*	0 0 0 0 ——— 0 0 $x(0)$ $x(0)$	C1 B41 OK4*	0 0 0 0 ——— $y(0)$ 0 $x(0)$ $y(0)$					$C\partial x$	0 0 0 0 ——— $y(0)$ $y(0) \cdot 2^{-k}$ $x(0)$ $y(0)$	C4 By_k B13	y_k $y(n+1)$ $x(n+1)$ $y(n+1)$ ——— y_k $y(n+1)$ $x(n+1)$ $y(n+1)$			11

*Operation not necessary, but does not interfere.

$c\partial$ = Sh　　B12 = D　　$Bx(0)_0 = Ex(0)_0$　　OK = RO　　$B\Delta x = D\Delta x$

$c_u = S_d$　　C = S (Signal)　　$By(0)_0 = Ey(0)_0$　　Cm = St　　subscript OKp = RO

TABLE 2 (Continued)

Cyclic calculation

C 4 ± 0 Bh_{1n}	h_1 . . . . $x(n)$ $y(n)$	-0		Δ	$\Delta x(n)$ $x(n)$ $y(n)$ $x(n+1)$	C 4 ± 0 Bh_{2n}	h_2 . . . . . . $y(n)$ $x(n+1)$	-0		Δ	$\Delta y(n)$ $y(n)$ $x(n+1)$ $y(n+1)$	Δ	$y_k - y(n+1)$ $y(n+1)$ $x(n+1)$ $y(n+1)$	Δ	$x_k - x(n+1)$ $x(n+1)$ $x(n+1)$ $y(n+1)$	00
	$\pm y(n)\cdot 2^{-k}$ $y(n)\cdot 2^{-k}$ $x(n)$ $y(n)$		$x(n+1)$ $x(n)\cdot 2^{-2k-1}$ $x(n)$ $y(n)$		$\Delta x(n)$ $x(n)$ $y(n)$ $x(n+1)$		$\pm x(n)\cdot 2^{-k}$ $x(n)\cdot 2^{-k}$ $y(n)$ $x(n+1)$		$y(n+1)$ $y(n)\cdot 2^{-2k-1}$ $y(n)$ $x(n+1)$		$\Delta y(n)$ $y(n)$ $x(n+1)$ $y(n+1)$		$y_k - y(n+1)$ $y(n+1)$ $x(n+1)$ $y(n+1)$		$x_k - x(n+1)$ $x(n+1)$ $x(n+1)$ $y(n+1)$	
C 3 B 23	h_1 $x(n)$ $x(n)$ $y(n)$	C 3 B 23	$x(n+1)$ $x(n)$ $x(n)$ $y(n)$			C 3 B 23	h_2 $y(n)$ $y(n)$ $x(n+1)$	C 3 B 23	$y(n+1)$ $y(n)$ $y(n)$ $x(n+1)$	C 3 B 13	$\Delta y(n)$ $y(n+1)$ $x(n+1)$ $y(n+1)$	C 3 BC_n	$y_k - y(n+1)$ 0 $x(n+1)$ $y(n+1)$	C3 BC_n	$x_k - x(n+1)$ 0 $x(n+1)$ $y(n+1)$	01
	$\mp y(n)\cdot 2^{-k}$ $x(n)$ $x(n)$ $y(n)$		$x(n+1)$ $x(n)$ $x(n)$ $y(n)$				$\pm x(n)\cdot 2^{-k}$ $y(n)$ $y(n)$ $x(n+1)$		$y(n+1)$ $y(n)$ $y(n)$ $x(n+1)$		$\Delta y(n)$ $y(n+1)$ $x(n+1)$ $y(n+1)$		$y_k - y(n+1)$ 0 $x(n+1)$ $y(n+1)$		$x_k - x(n+1)$ 0 $x(n+1)$ $y(n+1)$	
+ $C\partial 2_k + 1$	$x(n+1)$ . . . . $x(n)$ $y(n)$	B 12 OK	$x(n+1)$ $x(n)$ $y(n)$ $y(n)$	$B\Delta x$		+ $C\partial 2_k + 1$	$y(n+1)$ . . . . . . $y(n)$ $x(n+1)$	B 12 OK	$y(n+1)$ $y(n)$ $x(n+1)$ $x(n+1)$	$B\Delta y$				B13 C_n	$x_k - x(n+1)$ $y(n+1)$ $x(n+1)$ $y(n+1)$	10
	$x(n)\mp y(n)\cdot 2^{-k}$ $x(n)\cdot 2^{-2k-1}$ $x(n)$ $y(n)$		$x(n+1)_{okp}$ $x(n)$ $y(n)$ $y(n)$				$y(n)\pm x(n)\cdot 2^{-k}$ $y(n)\cdot 2^{-2k-1}$ $y(n)$ $x(n+1)$		$y(n+1)_{okp}$ $y(n)$ $x(n+1)$ $x(n+1)$						$x_k - x(n+1)$ $y(n+1)$ $x(n+1)$ $y(n+1)$	
		C1 B41 OK4	$x(n+1)$ $x(n)$ $y(n)$ $x(n+1)$	$C\partial k$				C1 B41 OK4	$y(n+1)$ $y(n)$ $x(n+1)$ $y(n+1)$	C4 By_k	y_k $y(n+1)$ $x(n+1)$ $y(n+1)$	C4 B23 Bx_k	x_k $x(n+1)$ $x(n+1)$ $y(n+1)$	$C\partial k$	$x_k - x(n+1)$ . . . . . . $x(n+1)$ $y(n+1)$	11
			$x(n+1)$ $x(n)$ $y(n)$ $x(n+1)$		$\Delta x(n)$ $x(n)\cdot 2^{-k}$ $y(n)$ $x(n+1)$				$y(n+1)$ $y(n)$ $x(n+1)$ $y(n+1)$		y_k $y(n+1)$ $x(n+1)$ $y(n+1)$		x_k $x(n+1)$ $x(n+1)$ $y(n+1)$		$x_k - x(n+1)$ $y(n+1)\cdot 2^{-k}$ $x(n+1)$ $y(n+1)$	
1000		1001		1010		1011		1100		1101		1110		1111		

(See key on page 280.)

(7) Table 2 only shows approximately in what places of the program the shifts Shk (by k places) or Sh2 k + 1 are performed.

(8) The remarks to the table show which numbers are located in Su, Sh, Re2, and Rel after performance of a given item of the program, with the position for machining of a straight line being shown above, and the position for the circle being shown below.

(9) In table 2 we understand the signal D41 to be both of the signals of the output from the summator to Rel--both $D41_d$ and $D41_0$. Which of these two

signals is delivered depends on the sign of the number in Su. It has already been shown above that following the transfer from Su into Rel, the last four digits in Su are discarded (on signal R04).

(10) In several of the table cells the reset and the output signals stand side by side. For example: S3 and D13, or S4 and Ex_k, or S1 and D41. /264

In these cases, actually, both signals are generated with the same position of the pulse counter, but the reset is still performed first, and then the transfer or entry. This follows from the fact that in the decoder the reset signals are formed by the series S50, while the transfer signals are formed by the series S180. Since the pulse S180 begins only with a delay of 50 μsec after the end of the pulse S50, as we see from the block diagram of the control unit in figure 8, the reset signal is performed first and then the transfer.

REFERENCES

1. Brik, V. A. Digital Computer for Program Control. Theory and Application of Discrete Automatic Systems (Tsifrovoye vychislitel'noye ustroystvo dlya programmnogo upravleniya. Teoriya i primeneniye diskretnykh avtomaticheskikh sistem). Trudy konferentsii 20-26 sentyabrya 1958, Izd. AN SSSR, 1960.
2. Interpolators Used in Machine Tool Program Control Systems (Interpolyatory, ispol'zuyemyye v sistemakh programmnogo upravleniya stankami). Otchet laboratorii No. 7, IAT AN SSSR, 1958.
3. Brik, V. A. Error Accumulation in Computations Using Digital Devices (Nakopleniye oshibok pri vychisleniyakh na tsifrovykh ustroystvakh). Avtomat. i telemekh, No. 5, 1960.
4. Ural Universal Automatic Computer, Technical Description (Universal'naya avtomaticheskaya tsifrovaya mashina "Ural." Tekhnicheskoye opisaniye). GOSINTI, 1958.

N66 34848

FAST-ACTING ELECTRONIC MULTIPLIERS

F. B. Gul'ko

One of the most important characteristics of multipliers is their response time. This requirement is imposed not only on the multipliers used in electronic simulators, but also those used in other fields such as in electric instrumentation (wattmeters, powermeters, etc.). /265

In the question of the speed of response of the multipliers we can identify two independent yet interrelated problems: (1) the design of the multipliers on the basis of low-inertia elements which permits obtaining fast response of the entire system as a whole and (2) analytic and experimental evaluation of the response time of the multipliers.

Relative to the statement of the second problem it is necessary to make certain remarks associated with refinement of the concepts of "response speed" and "passband" for the multipliers.

The fundamental criterion of the performance of the multiplier is the accuracy of the multiplication operation performed by it. It is evident that for every multiplier there exist two (for two inputs) classes of functions on which the multiplication operation is performed by a given multiplier with an error no greater than some specified quantity. The determination of these classes of functions as a function of the magnitude of the error is the general problem of the analysis of the multiplier. A similar general problem is the inverse problem of the determination of the maximal error for a given class of functions (which can be specified in the time domain or in the spectral domain).

At the present time it is not always possible to resolve these problems in the general case. Therefore, in practice the characteristics of the multipliers are computed and measured only for a limited class of functions, namely for the sinusoidal signals and for step-type signals. While for linear systems the results obtained with such computations and tests (i.e., amplitude-frequency and phase-frequency or transient characteristics) permit the study of the behavior of the systems in very different regimes, it is easy to show that for multiplier devices these data are in the general case insufficient.

Actually, if a multiplier is tested with the application to one input of a sinusoidal voltage and the application to the other input of a constant voltage (this form of test is widely used), we cannot make any judgement on the operation of the same device with the application of sinusoidal voltages to both inputs on the basis of the data obtained, because the output stage in /266

the second case will operate at a frequency double that attained in the first case.

It can be shown that with the testing of the multiplier using two sinusoidal signals the error will depend on the relationship of the phases of the signals. In particular, if the multiplier is built using quadrators, the tests with in-phase and out-of-phase signals can give different and completely unrelated values of the errors, because in these cases multiplication is accomplished as the result of the operation of different quadrators (squarers).

Thus the concept of "bandpass" for the multipliers has meaning only for a specific test method. A single test method has not yet been established, and the comparison of multipliers tested by different methods is therefore frequently difficult.

Let us now consider the factors which limit the passband[1] of certain multipliers. In direct action multipliers the passband is limited, as a rule, by the inertias of the input and output stages. As an example let us consider the multiplier based on the use of the Hall effect in semiconductors. A whole series of such multipliers has been described recently. Their primary advantages which have attracted attention to them are simplicity of construction, small size and high reliability. Finally, the multipliers of this type are practically inertialess with respect to one input. The essential deficiencies of these devices include the low output voltage (of the order of tenths of a volt) and the high temperature dependence (with the exception of the devices made using indium arsenide).

The simplest multiplier of this type is represented by the block diagram of figure 1a (here the multiplication sign denotes the multiplying part itself, which can be considered practically without delay up to 10^8 - 10^9 cps).

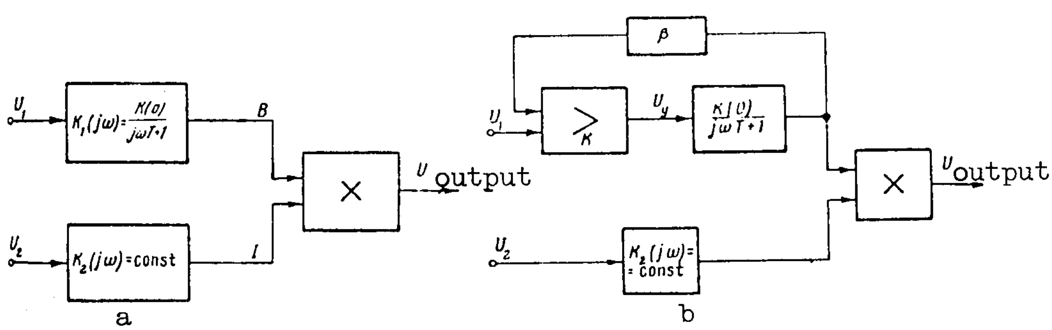

Figure 1. Multiplier using the Hall effect. a, Block diagram of simplest multiplier; b, block diagram of multiplier with negative inductive feedback.

---

[1]The concept of "passband" is defined in each specific case hereafter.

The inertial element representing the inductance coil, in principle, /267
can be nonlinear, which leads to additional error. To eliminate the nonlinearity we make use of a circuit with negative inductive feedback (ref. 1), where the inductance sensor is also a Hall sensor mounted in the gap of the electromagnet. The block diagram of this device is shown in figure 1b. We shall show that the circuit with negative feedback also reduces the dynamic error.

We define the limiting relative dynamic error ε as follows

$$\varepsilon = \frac{\sup |f_1(t) - f(t)|}{\sup |f(t)|},$$

where f(t) is the output signal which would be obtained in an ideal (giving no dynamic error) system; $f_1(t)$ is the output signal of the real system.

It is easy to verify that for the linear reproducing system with the tranfer function $K(j\omega)$ the dynamic error for a sinusoidal signal is

$$\varepsilon(\omega) = \frac{|K(j\omega) - K(0)|}{|K(0)|},$$

which for the inertial element gives

$$\varepsilon(\omega) = \sqrt{\frac{(\omega T)^2}{(\omega T)^2 + 1}}.$$

If we assume that the signal is applied to the multiplier through the inertialess input (fig. 1a) without distortion, the overall error of the multiplier will have the form[1]

ov = overall

$$\varepsilon_{ov} \leqslant \varepsilon(\omega) = \sqrt{\frac{(\omega T)^2}{1 + (\omega T)^2}}.$$

In the circuit with feedback (fig. 1b) the time constant of the inertial input in comparison with the open system must be reduced by a factor of $K\beta$ times; however, this is valid only when the amplifier operates in the zone of linearity.

---

[1]The equality sign in the equations for the total error obtains, in particular, with the application of a constant voltage to the second input.

Let us use $\overline{U}_y$ to denote the maximal output voltage of the amplifier with its operation in the linear zone, and $\overline{U}_1$ to denote the amplitude of the input voltage (at the inertial input) and let us introduce the coefficient

$$m = \frac{U_{\bar{y}}}{\overline{U}_1}\,(m \geqslant 1).$$

Then the critical frequency ω_{cr} at which the amplifier leaves the linear zone is determined by the equation

$$\omega_{cr} = \frac{1}{T}\sqrt{\frac{m^2 - 1}{1 - \left(\frac{m}{k\beta}\right)^2}}$$

or with $(K\beta)^2 \gg m^2$

$$\omega_{cr} \approx \frac{1}{T}\sqrt{m^2 - 1}.$$

With $\omega \leq \omega_{cr}$ the dynamic error of the multiplier (fig. 1b) can be /268
estimated as follows

$$\varepsilon_{ov} \leqslant \sqrt{\frac{(\omega T)^2}{(\omega T)^2 + (K\beta)^2}}$$

and with $\omega = \omega_{cr}$ (with account for $(K\beta)^2 \gg m^2$):

$$|\varepsilon_{ov}|_{\omega=\omega_{cr}} \leqslant \frac{\sqrt{m^2 - 1}}{K\beta}.$$

With the same frequency the error of the open circuit is

$$|\varepsilon_{ov}|_{\omega-\omega_{cr}} < \sqrt{1 - \frac{1}{m^2}}.$$

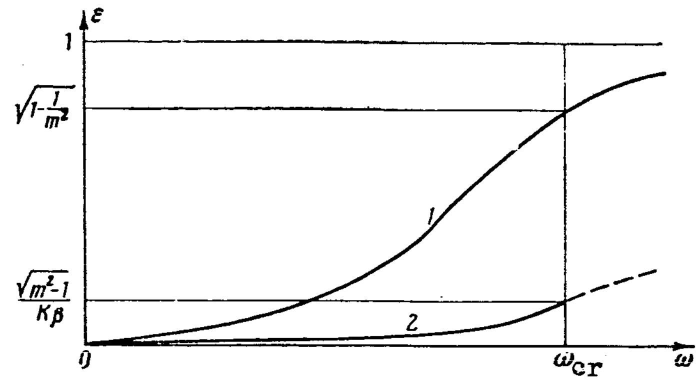

Figure 2. Variation of Hall effect multiplier error (as a function of frequency) without feedback (1) and with inductive feedback (2).

The limiting errors of the multipliers of figure 1a and 1b are represented as a function of the frequency in figure 2. As follows from the computation presented, in the multiplier with feedback, the passband diminishes with increase of the amplitude of the input signal $\bar{U}_1$.

Similar calculations can be made for other direct action multipliers with inertial elements at the input, for example, the electron-beam tube multiplier with crossed electrical and magnetic fields. Since the response speed of these systems is determined, in essence, by the rate of accumulation of energy in the magnetic (or electric) field, the possibilities of increasing their response speed are limited by the finite power of the signal sources.

In particular, the increase of the output power of the amplifier in the circuit of figure 1b would make it possible to increase the passband as a result of the increase of the linear zone (with increase of the output voltage), or would make it possible to reduce the number of turns of the coil and consequently the time constant T without reduction of the magnitude of the inductance in the gap (with increase of the output current).

Let us consider further the multipliers whose speed of response is limited primarily by the inertias of the output stages. An example of such a multiplier is the electron-beam tube with cylindrical beam (ref. 2). This tube has an electron gun which produces a cylindrical beam with quite uniform (across the section) current density, two pairs of deflection plates and a special metallic screen divided into four quadrants which are insulated from one another. In the absence of signals on the plates, the "image" of the beam on the screen is a circle with center at point O (fig. 3a) and the currents of all quadrants are equal. If we assign a plus sign to the currents of quadrants I and III and assign a minus sign to the currents of quadrants II and IV, the algebraic sum of the currents of the quadrants (total screen current) will be equal to zero. /269

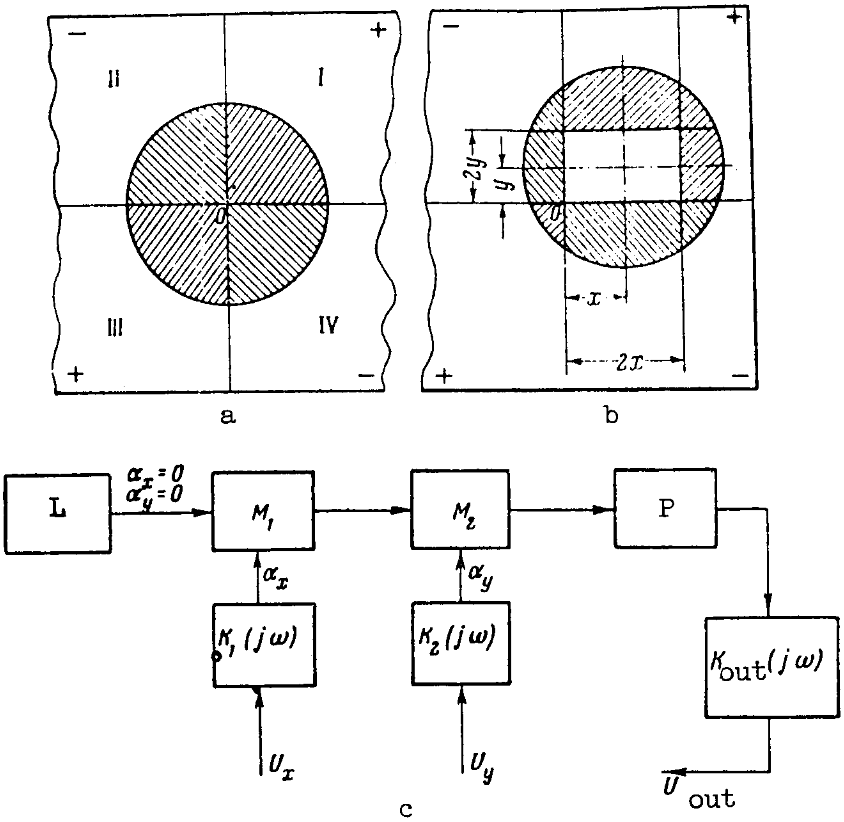

Figure 3. Multiplier using electron beam tube with cylindrical beam: a and b, mechanism of multiplication; c, design block diagram.

The signals U_x and U_y, applied to the plates, shift the "image" on the screen by the distances x and y proportional to these signals. From figure 3b we see that the algebraic sum of the currents in this case is proportional to the product xy, i.e., to the product of the signals U_x and U_y. As a result of a whole series of factors, primarily the nonuniform distribution of the current in the cross section of the beam, the static error of such a multiplier from the data of reference 2 is high (about 3 percent, including the zero drift during the measurement time of one hour).

The dynamic properties were determined with the application of sinusoidal signals to both inputs with the measurement of both dc and ac components at the output. The dc component remained constant up to frequencies of the order of 100 kcps, while the amplitude of the ac component was reduced by 3 db at a frequency of 70 kcps. This shows that in this case the dynamic error is determined primarily by the capacity at the output of the device, consisting of the capacitance between the screen quadrants and the capacitances of the summing (and also the measuring) circuit.

The dynamic characteristics of the electron-beam tube with cylindrical beam can be computed, using the block diagram of figure 3c, which presents the system for the creation of the beam L, the two deflection systems M_1 and M_2 with the corresponding transfer coefficients $K_1(j\omega)$ and $K_2(j\omega)$ (α_x and α_y are the deflections of the beam corresponding to voltages U_x and U_y), the device to convert the beam deflection into the output current P and the output stage $K_{out}(j\omega)$. It is essential that elements M_1, M_2 and P be considered inertialess (if the output capacitance of the tube is referred to the output stage), which considerably simplifies the analysis.

The large static error of the electron-beam tube with cylindrical beam makes it unpromising. The electron-beam tube with a hyperbolic field (ref. 3) has far greater possibilities. The multiplier using this tube is made with a closed circuit.

The principle of its operation is clear from figure 4a. The electron beam passing through the deflecting system I undergoes a deflection along the y-axis proportional to voltage U_1. In the second deflecting system, which creates the hyperbolic field, the beam is deflected along the x-axis, with the deflection being proportional to the product U_1U_2 with account for the sign. The third deflecting system, to which voltage U_3 is applied from the amplifier connected in the feedback circuit, deflects the beam so that its deflection at the screen along the x-axis is equal to zero. The screen is a metallic plate divided along the y-axis into two isolated parts. The voltage U_3, taken from the amplifier output is proportional to the product U_1U_2.

According to the data of reference 3, the static error of the device does not exceed 0.5 percent. An essential deficiency which reduces the accuracy and complicates the tuning is that the small error (0.5 percent) is not the result of the precise performance by all tube elements of the operations described above; just the reverse, the individual elements perform their operations with far less accuracy, but the inaccuracy is compensated by the other ele- /270 ments. Thus, the second deflecting system creates a beam deflection which is not exactly proportional to U_1U_2, but is somewhat greater, with the error proportional to $(U_1U_2)^2$. Moreover, a positive error is introduced by the edge effect of the deflection systems. The third deflection system gives a negative error of the order of 2.5 percent due to the reduction of the speed of the electrons which, being deflected from the z-axis, move in a field with a potential less than the accelerating field. The electrodes of the third deflection system are given a special shape in order to compensate for the remaining error.

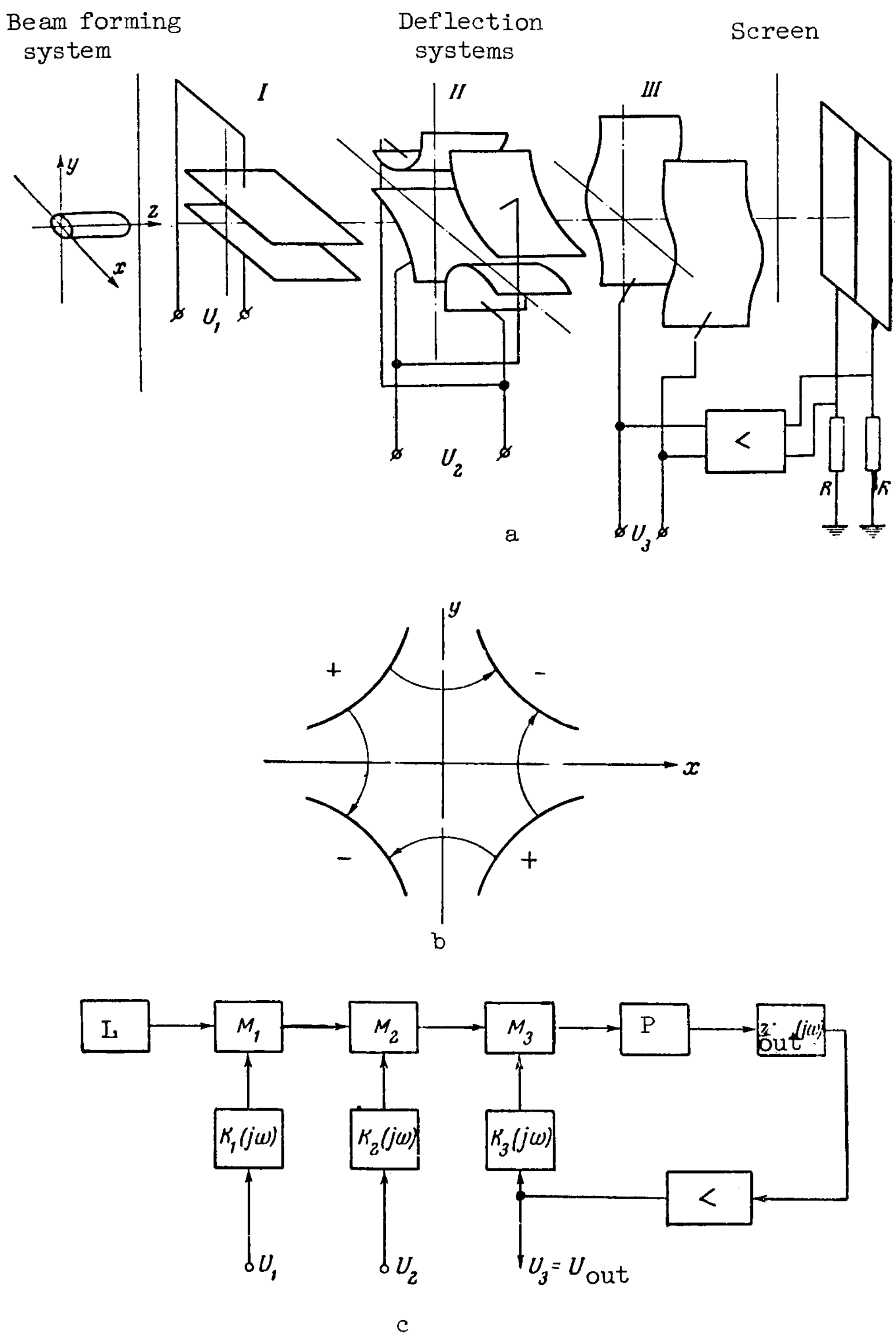

Figure 4. Multiplier using electron beam with hyperbolic field. a, multiplier circuit; b, second deflection system; c, design block diagram.

. The upper operating frequency of the device is 200 kcps (the test method is not described in reference 3). Computations show that with higher frequencies the inertia of the Z element begins to have an effect on the input of the amplifier, formed by resistors R, the output capacitance of the tube and the input capacitance of the amplifier. The block diagram of the multiplier using a tube with hyperbolic field is shown in figure 4c, where the notation is the same as in figure 3c.

The response speed of the multipliers made using quadrators is limited primarily by the capacitances of the quadratic converters themselves, and also by the parasitic capacitances of the circuit (especially in the circuits with diode converters). The compensation for these capacitances is quite complex, and no technique has been perfected for compensation so far. The investigation of reference 4 made an attempt to compensate for the capacitance of the diodes in a multiplier built using diode quadratic converters; the dynamic error of that device at 50 kcps reached 1.5 percent (with a static error of 0.3 percent), which indicates the low capabilities of such compensation. /272

It is evident that satisfactory compensation can be achieved only in the frequency range where the capacitive conductance remains considerably below the active conductance of the quadrator. Thus, from our data, the compensation in multipliers using thyrites, whose capacitance amounts to about 40-60 pF, is possible only in the frequency range up to several kcps.

Most promising from the point of view of construction of fast-response multipliers are the new quadratic functional converters, using special electron-beam tubes with a parabolic screen developed in the USA (ref. 5). The principle of operation of such a tube is shown in figure 5.

The flat electron beam leaving the system for the generation of beam 1 passes through deflection system 2 and strikes metallic collector 4. In the path of the beam there is screen 3 with a parabolic cutout. With application of a voltage to the deflection system the screen and collector currents vary, and this variation is proportional to the square of the applied voltage.

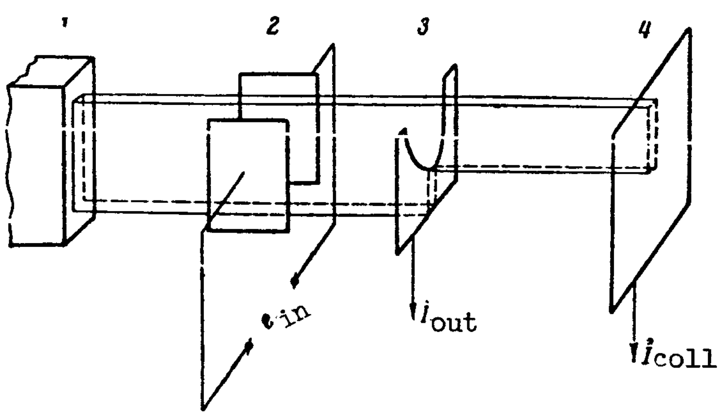

Figure 5. Electron beam tube with parabolic screen.

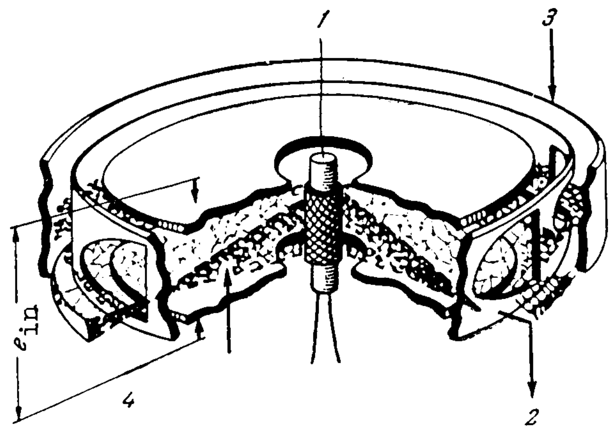

Figure 6. External view (a) and arrangement (b) of electron beam tube with parabolic screen. 1, Anode; 2, screen; 3, collector; 4, deflection plates.

Thus, if the screen current is taken as the output quantity, the equation of the converter can be written in the form

$$i_{out} = Ke_{in}^2 + i_0,$$

where K = 0.2 - 10 $\mu A/V^2$ for various tubes; e_{in} is the voltage applied to the deflection system; i_0 is the dc screen current, which can be compensated by suitable methods.

An external view of the electron-beam tube with parabolic screen is shown in figure 6a. The electron beam has the form of a flat disk, the deflection plates are also made in the form of disks (an additional dc voltage is applied to them to focus the beam properly). The collector and screen (fig. 6b) are cylinders with a whole series of parabolic cutouts made in the latter. Replacement of the single cutout by several parabolic cutouts produced a /273 considerable reduction of the error due to the nonuniform beam density along the y-axis and the slope of the beam to this axis.

The static error of a quadrator using this tube is no more than 1 percent (in practice, with input voltages to 35 V the error does not exceed 0.5 percent). The dynamic properties are quite high. The input capacitance is about 3 pF, output 13 pF. In the multipliers using such tubes (ref. 6) the passband with application of sinusoidal voltages to both inputs was found to be less than 90 kcps, but was limited primarily by the passband of the resolving amplifiers. According to the authors, the same tube can operate quite well up to medium wavelengths. However, with frequencies above 1 Mcps there appear additional error due to noise. Preliminary computations have shown that with a device passband of 5 Mcps, just the noise caused by the fluctuations in the space

charge produces an error, referred to the input, of the order of 0.3 V, i.e., with input voltages to 30 V it amounts to about 1 percent.

The possibilities being disclosed at the present time by the new electronic tubes for the design of multipliers with an error of less than 0.5 percent up to frequencies of the order of hundreds of kcps are of great interest and are worthy of considerable attention.

REFERENCES

1. Löfgren, L. Analog Multiplier Based on the Hall Effect. J. Appl. Phys., Vol. 29, No. 2, 1958.

2. Angelo, E. J. An Electron-beam Tube for Analog Multiplication. Rev. Scient. Instrum., 25, No. 3, 1954.

3. Schmidt, W. Hyperbolic Tube, an Electron Ray Tube for Multiplying in Analog Computers (Die Hyperfeldröhre, eine Elektronenstrahlröhre zum Multiplizieren in Analogie-Rechengeräten). Zeitschrift für angewandte Physik, Vol. 8, No. 2, January 1956.

4. Fischer, M. E. A Wide-band Analogue Multiplier Using Crystal Diodes and Its Application to the Study of a Nonlinear Differential Equation. Electronic Engng., 29, No. 358, 1957.

5. Soltes, A. S. A Wide-band Square-law Circuit Element. IRE Trans. on Electron Devices, ED-2, No. 2, 1955.

6. Miller, I. A., Soltes, A. S. and Scott, R. E. Wide-band Analog Function Multiplier. Electronics, 28, No. 2, 1955.

N66 34849

MODELING A CONTROLLABLE DELAY

Zh. A. Novosel'tseva

In the modeling of industrial control objects there frequently arises the need for the reproduction of a delay, due in the majority of the cases to the finite speed of transmission of a signal. At the present time the problem of modeling a constant delay has been quite well resolved, and various modeling methods (ref. 1) can be recommended depending on the delay time, the maximal frequency of the signal being delayed and the required accuracy. /274

However, in certain cases (for example, in the study of systems containing long pipelines with variable pumping capacity) it becomes necessary to reproduce a delay with a magnitude varying in accordance with some signal.

If we assume that no heat loss takes place inside the pipeline, the temperature of the coolant fluid at the outlet and inlet of the line are related by the expression

$$\theta_{out}(t) = \theta_{in}[t - \tau(t)], \tag{1}$$

where $\tau(t)$ is the variable delay which satisfies the condition

$$\int_{t-\tau(t)}^{t} v(t)\,dt = \text{const.} \tag{2}$$

In the last equation $v(t)$ denotes the velocity of movement of the coolant, while the constant in the right side corresponds to the line length. If the values of the temperature at the inlet are not defined at negative moments of time, equations (1) and (2) are valid only with $t - \tau(t) \geq 0$ and must be supplemented with the initial conditions $\theta_{out}(t) = \theta_{out\ initial}(t)$ for the initial moments of time. By differentiating equation (2) with respect to the parameter we obtain the equivalent implicit expression relative to τ

$$\tau'(t) = 1 - \frac{v(t)}{v(t-\tau)}\,. \tag{3}$$

The processes in the thermal portion of the energy system are slow; however, the fluid velocity varies over wide limits, and the range of permissible values of τ therefore amounts to 4-1,000 sec.

With respect to the principle of operation, the majority of the devices for the reproduction of a constant lag can be associated with the direct analogy models, since they model the signal delay process as a whole with provision by some method or other for a finite speed of transmission of the signal from the input to the output of the device. This is true for the devices for recording on magnetic tape and magnetic drum, for devices for electrostatic recording on a dielectric, and also for the delay lines using condensers which are commutated with the aid of keys and stepping switches. /275

Therefore, providing for the possibility of variation of the speed of transmission of the signal from the input to the output in accordance with equation (2), we can create a controllable lag unit on the basis of any of these devices. This task is resolved most simply in the last two types of devices, which require only the variation of the frequency of the controlling signal and modification of the interpolation circuit. A large magnitude of the time delay leads to the selection of the device where the input signal is stored on condensers, which are commutated by stepper switches.

During the time of recording (fig. 1), the condenser c_1 is connected to the source of the input signal, i.e., to the output of the resolving amplifier, through the current limiting resistor R. Since the charging time constant is small, we can consider that at the moment of disconnection the voltage across

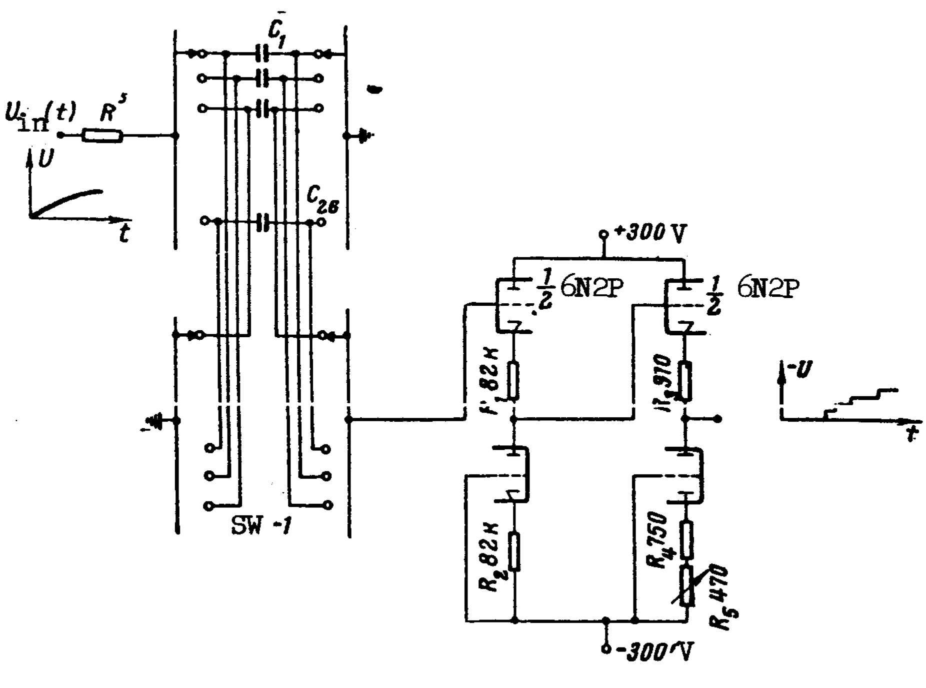

Figure 1. Record circuit. SW, Stepping Switch.

the condenser is equal to the input voltage. Thus, with commutation of the condensers C_1 - C_{26} with the aid of the stepping switch SW-1, the sequence of voltages on them forms a staircase curve corresponding to the input signal.

The problem of retention of the signal until the moment of readout is successfully resolved by the use of type MPGT polystyrene condensers and soldering of the condenser leads to series of switch contacts, separated from one another by a grounded series, which gives the effect of an "isolated ground."

In order to receive the readout of the delayed signal, the condensers are soldered to other series of the same stepping switch with some shift, for example, by 24 contacts. The arms of these series of the switch are connected with the input terminals of a cathode follower, which is used for readout.

The cathode follower circuit must provide for: (1) high input impedance; (2) low output impedance; (3) linearity range of ±100 V; (4) balancing relative to zero; (5) small zero drift.

In order to satisfy these conditions, the cathode follower in the device developed was made with a two-stage circuit, with the second half of the tube used as the cathode load in each stage. The first stage used the 6N2P tube operating with anode currents of the order of 60-100 μA and a filament voltage of 5.8 V, which permitted reduction of the grid current to a magnitude of the order of 10^{-11} A, i.e., reduction of voltage leakage across the condenser to an average value of 0.1 V per minute. The second stage used the 6N1P tube to provide adequate power; the linearity of the cathode follower was maintained with an accuracy of 1 percent in the range of ±100 V.

Readout was performed only at a time interval of τ after recording (here τ is the time expended on 24 steps of the switch, which must satisfy equation (2)). This requirement leads to the necessity for the design of a special control device.

The primary portion of the control circuit, shown in figure 2, is the integrator to which the controlling signal is applied. With increase of the integrator output voltage, the relay P_2 triggers first, closing the winding circuit of the stepping switch and then, when the voltage reaches 100 V, the winding circuit is broken and the stepping switch takes another step. Simultaneously the condenser in the integrator feedback circuit is discharged. This sequence of operations excludes the effect of the time of actuation of the stepping switch. /277

The moments of recording and readout of the signal are separated by the time τ, which satisfies the equation

$$K \int_{t_1-\tau(t_1)}^{t_1} U_{\text{contr}}(t)\,dt = 24 \cdot 100, \qquad (4)$$

where t_1 is the moment of readout.

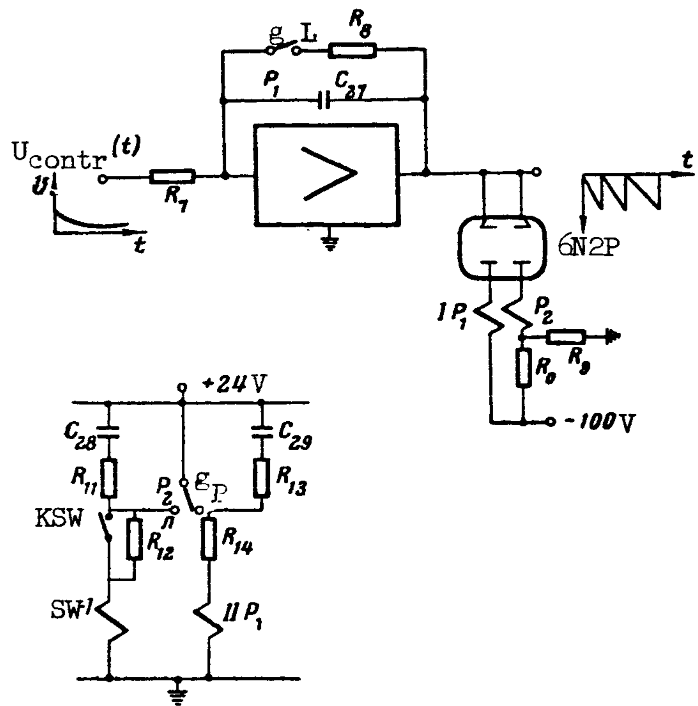

Figure 2. Control circuit.

By changing the relation of the integrator transmission coefficient K to the scale of the voltage $U_{contr}(t)$ we can obtain identity of equations (3) and (4).

Since at the output of the cathode follower there is obtained a delayed signal of staircase form, an interpolation circuit is used to improve the accuracy. The principle which is most easily realized is that of linear interpolation; however, this principle is not acceptable in our circuit in the form in which it is used in the conventional constant delay units. This is explained by the inconstancy of the period of the staircase curve, which is subject to interpolation.

With modeling of a variable delay the quasilinear interpolation must be accomplished in accordance with the equation

$$U(t) = U_2\left(\sum_{i=1}^{n} T_i\right) + K_1 \int\limits_{\sum_{i=1}^{n} T_i}^{t} [U_1(t) - U_2(t)]\, U_{contr}(t)\, dt, \qquad (5)$$

$$\sum_{i=1}^{n} T_i \leqslant t < \sum_{i=1}^{n+1} T_i,$$

where $U_1(t)$ is the staircase curve delayed by the time for 24 steps of the stepping switch;

$U_2(t)$ is the staircase curve delayed by 1 step relative to $U_1(t)$;

T_i is the time for the ith step of the switch.

Taking account of equation (4), we can show that with the selection $K_1 = K/100$ equation (5) is the interpolating formula for the function $U_2(t)$, because it coincides with it at the points of discontinuity. Consequently, the nature of the interpolation with the modeling of the controllable delay consists in the necessity for the use of an auxiliary multiplier, as follows from equation (5). As a quite simple multiplier we chose a servosystem using an irreversible stepping switch (this is possible since one of the cofactors is always positive).

According to equation (5), after obtaining the product $[U_1(t) - U_2(t)] \times U_{contr}(t)$, it is necessary to perform the integration in the indicated limits and the addition with the step function $U_2(t)$. For this we can use an integrator and summator, where the voltage on the output of the integrator plays the role of an "addendum" and is dropped at each moment of switching. However, as the first term in equation (5) we can make use directly of the voltage at the integrator output at the moment of switching; then equation (5) reduces to the form

$$U(t) = K_1 \int_0^t [U_1(t) - U_2(t)] U_{contr}(t)\, dt. \tag{6}$$

With this approach the number of resolving amplifiers in the interpolation circuit is reduced to one, and the danger of error accumulation is eliminated by the "trimming" of the voltage on the integrator to the required level at the moment of switching. For this use is made of the additional relay P_3, which operates synchronously with relay P_1 in the control circuit and switches the resolving amplifier from the integrator regime to the regime of a lag-lead element (fig. 3). /279

The amplitude error of the reproduction of the delayed signal can be divided into the error of reproduction of the nodal points and the error of interpolation. The first component of this error depends on the following factors: (1) the condenser leakages in the period between record and readout; (2) condenser leakages in the readout period; (3) nonlinearity of the cathode follower; (4) errors of the transmission coefficient of the output amplifier in the regime of a lag-lead element; (5) drift of the output amplifier.

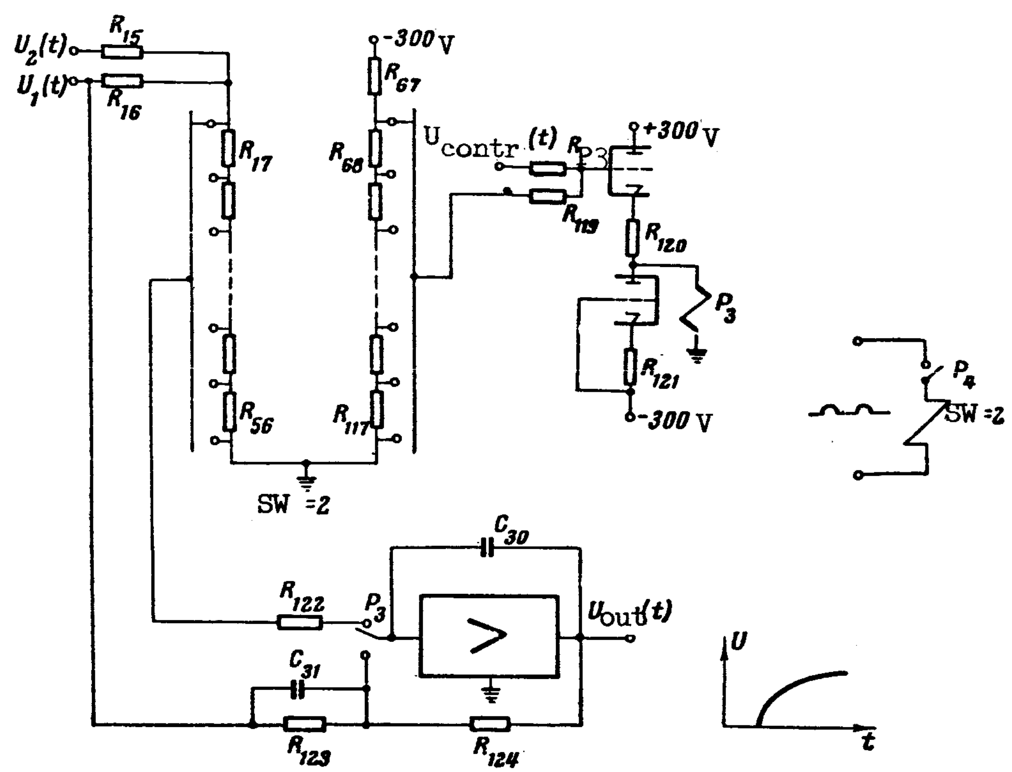

Figure 3. Interpolation circuit.

An evaluation of the effect of these factors shows that the first component of the error does not exceed 2 percent in amplitude.

As is known, the error with ideal linear interpolation is determined by the equation

$$\frac{U''_{max}\tau^2}{8} \leq \varepsilon. \tag{7}$$

In this case the magnitude of the acceptable error ε is usually specified and the maximal acceptable value of the signal frequency is determined as a function of the delay time τ. However, in the case of the reproduction of a variable delay such an estimate is not valid, because the derivatives of the input and delayed signals are different. Actually

$$[U(t-\tau)]'' = U''(t-\tau)(1-\tau')^2 - U'(t-\tau)\tau''. \tag{8}$$

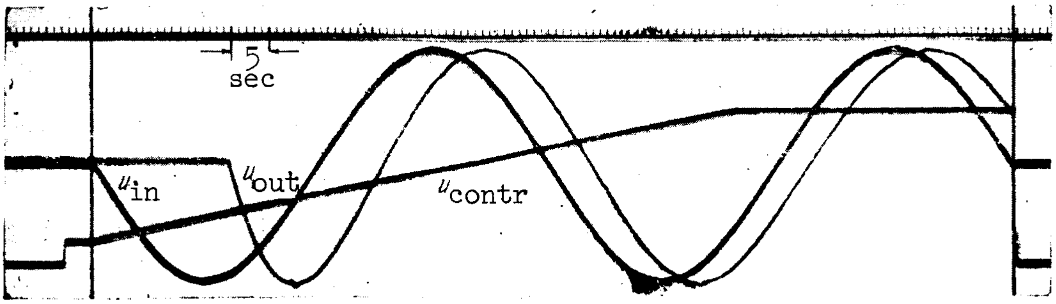

Figure 4. Oscillogram of delayed signal with linear law of variation of $U_{contr}(t)$.

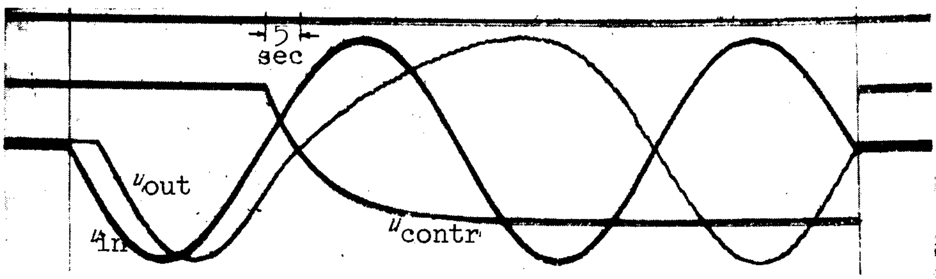

Figure 5. Oscillogram of delayed signal with exponential law of variation of $U_{contr}(t)$.

With a linear variation of the quantity τ

$$(\omega\tau)_{max\ var} = \frac{(\omega\tau)_{max\ const}}{|1 - \tau'|_{max}} . \tag{9}$$

Thus, in the reproduction of a variable delay with a specified accuracy and a specified time of delay, the range of acceptable values of the frequency is reduced sharply in comparison with the reproduction of a constant delay. The overall amplitude error of the device lies in the range of 4 percent.

Figures 4 and 5 present oscillograms of the reproduction of a variable controllable delay with a linear law of variation of the controlling signal with

$$U_{in}(t) = 100 \sin 0.1t$$

$$U_{cont}(t) = \begin{cases} 13.5 + t & t \leq 86.5 \text{ sec} \\ 100 & t > 86.5 \text{ sec} \end{cases}$$

and with variation of the controlling signal in accordance with an exponential law

$$U_{in}(t) = 100 \sin 0.114t$$

$$U_{cont}(t) = \begin{cases} 100 & t \leq 28 \text{ sec} \\ 86.5 \iota^{-\frac{t-28}{7.2}} + 13.5 & t > 28 \text{ sec.} \end{cases}$$

Conclusions

1. If the variation of the delay time is due to variation of the rate of transmission of the signal it is determined by equation /280

$$\int_{t-\tau}^{t} v(t)\,dt = \text{const.}$$

As a result the control circuit must contain an integrator.

2. In the modeling of a controllable delay, as a result of the inconstancy of the period of the staircase curve which is subject to interpolation, the interpolation formula must be altered, which requires the introduction of a multiplier into the circuit.

3. With a given value of the interpolation accuracy and maximal delay time, the range of acceptable values of the frequency of the input signal is reduced sharply in comparison with the modeling of a constant delay, depending on the rate and nature of the variation of the delay time.

4. The use of special cathode followers for the signal readout and the use of the method of continuous integration with correction at the end of each cycle for the formation of the output signal permits reduction of the number of resolving amplifiers in comparison with the analogous circuit for constant delay.

The unit developed for the controllable delay contains three cathode followers and two resolving amplifiers. The device provides for reproduction amplitude error of no more than 3 percent with

$$\omega\tau \leqslant \frac{6.8}{f_{(\tau', \tau'')}},$$

where in the case $\tau'' = 0$ $f_{(\tau')} = |1 - \tau'|_{max}$.

REFERENCE

1. Kogan, B. Ya. Electronic Simulators and Their Use for the Study of Automatic Control Systems (Elektronnyye modeliruyushchiye ustroystva i ikh primeneniye dlya issledovaniya sistem avtomaticheskogo regulirovaniya). Fizmatgiz, 1959.

N66 34850

ONE TYPE OF FUNCTIONAL CONVERTER WITH SEVERAL INPUTS

M. V. Rybashov

In the technology of mathematical modeling with the aid of electronic models, wide application has been made of the nonlinear functional converters of a single variable based on the piecewise-linear approximation of the function being reproduced. A typical representative of this class of converter is the circuit with potential-grounded diodes (refs. 1 and 2), shown in figure 1. /281

One electrode of each diode is connected to the summing point of the resolving amplifier RA, the second electrode is connected to the divider which is connected between the bus of the reference voltage U_{ref} and the bus of the input signal U_{in}. The pedestal voltages $U_1, \ldots, U_n$ form an increasing sequence $U_1 < U_2 <, \ldots, U_n$ (fig. 2) and, consequently, with increase of the input signal the diodes D_1, D_2, ..., D_i turn on sequentially.

Approximation is accomplished using the equation

$$U_{out} = -R_{fb} \cdot \sum_{i=1}^{n} \frac{1}{R_{i1}} \cdot U_{in} \cdot 1 (\alpha_i U_{in} - \beta_i U_{ref}),$$

(subscript fb = feedback)

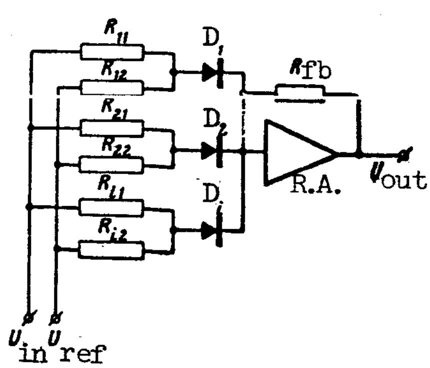

Figure 1

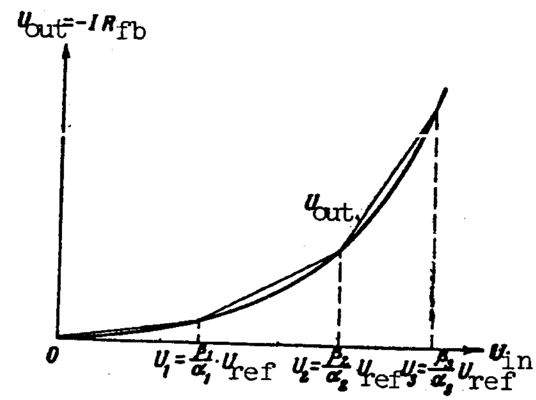

Figure 2

where the function $1\,(\alpha_i U_{in}-\beta_i U_{ref})$ for any i is determined as follows /282

$$1\,(\alpha_i U_{in}-\beta_i U_{ref}) = \begin{cases} 1 \text{ with } \alpha_i U_{in}-\beta_i U_{ref} > 0; \\ 0 \text{ with } \alpha_i U_{in}-\beta_i U_{ref} \leqslant 0, \end{cases}$$

where $\alpha_i = \frac{R_{i2}}{R_{i1}+R_{i2}}$. and $\beta_2 = \frac{R_{i1}}{R_{i1}+R_{i2}}$ are constants.

At the points i = 1, ..., n, for which the equality $\alpha_i U_{in}-\beta_i U_{ref} = 0$, is valid, the approximating function and the given function coincide. Between any two neighboring points i_k, i_{k+1} the approximating function varies linearly with variation of U_{in}.

Reference 3 proposes the use of such converters (it is true that the circuits considered differ somewhat from that shown in figure 1) as functional converters for two variables. This is possible if we make the reference voltage in the circuit the second independent variable. Actually, increase of the reference voltage by K times (figs. 1 and 3) leads to an increase of all approximating segments by the same factor. The function into which the new broken line is inscribed will be different from the previous one, although similar to it. From figure 1 we see that by suitable selection of U_{in} and U_{ref} we can arrive at any point of a quadrant in spite of this characteristic of the dependence of the function on the reference voltage.

Reference 3 also suggests a graphical method for the synthesis of such a functional converter. Similar to most graphical methods, this method does not give an answer to the possibility of realization of a function of a given form. The answer is obtained immediately as a result of the construction of the approximating graphs. This method can be utilized immediately, if the function is given graphically or in tabular form. However, in the case of analytic specification it is advisable to determine first the possibility of reproduction of the given function on such a converter and then to find the functional dependencies of its nonlinear circuits. The present study is devoted to these questions.

We note that if we make use of the reference input of the nonlinear feedback as the input of the third independent variable, the functional converter is capable of reproducing a function of three variables, of a narrow class, it is true, and if we connect this input with some other input of this same converter, it can reproduce different functions of two variables than when the reference voltage is fixed. This last technique expands the class of reproducible functions. Below we shall give examples of the determination of the functional dependencies of the input circuit and of the feedback, and we shall also give in broad outline the characteristic of the variation of the relative approximation error with variable reference voltages.

As we have mentioned, functions with two different reference voltages are similar, i.e., one is obtained from the other by variation of the scale along the coordinate axes. Let us establish the similarity equation.

Let us introduce some notations. We use x to denote the input voltage corresponding to U_{in} in circuit I. We take the value of the reference voltage equal to unity. With this condition the variation of the reference voltage by μ times will be equivalent to the application of a voltage equal to μ. We shall use $x_1, \ldots, x_n$ with $U_{ref} = 1$ to denote the values $(\beta_1/\alpha_1)\ U_{ref}, \ldots, (\beta_n/\alpha_n)\ U_{ref}$ corresponding to turn-on of the diodes.

Consider figure 3. Let $y = f(x)$ correspond to $U_{ref} = 1$. We increase the reference voltage by μ times; then all approximating chords will be increased by μ times. The point P is displaced to P', M to M', x_1 to x'_1. The angles formed between neighboring chords remain as before. We draw a broken line through the points O, P and M. We show that with increase of the number of chords approximating the curve $y = f(x)$ the broken line approximating the new function $y' = f'(x)$ tends to the function similar to $f(x)$.

The new function y' is given exactly at the points O, P', M', ... We express the values of y' at these points in terms of the values of the function y at the points O, P, M, taking account here that $x_i = x'_i/\mu$,

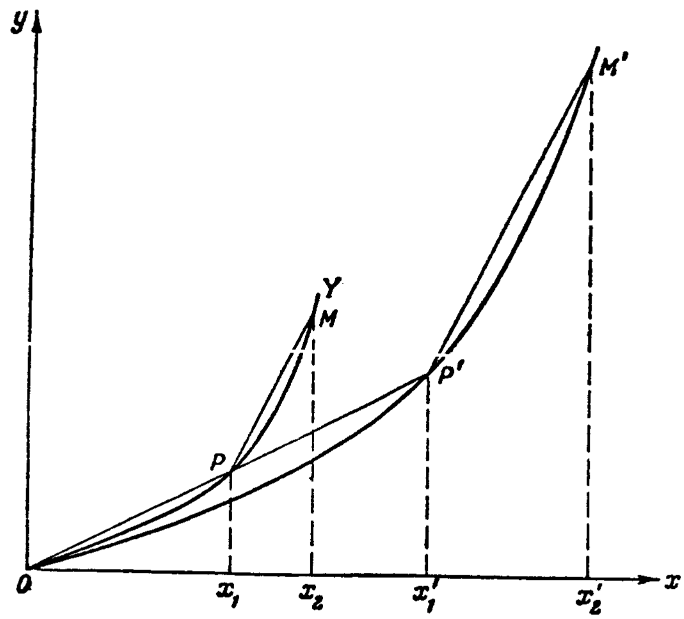

/283

Figure 3

$$
\left.\begin{aligned}
y'(x_1') &= \mu y\left(\frac{x_1'}{\mu}\right);\\
y'(x_2') &= y'(x_1') + \mu\left[y\left(\frac{x_2'}{\mu}\right) - y\left(\frac{x_1'}{\mu}\right)\right] = \mu y\left(\frac{x_1'}{\mu}\right) + \mu\left[y\left(\frac{x_2'}{\mu}\right) - y\left(\frac{x_1'}{\mu}\right)\right];\\
y'(x_i') &= \mu\left[\left(\frac{x_1}{\mu}\right) - y\left(\frac{x_0'}{\mu}\right)\right] + \mu\left[y\left(\frac{x_2'}{\mu}\right) - y\left(\frac{x_1'}{\mu}\right)\right] + \ldots + \mu\left[y\left(\frac{x_n'}{\mu}\right) - y\left(\frac{x'_{n-1}}{\mu}\right)\right].
\end{aligned}\right\} \tag{1}
$$

The last line is written for an arbitrary point with $y(x_0') \neq 0$. This equality can be written as follows

$$
y'(x_n') = \mu \sum_{i=0}^{n}\left[y\left(\frac{x_{i+1}'}{\mu}\right) - y\left(\frac{x_i'}{\mu}\right)\right]. \tag{2}
$$

If we now assume that the limit with infinite increase of the number of partitions (chords) of the broken line inscribed in y is the function y itself, from (2) it follows that

$$
y'(x) = \mu y\left(\frac{x}{\mu}\right),
$$

which proves the similarity.

Thus, increase of the reference voltage by μ times is equivalent to the multiplication by μ of a function of an argument, which is smaller by a factor of μ. Hereafter we introduce for the function y' the notation $F(x, \mu)$ as a function of two variables, having in mind the equality /284

$$
F(x, \mu) = \mu y\left(\frac{x}{\mu}\right) = \mu f\left(\frac{x}{\mu}\right). \tag{3}
$$

We note that for simplicity of analysis we have taken circuit II (ref. 2) (see table 1), in which the diodes operate on opening. It is evident that equation (3) is also valid for the circuit with blocking diodes. Also in the analysis we dropped the minus sign for the function y, which is due to the presence of the resolving amplifier.

Hereafter we shall not associate the analysis directly with any specific circuit for the connection of the diodes. The analyses will be equally valid for any of the circuits, if only in the circuit the formation of the family $F(x, \mu)$ takes place, using the method described above. We shall also assume that the circuit permits the reproduction of nonmonotonic functions in x in a single quadrant.

Let us consider some important properties of the function $F(x, \mu)$.

1. The function (more precisely, its envelope) is continuous in the combination of arguments x and μ if f(v) is continuous, where $v = \frac{x}{\mu}$, $\mu \neq 0$, which is obvious.

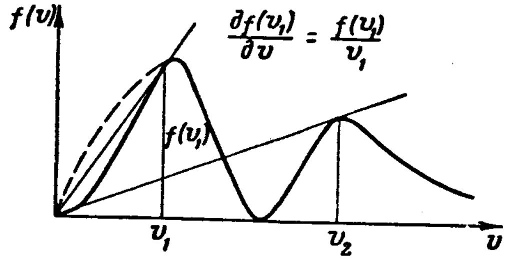

Figure 4

2. The sign of the function F (x, μ) is a function of the sign of x, which follows from the construction of the functional converter.

3. The extremal points in μ are determined by the equation

$$\frac{\partial F}{\partial \mu} = \frac{\partial f}{\partial v} v - f(v) = 0$$

or

$$\frac{f(v)}{v} = \frac{\partial f}{\partial v}\,.$$

The roots of the last equation correspond to the point of tangency of the straight lines drawn from the coordinate origin to the curve of the function f(v). From figure 4 we see that if the curve f(v) near the coordinate origin is convex downward, the number of extremal points is equal to the number of extremal points in x. If, however, it is convex upward, these numbers differ by unity.

4. For the functions F (x, μ) there can exist in the space (F, x, μ) only minima whose absolute value is always equal to zero.

Actually, the points at which the function can reach a smooth maximum (minimum) are determined by the system of equations

$$\frac{\partial F}{\partial \mu} = 0, \quad \frac{\partial F}{\partial x} = 0,$$

which is equivalent to the following system /285

$$\frac{\partial f}{\partial v} \cdot v - f(v) = 0;$$

$$\frac{\partial f}{\partial v} = 0.$$

Substituting the value of $\partial f/\partial v$ from the second equation into the first and considering that v is a bounded variable, we obtain

$$f\left(\frac{x}{\mu}\right)=0,$$

but with any relationships x and $\mu \neq 0$ of this equation the function F $(x, \mu) \equiv 0$, which proves the second part of our statement. The first half of the statement is obvious, since in order that the value F $(x, \mu) = 0$ be a maximum, it is necessary that the function F (x, μ) exist in the lower octants, which contradicts the chosen class of circuits.

Let us find all functional relations and certain of their characteristics which can be reproduced with different connections of nonlinearities (in the input circuit, in the feedback circuit, combined connection), and also with differing combinations of parallel connected inputs. In the future we shall make use of the following equation (ref. 1), which is valid for the circuit with two nonlinearities (fig. 5)

$$f_1(x_1)+f_2(x_2)=0, \tag{4}$$

where f_1 (x_1) is the nonlinearity in the input circuit from the signal x_1, which is subject to conversion; f_2 (x_2) is the nonlinearity of the feedback circuit from the output signal x_2. Equation (4) is valid for constant reference voltages of both nonlinear units.

In our case, equation (4) with account for (3) has the form

$$\mu_1 f_1\left(\frac{x_1}{\mu_1}\right)+\mu_2 f_2\left(\frac{x_2}{\mu_2}\right)=0.$$

This equation in essence must uniquely determine x_2 as the output quantity for the three variables x_1, μ_1, μ_2. From the theory of implicit functions it is known that for this it is necessary to satisfy the condition /286

$$\frac{\partial F(\mu_2, x_2)}{\partial x_2}\neq 0 \tag{5}$$

for all values of the variables appearing in it, with the possible exception of $\mu_2 = 0$ (the case is not of interest; there is no pedestal voltage). Circuit V can realize functions of three variables.

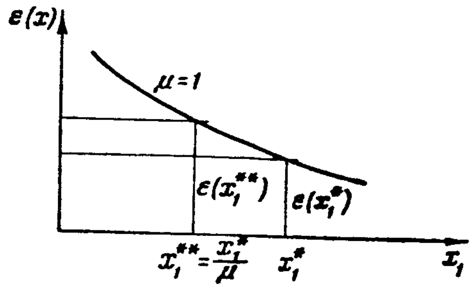

Figure 5

With $\mu_2 \neq 0$ this inequality is equivalent to

$$\frac{\partial f_2}{\partial v_2} \neq 0, \quad v_2 = \frac{x_2}{\mu_2}. \tag{6}$$

To this condition we must add the condition of static stability

$$\frac{\partial f_2}{\partial v_2} > 0. \tag{6'}$$

This last inequality includes condition (6).

Let us solve (5) relative to x_2

$$\frac{\mu_1}{\mu_2} \cdot f\left(\frac{x_1}{\mu_1}\right) = -f_2\left(\frac{x_2}{\mu_2}\right).$$

In view of (6) the function f_2 has the single inverse function Φ

$$\Phi = f_2^{-1}(v_2).$$

Taking account of what has been said and making use of equality (3), which is valid for this case also, we obtain

$$x_2(x_1, \mu_1, \mu_2) = -\mu_2 \cdot \Phi\left\{\frac{\mu_1}{\mu_2} \cdot f_1\left(\frac{x_1}{\mu_1}\right)\right\}. \tag{7}$$

In view of (6') the function $f_2(v_2)$ is monotonic and, consequently, the function $\Phi(\xi)$ where $\xi = \frac{\mu_1}{\mu_2} \cdot f_1\left(\frac{x_1}{\mu_1}\right)$, is also monotonic.

The resulting equation (7) is a very general structural equation for the functional converter with two nonlinearities (in the input circuit and the

feedback circuit) and with variable reference voltages. Without analyzing the circuit, this equation presents the answer to the question of whether such a reproduction of a function of a given form is possible or not. If the given function can be brought to the structure of the right side of (7), with account for the fact that Φ (ξ) > 0 everywhere in the region of variation of ξ, then in principle such a function can be reproduced by this converter. We further note that the independent variables μ_1, μ_2, x_1 themselves can be complex functions of a linear structure, i.e.,

$$\mu_1 = \sum_i \alpha_i u_i, \tag{8}$$

where u_i are the independent variables, α_i are the weighting factors. This follows directly from the properties of the functional converter. Various variants of the converter with the corresponding structural equations which they can reproduce are shown in table 1.

In comparison with the circuit I considered previously, circuit II can perform a more general functional dependence as a result of the additional /288 Φ operation, although this operation is quite limited (function Φ must be monotone). With the aid of this circuit we can realize a classical operation such as multiplication. The multiplication operation can be represented in the form

$$x_2 = \mu_1 \; x_1 = \left(\mu_1 \cdot \sqrt{\frac{x_1}{\mu_1}}\right)^2,$$

whence it follows that for its realization it is necessary to set

$$f_1(x_1) = \sqrt{x_1}, \;\; (\mu_1 = 1), \;\; \Phi^{-1} = f_2(x_2) = \sqrt{x_2}.$$

For simplicity the signs will be dropped here and hereafter.

Circuit III is a particular case of circuit I. With the aid of circuit IV we can realize the second classical operation of division.

The expression x_1/μ_2 can be represented as

$$x_2 = \frac{x_1}{\mu_2} = \mu_2 \left(\frac{\sqrt{x_1}}{\mu_2}\right)^2,$$

whence it follows that with $f_1 = \sqrt{x_1}$ and $\Phi^{-1} = f_2 = \sqrt{x_2}$ $(\mu_2 = 1)$ we have

$$x_2 = \frac{x_1}{\mu_2}.$$

TABLE 1

Block diagram	Structural formula for function being reproduced
I 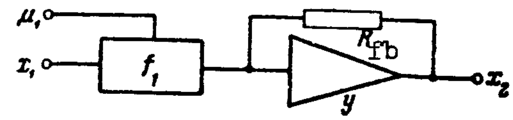	$x_2 = -\mu_1 f\left(\frac{x_1}{\mu_1}\right)$
II 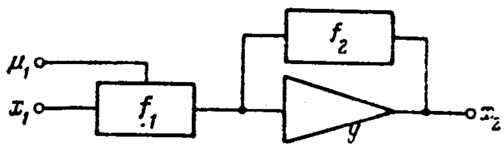	$x_2 = -\Phi\left\{\mu_1 f_1\left(\frac{x_1}{\mu_1}\right)\right\}$
III 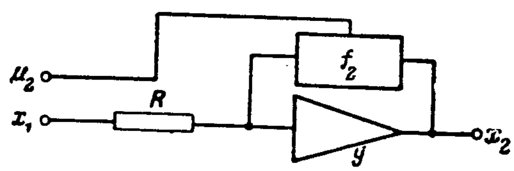	$x_2 = -\mu_2\Phi\left(\frac{x_1}{\mu_2}\right)$
IV 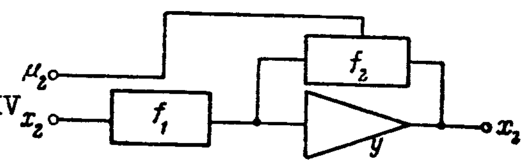	$x_2 = -\mu_2\Phi\left\{\frac{f_1(x_1)}{\mu_2}\right\}$
V 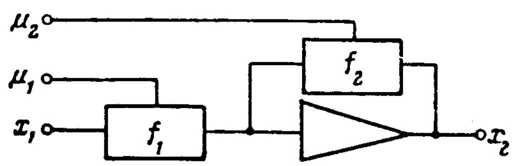	$x_2 = -\mu_2\Phi\left\{\frac{\mu_1}{\mu_2} f_1\left(\frac{x_1}{\mu_1}\right)\right\}$
VI 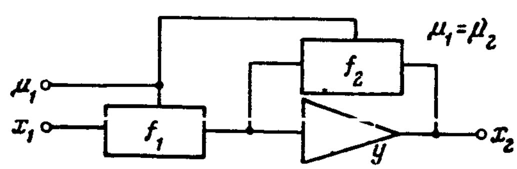	$x_2 = -\mu_1\Phi\left\{f_1\left(\frac{x_1}{\mu_1}\right)\right\}$
VII 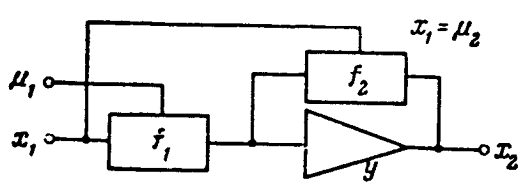	$x_2 = -x_1\Phi\left\{\frac{\mu_1}{x_1} f_1\left(\frac{x_1}{\mu_1}\right)\right\}$

Circuit V can realize a function of three variables. It is evident that the operations considered in the two preceding examples can be combined into a single group operation

$$x_2 = \frac{\mu_1 x_1}{\mu_2}$$

and we can perform it with the aid of this circuit.

Setting $f_1 = \sqrt{x_1}$, and $f_2 = \sqrt{x_2}$ (i.e., the same nonlinearities as in the preceding case), we obtain

$$x_2 = \mu_2 \left\{ \frac{\mu_1}{\mu_2} \left(\sqrt{\frac{x_1}{\mu_1}} \right) \right\}^2 = \frac{\mu_1 x_1}{\mu_2}.$$

Equations VI and VII are more general in comparison with I, since the latter is a particular case of them.

From all we have said, we see that the class of reproducible functions is very limited; however, if we make use of series and parallel connections of such converters, then their class can be expanded considerably.

Functions of many variables are frequently represented approximately in the form of a finite sum of the products of functions of a smaller number of variables.

Thus, for example, in references 4, 5 the terms of the approximation have the form

$$\zeta = \gamma(x)\eta(y).$$

Each term of this approximation can be obtained with the aid of two functional converters (in the limits of one octant).

Let us represent the operation ξ in the form

$$\zeta = \gamma(x)\eta(y) = \frac{1}{\eta(y)} \cdot \frac{\gamma_1^2(x)}{\dfrac{1}{\eta^2(y)}} = \mu\Phi\left(\frac{\gamma_1(x)}{\mu}\right),$$

where /289

$$\gamma_1(x) = \sqrt{\gamma(x)}.$$

Here we make use of circuit IV. To input μ we apply voltages from a functional converter which performs the operation

$$\mu = \frac{1}{\eta(y)}.$$

Let us find out how a variation of the variable μ affects the relative error of approximation in the circuit with a common nonlinear block. We use $x_2 = \mu f_1\left(\frac{x_1}{\mu}\right)$ to denote the exact function and $\tilde{x}_2 = \mu \cdot \tilde{f}_1\left(\frac{x_1}{\mu}\right)$ to denote its approximation. As an example let us assume the graph of the relative error of approximation of the function $f_1(x_1)$ with $\mu = 1$, shown in figure 5 (the graph gives the greatest relative deviations in modulus). Further let us form the relative error $\varepsilon(\mu, x_1)$ as a function of the two variables

$$\varepsilon(\mu, x) = \frac{x_2 - \tilde{x}_2}{x_2} = \frac{f_1\left(\frac{x_1}{\mu}\right) - \tilde{f}\left(\frac{x_1}{\mu}\right)}{f_1\left(\frac{x_1}{\mu}\right)}. \tag{9}$$

From (9) it follows that with fixed x_1^* and $\mu = 1$ we have the relative error $\varepsilon(x_1^*)$. Increase of μ is equivalent to reduction of x_1 by μ times. Here the error becomes equal to $\varepsilon(x_1^{**})$, where $x_1^{**} = \frac{x_1^*}{\mu}$ (we shift to the left on the graph). On this particular graph this leads to increase of the error. If $\varepsilon(x_1)$ is constant on the segment $[v_1, v_2]$, where $v = \frac{x_1}{\mu}$, then any combinations of x_1 and μ which do not lead v away from this segment do not alter the error.

From the analysis presented it follows that an important factor in the calculation of the nonlinearity is the selection of the function $\varepsilon(x_1^*)$ on the segment $[v_1, v_2]$, with which there will be guaranteed the specified relative error with any relationships of x_1 and μ from this segment.

We have considered above the circuit with a single nonlinear block. Now let us consider the circuit with two nonlinear blocks, for example circuit IV with $\mu_1 = \text{const}$, $\mu_2 = \text{var}$.

Let there be given the graph of the absolute errors of approximation (fig. 5) and also the graph of the approximation of the function $f_1(x_1)$ (fig. 2). From the latter graph it is easy to obtain the graph of the relative error of reproduction of the function Φ as the inverse function $f_2(x_2)$ for which it is sufficient to interchange the positions of the coordinate axes of figure 2 and read off conventionally the relative error. The total relative error

formed with the replacement of $x_2 = \mu_2\Phi\left(\frac{f_1(x_1)}{\mu_2}\right)$ by $\tilde{x}_2 = \mu_2\tilde{\Phi}\left(\frac{\tilde{f}_1(x_1)}{\mu_2}\right)$, can be represented as follows

$$\varepsilon(\mu, x_1) = \frac{\Phi\left(\frac{f_1(x_1) + \Delta f(x_1)}{\mu_2}\right) - \Phi\left(\frac{f_1(x_1)}{\mu_2}\right)}{\Phi\left(\frac{f_1(x_1)}{\mu_2}\right)} + \frac{\Phi\left(\frac{f_1(x_1)}{\mu_2}\right) - \tilde{\Phi}\left(\frac{f_1(x_1) + \Delta f_1(x_1)}{\mu_2}\right)}{\Phi\left(\frac{f_1(x_1)}{\mu_2}\right)},$$

where $\Delta f(x_1)$ is the absolute error with the replacement of $f_1(x_1)$.

In the last term we can ignore the error $\Delta f_1(x_1)$; then the final expres- /290
sion for $\varepsilon(\mu, x)$ takes the form

$$\varepsilon(\mu, x_1) = \frac{\Phi\left(\frac{f_1(x_1) + \Delta f_1(x_1)}{\mu_2}\right) - \Phi\left(\frac{f_1(x_1)}{\mu_2}\right)}{\Phi\left(\frac{f_1(x_1)}{\mu_2}\right)} + \frac{\Phi\left(\frac{f_1(x_1)}{\mu_2}\right) - \tilde{\Phi}\left(\frac{f_1(x_1)}{\mu_2}\right)}{\Phi\left(\frac{f_1(x_1)}{\mu_2}\right)} = \varepsilon_1 + \varepsilon_2,$$

where ϵ_1 and ϵ_2 are the errors of reproduction of $f_1(x_1)$ and $\Phi\left(\frac{f_1(x_1)}{\mu_2}\right)$, respectively.

The error ϵ_1 depends on the form of Φ, ϵ_2 varies in the same way as in the first case.

We can obtain the expressions for the errors in the remaining cases similarly. They also consist of two components, which is natural because the approximation is performed twice.

REFERENCES

1. Talantsev, A. D. Avtomat. i telemekh., Vol. 17, No. 2, 1956.

2. Kogan, B. Ya. Avtomat. i telemekh., Vol. 17, No. 12, 1956.

3. Messinger, H. F. Inst. Radio Eng. Convent. Record, Part 4, p. 150, 1955.

4. Shyra-Bura, M. R. Vychislitel'naya matematika (Computational Mathematics), No. 2, 1957.

5. Pike, E. W. and Silverberg, T. R. Designing Mechanical Computers. Machine Design, 24, No. 7, 8, 1952.

N66 34851

SOLUTION OF ONE TYPE OF LINEAR ALGEBRAIC EQUATION USING ELECTRONIC MODELS

M. V. Rybashov

Introduction

Several studies have been devoted to the solution of systems of linear algebraic equations with the use of electronic models (refs. 1-4). /291 The basic idea of these studies amounts to the construction of a dynamic system with an asymptotically stable rest position, having the property that the coordinates of this point satisfy the original system of linear algebraic equations

$$\sum_{k}^{n} a_{ik}x_k + b_i = 0, \ (i = 1, \ldots, n). \tag{1}$$

This dynamic system is assembled on the model, arbitrary initial conditions are selected, and at the end of the transient process, i.e., in the steady-state condition, the response is recorded. The references mentioned present regular methods for the construction of the systems of differential equations with these properties. In this case the systems of differential equations are usually linear with constant coefficients

$$\frac{dx_i}{dt} = \sum_{k}^{n} g_{ik}x_k + c_i, \ (i = 1, \ldots, n). \tag{2}$$

Here, as a rule, the matrix of the coefficients $\|g_{ik}\|$ is not equal to the original matrix $\|a_{ik}\|$. The same can be said of the columns $\|b_i\|$ and $\|c_i\|$. Actually, the basic problem of the cited references can be reduced to how to construct the new matrix of the coefficients with certain prespecified properties.

On the one hand, such a matrix must have roots with negative real parts in order to ensure asymptotic stability of the rest point of the system of equations (2); on the other hand, the transformation of the matrix $\|a_{ik}\|$ must

be such that the coordinates of the rest point satisfy the system of equations (1), for example, such a matrix could be the matrix of the form A'A.

Along with the problem of finding the roots, in practice we encounter the problem of tracking the roots $(x_1(t), \ldots, x_n(t))$ with the time-variable functions $b_1(t), \ldots, b_n(t)$. In essence this is the problem of the formation of the functions $x_1(t), \ldots, x_n(t)$, given implicitly by the system of equations

$$\sum_{k=1}^{n} a_{ik}x_k + b_i(t), \ (i = 1, \ldots, n). \tag{3}$$

The problem of formation of implicit functions in the general case /292 cannot be reduced to the problem of finding the roots. The trajectory $(x_1^*(t) \ldots, x_n^*(t))$, which is the solution of the system (2), in view of the inertial nature of the latter will not identically coincide with the trajectory of system (1). In this case there inevitably arises a dynamic error. However, we can pose the problem of the construction of such a system of differential equations for which this dynamic error will diminish in the course of time or will become zero with suitable initial conditions. The present paper is devoted to the solution of this problem.

1. Formulation and Solution of the Problem

Hereafter we shall consider the system of algebraic equations (3) in which all functions of time $b_i(t)$ are bounded and continuously differentiable. The solution of this system are the n functions $x_i = x_i(t)$, $(i = 1, \ldots, n)$, or, in other words, the vector-function $x(t)$. We shall use this notation everywhere hereafter. Let us pose the problem of constructing such a system of differential equations

$$\frac{dy}{dt} = \Phi_i(y_1, \ldots, y_n, b_1, \ldots, b_n), \ (i = 1, \ldots, n), \tag{4}$$

in which one of its partial solutions with the initial conditions

$$\left.\begin{array}{l} y_1^0 = x_1(0) \\ \cdots\cdots \\ y_n^0 = x_n(0) \end{array}\right\} \tag{5}$$

will be the vector-function x(t). This means that with $t \geq 0$ the following identity will be satisfied

$$y(t) \equiv x(t). \tag{6}$$

In this case the dynamic error stated in the introduction will also be equal identically to zero. Such a system of differential equations is easily constructed. At the same time the existence of the partial solution (6) to this system of equations is not sufficient for the practical use of this system as a tracking system. In practical conditions it is not possible to satisfy conditions (5) exactly. The initial conditions are always established with some error $\delta_i(0)$, $(i = 1, \ldots, n)$. In the general case, the solutions $\overline{y}_i(t)$, differing from (6), correspond to these initial conditions, which constitute the initial conditions

$$\overline{y}_1^0 = x_1(0) + \delta_1(0)$$
$$\cdots\cdots\cdots$$
$$\overline{y}_n^0 = x_n(0) + \delta_n(0).$$

The error $\delta(t) = |y(t) - \overline{y}(t)|$ then arises. System (4) can be considered workable and worthy of attention only in the case when $\max_t \delta(t)$ is sufficiently small, for example, of the same order as $\delta(0)$. It is still more desirable that

$$\lim_{t \to +\infty} \delta(t) = 0 \tag{7}$$

or, in other words, that the solution (5) be asymptotically stable.

The following system of differential equations satisfies both requirements /293

$$\frac{dy}{dt} = -y - A^{-1} \cdot \left(b + \frac{db}{dt}\right). \tag{8}$$

Here $\frac{dy}{dt}, y, b, \frac{db}{dt}$ denote the columnar matrices, respectively, of the derivatives $\frac{dy_i}{dt}$, the coordinates y_i, the functions $b_i(t)$ and their derivatives of the right sides of the system of equations (3). A^{-1} denotes the matrix which is the inverse of the matrix of the numbers $\|a_{ik}\|$.

Let us show that the solution y(t) = x(t), where

$$x(t) = -A^{-1}b \tag{9}$$

satisfies the matrix equation (8). To do this, let us substitute (9) in both sides of this equation. On the one hand, we have

$$\frac{dy}{dt} = \frac{dx}{dt} = -A^{-1}\frac{db}{dt}, \tag{10}$$

on the other hand

$$-y - A^{-1}\left(b + \frac{db}{dt}\right) = -x - A^{-1}\left(b + \frac{db}{dt}\right)$$
$$= A^{-1}b - A^{-1}\left(b + \frac{db}{dt}\right) = -A^{-1}\frac{db}{dt}.$$

Both sides of equation (8) are actually equal to one another. Let us show now that the error $\delta(t)$ decreases monotonically with the course of time. We compose the matrix equation relative to the variable $\bar{y} = x + \delta$

$$\frac{dx}{dt} + \frac{d\delta}{dt} = -(x+\delta) - A^{-1}\left(b + \frac{db}{dt}\right).$$

We substitute the solution (9) into this equation, taking account of (10). As a result we obtain the matrix differential equation for $\delta(t)$

$$\frac{d\delta}{dt} = -\delta.$$

Solving this equation, we obtain

$$\delta(t) = \delta(0)\cdot e^{-t} \to 0,\ t \to +\infty.$$

Thus the asymptotic stability of solution (6) is proved. With any initial conditions the solution of system (6) with the passage of time asymptotically approaches the solution (9). We can understand the essence of the constructed dynamic system using the following simple example. Let us use this method to solve equation

$$ax + b = 0. \tag{11}$$

We form the differential equation. According to (8), this equation is written as

$$\frac{dy}{dt} = -y - \frac{1}{a}\left(b + \frac{db}{dt}\right). \tag{12}$$

We form the transfer function $W(p) = \frac{y(p)}{b(p)}$. From (12) it follows that /294

$$W(p) = -\frac{1}{a} \cdot \frac{p+1}{p+1} = -\frac{1}{a},$$

i.e., if the smooth function b(t) starts from zero, system (12) is equivalent to the kinematic system with the transfer coefficient $-\frac{1}{a}$, which corresponds to original equation (11). The dynamic system (12) is a system with complete compensation, which is clearly seen from the course of the construction of transfer function W(p) (to reduction of the monomials p + 1).

2. Structural Diagram of the Setup of the Problem on the Model

To set up equation (8) on the electronic model requires preliminary computation of the inverse matrix A^{-1} and the multiplication of the matrices. It is evident that there is no sense in setting up the problem using equation (8), because the amount of the preliminary computational work will be commensurate with the direct solution of the problem using the Kramer rules and subsequent representation of the solution in the form

$$x_i(t) = \sum_{k=1}^{n} c_{ik} b_k, \ (i = 1, \ldots, n),$$

where c_{ik} are computed using the known rules. Therefore we reduce equation (8) to a form convenient for the formulation of the problem. By left-multiplying both sides of this equation by matrix A and considering that

$$A\frac{dy}{dt} + \frac{db}{dt} \equiv \frac{d(Ay + b)}{dt},$$

we obtain the transformed equation

$$\frac{d(Ay+b)}{dt}+Ay+b=0. \tag{13}$$

Let us collect equation (13) using the method of implicit functions. We introduce into the right side of this equation the term $\mu\dot{y}$, where μ is a small parameter. Then the equation being modeled is written in the form

$$\mu\frac{dy}{dt}=Ay+b+\frac{d(Ay+b)}{dt}. \tag{14}$$

The structural circuit of the setup for the formation of the single variable $y_i(t)$ with $\mu < 0$ is shown in figure 1. For the formation of the derivative

with respect to t of function Ay + b in this circuit, use is made of a differentiator, which can be quite coarse (fig. 2).

With modeling of differential equations using the method of implicit functions, the solution frequently differs strongly in some sense from the real solution. For example, there may be a loss of stability of the solution, which as a rule leads to increase of the error. Let us clarify in what cases we can make use of equation (13).

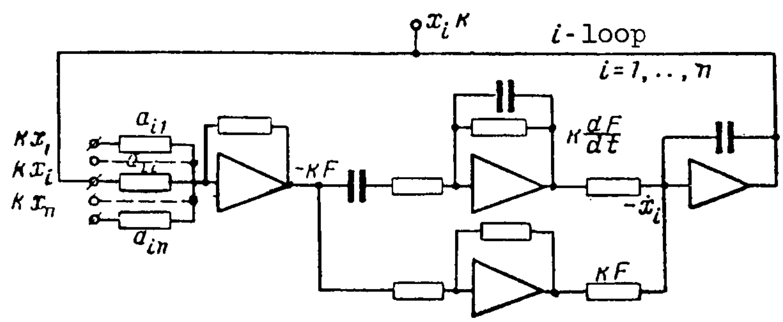

Figure 1

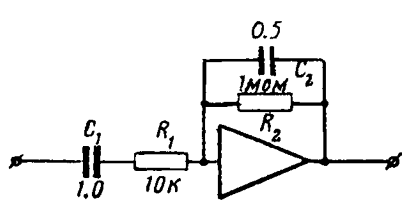

Figure 2

Consider the contracted equation

$$\mu \frac{du}{dt} = Ay + b.$$

Let us set without limiting generality $b \equiv 0$;

$$\mu \frac{dy}{dt} = Ay. \tag{14}$$

Further, let us assume that the coefficients of matrix A are sign-definite, for example positive, and that the system (14) with $\mu < 0$ has the stable rest point $y = 0$. In reference 5 it is shown that there exists a μ for which the system (14) will be stable with any physically existing operator of small parameters $D(p)$. This operator enters into equation (14) as follows /295

$$\mu py = D(p)Ay, \ p \equiv \frac{d}{dt}. \tag{15}$$

If we turn to equation (13), setting $b \equiv 0$, it is easy to see that this equation can be written in the form (15)

$$\mu py = (1 + p)Ay. \tag{16}$$

In the real circuit of the setup the physical operator $\frac{(1+p)}{Q(p)}$ will act, where $Q(p)$ is a fractionally rational operator. Thus, in view of this theorem, system (16) will be stable with suitable μ. If stability is achieved with unacceptable μ (the accuracy of the solution depends on μ), we must change over to equation

$$\alpha \cdot \frac{d(Ay + b)}{dt} + Ay + b = \mu \frac{dy}{dt},$$

where $\alpha < 1$. The derivation was made for $b \equiv 0$. However, for a linear system with constant coefficients, from the asymptotic stability with fixed b there follows stability of the solutions themselves with $b = b(t)$. As shown by experience, stability is observed not only with matrices A with sign-definite coefficients in which the roots have sign-definite real parts (in this case the shortened equation can always be made stable by selection of the sign of μ),

but also with any matrix A, if only by selection of the signs of y $\mu_1, \ldots, \mu_n$ in the contracted system we can achieve stability.

REFERENCES

/296

1. Gutenmakher, L. I., Gradshteyn, I. S. and Taft, V. A. Electrical Modeling of Physical Processes with the Aid of Matrix Circuits with Amplifiers (Elektricheskoye modelirovaniye fizicheskikh protsessov pri pomoshchi matrichnykh skhem s usilitelyami). Elektrichestvo, No. 3, 1946.

2. Gutenmakher, L. I., Korol'kov, N. V., et al. Handbook on the ELI Type Vacuum Tube Integrators (Rukovodstvo po elektronno-lampovym integratoram tipa ELI). Izd-vo AN SSSR, 1952.

3. Bruk, I. S. Electrical Minimizer (Elektricheskiy minimizator). Dokl. AN SSSR, Vol. 12, No. 4, 1948.

4. Korn, G. T. Electronic Analog Computers, I. L., 1955.

5. Rybashov, M. V. Methods of Solution of Linear Algebraic Equations on Models (Nekotoryye metody resheniya lineynykh algebraicheskikh uravneniy na modelyakh). Avtomat. i telemekh., No. 2, 1962.

N66 34852

SYNTHESIS OF CURRENT-SWITCHING CIRCUITS WITH CELL MATCHING USING p-n-p AND n-p-n TRANSISTORS

T. M. Aleksandridi

Introduction

In recent years descriptions of current-switching circuits using semi- /426
conductor triodes have appeared in several works (refs. 1 and 2). These circuits have very high reliability and speed of response and are at the present time among the most promising digital elements. A characteristic of these circuits is the purely potential connection between elements, which leads to the necessity for the introduction of various circuits for the matching of the input and output.

The method of matching circuits by alternation of cells constructed using p-n-p and n-p-n transistors is attractive in its simplicity and economy. However, several authors (ref. 2) indicate the difficulties which arise in the design of the logic circuits in this case.

The present paper suggests a logic apparatus based on the operations of Sheffer's stroke and the duality operation. This apparatus is very convenient for the analysis of circuits using the matching of triodes of the p-n-p and n-p-n types.

1. Switching Elements Which Realize the L_1 and L_7 Logical Operations

Let us consider the functional circuit of the current switch and its operation. Figure 1 shows the basic circuit of the current switch using the p-n-p type transistors. The triodes T_1 and T_2 are connected so that their emitters are joined and connected to the current source (the resistance R_1 is very large). The base of T_2 is connected to a constant potential, while to the base of T_1 a voltage is applied of either $+\Delta U$ or $-\Delta U$ relative to the base potential.

It is evident that if the potential $+\Delta U$ is applied to the base of T_1, the left triode will be off, and the entire current from the current generator will flow through T_2. If, however, $-\Delta U$ is applied to the base of T_1, this triode

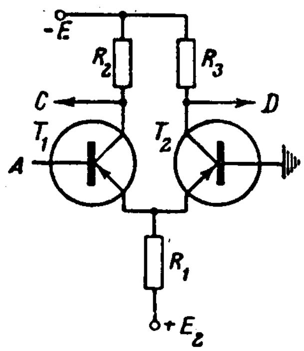

Figure 1

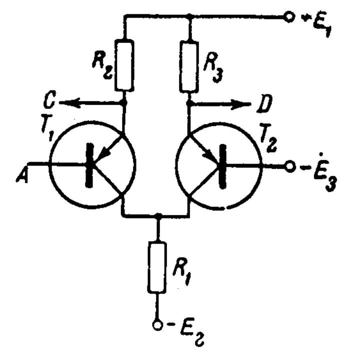

Figure 2

is turned on, while triode T_2 is turned off, in view of the fact that the potential on its emitter will be lower than on the base. In this case the entire current will flow through T_1. The output signal is taken from collector resistors R_2 and R_3. /427

Thus provision is made for the switching of current T_2 supplied by the generator from one triode to the other.

A similar circuit can be constructed using the n-p-n type transistors (fig. 2).

The principle of operation of the two circuits is identical; they differ only in the polarity of the supply sources. Therefore the signs of the voltage drops across the base of T_1, and the collector resistance in the circuit of figure 2 will be opposite to the corresponding differentials in the diagram of figure 1. As a result we can directly combine the inputs and outputs of the circuits of these two types, which is a tremendous technical convenience.

If we apply some function A to the input, it is evident that triode T_1 will perform the operation of inversion, while T_2 will perform the operation of repetition. Consequently, at the output C we have $\bar{A}$, and on D we have A.

The operation of these circuits will not be altered if the right triode, whose output repeats the input function, is replaced by a diode. This replacement is meaningful if in the future we are to use only one output of the current switching circuit. These circuits are shown in figures 3 and 4.

This version of the circuit has the advantage that it considerably reduces the power required by the circuit resulting from the current previously consumed by triode T_2 from source E_1. In addition there is a reduction of the number of triodes in the circuit.

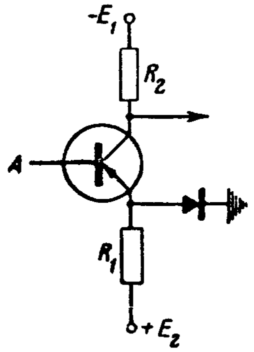

Figure 3

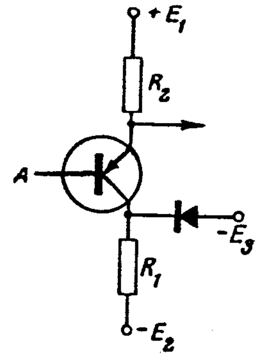

Figure 4

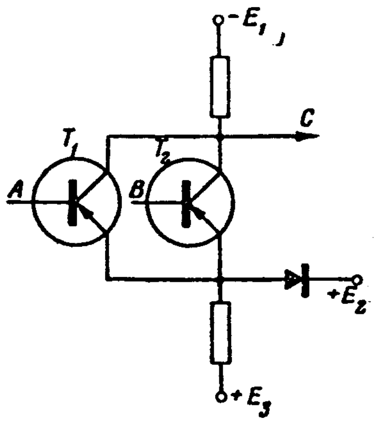

Figure 5

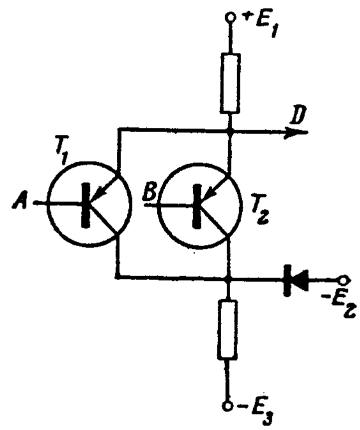

Figure 6

Figures 5 and 6 show the current switching circuits with two input triodes T_1 and T_2. The circuit of figure 5 uses triodes of the p-n-p type, while that of figure 6 uses triodes of the n-p-n type.

Let us consider the logical operations performed by these circuits.

We must keep in mind that at any point of the circuit, both at the input and the output, the more positive potential corresponds to 1 and the less positive potential corresponds to 0.

Thus, we have

$$+ \rightarrow 1,$$
$$- \rightarrow 0.$$

In figure 5 for the input

$$A,\ B = E_1 \rightarrow 1;$$
$$A,\ B = E_1 - 2\Delta U \rightarrow 0;$$

for the output

$$C = -E_1 \rightarrow 0;$$
$$C = -E_1 + 2\Delta U \rightarrow 1.$$

In figure 6 we have the analogous relations /428

$$A,\ B = -E_1 \rightarrow 0;\quad D = +E_1 \rightarrow 1;$$
$$A,\ B = -E_1 + 2\Delta U \rightarrow 1;\quad D = +E_1 - 2\Delta U \rightarrow 0.$$

We compile the tables of the dependence of the output function on the input variables for these two circuits. (Table 1 corresponds to the circuit of figure 5, table 2 is for the circuit of figure 6).

Table 3 presents all two-valued switching functions of two variables.

TABLE 1

A	B	C
0	0	1
0	1	1
1	0	1
1	1	0

TABLE 2

A	B	D
0	0	1
0	1	0
1	0	0
1	1	0

TABLE 3

A	B	L_0	L_1	L_2	L_3	L_4	L_5	L_6	L_7	L_8	L_9	L_{10}	L_{11}	L_{12}	L_{13}	L_{14}	L_{15}
0	0	0	1	0	1	0	1	0	1	0	1	0	1	0	1	0	1
0	1	0	0	1	1	0	0	1	1	0	0	1	1	0	0	1	1
1	0	0	0	0	0	1	1	1	1	0	0	0	0	1	1	1	1
1	1	0	0	0	0	0	0	0	0	1	1	1	1	1	1	1	1

From table 3 we see that the output function of the cell using the p-n-p triodes (table 1) is the $L_7(A, B)$ logical operation, while the output function of the cell using the n-p-n triodes (table 2) is the $L_1(A, B)$ logical operation. We note that we can connect several additional triodes in parallel with the input triode. In this case the cells using the p-n-p triodes will realize the same logical operation, but now as a function of several variables /429

$$L_7(A, B, \ldots, N).$$

The cells using the n-p-n triodes with several input triodes realizes the same logical operation $L_1(A, B, \ldots, N)$ of several input variables.

Since we are interested in the questions of the design of circuits using matching of the p-n-p and n-p-n triodes, it would be convenient in the logical studies to make use of the system of functions based on the L_1 and L_7 operations.

First of all it is necessary to establish whether or not the system of functions L_1, L_7 is "functionally complete" and to establish its primary properties. (As is known, the system of functions $L_1, L_2, \ldots, L_s$ is termed "functionally complete" if any function of the algebra of logic can be written in the form of an equation in terms of the functions $L_1, L_2, \ldots L_s$.)

2. The Logic Functions L_1 and L_7

The logic operation L_7 is termed the Sheffer stroke. Sheffer first showed in 1913 that the system of one of these functions is functionally complete (ref. 3). The logic operation L_1 is dual with relation to the L_7 operation.

As is known, the function $L^*(x_1, x_2, \ldots, x_n)$ is dual with respect to the function $L(x_1, x_2, \ldots, x_n)$, if there holds the equality

$$L^*(x_1, x_2, \ldots, x_n) = \overline{L}(\overline{x}_1, \overline{x}_2, \ldots, \overline{x}_n).$$

As examples of dual functions we can consider

(1) $L_{14} = L^*_8$ (conjunction is dual with respect to disjunction and vice versa);

(2) $L_6 = L_9^*$, etc.

The basic property of the dual functions is formulated in the "duality principle." If we have the logical function L, which is expressed in terms of function $f_1, f_2, \ldots, f_n$, to obtain the expressions for the dual function we must everywhere replace f_1 by the dual function f_1^*, f_2 by f_2^* etc., i.e.,

if

$$L(x_1, x_2, \ldots, x_n) = f[f_1(x_1, \ldots, x_n),\ f_2(x_2, \ldots, x_n) \ldots],$$

then

$$L^*(x_1, x_2, \ldots, x_n) = f^*[f_1^*,\ f_2^*, \ldots,\ f_n^*).$$

As a result of the duality principle the system of the single function L_1 is also functionally complete. /430

It is shown in reference 4 that the Sheffer function and its dual are unique binary operations, such that each of them forms all logical functions of two variables and, consequently, of any number of variables.

We emphasize that it is precisely in view of this fact that we can with the aid of a single standard current switching cell construct any logic circuits.

In his work Sheffer formulated the following axioms for the algebra of logic based on the L_7 (stroke) operation.

It is assumed that there is some class P_2 of binary functions and in it there is defined the operation $L_7(a, b) = a/b$.

To the class P_2 there belong at least two different elements a and b; then: $\frac{a}{b} \in P_2$.

The following axioms hold

1) $\overline{a} = a/a$;

2) $\overline{(\overline{a})} = a$;

3) $a/(b/\overline{b}) = \overline{a}$;

4) $a/(b/c) = (\overline{b}/a)/(\overline{c}/a)$.

From these axioms a series of corollaries is derived, i.e., equivalences, which we shall not present here. With the aid of these equivalences we can perform all conversions of the various logic equations in this calculus.

Exactly the same axioms can be written in terms of the duality function L_1, so that we obtain a calculus based on this logical operation.

3. Properties of the Calculus Based on L_1 and L_7 Operations

If we have available two elementary logic elements which realize functions L_1 and L_7, the circuits constructed on the basis of these two elements may have definite advantages compared with circuits using some single element.

In this connection it is necessary to study the properties of the complete system of functions L_1 and L_7. For simplicity all relations are given for functions of two variables.

In the system of functions L_1 and L_7 the following basic equivalences obtain, based on the Sheffer axioms and the duality principle (for the designation of logic operation L_1 we use the symbol $\mathbin{\text{ϟ}}$)

For L_7		For L_1	
$a/a = \bar{a};$	(1)	$a \mathbin{\text{ϟ}} a = \bar{a};$	(1')
$a/b = b/a;$	(2)	$a \mathbin{\text{ϟ}} b = b \mathbin{\text{ϟ}} a;$	(2')
$a/b/c = (\overline{a/b})/c;$	(3)	$a \mathbin{\text{ϟ}} b \mathbin{\text{ϟ}} c = (\overline{a \mathbin{\text{ϟ}} b}) \mathbin{\text{ϟ}} c;$	(3')
$a/(b/c) = (a/\bar{b})/(b/\bar{c});$	(4)	$a \mathbin{\text{ϟ}} (b \mathbin{\text{ϟ}} c) = (a \mathbin{\text{ϟ}} \bar{b}) \mathbin{\text{ϟ}} (a \mathbin{\text{ϟ}} \bar{c});$	(4')

The condition for replacement of operation L_7 by L_1 and vice versa is /431

$$\overline{a/b} = \bar{a} \mathbin{\text{ϟ}} \bar{b}. \tag{5}$$

The commutative property is

$$(a/b) \mathbin{\text{ϟ}} (\bar{c}/d) = (a/\bar{c}) \mathbin{\text{ϟ}} (b/d). \tag{6}$$

With the aid of these basic equivalences we can derive still other useful relations which facilitate the transformations of the equations.

Rules for the expansion of brackets

$$(a/b) \text{ϟ} (c/d) = (\overline{\bar{a} \text{ϟ} \bar{b}}) \text{ϟ} (\overline{\bar{c} \text{ϟ} \bar{d}}) = \bar{a} \text{ϟ} \bar{b} \text{ϟ} \bar{c} \text{ϟ} \bar{d}; \tag{7}$$

similarly

$$(a \text{ϟ} b)/(c \text{ϟ} d) = (\overline{\bar{a}/\bar{b}})/(\overline{\bar{c}/\bar{d}}) = \bar{a}/\bar{b}/\bar{c}/\bar{d}). \tag{7'}$$

Rules for removal from brackets

$$(\bar{a}/c) \text{ϟ} (\bar{a}/b) = (\bar{a}/\bar{a}) \text{ϟ} (b/c) = a \text{ϟ} (b/c); \tag{8a}$$

similarly

$$\left.\begin{aligned} &(\bar{a} \text{ϟ} \bar{c})/(\bar{a} \text{ϟ} b) = a/(b \text{ϟ} \bar{c}); \\ &(\bar{a} \text{ϟ} b) \text{ϟ} (\bar{a} \text{ϟ} \bar{c}) = a/(b/\bar{c}). \end{aligned}\right\} \tag{8b}$$

The derivation of this equality is based on the (5) axiom of Sheffer

$$\overline{a/(b/c)} = (\bar{b}/a)/(\bar{c}/a);$$

$$a/(b/c) = \overline{(\bar{b}/a)/(\bar{c}/a)} = (\overline{\bar{b}/a}) \text{ϟ} (\overline{\bar{c}/a}) = (b \text{ϟ} \bar{a}) \text{ϟ} (c/\bar{a}).$$

The same rule for the duality function

$$(\bar{a}/b)/(\bar{a}/c) = a \text{ϟ} (b \text{ϟ} c).$$

In addition, for the transformations it is useful to have in mind the following

$$a \text{ϟ} 0 = \bar{a}; \quad (9) \qquad a/0 = 1; \tag{9'}$$

$$a \text{ϟ} 1 = 0; \quad (10) \qquad a/1 = \bar{a}; \tag{10'}$$

$$a \text{ϟ} \bar{a} = 0; \quad (11) \qquad a/\bar{a} = 1. \tag{11'}$$

The validity of all statements presented above is easily verified with the aid of truth tables.

4. Canonical Expansion for Switching Functions in Terms of Operations L_1, L_7 (Normal L-Form)

It is known that every function of the algebra of logic can be written in the form of the conjunctive or disjunctive normal form.

Similarly, for any function of the algebra of logic we can construct the canonical expansion in terms of logic operations L_1 and L_7. We term this the canonical expansion of the normal L-form.

Let us assume that we have the function of the algebra of logic given in the form of table 4. /432

The construction of the canonical expansion can be performed by two methods.

1. Let us select all sets of input variables where function f is equal to 1; then for each set such that

$$f_i(x_1, x_2, \ldots, x_j, x_n) = 1, \text{ where } i = 1, 2, \ldots, k;\ j = 1, 2, \ldots, n,$$

we compose the expression of the form $(x_{i1} \lightning \bar{x}_{i2} \ldots \lightning x_{in})$, where for $x_{ij} = 0$

in the expression we take x_{ij}, and for $x_{ij} = 1$ in the expression we write $\bar{x}_{ij}$.

Then all such groups are combined with the same sign and the inversion is taken of the entire expression.

Finally the canonical expansion takes the form

$$f = \overline{(x_{11} \lightning \bar{x}_{12}, \ldots, \lightning x_{1n}) \lightning (\bar{x}_{21} \lightning x_{22}, \ldots, \lightning x_{2j} \lightning \bar{x}_{2n}) \lightning \lightning (x_{k1} \lightning \bar{x}_{k2}, \ldots, \lightning x_{kn})}. \tag{12}$$

TABLE 4

x_1	x_2	x_3	...	x_n	f
0	0	0	0	0	1
1	0	0	0	1	0
—	—	—	—	—	—
0	1	0	0	1	1

This algebraic equation is the form of the arbitrary function in terms of operation L_1.

2. Let us select in the tabular representation of the function all sets in which it takes the value "0". The meaning of the contents of operation L_7 amounts to the fact that at the output "zero" is obtained every time that the input variables take the value "1". Therefore, for each set such that

$f_i(\overline{x_{i1}}, \overline{x_{i2}}, \ldots, x_{in}) = 0$, we compose the expression $(\overline{x_{i1}}/\overline{x_{i2}}, \ldots, /x_{ij} - /x_{in})$, where

for $x_{ij} = 1$ we write the variable itself and for $x_{ij} = 0$ we take its inversion $\overline{x}_{ij}$.

Then all such groups are combined by the sign of the same operation, and the inversion is taken of the entire expression. Finally, the canonical expansion in terms of function L_7 takes the form

$$f = \overline{(x_{11}/x_{12}, \ldots, \overline{x}_{ij}/x_{1n})/(\overline{x}_{21}/x_{22}/, \ldots, \overline{x}_{2j})} \ldots . \tag{13}$$

In accordance with the equations presented above for the replacement of operations L_1 by L_7, we can obtain two more basic forms of the canonical expansion, where now the arbitrary logic function will be expressed in the form of an equation in terms of L_1 and L_7.

Thus, from (12) we obtain the following expression

$$f = \overline{(x_{11} \not\downarrow \overline{x}_{12} \not\downarrow, \ldots, x_{in})} / \overline{(x_{21} \not\downarrow x_{22}, \ldots, \not\downarrow x_{2j}, \ldots, x_{2n})} /; \tag{14}$$

similarly, from (13) we obtain the following

$$f = \overline{(x_{11}/\overline{x}_{12}, \ldots, x_{ij}/x_{in})} \not\downarrow \overline{(\overline{x}_{21}/x_{22}/, \ldots, \overline{x}_{2j})} \not\downarrow . \tag{15}$$

The normal L-forms (14) and (15) are convenient in the case when we have available elements which realize both the L_1 operation and the L_7 operation. /433

5. Examples of the Synthesis of Certain Logic Circuits

In the preceding sections we presented the technique for the construction of the algebraic expressions for arbitrary logic functions by means of the normal L-form. Now let us transform the normal L-form into a form which will

be convenient for the construction of a circuit from those elements which we have available. In the transformations of the algebraic expressions it is necessary to make use of the rules presented in section 3.

If as the standard elements we take those elements constructed of the triodes of the p-n-p and n-p-n types and using the circuits of figures 5 and 6, the rule for the transformation of the algebraic expression amounts to the necessity for reduction of the expression to such a form that the operations L_1 and L_7 alternate in the expression.

For example, expression (15) is written in this form. In order to construct a logic circuit with this expression, it is necessary mechanically to replace operation L_7 by a cell using triodes of the p-n-p type, and to /434 replace the operation L_1 by a cell using triodes of the n-p-n type. In this case there is automatic matching of the levels at the inputs and outputs of the cells.

Before turning to the consideration of the examples, for convenience let us introduce the schematic representation of the standard cells. Here we must limit the number of inputs of the standard cell. In actuality the question of the number of cell inputs is resolved by a whole series of technical considerations.

For simplicity of consideration, let us take a standard cell with two inputs. Figures 7 and 8 present functional circuits and the schematic representation of current switching cells with two inputs and with two outputs. Figure 8 corresponds to the cell using triodes of the p-n-p type, while figure 7 corresponds to the cell using triodes of the n-p-n type.

As the first example let us consider the construction of the circuit for a single-place summator with three inputs. The logic of its operation is given in table 5, where A, B are the terms; P is the carry from the preceding place; S is the sum; E is the carry into the following place.

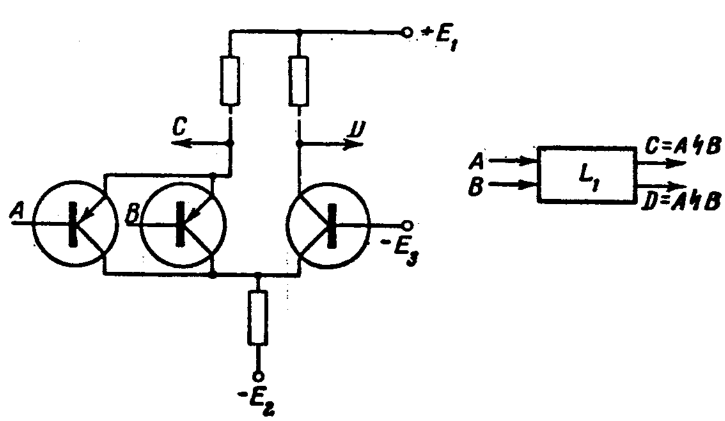

Figure 7

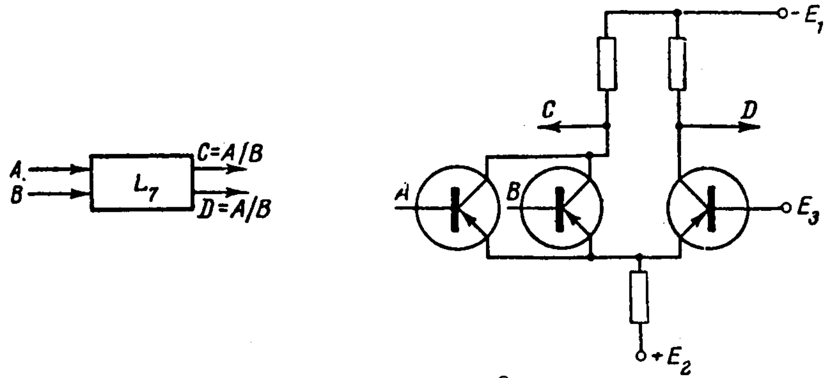

Figure 8

TABLE 5

A	B	P	S	E
0	0	0	0	0
1	0	0	1	0
0	1	0	1	0
0	0	1	1	0
0	1	1	0	1
1	0	1	0	1
1	1	0	0	1
1	1	1	1	1

Let us write on the basis of this table the normal form for the sum S

$$S = [(\bar{A} \text{ ϟ } \bar{B} \text{ ϟ } \bar{P}) \text{ ϟ } (\bar{A} \text{ ϟ } B \text{ ϟ } P)]/[(A \text{ ϟ } B \text{ ϟ } \bar{P})(A \text{ ϟ } B \text{ ϟ } P)].$$

In order to construct the circuit from the standard elements which we have selected, it is necessary to reduce this algebraic expression to the form such that operations L_1 and L_7 alternate. In addition, only functions of two input variables must appear in the expression.

Let us carry out this construction as an example. We transform each square bracket separately, using equalities (8b), (5), (3)

$$\left.\begin{aligned}
&[(\bar{A} \text{ ϟ } \bar{B} \text{ ϟ } \bar{P}) \text{ ϟ } (\bar{A} \text{ ϟ } B \text{ ϟ } P) = [\bar{A} \text{ ϟ } \overline{(\bar{B} \text{ ϟ } \bar{P})}] \text{ ϟ } [\bar{A} \text{ ϟ } \overline{(B \text{ ϟ } P)}] = \\
&\qquad = A/[\overline{(\bar{B} \text{ ϟ } \bar{P})} / \overline{(B \text{ ϟ } P)}] = A/\overline{[(\bar{P} \text{ ϟ } \bar{B}) \text{ ϟ } (P \text{ ϟ } B)]}; \\
&[(A \text{ ϟ } B \text{ ϟ } \bar{P}) \text{ ϟ } (A \text{ ϟ } \bar{B} \text{ ϟ } P)] = [A \text{ ϟ } \overline{(\bar{B} \text{ ϟ } \bar{P})}] \text{ ϟ } [A \text{ ϟ } \overline{(\bar{B} \text{ ϟ } P)}] = \\
&\qquad = \bar{A}/[\overline{(\bar{B} \text{ ϟ } \bar{P})}/\overline{(\bar{B} \text{ ϟ } P)}]; \\
&S = \overline{\{\bar{A} \text{ ϟ } [\overline{\overline{(\bar{P} \text{ ϟ } \bar{B})}/\overline{(\bar{P} \text{ ϟ } B)}}]\}}/\overline{\{A \mid [\overline{\overline{(P \text{ ϟ } \bar{B})}/\overline{(\bar{P} \text{ ϟ } B)}}]\}}.
\end{aligned}\right\} \quad (16)$$

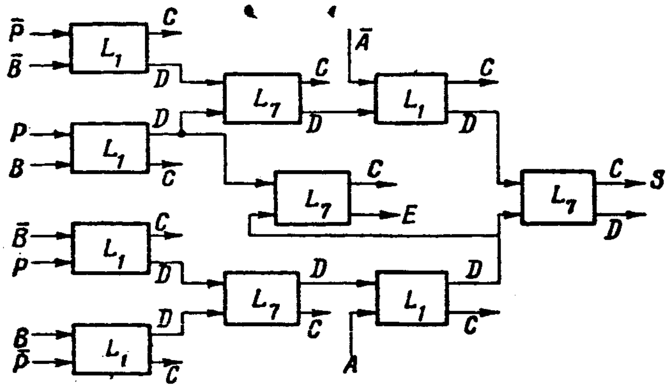

Figure 9

We write out and transform the normal L-form for E

$$
\left.
\begin{aligned}
&E = \overline{[(\bar{A}/\bar{B}/\bar{P})/(A/\bar{B}/\bar{P})/(\bar{A}/B/\bar{P})/(\bar{A}/\bar{B}/P)]} = \\
&= [(\bar{A}/\bar{B}/\bar{P})/(A/\overline{B}/\bar{P})] \lightning [(\bar{A}/B/\bar{P})/(\bar{A}/\bar{B}/P)]; \\
&[(\bar{A}/\bar{B}/\bar{P})/(A/\bar{B}/\bar{P})] = [\bar{P}/(A \lightning B)]/[\bar{P}/(\bar{A} \lightning B)] = \\
&\qquad = P \lightning [\bar{B}/(A/\bar{A})] = P \lightning B; \\
&[\bar{A}/B/\bar{P})/(\bar{A}/\bar{B}/P) = [\bar{A}/(\bar{B} \lightning P)]/[\bar{A}/(B \lightning \bar{P})] = \\
&\quad = A \lightning [(\bar{B} \lightning P) \lightning (B \lightning \bar{P})] = A \lightning \overline{[(\overline{\bar{B} \lightning P})/(\overline{B \lightning \bar{P}})]}; \\
&\quad E = \overline{(\overline{P \lightning B})/\overline{\{A \lightning \overline{[(\overline{\bar{B} \lightning P})/(\overline{B \lightning \bar{P}})]}\}}}.
\end{aligned}
\right\} \qquad (17)
$$

We have thus reduced the final expression for the sum and carry functions to a form where L_1 and L_7 operations alternate (certain operations with inversion). The corresponding logic diagram is shown in figure 9.

As the second example let us consider the construction of a decoder circuit using four input variables. The decoder will have 16 outputs, where the logic expressions for the output functions in terms of L_1 and L_7 will have the following form

$$
\begin{aligned}
&D_0 = A \lightning B \lightning C \lightning Q = (\overline{A/B}) \lightning (\overline{C_1 Q}); \\
&D_1 = \bar{A} \lightning \lightning B \lightning C \lightning Q = (A/\overline{B}) \lightning (\overline{C/Q}).
\end{aligned} \qquad (18)
$$

The equations for the remaining outputs of the decoder will obviously be obtained as further combinations from the input variables and their inversions.

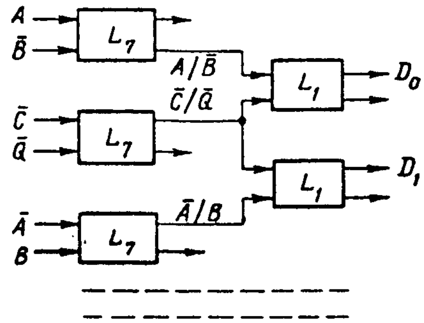

Figure 10

If we consider these equations in detail we see that each round bracket will be repeated in the logic equations for two outputs, i.e., in the construction of the circuit each such cell can be used twice.

As we see, the structure of the logic equations of the decoder is such that we can obtain an expression in which operations alternate in the pure form, without inversion. It is therefore convenient to construct these circuits from elements using triodes of the p-n-p and n-p-n types, where we can use cells with single output, replacing one triode by a diode. /436

Figure 10 shows the logic circuit of the decoder, constructed in accordance with expression (18) from the types of elements we selected.

REFERENCES

1. Harris, I. R. Direct-coupled Transistor Logic Circuitry. Trans. IRE on EC-7, Vol. 3, No. 1, 2, 1958.

2. Zalkind, A. B. and Pelenovich, I. I. Current Switching Devices Using Alloy Semiconductor Triodes (Pereklyuchateli toka na splavnykh poluprovodnikovykh triodakh). Voprosy radioelektroniki, No. 12, 1959.

3. Sheffer, H. M. A Set of Five Independent Postulates for Boolean Algebra With Application to Logical Constants. Trans. Amer. Math. Soc., Vol. 14, p. 481, 1913.

4. Zylinski, E. Tund. Math., Vol. 7, 203-209, 1925.

5. Lyubovich, L. A. and Ryabtsev, Yu. S. High-Speed Switching Circuits Using Transistor Current Switches (Bystrodeystvuyushchiye pereklyuchayushchiye skhemy na tranzistornykh pereklyuchatelyakh toka). Voprosy radioelektroniki, No. 12, 1959.

N66 34853

OBTAINING PARTICULAR NORMAL FORMS OF BOOLEAN FUNCTIONS WHICH DO NOT GIVE CONFLICTS IN CIRCUIT REALIZATIONS[1]

V. V. Vorzheva

Relay devices consist of relay elements which are functionally connected and which form a definite structure. The relay elements may be elements of the most varied physical nature, beginning with the electromechanical relays and terminating with the transistors and cryotrons. The problems of analysis and synthesis arise in the study of the structure of the relay devices. /437

Among the many problems of analysis and synthesis we frequently encounter the question of conflicts with the transition from one combination of states of the relay elements to another combination. With this transition there may occur at the output of the relay device either the momentary disappearance of a signal or the appearance of a false signal. In the device constructed using electromagnetic relays this form of conflict reduces to the conflict of the unlike contacts of the same relay.[2]

In the study of the relay devices we usually do not take into account the possible variations of the sequences of the interaction of the different contacts of the same relay, i.e., we start from the concept of ideal contacts, assuming that with actuation of the relay the closed contact opens simultaneously with the closure of the open contact. In this case a theoretically properly designed and analyzed circuit can make errors in practice.

This question has been considered by several authors in various articles. In particular these questions have been studied by Ioanin (ref. 1) and Huffman (ref. 2). In the works of these authors the basis taken is the method of constructing the circuits with ideal contacts, with subsequent study of the necessary and sufficient conditions which guarantee proper operation of the circuits with real contacts.

In the present article a new approach is taken to the question of obtaining structures which are free of conflicts. The problem is posed of

[1] This paper considers the problems of the analysis and synthesis of circuits operating with real contacts.

[2] It is assumed that there is no conflict between the relay elements themselves, i.e., in each cycle of operation one or several elements alter their state, if the sequence of their operation is not of importance.

excluding conflicts in the process of circuit synthesis rather than the exclusion of conflicts from circuits already designed.

The conditions of operation of the output of a relay device can be described by a Boolean function represented in conjunctive or disjunctive normal form. With the circuit realization of a Boolean function using electro- /438 mechanical relays, each variable corresponds to a normally open contact and its negation corresponds to a normally closed contact. The variables can take two values (0 and 1) to which two states of the contacts (open and closed) correspond. Hereafter we shall designate the value of the variable by its state.

Let us consider the principal normal disjunctive form of the Boolean function. It is the Boolean sum of the constituents of unity. Each constituent is the product of all variables or their negations, therefore it characterizes that state of the variables for which the Boolean function is equal to unity. This state is termed the operating state and corresponds to a closed circuit in the contact circuit. All possible combinations of states of the variables for which the conductance of the circuit must be equal to zero are termed forbidden states. The combinations of the states of the variables for which the conductance of the circuit is not defined in the statement of the problem are termed indifferent. Indifferent states can be used by the designer as additional operating states, if this simplifies the circuit.

Constituents which differ by the state of one variable are termed affines. Hereafter we shall say that there is affinity between two neighboring constituents.

In the synthesis of circuits we usually attempt to obtain that form of the Boolean function which contains the minimal number of occurrences of the variables (letters). In the contact circuit of the class Π this will correspond to the minimal number of contacts.

Let us consider the minimization of the normal forms of the Boolean functions (without the use of brackets). We shall make use of the minimization technique developed by Quine (ref. 3) and McCluskey (ref. 4).

	0	1	2	5	6	7
A	×	×				
B	×		×			
C		×		×		
D			×		×	
E				×		×
F					×	×

Figure 1

With minimization according to Quine we obtain the complete set of prime implicants. The number of letters in an implicant is termed its length. A prime implicant has minimal length. This means that with reduction of its length by even a single letter it begins to implicate forbidden states. The sum of all prime implicants is termed the general minimal form of the Boolean function F_{gm}. Each prime implicant is functionally equivalent to the Boolean sum of several constituents. We usually say that the prime implicant covers these constituents. If an implicant covers two neighboring constituents, we say that the implicant covers the corresponding neighborhood. By means /439
of the exclusion of a portion of the prime implicants from the general minimal form F_{gm}, we can obtain the particular minimal form F_{pm}, which also implicates the original Boolean function. To obtain F_{pm} it is convenient to make use of McCluskey's tables of coverings.

In the synthesis of the circuits we can obtain better results if we make use of the indifferent states. In this case, for obtaining F_{gm} we take all constituents corresponding to the operating and indifferent states.

Assume that in the synthesis of the circuits the operating conditions are described by the Boolean function

$$F = xyz + xy\bar{z} + \bar{x}\bar{y}\bar{z} + x\bar{y}z + \bar{x}\bar{y}z + \bar{x}y\bar{z}.$$

Let us find the general minimal form using Quine's method

$$F_{gm} = \bar{x}\bar{y} + \bar{x}\bar{z} + \bar{y}z + y\bar{z} + xz + xy$$

and let us compose the McCluskey table (fig. 1).

From the table we obtain the equation

$$\begin{aligned} F = {} & (A \vee B)(A \vee C)(B \vee D)(C \vee E)(D \vee F)(E \vee F) = \\ & = (A \vee BC)(D \vee BF)(E \vee CF) = ADE \vee BCDE \vee ABFE \vee \\ & \vee BCFE \vee ADCF \vee BCDF \vee ABCF \vee BCF = \\ & = ADE \vee BCF \vee BCDE \vee ABFE, \end{aligned}$$

which gives one of the possible particular minimal forms

$$F_{pm} = BCF = \bar{x}\bar{z} + xy + \bar{y}z.$$

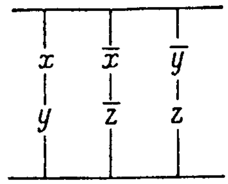

Figure 2

The circuit realization of this function is given in figure 2. In this circuit there is conflict for all three variables x, y and z.

Thus, with transition from the operating state $\bar{x}\ \bar{y}\ \bar{z}$ to the neighboring operating state $\bar{x}\ \bar{y}$ z, the real contacts $\bar{z}$ and z give brief interruptions of the circuit. Conflicts of this nature in multicyclic circuits can lead to disruption of the correct sequence of operation.

Consequently, in the relay devices it is not always possible to make use of the circuits which realize the particular minimal forms of the Boolean function. Hereafter, the forms of the Boolean function which give hardware circuits which are free of conflicts will be termed conflict-free Boolean functions.

Let us consider which forms of the Boolean function are free of conflict.

THEOREM. The general minimal form of the Boolean function is always free of conflict.

Conflict arises only when with the transition from one operating state to another neighboring operating state the variable and its negation do not change their state simultaneously. In the principal normal disjunctive form the /440
change of state of one variable corresponds to the fact that one operating constituent becomes equal to zero and the other becomes equal to one, but in this case there is an instant when both constituents are equal to zero. Combining of these two operating constituents leads to exclusion of the variable which is altering its state, i.e., to elimination of the conflict.

The general minimal form of the Boolean function is a complete listing of the prime implicants. The prime implicants are obtained as a result of combining neighboring constituents and the exclusion of one or several variables.

In the general minimal form, for each pair of neighboring operating constituents there is of necessity found a general prime implicant which covers them. This implies that the general minimal form of the Boolean function is free of conflicts.

There is the possibility of finding the particular minimal form F'_{pm}, which is conflict-free, from the general minimal form which is always free of conflicts, but is redundant in number of letters.

In some cases F'_{pm} coincides with F_{gm}, i.e., it is not always possible to exclude implicants from F_{gm} and thus avoid conflicts.

We shall make use of McCluskey's tables for obtaining F'_{pm}. Along the horizontals of McCluskey's table the operating constituents are located in strictly defined order with respect to affinity groups with retention of increasing order of the n-place binary numbers in each affine group, just as they are arranged in the process of obtaining the complete listing of implicants according to Quine. All prime implicants are arranged along the verticals, and crosses designate the intersections (coverings) of the implicants with the constituents. The form of McCluskey's table is given in the example presented above.

Let the length of the implicant L_i be the number of letters in the implicant and let the length of the constituent L_k be the number of letters in the constituent. Depending on the length, the implicant gives a different number of intersections (crosses) in McCluskey's table. This number is always equal to the power of two, since the intersections of the implicants with the constituents correspond to all possible combinations of the letters which are excluded in the formation of the implicant. Thus, for

$L_\kappa - L_i = 1$ the number of intersections $p = 2^1$;
$L_\kappa - L_i = 2$ the number of intersections $p = 2^2$;

$L_\kappa - L_i = n$ the number of intersections $p = 2^n$.

McCluskey's table has one important property: all 2^n intersections of any implicant are always arranged in increasing order of the n-place binary numbers. In order to obtain F'_{pm} from the general minimal form, any implicant can be excluded only in the case when each of all neighboring constituents, which are covered by this implicant, is covered by at least one other implicant.

The fact that in McCluskey's table the intersections of the implicant with the constituents are arranged in a strictly defined order facilitates the determination and verification of the coverings of the neighborhoods. Here we must take into account that if in the synthesis process use was made of differing states, the affinity between the indifferent constituents or the affinity between an operating and indifferent constituent are inessential, and in obtaining F'_{pm} they may not be covered by common implicants. In the synthesis of multicyclic circuits we can also consider as inessential those affinities which correspond to indifferent transitions from one state to another. /441

Let us consider which implicants or rows can be removed from the McCluskey table in the case when all the affinities are essential, and in what order it is most convenient to accomplish this process.

1. All the implicants of length $L_i = L_k$ must occur in F'_{pm} since each such implicant has the number of coverings $p = 1$ and consequently there do not exist any other implicants which cover the corresponding constituents.

2. All the implicants of length $L_i = L_k-1$ for which $p = 2$ also must occur in F'_{pm}. The implicant with $p = 2$ has a single affinity which can be covered only with a single shorter implicant, but in that case the implicant with $p = 2$ will be absent in the table, because it is a longer implicant having coverings which coincide with those of the shorter implicant.

3. From F_{gm} we can begin to exclude only the implicants of length $L_i = L_k-2$.

The implicant of any length $L_i < L_k-1$ can be excluded from F_{gm} only in the case when in each of the columns corresponding to its intersections the total number of intersections is not less than m, where $m = L_k-L_{in}$. In essence, m is the number of letters excluded during formation of the implicant, also equal to the number of neighborhoods which can be covered by the implicant being excluded.

Neighborhoods which can be covered by the implicant being excluded can be covered only by other implicants of the same length, because:

(1) no neighborhoods can be covered by an implicant of greater length, since both implicant of greater length and implicant of identical coverings with implicant of shorter length do not occur in the general minimal form;

(2) no neighborhoods can be covered by an implicant of shorter length, since in this case the excluded implicant would not occur in the general minimal form, because it is longer, having identical coverings with the shorter. In each column of the table, in addition to the intersection of the implicant being excluded, there must also be enough intersections of other implicants of the same length, so that with their aid it would be possible to cover all neighborhoods which are covered by the implicant being excluded, i.e., no less than m.

Thus, to obtain F_{pm} starting from McCluskey's table, it is necessary to label the rows which cannot be excluded according to the three rules formulated above. First we label the rows which have one or two intersections, then we look through the columns and label those rows which have one or two intersections with the columns being considered. Then we look for the columns

having three intersections, and if they all belong to the implicants with length $L_i = L_k-2$, one row can then be excluded, leaving of necessity two other rows. In this case we verify that all neighborhoods covered by the excluded implicant were covered by at least some one other implicant.

Finally, we verify the possibility of exclusion of the remaining unlabeled rows.

Let us consider an example of obtaining the particular minimal form of a Boolean function free from conflict.

Figure 3 presents McCluskey's table, where the prime implicants are denoted by the letters along the verticals. There are 26 in all. The operating constituents are arranged along the horizontals. Using the three rules presented above, we label with asterisks the implicants which cannot be removed from F'_{pm}. We look through the columns and find those in which there are one or two intersections. Such columns will be 2, 11, 19, 23 and 30. Let us label with asterisks all implicants which give intersections with these columns, i.e., implicants A, B, E, F, Q, S, T, U, W and Z. These implicants cannot be eliminated from F'_{pm}, because conflicts arise with their removal. /442

Then we look for the first column having three intersections. This is column 1, having intersections with implicants C, D and I. Implicant C can be removed from F'_{pm}, because all its neighbors are covered by other implicants, namely: the neighborhood 00 and 01 is covered by implicant D, the neighborhood 00 and 10 is covered by implicant E, neighborhood 01 and 11 is covered by implicant I, neighborhood 11 and 10 is covered by the two implicants J and K.

	0	1	2	4	8	16	5	6	9	18	20	24	7	11	13	14	19	21	25	26	28	15	23	27	29	30
* A																x										x
* B																	x						x			
- C	x(00)	x(01)	x(10)	x(11)																						
* D	x	x			x				x																	
* E	x		x	x				x																		
* F	x		x			x				x																
* G	x			x		x					x															
* H	x				x	x						x														
* I		x		x			x		x						x											
- J				x			x				x							x								
- K				x			x	x					x													
* L				x					x		x								x							
- M					x				x			x														
- N						x				x		x								x						
- O						x					x	x									x					
- P							x						x		x							x				
* Q							x						x					x					x			
* R							x								x			x							x	
* S								x					x			x						x				
* T									x					x	x							x				
* U									x					x					x					x		
* V									x						x				x						x	
* W										x							x			x				x		
* X											x							x			x				x	
* Y												x							x	x				x		
* Z												x								x	x					x

Figure 3

Consequently, one of the implicants J or K can be excluded. We label with an asterisk the implicants D, E, I and K. Then we proceed with the other columns having three intersections.

At the end of the procedure we find that the implicants C, J, M, N, O and P can be excluded in obtaining F'_{pm}.

Thus,

$$F'_{pm} = A + B + D + E + F + G + H + I + L + Q + R + \\ + S + T + U + V + W + X + Y + Z.$$

The resulting particular minimal form is free of conflicts.

As a second example we find F'_{pm}, if the conditions of operation of the circuit are described by the Boolean function

$$F = \underline{\bar{x}_1\bar{x}_2\bar{x}_3\bar{x}_4} + \bar{x}_1\bar{x}_2\bar{x}_3x_4 + \underline{\bar{x}_1\bar{x}_2x_3\bar{x}_4} + \\ + x_1\bar{x}_2\bar{x}_3\bar{x}_4 + \bar{x}_1x_2\bar{x}_3x_4 + \bar{x}_1x_2x_3\bar{x}_4 + \\ + \underline{x_1\bar{x}_2\bar{x}_3x_4} + \underline{x_1\bar{x}_2x_3\bar{x}_4} + \bar{x}_1x_2x_3x_4 + \\ + \underline{x_1\bar{x}_2x_3x_4} + x_1x_2\bar{x}_3x_4 + x_1x_2x_3\bar{x}_4 + x_1x_2x_3x_4.$$

By condition, the transitions from the states corresponding to the stressed constituents to other states and vice versa are indifferent; moreover consituents 2 and 11 are indifferent. /443

We use Quine's method to find the complete list of prime implicants and construct the table of coverings (fig. 4).

First we look through all columns and label with asterisks all implicants which give intersections with the columns having no more than two coverings. There are the rows B, C, D, F and G. The 0 column has two intersections, and both implicants A and B, which give these intersections, would in accordance with rule 1 have to occur in F'_{pm}, but in view of the fact that all affinities between constituents covered by implicant A are inessential, implicant A can be excluded. The implicants E, H and I remain unlabeled. They can all be excluded from F'_{pm}.

All affinities of implicant E are inessential, and for implicants H and I the only essential affinities are 10-11, which are respectively covered by implicants F and G.

As a result we obtain the following particular minimal form which is conflict-free

$$F'_{\mathrm{pm}} = B + C + D + F + G.$$

	0	1	2	8	5	6	9	10	7	11	13	14	15
A	×		×	×				×					
• B	×	×		×			×						
• C		×			×		×				×		
• D			×			×		×				×	
E				×			×	×		×			
• F					×				×		×		×
• G						×			×			×	×
H							×			×	×		×
I								×		×		×	×

Figure 4

Above we have considered the synthesis of circuits whose operating conditions are described by the disjunctive normal form of the Boolean function. In view of the duality law this same method can also be applied for obtaining the particular minimal forms, free from conflicts, starting from the conjunctive normal form of the Boolean function.

REFERENCES

1. Ioanin, G. Study of Circuits Operating with Real Contacts (Issledovaniye skhem rabotayushchikh s real'nymi kontaktami). IN: Materialy soveshchaniya po teorii ustroysto releynogo deystviya. No. 4, IAT AN SSSR, 1958.

2. Huffman, D. The Design and Use of Hazard-Free Switching Networks. J. Assoc. Comput. Machin., Vol. 4, No. 1, 1957.

3. Quine, W. A Way to Simplify Truth Functions. Am. Math. Monthly, Vol. 59, No. 8, 1952; Vol. 62, No. 9, 1955.

4. McCluskey, J. Minimization of Boolean Functions. Bell Syst. Tech. J., Vol. 35, No. 6, 1956.

METHODS OF MINIMIZATION AND CONSTRUCTION OF BRIDGE STRUCTURES FOR RELAY DEVICES

V. P. Didenko

Several studies devoted to the questions of the minimization of the /444 Boolean functions are known at the present time (refs. 1 and 2). In the majority of the methods, use is made of the relations familiar from Boolean algebra

$$fx + \bar{f}x = f;$$

$$\tilde{x} + \bar{\tilde{x}}f = \tilde{x} + f;$$

$$f + f = f;$$

$$x + xf = x.$$

The existing methods usually contain two stages for the construction of the minimal forms. In the first stage a determination (ref. 3) is made of the general minimal form or the reduced disjunctive normal form (rdnf). In the second stage, with the aid of sorting, the general minimal form is transformed into one of the particular minimal forms. In view of the complexity of the second stage, in practice we must frequently be satisfied with a function which is sufficiently close to the minimal form. The disjunctive normal form which realizes $f(x_1, x_2, \ldots, x_n)$ and has a minimal number of letters is termed the minimal form of the function $f(x_1, x_2, \ldots, x_n)$.

A different direction in the field of minimization of logic functions was developed in the work of Gavrilov (ref. 4). This method is based on comparison of the operating and forbidden states of the state table and the selection of the prime implicants, after which, with the aid of the table (ref. 2), we construct one or all of the minimal forms. The construction of the minimal form here is also associated with comparatively extensive sorting.

Therefore the author suggests a digital method which contains a relatively small number of operations and quite quickly leads to the construction of one of the minimal forms or a form sufficiently close to it.

1. The Number of Prime Implicants in the Minimal Form

The functions of algebra of logic can be considered as functions defined on the set E_n of all the vertices of an n-dimensional unit cube and taking the values 0 and 1.

Between the functions of logic algebra which depend on n-arguments /445 and the subsets E_n there exists a one-to-one correspondence (ref. 6), such that every function $f(x_1, \ldots, x_n)$ and subset $M_f \leqslant E_n$ correspond to one another, if

$$f(x_1, x_2, \ldots, x_n) = \begin{cases} 1 \text{ on } M_f; \\ 0 \text{ on } E_n \setminus M_f. \end{cases}$$

Let $f(x_1, x_2, \ldots, x_n)$ be given on the set E_n and take the values 0 and 1. There also exist the subsets M_1 and M_2, such that $M_1 \bigcup M_2 = E_n$; $M_1 \bigcap M_2 = 0$;

$$f(x_1, \ldots, x_n) = \begin{cases} 1 \text{ on } M_1; \\ 0 \text{ on } M_2. \end{cases}$$

In the more general case $M_1 \bigcup M_2 = M$ and

$$f(x_1, \ldots, x_n) = \begin{cases} 1 \text{ on } M_1; \\ 0 \text{ on } M_2; \\ \sim \text{ on } E_n \setminus M. \end{cases}$$

DEFINITION. Prime implicant φ_i is the name given to the conjunction of letters, such that there are simultaneously satisfied the conditions

$$\varphi_i \rightarrow \Sigma F_p; \ \varphi_i \,\&\, F_s \equiv 0$$

and with removal of even one letter from φ_i there become satisfiable simultaneously the conditions

$$\varphi_i' \rightarrow \Sigma F_p'; \ \varphi_i' \,\&\, F_s \neq 0,$$

where $\Sigma F_p'$ are the operating states;

ΣF_3 are the forbidden states.

Let us term the determinate ensemble $\sum_{i=1}^{q} F_{p_i}$, set in one-to-one correspondence with $\bigcup_{i=1}^{q} M_1$, such that $\Sigma\varphi_i \rightarrow \sum_{i=1}^{q} F_{p_j}$ and $\Sigma\varphi_i \& \Sigma F_{3_i} = 0$ (i.e., $\Sigma\varphi_i$ and ΣF_{3_i} are orthogonal) are the covering of $\bigcup_{i=1}^{q} M_1$

Let us term the number of operating combinations covered by the implicant φ_i Q--the power of the covering of φ_i. It is easy to see that implicants with a length (number of letters) $L_i = L_n$ have unit covering power. It is evident that with reduction of L_i and retention of $\varphi_i \rightarrow \Sigma F_p$; $\varphi_j \& \Sigma F_3 = 0$, the covering power increases, and with $L_i = L_{min}$ it is equal to

$$Q_{max} = 2^{n-L_{min}}.$$

Let us assume that in the function $f(x_1, x_2, \ldots, x_n)$ all n-arguments are essential; then, as shown in reference 8, the minimal forms of the completely defined Boolean functions with a number of variables n < 11 coincides with the particular minimal form containing the smallest number of terms satisfying the conditions

$$\sum_{i=1}^{q_{min}} \varphi_i \rightarrow \sum_{j=0}^{2^n-p-1} F_{p_j}; \ \sum_{i=1}^{q_{min}} F_i \& \sum_{r=p}^{2^n-1} F_{3_r} \equiv 0.$$

Let us denote the covering power of the implicants contained in the general minimal form by G_1. Then G_1 is determined from the expression /446

$$G_1 = \sum_{i=1}^{p} 2^{n-L_i}.$$

Let us place the general minimal form, and consequently G_1 also, in correspondence to some ensemble of constituents Q_1. It is not difficult to see that G_1/Q_1 is equal to the average number of coverings of each constituent.

Since the general minimal form contains k terms, the minimal number of terms H contained in F_{min} is determined from the expression

$$H = \frac{k}{\frac{G_1}{Q_1}} = \frac{Q_1 k}{G_1}.$$

Thus, in the general case we have

$$H \geqslant \frac{Q_1 k}{G_1}.$$

We determine the upper estimate of the number of prime implicants from the expression

$$\frac{Q_1 k}{G_1} + \frac{G_1}{2} = \frac{2Q_1 k + G_1^2}{2G_1}.$$

Consequently we have

$$\frac{2Q_1 \cdot k + G_1^2}{2G_1} \geqslant H \geqslant \frac{Q \cdot k}{G_1}.$$

2. Required Numbers of Sets and the Construction of Particular Minimal Forms

Every relay device has inputs and outputs (fig. 1). We denote the presence of signals on the device input by 1 and the absence of signals by 0. Then the conditions of operation of a relay device, both single-cycle and multicycle, can be described by a table of binary numbers.

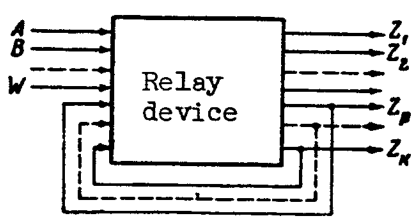

Figure 1

If we assign to the arguments $x_1, x_2, \ldots, x_n$, respectively, the weights $2^{n-1}, 2^{n-2}, \ldots, 2^0$ and substitute them in place of 1 in the corresponding combinations, the total weight will designate the number of the combination.

The sequence of variables $x_1, x_2, \ldots, x_n$ is termed basic (refs. 5 and 7), if each of them is assigned a weight in diminishing order, i.e., 2^{n-1}, /447 $2^{n-2}, \ldots, 2^0$.

By expansion of the base into its component elements we will understand the sequential identification of its even and odd elements in increasing order of their weights.

The even and odd whole numbers characterize the power of the variable x_i, i.e.,

$$x_i^{\sigma} = \begin{cases} x_i & \text{for } \sigma \text{ equal to an odd number of the set,} \\ \bar{x}_i & \text{for } \sigma \text{ equal to an even number of the set.} \end{cases}$$

The conversion from the base $x_1, x_2, \ldots, x_n$ to the base $x_1, x_2, \ldots, x_{n-1}$ is accompanied by the separation of the first variable in order of succession of the elements with respect to increasing weight with its subsequent exclusion from the numbers of the set. Let us use α_i and β_i to denote the odd numbers of the sets, respectively, of the operating and forbidden states, and $\bar{\alpha}_i, \bar{\beta}_i$ to denote the even numbers of the sets. Then the exclusion of the $\tilde{x}_i$ variable from the numbers of the sets is accomplished by the subtraction of unity from all odd numbers of the set and the division of the even and odd numbers of the set by 2.

Since the set numbers are mod-2-comparable, i.e.,

$$\alpha_i \equiv \beta_i \bmod 2;$$
$$\bar{\alpha}_i \equiv \bar{\beta}_i \bmod 2,$$

after separation from the base of the first variable in order of succession, the set numbers can again be partitioned into two groups, depending on which class of mod-2-residues they belong to.

We term the set number $\tilde{\alpha}_i$ essential, if for it

$$\bar{\alpha}_i = \beta_i - 1;$$
$$\alpha_i - 1 = \bar{\beta}_i$$

are realizable. It is not difficult to see that a variable is essential, if for it there exists at least one essential set number of the base being considered.

The following statement can be proved.

THEOREM. Prime implicants consist of variables corresponding to the essential numbers of the sets and only of them.

1. Taking as a base a definite permutation of the arguments $x_1, x_2, \ldots, x_n$, we determine all set numbers of this permutation. It is obvious that the parity of the set numbers will reflect the confirmation or negation of the variable x_n with the smallest weight.

2. Taking n-1 cyclic permutations, we determine for each of them the set numbers, starting from the set numbers of the preceding permutation, using the equations

$$\left.\begin{aligned} &\frac{\alpha_i - 1}{2} + 2^{n-1} = \alpha_i^1;\ \frac{\bar{\alpha}_i}{2} = \bar{\alpha}_i^1; \\ &\frac{\beta_i - 1}{2} + 2^{n-1} = \beta_1^i;\ \frac{\bar{\beta}_i}{2} = \bar{\beta}_i'. \end{aligned}\right\} \quad (1)$$

3. We compile the state table for the Ψ_i output, taking as the basis one of the n-bases, separating the set numbers for the first variable of the permutation into even and odd and inscribing the set numbers in the corresponding rows of the table. After this we compare the operating numbers of the sets with the forbidden numbers and enclose in circles the operating set numbers, for which the following equalities are satisfied

$$\left.\begin{aligned} &\bar{\alpha}_i = \beta_i - 1; \\ &\alpha_i - 1 = \bar{\beta}_i. \end{aligned}\right\} \quad (2)$$

4. We connect the essential numbers by the conjunction symbol and, setting in correspondence the variable as a function of the parity of the set numbers, we determine the prime implicants. /448

5. We check whether the implicants satisfy the condition

$$\varphi_l \,\&\, \sum F_3 \equiv 0.$$

If they do satisfy this condition they are written out in minimal form, and the states covered by them are stricken from the table.

6. If as a result of operation 5 all operating states are eliminated, the minimal form can be written out directly from the state table.

7. If after performance of operation 5 there remain in the state table implicants for which the conditions $\varphi_i' \to \Sigma F_p, \varphi_i' \to \Sigma F_3$, are simultaneously satisfiable, and in the table certain of the n-arguments are inessential, then, striking out one inessential variable, we determine the ω-table. After this we proceed for each of them just as in items 3, 4 and 7.

8. If after operation 5 there remain implicants in the table with the conditions that $\varphi_i' \to \Sigma F_p$, $\varphi_i' \to \Sigma F_3$, and all n-arguments are essential, the implicants of the form φ_1' must be extended by use of other essential numbers, so that $\varphi_i' \& \varphi_i'' = \varphi_{min}$.

This operation is accomplished as follows: we perform the combining of the essential set numbers only for the even base D_{x_1}, whose numbers were used in the performance of the separation. After this we strike out the even or odd operating states of the table which are covered by the implicants. Using the remaining unstricken even (odd) base set numbers, we make a determination of the neighbors in the opposite parity base D_{x_1} and then perform the carry and circling of the essential variables encountered in at least one of them. As a result we determine the implicants which cover simultaneously the even and odd numbers of the sets of the permutation taken as the base.

In case the state table is given by binary numbers rather than decimal, the essential set numbers can be determined by means of mod-2 addition of each operating combination in turn with all the forbidden combinations. Essential combinations will be those places of the binary set $\alpha_1, \ldots, \alpha_n$, which differ from the forbidden by one place (in this case zeros must be in the remaining places).

The process considered above for the construction of the particular minimal forms can be simplified. For this it is sufficient to partition all decimal numbers of the base set $D_{x_n, \ldots, x_1}$ into even and odd, writing under the even operating numbers (fig. 2) the even forbidden numbers, and under the odd--the odd forbidden numbers.

$\alpha_{i_1}, \alpha_{i_2}, \ldots, \alpha_{iq}$	$\bar{\alpha}_{i_1}, \bar{\alpha}_{i_2}, \ldots, \bar{\alpha}_{iq_2}$
$\beta_{i_1}, \beta_{i_2}, \ldots, \beta_{iq_3}$	$\bar{\beta}_{i_1}, \bar{\beta}_{i} \ldots, \bar{\beta}_{iq_4}$

Figure 2

After this, comparing $\alpha_i - 1$ for all i with $\bar{\beta}_{i_j}$ and $\bar{\alpha}_{i_j}$ with $\bar{\beta}_{i_j} - 1$, we circle the essential even and odd operating numbers. We denote the set of even numbers of the base D_{x_i} by $\mathfrak{M}_{D_{\bar{x}_i}}$, the set of odd by $\mathfrak{M}_{D_{x_i}}$. The following cases are possible if we take n-1 cyclic permutations relative to the /449
base and in each case separate all set numbers into even and odd

1. $\mathfrak{M}_{D_{\bar{x}_i}} = \mathfrak{M}_{D_{x_i}}$.

This means that the operating numbers of the odd and even parts of the base are neighbors. In this case the variable can be dropped as being inessential.

2. $\mathfrak{M}_{D_{\bar{x}_i}} \supset \mathfrak{M}_{D_{x_i}}$; $\mathfrak{M}_{D_{x_i}} \supset \mathfrak{M}_{D_{\bar{x}_i}}$.

This case indicates the presence of essential operating set numbers either in the even or in the odd parts of the base $D_{\tilde{x}_i}$. In this case, if the essential numbers are in the even part of the base $D_{\tilde{x}_i}$, then, correspondingly, the variable corresponding to the odd set numbers can be dropped, and vice versa.

3. $\mathfrak{M}_{D_{\bar{x}_i}} \cap \mathfrak{M}_{D_{x_i}} \equiv 0$.

This case indicates that all operating numbers are essential. Therefore, we shall place in correspondence with the even numbers x_i, and in correspondence with the odd $\bar{x}_i$.

4. $\mathfrak{M}_{D_{x_i}} \cap \mathfrak{M}_{D_{x_i}} \equiv \mathfrak{M}_{D_{\tilde{x}_i}} \not\equiv 0$.

This case is the most general; it is easy to see that cases 1-3 result from it. The fourth case indicates the presence of essential operating set numbers in both even and odd parts of the set and, moreover, the presence of the common portion.

The schematic representations of all cases are shown in figure 3a, b, c and d, respectively.

It is clear that, knowing the fundamental base and n-1 cyclic permutations, we can determine the new base for obtaining the minimal form with the smallest number of terms. We shall differentiate the following two possibilities.

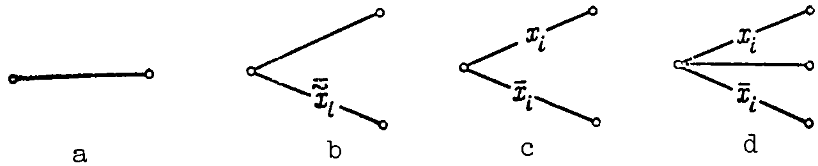

Figure 3

(1) Case 4 is absent in all cyclic permutations. The permutation from which we must start for the minimization must contain all variables corresponding to the 1st case--in the first place, to the 2nd case--in the second, to the 3rd case--in the third place. Within each place the ordering of the variables is unimportant.

(2) With the existence of the fourth condition it is necessary to determine the smallest quantity of set numbers which must be in the common portion. Actually, condition 4 indicates that there exist implicants which cover the essential numbers of the even and odd parts of the base $D_{\tilde{x}_i}$. At the same time the implicants can also cover certain inessential numbers of the even and /450 odd base. Therefore it is necessary to try to select for the covering of the essential set numbers of the even and odd parts of the base $D_{\tilde{x}_i}$ those implicants which will cover simultaneously the greatest number of neighbors among the inessential numbers, because otherwise a large quantity of numbers will appear in the common portion, which leads to a minimal form with an excessive number of terms. This implies that as the basic permutation in the general case it is necessary to select among the n-cyclic permutations that for which the following condition is satisfied

$$\mathfrak{M}_{D_{x_i}} \cap \mathfrak{M}_{D_{\tilde{x}_i}} \equiv \mathfrak{M}_{D_{\tilde{x}_i}\,\min},$$

where $\mathfrak{M}_{D_{\tilde{x}_i}\,\min}$ is the minimal number of elements of the common portion.

In the second step, after partition for each of the parts of the bases D'_{x_i} and $D'_{\tilde{x}_i}$ we again determine $\mathfrak{M}_{D'_{\tilde{x}_i}}$, etc. In this case it is necessary that we assign to each essential number of the original permutation $D_{\tilde{x}_i}$, after the operation $\frac{\alpha_i}{2}$ or $\frac{\alpha_i - 1}{2}$, has been performed on it, the essential number of that parity which contained at least one essential number in the given step. The minimal quantity of terms for the covering of the essential numbers of the even (odd) part of the base $D_{\tilde{x}_i}$ will thus be determined.

After this all covered set numbers of the original base are stricken out. The remaining uncovered set numbers of the even (odd) part of the base $D_{\tilde{x}_i}$

(if all numbers of the even (odd) part of the base are covered, we turn to the determination of the implicants for the odd (even)) are moved out into the common portion, for which the operation $\frac{\alpha_i - 1}{2}$; $\frac{\beta_i - 1}{2}$; $\left(\frac{\bar{\alpha}_i}{2}; \frac{\bar{\beta}_i}{2}\right)$ is performed, and their variable with the smallest weight of the base $D_{\tilde{x}_i}$ is dropped. Thereafter, we determine the implicants for the new base in exactly the same way, and so on, until all the numbers of the even (odd) part of the base D_{xi} are covered.

In this case a definite ensemble of numbers of the odd (even) part of the base D_{x_i} will simultaneously be covered. Then we turn to the determination of the implicants for the covering of the essential and the remaining uncovered set numbers of the odd (even) part of the original base $D_{\tilde{x}_i}$. In this case the same rules are used.

Let us consider examples for each of the four cases presented above.

EXAMPLE 1. Let there be given the function corresponding to case 1

$$F_1 = \left\{\frac{\Sigma\,(0,\ 2,\ 4,\ 6,\ 8,\ 10,\ 1,\ 3,\ 5,\ 7,\ 9,\ 11)}{\Sigma\ 12,\ 13,\ 14,\ 15,\ 18,\ 19,\ 28,\ 29]}\right\}_{x_1,\,x_2,\,x_3,\,x_4,\,x_5.}$$

The lowest weight 2 corresponds to the variable x_i. The missing numbers of the set of the base $D_{\tilde{x}_i}$ are indifferent or unusable. They are accounted for automatically.

The entire minimization process is represented in table 1.

TABLE 1

1	2		3		4		5	
	1	2			1	2		
$\tilde{x}_1$				0,2,4,6,8,10			1,3,5,7,9,11	
$\tilde{x}_2$				12,14,18,28 0,2,4			13,15,19,29 1,3,5	
$\tilde{x}_3$	$\bar{x}_3$			6,24 0,2			7,9 1	
$\tilde{x}_4$			1	4 0	$\bar{x}_4$		3,7 0	
$\tilde{x}_5$	$\bar{x}_5$		0	2	$\bar{x}_5$		2 0	1,3
				1				1

For the set numbers of the base $D_{\tilde{x}_i}$ there is no essential set number. Therefore the variable $\tilde{x}_1$ is dropped. In the second step all even and odd numbers with the exception of unity are divided by two and are grouped, depending on to what class with respect to mod-2 residues they belong. /451

There is also no essential set number for the base $D_{\tilde{x}_2}$. Therefore $\tilde{x}_2$ is dropped. For the base $D_{\tilde{x}_3}$ the essential set number is 2, since 2 = 3 - 1. Therefore we place in column 2 (table 1) the letter $\bar{x}_3$ corresponding to this set. Thereafter, the determination of the implicant for the set number 2 is performed only in the even part of the base $D_{\tilde{x}_3}$, because the letter x_3 must correspond to all odd numbers. We determine the set numbers of the base $D_{\tilde{x}_4}$, excluding $\tilde{x}_3$ by the operation $\frac{\bar{\alpha}_i}{2} : \frac{\bar{\beta}_i}{2}$. For the base $D_{\tilde{x}_4}$ there are no essential numbers, therefore the variable $\tilde{x}_4$ is excluded by the method indicated above. Finally, the letter $D_{\tilde{x}_5}$ corresponds to the base $\bar{x}_5$, i.e., the essential set number is 0. Further operations are terminated, since the even forbidden numbers are always absent.

We thus determined the minimal implicant $\bar{x}_3\bar{x}_5$. Omitting further reasoning, we construct the implicant $\bar{x}_4\bar{x}_5$. The minimal form F_{min} will be

$$F_{\min} = \bar{x}_3\bar{x}_5 + \bar{x}_4\bar{x}_5.$$

EXAMPLE 2. Let there be given the function corresponding to case 2

$$F_2 = \left\{\frac{\Sigma\,(0,\ 2,\ 4,\ 6,\ 8,\ 10,\ 18,\ 20,\ 24,\ 30,\ 13,\ 15,\ 21,\ 25,\ 29,\ 31)}{\Sigma\,[16,\ 22,\ 26,\ 3,\ 5,\ 7,\ 19,\ 23,\ 27]}\right\}_{x_1,\,x_2,\,x_3,\,x_4,\,x_5}.$$

We separate the numbers of the base $D_{\tilde{x}_i}$ into even and odd and construct table 2. It is easy to see that $\mathfrak{M}_{D_{x_1}} \supset \mathfrak{M}_{D_{\bar{x}_1}}$, because essential numbers, circled, appear only in column 3.

Since certain numbers are indifferent or unusable, it is necessary in covering the essential numbers of the base $D_{\bar{x}_1}$ 2, 4, 6, 18 simultaneously to cover (if this is possible) also the numbers 0, 8 and 10, for which there are no neighbors in column 5. After simultaneous covering of these numbers there

TABLE 2

1	2			3	4			5
	1	2	3		1	2	3	
$\tilde{x}_1$	$\bar{x}_1$	$\bar{x}_1$		0,2,4,6,8,10,18,20,24,30				13,15,21,25,29,31
$\tilde{x}_2$	x_2			16,22,26 1,3,9,5 | 2,0,4	$\bar{x}_2$	$\bar{x}_2$		3,5,7,19,23,27 6,10,12,14 | 7,15
$\tilde{x}_3$	$\bar{x}_3$			11,13 | 8 0,4,2 | 1 | 0,2 | 1	x_3		x_3	8,2 | 11,13,1,9,3 5 | 6 | 3,7
$\tilde{x}_4$	$\bar{x}_4$			6 | 5 | 6,4 | 5 0,2 | 1 | 0 | 1		x_4	x_4	1 | 4 | 5,1 | 6,0,4 2 | 3 | 1,3
$\tilde{x}_5$		$\bar{x}_5$		3 | 2 | 3 0	x_5			0 | 2,0 | 2,0 1
				1				0

will not be any need to introduce them into the common portion, in view of which we obtain the minimal number of terms. Performing at each step /452 the determination of the essential numbers and placing in correspondence to them in columns 2 and 4 (table 2) the corresponding letters as a function of their parity, we obtain five minimal implicants, which then represent the minimal form

$$F_{\min} = x_1 x_2 \bar{x}_3 \bar{x}_4 + \bar{x}_1 \bar{x}_5 + \bar{x}_2 x_3 x_5 + \bar{x}_2 x_4 + x_3 x_4.$$

EXAMPLE 3. Let there be given the function corresponding to case 3

$$F_3 = \left\{ \frac{\Sigma\,(0,\ 2,\ 4,\ 16,\ 24,\ 26,\ 7,\ 9,\ 11,\ 23,\ 29,\ 31)}{\Sigma\,[6,\ 8,\ 10,\ 22,\ 28,\ 30,\ 12,\ 13,\ 5,\ 17,\ 25,\ 27]} \right\}_{x_1,\, x_2,\, x_3,\, x_4,\, x_5}.$$

The determination of the implicants is presented in table 3. As we see from the table, in column 3 in the base $D_{\bar{x}_4}$ the number 2 is essential, /453 and in the base $D_{\bar{x}_3}$ the number 6 is essential. But this number was inessential for the base $D_{\bar{x}_2}$, while in the base $D_{\bar{x}_1}$ it does not coincide in parity with the number 1, for which the implicant is constructed. Therefore the number 6 is crossed out. After striking out the number 6 there are no more essential numbers in the base $D_{\tilde{x}_3}$ and the variable $\tilde{x}_3$ is dropped. We write out the minimal form directly from table 3

$$F_{3\min} = \bar{x}_1 \bar{x}_2 \bar{x}_4 + \bar{x}_1 \bar{x}_3 \bar{x}_4 + \bar{x}_1 \bar{x}_3 x_5 + x_1 x_2 x_3 + x_1 x_3 x_4 + x_1 x_4 \bar{x}_5.$$

TABLE 3

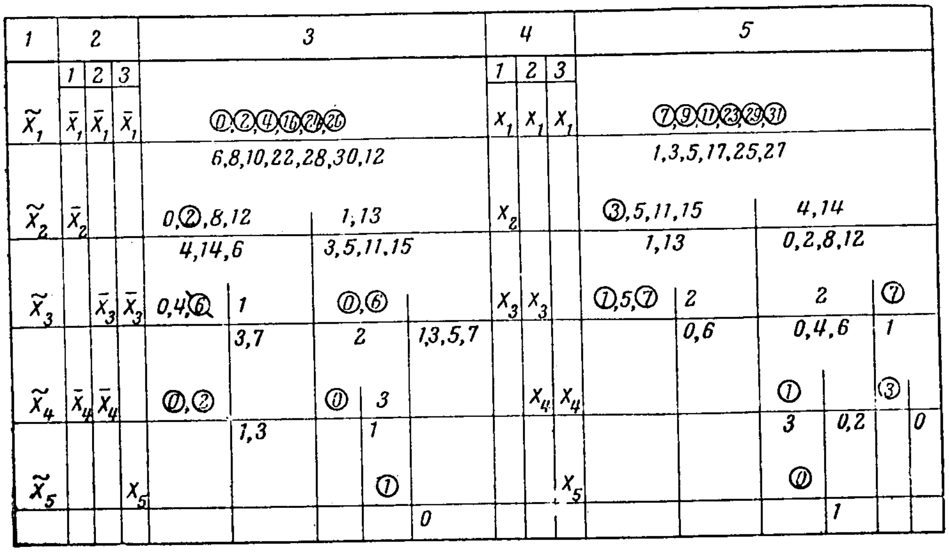

TABLE 4

	0	2	4	6	8	10	12	14	16	18	20	22	24	26	28	30	1	3	5	7	9	11	13	15	17	19	21	23	25	27	29	31
$\tilde{x}_1$	1	1	1	1	1	0	0	1	1	1	1	0	1	1	1	1	1	0	1	1	1	1	1	1	0	1	1	1	1	1	1	0
$\tilde{x}_2$	1	1	1	0	1	1	1	1	1	1	1	1	0	1	1	1	1	1	0	1	1	0	1	1	0	1	1	1	1	1	1	0
$\tilde{x}_3$	1	1	1	1	1	1	0	1	1	0	1	1	0	1	1	1	1	0	1	1	1	1	1	1	1	1	0	1	1	1	1	0
$\tilde{x}_4$	1	1	1	0	1	1	0	1	1	1	1	1	1	0	1	1	1	1	1	1	0	1	1	1.	0	1	1	1	1	1	1	0
$\tilde{x}_5$	1	1	1	0	1	1	1	1	1	1	0	1	0	1	1	1	1	0	1	1	1	1	0	1	1	1	1	1	1	1	1	0

EXAMPLE, corresponding to case 4. Let there be given the function

$$F_4 = \left\{ \frac{\Sigma\,(0,2,4,6,8,14,16,18,20,24,26,28,30,1,5,7,9,11,13,15,19,23,25,27,29)}{\Sigma\,[10,12,22,3,7,31]} \right\}_{x_1,\ldots,x_5}$$

Let us determine n - 1 cyclic bases from the given $D_{x_1,\ldots,x_5}$. To do this, we construct table 4, where unity corresponds to each operating number and zero corresponds to the forbidden number. Each successive set number is obtained from the preceding, using equations (1). Either one or zero corresponds to each of these numbers.

TABLE 5

1	2	3	4	5
	1 2 3 4 5		1 2 3 4	
$\tilde{x}_2$	$\tilde{x}_2$ $\tilde{x}_2$ $\tilde{x}_2$	0, 2, 4, 8, 10, 12, 14, 16, 18, 20, 22, 26, 28, 30 / 6, 24	$\tilde{x}_2$ $\tilde{x}_2$	1, 3, 7, 9, 13, 15, 19, 21, 23, 25, 27, 29 / 5, 11, 17, 31
$\tilde{x}_3$	$\tilde{x}_3$	0, 2, 4, 6, 8, 10, 14 / 12 ; 1, 5, 7, 9, 11, 13, 15 / 3	$\tilde{x}_3$ $\tilde{x}_3$	0, 4, 6, 12, 14 / 2, 8 ; 1, 3, 7 / 5, 15
$\tilde{x}_4$	$\tilde{x}_4$ $\tilde{x}_4$	0, 2, 4 / 6 ; 1, 3, 5, 7 ; 0, 2, 4 / 6 ; 3, 5, 7 / 1	$\tilde{x}_4$ $\tilde{x}_4$	0, 2, 6 / 4 ; 3, 7 / 1 ; 0 / 6, 4, 2 ; 1, 3 / 1, 7 ; 7 ; 2
$\tilde{x}_5$	$\tilde{x}_5$ $\tilde{x}_5$	0, 2 ; 1 / 3 ; 0 ; 1 / 3 ; 3, 7 / 0 ; 2	$\tilde{x}_5$ $\tilde{x}_5$	1, 3 ; 2, 0 ; 0 / 2 ; 1, 3 ; 0 ; 1 / 3
$\tilde{x}_1$	$\tilde{x}_1$	0 ; 1	$\tilde{x}_1$ $\tilde{x}_1$	0 / 1 ; 0 ; 1
$\tilde{x}_3$	$\tilde{x}_3$	9, 11, 13 / 3, 5, 15		
$\tilde{x}_4$	$\tilde{x}_4$ $\tilde{x}_4$	4, 6 / 2 2 ; 12, 2, 8 / 5		
$\tilde{x}_5$	$\tilde{x}_5$	1, 7 / 3 ; 1, 7 / 7 ; 6, 4, 2		
$\tilde{x}_1$	$\tilde{x}_1$ $\tilde{x}_1$	1 / 1 / 0 ; 0 / 1 ; 3 / 0		

It is easy to see from table 4 that the minimum of the intersection $\mathfrak{M}_{D_{x_i}} \cap \mathfrak{M}_{D_{\tilde{x}_i}}$ has the variable $\tilde{x}_2$. Therefore, we determine the minimal form from the base $D_{x_2, x_3, x_4, x_5, x_1}$. To do this, we construct table 5. In column 3 of table 5 for the base $D_{\tilde{x}_2}$ (labeled with circles) the essential numbers are 4, 10, 16 and 30. Dividing them and the remaining numbers by 2, we obtain the base $D_{\tilde{x}_3}$, in which for the even part there again appears the essential number 2, corresponding to the preceding essential number 4. Therefore, $\bar{x}_3$ is essential in the implicant. After this, excluding $\tilde{x}_3$, we transfer to the base $D_{\tilde{x}_4}$, in which none of the numbers previously essential is encircled. Therefore, we strike out the essential number 7, drop the variable $\tilde{x}_4$ and construct the implicant $\bar{x}_2, \bar{x}_3\,\bar{x}_5$.

In exactly the same way we strike out the numbers 13 and 0 in column 5. After determining the implicants which cover the essential numbers 4, 10, 16 and 30 of the base $D_{\tilde{x}_2}$, we label the inessential numbers simultaneously

covered by them. We move the numbers of the base $D_{\tilde{x}_2}$, which remain uncovered, into the common portion (see lower portion of table 5) and determine the implicants $x_3\bar{x}_4x_1 + x_4\bar{x}_5x_1$, simultaneously noting the numbers of the base $D_{\tilde{x}_2}$ covered by them. For the remaining uncovered numbers of the base $D_{\tilde{x}_2}$ we determine the new minimal form

$$F_4 \min = \bar{x}_2\bar{x}_3\bar{x}_5 + \bar{x}_2\bar{x}_4\bar{x}_1 + \bar{x}_2x_4x_5 + x_3\bar{x}_4x_1 + x_4\bar{x}_5x_1 + \\ + x_2\bar{x}_3x_5 + \bar{x}_4\bar{x}_5\bar{x}_1 + x_2x_3x_4\bar{x}_1,$$

having eight terms. Changing bases and striking out all particular minimal forms, which are longer in composition, we can obtain all minimal forms, if necessary.

3. Construction of Bridge Structures of Relay Contact Devices with Account for Alternate Paths as Primary Paths

At the present time the most advanced of the known methods for the construction of bridge structures of the (1-k)-pole relay devices are the cascade method and the graphical method (ref. 7).

However, these methods require considerable sorting of variants in order to select circuits with minimal structure and to avoid using alternate paths as primary paths. In the present paper the author makes an attempt to develop a method which takes account of the alternate paths as primary paths and which shortens the sorting. /455

In the construction of the circuits the connections are usually made between pairs of nodes. It is therefore advisable to consider the possible conditions for the connection of the nodes. To do this, we consider the (1-k)-pole circuit, in which we denote the inputs by $x_1, x_2, \ldots, x_n$, and the outputs by $z_1, \ldots, z_k$. Without restriction of generality we shall consider that the technique described below applies to both single-cycle and multicycle relay devices.

The conditions of operation of the (1-k)-pole relay device can be given in the form of table 6, where $\bar{\alpha}_{li}$ are the set numbers, corresponding to the numbers of the constituents of the permutation taken as the base, for example, $D_{x_1,x_2,\ldots,x_n}$, while the functions performed by the output reacting organs are given by means of 0 and 1 and are denoted by $F_{z_1}, \ldots, F_{z_k}$. /456

TABLE 6

	$\bar{\alpha}_{i_1}$	$\bar{\alpha}_{i_2}$	$\bar{\alpha}_{i_3}$	$\cdots$	$\bar{\alpha}_{i_i}$	$\cdots$	$\bar{\alpha}_{i_{n-1}}$	$\bar{\alpha}_{i_n}$	α_{i_1}	α_{i_2}	α_{i_3}	$\cdots$	α_{i_i}	$\cdots$	$\alpha_{i_{n-1}}$	α_{i_n}
F_{z_1}	1	1	1	$\cdots$	0	$\cdots$	0	0	0	0	0	$\cdots$	1	$\cdots$	1	1
F_{z_2}	0	1	1	$\cdots$	1	$\cdots$	0	1	1	0	1	$\cdots$	1	$\cdots$	0	0
$\vdots$	$\vdots$	$\vdots$	$\vdots$	$\vdots$	$\vdots$	$\vdots$	$\vdots$	$\vdots$	$\vdots$	$\vdots$	$\vdots$	$\vdots$	$\vdots$	$\vdots$	$\vdots$	$\vdots$
$F_{z_{k-1}}$	1	0	1	$\cdots$	1	$\cdots$	1	0	1	0	1	$\cdots$	0	$\cdots$	1	0
F_{z_k}	1	1	0	$\cdots$	0	$\cdots$	0	1	0	1	1	$\cdots$	1	$\cdots$	0	1

Let us denote the even part of the base of the first variable having the smallest weight by $D_{\bar{x}_i}$, and the odd part by D_{x_i}. Correspondingly, the set of elements consisting of zeros and ones and representing the conditions of operation z_i of the output are denoted by $\mathfrak{M}_{iD_{x_i}}$ and $\mathfrak{M}_{iD_{\bar{x}_i}}$, while z_j of the output are denoted by $\mathfrak{M}_{jD_{x_i}}$ and $\mathfrak{M}_{jD_{\bar{x}_i}}$. Then the possible conditions of connection of pairs of nodes at any r-step of construction of the circuit can be represented in table 7.

In the construction of the circuits by the methods indicated above (ref. 7), in the general case we require a minimum of n! sortings. However, in a particular case the optimal base may be completely determinate. Actually, let F_{z_1} depend essentially on the variables x_1, x_2, F_{z_2} on x_1, x_2, x_3, F_{z_3} on x_1, x_2, x_3, x_4, x_5 and so on; then $F_{z_1} \supset F_{z_2} \supset F_{z_3} \supset \ldots \supset F_{zk}$ and the optimal base is determined completely uniquely. For proof it is sufficient to assume the reverse order of arrangement of the arguments.

In the general case, as was shown above, to each of the $F_{z_1}, \ldots, F_{z_n}$ there can correspond the condition

$$\mathfrak{M}_{D_{x_i}} \cap \mathfrak{M}_{D_{\bar{x}_i}} = \mathfrak{M}_{D_{x_i}} \neq 0$$

on the assumption that each F_{z_i} output depends essentially on the n-arguments.

If we start the construction from the circuit input, then it is necessary to select at each stage

$$\mathfrak{M}_{D_{x_i}} \cap \mathfrak{M}_{D_{\bar{x}_i}} = \mathfrak{M}_{D_{\bar{x}_i}} = \min.$$

TABLE 7

N	Circuit notation for connection of node pairs	Conditions when connections are possible
I		$m_{iD\bar{\bar{x}}_i}=m_{jD\bar{\bar{x}}_i}$
II	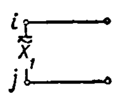	$m_{iD\bar{x}_i}=m_{jD\bar{x}_i}$ $m_{iD\bar{\bar{x}}_i}\cup m_{D\bar{\bar{x}}_i}=m_{iD\bar{x}_i}=m_{jD\bar{x}_i}$
III	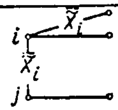	$m_{iD\bar{x}_i}=m_{jD\bar{x}_i}$ $m_{iD\bar{x}_i}\cup m_{jDx_i}\supset m_{iD\bar{x}_i}$
IV	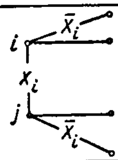	$m_{iDx_i}=m_{jDx_i}$ $m_{iDx_i}=m_{jDx_i}\supset m_{iD\bar{x}_i}\cup m_{jD\bar{x}_i}$
V	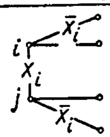	$m_{iDx_i}=m_{jDx_i}\subset m_{iD\bar{x}_i}\cap m_{jD\bar{x}_i}$
VI	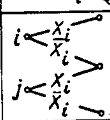	$m_{iD\bar{x}_i}=m_{jDx_i}$ $m_{iDx_i}=m_{jD\bar{x}_i}$
VII	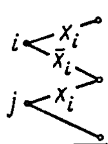	$m_{iD\bar{x}_i}=m_{jDx_i}$ $m_{jD\bar{x}_i}\supset m_{jDx_i}$ $m_{iDx_i}\not\supset m_{iD\bar{x}_i}$
VIII	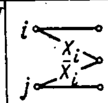	$m_{iDx_i}=m_{jD\bar{x}_i}$ $m_{iD\bar{x}_i}\supset m_{iDx_i}$ $m_{jDx_i}\supset m_{jD\bar{x}_i}$
IX	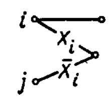	$m_{iDx_i}=m_{jD\bar{x}_i}$ $m_{jD\bar{x}_i}=0$ $m_{iD\bar{x}_i}\supset m_{iDx_i}$
X	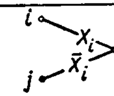	$m_{iDx_i}=m_{jD\bar{x}_i}$ $m_{iD\bar{x}_i}=0$; $m_{jDx_i}=0$
XI	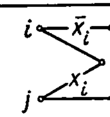	$m_{iDx_i}=m_{jD\bar{x}_i}$ $m_{iDx_i}\supset m_{iD\bar{x}_i}$ $m_{jD\bar{x}_i}\supset m_{jDx_i}$
XII	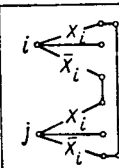	$m_{iDx_i}\setminus m_{iDx_i}\cap m_{iDx_i}=$ $=m_{jD\bar{x}_i}\setminus m_{jD\bar{x}_i}\cap m_{jDx_i}$ $m_{iD\bar{x}_i}\setminus m_{iDx_i}\cap m_{iD\bar{x}_i}=$ $=m_{jDx_i}\setminus m_{jD\bar{x}_i}\cap m_{jDx_i}$
XIII	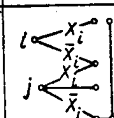	$m_{iDx_i}=m_{jD\bar{x}_i}\setminus m_{jD\bar{x}_i}\cap m_{jDx_i}$ $m_{iD\bar{x}_i}=m_{jDx_i}\setminus m_{jD\bar{x}_i}\cap m_{jDx_i}$
XIV	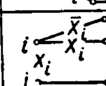	$m_{iD\bar{x}_i}\neq m_{jD\bar{x}_i}$ $m_{jD\bar{x}_i}=0$ $m_{jDx_i}\supset m_{iDx_i}$

. With construction from the output, i.e., from the reacting elements to the opposite terminal, it is necessary to determine at each stage

$$\mathfrak{M}_{D_{x_i}} \cap \mathfrak{M}_{D_{\bar{x}_i}} = \max,$$

since the variable which has a maximum in the common portion will have a minimum of essential set numbers. Therefore, taking n permutations at the first stage, we can identify that variable which has a minimum of the essential numbers. After this we perform all possible connections of nodes according to table 7 and exclude from consideration the identified variable. Then, taking n-2 cyclic permutations from the base which remains after exclusion of the variable, we again identify the variable having a minimum of essential numbers. If each variable has an identical quantity of essential numbers, their order is determined by the maximal coincidence of numbers and, consequently, a maximum of the circuit connections.

Using this construction we obtain a circuit which is sufficiently close in structure to the minimal circuit. In this case the number of sortings will not exceed $\frac{n^2+n}{2}$. With an equal quantity of essential variables, for certain groups of variables we can determine the best connection by inspection two steps ahead. By inspection one step ahead we determine the optimal conditions for the connection of the longest circuits, consisting of at least n-1 letters, consisting in the second step of n-2 letters, and thus obtain a circuit sufficiently close to optimal.

Let us consider the application of the method to an example. Let there be given base $D_{x_4,\ldots,x_1}$, where $\tilde{x}_1$ has the minimal weight 2^0. The conditions of operation of a (1-5)-terminal network are given by table 8, where the essential numbers are circled. /458

In computing the essential numbers we note that x_2 and x_1 have the minimal quantity of essential numbers. Noting that the variable x_3 gives more direct connections than $\tilde{x}_1$, we take $\tilde{x}_3$ as the separable variable. The first step of the construction with account for table 8 is shown in figure 4a. Excluding the variable $\tilde{x}_3$ and the bases x_3, x_4, x_1, x_2, we construct table 9 with account for the fact that

$$\overline{\mathfrak{M}}_{F_{z_1}} = \overline{\mathfrak{M}}_{F_{z_4}} \text{ and } \mathfrak{M}_{F_{z_1}} \cup \overline{\mathfrak{M}}_{F_{z_4}} \supset \overline{\mathfrak{M}}_{F_{z}}.$$

TABLE 8

	$\bar{x}_1$								x_1							
	0	2	4	6	8	10	12	14	1	3	5	7	9	11	13	15
F_{z_1}	1	0	1	0	1	1	0	1	1	0	1	0	1	1	1	1
F_{z_2}	0	1	0	1	1	0	1	0	0	1	1	0	1	0	1	0
F_{z_3}	1	0	1	0	1	1	0	1	1	0	1	0	0	1	0	1
F_{z_4}	0	1	0	1	0	0	1	1	0	1	0	1	0	1	0	1
F_{z_5}	1	0	1	0	1	1	0	0	1	0	0	0	1	1	1	1
	$\bar{x}_2$								x_2							
F_{z_1}	1	1	1	0	1	1	1	1	0	0	1	1	0	0	1	1
F_{z_2}	0	0	1	1	0	1	1	1	1	1	0	0	1	0	0	0
F_{z_3}	1	1	1	0	1	1	0	0	0	0	1	1	0	0	1	1
F_{z_4}	0	0	0	1	0	0	0	0	1	1	0	1	1	1	1	1
F_{z_5}	1	1	1	0	1	0	1	1	0	0	1	0	0	0	1	1
	$\bar{x}_3$								x_3							
F_{z_1}	1	1	1	1	0	1	0	1	1	0	1	1	0	1	0	1
F_{z_2}	0	1	0	1	1	0	1	0	0	1	1	1	1	0	0	0
F_{z_3}	1	1	1	0	0	1	0	1	1	0	1	0	0	1	0	1
F_{z_4}	0	0	0	0	1	0	1	1	0	1	0	0	1	1	1	1
F_{z_5}	1	1	1	1	0	1	0	1	1	0	0	1	0	0	0	1
	$\bar{x}_4$								x_4							
F_{z_1}	1	1	0	0	1	1	0	0	1	1	1	1	0	1	1	1
F_{z_2}	0	0	1	1	0	1	1	0	1	1	0	0	1	1	0	0
F_{z_3}	1	1	0	0	1	1	0	0	1	0	1	1	0	0	1	1
F_{z_4}	0	0	1	1	0	0	1	1	0	0	0	1	1	0	1	1
F_{z_5}	1	1	0	0	1	0	0	0	1	1	1	1	0	1	0	1

In table 9 the symbol $\sim$ designates those numbers which as a result of the direct connections are indifferent, but which can realize definite operating conditions with their connection with other nodes. The functions which approach the nodes 1, 1',..., 5 from the terminal F_1 by passing those connections, for which in the future the circuits leading to the terminal F_1, must be constructed, are shown in the table by the symbol $\tilde{0}$. This means that in addition to the forbidden state, alternate paths having operating states for this same number approach the given node. Therefore, in the connecting of the circuits it is necessary to pay particular attention to this in order to avoid the appearance of false paths.

Let us separate the variable $\tilde{x}_1$, because it has a minimum of the /459
essential numbers and, consequently, a maximum of identical states. Noting that $\mathfrak{M}_{1\bar{x}_1} = \mathfrak{M}_{1x_1}$; $\mathfrak{M}_{2\bar{x}_1} = \mathfrak{M}_{D_{x_1}} = \mathfrak{M}_{2'\bar{x}_1}$; $\mathfrak{M}_{1'\bar{x}_1} \supset \mathfrak{M}_{1''x_1}$; $\mathfrak{M}_{3'\bar{x}_1} = \mathfrak{M}_{3'x_1}$; $\mathfrak{M}_{4\bar{x}_1} \supset \mathfrak{M}_{4x_1}$,

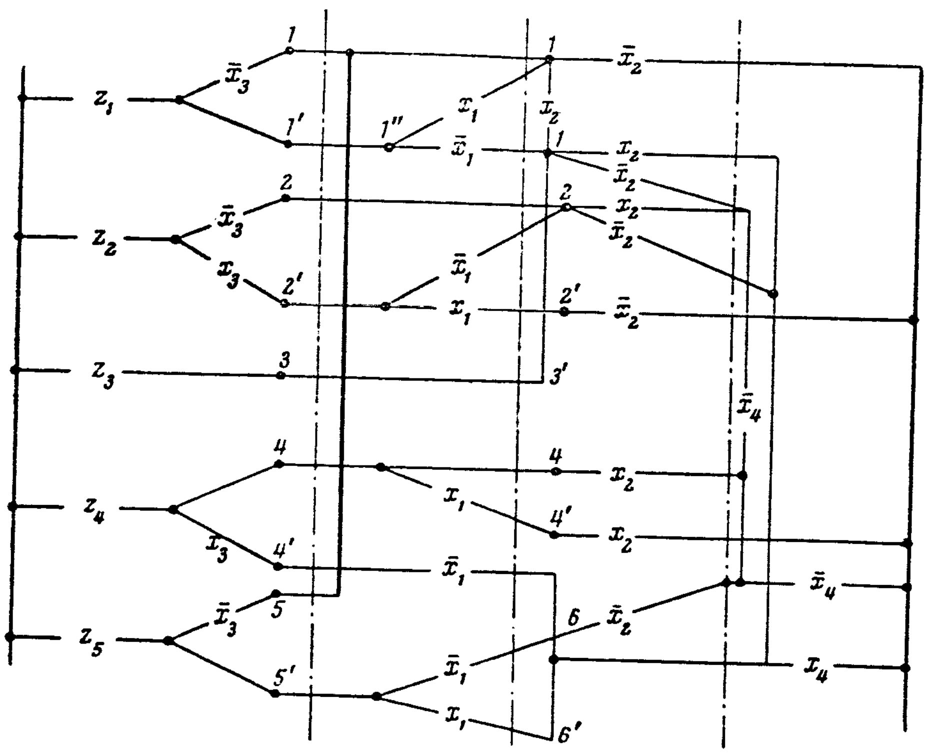

a b c d

Figure 4

we connect nodes 1 and 3, since $\mathfrak{M}_{1\bar{x}_1} = \mathfrak{M}_{3\bar{x}_1}$ with separation of $\bar{x}_1$ into the bridge. Let us connect $\mathfrak{M}_{1x_1}$ and $\mathfrak{M}_{1'x_1}$ with separation of the variable x_1 into a bridge. Furthermore, noting that $\mathfrak{M}_{1'\bar{x}_1} \supset \mathfrak{M}_{1'x_1}$, we make a direction connection from node 1'.

Noting that $\mathfrak{M}_{2\bar{x}_1} = \mathfrak{M}_{2x_1}$, we draw on the diagram (fig. 4) a direct lead from node 2; simultaneously taking into account that $\mathfrak{M}_{2\bar{x}_1} = \mathfrak{M}_{2'\bar{x}_1}$, we connect the direct lead through $\bar{x}_1$ with the point 2'.

In view of the equality $\mathfrak{M}_{1\bar{x}_1} = \mathfrak{M}_{3\bar{x}_1}$ node 3' is connected directly with node 1' and, noting that $\mathfrak{M}_{1'\bar{x}_1} = \mathfrak{M}_{3'\bar{x}_1}$, we separate $\bar{x}_1$ between nodes 1'-1". For node 4, in view of $\mathfrak{M}_{4\bar{x}_1} \supset \mathfrak{M}_{4x_1}$ we make a direct connection and simultaneously separate x_1, i.e., the set number 7 is essential. We connect node 4' through the contact $\bar{x}_1$ with node 5, and node 5' through x_1 with node 6' and, noting that $\mathfrak{M}_{4'\bar{x}_1} = \mathfrak{M}_{5'x_1}$, we connect nodes 5 and 6.

TABLE 9

NODE NO.	0	2	4	6	1	3	5	7
	$\bar{x}_4$				x_4			
1	~	~	0	0	1	~	~	~
1'	1	1	0	0	$\tilde{0}$	1	1	1
2	0	0	1	1	1	1	0	0
2'	0	1	1	0	1	1	0	0
3	~	~	0	0	1	0	~	~
3'	1	1	0	0	$\tilde{0}$	0	1	1
4	0	0	1	1	$\tilde{0}$	0	$\tilde{0}$	1
4'	0	0	~	~	1	0	1	~
5'	1	$\tilde{0}$	0	0	$\tilde{0}$	1	$\tilde{0}$	1
	$\bar{x}_1$				x_1			
1	~	0	1	~	~	0	~	~
1'	1	0	$\tilde{0}$	1	1	0	1	1
2	0	1	1	0	0	1	1	0
2'	0	1	1	0	1	0	1	0
3	~	0	1	~	~	0	0	~
3'	1	0	$\tilde{0}$	1	1	0	0	1
4	0	1	$\tilde{0}$	$\tilde{0}$	0	1	0	1
4'	0	~	1	1	0	~	0	~
5'	1	0	$\tilde{0}$	$\tilde{0}$	$\tilde{0}$	0	1	1
	$\bar{x}_2$				x_2			
1	~	1	~	~	0	~	0	~
1'	1	$\tilde{0}$	1	1	0	1	0	1
2	0	1	0	1	1	0	1	0
2'	0	1	1	1	1	0	0	0
3	~	1	~	0	0	~	0	~
3'	1	$\tilde{0}$	1	0	0	1	0	1
4	0	$\tilde{0}$	0	0	1	$\tilde{0}$	1	1
4'	0	1	0	0	~	1	~	~
5'	1	$\tilde{0}$	$\tilde{0}$	1	0	$\tilde{0}$	0	1

TABLE 10

NODE NO.	0	2	1	3
	$\bar{x}_2$		x_2	
1	1	1	0	~
1'	1	0	0	1
2	0	1	1	0
2'	1	1	0	0
3'	1	0	0	1
4	0	$\tilde{0}$	1	$\tilde{0}$
4'	0	0	~	1
5	0	1	$\tilde{0}$	1
6	1	$\tilde{0}$	0	$\tilde{0}$
6'	$\tilde{0}$	1	0	1
	$\bar{x}_4$		x_4	
1	1	0	1	~
1'	1	0	0	1
2	0	1	1	0
2'	1	0	1	0
3'	1	0	0	1
4	0	1	$\tilde{0}$	$\tilde{0}$
4'	0	~	1	1
5	0	$\tilde{0}$	1	1
6	1	0	$\tilde{0}$	$\tilde{0}$
6'	$\tilde{0}$	0	1	1

After this, constructing table 10 and carrying out the analyses described above, we will have the final circuit shown in figure 4a, b, c and d. The number of contacts in the resulting system is equal to 26. A check has shown that this number of contacts can be reduced to 25, but in this case the cascade separation of the variables is violated. /460

REFERENCES

1. Quine, W. The Problem of Simplifying Truth Functions. Am. Math. Monthly, Vol. 59, No. 8, 521, 1952.

2. McCluskey, J. Minimization of Boolean Functions. Bell. Syst. Techn. J., Vol. 35. No. 6, 1956.

3. Yablonskiy, S. V. Functional Constructions in n-Valued Logic (Funktsional'nyye postroyeniya v n-znachnoy logike). Trudy matem. in-ta im. V. A. Steklova, Izd-vo AN SSSR, 1958.

4. Gavrilov, M. A. Minimization of Boolean Functions Which Characterize Relay Circuits (Minimizatsiya bulevykh funktsiy, kharakterizuyushchikh releynyye tsepi). Avtomat. i telemekh., No. 9, 1959.

5. Roginskiy, V. N. Account for Unused States in the Synthesis of Relay-contact Circuits (Uchet neispol'zuyemykh sostoyaniy pri sinteze releyno-kontaktnykh skhem). Avtomat. i telemekh. Vol. 15, No. 3, 1954.

6. Zhuravlev, Yu. I. Separability of the Subsets of the Vertices of a Dimensional Unit Cube (Ob otdelimosti podmnozhestv vershin mernogo yedinichnogo kuba). Trudy matem. in-ta im. V. A. Steklova, Izd-vo AN SSSR, 1958.

7. Roginskiy, V. N. Elements of Structural Synthesis of Relay Control Circuits (Elementy strukturnogo sinteza releynykh skhem upravleniya). Izd-vo AN SSSR, 1959.

8. Zhuravlev, Yu. I. Various Concepts of the Minimality of Disjunctive Normal Forms (O razlichnykh ponyatiyakh minimal'nosti diz"yunktivnykh normal'nykh form). Izd-vo AN SSSR, Sibirskiy matematicheskiy zhurnal, Vol. 1, No. 4, 1960.

N66 34855

REALIZATION OF BOOLEAN FUNCTIONS AND VARIABLES ON CONTACTLESS LOGIC SWITCHES BY THE METHOD OF REDEFINITION

V. D. Kazakov and V. V. Naumchenko

Recently, in connection with the rapid development of computer technology and the increasingly complex devices of digital automation and remote control, the questions of the realization of the Boolean expressions have taken on exceptional importance. /461

However, the known methods for the construction of switching circuits corresponding to the complex Boolean expressions for a large number of variables require a very large number of relay elements (electron tubes, semiconductor elements, electromechanical relay contacts, and so on). In actuality, for the realization of a Boolean function we usually find its minimal (normal or bracketed) expression and then realize it with the aid of a collection of AND, OR, NOT logic elements.

Thus, for the realization of the symmetric function S_{10} (0, 2, 4, 6, 8)

of ten variables with the operating numbers 0, 2, 4, 6, 8 in the normal expression it would require 5,120 transistors or diodes and 513 resistors (with the realization of the minimal bracketed expression this function would require no less than 1,534 transistors or diodes). Therefore, until the present the complex functions, as a rule, have been realized by using electromechanical relays, which naturally has a negative effect on the response speed of the entire device.

The present paper proposes a different approach to the synthesis of relay circuits. It is known that in practice, particularly in the synthesis of multicyclic circuits, we are dealing either with ordered Boolean functions (symmetrical, for example) or with "incompletely defined" functions, i.e., functions whose values are not defined on all constituents. By "redefining" such functions we can bring them to a form which is convenient in some sense for us. In this direction redefinition to symmetric functions or to functions of the same class as the symmetric functions is very promising.

The realization of the symmetrical functions on contactless models of abstract neurons gives the possibility of realizing complex functions using a very small number of switching elements. More briefly, the AND and OR logic is replaced by the logic of the abstract neurons with a variable excitation threshold. This expansion of the logical techniques opens up new perspectives for the minimization of the Boolean functions.

1. Reduction of the State Table to a Form Convenient for Realization[1] /462

Redefinition of Functions to Symmetric Form

The probability that an arbitrarily given function is symmetrical can be computed approximately as the ratio of the number of symmetrical functions to the total number of functions of n variables

$$P_0 = \frac{2^{n+1}}{2^{2^n}}.$$

It is obvious that P_0 diminishes rapidly with increase of n. However, the number of "unused" states also usually increases rapidly with increase of n. Consequently, if we are dealing with "incompletely defined" functions having K "occupied" constituents, P_1 is increased correspondingly

$$P_1 = \frac{2^{n+1} \cdot 2^{(2^n - K)}}{2^{2^n}}.$$

Consequently, $P_1 = 1$ with $K = n + 1$.

Redefinition to Functions of the Same Class as Symmetrical

Redefinition to functions of the same class as symmetrical functions already requires a smaller number of unused states. The probability that an arbitrarily given function can be redefined to a function of the same class as a symmetrical function can be roughly represented as the ratio of the entire number of classes of the Boolean functions to the number of classes of the symmetrical functions[2]

$$P_2 = \frac{2^{n+1} \cdot 2^{(2^n - k)}}{\frac{2^{2^n - n}}{n!}} = \frac{n!}{2^{K-2n-1}}.$$

Whence $P \approx 1$ with $n = 4$ and $K = 14$, with $n = 6$ and $K = 23$, and with $n = 10$ and $K = 43$.

In the first and second case the redefinition procedure is very simple. To do this, we compose the table of operating and forbidden states and calculate

---

[1] Section 1 written by V. D. Kazakov.

[2] Here it is assumed that the power of the classes of all functions and of the classes of symmetric functions is approximately the same.

the weights of each row (i.e., the number of ones in each row). If the weights of the rows of the operating states do not coincide with the weights of the rows of the forbidden states, this means that the given conditions of operation can be expressed by symmetrical functions, whose operating numbers will be the weights of the rows of the operating states.

For example, in table 1 the weights of the operating states 2 and 4 do not have equals among the weights of the forbidden states 0, 1 and 3. In this case the given conditions of operation can be expressed by the symmetrical function

$$S_{2,4}(X_1, X_2, X_3, X_4).$$

For the redefinition of the given conditions of operation to a function of the same class as the symmetrical function we must perform the inversion of the columns (in all 2^n combinations) and must compare after each inversion /463
the weights of the rows of the operating and forbidden states (table 2).

If with some combination of the inverted columns the weights of the operating and forbidden states are found to be different, this will indicate that the obtained state table can be expressed (more precisely, redefined) in terms of a symmetrical function, as was done above. This means also that by inverting the corresponding inputs we can realize the given state table with the aid of a single symmetrical function.

TABLE 1

X_1	X_2	X_3	X_4	
0	1	1	0	2
0	1	0	1	2
1	0	0	1	2
1	1	1	1	4
0	0	0	0	0
1	0	0	0	1
1	1	1	0	3

TABLE 2

X_1	X_2	X_3	X_4		$\bar{X}_1$	X_2	X_3	X_4	
1	0	0	0	1	0	0	0	0	0
1	0	0	1	2	0	0	0	1	1
1	0	1	0	2	0	0	1	0	1
1	1	0	0	2	0	1	0	0	1
0	0	0	0	0	1	0	0	0	1
0	0	0	1	1	1	0	0	1	2
0	1	0	0	1	1	1	0	0	2

Redefinition by Exclusion of Inessential Variables

In some cases it will be possible to reduce the given state table to the symmetrical form by excluding rows with inessential variables. Thus, for example, the state table (table 3) after elimination of the column of the inessential variable X_2 can be expressed by the symmetrical function $S_{2,3}(X_1, X_3, X_4)$. It is evident that this expansion of the means for the conversion of the state table to the desired form gives us the possibility of further reduction of the number of unused states necessary for the redefinition.

For a verification of the possibility of the redefinition of the given state table to the symmetrical form we must perform 2^n exclusions of rows, with subsequent comparison of the weights of the rows of the operating (forbidden) states. /465

TABLE 3

X_1	X_2	X_3	X_4		Without X_2
0	0	1	1	2	2
1	1	0	1	3	2
1	0	1	0	2	2
1	1	1	1	4	3
0	1	0	1	2	1
0	1	1	0	2	1

Representation of a Given State Table by a Complex Symmetrical Function

By a complex symmetrical function in the present case we mean a symmetrical function with variables which can also be symmetrical functions. It is apparent that redefinition to this form of functions presents the greatest practical difficulty, although it also is the most universal means for the representation of an arbitrarily given state table in terms of a function of symmetrical form. The possibility of the representation of any state table in terms of symmetrical functions (with the assumption of inversion of the variables in them, i.e., of the inputs) is easy to perceive by the fact that any formula of predicate calculus can be expressed in terms of the operations AND $[S_2(X_1, X_2)]$, OR $[S_{1,2}(X_1, X_2)]$, and inversion. However, the problem of the most economical (in the sense of the number of elements) representation of a given function in terms of symmetrical functions is not trivial. We shall indicate only the simplest case of redefinition to the complex symmetrical function.

Expansion of a Given Table Using Separate Variables. In this case we partition the given table into 2^p subtables (where p is the number of variables in which the expansion is performed) and then we attempt to express each of the tables in terms of a symmetrical function.

TABLE 4

(a)

X_1	X_2	X_3	X_4	
0	0	0	0	0
0	0	0	1	1
0	0	1	0	1
0	1	0	1	2
0	1	1	0	2
1	0	1	1	3
1	0	1	0	2
1	0	0	1	2
1	1	1	1	4
0	1	1	1	3

(b)

X_2	X_1	X_3	X_4			X_2	X_1	X_3	X_4	
0	0	0	0	0		1	0	0	1	2
0	0	0	1	1	+	1	0	1	0	2
0	0	1	0	1						
0	1	1	1	3						
0	1	1	0	2		1	1	1	1	4
0	1	0	1	2		1	0	1	1	3

Let, for example, there be given the table of combinations shown in table 4a. Making an expansion of the table in the variable X_2, we obtain the two subtables 4b which are easily redefined to the symmetrical form.

Thus the given state table can be expressed by the complex symmetrical function /466

$$S_1\{S_2[S_{0,1,3}(X_1, X_3, X_4), X_2], S_2[S_1(X_1, X_3, X_4), X_2]\}.$$

These methods for the expression of state tables in terms of symmetrical functions and functions of the same class as the symmetrical are naturally not a complete listing of all possible simplifications. Our task consisted only in turning attention to this approach for minimization of relay structures, in which by means of the unused states the table is expressed in terms of some "ordered" function. We believe that this approach can prove itself in the synthesis of various sorts of decoders, distributors, counter cells and in the synthesis of circuits with a large (more than 8-10) number of variables, where as a rule we have a large number of unused states.

2. Realization of Symmetrical Boolean Functions of n Variables on Logic Switches[1]

As follows from the preceding section, a large portion of the Boolean functions of n variables which are used in practice can be, in the case of large n, reduced to symmetrical functions, if the number of unused states is sufficiently high.

In the realization of the functions of this class using the standard AND, OR and NOT elements, the characteristics of this class are hardly utilized. The resulting circuits are therefore very unwieldy. It is obvious that for the realization of the symmetrical functions we should make use of elements which also have (in some sense) the properties of symmetry. Such elements include, in particular, the McCullough-Pietz neurons having only excitatory filaments, which hereafter we shall term mixers.

As is known, the function realized by this neuron has the form

$$F(X_1, \ldots, X_k) = \sum_{j=p}^{k} S_j(X_1, \ldots, X_k),$$

where p is the neuron threshold, which is independent of the input variables; $S_j(X_1, \ldots, X_k)$ is the fundamental symmetrical function of index j.

With the realization of the symmetrical functions using elements of this form, with the condition of the use of still another element which is the Culbertson nerve cell with asymmetrical inputs, the following theorem is valid.

THEOREM 1. Any symmetrical function of n variables can be realized by a logic switch containing $E\left(\frac{n+1}{2}\right)$ mixers and one converter.

Any symmetrical function can be represented in the form of the sum of the fundamental symmetrical functions.

Let us prove theorem 1 for the very "worst" symmetrical function

$$F(X_1, X_2, \ldots, X_n) = \sum_{j=1}^{E\left(\frac{n+1}{2}\right)} S_{2j-1}(X_1, \ldots, X_n).$$

Let us consider the circuit of figure 1. On this diagram C_{2j} are mixers with the threshold $p = 2j$, $j = 1, \ldots, E\left(\frac{n+1}{2}\right)$; P_1 is a converter whose /467
threshold $p = 1$. The outputs of the mixers are applied to the inhibiting

[1] Section 2 was written by V. V. Naumchenko.

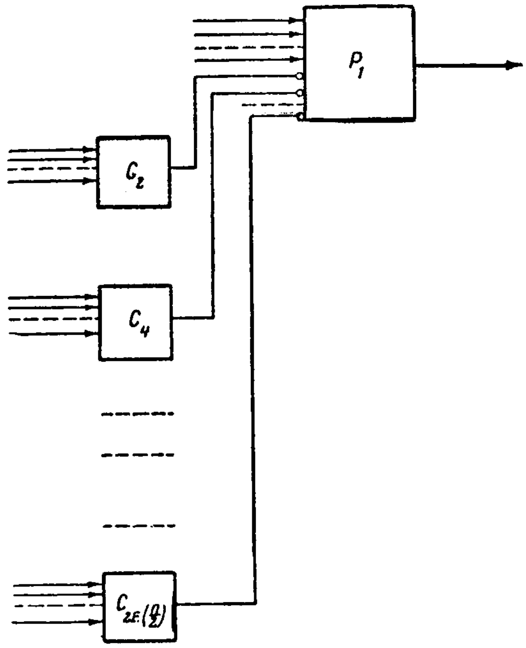

Figure 1

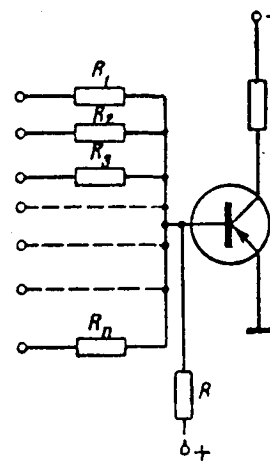

Figure 2

input filaments of the converter, the input variables are applied to the excitatory input filaments. The weight of each inhibitory filament is equal to two.

Thus the total weight of the excited inhibitory filaments of the converter with excitation of 2j input filaments of the mixers will also be equal to 2j. Consequently, the output of the converter will not be excited, because $k < l + p$ ($p = 1$, $k = l = 2j$). With excitation of an odd number of input filaments, the output of the converter will be excited, because $k = 2j + 1$ and, consequently, $k = l + p$, i.e., the excitation conditions are satisfied.

It is easy to see that any other symmetrical function $F(x_1, \ldots, x_n)$ is realized on the switch in which the number of mixers is less than or equal to $E\left(\frac{n+1}{2}\right)$.

The physical realization of the mixers can be accomplished with the most varied elements: magnetic cores, semiconductor triodes, etc.

Figure 2 shows the functional diagram of a mixer made with a transistor. This circuit operates stably with a number of input variables up to 10, and with certain limitations up to 15-20. Connection of these elements with others can be either capacitive or direct. The latter has certain advantages.

A symmetric function of ten variables: $F(X_1, \ldots, X_{10}) = S_{2,4,6,8,10}(X_1, \ldots, X_{10})$ was realized with elements of this form. The circuit contains

five type P15 transistors and 64 resistors. It operates with deviations of the supply voltage from nominal of ± 3 percent. For mixers whose threshold is equal to seven and higher, it is necessary to use resistors with a scatter of no more than 3 percent. With the use of silicon transistors (P101-P106), the circuit can operate stably with temperature variations from -15°C to + 55°C.

N66 34856

MINIMAL FORMS OF SYMMETRICAL BOOLEAN FUNCTIONS OF ANY NUMBER OF VARIABLES

V. D. Kazakov

The synthesis of relay systems involves the preliminary minimization /468 of the Boolean expressions describing the operating conditions of the circuits. The process of finding the minimal normal expressions (i.e. expressions of the form sp--sum of products, or ps--product of sums) usually presents considerable difficulty. However, in certain cases we can establish ahead of time that the function being minimized is symmetrical from the canonical representation of the function. Then the minimization process can be considerably simplified.

The present paper describes a method for directly obtaining the minimal normal forms of symmetrical functions which are given in the canonical representation or simply by the indication of the variables and indices ("operating numbers") of the function, and presents the required proofs.

Let us consider finding the sp-minimal forms of Boolean functions given in the canonical sp-form, since finding the ps-minimal forms of the Boolean functions given in the ps-form is an operation which is symmetrical relative to the signs · and +, while the case of finding the sp-minimal forms [from the canonical] ps-form and finding the ps-minimal forms from the canonical sp-form reduce to the first case by means of inversion, respectively, of the resulting minimal forms of the complement of the original function or of the complement itself.

Let us use $\mathfrak{A}_n(a_i, 0)$ to denote the group of elementary products consisting of a_i variables without negation and corresponding to all possible combinations of a_i with respect to n.

Similarly, let us use $\mathfrak{A}_n(0, a_j)$ to denote the group of elementary products consisting of a_j variables with negations and corresponding to all possible combinations of a_j with respect to n.

We shall consider that the elementary product A occurs in the elementary product B (notation[1] $A \subseteq B$), if B can be expressed as Ax, where x is the product of the variables not contained in A (in the case $A \doteq B$, x = 1).

[1]There is a difference between symbols $\in$ which is the inclusion of an element in a set and $\subset$ which is the occurrence of a portion of a set in a whole set.

Let $\mathfrak{F}_n(a_i, a_n - a_i)$ denote the fundamental symmetrical function of the n variables of index a_i.

It follows directly from the definition of the fundamental symmetrical function that each of the products $\Phi, [\Phi \in \mathfrak{F}_n(a_i, a_n - a_i), \mathfrak{F}_n(a_{i+1}, a_n - a_{i+1}), \ldots,$ $\mathfrak{F}_n, (a_n, 0)]$ has at least one corresponding product $A\,[A \in \mathfrak{A}_n(a_i, 0)]$, such that /469 $A \subseteq \Phi$, and, correspondingly, each of the products $\Phi', [\Phi' \in \mathfrak{F}_n(a_n - a_j, a_j),$ $\mathfrak{F}_n(a_n - a_{j+1}, a_{j+1}), \ldots, \mathfrak{F}_n(0, a_n)]$ has at least one corresponding product $A'\,[A' \in$ $\mathfrak{A}_n(0, a_j)]$, such that $A' \subset \Phi'$.

Let us denote by $\mathfrak{B}_n(a_i, a_j)$ that collection of nonrepeating elementary products[1] in which there is at least one product whose positive part[2] corresponds to any combination of n of the a_i, and at least one product whose negative part corresponds to any combination of n of the a_j, i.e., to each positive part $B\ [B \in \mathfrak{B}_n(a_i, a_j)]$ there corresponds one of the products $A\ [A \in \mathfrak{A}_n(a_i, 0)]$, and to each negative part B there corresponds one of the products $A'\,(A' \in \mathfrak{A}_n(0, a_j))$. At the same time, to each of the products $A\,[A \in \mathfrak{A}_n(a_i, 0)]$ there corresponds at least one positive part of $B\,[B \in \mathfrak{B}_n(a_i, a_j)]$, and to each of the products $A'\,[A' \in \mathfrak{A}_n(0, a_j)]$ there corresponds at least one negative part of $B\,[B \in \mathfrak{B}_n(a_i, a_j)]$.

It is evident that $\mathfrak{B}_n(a_i, a_j) \subseteq \mathfrak{A}_n(a_i, a_j)$.

Similar to the preceding, it follows from the definition of $\mathfrak{B}_n(a_i, a_j)$ that each of the products $\Phi\,[\Phi \in \mathfrak{F}_n(a_i, a_n - a_i), \mathfrak{F}_n(a_{i+1}, a_n - a_{i+1}), \ldots, \mathfrak{F}_n(a_n - a_j, a_j)]$ will have at least one product $B\,[B \in \mathfrak{B}_n(a_i, a_j)]$, corresponding to it, such that $B \subset \Phi$.

THEOREM: The Boolean function consisting of the sum of the products of Φ groups $\mathfrak{F}_n(a_i, a_n - a_i), \mathfrak{F}_n(a_{i+1}, a_n - a_{i+1}), \ldots, \mathfrak{F}_n(a_n - a_j, a_j)$ is equivalent to the function consisting of the sum of the products of the B group $\mathfrak{B}_n(a_i, a_j)$.

---

[1] By elementary products we mean those Boolean products in which each factor is one letter and in each product the variable is used no more than once.

[2] The positive part of the product is comprised of variables with negation in the given product.

Let us prove the theorem on the basis of the correspondence between the Boolean and logical functions.

At least one of the products $\mathfrak{F}_n(a_i, a_n - a_i), \ldots, \mathfrak{F}_n(a_n - a_j, a_j)$ occurs in each product of the groups $\mathfrak{B}_n(a_i, a_j)$, while each product of $\mathfrak{B}_n(a_i, a_j)$ occurs in the products of the group $\mathfrak{F}_n(a_i, a_n - a_i), \ldots, \mathfrak{F}_n(a_n - a_j, a_j)$ and only in them.

Since $A \subseteq B$ (occurrence) indicates $A \to B$ (implication) and it is known that the sum of the elementary conjunctions which imply certain terms of the disjunctive principal normal form of functions (and only them) is equivalent to the function represented by these terms, the theorem is proved.

Let us consider now in more detail the group of products $\mathfrak{B}_n(a_i, a_j)$. It is easy to see that it is defined uniquely only for the cases when $C_n^{a_i} = C_n^{a_j}$, i.e., when

$$
\begin{aligned}
&1)\ a_i = 0 \quad (C_n^0 = C_n^n);\\
&2)\ a_j = 0 \quad (C_n^n = C_n^0);\\
&3)\ a_i + a_j = a_n\,(C_n^{a_i} = C_n^{a_n - a_j}).
\end{aligned}
$$

For other values of a_i and a_j, the group $\mathfrak{B}_n(a_i, a_j)$ can be represented by a different number of products. Their maximal number max $\mathfrak{B}_n(a_i, a_j)$ is equal to $C_n^{a_i} \cdot C_n^{a_j}$. In this case all admissible combinations of products from max $\mathfrak{B}_n(a_i, a_j)$ with the products from $\mathfrak{A}_n(a_i, 0)$ occur in $\mathfrak{A}_n(0, a_j)$. In view of the uniqueness of the value of $C_n^{a_i+a_j} \cdot C_{a_i+a_j}^{a_i}$ the collection max $\mathfrak{B}_n(a_i, a_j)$ must be unique.

It also follows from the definition that the minimal representation min $\mathfrak{B}_n(a_i, a_j)$ cannot be smaller than one of the combinations $C_n^{a_i}$ or $C_n^{a_j}$, i.e., the number of terms of the group $\min \mathfrak{B}_n(a_i, a_j) = \max[C_n^{a_i}, C_n^{a_j}]$. It is evident /470 that in the case $C_n^{a_i} > C_n^{a_j}$ the group $\min \mathfrak{B}_n(a_i, a_j)$ is the collection of nonrepeating products whose positive part corresponds to the nonrepeating combinations of n of a_i, and the negative part corresponds to each combination of n of the a_j, where in view of the necessity to have the same number of positive and negative parts of the products and in view of the inequality $C_n^{a_i} > C_n^{a_j}$ in the second (negative) part there will be repeating nonuniquely

defined cofactors. In the case $C_n^{a_i} < C_n^{a_j}$ there will be repeating nonuniquely defined positive cofactors.

This fact leads to the nonuniqueness of the representation of $\min \mathfrak{V}_n(a_i, a_j)$.

COROLLARY 1. The minimal sp-expression of the symmetrical functions having the canonical representation

$$\mathfrak{F}_n(a_{i_1}, a_n - a_{i_1}) + \mathfrak{F}_n(a_{i_1+1}, a_n - a_{i_1+1}) + \ldots + \mathfrak{F}_n(a_{i_1+p_1}, a_n - a_{i_1+p_1}) +$$
$$+ \mathfrak{F}_n(a_{i_2}, a_n - a_{i_2}) + \mathfrak{F}_n(a_{i_2+1}, a_n - a_{i_2+1}) + \ldots + \mathfrak{F}_n(a_{i_2+p_2}, a_n - a_{i_2+p_2}) + \ldots +$$
$$+ \mathfrak{F}_n(a_{i_k}, a_n - a_{i_k}) + \mathfrak{F}_n(a_{i_k+1}, a_n - a_{i_k+1}) + \ldots + \mathfrak{F}_n(a_{i_k+p_k}, a_n - a_{i_k+p_k}),$$

is identical to the sum of the minimal representations of the groups

$$\min \mathfrak{V}_n(a_{i_s}, a_n - a_{i_s+p_s}),$$

where s = 1,..., k, i.e., it has the form

$$\min \mathfrak{V}_n(a_{i_1}, a_n - a_{i_1+p_1}) + \min \mathfrak{V}_n(a_{i_2}, a_n - a_{i_2+p_2}) + \ldots$$
$$\ldots + \min \mathfrak{V}_n(a_{i_k}, a_n - a_{i_k+p_k}).$$

COROLLARY 2. The minimal form of the symmetrical functions whose minimal form is $\mathfrak{A}_n(a_i, 0)$, $\mathfrak{A}_n(0, a_j)$, $\mathfrak{F}_n(a_i, a_n - a_i)$, is identical to the minimal form, i.e.,

$$\max \mathfrak{V}_n(a_i, 0) \equiv \min \mathfrak{V}_n(a_i, 0);$$
$$\max \mathfrak{V}_n(0, a_j) \equiv \min \mathfrak{V}_n(0, a_j);$$
$$\max \mathfrak{V}_n(a_i, a_n - a_i) \equiv \min \mathfrak{V}_n(a_i, a_n - a_i).$$

COROLLARY 3. The minimal form of the symmetrical functions (except for those stipulated in corollary 1) is not uniquely determined, i.e., there are several minimal forms for a single function.

COROLLARY 4. Knowing the form of the minimal forms of the symmetrical functions, we can determine the number of minimal forms of a single function.

To do this we must solve the combinatorial problem.

THE COMBINATORIAL PROBLEM. Assume that there are two groups of combinations C_n^a and C_n^b and that $C_n^a > C_n^b$. We are required to determine in how many ways we can compose C_n^a sets, in each of which there occurs one of the

combinations C_n^a (and there will not be any combination which occurs in more than one set) and one of the combinations of the group C_n^b (where one combination from the group C_n^b can occur in several sets, but each of them must occur in at least one set).

Moreover (in view of the elementary nature of the products $\mathfrak{B}_n(a, b)$), in the combinations C_n^a and C_n^b, which occur in a single set, there cannot be identical variables (having in mind that the combinations C_n^a and C_n^b are composed from the variables n). The problem is formulated similarly with $C_n^a < C_n^b$.

The number of such sets with given values of n, a and b (with n ≤ 5) and the lower estimate of this number with n > 5 is given by equations /471

$$(n-a)^{C_n^a} - (n-a)^{n-1} n \qquad (\text{ with } a > b);$$

$$(n-b)^{C_n^b} - (n-b)^{n-1} n \qquad (\text{ with } b > a).$$

Thus, finding the maximum of the number of sets K_{max} with given values of $n (n \leqslant 5)$ and the lower estimate of this number with n > 5 reduces to finding

$$K_{\max} = \max [(n-a)^{C_n^a} - (n-a)^{n-1} n]$$

with variable $a (a \leqslant n)$.

The numerical values are

$$K_{\max}^0 = 1; \quad K_{\max}^3 = 6; \quad K_{\max}^6 \geqslant 26\,624.$$
$$K_{\max}^1 = 1; \quad K_{\max}^4 = 32; \quad K_{\max}^{10} \geqslant 2^{12}(2^{39} - 10) \approx 10^{15}.$$
$$K_{\max}^2 = 1; \quad K_{\max}^5 = 704.$$

EXAMPLE 1. Let there be given the symmetrical function $S_6(0, 1, 2, 5)$ of the six variables a, b, c, d, e, f, which consists of the sum of the fundamental symmetrical functions of the indices 0, 1, 2, 5.

We are required to determine its minimal sp- and ps-expressions.

(a) Let us determine first the minimal sp-expressions. The given function consists of two arrays of fundamental symmetric functions: $\mathfrak{F}_6(0, 6)$, $\mathfrak{F}_6(1, 5)$, $\mathfrak{F}_6(2, 4)$ and $\mathfrak{F}_6(5.1)$.

Let us find the minimal expressions for the array $\mathfrak{F}_6(0. 6)$, $\mathfrak{F}_6(1. 5)$, $\mathfrak{F}_6(2. 4)$. According to the theorem just proved, $\mathfrak{B}_n(a_i, a_j)$ takes the form $\mathfrak{B}_6(0. 4)$. The group $\mathfrak{A}_n(a_i, 0)$ is empty in view of $a_i = 0$. The group $\mathfrak{A}_n(0, a_j)$ takes the form $\mathfrak{A}_6(0. 4) = \{\overline{abcd}, \overline{abce}, \overline{abde}, \overline{acde}, \overline{bcde}, \overline{abcf}, \overline{abde}, \overline{acdf}, \overline{bcdf}, \overline{abef}, \overline{acef}, \overline{bcef}, \overline{bdef}, \overline{cdef}\}$.

According to corollary 2, $\min \mathfrak{B}_n(0, a_j) \equiv \mathfrak{A}_n(0, a_j)$; consequently, the minimal expression for the first array will have the form of the sum of all products occurring in $\mathfrak{A}_6(0, 4)$.

Now let us determine the minimal sp-expressions $\mathfrak{F}_6(5. 1)$.

According to corollary 2, $\min \mathfrak{B}_6(5. 1) \equiv \mathfrak{F}_6(5. 1) = \{abcde\bar{f}, abcd\bar{e}f, abc\bar{d}ef, ab\bar{c}def, a\bar{b}cdef, abcd\overline{ef}\}$.

Whence the minimal expression for the given function has the form

$$\begin{aligned}\min S_6(0, 1, 2, 5) &= \min \mathfrak{B}_6(0.4) + \min \mathfrak{B}_6(5. 1) = \\ &= \overline{abcd} + \overline{abce} + \overline{abde} + \overline{acde} + \overline{bcde} + \overline{abcf} + \overline{abdf} + \\ &+ \overline{acdf} + \overline{bcdf} + \overline{abef} + \overline{acef} + \overline{bcef} + \overline{adef} + \overline{bdef} + \\ &+ \overline{cdef} + abcde\bar{f} + abcd\bar{e}f + abc\bar{d}ef + ab\bar{c}def + a\bar{b}cdef + \bar{a}bcdef.\end{aligned}$$

In the present case the minimal sp-expression for the given function has a unique representation, in view of the uniqueness of the representations $\mathfrak{B}_6(0. 4)$ and $\mathfrak{B}_6(5. 1)$.

(b) Now let us determine the minimal ps-expressions $S_6(0, 1, 2, 5)$. /472

To do this we find the minimal sp-expressions $S_6(3, 4)$ and, inverting them, we obtain the ps-minimal expressions $S_6(0, 1, 2, 5)$.

The minimal sp-expressions for the array $\mathfrak{F}_6(3, 3)$, $\mathfrak{F}_6(4, 2)$ have the form $\min \mathfrak{B}_6(3, 2)$, i.e., they are the sums of the products composed from the products of the groups $\mathfrak{A}_6(3, 0)$, $\mathfrak{A}_6(0,2)$:

$\mathfrak{A}_6(3,0) = \{abc,\ abd,\ abe,\ ace,\ bce,\ ade$ and so on (in all $C_6^3 = 20$ products) $\}$;

$\mathfrak{A}_6(0,2) = \{ab,\ ac,\ ad,\ ae,\ af,\ bc,\ bd$ and so on (in all $C_6^2 = 15$ products) $\}$.

In view of corollary 2 we have the nonuniqueness of the representation $\min \mathfrak{B}_6(3,2)$

$$\begin{aligned}\min \mathfrak{B}_6(3,2) &= abc\bar{e}\bar{f} + abd\bar{c}\bar{e} + abe\bar{d}\bar{f} + abf\bar{d}\bar{e} + acd\bar{b}\bar{e} + ace\bar{b}\bar{f} + acf\bar{b}\bar{d} + abe\bar{b}\bar{c} + \\ &+ adf\bar{b}\bar{c} + aef\bar{b}\bar{c} + bcd\bar{a}\bar{f} + bce\bar{a}\bar{f} + bcf\bar{a}\bar{d} + bde\bar{c}\bar{f} + bdf\bar{a}\bar{c} + bef\bar{c}\bar{d} + cde\bar{a}\bar{f} + \\ &+ cdf\bar{a}\bar{e} + cef\bar{a}\bar{d} + def\bar{a}\bar{b} = abc\bar{e}\bar{f} + abd\bar{c}\bar{e} + abe\bar{d}\bar{f} + abf\bar{d}\bar{e} + acd\bar{b}\bar{e} + ace\bar{b}\bar{f} + \\ &+ acf\bar{b}\bar{d} + ade\bar{b}\bar{c} + adf\bar{b}\bar{c} + aef\bar{b}\bar{c} + bcd\bar{a}\bar{e} + bce\bar{a}\bar{f} + bcf\bar{a}\bar{e} + bde\bar{c}\bar{f} + bdf\bar{a}\bar{e} + \\ &+ befcd + cde\bar{a}\bar{f} + cdf\bar{a}\bar{e} + cef\bar{a}\bar{d} + def\bar{a}\bar{b} = \dots\end{aligned}$$

Whence the minimal ps-expressions for the original function will be

$$\begin{aligned}\min \mathfrak{B}_6(0,1,2,5) &= (\bar{a}+\bar{b}+\bar{c}+e+f)(\bar{a}+\bar{b}+\bar{d}+c+e)\times \\ &\times(\bar{a}+\bar{b}+\bar{e}+d+f)(\bar{a}+\bar{b}+\bar{f}+d+e)(\bar{a}+\bar{c}+\bar{d}+b+e)(\bar{a}+\bar{c}+\bar{e}+b+f)\times \\ &\times(\bar{a}+\bar{c}+\bar{f}+b+d)(\bar{a}+\bar{d}+\bar{e}+b+c)(\bar{a}+\bar{d}+\bar{f}+b+c)(\bar{a}+\bar{e}+\bar{f}+b+c)\times \\ &\times(\bar{b}+\bar{c}+\bar{d}+a+f)(\bar{b}+\bar{c}+\bar{e}+a+f)(\bar{b}+\bar{c}+\bar{f}+a+d)(\bar{b}+\bar{d}+\bar{e}+c+f)\times \\ &\times(\bar{b}+\bar{d}+\bar{f}+a+c)(\bar{b}+\bar{e}+\bar{f}+c+d)(\bar{c}+\bar{d}+\bar{e}+a+f)(\bar{c}+\bar{d}+\bar{f}+a+e)\times \\ &\times(\bar{c}+\bar{e}+\bar{f}+a+d)(\bar{d}+\bar{e}+\bar{f}+a+b) = (\bar{a}+\bar{b}+\bar{c}+e+f)(\bar{a}+\bar{b}+\bar{d}+c+e)\times \\ &\times(\bar{a}+\bar{b}+\bar{e}+d+f)(\bar{a}+\bar{b}+\bar{f}+d+e)(\bar{a}+\bar{c}+\bar{d}+b+e)(\bar{a}+\bar{c}+\bar{e}+b+f)\times \\ &\times(\bar{a}+\bar{c}+\bar{f}+b+d)(\bar{a}+\bar{d}+\bar{e}+b+c)(\bar{a}+\bar{d}+\bar{f}+b+c)(\bar{a}+\bar{e}+\bar{f}+b+c)\times \\ &\times(\bar{b}+\bar{c}+\bar{d}+a+e)(\bar{b}+\bar{c}+\bar{e}+a+f)(\bar{b}+\bar{c}+\bar{f}+a+e)(\bar{b}+\bar{d}+\bar{e}+c+f)\times \\ &\times(b+d+f+a+e)(\bar{b}+\bar{e}+\bar{f}+c+d)(\bar{c}+\bar{d}+\bar{e}+a+f)(\bar{c}+\bar{d}+\bar{f}+a+e)\times \\ &\times(\bar{c}+\bar{e}+\bar{f}+a+d)(\bar{d}+\bar{e}+\bar{f}+a+b) = \dots\end{aligned}$$

EXAMPLE 2. Let there be given the function $S_4(0,2,3)$ of the variables a, b, c, d. We are required to find the minimal sp-expressions for this function.

We have the two arrays $\mathfrak{F}_4(0,4)$ and $\mathfrak{F}_4(2,2)$, $\mathfrak{F}_4(3,1)$. The minimal expression of the first array is

$$\min \mathfrak{F}_4(0,4) \equiv \min \mathfrak{B}_4(0,4) \equiv \mathfrak{A}_4(0,4) = \{\bar{a}\bar{b}\bar{c}\bar{d}\}.$$

The minimal expression of the second array is /473

$$\min\{\mathfrak{F}_4(2,2), \mathfrak{F}_4(3,1)\} \equiv \min \mathfrak{B}_4(2,1).$$

The representation of $\min \mathfrak{B}_6(2,1)$ is nonunique in view of the different number of products occurring in the groups $\mathfrak{A}_4(2,0)$ and $\mathfrak{A}_4(0,1)$ (corollary 2)

$$\mathfrak{A}_4(2,0) = \{ab, ac, ad, bc, bd, cd\};$$
$$\mathfrak{A}_4(0,1) = \{\overline{a}, \overline{b}, \overline{c}\,\overline{d}\}.$$

Whence $\min \mathfrak{B}_4(2,1)$ has the expressions $ab\bar{c} + ac\bar{d} + ad\bar{b} + bc\bar{a} + bd\bar{a} + ab\bar{c} + ac\bar{d} + ad\bar{b} + bc\bar{a} + bd\bar{a} + cd\bar{b} = ab\bar{c} + ac\bar{d} + ad\bar{b} + bc\bar{d} + bd\bar{c} + cd\bar{a} = ab\bar{c} + ac\bar{d} + ad\bar{b} + bc\bar{d} + bd\bar{a} + cd\bar{a} = \ldots$ and so on (32 expressions in all).

Whence the minimal sp-expressions are $S_4(0,2,3) = \min \mathfrak{B}_4(0,4) + \min \mathfrak{B}_4(2,1) = \bar{a}\bar{b}\bar{c}\bar{d} + ab\bar{c} + ac\bar{d} + ad\bar{b} + bc\bar{a} + bd\bar{a} + cd\bar{a} = \bar{a}\bar{b}\bar{c}\bar{d} + ab\bar{c} + ac\bar{d} + ad\bar{b} + bc\bar{a} + bd\bar{a} + cd\bar{b} = \bar{a}\bar{b}\bar{c}\bar{d} + ab\bar{c} + ac\bar{d} + ad\bar{b} + bc\bar{a} + bd\bar{c} + cd\bar{a} = \bar{a}\bar{b}\bar{c}\bar{d} + ab\bar{c} + acd + ad\bar{b} + bc\bar{d} + bd\bar{a} + cd\bar{a} = \ldots$
and so on (32 variants in all).

Translated for the National Aeronautics and Space Administration
by John F. Holman and Co. Inc.

"The aeronautical and space activities of the United States shall be conducted so as to contribute . . . to the expansion of human knowledge of phenomena in the atmosphere and space. The Administration shall provide for the widest practicable and appropriate dissemination of information concerning its activities and the results thereof."

—NATIONAL AERONAUTICS AND SPACE ACT OF 1958

NASA SCIENTIFIC AND TECHNICAL PUBLICATIONS

TECHNICAL REPORTS: Scientific and technical information considered important, complete, and a lasting contribution to existing knowledge.

TECHNICAL NOTES: Information less broad in scope but nevertheless of importance as a contribution to existing knowledge.

TECHNICAL MEMORANDUMS: Information receiving limited distribution because of preliminary data, security classification, or other reasons.

CONTRACTOR REPORTS: Technical information generated in connection with a NASA contract or grant and released under NASA auspices.

TECHNICAL TRANSLATIONS: Information published in a foreign language considered to merit NASA distribution in English.

SPECIAL PUBLICATIONS: Information derived from or of value to NASA activities. Publications include conference proceedings, monographs, data compilations, handbooks, sourcebooks, and special bibliographies.

TECHNOLOGY UTILIZATION PUBLICATIONS: Information on technology used by NASA that may be of particular interest in commercial and other nonaerospace applications. Publications include Tech Briefs; Technology Utilization Reports and Notes; and Technology Surveys.

Details on the availability of these publications may be obtained from:

SCIENTIFIC AND TECHNICAL INFORMATION DIVISION

NATIONAL AERONAUTICS AND SPACE ADMINISTRATION

Washington, D.C. 20546